# BIOENGINEERING AND BIOTECHNOLOGY APPROACHES IN CARDIOVASCULAR SCIENCES

EDITED BY: Jianyi Zhang, Vahid Serpooshan, James J. H. Chong and Philippe Menasché

PUBLISHED IN: Frontiers in Bioengineering and Biotechnology

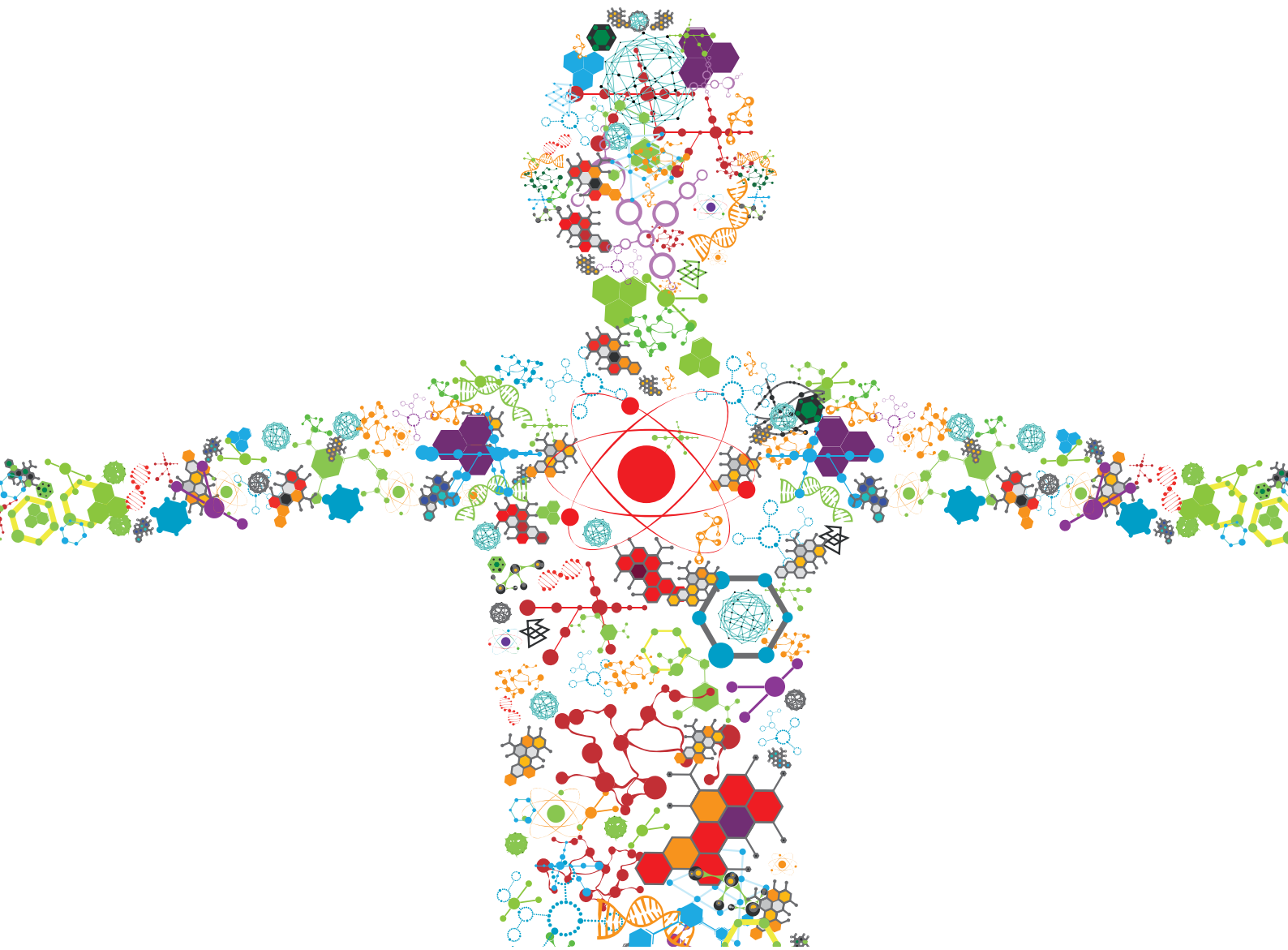

frontiers Research Topics

ISSN 1664-8714
ISBN 978-2-88971-462-9
DOI 10.3389/978-2-88971-462-9

## About Frontiers

Frontiers is more than just an open-access publisher of scholarly articles: it is a pioneering approach to the world of academia, radically improving the way scholarly research is managed. The grand vision of Frontiers is a world where all people have an equal opportunity to seek, share and generate knowledge. Frontiers provides immediate and permanent online open access to all its publications, but this alone is not enough to realize our grand goals.

## Frontiers Journal Series

The Frontiers Journal Series is a multi-tier and interdisciplinary set of open-access, online journals, promising a paradigm shift from the current review, selection and dissemination processes in academic publishing. All Frontiers journals are driven by researchers for researchers; therefore, they constitute a service to the scholarly community. At the same time, the Frontiers Journal Series operates on a revolutionary invention, the tiered publishing system, initially addressing specific communities of scholars, and gradually climbing up to broader public understanding, thus serving the interests of the lay society, too.

## Dedication to Quality

Each Frontiers article is a landmark of the highest quality, thanks to genuinely collaborative interactions between authors and review editors, who include some of the world's best academicians. Research must be certified by peers before entering a stream of knowledge that may eventually reach the public - and shape society; therefore, Frontiers only applies the most rigorous and unbiased reviews.
Frontiers revolutionizes research publishing by freely delivering the most outstanding research, evaluated with no bias from both the academic and social point of view. By applying the most advanced information technologies, Frontiers is catapulting scholarly publishing into a new generation.

## What are Frontiers Research Topics?

Frontiers Research Topics are very popular trademarks of the Frontiers Journals Series: they are collections of at least ten articles, all centered on a particular subject. With their unique mix of varied contributions from Original Research to Review Articles, Frontiers Research Topics unify the most influential researchers, the latest key findings and historical advances in a hot research area! Find out more on how to host your own Frontiers Research Topic or contribute to one as an author by contacting the Frontiers Editorial Office: frontiersin.org/about/contact

# BIOENGINEERING AND BIOTECHNOLOGY APPROACHES IN CARDIOVASCULAR SCIENCES

Topic Editors:
**Jianyi Zhang,** University of Alabama at Birmingham, United States
**Vahid Serpooshan,** Emory University, United States
**James J. H. Chong,** The University of Sydney, Australia
**Philippe Menasché,** Assistance Publique Hopitaux De Paris, France

**Citation:** Zhang, J., Serpooshan, V., Chong, J. J. H., Menasché, P., eds. (2021). Bioengineering and Biotechnology Approaches in Cardiovascular Sciences. Lausanne: Frontiers Media SA. doi: 10.3389/978-2-88971-462-9

# Table of Contents

frontiers in Bioengineering and Biotechnology

EDITORIAL
published: 20 August 2021
doi: 10.3389/fbioe.2021.746435

# Editorial: Bioengineering and Biotechnology Approaches in Cardiovascular Sciences

*Jianyi Zhang*[1,2]*, *Martin L. Tomov*[3], *James J. H. Chong*[4,5,6], *Philippe Menasché*[1,7] and *Vahid Serpooshan*[3,8,9]*

[1]Department of Biomedical Engineering, School of Medicine and School of Engineering, University of Alabama at Birmingham, Birmingham, AL, United States, [2]Division of Cardiovascular Diseases, Department of Medicine, School of Medicine, University of Alabama at Birmingham, Birmingham, AL, United States, [3]Department of Biomedical Engineering, Emory University School of Medicine and Georgia Institute of Technology, Atlanta, GA, United States, [4]Sydney Medical School, The University of Sydney, Sydney, NSW, Australia, [5]Centre for Heart Research, Westmead Institute for Medical Research, The University of Sydney, Sydney, NSW, Australia, [6]Department of Cardiology, Westmead Hospital, Sydney, NSW, Australia, [7]Department of Cardiovascular Surgery, Hôpital Européen Georges Pompidou, Université de Paris, PARCC, INSERM, Paris, France, [8]Department of Pediatrics, Emory University School of Medicine, Atlanta, GA, United States, [9]Children's Healthcare of Atlanta, Atlanta, GA, United States

**Keywords: bioengineering, biotechnologhy, cardiovascular medicine, tissue engieering, stem cell therapies**

OPEN ACCESS

***Edited and reviewed by:***
*Ranieri Cancedda, Independent Researcher, Genova, Italy*

***Correspondence:**
*Jianyi Zhang*
*jayzhang@uab.edu*
*Vahid Serpooshan*
*Vahid.serpooshan@bme.gatech.edu*

***Specialty section:***
*This article was submitted to Tissue Engineering and Regenerative Medicine, a section of the journal Frontiers in Bioengineering and Biotechnology*

***Received:*** *23 July 2021*
***Accepted:*** *04 August 2021*
***Published:*** *20 August 2021*

***Citation:***
*Zhang J, Tomov ML, Chong JJ H, Menasché P and Serpooshan V (2021) Editorial: Bioengineering and Biotechnology Approaches in Cardiovascular Sciences. Front. Bioeng. Biotechnol. 9:746435. doi: 10.3389/fbioe.2021.746435*

**Editorial on the Research Topic**

**Bioengineering and Biotechnology Approaches in Cardiovascular Sciences**

Medical science has often looked to the fields of bioengineering and biotechnology as tools that can facilitate the clinical translation of new therapeutic strategies. This Research Topic, *Bioengineering and Biotechnology Approaches in Cardiovascular Sciences*, focuses on cardiovascular bioengineering principles that seek to develop cells and tissues that fully recapitulate the functional properties of their native analogs. Early studies were frequently limited by a lack of cells, especially cardiomyocytes (CMs), but progress has accelerated since the development of techniques for reprogramming somatic cells into induced pluripotent stem cells (iPSCs) and then differentiating them into nearly any desired lineage. Here, we present a collection of 13 original research and review articles that provide the reader with a broad overview of recent discoveries and innovations that may expedite the use of bioengineered cells and tissues for therapeutic applications, disease modeling, and drug testing.

## CARDIAC THERAPY

With pluripotent cells and their differentiated progeny beginning to be investigated in patients, Menasché has reviewed their use from a clinical perspective. The number of patients enrolled in these early-phase trials has been too low to conclusively evaluate the efficacy of treatment, but concerns regarding the potential for treatment-related oncogenesis are largely resolved, and no other safety issues have been observed. The author also notes that most of the improvements associated with cell transplantation can be replicated *via* administration of the products that the cells produce and secrete in culture, and that the practical benefits of secretome administration could be advantageous for clinical applications. Furthermore, some evidence suggests that much of the benefit of myocardial cell therapy may be attributable to an acute immune response; Elde et al. briefly discuss how this new insight intersects with recent innovations in molecular and cell biology, biomaterials, biomechanics, and tissue engineering.

Much of the work in regenerative myocardial therapy has focused on CMs—the fundamental contractile units of the heart—and on the vascular cells that support them. However, Chen et al. discuss how cardiac fibroblasts (CFs) may contribute to myocardial regeneration by inducing CM proliferation and modulating the stiffness of the extracellular matrix. Notably, iPSCs retain many of the epigenetic characteristics present in the cells from which they were reprogrammed. Thus, iPSCs generated from CFs may be more suitable for cardiac therapy than those produced from other cell lineages. Conventional methods for iPSC-CM differentiation have been conducted in culture plates with two-dimensional (2D) cell sheets, but Kahn-Krell et al. introduce a three-dimensional (3D) differentiation protocol that is more suitable for commercial production. Their approach yields up to 1.5 million cells/mL, with an efficiency of greater than 98% and lower between-batch variability than traditional 2D protocols.

CFs have also been reprogrammed directly into CMs without passing through an intermediate iPSC stage, which suggests that the endogenous pool of CFs could serve as a source of new CMs for remuscularizing damaged myocardium. Riching and Song provide an in-depth review of direct CF-to-CM reprogramming, including the endogenous signaling pathways and epigenetic markers that influence reprogramming efficiency, as well as less extensive discussions of therapeutic revascularization and the transient induction of CM proliferation. Both direct and indirect reprogramming are discussed by Chingale et al., who also review the use of viral and non-viral vectors, methods for targeting reprogramming vectors and therapeutics to the heart, and how cell-derived proteins, exosomes, and microRNAs have been used to overcome limitations in cell production. They also highlight recent advancements in the manufacturing of cardiac patches *via* 3D bioprinting.

Cardiac function can also be compromised by disruptions in heart rhythm, and although electronic pacemakers can be life-saving, they cannot adapt to somatic growth or respond to physiological changes in the autonomic nervous system. Thus, this collection of articles also includes a report by Naumova and Lop, who review strategies for applying the principles of bioengineering and biotechnology to the development of biological pacemakers.

## TISSUE ENGINEERING

Many engineered tissues are produced by suspending cells within a biomaterial scaffold, but ensuring that the cells are homogenously distributed throughout the 3D scaffold can be challenging for constructs of clinically relevant sizes. Cunnane et al. have developed a semi-automated seeding device that can homogenously distribute up to 200 million cells along both the length and circumference of 10-cm long tissue-engineered vascular grafts (TEVGs). When transplanted into the carotid arteries of sheep, mechanical and histological assessments conducted 10 weeks later confirmed graft patency and indicated that the TEVG was being gradually remodeled with the native tissue.

Engineered tissue transplants are frequently secured in place with sutures or bioglues, which may fail to provide adequate adhesion strength or induce secondary damage, cytotoxicity, and adverse immune reactions. Chen et al. explore the mechanisms that influence transplant adhesion and then highlight the development of scaffolds that are intrinsically adhesive [i.e., adhesive tissue engineered scaffolds (ATESs)]. They also discuss some of the key challenges associated with the use of ATES in specific tissue engineering applications and strategies for both qualitatively and quantitatively monitoring adhesion. Furthermore, the integrity and function of transplanted tissues are crucially dependent on adequate vascularization. Although skeletal muscle myoblasts (SMMs) have been extensively studied for treatment of cardiac injury with little evidence of myocardial regeneration, they appear to improve recovery and limit remodeling by secreting cytokines that promote angiogenesis. Skeletal muscle fibroblasts (SMFs) also secrete pro-angiogenic cytokines. Thummarati and Kino-Oka demonstrate that the formation of endothelial networks in multilayered sheets of human SMMs and SMFs was greatest when 30–40% of the cells were SMFs. Thus, combinations of human SMFs and SMMs may improve the vascularity and transplantation efficiency of engineered tissues.

## PRECLINICAL AND *IN VITRO* MODELING

The clinical translation of new pharmaceutical and cell-based treatments is crucially dependent on the development of appropriate animal models. Shin et al., review the challenges associated with modeling the complexity of human ischemic cardiovascular disease in large animals, which include not only the anatomical and physiological differences between animals and humans, but also species-specific surgical modifications, limitations in sample size, and a lack of sufficient transparency in published reports. Large animal studies are also typically conducted in young, healthy animals and, consequently, fail to replicate the variations in age, comorbidity, and overall health observed in patients.

Because the clinical implications of observations in animals are limited by fundamental differences between humans and the model species, the results from animal studies are best interpreted in concert with those from experiments performed with engineered human tissue and organoid chips. These technologies are more physiologically relevant than conventional cell-culture models, because they are designed to replicate key properties of the native environment, including interactions among multiple cell types, mechanical stress, and other dynamic factors. Furthermore, since iPSCs can be differentiated from the somatic cells of each individual patient, chips constructed with iPSC-derived cells could be powerful tools for personalizing patient diagnosis and treatment. Chan and Huang review the design and construction of tissue chips and their application as models for studying the pathogenesis of cardiovascular disease and drug testing, while Zhao et al. discuss organoids and organoid chips, which mimic the even more complex structural and functional properties of entire organs. Organoid chips have already been used to model the

lung, kidney, and blood-brain barrier, but the functional and structural integrity of organoid models may be compromised by deficiencies in vascularity; thus, the authors include a detailed discussion of techniques such as 3D and 4D (i.e., 3D plus time) bioprinting that can be used to generate more extensive and sophisticated vascular networks.

## SUMMARY

The articles presented in this Research Topic provide a synopsis of many of the most recent advancements in cardiovascular cell and tissue bioengineering. The Editors are pleased to highlight this work and hope that it may help provide a foundation for future studies that could lead to the development of transformative new investigational tools and therapeutic approaches in the field of cardiovascular medicine.

## AUTHOR CONTRIBUTIONS

JZ, MLT, JJHC, PM, and VS contributed to the writing of this article.

## FUNDING

NIH grant number R00HL127295, NSF CAREER Award (no. 2044657), and the Marvin H. and Nita S. Floyd Research Fund Award to VS; NIH UO1 HL134764, RO1 HL114120, RO1 HL131017, RO1 HL149137, T32 EB032872 to JZ; NHMRC MRF1194139 to JC.

**Conflict of Interest:** The authors declare that the research was conducted in the absence of any commercial or financial relationships that could be construed as a potential conflict of interest.

**Publisher's Note:** All claims expressed in this article are solely those of the authors and do not necessarily represent those of their affiliated organizations, or those of the publisher, the editors and the reviewers. Any product that may be evaluated in this article, or claim that may be made by its manufacturer, is not guaranteed or endorsed by the publisher.

frontiers in Bioengineering and Biotechnology

ORIGINAL RESEARCH
published: 23 September 2020
doi: 10.3389/fbioe.2020.578140

# Effect of Co-culturing Fibroblasts in Human Skeletal Muscle Cell Sheet on Angiogenic Cytokine Balance and Angiogenesis

*Parichut Thummarati and Masahiro Kino-oka**

*Department of Biotechnology, Graduate School of Engineering, Osaka University, Osaka, Japan*

Skeletal muscle comprises a heterogeneous population of myoblasts and fibroblasts. Autologous skeletal muscle myoblasts are transplanted to patients with ischemia to promote cardiac regeneration. In damaged hearts, various cytokines secreted from the skeletal muscle myoblasts promote angiogenesis and consequently the recovery of cardiac functions. However, the effect of skeletal muscle fibroblasts co-cultured with skeletal muscle myoblasts on angiogenic cytokine production and angiogenesis has not been fully understood. To investigate these effects, production of vascular endothelial growth factor (VEGF) and hepatocyte growth factor (HGF) was measured using the culture medium of monolayers prepared from various cell densities (mono-culture) and proportions (co-culture) of human skeletal muscle myoblasts (HSMMs) and human skeletal muscle fibroblasts (HSMFs). HSMM and HSMF mono-cultures produced VEGF, whereas HSMF mono-culture produced HGF. The VEGF productivity observed in a monolayer comprising low proportion of HSMFs was two-fold greater than that of HSMM and HSMF mono-cultures. The production of VEGF in HSMMs but not in HSMFs was directly proportional to the cell density. VEGF productivity in non-confluent cells with low cell-to-cell contact was higher than that in confluent cells with high cell-to-cell contact. The dynamic migration of cells in a monolayer was examined to analyze the effect of HSMFs on myoblast-to-myoblast contact. The random and rapid migration of HSMFs affected the directional migration of surrounding HSMMs, which disrupted the myoblast alignment. The effect of heterogeneous populations of skeletal muscle cells on angiogenesis was evaluated using human umbilical vein endothelial cells (HUVECs) incubated with fabricated multilayer HSMM sheets comprising various proportions of HSMFs. Co-culturing HSMFs in HSMM sheet at suitable ratio (30 or 40%) enhances endothelial network formation. These findings indicate the role of HSMFs in maintaining cytokine balance and consequently promoting angiogenesis in the skeletal muscle cell sheets. This approach can be used to improve transplantation efficiency of engineered tissues.

**Keywords: skeletal muscle cell sheet, fibroblast co-culture, cytokine balance, myoblast alignment, angiogenesis, tissue engineering**

OPEN ACCESS

***Edited by:***
*Vahid Serpooshan, Emory University, United States*

***Reviewed by:***
*Karina Nakayama, Oregon Health & Science University, United States*
*Martin L. Tomov, Emory University, United States*

***Correspondence:**
*Masahiro Kino-oka*
*kino-oka@bio.eng.osaka-u.ac.jp*

***Specialty section:***
*This article was submitted to Tissue Engineering and Regenerative Medicine, a section of the journal Frontiers in Bioengineering and Biotechnology*

***Received:*** *30 June 2020*
***Accepted:*** *01 September 2020*
***Published:*** *23 September 2020*

***Citation:***
*Thummarati P and Kino-oka M (2020) Effect of Co-culturing Fibroblasts in Human Skeletal Muscle Cell Sheet on Angiogenic Cytokine Balance and Angiogenesis. Front. Bioeng. Biotechnol. 8:578140. doi: 10.3389/fbioe.2020.578140*

## INTRODUCTION

Transplantation of skeletal muscle myoblasts is a promising therapeutic strategy for myocardial infarction (Pagani et al., 2003). Easy availability and lack of immunologic barriers are the major advantages of using skeletal muscle myoblasts for transplantation (Dib et al., 2005b; Menasche, 2007). Furthermore, transplantation of autologous skeletal muscle myoblasts into the heart is reported to be safe and efficient in humans (Menasche et al., 2001; Durrani et al., 2010). Previous studies have revealed that various factors of skeletal muscle myoblasts induce angiogenesis and recruit the progenitors at the infarcted area, which result in the induction of cardiac tissue and recovery of heart function (Suzuki et al., 2001; Murtuza et al., 2004; Memon et al., 2005; Shirasaka et al., 2013). Additionally, the implantation of multilayered skeletal muscle myoblast sheets enhances angiogenesis both *in vitro* (Ngo et al., 2013) and *in vivo* (Sekiya et al., 2009; Miyagawa et al., 2017).

Similar to myoblasts, fibroblasts, which are the most common cell type in the connective tissues, can synthesize and secrete proangiogenic growth factors such as vascular endothelial growth factor (VEGF) and hepatocyte growth factor (HGF). In addition, fibroblasts synthesize extracellular matrix (ECM) components, such as collagen, fibronectin and proteoglycans that can promote angiogenesis in ischemia areas (Newman et al., 2011; Kendall and Feghali-Bostwick, 2014; Chapman et al., 2016). However, increased number of fibroblasts may result in excessive deposition of ECM and consequently fibrosis (Mann et al., 2011; Kendall and Feghali-Bostwick, 2014). Thus, co-transplantation of skeletal muscle myoblasts and a small proportion of fibroblasts can be a potential strategy for myocardial tissue regeneration. The proportion of fibroblasts and myoblasts in the skeletal tissue may vary depending on the tissue source, which may affect the therapeutic efficacy of transplantation. There is limited understanding of the effect of heterogeneous populations of skeletal muscle myoblasts and fibroblasts on cytokine production and angiogenesis.

Various potent growth factors are reported to function as angiogenic simulators in ischemic areas. VEGF, HGF, and basic fibroblast growth factor (bFGF or FGF2), which are direct proangiogenic markers that promote angiogenesis (Fallah et al., 2019; Laddha and Kulkarni, 2019), are experimentally demonstrated to improve cardiac functions. Combined delivery of HGF and VEGF to infarcted myocardium showed an increase of left ventricle (LV) wall thickness and capillary density, reduce myocardial infarction size and improve dilatation index (Makarevich et al., 2018). Clinical trials have demonstrated enhancing myocardial perfusion leading to a better cardiac function and well-tolerated following therapy with VEGF, HGF, and FGF2 (Atluri and Woo, 2008). VEGF exerts its physiological functions by binding to two homologous VEGF receptors, which are expressed on vascular endothelial cells (Carmeliet, 2005; Fallah et al., 2019). VEGF directly acts on the endothelial cells to enhance migration, increase permeability, and enhance survival during vascularization and angiogenesis (Zachary and Gliki, 2001). Injection of skeletal myoblasts with genetic modifications to upregulate the expression of VEGF was reported to effectively treat acute myocardial infarction through vasodilatory and angiogenic effects (Suzuki et al., 2001; Haider et al., 2004). However, this therapeutic strategy of gene transfer involves viral vectors, which are associated with adverse effects and ethical concerns (Kim et al., 2001). HGF, a potent mitogen for various cell types, including endothelial cells, promotes endothelial cell motility, interaction, branching morphogenesis, and/or tubular morphogenesis during angiogenesis and vascularization (Morimoto et al., 1991; Rosen et al., 1997). Furthermore, previous studies have demonstrated the therapeutic effects of HGF on myocardial infarction *in vivo* (Nakamura et al., 2000; Ueda et al., 2001; Jin et al., 2003; Liu et al., 2016). The HGF-engineered skeletal myoblasts promote angiogenesis, reduce myocardial fibrosis, and decrease apoptosis of cardiomyocytes (Yuan et al., 2008; Madonna et al., 2015). FGF2 is also reported to exert therapeutic effects in ischemia by regulating angiogenesis through regulation of various cell-cell interactions (Murakami and Simons, 2008) and other growth factors or chemokines, including VEGF (Masaki et al., 2002; Kanda et al., 2004) and HGF (Onimaru et al., 2002).

This study aimed to investigate the effect of co-coculturing human skeletal muscle fibroblasts (HSMFs) with human skeletal muscle myoblast (HSMM) sheets on cytokine balance and angiogenesis *in vitro*. Angiogenic cytokine productivity was measured in the monolayers prepared from various seeding densities (mono-culture) and proportions (co-culture) of HSMFs and HSMMs. The dynamic behavior of cells in the monolayer was analyzed to understand the mechanism underlying cytokine production in the skeletal muscle cells. The effect of co-culturing HSMFs in five-layered HSMM sheet on angiogenesis was evaluated using an *in vitro* angiogenesis model mimicking the transplantation area.

## MATERIALS AND METHODS

### Cell Culture and Preparation

In this study, human skeletal muscle cells (Lot. No. 6F4296; Lonza, Walkersville, Inc., Walkersville, MD, United States) that contain HSMMs and HSMFs were used for the experiments. The skeletal muscle cells were sub-cultured at 37°C and 5% $CO_2$ in skeletal cell growth medium-2 (SkGM-2; Lonza, Walkersville, MD, United States), which was formulated by combining SkBM-2 Basal Medium (Cat. No. CC-3246) and SkGM-2 SingleQuots Supplements and Growth Factors (Cat. No. CC-3244). The desmin-positive and desmin-negative cells were identified as HSMMs and HSMFs, respectively (Kino-oka et al., 2013). The proportion of HSMMs and HSMFs in the original human skeletal muscle cells or "pre-sorted cells" was 68.1 and 31.9%, respectively (**Supplementary Figure 1**).

The HSMMs and HSMFs were sorted using fluorescence-activated cell sorting (FACS). The pre-sorted cells were stained with Alexa Fluor 488-conjugated anti-CD56 (NCAM) antibody (Cat. No. 2191555, Sony, Sony Biotechnology, Inc., San Jose, CA, United States) at 5 μl to 1 × $10^6$ cells, following the

manufacturer's instructions. The cells were then sorted using a cell sorter (JZAN JR; Bay Bioscience, Co., Ltd., Japan) based on cell size and CD56-Alexa Fluor 488 fluorescence intensity (**Supplementary Figure 1D**). The sorted $CD56^+$ and $CD56^-$ cells (post-sorted cells) were cultured at 37°C and 5% $CO_2$ in SkGM-2 medium. The purity of pre-sorted cells and post-sorted cells was determined by culturing the cells in SkGM-2 medium for 24 h. Next, the cells were fixed with 4% formaldehyde (Wako Pure Chemical Industries, Tokyo, Japan) for 15 min and permeabilized with 0.5% Triton X-100 for 20 min. The cells were blocked with 1% bovine serum albumin (BSA) for 90 min and incubated with a mixture of anti-desmin antibody (Y66) (Cat. No. ab32362, Abcam, United States) at 1:250 dilution, and anti-fibroblast antibody (clone TE-7) (Cat. No. CBL271, Millipore, United States) at 1:100 dilution prepared in 1% (w/v) BSA at 4°C overnight. The cells were washed and immunolabeled with a mixture of Alexa Fluor 594 goat anti-rabbit IgG (Cat. No. A11001, Molecular Probes, Life Technologies, United States) at 1:250 dilution and Alexa Fluor 488 goat anti-mouse IgG (Cat. No. A11012, Molecular Probes, Life Technologies, United States) at 1:250 dilution prepared in 1% (w/v) BSA for 1 h at room temperature, followed by counterstaining with 4′-6-diamidino-2-phenylindole (DAPI) (Cat. No. D1306, Molecular Probes, Life Technologies, United States).

## Culturing HSMMs and HSMFs at Various Initial Cell Densities

The sorted HSMMs or HSMFs were cultured in SkGM-2 medium at various initial seeding densities ($X_0$) ($0.1 \times 10^5$, $0.8 \times 10^5$, and $3.5 \times 10^5$ cells/cm$^2$) inside a Teflon ring (area: 0.95 cm$^2$) placed in 24 well plates. The Teflon rings were removed after incubation at 37°C and 5% $CO_2$ for 24 h. The cultured medium was replaced every 24 h and collected at 72 h for measuring the levels of cytokines.

## Preparation of Monolayer With Various HSMM:HSMF Ratios

The sorted HSMMs were mixed with HSMFs in various proportions from 0 (no HSMF) to 100% HSMF (HSMF:HSMM ratios from 0:20 to 20:0) and seeded inside a Teflon ring (area: 0.95 cm$^2$) placed in 24 well plates at $X_0$ of $3.5 \times 10^5$ cells/cm$^2$. The cells were incubated for 24 h at 37°C and 5% $CO_2$ to form the monolayer. After 24 h, the Teflon rings were removed, and the culture medium was replaced with fresh medium. The cultured medium was collected at 72 h for cytokine measurement.

To prepare a monolayer for cell alignment analysis, the sorted HSMFs were stained with CellTracker Green CMFDA (Cat. No. C7025, Invitrogen, Thermo Fisher Scientific, United States). Next, the stained HSMFs were mixed with HSMMs and seeded ($X_0$ of $3.5 \times 10^5$ cells/cm$^2$) inside a Teflon ring (area: 0.95 cm$^2$) placed in 24 well plates. After 24 h, the Teflon rings were removed, and the culture medium was replaced with fresh medium. At 48 h, the attached cells were stained with NucBlue Live ReadyProbe Reagent (Hoechst 33342) (Cat. No. R37605, Molecular Probe, Life Technologies, United States), following the manufacturer's instructions.

## Quantitative Analysis of HSMM and HSMF Migration and Cell Alignment

**Figure 1** shows the analysis of cell migration and alignment data from cell tracking and time-lapse observation. Images of stained nuclei and HSMFs in the monolayer were captured every 1 for 24 h using the IN Cell Analyzer 2000 (GE Healthcare) under a 20X objective lens. The original images (1.5 mm × 1.5 mm) of stained cells were captured in an 8-bit gray scale with a resolution of 0.74 μm/pixel. The images were captured from three random areas from duplicate samples in the 24 well plates. For quantitative analysis, 100 nucleus-stained cells from the local density in three regions of interest (ROI; 0.8 mm × 0.8 mm) from duplicated samples were used. The cells from sequence images were measured at position (X,Y) using Image J software (Manual tracking plugin), and the data were visualized in a trajectory plot. The migration velocity ($\vec{v}$, μm/h) and directional angle [θ and θ′, degree (°)] were quantified as shown in **Figures 1B,C**, respectively. The frequency of migration angle of cells during 48–72 h of incubation was plotted in a histogram. The cell alignment index (CAI) was defined as the amount of variation (standard deviation, σ) of the migration angle of cells. A high σ value indicates a high degree of cell alignment disruption.

## Measurement of Cytokine Productivity

Cytokine levels were measured in the cultured medium collected from triplicate samples at 72 h. The levels of VEGF, HGF, and FGF2 were measured using the human VEGF Quantikine enzyme-linked immunosorbent assay (ELISA) assay (Cat. No. DVE00, R&D Systems, Inc., United States), human HGF ELISA Kit (Cat. No. KAC2211, Invitrogen, Thermo Fisher Scientific, United States), and human FGF Quantikine ELISA (Cat. No. DFB50, R&D Systems, Inc., United States), respectively, following the manufacturer's instructions. The Sf 21-expressed recombinant human VEGF165, *E. coli*-expressed recombinant human basic FGF and recombinant human HGF provided from the ELISA kits were used to establish the standard curve. The baseline levels of these cytokines in cultured media without cells were measured. At 72 h, the cells in monolayer were fixed with 4% paraformaldehyde and the nuclei were stained with DAPI (Cat. No. D1360, Invitrogen, Thermo Fisher Science, United States) to determine the total cell number in the monolayer. Cytokine productivity refers to the amount of cytokine (pg) produced per cell per hour (pg/cell × h) or per sheet (pg/sheet × day).

## Incubation of Five-Layered HSMM Sheets With Green Fluorescent Protein-Tagged Human Umbilical Vascular Endothelial Cells (GFP-HUVECs)

A five-layered HSMM sheet containing different proportions of HSMFs was fabricated according to a previous method (Nagamori et al., 2013). Briefly, the HSMMs and HSMFs were sub-cultured and mixed at various proportions of 0 (no HSMF), 10, 30, and 40% HSMF (HSMF:HSMM ratios of 0:20, 2:18, 6:14, and 8:12). The cells were seeded at $X_0$ of $3.5 \times 10^5$ cells/cm$^2$

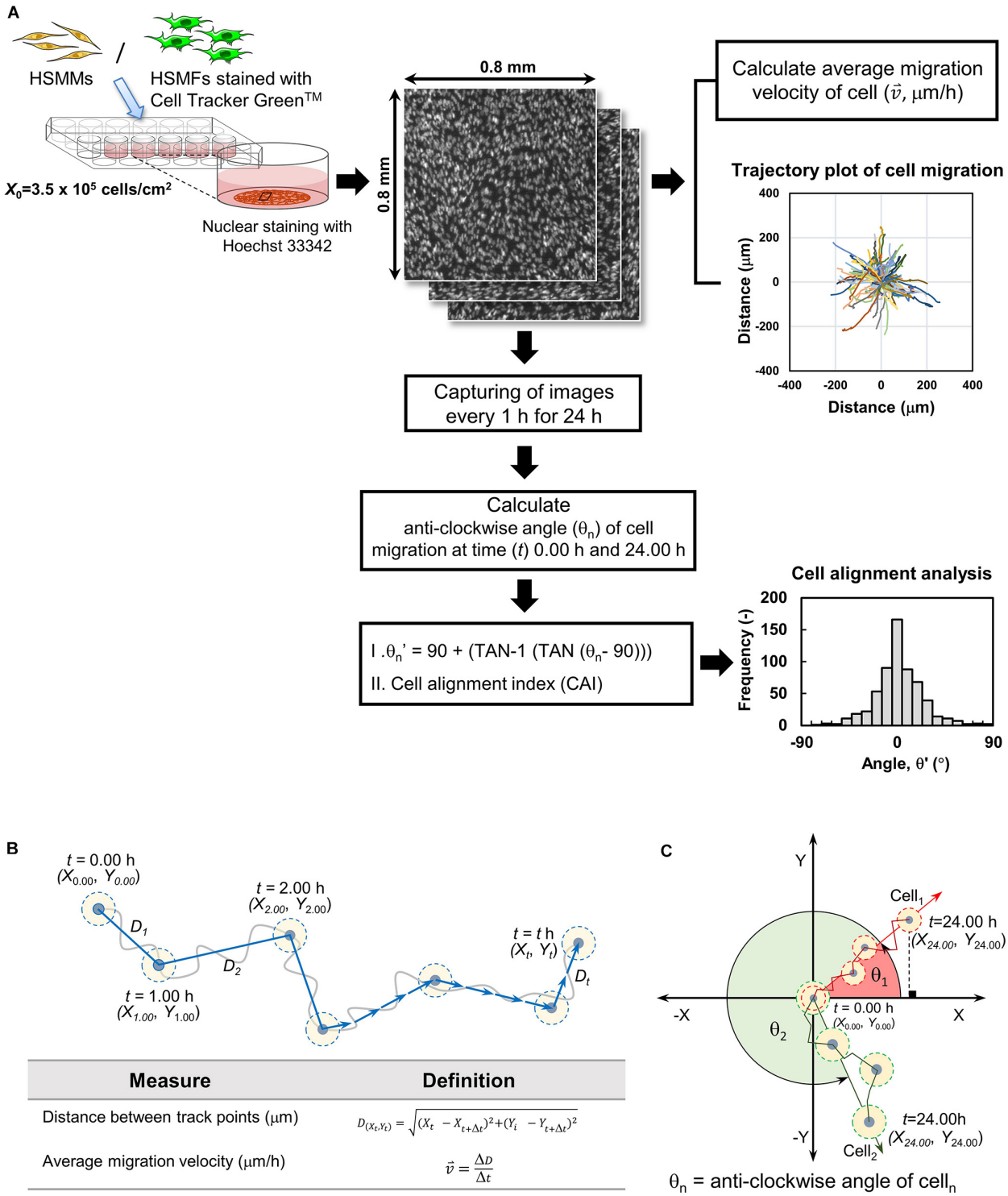


**FIGURE 1 |** Quantifying cell migration in monolayer using time-lapse image data analysis. **(A)** Diagram showing experimental procedure and data analysis of time-lapse images. The cells in the monolayer prepared using skeletal muscle cells with various proportion of human skeletal muscle fibroblast (HSMF) and human skeletal muscle myoblast (HSMM) were stained with Hoechst 33342. The images were captured every 1 h during 48–72 h of incubation. The positions (X,Y) of the nucleus were measured using Image J with Manual tracking plugin to evaluate the migration velocity ($\vec{v}$, μm/h), direction angle (θ′), and cell alignment index (CAI) for cell alignment analysis. **(B)** Cell positions at each hour were measured to calculate the distance between track point and average migration velocity. **(C)** The positions of the cell at origin ($t$ = 0.00 h) and at the end point ($t$ = 24.00 h) were measured to evaluate the anti-clockwise angle (θ′) of cell migration.

inside Teflon rings (0.95 $cm^2$) placed in the 24 well UpCell plates (CellSeed, Tokyo, Japan) with a temperature-responsive surface. The cells were incubated for 24 h at 37°C and 5% $CO_2$ to allow the formation of a monolayer sheet. To harvest the monolayer sheet, a gelatin stamp was overlaid onto the monolayer sheet in a well at 37°C. The temperature was decreased to 20°C, and the stamp was removed with the monolayer sheet from the bottom surface of the well. These steps were then repeated to sequentially harvest the monolayer sheets to form a multilayered construct. The multilayered sheet was transferred to the center of a 35 mm culture dish (ibidi GmbH, DE), which was seeded with GFP-HUVECs (Lot. No. 20100201001; Angio-Proteomie, MA, United States) ($X_0$ of 0.1 × $10^5$ cells/$cm^2$) in endothelial cell growth media-2 (EGM-2) at 37°C and 5% $CO_2$ for 24 h. At the sampling time ($t$), triplicate samples were harvested for quantitative analysis. During the incubation period, the medium was changed every day.

## Evaluation of GFP-HUVEC Network Formed Inside Multilayered HSMM Sheet

The images of eight positions in each sample were captured using a 10X objective lens of a confocal laser scanning microscope (FV-10i, Olympus, Tokyo, Japan). All images were converted to 8-bit gray scale with a size of 256 × 256 pixels covering an area of 1.27 mm × 1.27 mm. The images were processed (Image-Pro Plus; Media Cybernetics, Inc., Bethesda, MD, United States) using a low-pass filter for primary noise removal and binarization with a fixed intensity threshold. The threshold intensity was set as the average of the mode intensity and automatic threshold intensity. The binary images were subjected to skeletonization and secondary noise removal with a size threshold to remove items with a size of less than 16 pixels. The small branches were pruned in the objects. The total length of the network per image area ($L$; $cm^{-1}$) and the number of total tips of the network ($N_T$; tip/$cm^2$) were measured to estimate the degree of HUVEC network formation ($L/N$; cm/tip). The tips at the edge of the image were not counted.

## Statistical Analysis

All experimental data are expressed as mean ± standard deviation. Each experiment was performed on three independent sample ($n$ = 3) for quantitative analysis. The differences among multiple groups were evaluated using one-way analysis of variance (ANOVA), followed by Bonferroni or least-significant different (LSD) *post hoc* test (SPSS 26.0). The differences were considered statistically significant when the $P$-value was less than 0.01.

# RESULTS

## Effect of HSMF on Cytokine Productivity in HSMM Monolayer

Cytokine production in the monolayers prepared from skeletal muscle cells with various proportions of HSMF from no HSMF to 100% HSMF (HSMF:HSMM ratios from 0:20 to 20:0) was investigated after 72 h of culturing. The culture media of different groups were collected at 72 h to measure the levels of VEGF, HGF, and FGF2 (**Figure 2A**). VEGF productivity in monolayers derived from mono-cultures of HSMMs and HSMFs were 4.19 ± 0.10 × $10^{-5}$ and 4.18 ± 0.38 × $10^{-5}$ pg/cell × h, respectively. The VEGF productivity in the monolayer prepared from skeletal muscle cells with 15% (HSMF:HSMM ratio of 3:17) HSMF was approximately twofold higher (8.93 ± 0.45 × $10^{-5}$ pg/cell × h) than that in the monolayer prepared from mono-cultures of HSMF or HSMM ($P < 0.01$). The VEGF productivity decreased when the percentage of HSMF was higher than 15% (**Figure 2B**). In contrast to VEGF productivity, HGF productivity in the monolayer derived from HSMM mono-culture was low (0.33 ± 0.33 × $10^{-5}$ pg/cell × h). HGF productivity in the monolayer derived from HSMF mono-culture was 27.4 ± 2.27 × $10^{-5}$ pg/cell × h (**Figure 2C**). The baseline levels of VEGF and HGF in culture media without cells used in this experiment were 0.11 ± 0.19 and 0.05 ± 0.09 pg/ml, respectively. The levels of FGF2 were almost undetectable under all conditions (data not shown). These results indicate that varying the proportions of HSMM and HSMF in the skeletal cell monolayer differentially affected the production of cytokines. HGF was secreted only by HSMFs. The production of VEGF in the HSMM monolayers can be upregulated by introducing a small proportion of HSMFs.

## Effect of Cell Density on Cytokine Productivity in HSMMs and HSMFs

The effect of a small proportion of HSMFs in the HSMM monolayers on VEGF productivity was evaluated by examining the cell-to-cell contact. The productivities of VEGF in the sorted HSMMs cultured at low (0.1 × $10^5$ cells/$cm^2$), medium (0.8 × $10^5$ cells/$cm^2$), and high (3.5 × $10^5$ cells/$cm^2$) $X_0$ values, which resulted in varying degrees of cell-to-cell contacts, were compared with those of HSMFs. The productivity of VEGF in the monolayer derived from low $X_0$ value of HSMMs was 20.7 ± 1.46 × $10^{-5}$ pg/cell × h. However, the productivity of VEGF in the monolayers derived from medium and high $X_0$ values of HSMMs significantly decreased to 10.3 ± 0.07 × $10^{-5}$ ($P < 0.01$) and 5.18 ± 0.58 × $10^{-5}$ pg/cell × h ($P < 0.01$), respectively. The productivity of VEGF in the HSMF mono-culture varied, which was not related to $X_0$. The productivities of VEGF in the monolayer derived from low, medium, and high $X_0$ values of HSMFs were 2.18 ± 1.27 × $10^{-5}$, 6.90 ± 0.61 × $10^{-5}$, and 5.53 ± 0.60 × $10^{-5}$ pg/cell × h, respectively (**Figure 2D**). The productivity of HGF was high in the monolayer derived from HSMF mono-cultures at all $X_0$ values but was almost undetectable in the monolayer derived from HSMM mono-culture. The productivities of HGF in the monolayers derived from low, medium, and high $X_0$ values of HSMFs were 22.0 ± 0.39 × $10^{-5}$, 21.1 ± 4.47 × $10^{-5}$, and 24.3 ± 4.16 × $10^{-5}$ pg/cell × h, respectively. Additionally, the productivity of HGF was similar in the monolayers prepared from different $X_0$ values of HSMFs (**Figure 2E**). These results suggest that HSMF-mediated myoblast-myoblast contact disruption might promote VEGF production in HSMMs.

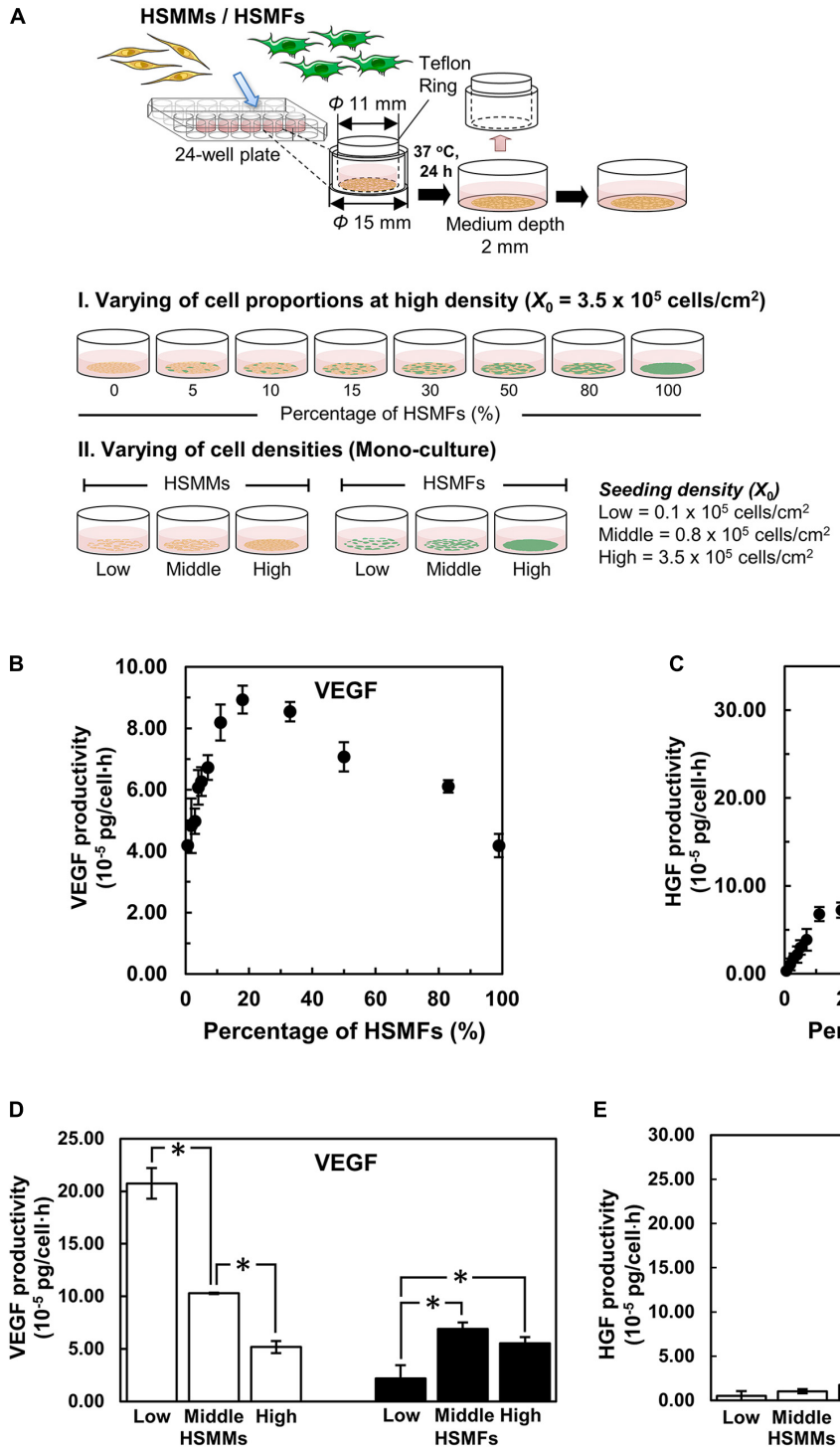


**FIGURE 2 |** Cytokine productivity in monolayers of skeletal muscle cells. **(A)** A schematic drawing shows the experimental design. The monolayers were prepared with various proportions of HSMFs and HSMMs (I) or using various initial seeding densities ($X_0$) of HSMFs or HSMMs (II). The culture medium of monolayers was collected at 72 h to measure the cytokine levels using enzyme-linked immunosorbent assay (ELISA). **(B)** Effect of co-culturing HSMFs and HSMMs with various proportions in a high initial density on vascular endothelial growth factor (VEGF) productivity and **(C)** hepatocyte growth factor (HGF) productivity. **(D)** The HSMMs and HSMFs were cultured various $X_0$ at 0.1 × 10$^5$ (low), 0.8 × 10$^5$ (middle) and 3.5 × 10$^5$ cells/cm$^2$ (high) for 72 h. The productivities of vascular endothelial growth factor (VEGF) and hepatocyte growth factor (HGF) **(E)** in the culture medium were measured. Data are represented as average cytokine productivity ± standard deviation from triplicate samples ($n$ = 3). *$P$ < 0.01; one-way analysis of variance (ANOVA), followed by Bonferroni *post hoc* test.

## Migration of HSMMs and HSMFs in the Monolayer

Next, the ability of HSMF in the HSMM monolayer to disrupt myoblast-to-myoblast contact was analyzed. Additionally, time-lapse analysis was performed to analyze the interaction and migration of HSMM and HSMF in the monolayer. The migration of HSMFs in the monolayer was hypothesized to disrupt the myoblast-to-myoblast contact, which may alter the directional migration and alignment of HSMMs. To verify this hypothesis, an HSMM monolayer containing CellTracker Green$^{TM}$-labeled HSMFs of 2% (HSMM:HSMF ratio of 1:49) was prepared to observe the individual HSMF cell migration behaviors. The nuclei of cells in the monolayer were stained with Hoechst 33342, and the cell migration was tracked during 48–72 h. Directional migration of HSMMs in the HSMF-free area was compared with that of HSMM in the HSMF-surrounded area (**Figure 3A**). The trajectory plot revealed that HSMMs in the HSMF-surrounded area exhibited random migration, whereas those in the HSMF-free area exhibited unidirectional migration (**Figure 3B** and **Supplementary Movie 1**). This indicated that HSMFs are involved in myoblast-to-myoblast contact disruption.

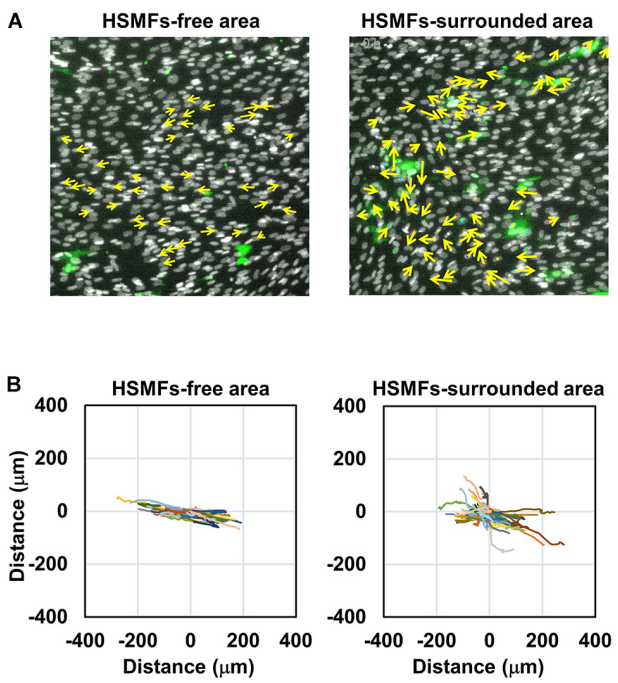


**FIGURE 3 |** Dynamic behavior of HSMM cell migration in the monolayer comprising a small proportion of HSMF population. **(A)** A HSMM cell monolayer comprising 2% HSMF was prepared to analyze the migration of HSMMs in the HSMF-free and HSMF-surrounded areas. The HSMFs were stained with CellTracker Green$^{TM}$ to distinguish them from HSMMs. All cells in the monolayer were stained with Hoechst 33342. The images were captured every 1 h during 48–72 h. Yellow arrow defines the direction of cell migration in the local area. **(B)** Representative trajectory plots showing directional migration of 100 HSMMs from each area. The direction and velocity of cell migration of 100 cells were measured at every position and plotted in the trajectory plot.

## Quantification of Cell Migration and Alignment in Monolayer Comprising Various HSMF Proportions

To confirm the role of HSMFs in myoblast-to-myoblast contact disruption, cell alignment in the monolayer prepared using HSMMs and various proportions of HSMFs was analyzed using an inverted microscope. The HSMM monolayer without HSMFs exhibited uniform cell alignment. The cell alignment was poor in some areas of the monolayer comprising a small proportion of HSMFs. The cell alignment was completely dysregulated in the monolayer comprising high proportion of HSMFs (**Supplementary Figure 2**). The HSMFs exhibited active migration in the monolayer comprising low proportions of HSMF (5 to 15% HSMF). Additionally, the migration velocity of HSMFs was significantly higher than that of HSMMs ($P < 0.01$). The migration velocity of HSMFs decreased when the proportion of HSMFs increased in the monolayer (**Figure 4A**). The trajectory plot of HSMM migration in the monolayer lacking HSMFs revealed unidirectional migration. The number of HSMMs exhibiting multidirectional migration increased with an increase in HSMF proportion (**Figure 4B** and **Supplementary Movie 2**). The HSMFs in the monolayer derived from skeletal muscle cells with 5, 10, and 15% HSMF exhibited active multidirectional migration (**Figure 4C** and **Supplementary Movie 2**). For quantitative analysis of cell alignment, the nucleus of HSMMs from three areas per sample was tracked to calculate the migration angle (θ') as a robust metric to judge overall alignment (**Figure 1A**). The θ' of HSMM migration in the monolayer comprising different HSMF proportions was plotted in a histogram (**Figure 5**). The degree of cell alignment disruption was determined by comparatively analyzing the standard deviation (σ) values, which indicate variation of directional migration (**Supplementary Figure 3**). Higher σ values indicate an increase in the myoblast alignment disruption level. The σ value of HSMM monolayer was 25.67 ± 4.67. The σ values of HSMFs in the monolayer derived from skeletal muscle cells with HSMF proportion of 5, 10, 15, 50 and 80% were 31.19 ± 9.52, 37.57 ± 3.27, 44.41 ± 5.70 (maximum σ value), 42.30 ± 3.43 and 43.73 ± 2.42, respectively. The staining of F-actin was performed to confirm the alignment disorder in HSMM monolayer containing 15% HSMF (**Supplementary Figure 6**). These results indicate that the HSMFs inhibit the myoblast-to-myoblast contact and consequently disrupt the myoblast alignment.

## Effect of HSMFs on GFP-HUVECs Network Formation in the Multilayered HSMM Sheet

The efficiency of HUVEC network formation in the HSMM sheets comprising various proportions of HSMF was evaluated using an *in vitro* angiogenesis assay mimicking the transplantation area *in vivo* (Nagamori et al., 2013). The five-layered sheet was prepared using skeletal muscle cells with 0, 10, 30, and 40% HSMF. The sheet was then co-cultured with GFP-HUVECs (**Figure 6A**). Fabricated HSMM sheets morphology

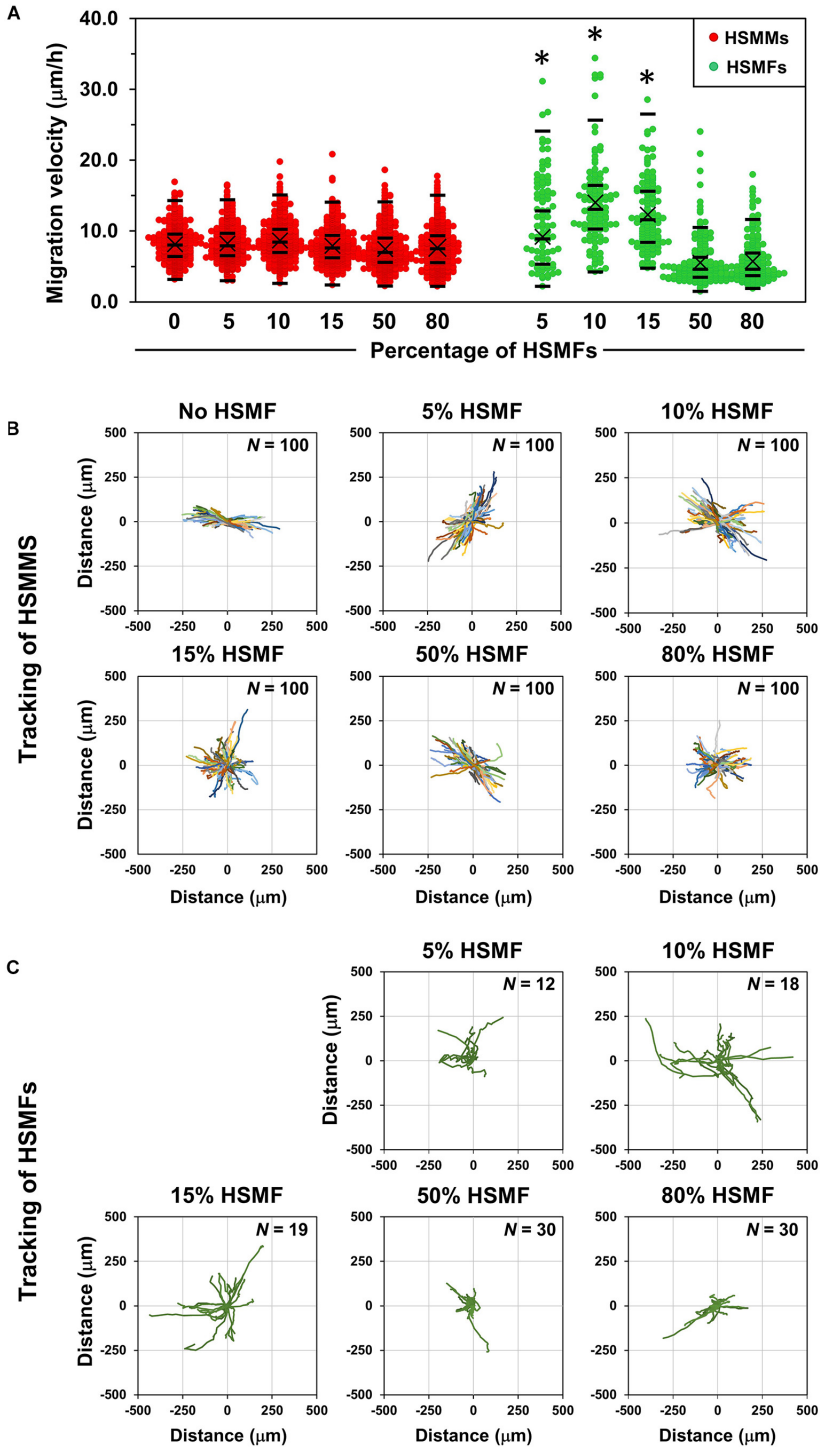


**FIGURE 4 |** Migration behaviors of HSMMs and human skeletal muscle fibroblasts (HSMFs) in a monolayer sheet comprising various proportion of HSMF. **(A)** Various proportions of HSMFs, which were stained with CellTracker Green$^{TM}$, were co-cultured with HSMM monolayer at an initial seeding density ($X_0$) of $3.5 \times 10^5$ cells/cm$^2$. All cells in the monolayer were stained with Hoechst 33342 before observation. The images were captured every 1 h, and the position of cells was used to determine the migration velocity of HSMFs and HSMMs. The migration velocity of HSMFs in the monolayer derived from skeletal cells with varying proportion of HSMFs (5 to 15% HSMF) was higher than that in the monolayer derived from skeletal cells with HSMFs of more than 15%. The migration velocity of HSMM was unaffected in the presence of HSMFs. **(B)** The trajectory plot represents HSMM migration direction and distance in the monolayer comprising various proportions of HSMFs during 48–72 h of incubation. Representative images show data obtained from 100 HSMMs from each local area. **(C)** Trajectory plot represents the migration of HSMFs in monolayer comprising various proportions of HSMFs during 48–72 h of incubation. *$P < 0.01$; one-way analysis of variance (ANOVA), followed by Least-Significant Different (LSD) *post hoc* test.

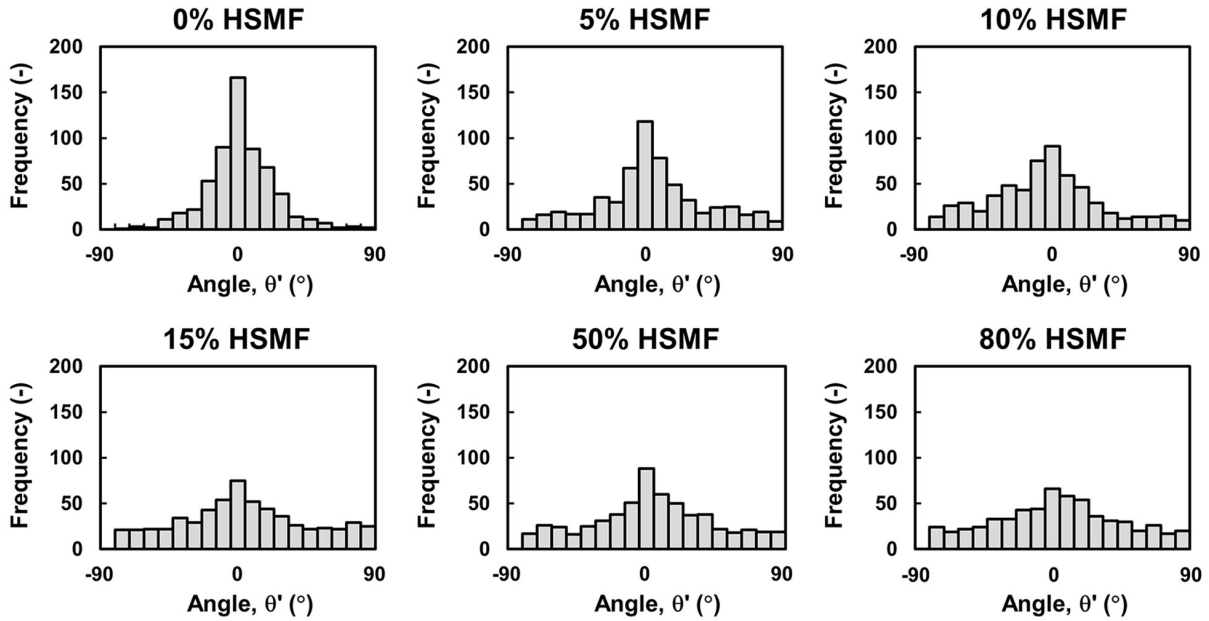


**FIGURE 5 |** Quantitative analysis of HSMM alignment at high density in the monolayer comprising various proportions of HSMFs. Various proportions of HSMFs, which were stained with CellTracker Green$^{TM}$, were co-cultured with HSMMs at an initial seeding density ($X_0$) of $3.5 \times 10^5$ cells/cm$^2$. All cells in the monolayer were stained with Hoechst 33342 before observation. The positions (X,Y) of the cell at the initial ($t$ = 0 h) and ending timepoints ($t$ = 24 h) were used to calculate the migration angle (θ′) and were plotted in a histogram. Data were obtained from 100 HSMMs in each area. Six random areas from duplicated samples were analyzed ($n$ = 600).

prepared by this method is shown in **Supplementary Figure 4A**. At $t$ = 0 h, HUVECs were initially localized at the bottom of the HSMM sheet and vertically migrate into the inner portion of the sheet to generate a flat network inside the sheet after several days co-incubation (**Supplementary Figure 4B**). The network formation of HUVECs in the five-layered HSMM sheets was analyzed for 216 h based on the $L$, $N_T$, and $L/N_T$ parameters. The $X_0$ value of HUVECs was $0.16 \pm 0.01 \times 10^5$ cells/cm$^2$. As shown in **Figure 6B**, the GFP-HUVECs exhibited single and round shapes at the beginning of the incubation period ($t$ = 0) However, early elongation of some GFP-HUVECs was observed in the sheets prepared using skeletal cells with HSMF proportions of 30 and 40%. **Figure 6C** shows the quantitative analysis of $L$, $N_T$, and $L/N_T$. At 24 h, the HUVECs exhibited elongation and were connected with each other in the HSMM sheets containing HSMFs. In contrast, the HUVECs exhibited poor connection with each other in HSMM sheets without HSMFs. The increase in elongation and connection resulted in increased $L$ and decreased $N_T$. At 48 h, early maturation of GFP-HUVECs was observed in the sheets prepared from skeletal cells with 30% HSMF. The maximum $L$ ($111.3 \pm 4.71$ cm$^{-1}$) and $L/N_T$ values ($0.05 \pm 0.01$ cm/tip) were observed at 48 h, which were higher than those observed at 24 h and other conditions. The sheet prepared from skeletal cells with 10% HSMF exhibited a maximum $L/N_T$ value of $0.034 \pm 0.02$ cm/tip, which was higher than the value at other time points of this condition. However, the elongation and smooth connection of GFP-HUVECs in sheet prepared from skeletal muscle cells with 40% HSMF, while the $L$ and $L/N_T$ values increased to a maximum of $115.76 \pm 5.59$ cm$^{-1}$ and $0.07 \pm 0.01$ cm/tip, respectively at 96 h although $L/N_T$ decreased in other conditions. This suggested late maturation of GFP-HUVEC network and indicated that different proportions of HSMFs in HSMM affect angiogenesis after transplantation in an *in vitro* angiogenesis assay.

## DISCUSSION

The use of skeletal muscle myoblasts for myocardial transplantation was first demonstrated by Menasche et al. (2003). Since then, several studies have reported safety, feasibility, and improved heart performance with skeletal muscle myoblast transplantation (Siminiak et al., 2004; Dib et al., 2005a; Gavira et al., 2006). Besides, the myoblasts are prepared as cell sheets, therefore, enhancing the cell transplant efficiency and induction of therapeutic potential (Hata et al., 2006). Skeletal muscle myoblast sheet transplantation has been evaluated for the safety and therapeutic efficiency, and showed no serious arrhythmia or changes in the frequency of ventricular extrasystole frequency (Sawa et al., 2015). Although the myoblast sheets have demonstrated their therapeutic effects by producing various paracrine factors (Pouzet et al., 2001), the effect of skeletal muscle cells comprising different proportions of myoblasts and fibroblasts on cytokine production and angiogenesis has not been elucidated. In the present study, we addressed the regulation of cytokine production by specific cell types in the skeletal muscle cell sheets. The primary human skeletal muscle cells comprise 68.1% of HSMMs and 31.9% of HSMFs as shown in

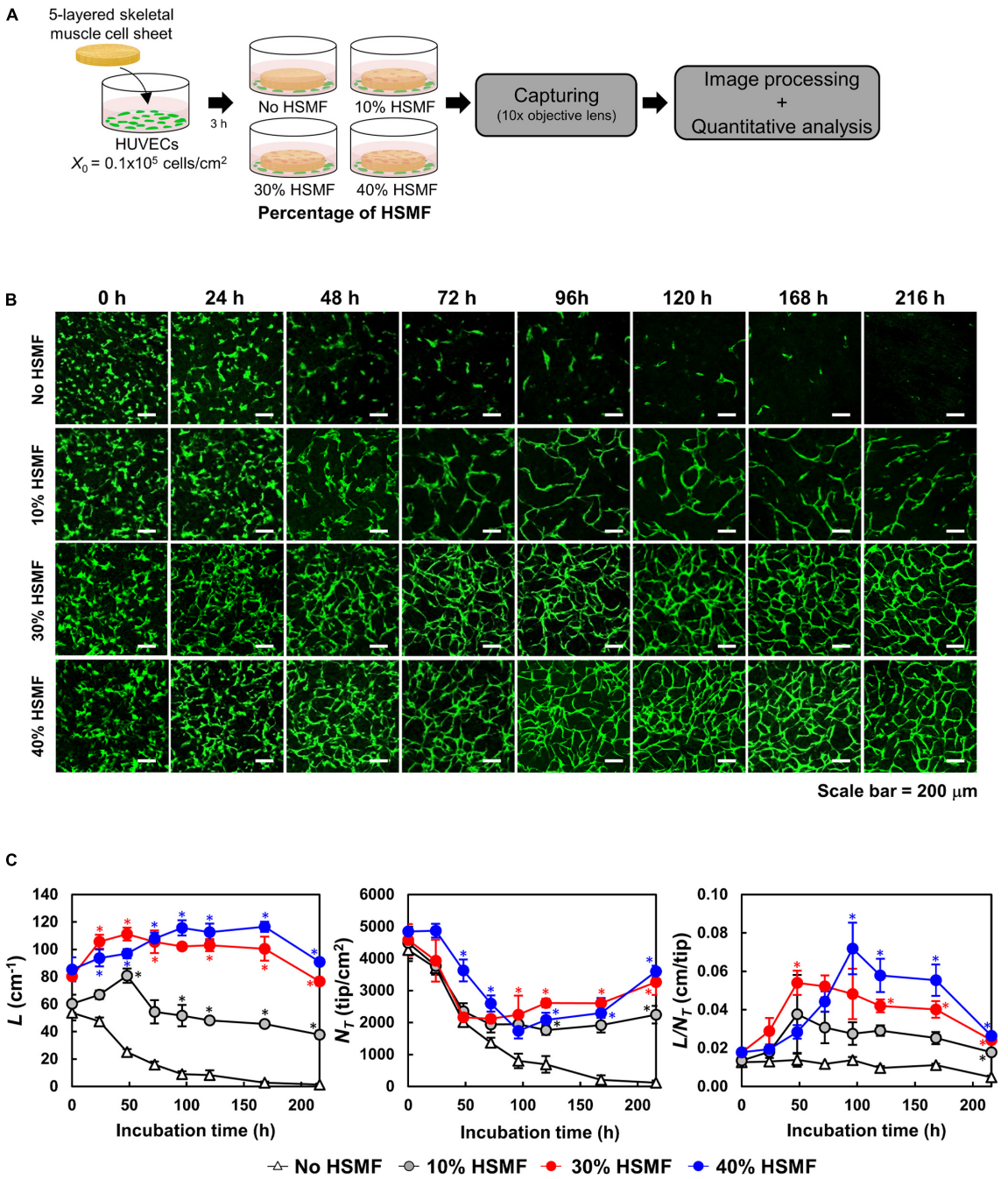


**FIGURE 6 |** Time course of human umbilical vein endothelial cell (HUVEC) network formation in the five-layered HSMM sheet comprising various proportions of human skeletal muscle fibroblast (HSMF). **(A)** Five-layered HSMM sheets with various proportions of HSMFs were prepared and co-cultured with green fluorescent protein-tagged HUVECs (GFP-HUVECs) and observed for 216 h. **(B)** Representative images of HUVEC morphology. Scale bar: 200 μm. **(C)** Evaluation of HUVEC network formation with image processing software. $L$, total length (cm$^{-1}$); $N_T$, total tip number (tip/cm$^2$); $L/N_T$, extent of network formation (cm/tip). The bars show the standard deviation (SD) ($n$ = 3). *$P$ < 0.01; one-way analysis of variance (ANOVA), followed by Bonferroni *post hoc* test.

**Supplementary Figure 1**, were sorted based on CD56 expression, which is a myogenic marker, on the cell surface. The purity of sorted populations was determined by immunostaining of desmin and TE-7. The monolayer was prepared using various densities (mono-culture) and proportions (co-culture) of HSMMs and HSMFs. VEGF production was observed in the mono-cultures of HSMMs and HSMFs, with low productivity. However, the presence of a small proportion of HSMF in the HSMM monolayer resulted in enhanced VEGF productivity with maximum productivity observed in the monolayer of skeletal

cells with 15% HSMF (**Figure 2B**). The production of HGF was observed only in the HSMF mono-culture (**Figure 2C**), whereas that of FGF2 was almost undetectable in the mono-cultures of both cell types (data not shown). Previous studies on primary human retinal pigment epithelial (RPE) cells have demonstrated that the expression of VEGF is highly upregulated at the edges of the scratched RPE layers after the physical disruption of RPE cell-to-cell interactions. This enhanced VEGF expression was correlated to delocalization of ZO-1, an important molecule for intercellular signal transduction in cells (Farjood and Vargis, 2017). Therefore, this study examined the role of cell-to-cell contact disruption in increasing the productivity of VEGF in the monolayers derived from HSMM and HSMF co-culture.

Then, the degree of cell-to-cell contact was evaluated by culturing the purified HSMMs and HSMFs at various $X_0$ values. At high $X_0$ value ($3.5 \times 10^5$ cells/cm$^2$), the cells were in contact with the neighboring cells. Conversely, at low $X_0$ value ($0.1 \times 10^5$ cells/cm$^2$), the cells exhibited decreased contact with the neighboring cells. This study demonstrated that VEGF productivity in the HSMM monolayer was inversely proportional to the cell density (**Figure 2D**). However, the productivity of other cytokines in the HSMM monolayer was not associated with cell density. Additionally, the productivity of cytokines in the HSMFs was not dependent on the cell density (**Figures 2D,E**). Therefore, these data suggest that myoblast-to-myoblast contact can regulate VEGF production in HSMMs. Next, the effect of HSMF in the HSMM monolayer on myoblast-to-myoblast contact disruption was evaluated using cell tracking and time-lapse analysis to examine the migration behaviors. The free HSMFs actively migrated and affected the HSMM directional migration without affecting the migration rate of HSMMs (**Figures 3**, **4A** and **Supplementary Movie 1**). HSMF migration in the monolayer was hypothesized to disrupt myoblast-myoblast contact, which alters the directional migration and alignment of HSMMs. The role of HSMF in HSMM alignment was evaluated by measuring the directional angle of cell migration, which was expressed as the CAI value, in the HSMM monolayers comprising various HSMF ratios. At low proportion in the HSMM monolayer, HSMFs exhibited active multidirectional migration. However, HSMFs exhibited inactive migration and aggregation at high proportion in the monolayer of skeletal cells with 50 and 80% HSMF (**Figure 4C**). In the pure HSMM monolayer, the HSMMs exhibited unidirectional migration. However, the presence of HSMFs increased the multidirectional migration of HSMMs

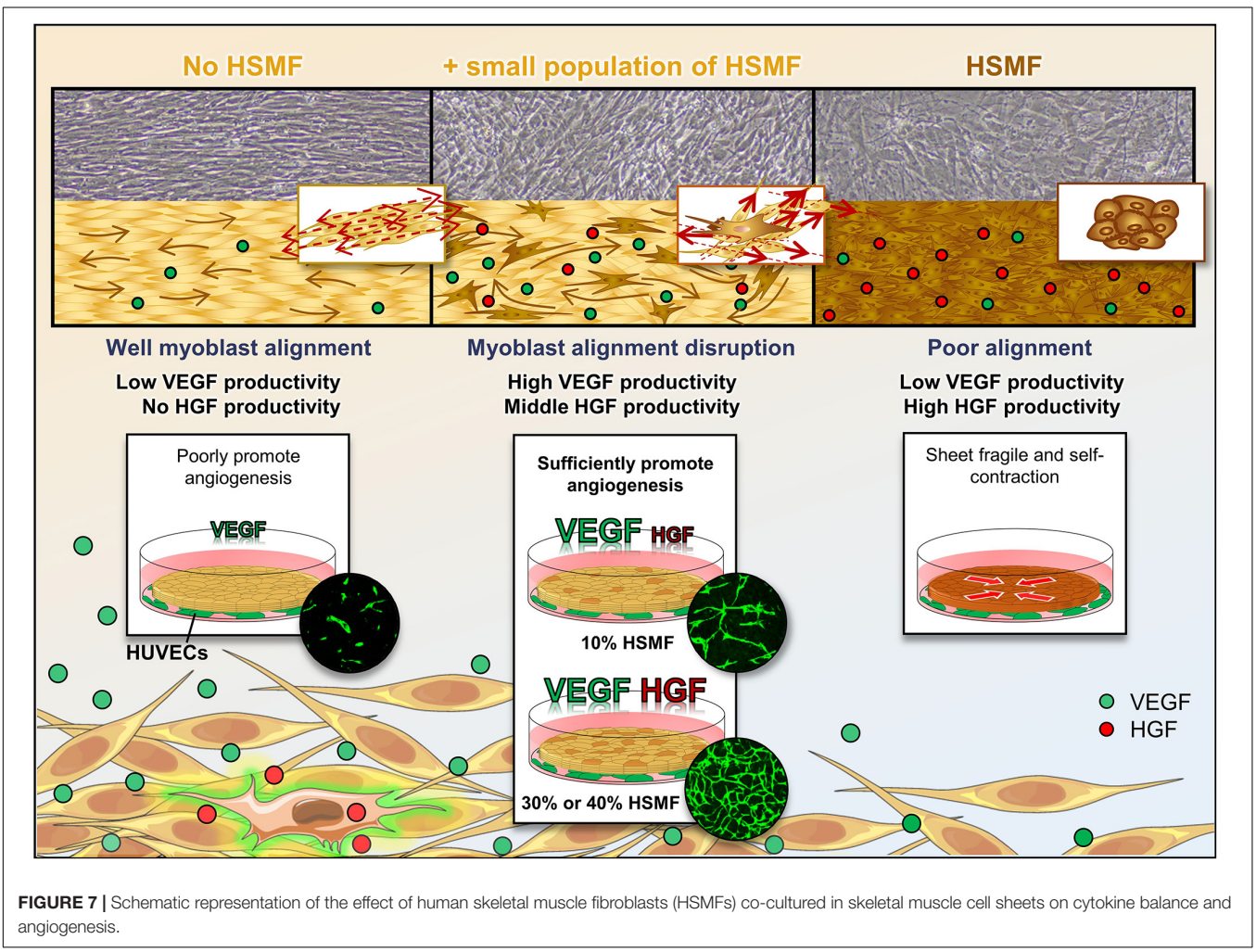


**FIGURE 7 |** Schematic representation of the effect of human skeletal muscle fibroblasts (HSMFs) co-cultured in skeletal muscle cell sheets on cytokine balance and angiogenesis.

(**Figure 3B**). In addition, the alignment disorder in monolayer containing low proportion of HSMF was confirmed by F-actin staining as shown in **Supplementary Figure 6**. Thus, the CAI values in the co-culture monolayer were higher than those in the mono-culture HSMM monolayer (**Figure 5**). These results support the hypothesis that the fibroblasts, which increase VEGF productivity in the HSMM monolayer, exhibit active migration and consequently disrupt the myoblast-to-myoblast contact. These findings indicate that HSMFs regulate the secretion of cytokines and that cytokine productivity is dependent on the proportion of HSMFs in the skeletal muscle sheets.

The effect of HSMFs in the skeletal muscle sheets on transplantation efficiency was evaluated using an *in vitro* angiogenesis assay. Five-layered HSMM sheets comprising various proportions of HSMFs were prepared and co-cultured with GFP-HUVECs (**Figure 6A**). The GFP-HUVECs in the HSMM sheet without HSMF exhibited elongation at an early time point but failed to connect and form a network. The presence of HSMFs enhanced the HUVEC network formation in HSMM sheets. However, the growth of GFP-HUVEC network was dependent on the proportion of HSMF and the levels of VEGF and HGF (**Figures 6B,C**). Various cytokines are involved in inducing angiogenesis. A previous study demonstrated that VEGF can increase blood vessel growth. However, the vessel was fragile and exhibited leakage. The combination of VEGF and HGF was reported to promote blood vessel growth and improve vessel integrity (Saif et al., 2010). In this study, the HUVECs initially exhibited network formation in the sheets prepared from skeletal cells with 10% HSMF, which markedly decreased over time. In contrast, the GFP-HUVECs in the sheets prepared from skeletal cells with 30 and 40% HSMF exhibited higher connectivity than those in sheets prepared from skeletal cells with 10% HSMF. The level of HGF under these conditions may be sufficient to promote strong connection among HUVECs when the VEGF productivity was similar. Moreover, HGF and VEGF levels may affect the time of network maturation. The maturation of HUVEC network in the sheet prepared from skeletal cells with 30% HSMF was observed at 48 h with maximum $L/N_T$ value, whereas that in the sheets prepared from skeletal cells with 40% HSMF was observed at 96 h. The HUVEC network at 96 h was more stable than that at 48 h. The late maturation of the HUVEC network maybe due to low VEGF productivity and the stability of the network maybe due to high productivity of HGF.

The cytokine productivity was also measured from cultured media of five-layered HSMM sheets containing various proportion of HSMF co-incubated with GFP-HUVECs. The VEGF productivity in five-layered HSMM sheets containing 10% HSMF was three-fold greater than that of five-layered HSMM sheets without HSMF (**Supplementary Figure 5A**). The highest HGF productivity was observed in five-layered HSMM sheets containing 40% HSMF (**Supplementary Figure 5B**). Although levels of the VEGF and HGF increase in serum of myocardial infarction patients (Kubota et al., 2004; Seko et al., 2004; Atluri and Woo, 2008; Huang et al., 2020), it is noteworthy that the amount of these cytokines secreted from the five-layered HSMM sheets co-cultured with HSMFs were much higher, suggesting the ability of the five-layered HSMM sheets in induction of angiogenesis toward the injure site.

This study did not evaluate the effect of ECM protein deposition on HSMM sheets comprising various ratios of HSMFs. Hence, the effects of ECM in promoting HUVEC network formation and supporting network stability cannot be excluded. In this study, the sheets prepared from skeletal cells with HSMF higher than 50% were not comparatively analyzed. The sheets containing a high proportion of HSMFs were fragile and self-contracted during preparation, which can be attributed to the aggregation of HSMFs at high proportions (**Figures 4A,C** and **Supplementary Movie 2**) due to the strong connection between HSMFs.

## CONCLUSION

This study demonstrated that different ratios of HSMM and HSMF differentially affect cytokine balance and angiogenesis as showed in **Figure 7**. Fibroblasts secrete high levels of HGF and promote VEGF production in HSMM to maintain cytokine balance, which is potentially mediated through inhibition of active HSMM migration that results in the loss of myoblast-to-myoblast contact. The co-culture of HSMF and HSMM at a suitable ratio promotes angiogenesis and cytokine production. The findings of this study can be used to improve the efficiency of HSMM sheets or engineered tissue for transplantation and highlights the role of fibroblasts in VEGF secretion regulation from adjacent tissue.

## DATA AVAILABILITY STATEMENT

The raw data supporting the conclusions of this article will be made available by the authors, without undue reservation.

## AUTHOR CONTRIBUTIONS

PT performed the experiments, data analysis and interpretation, and drafted and finally edited manuscript. MK significantly contributed to revise the manuscript and supervised the project. All authors designed the experiments and discussed the results and approved the final version of the manuscript.

## ACKNOWLEDGMENTS

The authors acknowledge Assoc. Prof. Dr. Eiji Nagamori (Department of Biomedical Engineering, Osaka Institute of Technology), Iwata Toshihiko, and Iwahashi Atsushi for their support in the experiment.

## SUPPLEMENTARY MATERIAL

The Supplementary Material for this article can be found online at: https://www.frontiersin.org/articles/10.3389/fbioe.2020.578140/full#supplementary-material

## REFERENCES


Atluri, P., and Woo, Y. J. (2008). Pro-angiogenic cytokines as cardiovascular therapeutics: assessing the potential. *BioDrugs* 22, 209–222. doi: 10.2165/00063030-200822040-00001

Carmeliet, P. (2005). VEGF as a key mediator of angiogenesis in cancer. *Oncology* 69 (Suppl. 3), 4–10. doi: 10.1159/000088478

Chapman, M. A., Meza, R., and Lieber, R. L. (2016). Skeletal muscle fibroblasts in health and disease. *Differentiation* 92, 108–115. doi: 10.1016/j.diff.2016.05.007

Dib, N., McCarthy, P., Campbell, A., Yeager, M., Pagani, F. D., et al. (2005a). Feasibility and safety of autologous myoblast transplantation in patients with ischemic cardiomyopathy. *Cell Transplant.* 14, 11–19. doi: 10.3727/000000005783983296

Dib, N., Michler, R. E., Pagani, F. D., Wright, S., Kereiakes, D. J., et al. (2005b). Safety and feasibility of autologous myoblast transplantation in patients with ischemic cardiomyopathy: four-year follow-up. *Circulation* 112, 1748–1755. doi: 10.1161/CIRCULATIONAHA.105.547810

Durrani, S., Konoplyannikov, M., Ashraf, M., and Haider, K. H. (2010). Skeletal myoblasts for cardiac repair. *Regen Med.* 5, 919–932. doi: 10.2217/rme.10.65

Fallah, A., Sadeghinia, A., Kahroba, H., Samadi, A., Heidari, H. R., et al. (2019). Therapeutic targeting of angiogenesis molecular pathways in angiogenesis-dependent diseases. *Biomed. Pharmacother.* 110, 775–785. doi: 10.1016/j.biopha.2018.12.022

Farjood, F., and Vargis, E. (2017). Physical disruption of cell-cell contact induces VEGF expression in RPE cells. *Mol. Vis.* 23, 431–446.

Gavira, J. J., Herreros, J., Perez, A., Garcia-Velloso, M. J., Barba, J., et al. (2006). Autologous skeletal myoblast transplantation in patients with nonacute myocardial infarction: 1-year follow-up. *J. Thorac, Cardiovasc, Surg.* 131, 799–804. doi: 10.1016/j.jtcvs.2005.11.030

Haider, H., Ye, L., Jiang, S., Ge, R., Law, P. K., et al. (2004). Angiomyogenesis for cardiac repair using human myoblasts as carriers of human vascular endothelial growth factor. *J. Mol. Med.* 82, 539–549. doi: 10.1007/s00109-004-0546-z

Hata, H., Matsumiya, G., Miyagawa, S., Kondoh, H., Kawaguchi, N., et al. (2006). Grafted skeletal myoblast sheets attenuate myocardial remodeling in pacing-induced canine heart failure model. *J. Thorac. Cardiovasc. Surg.* 132, 918–924. doi: 10.1016/j.jtcvs.2006.01.024

Huang, A., Qi, X., Cui, Y., Wu, Y., Zhou, S., and Zhang, M. (2020). Serum VEGF: diagnostic value of acute coronary syndrome from stable angina pectoris and prognostic value of coronary artery disease. *Cardiol. Res. Pract.* 2020:6786302. doi: 10.1155/2020/6786302

Jin, H., Yang, R., Li, W., Ogasawara, A. K., Schwall, R., et al. (2003). Early treatment with hepatocyte growth factor improves cardiac function in experimental heart failure induced by myocardial infarction. *J. Pharmacol. Exp. Ther.* 304, 654–660. doi: 10.1124/jpet.102.041772

Kanda, S., Miyata, Y., and Kanetake, H. (2004). Fibroblast growth factor-2-mediated capillary morphogenesis of endothelial cells requires signals via Flt-1/vascular endothelial growth factor receptor-1: possible involvement of c-Akt. *J. Biol. Chem.* 279, 4007–4016. doi: 10.1074/jbc.M307569200

Kendall, R. T., and Feghali-Bostwick, C. A. (2014). Fibroblasts in fibrosis: novel roles and mediators. *Front. Pharmacol.* 5:123. doi: 10.3389/fphar.2014.00123

Kim, C. K., Haider, K. H., and Lim, S. J. (2001). Gene medicine : a new field of molecular medicine. *Arch. Pharm. Res.* 24, 1–15. doi: 10.1007/bf02976486

Kino-oka, M., Kim, J., Kurisaka, K., and Kim, M. H. (2013). Preferential growth of skeletal myoblasts and fibroblasts in co-culture on a dendrimer-immobilized surface. *J. Biosci. Bioeng.* 115, 96–99. doi: 10.1016/j.jbiosc.2012.08.012

Kubota, T., Namiki, A., Fukazawa, M., Ishikawa, M., Moroi, M., et al. (2004). Concentrations of hepatocyte growth factor, basic fibroblast growth factor, and vascular endothelial growth factor in pericardial fluid and plasma. *Jpn Heart J.* 45, 989–998. doi: 10.1536/jhj.45.989

Laddha, A. P., and Kulkarni, Y. A. (2019). VEGF and FGF-2: promising targets for the treatment of respiratory disorders. *Respir. Med.* 156, 33–46. doi: 10.1016/j.rmed.2019.08.003

Liu, J., Wu, P., Wang, Y., Du, Y., Nan, A., Liu, S., et al. (2016). Ad-HGF improves the cardiac remodeling of rat following myocardial infarction by upregulating autophagy and necroptosis and inhibiting apoptosis. *Am. J. Transl. Res.* 8, 4605–4627.

Madonna, R., Cadeddu, C., Deidda, M., Giricz, Z., Madeddu, C., Mele, D., et al. (2015). Cardioprotection by gene therapy: a review paper on behalf of the working group on drug cardiotoxicity and cardioprotection of the italian society of cardiology. *Int. J. Cardiol.* 191, 203–210. doi: 10.1016/j.ijcard.2015.04.232

Makarevich, P. I., Dergilev, K. V., Tsokolaeva, Z. I., Boldyreva, M. A., Shevchenko, E. K., Gluhanyuk, E. V., et al. (2018). Angiogenic and pleiotropic effects of VEGF165 and HGF combined gene therapy in a rat model of myocardial infarction. *PLoS One* 13:e0197566. doi: 10.1371/journal.pone.0197566

Mann, C. J., Perdiguero, E., Kharraz, Y., Aguilar, S., Pessina, P., Serrano, A. L., et al. (2011). Aberrant repair and fibrosis development in skeletal muscle. *Skelet. Muscle* 1:21. doi: 10.1186/2044-5040-1-21

Masaki, I., Yonemitsu, Y., Yamashita, A., Sata, S., Tanii, M., Komori, K., et al. (2002). Angiogenic gene therapy for experimental critical limb ischemia: acceleration of limb loss by overexpression of vascular endothelial growth factor 165 but not of fibroblast growth factor-2. *Circ. Res.* 90, 966–973. doi: 10.1161/01.res.0000019540.41697.60

Memon, I. A., Sawa, Y., Fukushima, N., Matsumiya, G., Miyagawa, S., Taketani, S., et al. (2005). Repair of impaired myocardium by means of implantation of engineered autologous myoblast sheets. *J. Thorac. Cardiovasc. Surg.* 130, 1333–1341. doi: 10.1016/j.jtcvs.2005.07.023

Menasche, P. (2007). Skeletal myoblasts as a therapeutic agent. *Prog. Cardiovasc. Dis.* 50, 7–17. doi: 10.1016/j.pcad.2007.02.002

Menasche, P., Hagege, A. A., Scorsin, M., Pouzet, B., Desnos, M., et al. (2001). Myoblast transplantation for heart failure. *Lancet* 357, 279–280. doi: 10.1016/S0140-6736(00)03617-5

Menasche, P., Hagege, A. A., Vilquin, J. T., Desnos, M., Abergel, E., et al. (2003). Autologous skeletal myoblast transplantation for severe postinfarction left ventricular dysfunction. *J. Am. Coll. Cardiol.* 41, 1078–1083. doi: 10.1016/s0735-1097(03)00092-5

Miyagawa, S., Domae, K., Yoshikawa, Y., Fukushima, S., Nakamura, T., et al. (2017). Phase I clinical trial of autologous stem cell-sheet transplantation therapy for treating cardiomyopathy. *J. Am. Heart Assoc.* 6:4. doi: 10.1161/JAHA.116.003918

Morimoto, A., Okamura, K., Hamanaka, R., Sato, Y., Shima, N., et al. (1991). Hepatocyte growth factor modulates migration and proliferation of human microvascular endothelial cells in culture. *Biochem. Biophys. Res. Commun.* 179, 1042–1049. doi: 10.1016/0006-291x(91)91924-2

Murakami, M., and Simons, M. (2008). Fibroblast growth factor regulation of neovascularization. *Curr. Opin. Hematol.* 15, 215–220. doi: 10.1097/MOH.0b013e3282f97d98

Murtuza, B., Suzuki, K., Bou-Gharios, G., Beauchamp, J. R., Smolenski, R. T., et al. (2004). Transplantation of skeletal myoblasts secreting an IL-1 inhibitor modulates adverse remodeling in infarcted murine myocardium. *Proc. Natl. Acad. Sci. U.S.A.* 101, 4216–4221. doi: 10.1073/pnas.0306205101

Nagamori, E., Ngo, T. X., Takezawa, Y., Saito, A., Sawa, Y., et al. (2013). Network formation through active migration of human vascular endothelial cells in a multilayered skeletal myoblast sheet. *Biomaterials* 34, 662–668. doi: 10.1016/j.biomaterials.2012.08.055

Nakamura, T., Mizuno, S., Matsumoto, K., Sawa, Y., Matsuda, H., and Nakamura, T. (2000). Myocardial protection from ischemia/reperfusion injury by endogenous and exogenous HGF. *J. Clin. Invest.* 106, 1511–1519. doi: 10.1172/JCI10226

Newman, A. C., Nakatsu, M. N., Chou, W., Gershon, P. D., and Hughes, C. C. (2011). The requirement for fibroblasts in angiogenesis: fibroblast-derived matrix proteins are essential for endothelial cell lumen formation. *Mol. Biol. Cell.* 22, 3791–3800. doi: 10.1091/mbc.E11-05-0393

Ngo, T. X., Nagamori, E., Kikuchi, T., Shimizu, T., Okano, T., et al. (2013). Endothelial cell behavior inside myoblast sheets with different thickness. *Biotechnol. Lett.* 35, 1001–1008. doi: 10.1007/s10529-013-1174-x

Onimaru, M., Yonemitsu, Y., Tanii, M., Nakagawa, K., Masaki, I., et al. (2002). Fibroblast growth factor-2 gene transfer can stimulate hepatocyte growth factor expression irrespective of hypoxia-mediated downregulation in ischemic limbs. *Circ. Res.* 91, 923–930. doi: 10.1161/01.res.0000043281.66969.32

Pagani, F. D., DerSimonian, H., Zawadzka, A., Wetzel, K., Edge, A. S., et al. (2003). Autologous skeletal myoblasts transplanted to ischemia-damaged myocardium in humans. Histological analysis of cell survival and differentiation. *J. Am. Coll. Cardiol.* 41, 879–888. doi: 10.1016/s0735-1097(03)00081-0

Pouzet, B., Ghostine, S., Vilquin, J. T., Garcin, I., Scorsin, M., et al. (2001). Is skeletal myoblast transplantation clinically relevant in the era of angiotensin-converting enzyme inhibitors? *Circulation* 104(12 Suppl. 1), I223–I228.

Rosen, E. M., Lamszus, K., Laterra, J., Polverini, P. J., Rubin, J. S., and Goldberg, I. D. (1997). HGF/SF in angiogenesis. *Ciba Found Symp.* 212, 215–226; discussion 227–219. doi: 10.1002/9780470515457.ch14

Saif, J., Schwarz, T. M., Chau, D. Y., Henstock, J., Sami, P., et al. (2010). Combination of injectable multiple growth factor-releasing scaffolds and cell therapy as an advanced modality to enhance tissue neovascularization. *Arterioscler. Thromb. Vasc. Biol.* 30, 1897–1904. doi: 10.1161/ATVBAHA.110.207928

Sawa, Y., Yoshikawa, Y., Toda, K., Fukushima, S., Yamazaki, K., et al. (2015). Safety and efficacy of autologous skeletal myoblast sheets (TCD-51073) for the treatment of severe chronic heart failure due to ischemic heart disease. *Circ. J.* 79, 991–999. doi: 10.1253/circj.CJ-15-0243

Sekiya, N., Matsumiya, G., Miyagawa, S., Saito, A., Shimizu, T., et al. (2009). Layered implantation of myoblast sheets attenuates adverse cardiac remodeling of the infarcted heart. *J Thorac. Cardiovasc. Surg.* 138, 985–993. doi: 10.1016/j.jtcvs.2009.02.004

Seko, Y., Fukuda, S., and Nagai, R. (2004). Serum levels of endostatin, vascular endothelial growth factor (VEGF) and hepatocyte growth factor (HGF) in patients with acute myocardial infarction undergoing early reperfusion therapy. *Clin. Sci.* 106, 439–442. doi: 10.1042/CS20030365

Shirasaka, T., Miyagawa, S., Fukushima, S., Saito, A., Shiozaki, M., et al. (2013). A slow-releasing form of prostacyclin agonist (ONO1301SR) enhances endogenous secretion of multiple cardiotherapeutic cytokines and improves cardiac function in a rapid-pacing-induced model of canine heart failure. *J. Thorac. Cardiovasc. Surg.* 146, 413–421. doi: 10.1016/j.jtcvs.2012.10.003

Siminiak, T., Kalawski, R., Fiszer, D., Jerzykowska, O., Rzezniczak, J., et al. (2004). Autologous skeletal myoblast transplantation for the treatment of postinfarction myocardial injury: phase I clinical study with 12 months of follow-up. *Am. Heart J.* 148, 531–537. doi: 10.1016/j.ahj.2004.03.043

Suzuki, K., Murtuza, B., Smolenski, R. T., Sammut, I. A., Suzuki, N., et al. (2001). Cell transplantation for the treatment of acute myocardial infarction using vascular endothelial growth factor-expressing skeletal myoblasts. *Circulation* 104(12 Suppl. 1), I207–I212. doi: 10.1161/hc37t1.094524

Ueda, H., Nakamura, T., Matsumoto, K., Sawa, Y., Matsuda, H., and Nakamura, T. (2001). A potential cardioprotective role of hepatocyte growth factor in myocardial infarction in rats. *Cardiovasc. Res.* 51, 41–50. doi: 10.1016/s0008-6363(01)00272-3

Yuan, B., Zhao, Z., Zhang, Y. R., Wu, C. T., Jin, W. G., Zhao, S., et al. (2008). Short-term safety and curative effect of recombinant adenovirus carrying hepatocyte growth factor gene on ischemic cardiac disease. *In Vivo* 22, 629–632.

Zachary, I., and Gliki, G. (2001). Signaling transduction mechanisms mediating biological actions of the vascular endothelial growth factor family. *Cardiovasc. Res.* 49, 568–581. doi: 10.1016/s0008-6363(00)00268-6

**Conflict of Interest:** The authors declare that the research was conducted in the absence of any commercial or financial relationships that could be construed as a potential conflict of interest.

frontiers in Bioengineering and Biotechnology

BRIEF RESEARCH REPORT
published: 23 October 2020
doi: 10.3389/fbioe.2020.597847

# Development of a Semi-Automated, Bulk Seeding Device for Large Animal Model Implantation of Tissue Engineered Vascular Grafts

*Eoghan M. Cunnane[1,2†], Katherine L. Lorentz[1†], Lorenzo Soletti[1], Aneesh K. Ramaswamy[1], Timothy K. Chung[1], Darren G. Haskett[3], Samuel K. Luketich[3], Edith Tzeng[4], Antonio D'Amore[3,5], William R. Wagner[1,3,4,6], Justin S. Weinbaum[1,3,7] and David A. Vorp[1,3,4,6,8,9]**

[1] Department of Bioengineering, University of Pittsburgh, Pittsburgh, PA, United States, [2] Tissue Engineering Research Group, Department of Anatomy, Royal College of Surgeons in Ireland, Dublin, Ireland, [3] McGowan Institute for Regenerative Medicine, University of Pittsburgh, Pittsburgh, PA, United States, [4] Department of Surgery, University of Pittsburgh, Pittsburgh, PA, United States, [5] RiMED Foundation, Palermo, Italy, [6] Department of Chemical and Petroleum Engineering, University of Pittsburgh, Pittsburgh, PA, United States, [7] Department of Pathology, University of Pittsburgh, Pittsburgh, PA, United States, [8] Department of Cardiothoracic Surgery, University of Pittsburgh, Pittsburgh, PA, United States, [9] Clinical and Translational Sciences Institute, University of Pittsburgh, Pittsburgh, PA, United States

OPEN ACCESS

**Edited by:**
*Vahid Serpooshan, Emory University, United States*

**Reviewed by:**
*Toshiharu Shinoka, Nationwide Children's Hospital, United States*
*Vasif Nejat Hasirci, Acıbadem University, Turkey*

***Correspondence:**
*David A. Vorp*
*vorp@pitt.edu*

*[†]These authors share first authorship*

**Specialty section:**
*This article was submitted to Tissue Engineering and Regenerative Medicine, a section of the journal Frontiers in Bioengineering and Biotechnology*

**Received:** *22 August 2020*
**Accepted:** *07 October 2020*
**Published:** *23 October 2020*

**Citation:**
*Cunnane EM, Lorentz KL, Soletti L, Ramaswamy AK, Chung TK, Haskett DG, Luketich SK, Tzeng E, D'Amore A, Wagner WR, Weinbaum JS and Vorp DA (2020) Development of a Semi-Automated, Bulk Seeding Device for Large Animal Model Implantation of Tissue Engineered Vascular Grafts. Front. Bioeng. Biotechnol. 8:597847. doi: 10.3389/fbioe.2020.597847*

Vascular tissue engineering is a field of regenerative medicine that restores tissue function to defective sections of the vascular network by bypass or replacement with a tubular, engineered graft. The tissue engineered vascular graft (TEVG) is comprised of a biodegradable scaffold, often combined with cells to prevent acute thrombosis and initiate scaffold remodeling. Cells are most effectively incorporated into scaffolds using bulk seeding techniques. While our group has been successful in uniform, rapid, bulk cell seeding of scaffolds for TEVG testing in small animals using our well-validated rotational vacuum technology, this approach was not directly translatable to large scaffolds, such as those required for large animal testing or human implants. The objective of this study was to develop and validate a semi-automated cell seeding device that allows for uniform, rapid, bulk seeding of large scaffolds for the fabrication of TEVGs appropriately sized for testing in large animals and eventual translation to humans. Validation of our device revealed successful seeding of cells throughout the length of our tubular scaffolds with homogenous longitudinal and circumferential cell distribution. To demonstrate the utility of this device, we implanted a cell seeded scaffold as a carotid interposition graft in a sheep model for 10 weeks. Graft remodeling was demonstrated upon explant analysis using histological staining and mechanical characterization. We conclude from this work that our semi-automated, rotational vacuum seeding device can successfully seed porous tubular scaffolds suitable for implantation in large animals and provides a platform that can be readily adapted for eventual human use.

**Keywords: vascular tissue engineering, sheep model, carotid implantation, mesenchyaml stem cells, bulk seeding**

## INTRODUCTION

Cardiovascular disease remains the primary cause of global death and encompasses disorders of the heart and blood vessels (Mendis et al., 2011; Benjamin et al., 2017). The vessels most frequently affected by cardiovascular disease are the coronary and peripheral arteries which require revascularization surgeries to treat occlusion and distal ischemia, respectively (Goodney et al., 2009; Alexander and Smith, 2016). Stent deployment is effective in the revascularization of localized obstructions; however diffuse obstructions require bypass surgery. The saphenous vein and internal mammary artery are the gold standard bypass conduits for small diameter vessels (<6 mm diameter) of the coronary and peripheral arteries, respectively. However, saphenous veins are often unavailable or unsuitable and frequently fail due to intimal hyperplasia (Isenberg et al., 2006), while the failure of mammary artery grafts due to occlusion is a persistent issue (Harskamp et al., 2015). Furthermore, synthetic grafts are not a viable treatment option for small diameter vessels due to high rates of acute thrombosis (Klinkert et al., 2004; Desai et al., 2011).

The advancement of tissue engineered vascular grafts (TEVGs) in recent years, and their ability to form functional neo-vessels, presents as a promising clinical option for the treatment of vascular disease (Cunnane et al., 2018). TEVGs often incorporate cells into biodegradable scaffolds through various cell-seeding techniques (Villalona et al., 2010; Weinbaum et al., 2020), and the presence of cells has demonstrated improved TEVG patency rates through reduced thrombosis and stenosis (Nieponice et al., 2010; Soletti et al., 2011; Krawiec et al., 2016, 2017; Haskett et al., 2018).

In order to achieve homogenous incorporation of cells within TEVG scaffolds, bulk seeding techniques have come to be preferred over the simpler drip or static seeding techniques first used to impregnate scaffolds with cells (Soletti et al., 2006). However, the majority of work to date has focused on seeding TEVGs intended for implant in small animal models (Nieponice et al., 2008; Hibino et al., 2011; Udelsman et al., 2011, 2014). The generation of cell-based, larger sized TEVGs (∼4 mm inner diameter, ∼100 mm length) suitable for testing in large animal models or eventual translation to the clinic requires scale-up of both the scaffold and the bulk seeding system. Additionally, to ensure regulatory approval and effective clinical translation, a semi-automated bulk cell seeding device that can create a reproducible TEVG is required. To this end, the purpose of this work was to develop and validate a semi-automated, rapid, bulk seeding device that results in homogenous cell distribution within large scaffolds intended for use as "human-sized" TEVGs. We demonstrate the utility of the device by bulk seeding a scaffold with adipose derived stromal cells and implanting the resulting construct in a sheep model to examine patency and remodeling over a 10-week period.

**Abbreviations:** DMSO, dimethyl sulfoxide; FBS, fetal bovine serum; H&E, hematoxylin and eosin; hADMSC, human adipose derived stem cell; PBS, phosphate buffered saline; sSVF, sheep stromal vascular fraction; TEVG, Tissue engineered vascular graft; VVG, Verhoeff van Gieson.

## METHODS

### Design of the Translating-Rotating Seeding Device

The design of our novel bulk seeding device for large, "human-sized" scaffolds was first conceived during the doctoral dissertation work of Soletti (2008). It is based on our lab's previously published and validated custom rotational vacuum seeding device which has been used to produce TEVGs for small animal testing (Nieponice et al., 2010; Soletti et al., 2011; Krawiec et al., 2016, 2017; Haskett et al., 2018). The common concept is to achieve bulk seeding of rotating, porous, tubular scaffolds via local luminal delivery of cells under applied vacuum. The new system presented herein adds a cell-releasing "Diffuser" equipped with eight equi-spaced radial nozzles attached to a "Stylet" arm. The Stylet drives the Diffuser coaxially along the longitudinal axis of the tubular scaffold and transports cell suspension from a syringe, locally to the scaffold lumen while the scaffold rotates under an applied vacuum (**Figures 1A,B**). The locally delivered cells are drawn into the wall of the scaffold, via the applied vacuum, through the interconnected pore network, to ensure even radial cell distribution (**Figure 1C**). The linear displacement of the Diffuser ensures even longitudinal cell distribution, while the rotation of the scaffold ensures even circumferential distribution.

Linear translation of the Stylet/Diffuser is achieved using a stepper motor ("Motor 1") attached to a sliding stage. Rotation of the scaffold is achieved using an additional stepper motor ("Motor 2") connected to a mounting tee located distally to the scaffold ("Distal Tee"). The Distal Tee is connected to the proximal mounting tee ("Proximal Tee") via a bracket that transfers the rotational momentum (**Figures 1D,E**). Two PTFE supports are attached to the ends of the tees to allow for mounting of the scaffold within the vacuum chamber. A syringe pump supplies the cell suspension to the Diffuser, through the Stylet. Both the pump and the motors are controlled using a custom Labview program (National Instruments, TX, United States) that allows for control of the Stylet translation speed, the scaffold rotation speed and the syringe pump infusion rate. Additional detail regarding the device, shear stress on the seeded cells and sterilization of the device is provided in **Supplementary Material**.

### Scaffold Design

The biodegradable, bi-layered, elastomeric scaffolds used in this study are manufactured from poly(ester urethane)urea (PEUU) as described previously (Nieponice et al., 2010; He et al., 2011, 2010; Krawiec et al., 2016). The porous inner layer of the scaffold was created using thermally induced phase separation in a tubular mold. The inner layer was then coated by electrospinning an additional layer of PEUU for mechanical stability. Scaffolds are tubular, 4.7 mm inner diameter, 5.2 mm outer diameter, and 10 cm in length, to approximate the shape and size of a human coronary or peripheral artery. The structural and morphological properties of the scaffold have been fully characterized previously (Soletti et al., 2010). Briefly, the inner

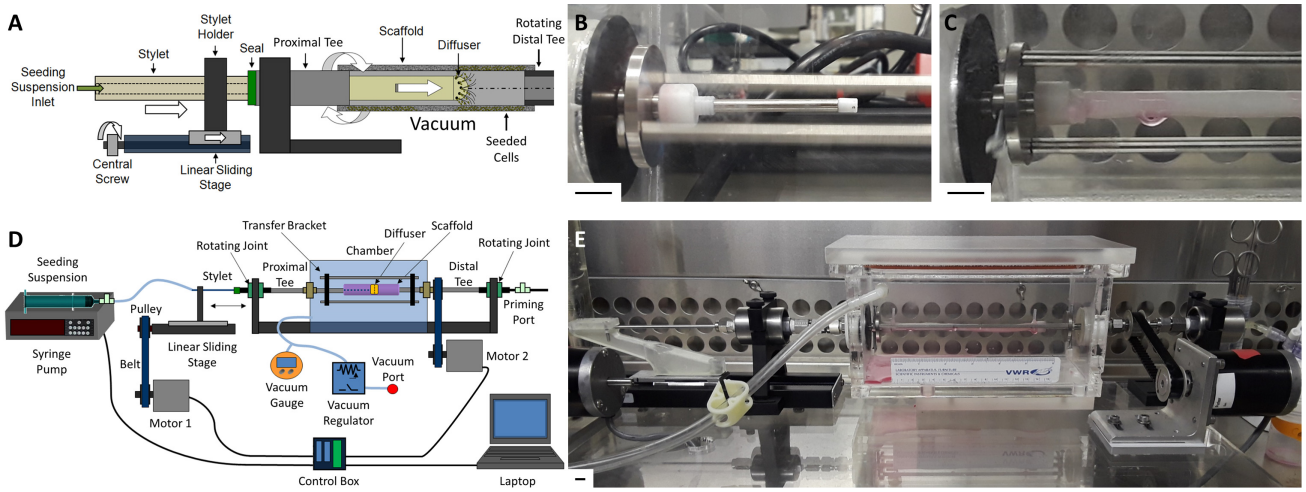


**FIGURE 1 |** Overview of translating-rotating seeding device. **(A)** Schematic of the linear sliding stage system used to translate the Stylet/Diffuser component within the rotating scaffold lumen during seeding under vacuum. **(B)** Image of the Stylet/Diffuser system emerging from the proximal mounting tee. **(C)** Image of a mounted scaffold with the Diffuser infusing cell suspension within the scaffold lumen. **(D)** Schematic and **(E)** image of the novel cell seeding device developed in this study to bulk seed human-sized tubular scaffolds. Scale bars depict 1 cm.

layer of the scaffold has a pore size measuring 123 ± 20 μm (mean ± SD), the outer layer has a pore size measuring 5.1 ± 3.2 μm, while the diameter of the outer layer nanofibers is 743 ± 201 nm. Scanning electron microscope images of the scaffold can be found in **Supplementary Material** and also in Soletti et al. (2010).

## Bulk Seeding Validation

### Cell Source and Culture

PEUU scaffolds were bulk seeded with human adipose derived mesenchymal stem cells (hADMSCs) to validate the seeding device. The hADMSCs were obtained commercially (Rooster Bio, Inc., Frederick, MD, RoosterVial-hAD-1M MSC Lot #00097) and cultured in supplemented growth media (RoosterBio, SU0005, GM) until passage 2. The hADMSCs were then frozen in freezing media [90% FBS (Atlanta Biologics) and 10% DMSO (Sigma)] until ready for use. For each seeding study, a stock of 1 million hADMSCs was thawed into a 175 $cm^2$ flask (Falcon) and cultured for 3 days in 15 mL of GM. Media was replaced after 16 h to remove residual DMSO. After 3 days of culture, 6 million cells were passed into two 5-layer tower flasks (equivalent to approximately 3,500 cells/$cm^2$) and cultured for 72 h in 75 mL of GM. The cells were then passed into 10, 5-layer tower flasks and cultured for a further 72 h in 75 mL of GM per flask to obtain approximately 200 million cells for seeding.

A cell number of 200 million was chosen as it approximates the cell density (cell number per volume of scaffold material) employed in our previous small animal studies. Those studies demonstrated that a cell density in excess of 400 cells per $cm^3$ of scaffold material prevents acute thrombosis and initiates positive scaffold remodeling upon implantation (Krawiec et al., 2017; Haskett et al., 2018). We therefore targeted a cell density in excess of 400 cells per $cm^3$ of material as our cell seeding density, which requires approximately 200 million cells for a 12 cm scaffold with 4.7 mm inner diameter and 5.2 mm outer diameter. The calculations used to determine cell seeding density are provided in **Supplementary Material**.

### Cell Seeding

The performance of the cell seeding device was examined by seeding PEUU scaffolds (10 cm in length) with approximately 200 million hADMSCs suspended in 30 mL of GM and characterizing the longitudinal and circumferential distribution of cells in the seeded scaffold. Linear translation speed was varied (2.5, 5, and 7.5 mm/s) to examine the effect of diffuser displacement rate on cell distribution. The dispensed volume was kept consistent across displacement rates by varying the number of complete cycles through the scaffold lumen (2, 4, and 6 cycles for 2.5, 5, and 7.5 mm/s, respectively). The remaining seeding parameters were kept constant (flow rate = 12.5 mL/min, rotation speed = 60 rpm, and applied vacuum = −127 mmHg). Seeding efficiency was calculated using the following expression (Wendt et al., 2003; Zhao and Ma, 2005):

$$\frac{\textit{Cell Number in Suspension Before Seeding} - \textit{Cell Number in Suspension After Seeding}}{\textit{Cell Number in Suspension Before Seeding}} \times 100.$$

After seeding, 1.5 cm of material was trimmed from the scaffold ends and discarded. Scaffolds were placed in 20 mL of GM and incubated overnight to facilitate cell adhesion under static conditions. Scaffolds were then sectioned into 1 cm segments and labeled L1 to L7 (**Figure 2A**). The segments were bisected longitudinally with one half reserved for histological staining (to visualize cell nuclei), and the other half reserved to assess cell metabolic activity (**Figure 2B**). Metabolic activity was used as a surrogate marker to assess the distribution of cells within the seeded scaffold.

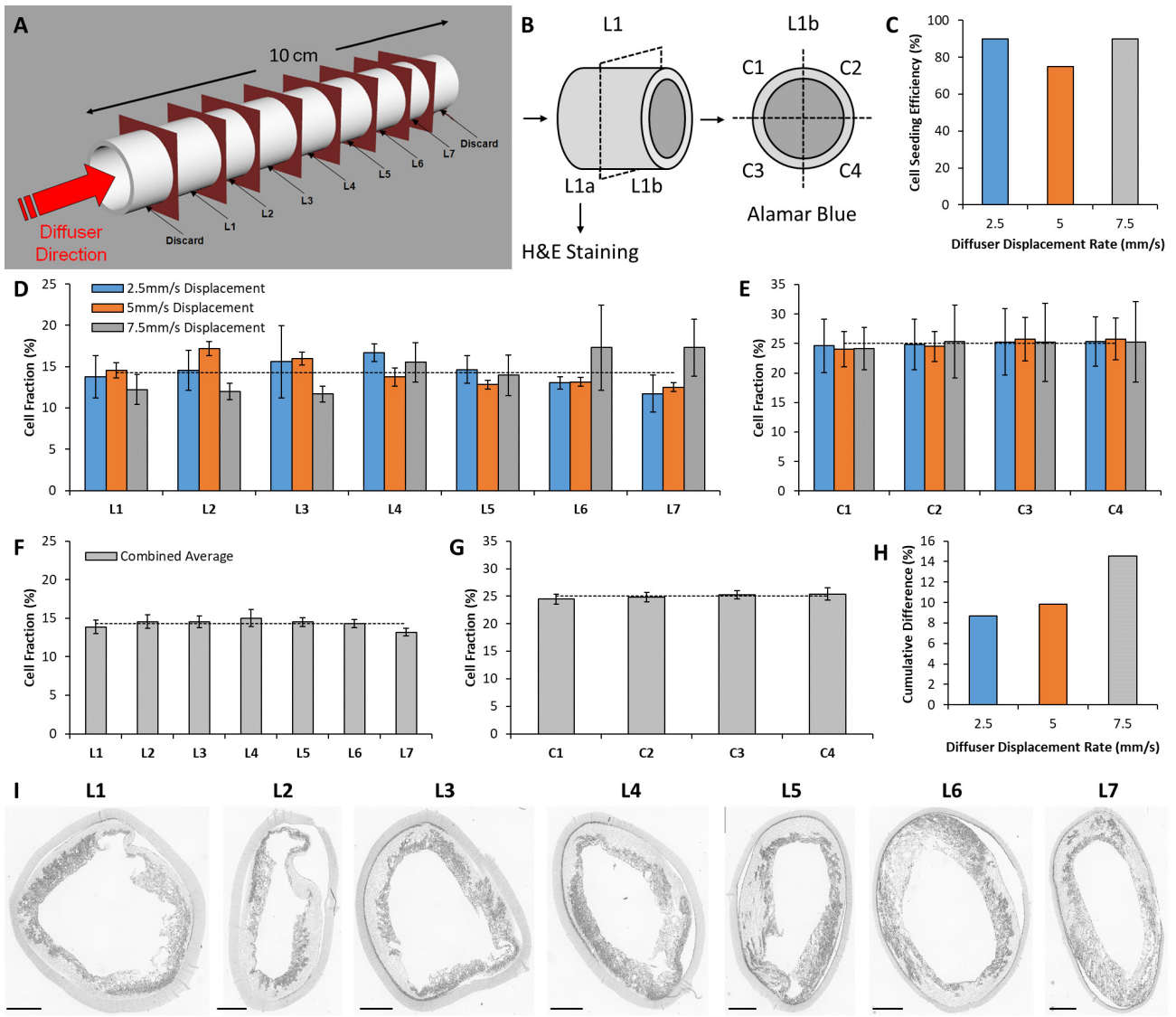


**FIGURE 2 |** *In vitro* analysis of seeding device performance. **(A)** Schematic of the sectioning technique used to quantitatively assess the distribution of cells seeded within scaffolds using the novel seeding device. **(B)** Separation of each section for histological staining and metabolic activity assessment. Cell metabolic activity assay sections were further divided into quadrants to estimate circumferential cell distribution within the scaffold. **(C)** Scaffold seeding efficiency for each seeding configuration examined in this study. **(D)** Longitudinal distribution of cells across seven longitudinal sections for each seeding configuration. The dashed line indicates ideal cell distribution. **(E)** Circumferential distribution of cells across four quadrants for each seeding configuration. **(F)** Combined average of all three seeding configurations for longitudinal, and **(G)** circumferential distribution. **(H)** Cumulative difference between longitudinal cell distribution and the ideal distribution for each seeding configuration. **(I)** H&E staining of the seeded scaffold (seeded at a Diffuser displacement speed of 2.5 mm/s) to visualize the distribution of cells within the scaffold pores. Scale bars depict 1 mm.

## Histologic Evaluation

Seeded scaffold segments intended for histological analysis were fixed in 4% paraformaldehyde and sectioned at a thickness of 10 μm using a microtome. Sections were stained with hematoxylin and eosin (H&E) to mark cell nuclei and determine hADMSC distribution in the scaffolds. Imaging was performed on a Nikon Eclipse 90i microscope (Nikon, Tokyo, Japan). Quantification of cell nuclei number was performed using the intensity threshold and particle count features available in ImageJ (Fiiji, public domain) (Soletti et al., 2011).

## Metabolic Activity

Seeded scaffold segments intended for cell metabolic activity assessment were further sectioned into quadrants (labeled C1–C4) and each quadrant was placed in a well of a 48-well plate containing 500 μL of GM and 50 μL of Alamar Blue solution (Sigma). The quadrants were incubated for 4 h at 37°C, then removed from the Alamar Blue solution and squeezed to drain any remaining solution. The absorbance of the solution was read at 570 nm relative to 600 nm with a microplate reader (model 680, Bio-Rad, Hercules,

CA, United States) and the absorbance of Alamar blue solution incubated with an unseeded scaffold section was subtracted as a blank control. The longitudinal distribution of cell metabolic activity was determined by pooling all four quadrants from the same longitudinal segment for segments L1–L7. The circumferential distribution of cell metabolic activity was estimated by pooling one quadrant from each longitudinal segment for quadrants C1–C4. However, circumferential distribution should only be regarded as an estimate as one quadrant from each longitudinal section was selected and pooled at random.

## *In vivo* Evaluation

### Cell Source, Isolation, and Culture

Sheep stromal vascular fraction (sSVF) was selected as the cell source be to seeded within the PEUU scaffold intended for implant as we have previously demonstrated that the inclusion of such cells limits acute thrombosis and promotes positive vascular remodeling when incorporated into tubular PEUU scaffolds in a small animal model (Krawiec et al., 2017; Haskett et al., 2018). sSVF was obtained from the adipose tissue of a single donor sheep. Autologous cells were not used as sufficient adipose tissue could not be harvested from the same animal without seriously compromising animal health. Furthermore, our group has shown that autologous cells harvested from patients at risk of developing cardiovascular disease and requiring a bypass (e.g., diabetic or elderly patients) are not capable of generating viable TEVGs *in vivo*, with the implants predisposed to failure due to acute thrombosis (Krawiec et al., 2015, 2016).

The sSVF was isolated using previously described methods (Krawiec et al., 2017; Haskett et al., 2018). Briefly, adipose tissue was cut into approximately 10 cc portions and placed into separate 50 cc conical tubes. Each piece was minced and combined with a collagenase solution [Hanks' Balanced Salt Solution (Invitrogen, Carlsbad, CA) containing 3.5% bovine serum albumin (Millipore, Charlottesville, VA) and 1 mg/mL collagenase type II (Worthington, Lakewood, NJ)]. Tubes were then incubated at 37°C with agitation for 1 h. Digested tissue was filtered through sterile gauze to remove undigested tissue fragments and then centrifuged at 400 × g for 10 min at ambient temperature. After centrifugation, the cell pellet was resuspended in an $NH_4Cl$-based buffer (Beckman Coulter, Miami, FL) to lyse red blood cells. The resulting cell suspension was filtered through a 500 μm sieve and centrifuged at 400 × g for 10 min at ambient temperature. The resulting pellet was resuspended in defined culture media [1:1 Dulbecco's modified Eagle's medium (DMEM, Gibco) to DMEM/F12 (Gibco) with 10% fetal bovine serum (Atlanta Biologics), antibiotics (1% penicillin/streptomycin, 0.5% Fungizone, 0.1% gentamycin), and 10 μL/L dexamethasone] and plated in collagen-coated (rat tail, Sigma) 175 $cm^2$ flasks. Upon becoming 80% confluent, the cells were removed from the plate using trypsin and expanded up to passage 4 in collagen coated 5-layer tower flasks using the same protocol outlined in section " Cell Source and Culture."

### Scaffold Implantation and Explant

Twenty four hours prior to implantation, a 12 cm PEUU scaffold was seeded with 200 million sSVF cells. The Diffuser speed was set to 2.5 mm/s for two cycles as this was shown to be the optimal displacement speed following validation testing (see section "Bulk Seeding Validation"). After overnight incubation in defined culture media, the scaffold was transported to the surgical facility and maintained in defined culture media until implantation.

The neck of a 9-month-old Suffolk sheep was prepared for surgery (Rojo Stock Farm, New Castle, PA). Prior to surgery, atropine (0.03–0.06 mg/kg), oxytetracycline (20–27 mg/kg), and heparin (5,000 IU) was administered. Morphine (0.2–0.5 mg/kg) was given as an analgesic and anesthesia was maintained with isoflurane (1.5–5% inhaled). A 14 cm incision was made in the skin running longitudinally along the medial border of the sternocleidomastoid muscle. A 10 cm portion of the carotid artery was isolated and exposed. The segment of isolated artery was clamped at each end using vascular clamps and an 8 cm length of carotid artery was excised. A 9 cm portion of the seeded scaffold was implanted as a carotid interposition graft. Both ends were oblique anastomoses sutured with a continuous running suture technique using 7-0 prolene sutures (Ethicon 8696G, Cincinnati, OH). The clamps were then removed, and the flow was confirmed using ultrasound. The muscle and skin layers were closed separately using a 2-0 and 3-0 vicryl running suture respectively (Ethicon J317H and J316H, Cincinnati, OH).

After 10 weeks, the sheep was prepared for explant and euthanized as approved by the Institutional Animal Care and Use Committee. The initial incision site was re-opened, and the graft was isolated. The graft and a small portion of the proximal and distal carotid artery was harvested (**Figure 3A**). The graft was processed by sectioning it into seven separate segments (sections L1–L7) (**Figure 3B**). The segments were further bisected longitudinally with one half reserved for mechanical characterization and the other half reserved for histological staining.

### Mechanical Characterization

Explanted graft ring segments intended for mechanical characterization were mounted on two parallel pins clamped within an Instron tensile tester (Instron, #5543A, Norwood, MA) and a preload of 0.01 N was applied. Each ring segment was extended at a displacement rate of 1 mm/min up to 20% strain for 5 cycles to precondition the tissue and then immediately extended until failure at the same rate. The mechanical properties of the explanted graft were compared to adjacent carotid artery tissue and unseeded PEUU scaffold material. The force-extension curves were converted to stress-strain curves using the following expressions (Macrae et al., 2016):

$$\text{Stress, } \sigma = \frac{F}{2A_o}; \quad \text{Strain, } \varepsilon = \frac{L + \pi r_w}{L_o + \pi r_w} - 1$$

Stress and strain measurements are obtained from twice the original cross-sectional area (Ao) of the test specimen, the force (F) measured during each mechanical test, the sample

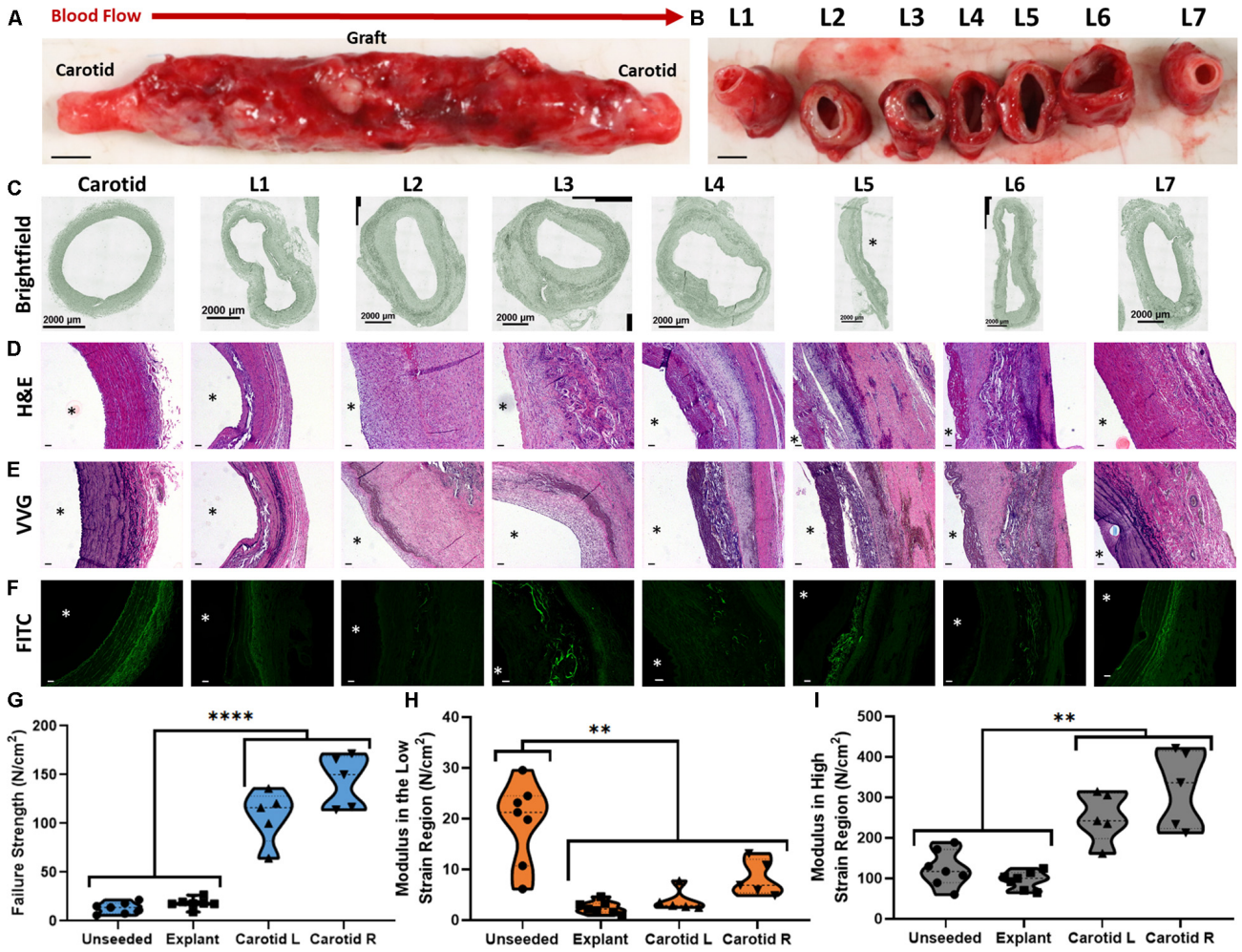


**FIGURE 3 |** Large animal implantation and explant analysis of a large seeded construct. **(A,B)** Macroscopic image of the explanted TEVG (**A**, intact and **B**, longitudinally sectioned) after 10 weeks as a carotid interposition graft in a sheep model. Scale bars depict 5 mm. **(C)** Brightfield images of sections L1 to L7. **(D)** H&E staining of sections L1 to L7 demonstrating cellular distribution in the graft and neo-intima formation. **(E)** VVG staining of sections L1 to L7 demonstrating elastin distribution in the graft neo-tissue. **(F)** Auto-fluorescence of the PEUU material remaining in the graft. Scale bars depict 100 µm. **(G)** Failure strength, **(H)** modulus in the low strain region and **(I)** modulus in the high strain region for the unseeded scaffold, the explanted TEVG and the native carotid arterial tissue. ** indicates statistical significance at $p < 0.01$ and **** indicates statistical significance at $p < 0.0001$.

gauge length in the loaded (L) and unloaded configuration (Lo), and the radius of the mounting pins ($r_w$). Two separate moduli are calculated using the slopes of the linear portions of the mechanical response curve in the low- and high-strain regions. The transition point between low and high strain is defined as the point of the stress–strain curve with the maximum normal distance from the global secant, the line spanning from the origin to the end of the curve (Holzapfel, 2006; Cunnane et al., 2016). This equates to dividing the curve into three equal parts and treating the initial and final thirds of the curve as the low- and high-strain regions respectively.

### Explant Staining

Explant segments intended for histological staining were sliced into 5 µm sections and stained for cell and elastin distribution using H&E and Verhoeff van Gieson (VVG) staining, respectively. Staining was performed by the Histology Core at the McGowan Institute for Regenerative Medicine. Stained sections were imaged using a Nikon 90i upright microscope. Prior to sectioning the explant for histological examination, the carotid artery tissue was separated from the TEVG along the anastomosis to ensure that sections L1–L7 reflect the structure of the explanted graft.

## Statistics

Statistical analysis was performed using GraphPad Prism 8 (GraphPad Software, San Diego, CA, United States). Data normality was examined using Shapiro-Wilk tests. Ordinary one-way ANOVA analysis was used to identify significant differences between more than two groups of variables. A $p$-value of less than 0.05 was considered statistically significant.

# RESULTS

## Bulk Seeding Validation

Cell seeding efficiency for each diffuser displacement speed is displayed in **Figure 2C**. Efficiency was 90% for both 2.5 and 7.5 mm/s, and 75% for 5 mm/s. **Figures 2D,E** display the longitudinal and circumferential distribution of cell metabolic activity (section "Metabolic Activity") within each scaffold, respectively. No intra-sample variance was observed for longitudinal or circumferential distribution ($p > 0.05$). The dashed lines in **Figures 2D,E** indicate the cell distribution within a theoretical sample that exhibits perfectly homogenous cell distribution (longitudinal = 14.29%, circumferential = 25%). The cell distribution of all samples is combined in **Figures 2F,G** to examine the pooled longitudinal and circumferential cell distribution over the three samples. The cumulative difference of each longitudinal section from the ideal distribution is displayed in **Figure 2H** for each diffuser displacement speed. The cumulative difference is 8.67, 9.81, and 14.57% for 2.5, 5, and 7.5 mm/s, respectively.

**Figure 2I** displays grayscale images of H&E staining that illustrate the cell distribution in sections obtained from the scaffold seeded at 2.5 mm/s. Qualitative assessment reveals the retention of cells within the scaffold structure. The cells are restricted to the inner layer of the scaffold and are unable to penetrate the outer layer due to the small pore size exhibited by the outer electrospun layer.

## Pilot *in vivo* Testing of a Cell Seeded TEVG Construct

The seeded construct was well-tolerated as a TEVG implant by the recipient animal over the 10-week period. The animal recovered fully from the surgery, demonstrating good health after 10 days and throughout the remainder of the study. Ultrasounds performed at weekly intervals confirmed longitudinal patency of the graft. Staining of the explanted graft revealed cell integration, scaffold degradation and neo tissue formation (**Figures 3C–F**).

H&E staining of all sections revealed cell-rich neo-intimal layer formation along the lumen of the explant (**Figure 3D**). VVG staining allows for differences in neo-tissue composition to be identified along the length of the scaffold. Ordered, stratified laminae of elastin can be seen in sections L1 and L7. Conversely, elastin is largely absent from sections L2, L3, and L6, while elastin appears in a disorganized fashion in sections L4 and L5 (**Figure 3E**).

Images depicting auto-fluorescence of the PEUU scaffold in the FITC channel reveal varying levels of scaffold degradation in each section (**Figure 3F**). It can be observed that sections L3, L4, and L5 exhibit the largest quantity of remaining scaffold material. This is intuitive as these sections represent the center of the scaffold which would be exposed to less endogenous enzymes capable of dissolving the PEUU.

**Figures 3G–I** display the mechanical characteristics of the unseeded scaffold, the explanted graft and the native carotid artery tissue. The data is presented as failure strength, and moduli in the low and high strain regions. The failure strength of the unseeded scaffold and the explanted graft are lower than the native tissue ($p < 0.0001$) (**Figure 3G**). However, the failure strength of the unseeded scaffold and explant are still above normal levels of physiological circumferential stress present in human common carotid arteries during diastole ($13.37 \pm 2.62$ and $18.09 \pm 2.21$ vs. $6.3 \pm 2.3$ N/cm$^2$) (Kamenskiy et al., 2012). Furthermore, no portion of the explant underwent rupture, highlighting the adequacy of the graft strength. The modulus of the explant in the low strain region is lower than the unseeded scaffold ($2.5 \pm 0.53$ vs. $19.3 \pm 3.77$ N/cm$^2$, $p < 0.0001$), indicating that the modulus decreases after the implant period (**Figure 3H**). This change in modulus is likely due to the resorption of the PEUU material coupled with the synthesis of elastic fibers, which combine to decrease the modulus of the graft to a more physiological level. The modulus of the explant in the high strain region remains similar to the unseeded scaffold due to the persistence of the electrospun layer ($95.74 \pm 9.51$ vs. $123.64 \pm 20.74$ N/cm$^2$, $p > 0.05$), but both are still below the values observed for the native tissue ($253.1 \pm 27.72$ and $322.49 \pm 43.17$ N/cm$^2$, $p < 0.01$) (**Figure 3I**).

# DISCUSSION

We have successfully developed and validated a semi-automated device that allows for rapid, bulk seeding of large tubular scaffolds with cells. Furthermore, we have demonstrated the utility of this device by evaluating the *in vivo* remodeling of a cell seeded TEVG construct in a large animal pilot study. Validation of our device revealed successful seeding of hADMSCs throughout the full length of our PEUU scaffolds with homogenous longitudinal and circumferential cell distribution. Using our validated cell seeding device, approximately 200 million sSVF cells were incorporated into a 12 cm PEUU scaffold, which was cut to 9 cm and implanted as a carotid interposition graft in a sheep model. The seeded graft remained patent, exhibited signs of scaffold degradation and initiated neo-tissue formation throughout the length of the graft after 10 weeks *in vivo*.

Static, quasi-static, rotational, bioreactor and vacuum cell seeding approaches have all been previously employed to incorporate cells into tubular scaffolds for the purpose of developing TEVGs (as reviewed in Weinbaum et al., 2020). Our rotational, vacuum cell seeding approach offers considerable advantages over alternative cell seeding techniques. Rotational, vacuum seeding achieves much higher seeding efficiencies and more even cell distributions compared static loading (Hibino et al., 2010; Roh et al., 2010; Lee et al., 2016), does not require the cell or scaffold modifications that quasi-static seeding techniques necessitate (Tiwari et al., 2003; Sagnella et al., 2005; Perea et al., 2006; Shimizu et al., 2007; Campagnolo et al., 2016), is far faster than bioreactor techniques (Sodian et al., 2002; Zhao and Ma, 2005; Inoguchi et al., 2007; Melchiorri et al., 2016), and offers improved cell distribution and cell viability compared to techniques that employ exclusively rotational (Nasseri et al., 2003; Godbey et al., 2004; Hsu et al., 2005; Aper et al., 2016)

or vacuum approaches (van Wachem et al., 1990; Udelsman et al., 2011; Kurobe et al., 2015). This study advances the current state-of-the-art for rotational, vacuum cell seeding by scaling our cell seeding technology into a novel semi-automated seeding device that is capable of fabricating reproducible human-sized, cell-seeded TEVG constructs. The technology presented herein therefore has considerable implications for TEVG research that incorporates cells into tubular scaffolds, as our semi-automated seeding approach and promising pilot *in vivo* data increase the likelihood of securing regulatory approval and effective clinical translation of our TEVG technology.

This present study has a number of limitations. Firstly, the pilot study only performs a single implantation. The primary objective of this manuscript was to describe our novel seeding device and validate it by determining if it can produce cell seeded TEVG constructs of a size necessary for human (and large animal) implantation. We then performed an initial pilot implantation study as a secondary objective to investigate if our novel seeding device can produce TEVGs that do not undergo acute thrombosis and initiate neo-tissue formation *in vivo*, prior to transitioning toward a multi-animal study. Future studies will increase implant numbers to examine the reliability of this approach and build confidence toward a dependable clinical treatment option. Secondly, longer explant time points are required to provide a more robust picture of graft longevity in terms of sustained patency and long-term remodeling. The presence of organized elastin at the edges of our explanted TEVG, and the absence of organized elastin toward the center of the graft, suggests that the seeded construct is still undergoing remodeling, and that longer time point studies are required to fully characterize neo-tissue formation and mechanics once the scaffold has completely remodeled. However, the presence of physiologically relevant elastin formation in the outer sections of the explant is promising for the future of our cell seeding device and TEVG technology. Furthermore, it has previously been shown that the PEUU material used to fabricate the scaffolds in this study undergoes an approximate 50% reduction in molecular weight over an 8-week period (Guan et al., 2002), and the presence of PEUU mass at 10 weeks (**Figure 3**) further suggests that longer time point studies are required to characterize the remodeling of our TEVG up to the point where all of the scaffold material has been resorbed. Future studies should therefore seek to characterize explanted TEVGs after at least 6 months *in vivo* to better understand the effects of vascular remodeling and scaffold degradation on long-term graft viability. Finally, our construct was implanted as a carotid graft which is a straight configuration. However, many bypass grafts in clinical practice must be bent and curved around obstructions. Future studies must demonstrate the grafts ability to withstand kinking in complex configurations *in vivo* (Van Epps et al., 2009) or the possibility to modify the scaffold structure in order to mitigate mechanical instability such as kinking or buckling.

With respect to future practice, this study brings TEVG technology closer to clinical translation in two ways. Firstly, the development of our seeding device will allow us to create and test clinically relevant grafts in a reproducible manner, thus accelerating the clinical translation of small-diameter arterial TEVGs. Secondly, the human-sized TEVG that we generated in this pilot study using our scaffold-seeding technology undergoes full cellularization, partial degradation and positive matrix remodeling after 10 weeks *in vivo* therefore demonstrating that our novel TEVG cell-seeding technology warrants further investigation via increased implant numbers and longer explant time points to fully understand the clinical potential of this promising treatment modality.

## CONCLUSION

Our novel, semi-automated, bulk seeding device makes it possible to rapidly generate "human-sized" cell-seeded, tubular TEVG constructs. Our *in vitro* results demonstrate that the novel device allows for uniform longitudinal and circumferential cell seeding. Our pilot *in vivo* results demonstrate graft patency, scaffold degradation and neo-tissue formation within the TEVG seeded construct using the presented device. The findings of this study support our hypothesis that it is possible to use an automated system to generate "human-sized" TEVGs capable of positive vascular remodeling in a large animal model.

## DATA AVAILABILITY STATEMENT

The raw data supporting the conclusions of this article will be made available by the authors, without undue reservation, to any qualified researcher.

## ETHICS STATEMENT

The animal study was reviewed and approved by the University of Pittsburgh Institutional Animal Care and Use Committee.

## AUTHOR CONTRIBUTIONS

EC and KL: concept generation, literature review, experimental work, and manuscript writing. LS, ET, AD'A, and SL: concept generation, experimental work, and critical review of the manuscript. AR: experimental work and critical review of the manuscript. DH: concept generation, literature review, experimental work, and critical review of the manuscript. WW, JW, and DV: concept generation and critical review of manuscript. All authors contributed to the article and approved the submitted version.

## FUNDING

This work was funded by the European Union's Horizon 2020 Research and Innovation Program under the Marie Skłodowska-Curie Grant Agreement No. 708867 awarded to EC, the National Institute of Health Vascular Training Grant awarded to DH (T32 HL098036; PI: ET), the RiMED Foundation grant

awarded to AD'A, and the National Institute of Health under Grant Agreement Nos. R21HL130784, R61HL154102, and R01AG061430 awarded to DV.

## ACKNOWLEDGMENTS

We would like to acknowledge Patrick Iyasele for assistance with mechanical testing of the explanted tissue, Siddarth Madala for assistance with LabVIEW programming of the large seeding device, Jonathan Vande Geest for donation of the sheep used in the pilot study, and the McGowan Institute for Regenerative Medicine Preclinical Surgical Staff.

## SUPPLEMENTARY MATERIAL

The Supplementary Material for this article can be found online at: https://www.frontiersin.org/articles/10.3389/fbioe.2020.597847/full#supplementary-material

## REFERENCES

Alexander, J. H., and Smith, P. K. (2016). Coronary-Artery Bypass Grafting. *N Engl. J. Med.* 374(20), 1954–64. doi: 10.1056/NEJMra1406944.

Aper, T., Wilhelmi, M., Gebhardt, C., Hoeffler, K., Benecke, N., Hilfiker, A., and Haverich, A. (2016). Novel Method for the Generation of Tissue-Engineered Vascular Grafts Based on a Highly Compacted Fibrin Matrix. *Acta Biomater.* 29, 21–32. doi: 10.1016/j.actbio.2015.10.012.

Benjamin, E. J., Blaha, M. J., Chiuve, S. E., Cushman, M., Das, S. R., Deo, R., et al. (2017). Heart Disease and Stroke Statistics' 2017 Update: A Report from the American Heart Association. *Circulation* 135(10), e146–e603. doi: 10.1161/CIR.0000000000000485

Campagnolo, P., Gormley, A. J., Chow, L. W., Géraldine Guex, A., Parmar, P. A., Puetzer, J. L., Steele, J A.M. (2016). Pericyte Seeded Dual Peptide Scaffold with Improved Endothelialization for Vascular Graft Tissue Engineering. *Adv. Health. Mater.* 5(23), 3046–3055. doi: 10.1002/adhm.201600699

Cunnane, E.M., Mulvihill, J.J.E., Barrett, H.E., Hennessy, M.M., Kavanagh, E.G., and Walsh, M.T. (2016). Mechanical Properties and Composition of Carotid and Femoral Atherosclerotic Plaques: A Comparative Study. *J. Biomech.* 49 (15), 3697–3704. doi: 10.1016/j.jbiomech.2016.09.036.

Cunnane, E. M., Weinbaum, J. S., O'Brien, F. J., and Vorp, D A. (2018). Future Perspectives on the Role of Stem Cells and Extracellular Vesicles in Vascular Tissue Regeneration. *Front. Cardiovasc. Med.* 5:58. doi: 10.3389/fcvm.2018.00086.

Desai, M., Seifalian, A. M., and Hamilton, G. (2011). Role of Prosthetic Conduits in Coronary Artery Bypass Grafting. *Eur. J. Card. Thor. Surg.* 40(2), 394–98. doi: 10.1016/j.ejcts.2010.11.050.

Van Epps, J. S., Chew, D. W., and Vorp, D A. (2009). Effects of Cyclic Flexure on Endothelial Permeability and Apoptosis in Arterial Segments Perfused Ex Vivo. *J. Biomech. Engin.* 131:101005. doi: 10.1115/1.3192143.

Godbey, W. T., Stacey Hindy, B. S., Sherman, M. E., and Atala, A. (2004). A Novel Use of Centrifugal Force for Cell Seeding into Porous Scaffolds. *Biomaterials* 25(14), 2799–2805. doi: 10.1016/j.biomaterials.2003.09.056.

Goodney, P. P., Beck, A. W., Nagle, J., Gilbert Welch, H., and Zwolak, R M. (2009). National Trends in Lower Extremity Bypass Surgery, Endovascular Interventions, and Major Amputations. *J. Vascu. Surg.* 50(1), 54–60. doi: 10.1016/j.jvs.2009.01.035.

Guan, J., Sacks, M. S., Beckman, E. J., and Wagner, W R. (2002). Synthesis, Characterization, and Cytocompatibility of Elastomeric, Biodegradable Poly(Ester-Urethane)Ureas Based on Poly(Caprolactone) and Putrescine. *J. Biomed. Mater. Res.* 61(3), 493–503. doi: 10.1002/jbm.10204.

Harskamp, R. E., Alexander, J. H., Ferguson, T B. Jr., Hager, R., Mack, M. J., Englum, B., et al. (2015). Frequency and Predictors of Internal Mammary Artery Insights From the Project of Ex-Vivo Vein Graft Engineering Via, *Circulation* 133, 131–38. doi: 10.1161/CIRCULATIONAHA.115.015549.

Haskett, D. G., Saleh, K. S., Lorentz, K. L., Josowitz, A. D., Luketich, S. K., Weinbaum, J. S., Kokai, L. E., et al. (2018). An Exploratory Study on the Preparation and Evaluation of a 'Same-Day' Adipose Stem Cell–Based Tissue-Engineered Vascular Graft. *J. Thor. Cardiovas. Surg.* 156(5), 1814–1822.e3. doi: 10.1016/j.jtcvs.2018.05.120.

He, W., Nieponice, A., Hong, Y., Wagner, W. R., and Vorp, D A. (2011). Rapid Engineered Small Diameter Vascular Grafts from Smooth Muscle Cells. *Cardiovas. Engin. Technol.* 2(3), 149–59. doi: 10.1007/s13239-011-0044-8.

He, W., Nieponice, A., Soletti, L., Hong, Y., Gharaibeh, B., Crisan, M., et al. (2010). Pericyte-Based Human Tissue Engineered Vascular Grafts. *Biomaterials* 31(32), 8235–8244. doi: 10.1016/j.biomaterials.2010.07.034

Hibino, N., Yi, T., Duncan, D. R., Rathore, A., Dean, E., Naito, Y., et al. (2011). A Critical Role for Macrophages in Neovessel Formation and the Development of Stenosis in Tissue-Engineered Vascular Grafts. *FASEB J.* 25(12), 4253–4263. doi: 10.1096/fj.11-186585

Hibino, N., McGillicuddy, E., Matsumura, G., Ichihara, Y., Naito, Y., Breuer, C., and Shinoka, T. (2010). Late-Term Results of Tissue-Engineered Vascular Grafts in Humans. *J. Thor. Cardiovas. Surg.* 139(2), 431–6. doi: 10.1016/j.jtcvs.2009.09.057.

Holzapfel, G A. (2006). Determination of Material Models for Arterial Walls from Uniaxial Extension Tests and Histological Structure. *J. Theor. Biol.* 238(2), 290–302. doi: 10.1016/j.jtbi.2005.05.006

Hsu, S. H., Tsai, I. J., Lin, D. J., and Chen, D. C. (2005). The Effect of Dynamic Culture Conditions on Endothelial Cell Seeding and Retention on Small Diameter Polyurethane Vascular Grafts. *Med. Engin. Phys.* 27(3), 267–72. doi: 10.1016/j.medengphy.2004.10.008.

Inoguchi, H., Tanaka, T., Maehara, Y., and Matsuda, T. (2007). The Effect of Gradually Graded Shear Stress on the Morphological Integrity of a Huvec-Seeded Compliant Small-Diameter Vascular Graft. *Biomaterials* 28(3), 486–95. doi: 10.1016/j.biomaterials.2006.09.020.

Isenberg, B. C., Williams, C., and Tranquillo, R T. (2006). Small-Diameter Artificial Arteries Engineered in Vitro. *Circul. Res.* 98(1), 25–35. doi: 10.1161/01.RES.0000196867.12470.84

Kamenskiy, A. V., Dzenis, Y. A., MacTaggart, J. N., Lynch, T. G., Jaffar Kazmi, S. A., and Pipinos, I I. (2012). Nonlinear Mechanical Behavior of the Human Common, External, and Internal Carotid Arteries in Vivo. *J. Surg. Res.* 176(1), 329–36. doi: 10.1016/j.jss.2011.09.058.

Klinkert, P., Post, P. N., Breslau, P. J., and van Bockel, J. H. (2004). Saphenous Vein versus PTFE for Above-Knee Femoropopliteal Bypass. A Review of the Literature. *Eur. J. Vascu. Endovas. Surg.* 27(4), 357–62. doi: 10.1016/j.ejvs.2003.12.027.

Krawiec, J. T., Liao, H. T., Kwan, L. Y.,D'Amore, A., Weinbaum, J. S., Peter Rubin, J. (2017). Evaluation of the Stromal Vascular Fraction of Adipose Tissue as the Basis for a Stem Cell-Based Tissue-Engineered Vascular Graft. *J. Vascu. Surg.* 66(3), 883–890.e1. doi: 10.1016/j.jvs.2016.09.034.

Krawiec, J. T., Weinbaum, J. S., Liao, H. T., Ramaswamy, A. K., Pezzone, D. J., Josowitz, A D. (2016). In Vivo Functional Evaluation of Tissue-Engineered Vascular Grafts Fabricated Using Human Adipose-Derived Stem Cells from High Cardiovascular Risk Populations. *Tissue Engin. Part A* 22(9–10), 765–775. doi: 10.1089/ten.tea.2015.0379

Krawiec, J. T., Weinbaum, J. S., St Croix, C. M., Phillippi, J. A., Watkins, S. C., Rubin, J. P., and Vorp, D A. (2015). A Cautionary Tale for Autologous Vascular Tissue Engineering: Impact of Human Demographics on the Ability of Adipose-Derived Mesenchymal Stem Cells to Recruit and Differentiate into Smooth Muscle Cells. *Tissue Engin. Part A* 21, 426–37. doi: 10.1089/ten.tea.2014.0208.

Kurobe, H., Maxfield, M. W., Naito, Y., Cleary, M., Stacy, M. R., Solomon, D., Rocco, K. A., et al. (2015). Comparison of a Closed System to a Standard Open Technique for Preparing Tissue-Engineered Vascular Grafts. *Tissue Engin. Part C Methods* 21(1), 88–93. doi: 10.1089/ten.tec.2014.0160

Lee, Y. U., Mahler, N., Best, C. A., Tara, S., Sugiura, T., Lee, A. Y., Yi, T., Hibino, N. (2016). Rational Design of an Improved Tissue-Engineered Vascular Graft:

Determining the Optimal Cell Dose and Incubation Time. *Regener. Med.* 11(2), 159–167. doi: 10.2217/rme.15.85

Macrae, R. A., Miller, K., and Doyle, B. J. (2016). Methods in Mechanical Testing of Arterial Tissue: A Review. *Strain* 52(5), 380–399. doi: 10.1111/str.12183

Melchiorri, A. J., Bracaglia, L. G., Kimerer, L. K., Hibino, N., and Fisher, J P. (2016). In Vitro Endothelialization of Biodegradable Vascular Grafts Via Endothelial Progenitor Cell Seeding and Maturation in a Tubular Perfusion System Bioreactor. *Tissue Engin. Part C Methods* 22(7), 663–70. doi: 10.1089/ten.tec.2015.0562.

Mendis, S., Puska, P., and Norrving, B. (2011). "*Global Atlas on Cardiovascular Disease Prevention and Control*," in *World Health Organization*, eds Mendis S, Puska P, Norrving B, (*World Health Organization*: Geneva).

Nasseri, B. A., Pomerantseva, I., Kaazempur-Mofrad, M. R., Sutherland, F W.H., Perry, T., Ochoa, E. (2003). Dynamic Rotational Seeding and Cell Culture System for Vascular Tube Formation. *Tissue Engin.* 9(2), 291–299. doi: 10.1089/107632703764664756

Nieponice, A., Soletti, L., Guan, J.,Deasy, B. M., Huard, J., Wagner, W. R., and Vorp, D A. . (2008). Development of a Tissue-Engineered Vascular Graft Combining a Biodegradable Scaffold, Muscle-Derived Stem Cells and a Rotational Vacuum Seeding Technique. *Biomaterials* 29(7), 825–833. doi: 10.1016/j.biomaterials.2007.10.044

Nieponice, A., Soletti, L., Guan, J., Hong, Y., Gharaibeh, B., Maul, T M. et al. (2010). In Vivo Assessment of a Tissue-Engineered Vascular Graft Combining a Biodegradable Elastomeric Scaffold and Muscle-Derived Stem Cells in a Rat Model. *Tissue Engin. Part A* 16(4), 1215–1223. doi: 10.1089/ten.TEA.2009.0427

Perea, H., Aigner, J., Hopfner, U., and Wintermantel, E. (2006). Direct Magnetic Tubular Cell Seeding: A Novel Approach for Vascular Tissue Engineering. *Cells Tissues Organs.* 183(3), 156–165. doi: 10.1159/000095989

Roh, J. D., Sawh-Martinez, R., Brennan, M. P., Jay, S. M., Devine, L., Rao, D. A., et al. (2010). Tissue-Engineered Vascular Grafts Transform into Mature Blood Vessels via an Inflammation-Mediated Process of Vascular Remodeling. *Proc. Natl. Acad. Sci.* 107(10), 4669–4674. doi: 10.1073/pnas.0911465107

Sagnella, S., Anderson, E., Sanabria, N., Marchant, R. E., and Kottke-Marchant, K. (2005). Human Endothelial Cell Interaction with Biomimetic Surfactant Polymers Containing Peptide Ligands from the Heparin Binding Domain of Fibronectin. *Tissue Engin.* 11, 226–36. doi: 10.1089/ten.2005.11.226.

Shimizu, K., Ito, A., Arinobe, M., Murase, Y., Iwata, Y., Narita, Y., et al. (2007). Effective Cell-Seeding Technique Using Magnetite Nanoparticles and Magnetic Force onto Decellularized Blood Vessels for Vascular Tissue Engineering. *J. Biosci. Bioengin.* 103(5), 472–478. doi: 10.1263/jbb.103.472

Sodian, R., Lemke, T., and Fritsche, C. (2002). Tissue-Engineering Bioreactors: A New Combined Cell-. *Tissue Engin.* 8(5), 863–70.

Soletti, L. (2008). *Development of a Stem Cell-Based Tissue Engineered Vascular Graft.* ProQuest Dissertations and Theses, (Indiana: University Bloomington), 1–404.

Soletti, L., Hong, Y., Guan, J., Stankus, J. J., El-Kurdi, M. S., Wagner, W R. and Vorp, D A. (2010). A Bilayered Elastomeric Scaffold for Tissue Engineering of Small Diameter Vascular Grafts. *Acta Biomater.* 6(1), 110–122. doi: 10.1016/j.actbio.2009.06.026

Soletti, L., Nieponice, A., Guan, J., Stankus, J. J., Wagner, W. R., and Vorp, D A. (2006). A Seeding Device for Tissue Engineered Tubular Structures. *Biomaterials* 27(28), 4863–70. doi: 10.1016/j.biomaterials.2006.04.042.

Soletti, L., Nieponice, A., Hong, Y., Ye, S. H., Stankus, J. J., Wagner, W. R., and Vorp, D A. (2011). In Vivo Performance of a Phospholipid-Coated Bioerodable Elastomeric Graft for Small-Diameter Vascular Applications. *J. Biomed. Mater. Res. Part A* 96, 436–48. doi: 10.1002/jbm.a.32997.

Tiwari, A., Punshon, G., Kidane, A., Hamilton, G., and Seifalian, A M. (2003). Magnetic Beads (Dynabead$^{TM}$) Toxicity to Endothelial Cells at High Bead Concentration: Implication for Tissue Engineering of Vascular Prosthesis. *Cell Biol. Toxicol.* 19, 265–72. doi: 10.1023/B:CBTO.0000004929.37511.ed.

Udelsman, B., Hibino, N., Villalona, G. A., McGillicuddy, E., Nieponice, A., Sakamoto, Y., Matsuda, S., Vorp, D A. (2011). Development of an Operator-Independent Method for Seeding Tissue-Engineered Vascular Grafts. *Tissue Engin. Part C Methods* 17(7), 731–736. doi: 10.1089/ten.tec.2010.0581

Udelsman, B. V., Khosravi, R., Miller, K. S., Dean, E. W., Bersi, M. R., Rocco, K., Yi, T. (2014). Characterization of Evolving Biomechanical Properties of Tissue Engineered Vascular Grafts in the Arterial Circulation. *J. Biomech.* 47(9), 2070–2079. doi: 10.1016/j.jbiomech.2014.03.011

Villalona, G. A, Udelsman, B., Duncan, D. R., McGillicuddy, E., Sawh-Martinez, R. F., Hibino, N. (2010). Cell-Seeding Techniques in Vascular Tissue Engineering. *Tissue Engin. Part B Rev.* 16(3), 341–350. doi: 10.1089/ten.TEB.2009.0527

van Wachem, P. B., Stronck, J. W.S., Koers-Zuideveld, R., Dijk, F., and Wildevuur, C. R.H. (1990). Vacuum Cell Seeding: A New Method for the Fast Application of an Evenly Distributed Cell Layer on Porous Vascular Grafts. *Biomaterials* 11, 602–6. doi: 10.1016/0142-9612(90)90086-6.

Weinbaum, J. S., Haskett, D. G., Mandelkern, T. F., and Vorp, D A. (2020). "Advances in Cell Seeding of Tissue Engineered Vascular Grafts," in *Tissue-Engineered Vascular Grafts*, eds B. Walpoth, H. Bergmeister, G. Bowlin, D. Kong, J. Rotmans, and P. Zilla, (Cham: Springer International Publishing) 1–25.

Wendt, D., Marsano, A., Jakob, M., Heberer, M., and Martin, I. (2003). Oscillating Perfusion of Cell Suspensions through Three-Dimensional Scaffolds Enhances Cell Seeding Efficiency and Uniformity. *Biotechnol. Bioengin.* 84(2), 205–14. doi: 10.1002/bit.10759.

Zhao, F., and Ma, T. (2005). Perfusion Bioreactor System for Human Mesenchymal Stem Cell Tissue Engineering: Dynamic Cell Seeding and Construct Development. *Biotechnol. Bioengin.* 91(4), 482–93. doi: 10.1002/bit.20532.

**Conflict of Interest:** The authors declare that the research was conducted in the absence of any commercial or financial relationships that could be construed as a potential conflict of interest.

frontiers in Bioengineering and Biotechnology

REVIEW
published: 26 October 2020
doi: 10.3389/fbioe.2020.601560

# Cell Therapy With Human ESC-Derived Cardiac Cells: Clinical Perspectives

*Philippe Menasché*[1,2]*

[1] Department of Cardiovascular Surgery, Hôpital Européen Georges Pompidou, Paris, France, [2] PARCC, INSERM, University of Paris, Paris, France

In the ongoing quest for the "ideal" cell type for heart repair, pluripotent stem cells (PSC) derived from either embryonic or reprogrammed somatic cells have emerged as attractive candidates because of their unique ability to give rise to lineage-specific cells and to transplant them at the desired stage of differentiation. The technical obstacles which have initially hindered their clinical use have now been largely overcome and several trials are under way which encompass several different diseases, including heart failure. So far, there have been no safety warning but it is still too early to draw definite conclusions regarding efficacy. In parallel, mechanistic studies suggest that the primary objective of "remuscularizing" the heart with PSC-derived cardiac cells can be challenged by their alternate use as *ex vivo* sources of a biologically active extracellular vesicle-enriched secretome equally able to improve heart function through harnessing endogenous repair pathways. The exclusive use of this secretome would combine the advantages of a large-scale production more akin to that of a biological medication, the likely avoidance of cell-associated immune and tumorigenicity risks and the possibility of intravenous infusions compatible with repeated dosing.

**Keywords: embryonic stem cell, cardiac cell, heart failure, ischemic heart, induced pluripoten stem cell**

OPEN ACCESS

***Edited by:***
*Martijn van Griensven, Maastricht University, Netherlands*

***Reviewed by:***
*Hidetoshi Masumoto, RIKEN Center for Biosystems Dynamics Research (BDR), Japan*
*Richard Lee, Harvard University, United States*
*Jop Van Berlo, University of Minnesota Twin Cities, United States*

***Correspondence:**
*Philippe Menasché*
*philippe.menasche@aphp.fr*

***Specialty section:***
*This article was submitted to Tissue Engineering and Regenerative Medicine, a section of the journal Frontiers in Bioengineering and Biotechnology*

***Received:*** *01 September 2020*
***Accepted:*** *02 October 2020*
***Published:*** *26 October 2020*

***Citation:***
*Menasché P (2020) Cell Therapy With Human ESC-Derived Cardiac Cells: Clinical Perspectives. Front. Bioeng. Biotechnol. 8:601560. doi: 10.3389/fbioe.2020.601560*

## WHY PLURIPOTENT STEM CELLS?

### Rationale for the Use of Cardiac-Committed Cells

So far, it is fair to acknowledge that no one can claim that a given cell type has unequivocally demonstrated its superiority over another for inducing heart repair and the attendant improvement in left ventricular function. Nevertheless, the few comparative experimental studies which have been published suggest the interest of using cells which are phenotypically matched to those of the organ to be repaired and thus highlight the potential benefits of cardiac-committed cells. A first comparison of human induced pluripotent stem cell (iPSC)-derived cardiomyocytes versus human mesenchymal stromal cells (MSC) injected 30 min after permanent coronary artery ligation in rats reported that the former tended to improve left ventricular function to a greater extent and significantly reduced fibrosis compared with MSC (Citro et al., 2014). In a subsequent head-to-head comparison of different human stem cell types, cardiosphere-derived cells were found superior to MSC from bone marrow and adipose tissue and to bone marrow-derived mononuclear cells (BMMNCs) for improving post-infarction cardiac function and cell engraftment in a mouse model also treated just after ligation of the left anterior descending artery (Li et al., 2012). Likewise, human embryonic stem cell (ESC)-derived cardiomyocytes and mesodermal cardiovascular progenitors were found to similarly improve post-infarction systolic function in contrast to BMMNCs in rat

hearts treated 4 days after a 60 min period of coronary artery occlusion (Fernandes et al., 2015). In keeping with these data, the more recent pig study of Ishida et al. (2019) shows that in comparison of skeletal myoblasts and MSC, iPSC-derived cardiomyocytes (all cells being of human origin) yielded the best outcomes with regard to regional function, oxidative metabolism, vascular density and limitation of apoptosis. However, an opposite conclusion emerged from another comparative study of iPS derivatives where MSC were found superior to cardiomyocytes for the improvement of cardiac function in heart failure, an effect primarily attributed to their immunomodulatory effects (Liao et al., 2019). This discrepancy could be related to very specific features of this protocol: the induction of heart failure by coronary artery occlusion associated with rapid pacing, a setting known for its instability and the intensity of neuro-hormonal stimulation (Yarbrough, 2003); the use of different PSC sources (ESC for cardiomyocytes and iPSC for MSC); the application of a uniform immunosuppression regimen to MSC and cardiomyocytes whereas the former are known to be more immune evasive, which was indeed reflected in that study by their lower expression of Human Leukocyte Antigen (HLA)-II; the greater susceptibility of ESC-derived cardiomyocytes to an immune response could thus have accounted for their lower rate of survival and their (slightly) inferior functional performance. In brief, these data are difficult to interpret because of all these confounders and do not challenge the concept that an optimal therapeutic benefit likely requires that both transplanted and host cells belong to the same lineage.

In practice, adult tissue sources of cardiac cells are limited to cardiospheres and c-*kit*$^+$ cardiac stem cells (CSC) whose harvest from heart tissue does not equate to their cardiac lineage commitment. Cardiospheres are agglomerates of several cell types, predominantly MSC, harvested from the right ventricle by an endomyocardial biopsy (Smith et al., 2007) with a subsequent intracoronary delivery while c-*kit*$^+$ CSC are grown from a right appendage biopsy taken during a coronary artery bypass operation before being also reinjected into the coronary arteries. However, the first have failed to show benefits in an ischemic cardiomyopathy phase II trial which was prematurely interrupted in April, 2017 for futility; however, the use of these cells in Duchenne muscular dystrophy has yielded an encouraging efficacy signal (Taylor et al., 2019) which needs to be confirmed by the ongoing HOPE-II study, planned to randomize 84 non-ambulatory and ambulatory patients with Duchenne muscular dystrophy to intravenous infusions of either 150 million cardiosphere-derived cells every 3 months for a total of 4 doses or placebo. The use of c-*kit*$^+$ CSC has been largely based on preclinical data now considered to be in part fraudulent[1] and there is some consensus that these cells are rather endowed with an angiogenic potential (van Berlo et al., 2014). Four trials are currently registered in the ClinicalTrials.gov website, of which one (CONCERT-HF) which has tested transendocardial injections of autologous MSC, c-*kit*$^+$ CSC, alone or in combination, in patients with ischemic heart failure, was temporarily paused in October, 2018. Among the remaining 3 studies, only one, the CHILD trial, which assesses the effects of intramyocardial injection of autologous c-*kit*$^+$ cells in 32 patients with hypoplastic left heart syndrome, is currently recruiting. A second one (TAC-HF-II) planned to test transendocardial injection of autologous MSC alone or in combination with CSC in 55 patients with ischemic left ventricular dysfunction, has not yet started recruiting. The third trial (JOKER) was designed to assess the effects an intracoronary infusion of autologous c-*kit*$^+$ cells expanded from a right appendage biopsy taken during coronary surgery in a small group of six patients still presenting a left ventricular ejection fraction $< 40\%$ after their revascularization; it is reported active but not recruiting. Outcomes of these trials will hopefully shed some light on the place of these cells in the context of cell-based heart repair.

## Interest of PSC as a Source of Cardiac-Committed Cells

Given the limitations of these adult sources of cardiac-committed cells, it has looked sound to consider the alternate use of pluripotent stem cells (PSC) to leverage their intrinsic ability to generate lineage-specific cells in response to appropriate cues and thus coax them toward a cardiac differentiation pathway. Since the seminal work of Caspi et al. (2007) showing that ESC-derived cardiomyocytes improved myocardial performance in chronically infarcted rats, a flurry of studies have confirmed the functional efficacy of PSC cardiac derivatives. This has been a strong incentive for developing multiple and various techniques for PSC scale-up and differentiation, the detailed description of which is beyond the scope of this article (for a recent review, see Le and Hasegawa, 2019). Enough is to say that the extensive documentation on the raw products required for a regulatory approval makes highly desirable to use the most straightforward and cost-effective procedures, which has guided our choice of an only two cytokine-based technique described below. Another advantage of PSC is their scalability which is critical particularly if the objective is the "remuscularization" of extensively scarred post-infarction myocardial areas (as discussed below). One could argue that this property is shared by MSC but it is not totally true as there is some evidence that increasing the number of MSC passages can shift their phenotype toward an aging pattern translating into an impaired functionality of the cells (Yin et al., 2019).

The ability to control the differentiation pathway of PSC gives the flexibility of "freezing" it at the desired stage and thus provides the option of transplanting early progenitor cells or more mature cardiomyocytes. Each of these cell types has advantages and inconvenient. Early progenitors feature a greater plasticity which could allow them to differentiate in both cardiac and vascular cells and their predominant reliance on anaerobic glycolysis might enhance their survival in a poorly oxygenated environment. This assumption is supported by the findings of Halbach et al. (2014) that the highest persistence and grade of electrical coupling of intramyocardially transplanted fetal cardiomyocytes from different developmental stages is achieved by intermediate cells (days 14.5) compared with earlier and later

[1]News at a glance. *Science* 362, 268–270. doi: 10.1126/science.362.6412.268

stages (days 9.5 and 18.5, respectively). An additional feature of early progenitor cells is their greater secretory profile (Agarwal et al., 2017; El Harane et al., 2018), which can be an advantage if one relies on a predominant paracrine mechanism of action (see below). At the opposite, an early progenitor cell population can still be "contaminated" by pacemaker cells behaving as foci of automaticity and thus predisposing to arrhythmias (Ichimura et al., 2020). Conversely, this issue is addressed by the use of more mature cardiomyocytes which are thought to be endowed with a greater force-generating potential but, in turn, may be more susceptible to death once transplanted in hypovascularized areas because of their reliance on oxidative phosphorylation. At the end, it is fair to admit that currently the few studies which have compared different stage-specific cardiac differentiated cells have failed to provide unequivocal evidence for the superiority of one type over the other (Fernandes et al., 2015; Ye et al., 2015).

## The ESCORT Trial

Our choice has been to transplant early progenitors differentiated from ESC in the ESCORT trial (NCT02057900) which was a first-in-man safety study of 6 patients with severe ischemic left ventricular dysfunction (median left ventricular ejection fraction: 26%; IQR: 22–32%) and in whom the cell therapy treatment was combined with a coronary artery bypass (Menasché et al., 2018). The trial was based on 10 years of preclinical studies in rodents and non-human primates (Bellamy et al., 2015; Menasché et al., 2015). Pluripotent ESC were first scaled-up to generate a master/working cell bank from which cells were collected, thawed, expanded in a defined medium on clinical-grade feeder cells (irradiated human foreskin fibroblasts) and then committed toward a mesodermal-cardiac lineage by a 4-day exposure to two cytokines (bone morphogenetic protein-2 and a FGF inhibitor) according to Good Manufacturing Practice (GMP) standards. As roughly 44% of the cells only responded to the cardio-instructive cues, a purification step was mandatory. The expression of stage-specific embryonic antigen (SSEA)-1, was then taken as a marker for loss of pluripotency and immunomagnetic sorting using a microbead-coupled anti-SSEA-1 antibody was used for selecting the committed cells. This resulted in the harvest of a highly purified population of SSEA-$1^+$ cells characterized by a knock-down of the pluripotency gene *Nanog* and a parallel upregulation of the cardiac transcription factor *Isl-1*. These two markers, assessed by qPCR, were among the release criteria, with thresholds set as $<0.1\%$ and $> 5\%$, respectively, expressed as fold changes relative to the undifferentiated population. Additional lot release criteria included cell viability and purity, with thresholds set at 90 and 95%, respectively, which were fully met for all the patients [median viability and purity rates of 96% (IQR: 96–96%) and 97.5% (IQR: 95.5–98.7%), respectively]. SSEA-$1^+$ progenitor cells were then embedded into a fibrin patch generated by first mixing them with fibrinogen followed by addition of thrombin to induce rapid polymerization of the gel (fibrinogen and thrombin were components of a clinically used surgical glue). Finally, during the surgical procedure, a 20 $cm^2$ piece of autologous pericardium was harvested and sutured to the epicardium along one-half the borders of the infarct area, thereby creating a pocket into which the cell-loaded fibrin patch was simply slipped. The free edge of the pericardial flap was then stitched to the remaining half of the infarct circumference, thereby enclosing the fibrin patch and ensuring its stability. The use of the pericardium was based on the assumption that it could act as a natural bioreactor providing growth factors to the underlying cellular graft and thus contributing to enhance early cell survival (**Figures 1**, **2**). A median dose of SSEA-$1^+$ *Isl-1* cardiovascular progenitors of 8.2 million (IQR: 5–10 million) was delivered without any adverse intraoperative events. The primary end point was safety at 1 year, primarily assessed on (1) cardiac teratoma or remote tumor tracked by whole body computed tomography and fluorine-18 deoxyglucose positron emission tomography scans, (2) arrhythmias, detected by serial interrogations of the cardioverter-defibrillator implanted in all patients, and (3) alloimmunization, assessed by the presence of donor-specific antibodies. All patients had an uneventful post-operative course, except for one who died shortly after the operation from multiple comorbidities. With a maximum follow-up of 6 years, no patient presented an adverse event that could be related to the cells and/or the patch. While it would be meaningless to draw conclusions regarding efficacy, enough is to say that an encouraging signal was provided by a significant improvement of the wall motion of the cell/patch-treated segments during follow-up with a score that decreased from $4.2 \pm 0.8$ at baseline to $2.5 \pm 0.4$ at 1 year ($p = 0.004$ by the mixed model ANOVA on ranks). Of note, in 3 of the 4 patients who contributed these 1-year data, the treated segments had not been revascularized but, again, this cannot be taken as definite proof of efficacy because of the confounding effect of concomitant revascularization. Since we were not expecting a long-term cellular engraftment and primarily relied on a paracrine mechanism of action (see below), patients were only immunosuppressed transiently and while the initial planning was to give the drugs for 2 months, the duration was shortened to 1 month from the second patient onward. Drugs were given at a relatively low dosing (target trough levels of cyclosporine: 100–150 ng/ml; mycophenolate mofetil, 2 g/day) since our pre-operative mixed lymphocyte reaction assays had shown that SSEA-$1^+$ cells are weakly immunogenic.

## Other PSC Clinical Trials

Other investigators have made the different choice of transplanting PSC-derived cardiomyocytes at a later stage of differentiation (although their persistent fetal-like phenotype precludes their assimilation to *bona fide* myocardium-resident cardiomyocytes) and have switched to iPSC as the source cells for practicality and/or ethical reasons. Once differentiated, iPSC-derived cardiomyocytes share with ESC the ability to improve the function of infarcted hearts (Lee et al., 2017) but also the lack of long term engraftment (Okano and Shiba, 2019). The use of iPSC has been aggressively promoted by those who oppose ESC for religious reasons with the premise that they could be differentiated from the patient's own somatic cells, thereby obviating the use of immunosuppression. This argument is no longer tenable since there is a consensus that iPSC for clinical purposes should rather be harvested from healthy donors, i.e., in an allogeneic mode, to improve safety and potency and decrease costs. This is actually the case for two trials in patients with ischemic heart failure: one in Japan aims

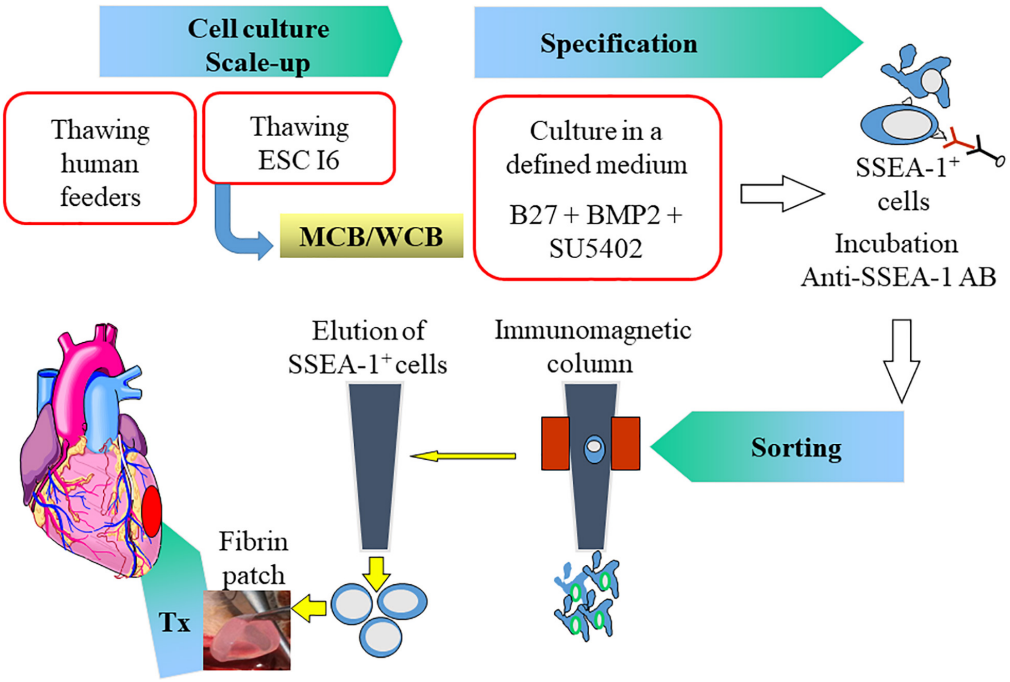


**FIGURE 1 |** Summary of the protocol in the ESCORT trial. Human Embryonic Stem Cells (ESC) from the I6 cell line were expanded on human feeders to generate a Master/Working Cell Bank (MCB/WCB). Expanded pluripotent stem cells (scale-up) were then cardiac-committed (specification) by a 4-day exposure to Bone Morphogenetic Protein (BMP)-2 and a Fibroblast Growth Factor inhibitor (SU5402) in B27 medium. Committed cells express the Stage-Specific Embryonic Antigen (SSEA)-1 indicating their loss of pluripotency and could thus be immune-magnetically sorted using an anti SSEA-1 antibody. The SSEA-1 enriched cardiovascular progenitor cell population was then embedded in a fibrin patch which was transplanted onto the epicardium of the infarct area. AB: antibody; Tx: transplantation.

at grafting *allogeneic* iPSC-derived cardiomyocytes in 10 patients with a severe cardiomyopathy under the form of cell sheets prepared according to a well-documented technology (Guo et al., 2020). The announcement of the first operation in this series has been made in the lay press in January, 2020[2], but at the time of this writing, this trial is not registered on University Hospital Medical Information Network (UMIN CTR), Japan[3] and only its 3-patient roll-in phase is listed as terminated (UMIN000032989). The second trial which is in preparation in Germany plans to graft engineered heart constructs (Tiburcy et al., 2017) made of iPSC-derived cardiomyocytes and collagen in patients with end-stage heart failure. Of note, in these two studies, cell therapy will be used as a stand-alone procedure which will allow a true assessment of its effects without the confounding effect of an associated procedure and also makes possible a less invasive approach by a small left thoracotomy. Conversely, another trial (HEAL-CHF, NCT03763136), in China, should include five participants with ejection fractions between 30 and 45% who will be injected intramyocardially with 100 million *allogeneic* iPSC-derived cardiomyocytes but in conjunction with coronary artery bypass grafting. This study is currently recruiting. A last trial planned to include 3 patients with chronic heart failure and in whom *autologous* iPSC-derived cardiomyocytes would be delivered intravenously has been registered in ClinicalTrials.gov in November 2018 (NCT03759405) but has surprisingly not yet started recruiting.

## The Issue of Dosing

A critically relevant issue raised by transplantation of PSC-derived cardiomyocytes, regardless of their ESC or iPSC source, is their optimal dosing. Several factors have to be taken into account, including the mass of lost myocardium, particularly if the objective is its remuscularization (as discussed below), the rate of cell attrition and the possible proliferation of the surviving cells although the latter factor is of unlikely clinical relevance because of the consistent finding of the absence of sustained cell engraftment. In a meta-analysis of stem cells in large animal studies (primarily performed in pigs), cells doses were extremely variable, ranging from $5 \times 10^5$ to $25 \times 10^6$ for c-*kit* CSC, from $1.3 \times 10^6$ to $1 \times 10^7$ for cardiospheres and also averaged $1 \times 10^7$ for Sca-1 + CSC. Interestingly, in the only dose-escalating study of cardiospheres (Yee et al., 2014), the highest dose (150 million) was found superior to the lower ones when the assessment was made 4 weeks after treatment but the benefit on global and regional left ventricular function (versus a control group) was lost in a subsequent cohort receiving this high dose but assessed at a later time point (8 weeks). In a Phase II dose-escalation study of allogeneic mesenchymal precursor cells in patients with ischemic or non-ischemic heart failure (Perin et al., 2015), the best outcomes were yielded by

[2]https://www.japantimes.co.jp/news/2020/01/28/national/science-health/osaka-university-transplants-ips-cell-based-heart-cells-worlds-first-clinical-trial/
[3]https://www.umin.ac.jp/ctr/

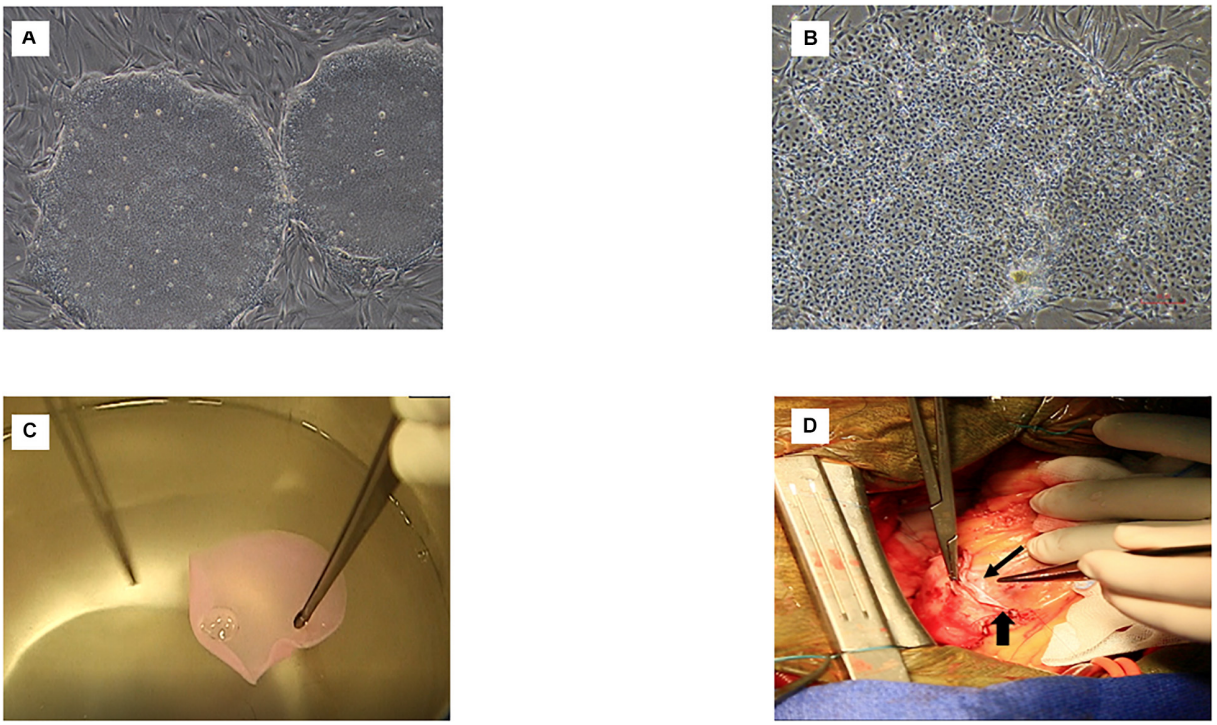


**FIGURE 2 |** Main steps of the procedure in the ESCORT trial. **(A)** Pluripotent ESC of the I6 cell line. **(B)** Cardiovascular progenitors at the completion of the 4-day specification step. **(C)** Fibrin patch loaded with the cardiovascular progenitors (intra-operative picture showing the rinsing of the patch before its implantation in the patient). **(D)** Final step: the cell-loaded patch has been delivered onto the epicardium of the infarct area and is partly covered by a pericardial flap already sutured along one-half the infarct circumference, thereby creating a pocket (between the flap and the epicardium) inside which the patch has been slid; the long and thin arrow indicates the border of the patch. The short and wider arrow indicates the suture line of the pericardial flap to the epicardium. Once the cell-loaded fibrin patch seats within the pocket, this suture line will be completed along the remaining one-half of the infarct circumference to enclose it completely, thereby ensuring its stability while providing some trophic support to the underlying fibrin patch.

the highest dose (150 million versus 25 and 75 million) and a similar dose-dependent response (better with 100 versus 20 million cells) has been reported in the TRIDENT trial in which allogeneic bone marrow-derived-MSC were delivered in patients with ischemic cardiomyopathy (Florea et al., 2017). These data are consistent with those of a metaanalysis of 914 MSC clinical trials (for all types of indications) in which the minimal effective dose ranged between 100 and 150 million cells (Kabat et al., 2020). Admittedly, however, none of these clinical studies have used PSC derivatives. Looking exclusively at those transplanted in non-human primate models generates conflicting results. Chong et al. (2014) reported an extensive remuscularization of the infarcted myocardium injected with $1 \times 10^9$ ESC-derived cardiomyocytes but the small sample size precluded any meaningful functional assessment. Conversely, despite injecting a similar cell number, Romagnuolo et al. (2019) failed to show a benefit on infarct size or global left ventricular function (with no correlation between cardiomyocyte purity and graft size) after 4 weeks. In contrast, Liu Y.-W. et al. (2018) reported a functional benefit following transplantation of a slightly lower dose ($7.5 \times 10^8$) of ESC-derived cardiomyocytes and in the study of Shiba et al. (2016), a post-transplantation improvement of contractile function at 4 and 12 weeks could even be yielded by an almost twofold lower dose dose ($4 \times 10^8$ iPSC-derived cardiomyocytes). Finally, in another study using ESC-derived cardiovascular progenitors, a much lower dose ($1 \times 10^7$) also improved heart function provided the immunosuppression regimen was appropriate (Zhu et al., 2018). Put together, these data suggest that the highest doses are not necessarily the most effective, particularly in view of the risk of arrhythmias outlined in the next section, and although the issue of the optimal dosing is still open, they tend to support the earlier experimental findings that even though increasing the dose of ESC translates into an increased graft size, this may not reflected by an improvement in heart function (van Laake et al., 2009).

## HOW DO PSC-DERIVED CARDIAC CELLS WORK?

### The "Remuscularization" Hypothesis

A logical objective of using PSC-derived cardiac cells is to structurally replace host cardiomyocytes which have been irreversibly damaged. This forms the basis of the "remuscularization" concept which entails the transplantation of cardiomyocytes, as mature as they can, or cardiac progenitors expected to complete their differentiation under the influence of local cues. The goal is that these cells stably engraft and

seamlessly couple with host cardiomyocytes enabling the cellular graft to synchronously contribute to heart pump function while avoiding electrical instability. Several studies in both rodents and large animals, including non-human primates, have documented histologically the feasibility of generating large grafts recolonizing part of the scar tissue and predominantly made of cardiomyocytes, with evidence for their progressive maturation over time, an electrical coupling with host cardiomyocytes, as assessed by fluorescent calcium indicators (despite an often low connexin-43 immunoreactivity) and an associated improvement of left ventricular function of varying degree demonstrated by magnetic resonance imaging (Liu Y.-W. et al., 2018; Romagnuolo et al., 2019) or echocardiography and micro computerized tomography (Chong et al., 2014; Shiba et al., 2016). Despite being intellectually sound and attractive, this approach raises two major clinically relevant challenges: maintenance of long term cell survival and arrhythmias.

## Cell Survival

If one targets the generation of a new myocardial tissue, it is expected that the grafted cells will remain engrafted and alive over time. Unfortunately, cells tend to die rapidly following transplantation, which has led to the investigation of multiple empowering strategies, primarily based on chemical or physical (heat shock) preconditioning and genetic engineering (Mohsin et al., 2011), but these approaches have been challenging to translate clinically, most likely because of their complexity, cost and difficulties to meet regulatory standards. In practice, three main factors of cell death have been identified. The first is the loss of cell anchorage to an extracellular matrix which occurs at the time of their usual dissociation before injection; this can be addressed by incorporation of the cells in a biomaterial which has a dual interest: (1) it provides a three-dimensional template conducive to extracellular matrix secretion enhancing cell cohesiveness, and (2) it acts as a shielding structure that increases cell retention. It is beyond the scope of this article to discuss the choice of biomaterials. Suffice is to say that if they are considered for catheter-based delivery, they should feature shear-thinning properties allowing their injection followed by an *in situ* gelation to improve retention of the matrix-encapsulated cells (Ban et al., 2014), whereas, they should have mechanical properties allowing to generate an easily manipulable patch if they are poised to an intraoperative epicardial application, as in the ESCORT trial and others. A second factor of cell death is the hostile nature of the environment they are implanted in, with a mix of inflammatory, hypovascularized and scarred areas which makes challenging for the transplanted cells to survive. One way of addressing this issue is to co-transplant them with supportive vascular and/or stromal cells to provide trophic and structural support. The critical role of non-cardiac cells (at a roughly 30% ratio) for increasing the therapeutic potential of iPSC-derived cardiomyocytes has been established (Iseoka et al., 2018) and further confirmed recently by the ability of ESC-derived epicardial cells co-transplanted with ESC-derived cardiomyocytes to enhance cardiac graft size and heart function in athymic rats treated 4 days after a 60 min coronary artery ligation (Bargehr et al., 2019). The study by Gao et al. (2018) is of even greater clinical relevance in that it used a large animal (porcine) model to establish the functional benefits of a composite patch construct made of iPSC-derived cardiomyocytes, endothelial and smooth muscle cells. In the clinics, these co-transplantation are technically doable as exemplified by the TAC-HF-II and the Japanese iPS sheet trials but they may complicate the cell manufacturing process. A third, and possible, the most challenging cause of cell death, is rejection of these allogeneic PSC derivatives. Currently, only drug-based immunosuppression is used to prevent rejection but despite the persisting uncertainties regarding the optimal drug regimen, it is admitted that these drugs are fraught with side-effects which may lead to their discontinuation with an attendant loss of the grafted cells (Guan et al., 2020). A variant of this approach could be a "biological" immunomodulation by co-transplantation of MSC which have been shown, at least in a subcutaneous implantation model, to control allogeneic iPSC-CM rejection via regulatory T cells and cell-cell contact with activated lymphocytes (Yoshida et al., 2020), however, because MSC are immune evasive and not immune privileged, they can only extend the survival of the co-transplanted iPSC-derived cardiomyocytes without preventing their ultimate disappearance (Yoshida et al., 2020).

## Arrhythmias

A major concern raised by non-human primate studies in which ESC-derived cardiomyocytes have been transplanted has been the occurrence of ventricular arrhythmias (Chong et al., 2014; Shiba et al., 2016; Liu Y.-W. et al., 2018; Romagnuolo et al., 2019), some of which were life-threatening. Different mechanisms have been hypothesized but rather then re-entry induced by tracks of slow conduction, it seems that focal activation at the graft/host interface is a key trigger of these events (Liu Y.-W. et al., 2018; Romagnuolo et al., 2019). Of note, arrhythmias have usually been observed early, i.e., during the first post-transplantation weeks with a progressive diminution onward which could reflect a progressive *in situ* maturation of the graft toward a ventricular-like pattern. This supports the transplantation of a homogeneous population of cells featuring a mature electrophysiological phenotype but also emphasizes the importance of ensuring that the graft is appropriately purged from all cells which could still feature a pace-maker phenotype.

In an attempt to circumvent these issues while still targeting remuscularization of the diseased heart, other strategies have been developed which overall try either to reset the clock by restoring the ability of endogenous cardiomyocytes to divide or to convert host fibroblasts into new cardiomyocytes (reviewed in Sadek and Olson, 2020). The discussion of these strategies is beyond the scope of this paper but the important point is that a cell-induced improvement of function, which is the ultimate main objective, is not automatically correlated with an increase of the contractile cell pool. This has been well demonstrated in a mouse model of myocardial infarction where transplanted cardiovascular progenitor cells expressing a doxycycline-inducible *MYC* construct were shown to proliferate in the myocardium and then, following doxycycline removal, to differentiate in cardiomyocytes, endothelial and smooth muscle cells, leading to the formation of large grafts from the

transplanted cells but without improvement of the contractile function (even though fibrosis was reduced) (Schwach et al., 2020). These data are in line with those published more than 10 years ago by van Laake et al. (2009) who had shown, in a mouse model, that post-infarction cardiac function was not improved by increasing graft size but rather seemed to be largely contributed by augmentation of the vascular density. Put together, these results are thus suggestive that other mechanisms than generation of new cardiomyocytes are involved in cell-induced improvement of outcomes, thereby lending support to the paracrine hypothesis.

## The Paracrine Hypothesis

Aside from "remuscularization," a second mechanism whereby PSC-derived cardiac cells could act is paracrine signaling, i.e., the release of factors harnessing endogenous repair pathways (Garbern and Lee, 2013).

### Evidence for a Paracrine Mechanism of Action

This hypothesis is strongly supported by three lines of reasoning. First, there is a consistent temporal discrepancy between the physical presence of cells in the transplanted tissue and the functional outcomes, i.e., an improvement in heart function is commonly demonstrated at a time where all grafted cells have disappeared. This applies to PSC cardiac derivatives as well. Thus, Riegler et al. (2015) found no difference in cardiac function between chronically infarcted rats transplanted with human ESC-derived cardiomyocytes mixed with collagen and those in which cells had previously been made non-viable by irradiation, thereby suggesting that cell engraftment was not directly responsible for functional improvements. Likewise, differences in ESC graft size have been shown not to translate into differences in the preservation of post-infarction heart function which further supports the idea that remuscularization may not be the key driver of the cell-associated therapeutic benefit (van Laake et al., 2009; Luo et al., 2014). More recently, ESC-derived cardiovascular progenitor cells were reported to improve function of infarcted and adequately immunosuppressed non-human primates at a time where cells are no longer detectable (Zhu et al., 2018). Admittedly, another macaque study has reported the persistence of substantial grafts until 3 months after transplantation, possibly because of the use of more differentiated cardiomyocytes, but the scarcity of their connexin-43 expression still makes uncertain a functionally effective coupling with host cardiomyocytes (Liu Y.-W. et al., 2018) and this concern is strengthened by the finding of scar tissue isolating ESC- and iPSC-cardiomyocyte grafts from the host myocardium of infarcted rats, which makes unlikely their direct contribution to cardiac contractility (van Laake et al., 2009; Lee et al., 2017). Second, cells are known to release a myriad of cytokines, growth factors and other biologics, many of them being packaged in extracellular vesicles (exosomes and microparticles) which can modulate the function of recipient cells through the delivery of their cargo (Patil et al., 2019) and this mechanism also pertains to vesicles released by PSC (Yuan et al., 2009). Extracellular vesicles can then shift recipient cell signaling pathways toward cardiac repair through multiple mechanisms, primarily mitigation of apoptosis, inflammation and fibrosis and stimulation of angiogenesis (Garikipati et al., 2018; Zhao et al., 2019), while the re-induction of a mitotic cycle of native cardiomyocytes leading to an increased contractile cell pool remains more controversial. Third, the extracellular vesicle-enriched secretome of stem cell-derived cardiac cells (or of MSC) recapitulates (and even sometimes outweighs) the beneficial effects of their parental cells an observation which has now been made across a wide variety of preclinical cardiac (Kervadec et al., 2016; Adamiak et al., 2018; El Harane et al., 2018; Rogers et al., 2019) and non-cardiac disease models (reviewed in Desgres and Menasché, 2019) and is consistent with the finding of an overlap of the microRNA profiles between iPSC-cardiomyocytes (Santoso et al., 2020) or MSC (Shao et al., 2017) and their respective exosomes.

Relying on a paracrine mechanism of action implies that cells behave as platforms releasing bioactive molecules and will remain only transiently in the grafted tissue; however, as nobody still knows exactly how long is enough for the cells to release the factors underpinning their therapeutic benefits, the use of adjunctive biomaterials to extend their residency time can still be justified (Chen et al., 2018; Waters et al., 2018; Han et al., 2019). Importantly, rejection does not need to be prevented any longer; it should only be delayed, which implies a short-duration of immunosuppression and consequently reduces the risk of drug-induced side effects. We previously mentioned that in the ESCORT trial, immunosuppressive drugs were only given for 1 month with good tolerance and the Japanese trial entailing the use of iPSC-derived cardiomyocyte cell sheets has likewise planned a limited period (3 months) of immunosuppression.

### Use of the PSC Secretome

#### *Advantages*

The assumption that most, if not all, of the cardioprotective effects of stem cells can be duplicated by the exclusive use of their secretome has logically led to consider the latter as the only therapeutics that could be delivered. This approach has distinct clinically relevant advantages, including (1) a standardized pharma-like manufacturing process, (2) a likely lack of immunogenicity, provided the cells of origin themselves express little, if any, of the HLA I and II, which is the case for iPSC-derived cardiovascular progenitors (Lima Correa et al., 2020), and (3) a functional stability under cryo-storage compatible with an off-the-shelf availability. However, these presumed benefits have to be compounded by the still limited number of large animal proof-of-concept studies (Timmers et al., 2011; Gallet et al., 2017) and the absence, so far, of clinical trials allowing a thorough assessment of this approach in the context of heart failure.

#### *Challenges*

Regardless of the cautionary words above, the translational use of the secretome requires to address at least four main challenges, the first of which is the choice of the parental cells. Although the RNA and protein cargo of undifferentiated ESC (Khan et al., 2015) and iPSC (Bobis-Wozowicz et al., 2015) has shown cardio-protective effects both *in vitro* and in animal models of myocardial infarction, the clinical use of such a secretome would likely raise safety issues because of its possible enrichment

with pluripotency markers (Ratajczak et al., 2006), which rather leads to privilege more differentiated cells as the source material. In this context, and in parallel to what has been shown for cells, the bioactivity of the secretome of cardiac-committed cells outweighs that of non-cardiac cells (Barile et al., 2018), possibly because the released factors are better tailored to the specific biology of the target cardiac tissue; even within the cardiac cell population, the secretome released by early progenitor cells seems to feature superior cardioprotective properties (Agarwal et al., 2017; Könemann et al., 2019) and these data are in line with our observations (El Harane et al., 2018) and those of others (Malik et al., 2013) that untreated adult cardiomyocytes secrete minimal amounts of exosomes. These findings strongly rationalize the choice of PSC as the parental cells because of the dual possibility of differentiating them into cardiac-committed cells and stopping the differentiation process at an early developmental stage. For this reason, our next clinical trial will entail the administration of an extracellular vesicle-enriched secretome of iPSC-derived cardiovascular progenitor cells (El Harane et al., 2018). A second challenge is the mode of delivery of the secretome. If direct intramyocardial injections are considered, a one-shot delivery without any additional carrier exposes to a rapid wash-out and an attendant loss of efficacy. Thus, the incorporation of the cell-produced biologics into biomaterials enabling a sustained release (Chen et al., 2018; Waters et al., 2018), much like for traditional stem cell therapy, can be an effective means of extending their retention and improving outcomes and this concept applies to PSC-derived cardiac cells (Liu B. et al., 2018). Here, a distinct advantage of cell-derived biologics is that they can be successfully embedded into scaffolds suitable for long-term cryopreservation and immediate availability, thereby overcoming survival and storage issues associated with the use of cells (Huang et al., 2020). However, a more appealing means of leveraging the acellular nature of the secretome is to deliver it intravenously. Although a limited amount of the injectate may then reach the target organ, the intravenous route is yet associated with a functional benefit which has been demonstrated across a wide variety of preclinical models of acute myocardial infarction (Timmers et al., 2011; Ciullo et al., 2019), Duchenne (Rogers et al., 2019) and chemotherapy-induced (Singla et al., 2012; Vandergriff et al., 2015; Sun et al., 2018; Milano et al., 2019) cardiomyopathies, as well as in non-cardiac disease models. One postulated mechanism of action of these intravenously injected EV-enriched secretomes is that following their predominant uptake by macrophages (Morishita et al., 2017) and liver sequestration (Wiklander et al., 2015), they could act like cells through a systemic modulation of inflammation triggering tissue-protective signals which are then conveyed to the target organ by the circulating cells (Walker et al., 2012). It is clear that the intravenous route has clinically relevant advantages: it is simple as it does not require costly equipment and facilities; more importantly, it is non-invasive and as such allows repeated administrations, which could be critical for optimizing the therapeutic benefit, as suggested by the finding that repeated administrations of transplanted cells are superior to the single administration of an equivalent cumulative dose (Tang et al., 2018). Of note, while all modes of cells/cell products delivery target the same objective, i.e., an improvement in heart function along with a reversal of adverse ventricular remodeling, they might conceivably reach this goal through different mechanisms of action, i.e., the predominant replenishment of the contractile cell pool along with an increased angiogenesis in the case of direct intramyocardial cardiac cell implantation as opposed to a systemic regulation of inflammation following intravenous infusions.

The last two translational challenges raised by the use of the cellular secretome are its degree and method of purification as well as the characterization of its content. However, these issues are not specific for PSC used as the parental cells and their discussion is beyond the scope of this chapter (for reviews, see Andriolo et al., 2018; Théry et al., 2018).

## A Common Mechanism-Independent Issue: Safety

Regardless of the putative mechanism of action, safety is obviously a key issue because the presence in the cell product of still undifferentiated and/or transformed cells could lead to their uncontrolled proliferation and give rise to a teratoma or a terato-carcinoma. The opponents of ESC have obviously rushed on this risk to demonize ESC (Wysoczynski and Bolli, 2020) in contempt of the actual data which show that although the first five patients to receive ESC derivatives, in this case oligodendrocytes for spinal cord injury, are now at 8 years of their treatment without any warning signal (Press release from Asterias Biotherapeutics Inc., January 24, 2019). Likewise, the first patient of the ESCORT trial has now a more than 5 year-follow up and is doing well without any abnormality on imaging studies (computerized tomography and $^{18}$F-FDG positron emission tomography scans). Nevertheless, it is obviously critical to purify the differentiated cells to ensure that they are no longer contaminated with unwanted and still pluripotent cells.

Multiple purification methods have been developed (reviewed in Ban et al., 2017; Moon et al., 2017), of which only a sorting based on surface markers is currently suitable for large-scale GMP-compliant applications. In the ESCORT trial, we used SSEA-1 as a marker for cells which were no longer undifferentiated and used magnetic bead-bound anti-SSEA-1 antibodies for selecting them. Even though this mode of immunomagnetic positive selection has been used for years for enriching in hematopoietic cell populations, a negative mode of selection targeting markers for pluripotency (Tang et al., 2011) is more appealing in that it would allow the final cell therapy product for patient use to remain magnetic bead-free. Other strategies based on microfluidics or field-flow fractionation are currently investigated and might be of interest if they can be scaled-up under GMP conditions. Of note, selection of the cardiac-committed cells is primarily relevant to the use of cardiovascular progenitors where stage-specific markers have to be used (*Isl-1* in the ESCORT trial) since an extended period of culture is expected to yield an almost pure population of cardiomyocytes whose identity can be confirmed by a battery of markers (Flk-1, PDGFR- α, signal-regulatory protein alpha [(SIRPA)] and vascular cell adhesion molecule 1 (VCAM1)]

and which, in principle, does not harbor undifferentiated cells any longer.

However, regardless of the cell culture strategy, it is mandatory to ensure that the final product which will be delivered to the patient has no tumorigenic potential. This first implies *in vitro* checking for its genetic stability to eliminate the occurrence of cancer-driving mutations that can be induced by culture conditions and time in culture (Goldring et al., 2011; Oliveira et al., 2014). Several quality control metrics have been proposed to ensure that oncogenic networks have not been activated (reviewed in Assou et al., 2018). As an example, the cardiovascular SSEA-1$^{+}$ cells used in the ESCORT trial were assessed by karyotyping, fluorescence *in situ* hybridization (FISH) and array comparative genomic hybridization (aCGH). Of note, iPSC may be more prone to genetic/epigenetic alterations than ESC because of the potential of mutations already present in the parental cells from which they are reprogrammed (Ben-David and Benvenisty, 2011; Oliveira et al., 2014), with the caveat that it can be difficult to establish a correlation between genetic modifications of the cells and the actual risk that will form a tumor *in vivo*. Maybe, in the future, the organs-on-chip technology will provide a human-like micro-environment more suitable for an accurate risk prediction. The identity of the cardiac-committed product also needs to be tested by lineage-specific markers, usually by flow cytometry and/or gene sequencing, in particular to ensure that pluripotency genes have been appropriately knocked down. It may also be advisable to enrich the risk analysis with assays evaluating the potential of the cells to cause genotoxicity and chromosomal damage.

Despite the utility of these *in vitro* tests, tumorigenicity studies in animals still represent a major pillar of the preclinical safety assessment. Several factors have then to be taken into consideration, which include the number of cells to be inoculated, the duration of follow-up, the site of transplantation and the limit of detection of the relevant assays (Sato et al., 2019). The choice of the animal model is particularly critical, keeping in mind that most studies entail transplanting human cells into rodents and, as such, should be interpreted cautiously since xenotransplantation is less likely to induce teratomas than allografts (Erdö et al., 2003). This has been the main argument for us to test Rhesus ESC-derived cardiovascular progenitors in infarcted Rhesus monkeys with the premise that such an intraspecies transplantation would sensitize the potential occurrence of a tumor (Blin et al., 2010). Importantly, these teratoma experiments should include spiking experiments with different ratios of undifferentiated/lineage-committed cells to identify the threshold above which a tumor occurs and thus helps defining lot release criteria (Priest et al., 2015). This information is a critical component of the risk assessment. Finally, off-target adverse effects have to be ruled out by biodistribution studies.

# PERSPECTIVES

## Remuscularization

For those who remain committed to use PSC-derived cardiac-committed cells as physical and expectedly permanent substitutes for the lost cardiomyocytes, there are at least three areas of research which need to be prioritized. The first is to define the optimal stage of differentiation at which cells should be transplanted. As mentioned above, there are no robust arguments favoring early progenitors versus more mature cardiomyocytes but, assuming that the latter could more efficiently increase pump function, it is mandatory to address the risk of arrhythmias by optimizing the maturation state of the transplanted cardiomyocytes and thus mitigate an electrical mismatch at the graft/host interface (Romagnuolo et al., 2019); this can be achieved by a variety of strategies including co-culture with endothelial cells, prolongation of the culture time, control of the composition, topography and stiffness of the extracellular matrix, mechanical and electrical stimulation (Le and Hasegawa, 2019). The second area of research pertains to the development of strategies allowing an immune tolerance of these allogeneic cells in order to avoid the use of high doses of immunosuppressive drugs and their cohort of adverse effects. In this setting, the use of HLA-haplotyped cell lines (Neofytou et al., 2015) could be helpful by allowing a better match between the grafted cells and the immune profile of the recipient and is clinically doable as HLA-matched cells are currently transplanted in a Parkinson trial: https://upload.umin.ac.jp/cgi-open-bin/ctr_e/ctr_view.cgi?recptno=R000038278. However, the most conceptually attractive option could be the use of gene editing to generate cell lines no longer expressing HLA-I and -II antigens but engineered to express molecules preventing cell destruction by Natural Killer cells (Xu H. et al., 2019), provided that the efficacy and safety of these "universal" cell lines can be validated. One step further, co-transplanting cardiomyocytes and dendritic cells derived from the *same* PSC line might induce a selective tolerance to T cells reactive to the alloantigens expressed by the PSC derivatives. In the context of these efforts to "lighten" immunosuppressive regimens, another approach, possibly easier to implement in the clinics, could be the use of regulatory T cells or even their derived exosomes which have been shown to successfully extend liver graft survival (Chen et al., 2019).

Finally, even though the success of pro-survival approaches could enable a prolonged engraftment of the cells, it is likely that their number will progressively decrease over time. This assumption is supported by the finding that cardiac function was significantly improved in mice injected with ESC-derived cardiomyocytes at 4 weeks after transplantation but that this benefit was not retained at 3 months (van Laake et al., 2007), thereby suggesting that maintenance of a therapeutic effect likely requires repeated administrations. In the clinics, this can only be achieved, easily and safely, by intravenous injections. Admittedly, however, intravenously injected ESC-derived endothelial cells or iPSC-derived neural stem cells have been therapeutically effective in ischemic hindlimb (Huang et al., 2010) and amyotrophic lateral sclerosis (Nizzardo et al., 2014) models, respectively, without causing short-term adverse events, but one could be concerned about the safety of a systemic delivery of PSC derivatives and it is uncertain that such a strategy would be approved by the regulators (it might be the reason why the Chinese trial mentioned above and which had planned intravenous infusions of iPSC-derived cardiomyocytes in 3 heart

failure patients has not yet started 18 months after its official registration). In this context, an innovative approach has been proposed which consists of implanting an epicardial device connected to a subcutaneous port which can be periodically replenished with. The extent to which this system, which has shown promising results in a rodent model of myocardial infarction (Whyte et al., 2018), can be translated clinically remains to be established.

## Paracrine Signaling

Reliance on a paracrine mechanism of action logically leads to consider to exclusively deliver the cellular secretome even though its effects on *in vitro* potency assays may not be representative of what happens when it is directly released by the parental cells *in vivo*. This limitation, however, may not be so relevant as demonstrated almost 10 years ago by Timmers et al. (2011) who showed, in a pig model of myocardial infarction, the protective effects of the intravenously infused conditioned medium (only clarified and concentrated) of ESC-derived MSC. Further confirmation has been brought more recently in a rat model of myocardial infarction in which a single intramyocardial injection of the total conditioned media released by neonatal human CSC was significantly more effective functionally than either the parental cells of their purified exosomal fraction (Sharma et al., 2017). Nevertheless, one area of research is to identify the key drivers of the biological effects of the cellular secretome and many different miRNAs and proteins have been reported as the most effective candidates. While it is tempting to identify a short list of compounds in the perspective of synthetizing them as a multi-targeted drug, it could indeed be counter-productive to deconstruct the cargo of the secretome because of the multiplicity of its components and their possible interactions leading to synergistic effects, notwithstanding the challenge of artificially recapitulating a complex repertoire of bioactive molecules. Another reason for keeping the whole extracellular vesicle payload intact is that it can be shuttled in the recipient cells without the risk of degradation because of the protection afforded by the lipid bilayer of the vesicles whereas it is unlikely it would still be the case if its individual components had to be delivered individually. A second area of research pertains to the means of "priming" the parental cells during the culture period to enrich the extracellular vesicle package with proteins and other biologics that can bolster their biological effects (Wiklander et al., 2019; Xu R. et al., 2019; Yuan et al., 2019). A third clinically relevant perspective pertains to the optimized delivery of the cellular secretome. Although using source cells which share the same repertoire of surface receptors as those of the target tissue can yet be therapeutically beneficial, as discussed above, a greater benefit could likely be yielded by a more selective targeting of the injectate toward the heart, which can be achieved by two different approaches. The first consists of engineering the parental cells to make them overexpressing receptors expected to traffic to their extracellular vesicles and whose display on the external part of the vesicular membrane can enhance recognition by target cells, docking and vesicle uptake. This strategy has been shown successful for promoting homing of intravenously injected exosomes derived from cardiac progenitor cells overexpressing CXCR4 to enhance interaction of this receptor with its SDF-1α ligand which is upregulated in ischemic tissues (Ciullo et al., 2019). This approach, however, is challenged by the risk of peptide degradation (Hung and Leonard, 2015), hence the interest of an alternate approach based on the direct engineering of the secreted vesicles by anchorage of cardiac-specific peptides to their membrane (Vandergriff et al., 2018) or modifications of their glysosylation pattern to promote binding to endothelial selectins (Sackstein, 2009; Lo et al., 2016). A last clinically relevant issue is dosing. There is consistent evidence that the effects of extracellular vesicles are dose-dependent (Kervadec et al., 2016) while the apparently low number of miRNA carried by exosomes (Chevillet et al., 2014) likely requires large amounts of them to be transferred to convey a significant biological effect, particularly following a systemic delivery. Different metrics can be considered here such as an absolute number of particles, a protein concentration, the vesicle number to protein ratio or a "cell equivalent," i.e., the amount of particles assumed to be released by a given number of the parental cells but no consensus has emerged yet.

In conclusion, while iPSC look more attractive for disease modeling and drug screening, both ESC and iPSC share the same potential for inducing heart repair and possibly regeneration. For reasons related to practicality, iPSC-derived cardiac-committed cells, regardless of their stage of differentiation, may provide a better cost-effective model, particularly if they are primarily used as *ex vivo* biofactories producing a biologically active secretome which would then represent the therapeutics delivered to the patient. This approach would allow to leverage the cardioprotective potential of PSC derivatives while overcoming the safety issues that might be associated with their direct delivery. Future clinical studies will tell whether such an expectation can be really met. In the meantime, the observation that by the end of 2019, there were at least 54 registered trials testing PSC derivatives (Kobold et al., 2020) provides compelling evidence that regardless of the cell source (ESC or iPSC), the clinical indication and the delivery strategy, PSC-derived lineage-specific cells have now integrated the armamentarium of therapies against a wide variety of diseases.

## AUTHOR CONTRIBUTIONS

PM wrote the manuscript.

## ACKNOWLEDGMENTS

I thank the French Ministry of Health (Programme Hospitalier de Recherche Clinique PCR11001, P100303) and Assistance Publique-Hôpitaux de Paris, l'Institut National de la Recherche Médicale (Inserm), the LabEx REVIVE (ANR-10-LABX-73), the French Association Against Myopathies (EVEDOX, Application #22378), the Fondation de France (FDF/2014 00047970), the Fondation pour la Recherche Médicale (PME20180639496), and the Fondation de l'Avenir (AP-RM-18-017) for their funding support.

## REFERENCES


Adamiak, M., Cheng, G., Bobis-Wozowicz, S., Zhao, L., Kedracka-Krok, S., Samanta, A., et al. (2018). Induced pluripotent stem cell (iPSC)-Derived extracellular vesicles are safer and more effective for cardiac repair than iPSCs. *Circ. Res.* 122, 296–309. doi: 10.1161/CIRCRESAHA.117.311769

Agarwal, U., George, A., Bhutani, S., Ghosh-Choudhary, S., Maxwell, J. T., Brown, M. E., et al. (2017). Experimental, systems, and computational approaches to understanding the microrna-mediated reparative po-tential of cardiac progenitor cell–derived exosomes from pediatric pa-tientsnovelty and significance. *Circ. Res.* 120, 701–712. doi: 10.1161/CIRCRESAHA.116.309935

Andriolo, G., Provasi, E., Lo Cicero, V., Brambilla, A., Soncin, S., Torre, T., et al. (2018). Exosomes from human cardiac progenitor cells for therapeutic applications: development of a GMP-Grade manufacturing method. *Front. Physiol.* 9:1169. doi: 10.3389/fphys.2018.01169

Assou, S., Bouckenheimer, J., and De Vos, J. (2018). Concise review: assessing the genome integrity of human induced pluripotent stem cells: what quality control metrics? *Stem Cells* 36, 814–821. doi: 10.1002/stem.2797

Ban, K., Bae, S., and Yoon, Y.-S. (2017). Current strategies and challenges for purification of cardiomyocytes derived from human pluripotent stem cells. *Theranostics* 7, 2067–2077. doi: 10.7150/thno.19427

Ban, K., Park, H.-J., Kim, S., Andukuri, A., Cho, K.-W., Hwang, J. W., et al. (2014). Cell therapy with embryonic stem cell-derived cardiomyocytes encapsulated in injectable nanomatrix gel enhances cell engraftment and promotes cardiac repair. *ACS Nano* 8, 10815–10825. doi: 10.1021/nn504617g

Bargehr, J., Ong, L. P., Colzani, M., Davaapil, H., Hofsteen, P., Bhandari, S., et al. (2019). Epicardial cells derived from human embryonic stem cells augment cardiomyocyte-driven heart regeneration. *Nat. Biotechnol.* 37, 895–906. doi: 10.1038/s41587-019-0197-9

Barile, L., Cervio, E., Lionetti, V., Milano, G., Ciullo, A., Biemmi, V., et al. (2018). Cardioprotection by cardiac progenitor cell-secreted exosomes: role of pregnancy-associated plasma protein-A. *Cardiovasc. Res.* 114, 992–1005. doi: 10.1093/cvr/cvy055

Bellamy, V., Vanneaux, V., Bel, A., Nemetalla, H., Emmanuelle Boitard, S., Farouz, Y., et al. (2015). Long-term functional benefits of human embryon-ic stem cell-derived cardiac progenitors embedded into a fibrin scaffold. *J. Heart Lung Transplant.* 34, 1198–1207. doi: 10.1016/j.healun.2014.10.008

Ben-David, U., and Benvenisty, N. (2011). The tumorigenicity of human embryonic and induced pluripotent stem cells. *Nat. Rev. Cancer* 11, 268–277. doi: 10.1038/nrc3034

Blin, G., Nury, D., Stefanovic, S., Neri, T., Guillevic, O., Brinon, B., et al. (2010). A purified population of multipotent cardiovascular progenitors derived from primate pluripotent stem cells engrafts in postmyocardial infarcted nonhuman primates. *J. Clin. Invest.* 120, 1125–1139. doi: 10.1172/JCI40120

Bobis-Wozowicz, S., Kmiotek, K., Sekula, M., Kedracka-Krok, S., Kamycka, E., Adamiak, M., et al. (2015). Human induced pluripotent stem cell-derived microvesicles transmit RNAs and proteins to recipient mature heart cells modulating cell fate and behavior: hiPSC-MVs Transmit RNAs and proteins to heart cells. *Stem Cells* 33, 2748–2761. doi: 10.1002/stem.2078

Caspi, O., Huber, I., Kehat, I., Habib, M., Arbel, G., Gepstein, A., et al. (2007). Transplantation of human embryonic stem cell-derived cardiomyocytes improves myocardial performance in infarcted rat hearts. *J. Am. Coll. Cardiol.* 50, 1884–1893. doi: 10.1016/j.jacc.2007.07.054

Chen, C. W., Wang, L. L., Zaman, S., Gordon, J., Arisi, M. F., Venkataraman, C. M., et al. (2018). Sustained release of endothelial progenitor cell-derived extracellular vesicles from shear-thinning hydrogels improves angiogene-sis and promotes function after myocardial infarction. *Cardiovasc. Res.* 114, 1029–1040. doi: 10.1093/cvr/cvy067

Chen, L., Huang, H., Zhang, W., Ding, F., Fan, Z., and Zeng, Z. (2019). exosomes derived from T regulatory cells suppress CD8+ Cytotoxic T Lympho-cyte proliferation and prolong liver allograft survival. *Med. Sci. Monit.* 25, 4877–4884. doi: 10.12659/MSM.917058

Chevillet, J. R., Kang, Q., Ruf, I. K., Briggs, H. A., Vojtech, L. N., Hughes, S. M., et al. (2014). Quantitative and stoichiometric analysis of the microRNA content of exosomes. *Proc. Natl. Acad. Sci. U.S.A.* 111, 14888–14893. doi: 10.1073/pnas.1408301111

Chong, J. J. H., Yang, X., Don, C. W., Minami, E., Liu, Y.-W., Weyers, J. J., et al. (2014). Human embryonic-stem-cell-derived cardiomyocytes regenerate non-human primate hearts. *Nature* 510, 273–277. doi: 10.1038/nature13233

Citro, L., Naidu, S., Hassan, F., Kuppusamy, M. L., Kuppusamy, P., Angelos, M. G., et al. (2014). Comparison of human induced pluripotent stem-cell derived cardiomyocytes with human mesenchymal stem cells following acute myocardial infarction. *PLoS One* 9:e116281. doi: 10.1371/journal.pone.0116281

Ciullo, A., Biemmi, V., Milano, G., Bolis, S., Cervio, E., Fertig, E. T., et al. (2019). Exosomal expression of CXCR4 targets cardioprotective vesicles to myocardial infarction and improves outcome after systemic Ad-ministration. *Int. J. Mol. Sci.* 20:468. doi: 10.3390/ijms20030468

Desgres, M., and Menasché, P. (2019). Clinical translation of pluripotent stem cell therapies: challenges and considerations. *Cell Stem Cell* 25, 594–606. doi: 10.1016/j.stem.2019.10.001

El Harane, N., Kervadec, A., Bellamy, V., Pidial, L., Neametalla, H. J., Perier, M.-C., et al. (2018). Acellular therapeutic approach for heart failure: in vitro production of extracellular vesicles from human cardiovascular progeni-tors. *Eur. Heart J.* 39, 1835–1847. doi: 10.1093/eurheartj/ehy012

Erdö, F., Bührle, C., Blunk, J., Hoehn, M., Xia, Y., Fleischmann, B., et al. (2003). Host-dependent tumorigenesis of embryonic stem cell transplantation in experimental stroke. *J. Cereb. Blood Flow Metab.* 23, 780–785. doi: 10.1097/01.WCB.0000071886.63724.FB

Fernandes, S., Chong, J. J. H., Paige, S. L., Iwata, M., Torok-Storb, B., Keller, G., et al. (2015). Comparison of human embryonic stem cell-derived car-diomyocytes, cardiovascular progenitors, and bone marrow mononu-clear cells for cardiac repair. *Stem Cell Rep.* 5, 753–762. doi: 10.1016/j.stemcr.2015.09.011

Florea, V., Rieger, A. C., DiFede, D. L., El-Khorazaty, J., Natsumeda, M., Banerjee, M. N., et al. (2017). Dose comparison study of allogeneic mesenchymal stem cells in patients with ischemic cardiomyopathy (The TRIDENT Study). *Circ. Res.* 121, 1279–1290. doi: 10.1161/CIRCRESAHA.117.311827

Gallet, R., Dawkins, J., Valle, J., Simsolo, E., de Couto, G., Middleton, R., et al. (2017). Exosomes secreted by cardiosphere-derived cells reduce scarring, attenuate adverse remodelling, and improve function in acute and chronic porcine myocardial infarction. *Eur. Heart J.* 38, 201–211. doi: 10.1093/eurheartj/ehw240

Gao, L., Gregorich, Z. R., Zhu, W., Mattapally, S., Oduk, Y., Lou, X., et al. (2018). Large cardiac muscle patches engineered from human induced-pluripotent stem cell–derived cardiac cells improve recovery from myocardial infarction in swine. *Circulation* 137, 1712–1730. doi: 10.1161/CIRCULATIONAHA.117.030785

Garbern, J. C., and Lee, R. T. (2013). Cardiac stem cell therapy and the promise of heart regeneration. *Cell Stem Cell* 12, 689–698. doi: 10.1016/j.stem.2013.05.008

Garikipati, V. N. S., Shoja-Taheri, F., Davis, M. E., and Kishore, R. (2018). Ex-tracellular vesicles and the application of system biology and computational modeling in cardiac repair. *Circ. Res.* 123, 188–204. doi: 10.1161/CIRCRESAHA.117.311215

Goldring, C. E. P., Duffy, P. A., Benvenisty, N., Andrews, P. W., Ben-David, U., Eakins, R., et al. (2011). Assessing the safety of stem cell therapeutics. *Cell Stem Cell* 8, 618–628. doi: 10.1016/j.stem.2011.05.012

Guan, X., Xu, W., Zhang, H., Wang, Q., Yu, J., Zhang, R., et al. (2020). Transplantation of human induced pluripotent stem cell-derived cardiomyo-cytes improves myocardial function and reverses ventricular remodeling in infarcted rat hearts. *Stem Cell Res. Ther.* 11:73. doi: 10.1186/s13287-020-01602-0

Guo, R., Morimatsu, M., Feng, T., Lan, F., Chang, D., Wan, F., et al. (2020). Stem cell-derived cell sheet transplantation for heart tissue repair in myocardial infarction. *Stem Cell Res. Ther.* 11:19. doi: 10.1186/s13287-019-1536-y

Halbach, M., Baumgartner, S., Sahito, R. G. A., Krausgrill, B., Maass, M., Peinkofer, G., et al. (2014). Cell persistence and electrical integration of transplanted fetal cardiomyocytes from different developmental stages. *Int. J. Cardiol.* 171, e122–e124. doi: 10.1016/j.ijcard.2013.12.115

Han, C., Zhou, J., Liang, C., Liu, B., Pan, X., Zhang, Y., et al. (2019). Human umbilical cord mesenchymal stem cell derived exosomes encapsulated in functional peptide hydrogels promote cardiac repair. *Biomater. Sci.* 7, 2920–2933. doi: 10.1039/C9BM00101H

Huang, K., Ozpinar, E. W., Su, T., Tang, J., Shen, D., Qiao, L., et al. (2020). An off-the-shelf artificial cardiac patch improves cardiac repair after myocardial infarction in rats and pigs. *Sci. Transl. Med.* 12:eaat9683. doi: 10.1126/scitranslmed.aat9683

Huang, N. F., Niiyama, H., Peter, C., De, A., Natkunam, Y., Fleissner, F., et al. (2010). Embryonic stem cell-derived endothelial cells engraft into the is-chemic hindlimb and restore perfusion. *Arterioscler. Thromb. Vasc. Biol.* 30, 984–991. doi: 10.1161/ATVBAHA.110.202796

Hung, M. E., and Leonard, J. N. (2015). Stabilization of Exosome-targeting Peptides via Engineered Glycosylation. *J. Biol. Chem.* 290, 8166–8172. doi: 10.1074/jbc.M114.621383

Ichimura, H., Kadota, S., Kashihara, T., Yamada, M., Ito, K., Kobayashi, H., et al. (2020). Increased predominance of the matured ventricular subtype in embryonic stem cell-derived cardiomyocytes in vivo. *Sci. Rep.* 10:5268. doi: 10.1038/s41598-020-68373-9

Iseoka, H., Miyagawa, S., Fukushima, S., Saito, A., Masuda, S., Yajima, S., et al. (2018). Pivotal role of non-cardiomyocytes in electromechanical and therapeutic potential of induced pluripotent stem cell-derived engi-neered cardiac tissue. *Tissue Eng Part A* 24, 287–300. doi: 10.1089/ten.TEA.2016.0535

Ishida, M., Miyagawa, S., Saito, A., Fukushima, S., Harada, A., Ito, E., et al. (2019). Transplantation of human-induced pluripotent stem cell-derived cardiomyocytes is superior to somatic stem cell therapy for restoring cardiac function and oxygen consumption in a porcine model of myocardial infarction. *Transplantation* 103, 291–298. doi: 10.1097/TP.0000000000002384

Kabat, M., Bobkov, I., Kumar, S., and Grumet, M. (2020). Trends in mesenchy-mal stem cell clinical trials 2004-2018: Is efficacy optimal in a narrow dose range? *Stem Cells Transl. Med.* 9, 17–27. doi: 10.1002/sctm.19-0202

Kervadec, A., Bellamy, V., El Harane, N., Arakélian, L., Vanneaux, V., Cacciapuoti, I., et al. (2016). Cardiovascular progenitor–derived extracellular vesicles recapitulate the beneficial effects of their parent cells in the treatment of chronic heart failure. *J. Heart Lung Trans Plantation* 35, 795–807. doi: 10.1016/j.healun.2016.01.013

Khan, M., Nickoloff, E., Abramova, T., Johnson, J., Verma, S. K., Krishnamurthy, P., et al. (2015). Embryonic stem cell-derived exosomes promote en-dogenous repair mechanisms and enhance cardiac function following myocardial infarction. *Circ. Res.* 117, 52–64. doi: 10.1161/CIRCRESAHA.117.305990

Kobold, S., Guhr, A., Mah, N., Bultjer, N., Seltmann, S., Seiler Wulczyn, A. E. M., et al. (2020). A manually curated database on clinical studies in-volving cell products derived from human pluripotent stem cells. *Stem Cell Rep.* 15, 546–555. doi: 10.1016/j.stemcr.2020.06.014

Könemann, S., Sartori, L. V., Gross, S., Hadlich, S., Kühn, J.-P., Samal, R., et al. (2019). Cardioprotective effect of the secretome of Sca-1+ and Sca-1- cells in heart failure: not equal, but equally important? *Cardiovas. Res.*. 116, 566–575. doi: 10.1093/cvr/cvz140

Le, M. N. T., and Hasegawa, K. (2019). Expansion culture of human pluripotent stem cells and production of cardiomyocytes. *Bioengineering* 6:48. doi: 10.3390/bioengineering6020048

Lee, W. H., Chen, W.-Y., Shao, N.-Y., Xiao, D., Qin, X., Baker, N., et al. (2017). Comparison of non-coding RNAs in exosomes and functional efficacy of human embryonic stem cell- versus induced pluripotent stem cell-derived cardiomyocytes. *Stem Cells* 35, 2138–2149. doi: 10.1002/stem.2669

Li, T.-S., Cheng, K., Malliaras, K., Smith, R. R., Zhang, Y., Sun, B., et al. (2012). Direct comparison of different stem cell types and subpopulations reveals superior paracrine potency and myocardial repair efficacy with cardiosphere-derived cells. *J. Am. Coll. Cardiol.* 59, 942–953. doi: 10.1016/j.jacc.2011.11.029

Liao, S., Zhang, Y., Ting, S., Zhen, Z., Luo, F., Zhu, Z., et al. (2019). Potent im-munomodulation and angiogenic effects of mesenchymal stem cells versus cardiomyocytes derived from pluripotent stem cells for treatment of heart failure. *Stem Cell Res. Ther.* 10:78. doi: 10.1186/s13287-019-1183-3

Lima Correa, B., El Harane, N., Gomez, I., Rachid Hocine, H., Vilar, J., Desgres, M., et al. (2020). Extracellular vesicles from human cardiovascular pro-genitors trigger a reparative immune response in infarcted hearts. *Cardi Ovasc. Res.* 12:cvaa028. doi: 10.1093/cvr/cvaa028

Liu, B., Lee, B. W., Nakanishi, K., Villasante, A., Williamson, R., Metz, J., et al. (2018). Cardiac recovery via extended cell-free delivery of extracellular vesicles secreted by cardiomyocytes derived from induced pluripotent stem cells. *Nat. Biomed. Eng.* 2, 293–303. doi: 10.1038/s41551-018-0229-7

Liu, Y.-W., Chen, B., Yang, X., Fugate, J. A., Kalucki, F. A., Futakuchi-Tsuchida, A., et al. (2018). Human embryonic stem cell-derived cardiomyocytes restore function in infarcted hearts of non-human primates. *Nat. Biotechnol.* 36, 597–605. doi: 10.1038/nbt.4162

Lo, C. Y., Weil, B. R., Palka, B. A., Momeni, A., Canty, J. M., and Neelamegham, S. (2016). Cell surface glycoengineering improves selectin-mediated ad-hesion of mesenchymal stem cells (MSCs) and cardiosphere-derived cells (CDCs): pilot validation in porcine ischemia-reperfusion model. *Bio Mater.* 74, 19–30. doi: 10.1016/j.biomaterials.2015.09.026

Luo, J., Weaver, M. S., Dennis, J. E., Whalen, E., Laflamme, M. A., and Allen, M. D. (2014). Targeting survival pathways to create infarct-spanning bridges of human embryonic stem cell-derived cardiomyocytes. *J. Thorac. Car Diovasc. Surg.* 148, 3180.e1–3188.e1. doi: 10.1016/j.jtcvs.2014.06.087

Malik, Z. A., Kott, K. S., Poe, A. J., Kuo, T., Chen, L., Ferrara, K. W., et al. (2013). Cardiac myocyte exosomes: stability, HSP60, and proteomics. *Am. J. Physiol. Heart Circ. Physiol.* 304, H954–H965. doi: 10.1152/ajpheart.00835.2012

Menasché, P., Vanneaux, V., Fabreguettes, J.-R., Bel, A., Tosca, L., Garcia, S., et al. (2015). Towards a clinical use of human embryonic stem cell-derived cardiac progenitors: a translational experience. *Eur. Heart J.* 36, 743–750. doi: 10.1093/eurheartj/ehu192

Menasché, P., Vanneaux, V., Hagège, A., Bel, A., Cholley, B., Parouchev, A., et al. (2018). Transplantation of human embryonic stem cell-derived cardiovascular progenitors for severe ischemic left ventricular dys-function. *J. Am. Coll. Cardiol.* 71, 429–438. doi: 10.1016/j.jacc.2017.11.047

Milano, G., Biemmi, V., Lazzarini, E., Balbi, C., Ciullo, A., Bolis, S., et al. (2019). Intravenous administration of cardiac progenitor cell-derived exosomes protects against doxorubicin/trastuzumab-induced cardiac toxicity. *Cardiovasc. Res.* 116, 383–392. doi: 10.1093/cvr/cvz108

Mohsin, S., Siddiqi, S., Collins, B., and Sussman, M. A. (2011). Empowering adult stem cells for myocardial regeneration. *Circ. Res.* 109, 1415–1428. doi: 10.1161/CIRCRESAHA.111.243071

Moon, S.-H., Bae, D., Jung, T.-H., Chung, E.-B., Jeong, Y.-H., Park, S.-J., et al. (2017). From bench to market: preparing human pluripotent stem cells derived cardiomyocytes for various applications. *Int. J. Stem Cells* 10, 1–11. doi: 10.15283/ijsc17024

Morishita, M., Takahashi, Y., Nishikawa, M., and Takakura, Y. (2017). Pharmacokinetics of exosomes-an important factor for elucidating the biologi-cal roles of exosomes and for the development of exosome-based therapeutics. *J. Pharm. Sci.* 106, 2265–2269. doi: 10.1016/j.xphs.2017.02.030

Neofytou, E., O'Brien, C. G., Couture, L. A., and Wu, J. C. (2015). Hurdles to clinical translation of human induced pluripotent stem cells. *J. Clin. In Vest* 125, 2551–2557. doi: 10.1172/JCI80575

Nizzardo, M., Simone, C., Rizzo, F., Ruggieri, M., Salani, S., Riboldi, G., et al. (2014). Minimally invasive transplantation of iPSC-derived ALDHhiSSCloVLA4+ neural stem cells effectively improves the phenotype of an amyotrophic lateral sclerosis model. *Hum. Mol. Genet.* 23, 342–354. doi: 10.1093/hmg/ddt425

Okano, S., and Shiba, Y. (2019). Therapeutic potential of pluripotent stem cells for cardiac repair after myocardial infarction. *Biol. Pharma Ceut. Bull.* 42, 524–530. doi: 10.1248/bpb.b18-00257

Oliveira, P. H., da Silva, C. L., and Cabral, J. M. S. (2014). Concise review: ge-nomic instability in human stem cells: current status and future challeng-es. *Stem Cells* 32, 2824–2832. doi: 10.1002/stem.1796

Patil, M., Henderson, J., Luong, H., Annamalai, D., Sreejit, G., and Krishnamurthy, P. (2019). The art of intercellular wireless communications: exosomes in heart disease and therapy. *Front. Cell Dev. Biol.* 7:315. doi: 10.3389/fcell.2019.00315

Perin, E. C., Borow, K. M., Silva, G. V., DeMaria, A. N., Marroquin, O. C., Huang, P. P., et al. (2015). A Phase II dose-escalation study of allogeneic mesenchymal precursor cells in patients with ischemic or nonischemic heart failurenovelty and significance. *Circ. Res.* 117, 576–584. doi: 10.1161/CIRCRESAHA.115.306332

Priest, C. A., Manley, N. C., Denham, J., Wirth, E. D., and Lebkowski, J. S. (2015). Preclinical safety of human embryonic stem cell-derived oligodendrocyte progenitors supporting clinical trials in spinal cord injury. *Regen. Med.* 10, 939–958. doi: 10.2217/rme.15.57

Ratajczak, J., Miekus, K., Kucia, M., Zhang, J., Reca, R., Dvorak, P., et al. (2006). Embryonic stem cell-derived microvesicles reprogram hematopoietic progenitors: evidence for horizontal transfer of mRNA and protein deliv-ery. *Leukemia* 20, 847–856. doi: 10.1038/sj.leu.2404132

Riegler, J., Tiburcy, M., Ebert, A., Tzatzalos, E., Raaz, U., Abilez, O. J., et al. (2015). Human engineered heart muscles engraft and survive long term in a rodent myocardial infarction model. *Circ. Res.* 117, 720–730. doi: 10.1161/CIRCRESAHA.115.306985

Rogers, R. G., Fournier, M., Sanchez, L., Ibrahim, A. G., Aminzadeh, M. A., Lewis, M. I., et al. (2019). Disease-modifying bioactivity of intravenous cardiosphere-derived cells and exosomes in mdx mice. *JCI Insight* 4:e125754. doi: 10.1172/jci.insight.125754

Romagnuolo, R., Masoudpour, H., Porta-Sánchez, A., Qiang, B., Barry, J., Laskary, A., et al. (2019). Human embryonic stem cell-derived cardiomy-ocytes regenerate the infarcted pig heart but induce ventricular tach-yarrhythmias. *Stem Cell Rep.* 12, 967–981. doi: 10.1016/j.stemcr.2019.04.005

Sackstein, R. (2009). Glycosyltransferase-programmed stereosubstitution (GPS) to create HCELL: engineering a roadmap for cell migration. *Immunol. Rev.* 230, 51–74. doi: 10.1111/j.1600-065X.2009.00792.x

Sadek, H., and Olson, E. N. (2020). Toward the goal of human heart regenera-tion. *Cell Stem Cell* 26, 7–16. doi: 10.1016/j.stem.2019.12.004

Santoso, M. R., Ikeda, G., Tada, Y., Jung, J., Vaskova, E., Sierra, R. G., et al. (2020). Exosomes from induced pluripotent stem cell–derived cardio-myocytes promote autophagy for myocardial repair. *J. Am. Heart Assoc.* 9:e014345. doi: 10.1161/JAHA.119.014345

Sato, Y., Bando, H., Di Piazza, M., Gowing, G., Herberts, C., Jackman, S., et al. (2019). Tumorigenicity assessment of cell therapy products: the need for global consensus and points to consider. *Cytotherapy* 21, 1095–1111. doi: 10.1016/j.jcyt.2019.10.001

Schwach, V., Gomes Fernandes, M., Maas, S., Gerhardt, S., Tsonaka, R., van der Weerd, L., et al. (2020). Expandable human cardiovascular progenitors from stem cells for regenerating mouse heart after myocardial infarction. *Cardiovasc. Res.* 116, 545–553. doi: 10.1093/cvr/cvz181

Shao, L., Zhang, Y., Lan, B., Wang, J., Zhang, Z., Zhang, L., et al. (2017). MiRNA-sequence indicates that mesenchymal stem cells and exosomes have similar mechanism to enhance cardiac repair. *BioMed Res. Int.* 2017, 1–9. doi: 10.1155/2017/4150705

Sharma, S., Mishra, R., Bigham, G. E., Wehman, B., Khan, M. M., Xu, H., et al. (2017). A deep proteome analysis identifies the complete secretome as the functional unit of human cardiac progenitor cells. *Circ. Res.* 120, 816–834. doi: 10.1161/CIRCRESAHA.116.309782

Shiba, Y., Gomibuchi, T., Seto, T., Wada, Y., Ichimura, H., Tanaka, Y., et al. (2016). Allogeneic transplantation of iPS cell-derived cardiomyocytes regenerates primate hearts. *Nature* 538, 388–391. doi: 10.1038/nature19815

Singla, D. K., Ahmed, A., Singla, R., and Yan, B. (2012). Embryonic stem cells improve cardiac function in doxorubicin-induced cardiomyopathy mediated through multiple mechanisms. *Cell Transplant* 21, 1919–1930. doi: 10.3727/096368911X627552

Smith, R. R., Barile, L., Cho, H. C., Leppo, M. K., Hare, J. M., Messina, E., et al. (2007). Regenerative potential of cardiosphere-derived cells expanded from percutaneous endomyocardial biopsy specimens. *Circulation* 115, 896–908. doi: 10.1161/CIRCULATIONAHA.106.655209

Sun, X., Shan, A., Wei, Z., and Xu, B. (2018). Intravenous mesenchymal stem cell-derived exosomes ameliorate myocardial inflammation in the dilated cardiomyopathy. *Biochem. Biophys. Res. Commun.* 503, 2611–2618. doi: 10.1016/j.bbrc.2018.08.012

Tang, C., Lee, A. S., Volkmer, J.-P., Sahoo, D., Nag, D., Mosley, A. R., et al. (2011). An antibody against SSEA-5 glycan on human pluripotent stem cells enables removal of teratoma-forming cells. *Nat. Biotechnol.* 29, 829–834. doi: 10.1038/nbt.1947

Tang, X.-L., Nakamura, S., Li, Q., Wysoczynski, M., Gumpert, A. M., Wu, W.-J., et al. (2018). Repeated administrations of cardiac progenitor cells are superior to a single administration of an equivalent cumulative dose. *J Am Heart Assoc.* 7:e007400. doi: 10.1161/JAHA.117.007400

Taylor, M., Jefferies, J., Byrne, B., Lima, J., Ambale-Venkatesh, B., Ostovaneh, M. R., et al. (2019). Cardiac and skeletal muscle effects in the randomized HOPE-Duchenne trial. *Neurology* 92, e866–e878. doi: 10.1212/WNL.0000000000006950

Théry, C., Witwer, K. W., Aikawa, E., Alcaraz, M. J., Anderson, J. D., Andriantsitohaina, R., et al. (2018). Minimal information for studies of extra-cellular vesicles 2018 (MISEV2018): a position statement of the Interna-tional society for extracellular vesicles and update of the MISEV2014 guidelines. *J. Extracell. Vesicles* 7:1535750. doi: 10.1080/20013078.2018.1535750

Tiburcy, M., Hudson, J. E., Balfanz, P., Schlick, S., Meyer, T., Chang Liao, M.-L., et al. (2017). Defined engineered human myocardium with advanced maturation for applications in heart failure modeling and repair. *Cir Culation* 135, 1832–1847. doi: 10.1161/CIRCULATIONAHA.116.024145

Timmers, L., Lim, S. K., Hoefer, I. E., Arslan, F., Lai, R. C., van Oorschot, A. A. M., et al. (2011). Human mesenchymal stem cell-conditioned medium improves cardiac function following myocardial infarction. *Stem Cell Res.* 6, 206–214. doi: 10.1016/j.scr.2011.01.001

van Berlo, J. H., Kanisicak, O., Maillet, M., Vagnozzi, R. J., Karch, J., Lin, S.-C. J., et al. (2014). c-kit+ cells minimally contribute cardiomyocytes to the heart. *Nature* 509, 337–341. doi: 10.1038/nature13309

van Laake, L. W., Passier, R., den Ouden, K., Schreurs, C., Monshouwer-Kloots, J., Ward-van Oostwaard, D., et al. (2009). Improvement of mouse cardiac function by hESC-derived cardiomyocytes correlates with vascularity but not graft size. *Stem Cell Res.* 3, 106–112. doi: 10.1016/j.scr.2009.05.004

van Laake, L. W., Passier, R., Monshouwer-Kloots, J., Verkleij, A. J., Lips, D. J., Freund, C., et al. (2007). Human embryonic stem cell-derived cardiomy-ocytes survive and mature in the mouse heart and transiently improve function after myocardial infarction. *Stem Cell Res* 1, 9–24. doi: 10.1016/j.scr.2007.06.001

Vandergriff, A., Huang, K., Shen, D., Hu, S., Hensley, M. T., Caranasos, T. G., et al. (2018). Targeting regenerative exosomes to myocardial infarction us-ing cardiac homing peptide. *Theranostics* 8, 1869–1878. doi: 10.7150/thno.20524

Vandergriff, A. C., de Andrade, J. B. M., Tang, J., Hensley, M. T., Piedrahita, J. A., Caranasos, T. G., et al. (2015). Intravenous cardiac stem cell-derived exosomes ameliorate cardiac dysfunction in doxorubicin induced dilated cardiomyopathy. *Stem Cells Int.* 2015, 1–8. doi: 10.1155/2015/960926

Walker, P. A., Shah, S. K., Jimenez, F., Aroom, K. R., Harting, M. T., and Cox, C. S. (2012). Bone marrow–derived stromal cell therapy for traumatic brain injury is neuroprotective via stimulation of non-neurologic organ sys-tems. *Surgery* 152, 790–793. doi: 10.1016/j.surg.2012.06.006

Waters, R., Alam, P., Pacelli, S., Chakravarti, A. R., Ahmed, R. P. H., and Paul, A. (2018). Stem cell-inspired secretome-rich injectable hydrogel to repair injured cardiac tissue. *Acta Biomater.* 69, 95–106. doi: 10.1016/j.actbio.2017.12.025

Whyte, W., Roche, E. T., Varela, C. E., Mendez, K., Islam, S., O'Neill, H., et al. (2018). Sustained release of targeted cardiac therapy with a replenishable implanted epicardial reservoir. *Nat. Biomed. Eng.* 2, 416–428. doi: 10.1038/s41551-018-0247-5

Wiklander, O. P. B., Brennan, M. Á, Lötvall, J., Breakefield, X. O., and El An-daloussi, S. (2019). Advances in therapeutic applications of extracellular vesicles. *Sci. Transl. Med.* 11:eaav8521. doi: 10.1126/scitranslmed.aav8521

Wiklander, O. P. B., Nordin, J. Z., O'Loughlin, A., Gustafsson, Y., Corso, G., Mäger, I., et al. (2015). Extracellular vesicle in vivo biodistribution is de-termined by cell source, route of administration and targeting. *J. Extracell Vesicles* 4:26316.

Wysoczynski, M., and Bolli, R. (2020). A realistic appraisal of the use of embryonic stem cell-based therapies for cardiac repair. *Eur. Heart J.* 41, 2397–2404. doi: 10.1093/eurheartj/ehz787

Xu, H., Wang, B., Ono, M., Kagita, A., Fujii, K., Sasakawa, N., et al. (2019). Targeted Disruption of HLA Genes via CRISPR-Cas9 Generates iPSCs with Enhanced Immune Compatibility. *Cell Stem Cell* 24, 566.e1–578.e1. doi: 10.1016/j.stem.2019.02.005

Xu, R., Zhang, F., Chai, R., Zhou, W., Hu, M., Liu, B., et al. (2019). Exosomes derived from pro-inflammatory bone marrow-derived mesenchymal stem cells reduce inflammation and myocardial injury via mediating macrophage polarization. *J. Cell. Mol. Med.* 23, 7617–7631. doi: 10.1111/jcmm.14635

Yarbrough, W. (2003). Large animal models of congestive heart failure: a critical step in translating basic observations into clinical applications. *J. Nucl. Cardiol.* 10, 77–86. doi: 10.1067/mnc.2003.16

Ye, J., Gaur, M., Zhang, Y., Sievers, R. E., Woods, B. J., Aurigui, J., et al. (2015). Treatment with hESC-derived myocardial precursors improves cardiac function after a myocardial infarction. *PLoS One* 10:e0131123. doi: 10.1371/journal.pone.0131123

Yee, K., Malliaras, K., Kanazawa, H., Tseliou, E., Cheng, K., Luthringer, D. J., et al. (2014). Allogeneic cardiospheres delivered via percutaneous transen-docardial injection increase viable myocardium, decrease scar size, and attenuate cardiac

dilatation in porcine ischemic cardiomyopathy. *PLoS One* 9:e113805. doi: 10.1371/journal.pone.0113805

Yin, J. Q., Zhu, J., and Ankrum, J. A. (2019). Manufacturing of primed mesenchymal stromal cells for therapy. *Nat. Biomed. Eng.* 3, 90–104. doi: 10.1038/s41551-018-0325-8

Yoshida, S., Miyagawa, S., Toyofuku, T., Fukushima, S., Kawamura, T., Kawamura, A., et al. (2020). Syngeneic mesenchymal stem cells reduce im-mune rejection after induced pluripotent stem cell-derived allogeneic cardiomyocyte transplantation. *Sci. Rep.* 10:4593. doi: 10.1038/s41598-020-58126-z

Yuan, A., Farber, E. L., Rapoport, A. L., Tejada, D., Deniskin, R., Akhmedov, N. B., et al. (2009). Transfer of microRNAs by embryonic stem cell mi-crovesicles. *PLoS One* 4:e4722. doi: 10.1371/journal.pone.0004722

Yuan, O., Lin, C., Wagner, J., Anderson, J. S., Archard, J. A., Deng, P., et al. (2019). Exosomes derived from human primed mesenchymal stem cells induce mitosis and potentiate growth factor secretion. *Stem Cells Dev.* 28, 398–409. doi: 10.1089/scd.2018.0200

Zhao, J., Li, X., Hu, J., Chen, F., Qiao, S., Sun, X., et al. (2019). Mesenchymal stromal cell-derived exosomes attenuate myocardial ischaemia-reperfusion injury through miR-182-regulated macrophage polarization. *Cardiovasc. Res.* 115, 1205–1216. doi: 10.1093/cvr/cvz040

Zhu, K., Wu, Q., Ni, C., Zhang, P., Zhong, Z., Wu, Y., et al. (2018). Lack of Re-muscularization following transplantation of human embryonic stem cell-derived cardiovascular progenitor cells in infarcted nonhuman primates. *Circ. Res.* 122, 958–969. doi: 10.1161/CIRCRESAHA.117.311578

**Conflict of Interest:** The author declares that the research was conducted in the absence of any commercial or financial relationships that could be construed as a potential conflict of interest.

frontiers in Bioengineering and Biotechnology

SYSTEMATIC REVIEW
published: 27 January 2021
doi: 10.3389/fbioe.2020.637538

# Cardiac Regeneration: New Insights Into the Frontier of Ischemic Heart Failure Therapy

*Andrew S. Riching*[1,2,3,4] *and Kunhua Song*[1,2,3,4]*

[1] Division of Cardiology, Department of Medicine, University of Colorado Anschutz Medical Campus, Aurora, CO, United States, [2] Gates Center for Regenerative Medicine and Stem Cell Biology, University of Colorado Anschutz Medical Campus, Aurora, CO, United States, [3] The Consortium for Fibrosis Research & Translation, University of Colorado Anschutz Medical Campus, Aurora, CO, United States, [4] Pharmacology Graduate Program, University of Colorado Anschutz Medical Campus, Aurora, CO, United States

Ischemic heart disease is the leading cause of morbidity and mortality in the world. While pharmacological and surgical interventions developed in the late twentieth century drastically improved patient outcomes, mortality rates over the last two decades have begun to plateau. Following ischemic injury, pathological remodeling leads to cardiomyocyte loss and fibrosis leading to impaired heart function. Cardiomyocyte turnover rate in the adult heart is limited, and no clinical therapies currently exist to regenerate cardiomyocytes lost following ischemic injury. In this review, we summarize the progress of therapeutic strategies including revascularization and cell-based interventions to regenerate the heart: transiently inducing cardiomyocyte proliferation and direct reprogramming of fibroblasts into cardiomyocytes. Moreover, we highlight recent mechanistic insights governing these strategies to promote heart regeneration and identify current challenges in translating these approaches to human patients.

**Keywords: ischemic heart disease, cardiac reprogramming, cardiomyocyte proliferation, cardiac regeneration, revascularization**

OPEN ACCESS

***Edited by:***
*Vahid Serpooshan, Emory University, United States*

***Reviewed by:***
*Ahmed Mahmoud, University of Wisconsin-Madison, United States*
*Vivek Pratap Singh, Baylor College of Medicine, United States*

***Correspondence:**
*Kunhua Song*
*kunhua.song@cuanschutz.edu*

***Specialty section:***
*This article was submitted to Tissue Engineering and Regenerative Medicine, a section of the journal Frontiers in Bioengineering and Biotechnology*

***Received:*** *03 December 2020*
***Accepted:*** *29 December 2020*
***Published:*** *27 January 2021*

***Citation:***
*Riching AS and Song K (2021) Cardiac Regeneration: New Insights Into the Frontier of Ischemic Heart Failure Therapy. Front. Bioeng. Biotechnol. 8:637538. doi: 10.3389/fbioe.2020.637538*

## INTRODUCTION

Cardiovascular diseases (CVD) are the leading cause of death worldwide, accounting for nearly one-third (∼18 million) of all global deaths annually (Roth et al., 2017). Approximately half of all CVD-related deaths are caused by ischemic heart disease (IHD), which results in loss of cardiomyocytes (CMs) within the myocardium leading to ventricular dysfunction and heart failure (HF). Numerous pharmacotherapies, implantable devices, and surgical techniques have been pioneered over the last five decades to salvage the myocardium and prevent pathological remodeling, dramatically improving patient outcomes and quality of life following the development of HF (Benjamin et al., 2017; Jones et al., 2019). However, HF mortality rates have begun to plateau (Roth et al., 2017), likely because existing interventions only slow disease progression but are incapable of reversing it. This stems from the fact that adult mammalian hearts exhibit minimal regenerative capacity due to the relative inability of CMs within the adult heart to reenter the cell cycle, and an apparent absence of a stem cell population that can repopulate all cell types within the heart following injury (Hashimoto et al., 2018; Sadek and Olson, 2020).

Shortly after birth, CMs in mammalian hearts undergo DNA synthesis and cell cycle exit. In rodents, this process occurs within the first few days after birth. Following DNA synthesis, ∼75% of rodent CMs undergo nuclear division, resulting in diploid, binucleate CMs. In contrast, the

majority of CMs in human hearts remain mononucleate but are tetraploid or polyploid (Laflamme and Murry, 2011). CM ploidy also increases during CM hypertrophy (Laflamme and Murry, 2011), though it remains unclear if increased ploidy is a cause or consequence of hypertrophic growth (Derks and Bergmann, 2020). Until the last two decades, it was generally well-accepted that CMs that exited the cell cycle are quiescent and unable to reenter the cell cycle and complete mitosis. However, more recent evidence based on incorporation of nuclear bomb-derived $^{14}C$ into CM DNA revealed that CM turnover rate in humans is approximately 1% at age 25, and declines to <0.45% past age 75 (Bergmann et al., 2009, 2015). These data indicate that approximately half of the CMs within the heart are generated postnatally (Bergmann et al., 2015). Similarly, it has been observed that CMs in adult mice replenish at a rate of ∼0.76%/year, a rate that continues to decline with age (Senyo et al., 2013). Moreover, this rate increases up to 4-fold following myocardial infarction (MI) (Senyo et al., 2013), though whether these new proliferating myocytes arise from existing CMs or cardiac progenitor cells (CPCs) remains somewhat unclear. To determine the origin of these newly proliferating CMs, Hsieh et al. crossed mice harboring a floxed LacZ-polyA sequence followed by GFP under control of the *Actb* promoter with a tamoxifen inducible *Myh6*-Cre mouse line. Adult animals were pulsed with tamoxifen for 14 days to specifically label CMs with GFP while non-myocytes were labeled with LacZ; due to labeling inefficiency, ∼82% of CMs expressed GFP while 18% expressed LacZ. During normal aging, these percentages remained relatively constant. However, following MI, the GFP positive percentage of CMs decreased to ∼68% whereas the LacZ positive population increased to ∼35%, suggesting that a CPC population gave rise to new CMs in response to injury (Hsieh et al., 2007). In contrast, using four independent interleaved reporter lines generating mutually exclusive fluorescent labeling of CMs and non-myocytes by Cre-*lox*P/Dre-*rox* recombinase activity, Li et al. observed that while new myocytes are derived from non-myocytes in embryonic mice, new myocytes in adult mice arise only from existing CMs following MI (Li et al., 2018). Regardless of the origin of new CMs post-MI, the progressive deterioration of heart function and continual fibrotic deposition clearly indicate that the rate at which CMs replenish in adult mammals is insufficient for cardiac regeneration. In this review, we evaluate the progress of three strategies to promote cardiac repair: (1) revascularization, (2) inducing CM proliferation, and 3) direct reprogramming of fibroblasts into CMs (**Figure 1**). We do not discuss stem cell-based strategies to improve heart function post-MI, as they have been extensively reviewed elsewhere in this special issue (Menasche, 2020).

## STRATEGIES FOR CARDIAC REPAIR

### Infarct Revascularization

A key development in the treatment of heart failure post-MI was the pioneering of surgical intervention to revascularize the infarcted myocardium via removal of coronary artery occlusions. Evidence that myocardial reperfusion could reduce infarct size dates back to the early 1970s (Ginks et al., 1972), but widespread clinical adaptation of reperfusion was not seen for several more decades. Three primary methods of infarct revascularization remain in use today; enzymatic fibrinolysis/thrombolysis, coronary artery bypass graft (CABG), and percutaneous coronary intervention (PCI; also referred to as percutaneous transluminal coronary angioplasty). Early thrombolysis relied on intravenous delivery of streptokinase (SK) isolated from certain strains of streptococci. The fibrinolytic properties of SK had been described as early as 1933 (Tillett and Garner, 1933), but nearly three decades passed before SK was administered in patients following ST elevation MI (STEMI) (Boucek and Murphy, 1960). Furthermore, it took additional 26 years to establish clinical benefit. The GISSI trial established that administration of SK reduced mortality by 18% compared to control. In a subgroup analysis, SK administration within 3 h of MI exhibited even greater reduction in mortality whereas later administration of SK (9–12 h post-MI) were not associated with reduced mortality [(Gissi), G.I.P.L.S.D.S.N.I.M, 1986]. The TIMI phase I trial demonstrated that recombinant tissue plasminogen activator (rtPA) was nearly twice as effective at recanalizing coronary arteries as SK (Chesebro et al., 1987). Combination therapy of SK and aspirin further reduced mortality compared to SK or aspirin individually [(Isis-2), S.I.S.O.I.S.C.G, 1988]. Thus, these seminal trials demonstrated that myocardial preservation via recanalization could reduce mortality and improve patient outcomes.

Surgical intervention to improve vessel patency also emerged during this period. The first successful coronary vessel graft was performed in 1960 by Robert Goetz in which a patient's right internal thoracic artery was grafted to their right coronary artery. This patient lived an additional 13 months and upon autopsy, the graft was still intact and patent (Goetz et al., 1961). In 1968, the first graft of the left internal thoracic artery to the left anterior descending artery was performed by Green et al. (1968), which set the precedence for the modern CABG procedure (Melly et al., 2018). While CABG remains one of the most performed coronary procedures today with established long-term benefits, it is highly invasive which presents significant risks and discomfort to patients (Melly et al., 2018). Within a decade of George Green's procedure, the first PCI procedures were performed by Andreas Gruntzig by advancing a catheter with an expandable balloon tip through the femoral artery and into an occluded coronary artery in five patients (Gruntzig, 1978). Following PCI, the placement of bare metal stents (BMS) or drug-eluting stents (DES) quickly became the standard of care to combat restenosis (Melly et al., 2018). Stent placement was deemed superior to angioplasty alone for target vessel revascularization and for reducing major adverse cardiac events (Zhu et al., 2001). However, stents themselves can lead to scar formation and restenosis (in the case of BMS) (Weintraub et al., 2013) or thrombus formation (in the case of DES) (Finn et al., 2007). Thus, dual antiplatelet therapy (DAPT), typically consisting of aspirin and P2Y12 receptor blockers (clopidogrel, ticagrelor, and prasugrel), is recommended after stent placement for at least 1 year (reviewed in Weintraub et al., 2013). The AMIHOT II study demonstrated that in conjunction with PCI, intracoronary delivery of supersaturated oxygen ($SSO_2$) further reduced infarct

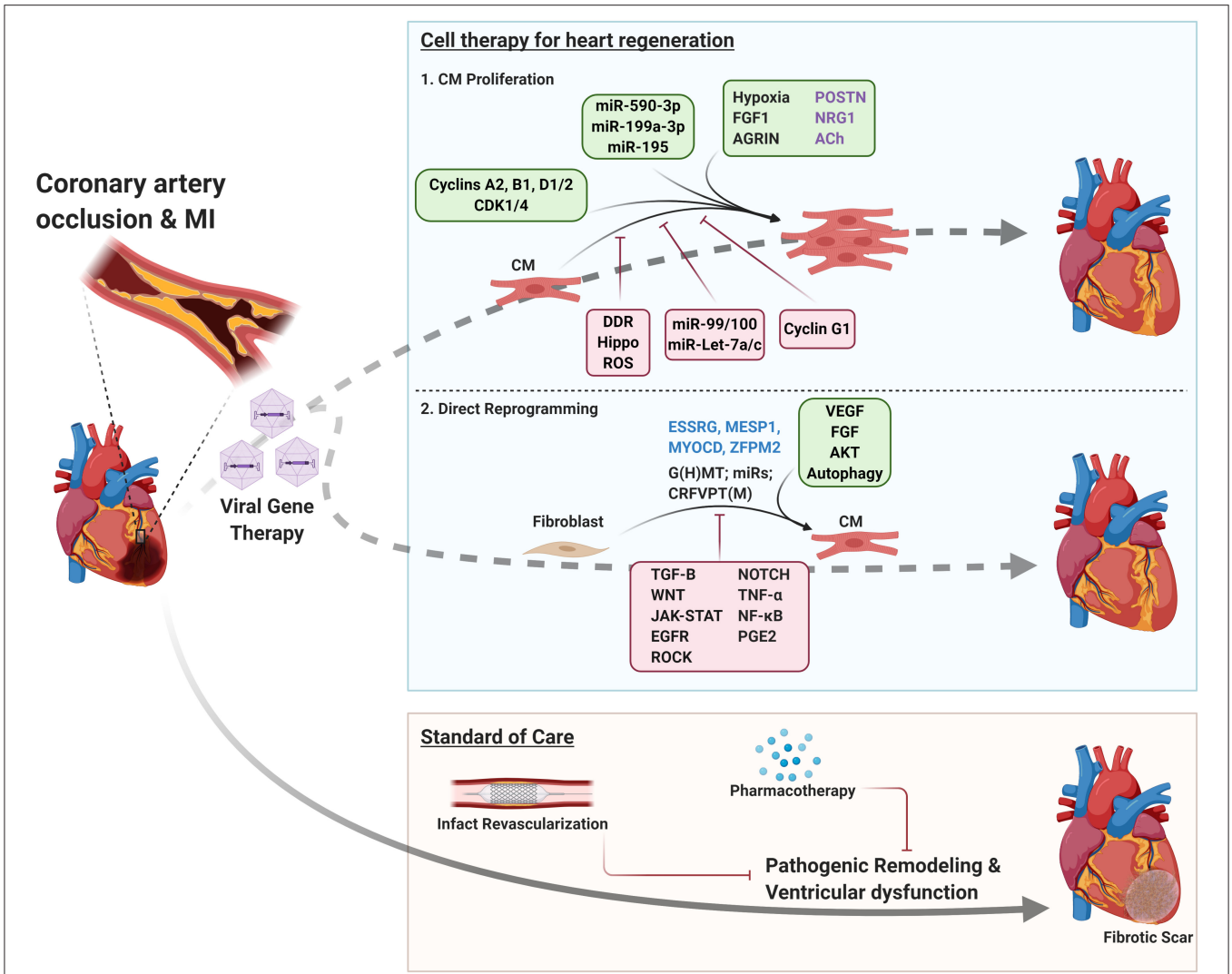


**FIGURE 1 |** Therapeutic strategies for ischemic heart disease. Tan box; Standard of care: Following MI, patients undergo infarct revascularization and begin pharmacotherapy to slow disease progression, but ultimately develop heart failure and progressive fibrosis. Blue box; Cell therapy for heart regeneration: schematic indicating factors that regulate CM proliferation and direct reprogramming of fibroblasts to CMs to regenerate the myocardium following MI. Green boxes indicate environmental, signaling, and genetic factors that promote CM proliferation/fibroblast reprogramming. Red boxes indicate factors that impair these processes. Factors that have conflicting reports regarding their roles in inducing CM proliferation are listed in purple text. Blue text indicates factors that enhance direct reprogramming in human fibroblasts. DDR, DNA damage response; G(H)MT, *G*ATA4, (*H*AND2), *M*EF2C, *T*BX5; CRFVPT(M), *C*HIR99021, *R*epSox, *F*orskolin, *V*alproic acid, *P*arnate, *T*TNPB, (Rolipra*m*).

size (Stone et al., 2009). A follow-up trial showed that delivery of $SSO_2$ via the left main coronary artery for 60 min after PCI in STEMI patients was associated with a favorable safety profile (David et al., 2019). Based on these trials, the FDA approved $SSO_2$ therapy in 2019 as an add-on therapy following PCI in STEMI patients.

Many clinical trials have focused on comparing different revascularization strategies to establish which technique should be used in specific patient populations. Based on a meta-analysis of data from 23 trials, PCI and stent placement was deemed superior to thrombolysis at reducing mortality, reinfarction, or stroke in STEMI patients (Keeley et al., 2003). However, not all care facilities are equipped to perform PCI, limiting patients' access. Thus, if patients cannot undergo PCI in a timely manner (within 2 h of acute MI), thrombolysis may be performed instead (O'gara et al., 2013). Following successful revascularization via thrombolysis, transfer to a PCI-capable facility and subsequent catheterization within 24 h of acute MI may further improve revascularization and patient outcome (Al Shammeri and Garcia, 2013; O'gara et al., 2013). Several clinical trials have also focused on comparing PCI to CABG. Though PCI is much less invasive, is associated with lower risks at the time of procedure, and was shown to be non-inferior to CABG in the short term (1–3 years), CABG is associated with superior long-term (>5 years) survival (reviewed in Melly et al., 2018; Ruel et al., 2018). Based on the outcomes from these trials, PCI followed by stent placement and

DAPT is the preferred method of revascularization in STEMI patients according to the 2013 ACCF/AHA guidelines. If patients cannot be transferred to a PCI-capable facility in a timely manner, thrombolysis may be performed. Transfer to a PCI-capable facility within 24 h of acute MI may be recommended following successful thrombolysis. CABG is recommended as an alternative to PCI in patients with complex lesions or coronary vasculature intolerant to catheterization (O'gara et al., 2013).

Myocardial reperfusion is estimated to salvage >50% of the myocardium that otherwise would be lost due to infarction (Yellon and Hausenloy, 2007; Frohlich et al., 2013). Furthermore, the advent of revascularization halved in-hospital mortality following acute MI (Braunwald, 2012). However, reperfusion itself causes myocardial damage. It has been postulated that an additional 50 to 80% of the myocardium could be spared if reperfusion injury could be prevented (Yellon and Hausenloy, 2007; Frohlich et al., 2013). Reperfusion injury is likely a significant contributing factor for in-hospital mortality and the development of HF following acute MI (Yellon and Hausenloy, 2007). Oxidative stress, increased intracellular calcium levels, rapid return to physiological pH, and leukocyte invasion have all been linked to causing reperfusion injury in animal models (reviewed in Yellon and Hausenloy, 2007), but targeting these processes has not led to any FDA-approved therapies to date. Thus, exploring new ways to reduce myocardial damage caused by reperfusion may further reduce patient morbidity and mortality.

Infarct revascularization and optimization of pharmacological therapies have radically transformed the treatment and management of post-MI HF. Moreover, these interventions have dramatically reduced mortality, from 5 year mortality rates of 70% in men and 57% in women prior to 1970 (Levy et al., 2002) to <45% between 2000 and 2010 (Benjamin et al., 2017; Jones et al., 2019). It has been argued that numerous pharmacological therapies including renin-angiotensin-aldosterone system inhibitors, dual angiotensin receptor/neprilysin inhibitors, and β-adrenergic receptor antagonists (β-blockers) are significantly underutilized in the HF patient population. Optimizing pharmacotherapy in this population could prevent tens of thousands of deaths per year in the United States alone (Anand, 2018). In contrast, some argue that the strength of β-blocker recommendations in particular should be reevaluated. Most β-blocker trials that demonstrated a reduction in overall mortality were performed prior to reperfusion interventions becoming standard clinical practice following MI. In the reperfusion era, β-blockers have no mortality benefit but are associated with a 30% reduction in recurrent MI and a 20% reduction in angina at the expense of 10% increased risk of worsening heart failure and a 30% increased risk of cardiogenic shock (Bangalore et al., 2014). Risk reduction of recurrent MI and angina appeared to be most significant in the short term (<30 days), thus short-term β-blocker therapy post-MI may maximize benefits while mitigating risks to patients. While the therapies outlined above have proven successful in improving patient survival and slowing HF progression, no current therapy or intervention is able to regenerate CMs lost during MI or reverse cardiac fibrosis.

## CM Proliferation

### Zebrafish Heart Regeneration

In contrast to mammals, amphibian and teleost CMs are able to reenter the cell cycle, resulting in CM mitosis and partial or full heart regeneration upon injury (reviewed in Kikuchi and Poss, 2012; Porrello and Olson, 2014; Gonzalez-Rosa et al., 2017). Heart regeneration in zebrafish is particularly well-established. Following ∼20% resection of the ventricle, a fibrin clot forms to seal the ventricular wound, which is ultimately replaced by proliferating CMs over the course of 60 days (Poss et al., 2002). Heart regeneration has also been observed following cryoinjury, wherein a copper filament is cooled with liquid nitrogen and placed against approximately 25% of the ventricle to induce myocardial damage. In this model, CMs die via necrosis and apoptosis rather being removed surgically, which represents a more physiologically relevant model of myocardial damage. Following cryoinjury, necrotic tissue was replaced by fibrotic scar tissue before being replaced by newly proliferated CMs, resulting in full heart regeneration after ∼130 days (Gonzalez-Rosa et al., 2011). A third model of myocardial damage, in which diptheria toxin A chain (DTA) is expressed specifically in CMs via tamoxifen inducible *Myl7*-Cre resulted in ablation of ∼60% of ventricular CMs. Remarkably, CM proliferation was induced within 1 week of genetic ablation, resulting in full replenishment of lost CMs and restored heart function (Wang et al., 2011).

Though immunofluorescent staining indicated CMs undergo DNA synthesis and mitosis in these models, whether newly generated CMs arose from existing CMs or differentiated from CPCs remained unclear. Using a tamoxifen inducible GFP reporter under the control of the Cmlc2a (*Myl7*) promoter, Jopling et al. permanently labeled CMs 48 h post-fertilization. Following ventricular resection, regenerated tissue was uniformly GFP positive, indicating new CMs were derived from existing CMs (Jopling et al., 2010). More GFP/ bromodeoxyuridine (BrdU) double positive CMs were detected in injured animals than uninjured controls, which was accompanied by upregulation of the cell cycle progression regulator polo like kinase 1 (Plk1). Moreover, proliferating CMs displayed disassembled sarcomeres and reduced cell-cell contact but did not upregulate Hand2/Nkx2.5 expression indicating only limited CM de-differentiation occurred in response to injury (Jopling et al., 2010). Following ventricular resection, CMs upregulated expression of a *gata4:EGFP* reporter in the subepicardial ventricular layer prior to the injury site. Moreover, EGFP expression preceded induction of DNA synthesis and proliferation. Proliferating CMs initially uncoupled from the conduction system but reintegrated after apical regeneration (Kikuchi et al., 2010). Mechanistically, cell cycle reentry is influenced by cellular signaling (reviewed in Gonzalez-Rosa et al., 2017). For example, following injury, expression of the retinoic acid synthesizing enzyme Raldh2 was induced in the endocardium. Degradation of retinoic acid (RA) by inducible expression of Cyp26a1 or inducing expression of dominant negative Raldh2 reduced CM proliferation by >85%. However, administration of exogenous RA was insufficient to induce proliferation in CMs (Kikuchi et al., 2011). Notch1b and DeltaC were upregulated 1 day following ventricular

resection, and remained elevated through day 7 post-amputation, indicating activation of Notch precedes heart regeneration (Raya et al., 2003). Moreover, inhibition of Notch signaling blunted CM proliferation following ventricular resection (Zhao et al., 2014). Finally, Neuregulin 1 (Nrg1) expression was strongly induced following genetic ablation of CMs (Gemberling et al., 2015). Myocardial overexpression of Nrg1 strongly induced CM proliferation, even in the absence of injury, resulting in cardiomegaly and dramatic thickening of the ventricular wall. In contrast, inhibition of Erbb2, an Nrg1 co-receptor, blocked CM proliferation in response to injury (Gemberling et al., 2015). Further elucidation of the mechanisms that induce CM proliferation in zebrafish may lead to novel strategies to induce CM proliferation in humans post-MI.

## Neonatal Heart Regeneration

Despite limited regeneration in adults, remarkably, a brief window exists during which partial or complete regeneration occurs after injury in neonatal mammals. Neonatal mice exhibit full heart regeneration following resection of 15% of the ventricle 1 day after birth (postnatal day 1; P1) (Porrello et al., 2011b). Troponin T positive CMs in resected hearts displayed significant increases in phosphorylated Histone H3 and Aurora B kinase, markers indicative of mitosis and cytokinesis, respectively. CM proliferation peaked 1 week after resection, and mitotic cells were detected not only at the site of injury, but throughout the heart. To determine the origin of proliferating CMs, Porrello et al. utilized a Rosa26-LacZ reporter under the control of tamoxifen inducible αMHC-Cre to generate LacZ positive CMs. Neonatal animals were dosed a single pulse of tamoxifen at birth to label CMs and apical resection was performed at P1. Regeneration following resection did not change the percentage of LacZ positive cells indicating new CMs were derived from existing CMs, not CPCs. In contrast to resection at P1, resection at P7 instead resulted in the development of a fibrotic scar (Porrello et al., 2011b), coinciding with previous observations that CM binucleation begins at P4 and is followed by cell cycle exit (Li et al., 1996). Additional evidence shows that a second proliferative burst of CMs occurs at P15 in mice, which corresponds to pre-adolescence in humans. During this period, both heart weight and CM number increase by ∼40% (Naqvi et al., 2014). Notably, this proliferative burst could be entirely suppressed by inhibiting thyroid hormone (T3) biosynthesis whereas T3 administration doubled the number of BrdU positive cells in isolated CMs, indicating increased DNA synthesis. P15 animals also exhibited partial heart regeneration post-MI; infarction size in P15 animals was smaller than in P21 animals and functional parameters were only modestly reduced in P15 animals but severely compromised in P21 animals (Naqvi et al., 2014). More recently, it has also been demonstrated that P2 pigs exhibit significant cardiac regeneration but P3 or P14 pigs instead form fibrotic scars following MI (Ye et al., 2018). As observed in murine neonates, CMs in P2 pigs undergo DNA synthesis and cytokinesis, evidenced by BrdU incorporation and Aurora B kinase staining. These studies indicate that like amphibians and teleosts, mammalian hearts also possess significant regenerative capacity, but this capacity is lost shortly after birth.

## Mechanisms Governing Mammalian CM Proliferation

Numerous extracellular factors have been shown to regulate CM proliferation during development and disease. In mice, increased reactive oxygen species (ROS) production and a switch from glycolysis to oxidative phosphorylation occurs shortly after birth, correlating to the interval during which CMs exit the cell cycle. Hypoxia, ROS scavenging, or inhibition of the DNA damage response all prolonged the interval during which postnatal mice hearts could regenerate following injury (Puente et al., 2014). Moreover, fate mapping of hypoxic CMs by fusing the oxygen-dependent degradation domain of HIF-1α to tamoxifen inducible Cre, resulting in fluorescent labeling of hypoxic CMs, indicated that these CMs are more proliferative and tend to be mononucleated compared to normoxic CMs, evidenced by increased labeling by cell cycle and DNA synthesis markers Ki67 and BrdU (Kimura et al., 2015). By RNA-seq, hypoxic CMs upregulated Cyclin-dependent kinase (CDK)/cyclin genes and downregulated negative cell cycle regulators including *Meis1*. Gradual exposure to severe hypoxia (7% $O_2$) reduced oxidative phosphorylation and DNA damage post-MI, which coincided with induction of CM proliferation compared to normoxia. Further, hypoxia reduced fibrotic area and improved ventricular function 1 week after infarction (Nakada et al., 2017). Additionally, extracellular matrix (ECM) components such as the fibroblast-derived protein periostin (POSTN) may regulate CM proliferation. Administration of truncated recombinant human POSTN increased BrdU incorporation in adult rat CMs 14-fold compared to non-stimulated CMs (Kuhn et al., 2007). Myocardial delivery of POSTN via Gelfoam patch increased ejection fraction (EF) and reduced scar size 12 weeks post-MI in rats whereas untreated rats showed no functional improvement and displayed extensive scarring. Additionally, the number of CMs undergoing mitosis increased 40-fold in POSTN treated animals. POSTN knockout (KO) impaired myocardial regeneration in neonatal mice, evidenced by increased fibrosis, reduced ventricular function, and reduced CM proliferation 3 weeks post-MI (Chen et al., 2017). In contrast, Lorts et al. did not observe increased DNA synthesis, mitosis, or cytokinesis in neonatal mouse or rat CMs following 2–3 day treatment with full length POSTN. Moreover, neither genetic deletion nor overexpression altered CM proliferation *in vivo* post-MI (Lorts et al., 2009). Thus, the contexts in which POSTN regulates cardiac regeneration and CM proliferation require further exploration. Finally, KO of the ECM protein agrin impaired cardiac regeneration in P1 mice following ventricular resection whereas intramyocardial injection of agrin induced CM cell cycle reentry in juvenile and adult hearts resulting in reduced scar area and significant improvement in ventricular function post-MI (Bassat et al., 2017).

As in zebrafish, diverse signaling pathways and growth factors have been shown to induce CM proliferation in both neonates and adult animals. Inhibition of p38 alongside fibroblast growth factor 1 (FGF1) stimulation improved ventricular function and reduced fibrosis in rats post-MI, which was accompanied by increased CM mitosis and angiogenesis (Engel et al., 2006). Inhibition of p38 alone also increased proliferation of both neonatal and adult rat CMs, and potentiated proliferation

induced by other ligands including NRG1, FGF1, and interleukin 1 β (IL-1β) (Engel et al., 2005). Furthermore, CM-specific genetic deletion of p38α nearly doubled the percentage of mitotic CMs in neonatal mice. NRG1 induced proliferation in neonatal rat CMs and improved cell viability and survival in both neonatal and adult rat CMs (Zhao et al., 1998). Additionally, NRG1β induced CM proliferation in mononucleated but not binucleated adult rat and mouse CMs *in vitro* and *in vivo* (Bersell et al., 2009). Genetic lineage tracing confirmed that proliferating CMs arose from existing CMs rather than progenitor cells. Further, NRG1 injection attenuated fibrosis, improved EF, and decreased compensatory hypertrophy post-MI (Bersell et al., 2009). Single or dual administration of NRG1 and FGF1 via microparticle injection improved heart function and reduced fibrosis post-MI in rats (Formiga et al., 2014). Either growth factor alone or in combination also increased vasculogenesis in infarcted hearts, but only NRG1 increased the number of Ki67 positive CMs. A follow up study demonstrated that microparticle delivery of NRG1 and FGF1 also improved ventricle function and infarct vasculogenesis post-MI in pigs (Garbayo et al., 2016). While FGF1 administration did not affect fibrosis, NRG1 administration reduced scar area. In contrast to these studies, Reuter et al. did not observe increased CM DNA synthesis post-infarction in mice administered NRG1, and even observed reduced CM DNA synthesis in the uninjured heart (Reuter et al., 2014). Nevertheless, short term NRG1 administration showed promising trends in improving left ventricular EF (LVEF) and reducing end systolic and diastolic volume in human patients in a phase II clinical trial (Gao et al., 2010). However, whether these favorable trends resulted from increased CM proliferation, vasculogenesis, or additional affects by NRG1 to prevent cardiac remodeling requires further investigation.

Cardiac regeneration requires sympathetic reinnervation following injury. Chemical sympathectomy via 6-Hydroxydopamine hydrobromide (6-OHDA) resulted in extensive fibrosis and a lack of cardiac regeneration in P2 neonatal mice (White et al., 2015). Similarly, transgenic overexpression of Semaphorin3aa resulted in hypo-innervation in zebrafish hearts and greatly impaired regeneration following ventricular resection (Mahmoud et al., 2015). Pharmacological inhibition of cholinergic nerve function by the non-selective muscarinic receptor antagonist atropine or the type 2 muscarinic (M2) receptor-specific antagonist methoctramine impaired heart regeneration and reduced CM proliferation in both zebrafish and neonatal mice. Moreover, removal of the left vagus nerve impaired cardiac regeneration in P1 mice post-MI, which could be rescued by administration of NRG1 and nerve growth factor (NGF) (Mahmoud et al., 2015). Intriguingly, vagal nerve stimulation was found to promote long term survival in rats post-MI (Li et al., 2004). However, disappointingly, the INOVATE-HF trial concluded that vagal nerve stimulation was not associated with increased survival or reduced HF events in humans (Gold et al., 2016).

Suppression of the conserved Hippo signaling pathway has also been demonstrated to induce CM proliferation and regulate heart development. Activation of this pathway triggers a kinase cascade leading to phosphorylation of Yes-associated Protein (YAP), resulting in nuclear exclusion and subsequent degradation. Inactivation of this kinase cascade allows active (non-phosphorylated) YAP to translocate to the nucleus and regulate transcription with its coactivator TEA Domain Transcription Factor 1 (TEAD1). CM-specific KO of *Lats1/2*, which directly phosphorylate YAP, induced CM DNA synthesis, cell cycle reentry, and cytokinesis in adult mouse hearts (Heallen et al., 2013). Similarly, CM-specific KO of *Salvadore* (*Salv*), a scaffold protein that mediates the phosphorylation and activation of LATS1/2 by upstream kinases MST1/2, also induced CM proliferation in adult mice. Both *Salv* and *Lats1/2* KO animals displayed reduced scar area and improved ventricular function following ventricular resection at P8, a time point typically past the regenerative window in neonatal mice. *Salv* KO also reduced fibrotic area and improved ventricular function following coronary artery ligation in adult mice (Heallen et al., 2013; Leach et al., 2017), and resulted in upregulation of an inducer of mitophagy, Parkin (Park2). *Park2* KO blocked regeneration in adult *Salv*-KO mice post-MI (Leach et al., 2017). Paired-like homeodomain transcription factor 2 (Pitx2) was also induced in the border zone of adult mice harboring CM-specific *Salv*-KO post-MI. Pitx2 was observed to co-regulate ROS-related genes along with YAP. Interestingly, double KO of *Pitx2* and *Salv* in adult mice prevented cardiac regeneration post-MI, but regeneration could be restored by treatment with the antioxidant N-acetyl cysteine (Tao et al., 2016). *Salv* KO driven by *Nkx2-5*-Cre resulted in cardiomegaly in neonatal mice and increased phosphorylation of Histone H3 during development (Heallen et al., 2011). In support of these studies, *Yap1* KO (Von Gise et al., 2012) or dual KO of *Yap1* and *Taz* (Xin et al., 2013) resulted in embryonic lethality due to severe ventricular hypoplasia. *Yap1* KO alongside *Taz* haploinsufficiency resulted in viable embryos, but surviving animals exhibited markedly reduced CM proliferation and developed severe lethal cardiomyopathy within the first 2 weeks of life (Xin et al., 2013). Transgenic overexpression of constitutively active (phospho-null) YAP S112A induced CM proliferation post-MI in P7 and P49 mice resulting in reduced fibrosis and improved ventricular function (Xin et al., 2013). Similarly, overexpression of S127A YAP induced CM proliferation in embryonic mice and in isolated neonatal CMs, coinciding with induction of cell cycle genes *Ccna2*, *Ccnb1*, and *Cdc2* (Von Gise et al., 2012). Mice overexpressing constitutively active YAP developed lethal cardiomegaly due to CM hyperplasia. These pro-proliferative effects were mediated via the interaction between YAP and TEAD1. Embryonic mice expressing YAP S79A, a mutation that abolished the interaction between YAP and TEAD1, exhibited marked hypoplasia, comparable to *Yap1* KO embryos (Von Gise et al., 2012).

Forced expression of cyclins and CDK proteins have shown promise in inducing CM cell cycle reentry. Embryonic mice specifically overexpressing Cyclin A2 in CMs led to cardiomyocyte hyperplasia and cardiomegaly (Chaudhry et al., 2004). CMs retained proliferative potential after birth, demonstrated by significantly elevated proliferating cell nuclear

antigen (PCNA) and phosphorylated Histone H3 signal compared to control animals at P7 and P14, which corresponded to a greater population of mononucleated CMs (Chaudhry et al., 2004). Moreover, Cyclin A2 adenoviral overexpression improved LVEF in adult pigs post-MI, which was accompanied by increased percentages of CMs positive for phosphorylated Histone H3 and Ki-67 (Shapiro et al., 2014). Further, Cyclin A2 overexpression reduced the collagen/muscle density ratio, indicating reduced fibrosis vs. Adeno-Null control. Transgenic overexpression of Cyclin D2, but not Cyclin D1 or D3 resulted in DNA synthesis following cardiac injury in mice, which correlated to reduced infarct size and increased CM numbers detected within the infarct 5 months post-MI (Pasumarthi et al., 2005). The newly regenerated myocardium electrically coupled with the surrounding heart tissue, and cardiac function in Cyclin D2 transgenic animals was indistinguishable from sham-operated mice 6 months post-MI whereas heart function in control animals continued to decline (Hassink et al., 2008). Overexpression of the combination of CDK1, CDK4, Cyclin B1, and Cyclin D1 resulted in cell division in up to 20% of adult CMs expressing all four proteins (Mohamed et al., 2018). Moreover, adenoviral intramyocardial delivery of these cell cycle regulators before or 1 week after coronary artery ligation reduced scar size and resulted in near complete restoration of heart function 12 weeks post-MI whereas animals injected with control virus displayed extensive fibrotic scarring and poor heart function. Additionally, CDK1 and Cyclin B1 overexpression could be replaced by pharmacologic inhibition of Wee1 and transforming growth factor (TGF)-β (Mohamed et al., 2018). Silencing of cell cycle proteins in adult CMs is facilitated by Retinoblastoma (Rb) and Retinoblastoma-like protein 2 (p130). CM-specific KO of *Rb1* in p130 deficient mice impaired recruitment of heterochromatin protein 1 (HP1)-γ, resulting in de-repression of cell cycle genes including *Cyce1*, *E2f1*, *Cycb1*, *cdc2*, *cdc25c*, *Plk1*, and *Aurkb*, which coincided with increased cytokinesis in isolated adult CMs (Sdek et al., 2011). In contrast, overexpression of Cyclin G1 induced DNA synthesis and nuclear division, but inhibited cytokinesis in neonatal rat CMs, thereby inducing polyploidy but not proliferation (Liu et al., 2010). Acute pressure overload by transverse aortic constriction (TAC) induces CM hypertrophy and increases polynucleation of CMs. However, *Ccng1* KO mice did not exhibit increased numbers of polynucleated CMs after TAC (Liu et al., 2010). Thus, overexpression of Cyclins A2, B1, and D2, and CDK1 and 4 promote CM cell cycle reentry while expression of Cyclin G1 instead seems to play a role in binucleation.

Recently, several groups have established the involvement of microRNAs (miRs) in regulating cell cycle and proliferation in CMs. Eulalio et al. utilized high content microscopy to identify 204 miRs that induced proliferation in neonatal rat CMs, evidenced by triple staining with Ki67, EdU, and α-actinin (Eulalio et al., 2012). Two of these candidate miRs (miR-590-3p and miR-199a-3p) also induced proliferation in adult rat CMs. Transcriptome profiling by RNA-seq revealed these miRs upregulated expression of genes related to cell cycle, cell growth and proliferation, and DNA replication, recombination, and repair. Additionally, *in vivo* transfection or adeno-associated virus (AAV)9-mediated intramyocardial delivery of these miRs increased ventricular wall thickness and resulted in gross enlargement of neonatal rat hearts, coinciding with marked increases in EdU incorporation and H3 phosphorylation in CMs. AAV9 miR injection also preserved ventricular function and reduced scar size following coronary artery ligation, which was accompanied by increased numbers of EdU positive CMs (Eulalio et al., 2012). A follow up study demonstrated that AAV6-miR-199a-1 intramyocardial delivery also improved ventricular function and reduced infarct size and fibrosis after 1 month in a porcine ischemia/reperfusion injury model (Gabisonia et al., 2019). Functional improvement correlated to increased detection of BrdU, Ki67, and phosphorylated H3 in CMs. In contrast, several miRs have also been demonstrated to suppress CM proliferation. CM-specific transgenic overexpression of the miR-15 family member miR-195 resulted in congenital heart defects including ventricular septal defects and right ventricle hypoplasia in neonatal mice (Porrello et al., 2011a). Gross heart size was reduced, and animals that did not die during development developed lethal cardiomyopathy by 5 to 6 months of age. Hearts at P1 had fewer mitotic CMs but increased numbers of binucleated/multinucleated CMs. The authors established that miR-195 directly targets *Chek1*, resulting in failure of CMs to progress through the G2 checkpoint and undergo mitosis. Administration of locked nucleic acid (LNA)-modified anti-miRs targeting both miR-15b and miR-16 resulted in downregulation of all miR-15 family members and extended the proliferative window of CMs in postnatal mice through P12 (Porrello et al., 2011a). CM-specific transgenic overexpression of miR-195 also blunted cardiac regeneration in P1 neonatal mice following coronary artery ligation (Porrello et al., 2013). In contrast, antagonizing miR-195 by administering LNA-modified anti-miRs prior to MI resulted in partial restoration of cardiac function following ischemia/reperfusion injury in P21 mice. Aguirre et al. observed downregulation of ∼60 miRs following ventricular resection in zebrafish, including the miR-99/100 and let-7a/c families, which are well-conserved across species (Aguirre et al., 2014). MiR-99/100 mimic resulted in defective heart regeneration whereas antagomiR-99/100 induced strong proliferation and enlargement of the heart in uninjured zebrafish. Notably, these miRs are not downregulated upon injury in mammals. Lentiviral silencing of miR-99/100 and/or miR-Let-7a/c in adult mice induced CM dedifferentiation, evidenced by sarcomere disassembly and upregulation of GATA4, which was accompanied by H3 phosphorylation. These effects were all enhanced by hypoxia. Antagonizing miR-99/100 and miR-Let-7a/c resulted in improved ventricular function, reduced scar size, and increased CM proliferation in adult mice following coronary artery ligation (Aguirre et al., 2014).

While specific mechanisms and contexts during which these diverse factors regulate CM proliferation in response to injury remain elusive, collectively, these

studies illustrate that inducing CM proliferation represents a promising strategy to regenerate the myocardium following MI.

## Fibroblast Reprogramming

While CMs occupy an estimated 70% of the ventricular volume (Tang et al., 2009) they account for only 25–35% of the total number of cells residing in the heart (Nag, 1980; Bergmann et al., 2015). The non-myocyte fraction is comprised primarily of endothelial cells, immune cells, and cardiac fibroblasts (CFs), the latter of which comprise ∼15% of the non-myocyte cell population and ∼11% of the total cells residing in the heart (Pinto et al., 2016). Upon ischemic injury, CFs are activated by biochemical and mechanical cues triggering migration and expansion into the infarct and border zone. Activated CFs secrete extracellular matrix (ECM) proteins to produce a fibrotic scar, which is integral to prevent myocardial rupture following loss of CMs due to ischemia (reviewed in Davis and Molkentin, 2014; Travers et al., 2016; Tallquist and Molkentin, 2017; Humeres and Frangogiannis, 2019). However, persistent CF activation leads to progressive fibrosis, which in turn worsens heart function post-MI. Thus, CFs serve as an ideal pool of cells to reprogram to repopulate the infarct with CMs and mitigate the chronic deposition of ECM.

The first evidence of fibroblast reprogramming was observed in 1987 wherein transfection of a single cDNA containing the coding region of the *MyoD1* gene was found to convert multiple fibroblast cell lines into skeletal muscle myoblasts (Davis et al., 1987). MyoD was later found to induce skeletal muscle differentiation not only in dermal fibroblasts, but also chondroblasts, smooth muscle, and retinal pigmented epithelial cells with varying degrees of efficiency. While retinal pigmented epithelial cells demonstrated lower differentiation efficiency than cells from mesodermal lineages, they still displayed prominent striation, multinucleation, and growth arrest, all key features of skeletal muscle morphogenesis (Choi et al., 1990). Thus, MyoD was established as a "master regulator" of skeletal muscle differentiation.

Unfortunately, to date, no parallel "master regulator" of cardiac muscle differentiation has been identified. However, the landmark discovery that iPSCs can be generated from fibroblasts via transcription factor (TF) overexpression (Takahashi and Yamanaka, 2006; Takahashi et al., 2007) generated interest in identifying combinations of TFs that cooperatively reprogram fibroblasts into terminally differentiated cells including neurons (Vierbuchen et al., 2010), hepatocytes (Huang et al., 2011), and CMs (Ieda et al., 2010). Ieda et al. identified TFs enriched in CMs compared to CFs by microarray and selected 14 which resulted in embryonic lethality due to cardiac defects when mutated for further analysis. Serial removal of individual TFs identified a cardiomyogenic core consisting of GATA4, MEF2C, and TBX5 (GMT) which induced ∼4.8% of neonatal CFs to express the cardiac isoform of Troponin T (cTnT). Moreover, a small population of these $cTnT^+$ cells exhibited spontaneous calcium transients and visible beating after 4 to 5 weeks in culture (Ieda et al., 2010). GMT transduction generated similar results upon delivery to dermal (tail tip) fibroblasts (TTFs), though the frequency of calcium oscillations was reduced. Subsequent studies confirmed that GMT, though inefficient, is sufficient to reprogram a subpopulation of mouse embryonic fibroblasts (MEFs), neonatal mouse CFs and TTFs, and adult mouse or rat CFs and TTFs both *in vitro* and *in vivo* (Chen et al., 2012; Mathison et al., 2012; Qian et al., 2012; Ma et al., 2015). **Table 1** summarizes GMT-based reprogramming strategies.

### Optimizing the Combination of Reprogramming Factors

Although GMT expression is sufficient to induce expression of cardiac sarcomere proteins, the generation of functional induced CMs (iCMs) is inefficient. Thus, numerous studies focused on optimizing the combination of TFs to increase the yield of functional iCMs. The addition of HAND2 to GMT (GHMT) increased the percentage of cells expressing both cTnT and the αMHC-GFP reporter 3- to 5-fold compared to GMT (9.2% vs. 2.9% in adult TTFs, 6.8% vs. 1.4% in adult CFs) (Song et al., 2012). Additionally, ∼1% of total cells (∼5% of reprogrammed cells) formed well-organized sarcomeres following GHMT transduction (Nam et al., 2014). Intriguingly, the original 14 factor screen performed by Ieda et al. indicated removal of HAND2 enhances reprogramming efficiency (Ieda et al., 2010), thus the role of HAND2 in promoting cardiac reprogramming was initially controversial. However, follow up studies from several groups have conclusively demonstrated that the inclusion of HAND2 markedly improves reprogramming efficiency, at least in part through more efficient upregulation of cardiac TF, ion channel, and sarcomere genes and suppression of cell cycle genes. These genetic changes correlate to more organized sarcomere formation, increased calcium flux, and generation of increased numbers of beating cells (Umei et al., 2017; Zhang et al., 2019a,b; Wang et al., 2020b). GHMT-based reprogramming strategies are summarized in **Table 2**.

Overexpression of Myocardin (MYOCD) alongside MEF2C and TBX5 generated similar numbers of cTnT/αMHC-GFP double positive cells as GMT in both neonatal CFs and TTFs, but also upregulated mRNA expression of *Myh6, Myl2, Actc1, Nkx2-5,* and *Scn5a* whereas GMT only upregulated expression of *Myh6* and modestly upregulated *Actc1* expression (Protze et al., 2012). Addition of NKX2.5 to GHMT greatly improved the percentage of cells exhibiting calcium transients compared to GMT alone (1.6% vs. 0.03% in MEFs, 4.5% vs. 1% in adult CFs) (Addis et al., 2013). Expression of a MyoD transactivation domain—MEF2C ($MM_3$) fusion protein alongside GHT ($MM_3$-GHT) increased the generation of beating cells by 18-fold compared to GHMT in MEFs (3.2–3.5% vs. 0.2% based on the number of cells seeded) and generated detectable numbers of beating cells in neonatal TTFs. Furthermore, $MM_3$-GHT increased the number of cTnT positive cells compared to GHMT (20.9% vs. 12.6% in MEFs, 29.3% vs. 11.2% in TTFs) (Hirai et al., 2013). Addition of MYOCD, Serum response factor (SRF), Mesoderm Posterior BHLH Transcription Factor 1 (MESP1), and the SWItch/sucrose non fermentable (SWI/SNF) complex subunit BAF60C (encoded by *Smarcd3*) to GMT enhanced expression of the αMHC-GFP reporter as well as *Actc1, Tnnt2, Myl2, Myh6,* and *Myh7* mRNA

**TABLE 1 |** *In vitro* and *in vivo* efficiencies of GMT-based reprogramming strategies.

| Reprogramming strategy | | | Fibroblast origin | | | Efficiency | | | Study |
|---|---|---|---|---|---|---|---|---|---|
| **Core factors** | **Species** | **Additional factors** | **Embryonic** | **Dermal** | **Cardiac** | **Cardiac marker expression** | **Spontaneously beating cells** | **Reprogramming *in vivo*** | **Authors** |
| GMT | Mouse | None | | X | X | 4% cTnT/αMHC-GFP$^+$ (CFs); 2.5% cTnT/αMHC-GFP$^+$ (TTFs) | Rare | Rare detection of reprogrammed cells in hearts | Ieda et al., 2010 |
| | | Polycistronic delivery | | | X | 3–7% αMHC-GFP$^+$ | Not discussed | ∼1% GFP/α-actinin$^+$ following GMT+GFP injection into infarct | Inagawa et al., 2012 |
| | | +Thymosin β4 | | | X | N/A | N/A | GMT vs. DsRed<br>EF = 25% vs. 16%; Fibrosis reduced 75% | Qian et al., 2012 |
| | | None | | X | X | 35% GFP$^+$ Tnnt2-Cre/Rosa26 mTmG reporter TTFs | Not detected | Cardiac gene expression detected in reprogrammed cells | Chen et al., 2012 |
| | | +MyoCD, SRF, MESP1, and SMARCD3 | X | | | 2.4% αMHC-GFP$^+$ | Not detected | N/A | Christoforou et al., 2013 |
| | | +miR-133 | X | | X | 20% α-actinin$^+$, 12% cTnT$^+$ (MEFs); 3.5% cTnT$^+$ (TTFs) | ∼7-fold enhanced by miR-133 vs. GMT alone | N/A | Muraoka et al., 2014 |
| | | Polycistronic delivery | | X | X | 3–4% cTnT/αMHC-GFP$^+$ (neonatal CFs) | ∼10-fold enhanced by polycistronic delivery vs. previous studies | N/A | Wang et al., 2015a |
| | | +FGF2/FGF10/VEGF (FFV) | X | X | | 1% cTnT/αMHC-GFP$^+$ | ∼20-fold enhanced by FFV vs. GMT alone | N/A | Yamakawa et al., 2015 |
| | | Polycistronic delivery | | | X | N/A | N/A | Polycistronic GMT vs. DsRed<br>EF = ∼38% vs. 17%; FS = ∼18.4% vs. ∼7.5%; Fibrotic area = ∼20% vs. ∼40% | Ma et al., 2015 |
| | | Polycistronic delivery +shBmi1 | X | X | X | 22% cTnT/αMHC-GFP$^+$ (neonatal CFs) | 2-fold enhanced by shBmi1 | N/A | Zhou et al., 2016 |
| | | Polycistronic delivery +TGF-β/WNT inhibition | | | X | 16% cTnT/αMHC-GFP$^+$ (neonatal CFs) | ∼40% of cells seeded | GMT ± inhibitors vs. DsRed<br>EF = ∼35% vs. 20%; Fibrotic area = ∼15% vs. ∼39% | Mohamed et al., 2017 |
| | | Polycistronic delivery +shPbtb1 | | | X | 45% cTnT/αMHC-GFP$^+$ | Not discussed | N/A | Liu et al., 2017 |
| | | Polycistronic Sendai viral delivery | X | X | X | 10% cTnT$^+$ | ∼50% of MEFs seeded; ∼10% of total cells | Polycistronic GMT vs. GFP<br>EF = ∼35% vs. ∼25%; FS = ∼15% vs. ∼10%; Reduced fibrosis | Miyamoto et al., 2018 |
| | | Polycistronic delivery +shBcor | X | | X | ∼9–16% cTnT/αMHC-GFP$^+$ (CFs); ∼1.2% cTnT/αMHC-GFP$^+$ (MEFs) | Not discussed | N/A | Zhou et al., 2018 |

*(Continued)*

**TABLE 1** | Continued

| Reprogramming strategy | | | Fibroblast origin | | | Efficiency | | | Study |
|---|---|---|---|---|---|---|---|---|---|
| **Core factors** | **Species** | **Additional factors** | **Embryonic** | **Dermal** | **Cardiac** | **Cardiac marker expression** | **Spontaneously beating cells** | **Reprogramming *in vivo*** | **Authors** |
| | | Alternate MEF2C isoforms | X | X | X | 5% cTnT/αMHC-GFP$^+$ (MEFs); 4% cTnT/αMHC-GFP$^+$ (CFs); 1.25% cTnT/αMHC-GFP$^+$ (TTFs) | Not discussed | N/A | Wang et al., 2020b |
| | | Polycistronic delivery +shBeclin1 | X | X | X | 6% cTnT$^+$ (MEFs); 20% cTnT$^+$ (CFs); 5% cTnT+ (TTFs) | ∼3-fold enhanced by shBeclin1 | Polycistronic GMT ± Beclin$^{\pm/-}$ vs. DsRed<br>EF = ∼40% vs. ∼20%; FS = ∼29% vs. ∼10%; Fibrotic area = 25% vs. 45% | Wang et al., 2020c |
| | Rat | +VEGF | | X | X | 7% cTnT$^+$ | Not discussed | GMT ± VEGF vs. GFP<br>EF = 63% vs. 48%; Fibrotic area = 12% vs. 24% | Mathison et al., 2012 |
| | | Polycistronic delivery +VEGF | | | X | 7.5% cTnT$^+$ | Not discussed | GMT ± VEGF vs. GFP;<br>EF = 48% vs. 39%; Fibrosis = 21% vs. 31% | Mathison et al., 2014 |
| | | None | | | X | 5% cTnT$^+$ | Not discussed | N/A | Singh et al., 2016 |
| | | +VEGF and adenoviral GMT delivery | | | X | 6.9% cTnT$^+$ | Not discussed | Ad-GMT±VEGF vs. Ad-Null;<br>EF (Change from baseline); +21% vs. −0.4% | Mathison et al., 2017 |
| | | +HDAC/WNT inhibition and Retinoic Acid | | | X | 23% cTnT$^+$ | Not detected | N/A | Singh et al., 2020 |

**TABLE 2 |** *In vitro* and *in vivo* efficiencies of GHMT-based reprogramming strategies.

| Reprogramming strategy | | | Fibroblast origin | | | Efficiency | | | Study |
|---|---|---|---|---|---|---|---|---|---|
| **Core factors** | **Species** | **Additional factors** | **Embryonic** | **Dermal** | **Cardiac** | **Cardiac marker expression** | **Spontaneously beating cells** | **Reprogramming *in vivo*** | **Authors** |
| GHMT | Mouse | None | | X | X | 6.8% cTnT/αMHC-GFP$^+$ (CFs), 9.2% cTnT/αMHC-GFP$^+$ (TTFs) | 0.2% of iCMs with sarcomeres that also express cTnT, αMHC-GFP | GHMT vs. GFP | Song et al., 2012 |
| | | | | | | | | EF = 57% vs. 29% at 12 weeks; Fibrotic area reduced 50% | |
| | | +NKX2.5 | X | | X | cTnT-GCaMP activity induced in 1.6% of MEFs and 4% of CFs | Rare | N/A | Addis et al., 2013 |
| | | Fusion of MyoD transactivation domain to MEF2C | X | X | | 20.9% cTnT$^+$ (MEFs, Day 7), 29.3% cTnT$^+$ (TTFs, Day 20) | 3.2–3.5% of seeded MEFs; 0.025% of seeded TTFs | N/A | Hirai et al., 2013 |
| | | +NKX2.5 and TGF-β inhibition | X | | X | cTnT-GCaMP activity induced in 17% of MEFs and 9.3% of CFs | ∼5-fold enhanced by TGF-β inhibition | N/A | Ifkovits et al., 2014 |
| | | None | X | X | X | 1.2% sarcomere positive | 0.16% of reprogrammed MEFs | N/A | Nam et al., 2014 |
| | | Fusion of MyoD transactivation domain to MEF2C + Ezh2 or G9a/GLP inhibition | X | | | 17% cTnT/Hcn4$^+$ | 23% (Ezh2 inhibition) or 20% (G9a/GLP inhibition) of reprogrammed MEFs | N/A | Hirai and Kikyo, 2014 |
| | | +miR-1, miR-133, and TGF-β inhibition | X | X | X | 64% α-actinin$^+$, 67% cTnT$^+$ (MEFs); 18% α-actinin$^+$, 18% cTnT$^+$ (CFs); 30% α-actinin$^+$, 35% cTnT$^+$ (TTFs) | 60% of total cells at Day 11 (MEFs); 2.5% of total cells (CFs); 4% of total (TTFs) | N/A | Zhao et al., 2015 |
| | | +AKT1 | X | X | X | 25% cTnT/αMHC-GFP$^+$ (MEFs); 5% cTnT/αMHC-GFP$^+$ (CFs); 5% cTnT/αMHC-GFP$^+$ (TTFs) | 50% of seeded MEFs at Day 21; 0.8% of seeded CFs; 0.5% of seeded TTFs | N/A | Zhou et al., 2015 |
| | | +AKT1 and γ-secretase inhibition | X | X | | 70% α-actinin+, 65% cTnT+ (MEFs) | 40% of seeded MEFs at Day 18 | N/A | Abad et al., 2017 |
| | | +AKT1 and ZNF281 | | X | | 28% cTnT/αMHC-GFP$^+$ | 10% of seeded TTFs after 4 weeks | N/A | Zhou et al., 2017 |
| | | None | X | | | 13-16% cTnT$^+$ | ∼4-fold enhanced vs. GMT | N/A | Umei et al., 2017 |
| | | Sendai viral delivery | | X | | 22% cTnT$^+$ | ∼20-fold enhanced by sendai viral delivery vs. retroviral | N/A | Miyamoto et al., 2018 |
| | | +AKT1 and EGFR/JAK inhibition | X | X | X | 32% cTnT/αMHC-GFP$^+$ (MEFs); 20% cTnT/αMHC-GFP$^+$ (CFs); 20% cTnT/αMHC-GFP$^+$ (TTFs) | ∼2-fold enhanced by EGFR/JAK inhibition | N/A | Hashimoto et al., 2019 |
| | | Polycistronic delivery +TGF-β inhibition | X | | | 80% α-actinin$^+$ | ∼8-fold enhanced vs. GMT | N/A | Zhang et al., 2019a |
| | | Polycistronic delivery +TGF-β inhibition | X | | | 25% Titin-eGFP/α-actinin$^+$ | ∼6-fold enhanced vs. GMT | N/A | Zhang et al., 2019b |
| | | Alternatively spliced MEF2C isoforms | X | X | X | 5% cTnT/αMHC-GFP$^+$ (MEFs), 1.8% cTnT/αMHC-GFP$^+$ (CFs), 1% cTnT/αMHC-GFP$^+$ (TTFs) | Not discussed | N/A | Wang et al., 2020b |
| | | +miR-1, miR-133, and SMAD7 | X | | | 80% α-actinin$^+$ | ∼40% of seeded MEFs at Day 13 | N/A | Riching et al., 2021 |

expression in MEFs compared to GMT alone (Christoforou et al., 2013).

Alternative reprogramming strategies have also been shown to generate induced CPCs (iCPCs), which are then capable of undergoing differentiation toward the CM lineage. Generation of multipotent iCPCs may offer additional benefits for heart regeneration as they have the potential to differentiate into endothelial and smooth muscle cells, thereby promoting vasculogenesis. Further, while iCMs rapidly exit the cell cycle upon reprogramming, iCPCs remain proliferative until they differentiate into CMs (reviewed in Klose et al., 2019; Lopez-Muneta et al., 2020). Overexpression of OCT4, KLF4, SOX2, and C-MYC in MEFs, which is well-known to generate iPSCs (Takahashi and Yamanaka, 2006; Takahashi et al., 2007), was observed to generate small clusters of contracting colonies by day 18 in the absence of leukemia inhibitor factor (LIF) (Efe et al., 2011). Notably, the emergence of contracting colonies was too early for cells to reprogram to iPSCs and then differentiate to CMs. Instead, Efe et al. observed that pluripotency markers including *Nanog* were never upregulated, but induction of cardiac progenitor genes *Mesp1, Isl1,* and *Gata4* occurred after 1 week suggesting reprogramming bypassed pluripotency and generated iCPCs. Inhibition of the JAK-STAT pathway and BMP4 stimulation starkly enhanced the generation of cardiac progenitors, resulting in ∼80-fold more contracting colonies than TF overexpression alone (Efe et al., 2011). Moreover, the authors found that removal of C-MYC did not negatively influence reprogramming toward cardiac lineages. Strikingly, KLF4 and SOX2 overexpression could be replaced by the addition of small molecules *S*B431542 (TGF-β inhibitor), *C*HIR99021 (GSK3β inhibitor/WNT activator), *p*arnate (monoamine oxidase inhibitor), and *f*orskolin (adenylyl cyclase agonist) (SCPF), resulting in the generation of cardiac progenitors from overexpression of OCT4 alone alongside SCPF treatment (Wang et al., 2014). Treating MEFs with the combination of CHIR99021, 616452 (TGF-β inhibitor), parnate, forskolin, valproic acid (VPA, class I histone deacetylase inhibitor), TTNPB (synthetic RA analog), and DZNep (epigenetic modulator) resulted in the generation of iPSCs in the absence of TF overexpression (Hou et al., 2013). However, omitting DZNep and bFGF and treating MEFs with only *C*HIR99021, *R*epSox (TGF-β inhibitor), *f*orskolin, *V*PA, *p*arnate, and *T*TNPB (CRFVPT) instead resulted in the generation of beating colonies that bypassed pluripotency and expressed cardiac precursor markers including *Sca-1, Abcg2*, *Wt1*, *Flk1*, and *Mesp1* (Fu et al., 2015). Treatment of neonatal TTFs with CRFVPT also generated beating colonies, but to a lesser extent than MEFs. Inclusion of rolipram (PDE4 inhibitor) increased the yield of beating colonies in TTFs by >2-fold compared to CRFVPT alone (Fu et al., 2015). Strategies to promote iCM, iCPC, and iPSC reprogramming are illustrated in **Figure 2**.

## Reprogramming via miRs

As an alternative to transcription factor overexpression, several groups explored microRNA (miR) delivery to drive cardiac reprogramming. The combination of miR-1, miR-133, miR-208, and miR-499 induced expression of the αMHC-CFP reporter in 1.5 to 7.7% of neonatal CFs (Jayawardena et al., 2012). Delivery of this miR combination induced endogenous expression of GHMT in neonatal CFs indicating miRs may be an alternative delivery source to upregulate expression of reprogramming factors (Dal-Pra et al., 2017). The addition of miRs to TF cocktails have also led to increased reprogramming efficiency. The addition of miR-133 to GMT generated 6-fold more calcium transients and 7-fold more spontaneously contracting cells than GMT alone, and accelerated the reprogramming process by 2 weeks in MEFs. Moreover, GMT + miR-133 increased the percentage of cells expressing sarcomere proteins α-actinin and cTnT by 4- to 7-fold vs. GMT in both MEFs and adult CFs (Muraoka et al., 2014). Similarly, addition of miR-1 and miR-133 to GHMT dramatically increased the percentage of spontaneously contracting cells vs. GHMT alone (∼12% vs. <0.5%) (Zhao et al., 2015). This increase in reprogramming efficiency induced by miR-1 and miR-133 was accompanied by significant upregulation of cardiac gene signatures and a concomitant repression of pro-fibrotic genes. Non-GMT/GHMT based reprogramming strategies are summarized in **Table 3**.

## Ensuring Expression and Optimal Stoichiometry of Reprogramming Factors

The increasing number of factors required to promote fibroblast reprogramming generated concern that simultaneous transduction of three or more viral vectors into the same cell was inefficient and could represent a technical barrier to achieving optimal reprogramming. Thus, polycistronic expression vectors containing GMT separated by "self-cleaving" 2A peptides were developed to ensure all three reprogramming factors were transduced into the same cell (Inagawa et al., 2012). Transduction of polycistronic GMT nearly doubled the percentage of adult rat CFs expressing cTnT compared to individual G/M/T delivery (7.5% vs. 4%) (Mathison et al., 2014). An inherent property of polycistronic expression systems is that the splicing order of genes affects protein expression levels. Thus, polycistronic vectors containing all possible splicing orders of GMT were developed to determine the optimal expression levels for each reprogramming factor. Combinations that resulted in relatively higher levels of MEF2C and lower levels of GATA4 and TBX5 (M-G-T, M-T-G) induced expression of cTnT and the αMHC-GFP reporter in ∼3–4% of reprogrammed neonatal CFs. In contrast, individual G/M/T overexpression resulted in expression of cTnT and the αMHC-GFP reporter in only ∼0.3% of cells, and splicing orders that resulted in low MEF2C expression produced even lower percentages of cTnT and αMHC-GFP positive cells than individual G/M/T overexpression (Wang et al., 2015a,b).

Given the role of HAND2 in increasing reprogramming efficiency, quad-cistronic vectors were also generated to determine optimal expression levels for HAND2 alongside GMT. Relatively higher levels of GMT and lower levels of HAND2 (M-G-T-H/M-G-H-T) significantly improved the percentage of α-actinin positive cells reprogrammed from MEFs compared to vectors with relatively higher levels of HAND2 (H-M-G-T) or compared to M-G-T alone. Further, M-G-T-H/M-G-H-T both increased the number of sarcomere positive cells by 5-fold

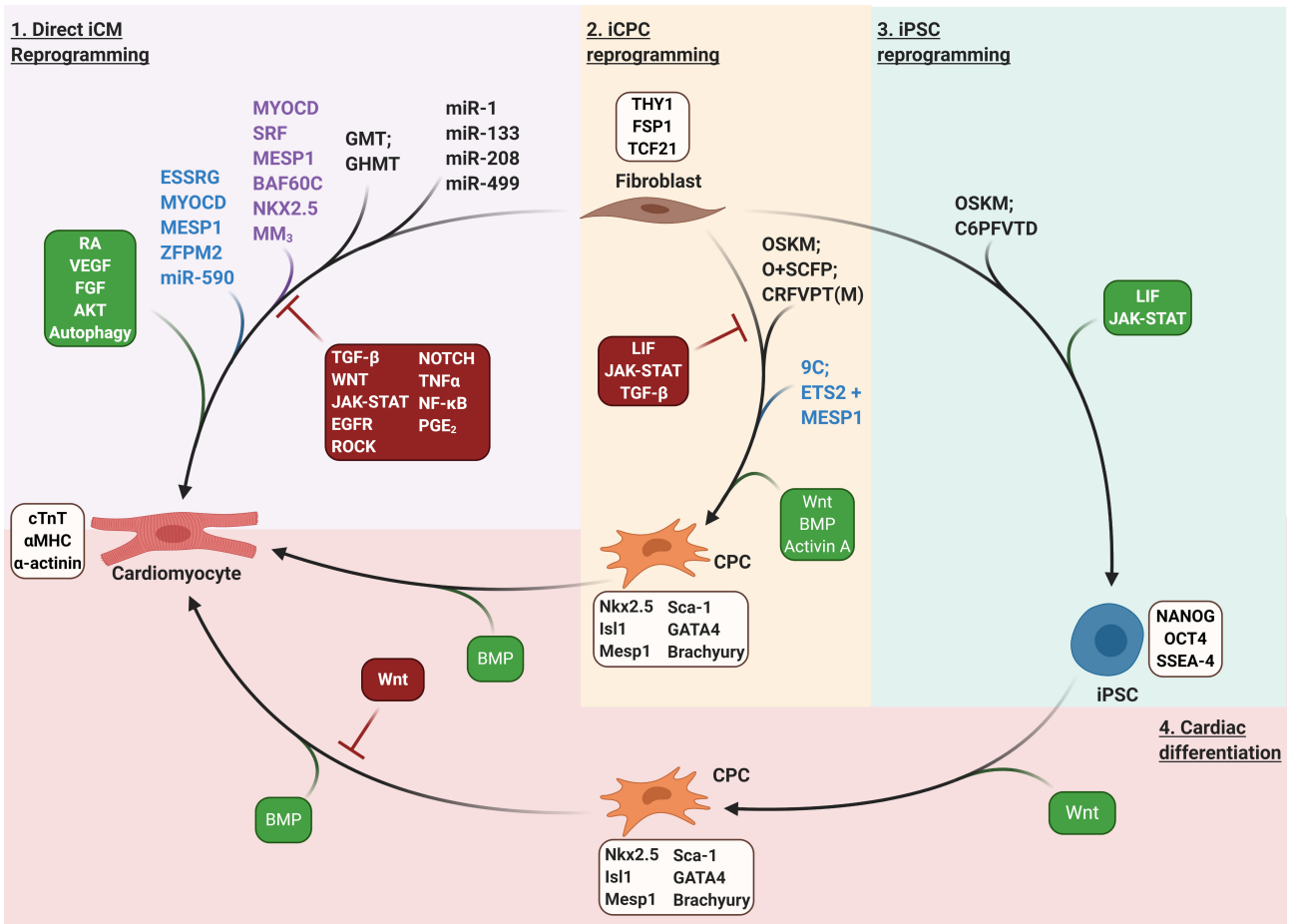


**FIGURE 2 |** Fibroblast reprogramming strategies. Purple shaded region: direct iCM reprogramming. GMT/GHMT, *GATA4*, *MEF2C*, *TBX5*/*GATA4*, *HAND2*, *MEF2C*, *TBX5*; $MM_3$, MYOD transactivation domain—MEF2C fusion protein. Tan shaded region: iCPC reprogramming; OSKM, *OCT4*, *SOX2*, *KLF4*, *C-MYC*; O+SCFP, *OCT4* + *SB431542*, *CHIR99021*, *Forskolin*, and *Parnate*; CRFVPT(M), *CHIR99021*, *RepSox*, *Forskolin*, *Valproic acid*, *Parnate*, *TTNPB*, and (Rolipram); 9C; CHIR99021, BIX01294, A-83-01, AS8351, SC1, OAC2, Y27632, SU16F, and JNJ10198409. Green shaded region: iPSC reprogramming. C6PFVTD; *CHIR99021*, *616452*, *Parnate*, *Forskolin*, *Valproic Acid*, *TTNPB*, and *DZnep*. Red shaded region: cardiac differentiation of pluripotent or multipotent stem cells to generate CMs. Lineage specific markers for each cell type are listed in light brown boxes. Purple text indicates factors that enhance reprogramming of rodent fibroblasts. Blue text indicates factors that enhance reprogramming of human fibroblasts. Signaling pathways that enhance or inhibit reprogramming are depicted in green or red boxes, respectively.

compared to M-G-T, but M-G-T-H resulted in a 6-fold increase in the number of beating cells vs. M-G-T whereas M-G-H-T only modestly increased the number of beating cells (Zhang et al., 2019b; Zhang and Nam, 2020). Sendai viral (SeV) delivery of polycistronic G-M-T robustly increased expression of GMT reprogramming factors compared to retroviral delivery in MEFs, which correlated to a 5-fold increase in the percentage of cells expressing cTnT and nearly a 100-fold increase in the generation of contracting cells after 6 weeks in culture (Miyamoto et al., 2018). Curiously, retroviral delivery of polycistronic M-G-T did not enhance reprogramming efficiency compared to individual G/M/T (∼2% cTnT positive cells vs. ∼3% in G/M/T), but did moderately enhance expression of cardiac genes *Actc1* and *Myocd* in MEFs. Thus, the enhanced reprogramming efficiency by polycistronic delivery observed in previous studies may be specific to postnatal and adult cardiac and dermal fibroblasts rather than embryonic fibroblasts.

Alternative splicing of the *Mef2c* gene gives rise to expression of multiple isoforms. Recent comparative analysis identified two primary isoforms used in most previous fibroblast reprogramming studies generated by alternative splicing of exon 3. Overexpression of polycistronic M-G-T including *Mef2c* containing exon 3 α2 resulted in nearly double the percentage of cells expressing the αMHC-GFP and cTnT compared polycistronic delivery including *Mef2c* containing exon 3 α1, though this increase in reprogramming efficiency was only observed in MEFs and not CFs or TTFs (Wang et al., 2020b). This observation may help resolve the discrepancies in reprogramming efficiencies demonstrated using the same TF cocktails in different laboratories.

## Signaling Pathways That Influence Reprogramming

Numerous signaling pathways also dramatically influence the efficiency of cardiac reprogramming (**Figure 3**). Inhibition of the

**TABLE 3 |** *In vitro* and *in vivo* efficiencies of non-GMT/GHMT-based reprogramming strategies.

| Reprogramming strategy | | | Fibroblast origin | | | Efficiency | | | Study |
|---|---|---|---|---|---|---|---|---|---|
| **Species** | **Core factors** | **Additional factors** | **Embryonic** | **Dermal** | **Cardiac** | **Cardiac marker expression** | **Spontaneously beating cells** | **Reprogramming *in vivo*** | **Authors** |
| Mouse | miRs | miR-1, miR-133, miR-208, miR-499 +JAK inhibition | | | X | 13.4–28% αMHC-GFP$^+$ | 1% of total cells | ∼1% cTnT/Fsp1-TdTomato double positive | Jayawardena et al., 2012 |
| | | miR-1, miR-133, miR-208, miR-499 | | | X | N/A | N/A | miR combination vs. miR negative control<br>FS = 30% VS. 20% at 12 weeks; Fibrotic area = 10% vs. 25% | Jayawardena et al., 2015 |
| | Non-GMT/GHMT Transcription factors | MYOCD, MEF2C, TBX5 | X | X | X | 2.5% cTnT/αMHC-TdTomato$^+$ | Rare | N/A | Protze et al., 2012 |
| | | OCT4, KLF4, SOX2, C-MYC + JAK inhibition and BMP4 stimulation | X | X | | 39% cTnT$^+$ (MEFs) | 120% of seeded cells, ∼37% of total cells (MEFs) | N/A | Efe et al., 2011 |
| | Small Molecules | CHIR99021, RepSox, Forskolin, VPA, Parnate, and TTNPB (CRFVPT); CRFVPT + rolipram (CRFVPTM); LIF after day 16 | X | X | | 14.5% α-actinin$^+$, 9% αMHC$^+$ (MEFs) | ∼100 beating clusters from 50,000 starting cells (MEFs); Generation of beating cells ∼2-fold enhanced by rolipram (TTFs) | N/A | Fu et al., 2015 |
| | | CRFVPTM | | | X | N/A | N/A | CRFVPTM vs. vehicle;<br>EF = ∼35% vs. ∼23%; FS = ∼18% vs. ∼10% after 7 weeks | Huang et al., 2018 |
| | | CRFVPTM + PTC-209 | X | | X | 42% αMHC$^+$ (MEFs), 10% αMHC$^+$ (CFs) | ∼20% enhanced by PTC-209 | N/A | Testa et al., 2020 |

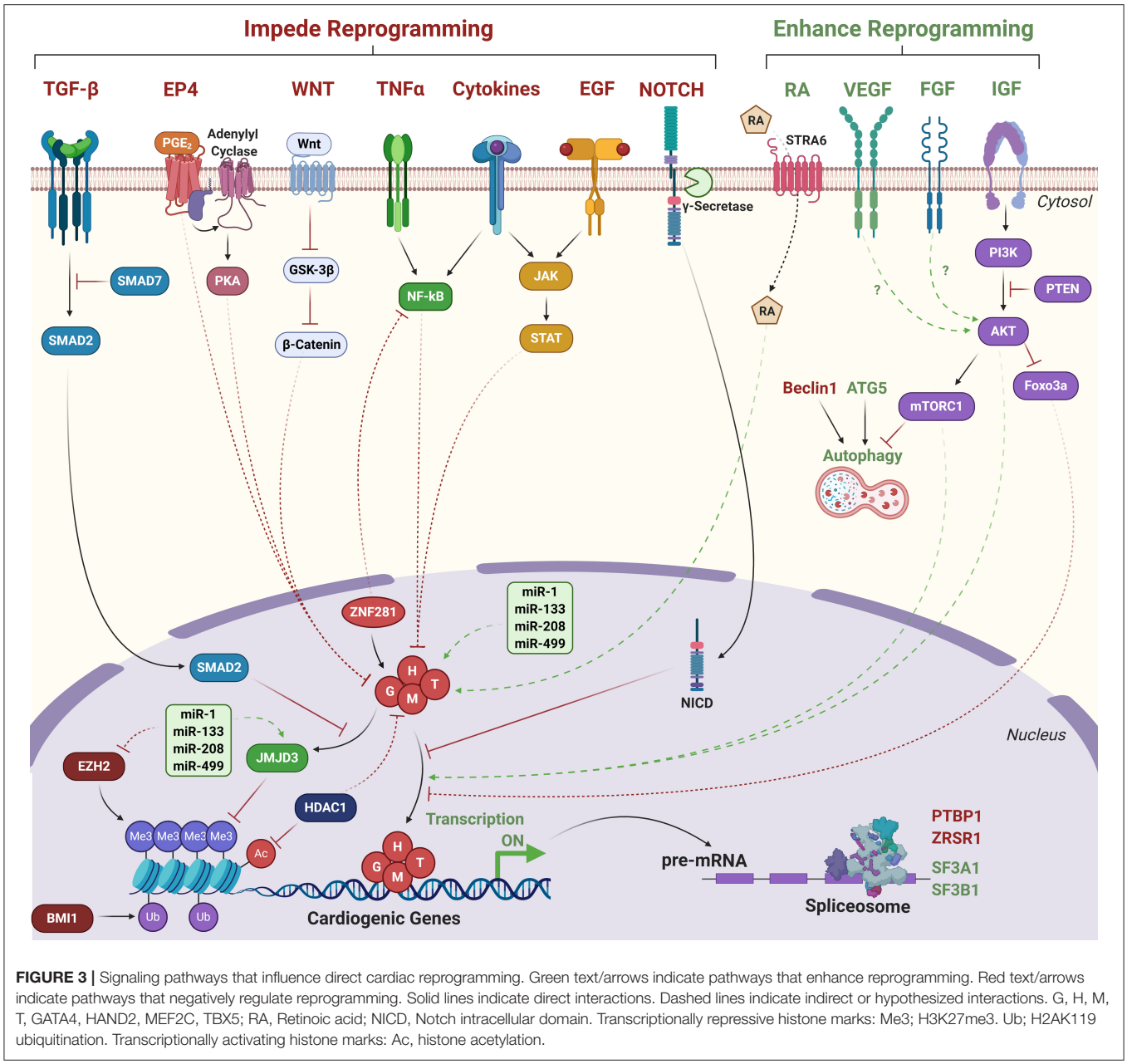


**FIGURE 3 |** Signaling pathways that influence direct cardiac reprogramming. Green text/arrows indicate pathways that enhance reprogramming. Red text/arrows indicate pathways that negatively regulate reprogramming. Solid lines indicate direct interactions. Dashed lines indicate indirect or hypothesized interactions. G, H, M, T, GATA4, HAND2, MEF2C, TBX5; RA, Retinoic acid; NICD, Notch intracellular domain. Transcriptionally repressive histone marks: Me3; H3K27me3. Ub; H2AK119 ubiquitination. Transcriptionally activating histone marks: Ac, histone acetylation.

JAK-STAT pathway enhanced the percentage of reprogrammed CFs expressing αMHC-CFP by >4-fold following miR-1, miR-133, miR-208, and miR-499 delivery (Jayawardena et al., 2012). TGF-β inhibition increased the percentage of cells exhibiting calcium transients by >3-fold in both GHMT + NKX2.5- and GHMT-reprogrammed MEFs vs. DMSO control. Similarly, TGF-β inhibition or ROCK inhibition increased the generation of beating cells in MEFs transduced with GHMT + miR-1 + miR-133 by 4- to 6-fold, resulting in up to 60% beating iCMs by Day 11 (Zhao et al., 2015; Riching et al., 2018). Stimulation with TGF-β1 or TGF-β2, but not Activin A, blunted the effects of TGF-β inhibition (Ifkovits et al., 2014). Treatment with FGF2, FGF10, and VEGF (FFV) resulted in a ∼20-fold increase in the number of beating cells generated by GMT transduction in MEFs compared to fetal bovine serum, and WNT inhibition alongside FFV treatment further increased the beating cell yield 4-fold vs. FFV alone (Yamakawa et al., 2015).

Dual inhibition of TGF-β and WNT signaling increased the number of contracting cells generated by polycistronic GMT overexpression in neonatal CFs by ∼8-fold vs. GMT alone, resulting in ∼40% contracting cells after 7 weeks of culture (Mohamed et al., 2017). Dual inhibition of histone deacetylases (HDACs) and WNT signaling alongside administration of RA increased expression of cTnT by ∼7-fold compared to GMT alone in rat CFs, which coincided with increased expression of cardiac genes including *Gata4*, *Mef2c*, *Tbx5*, *Tnnt2*, *Nkx2-5*, and

*Myh6* (Singh et al., 2020). Notably, though neither compound treated reprogrammed cells nor untreated cells spontaneously contracted in culture, GMT-reprogrammed cells treated with HDAC/WNT inhibitors and RA synchronously contracted following 4 week coculture with neonatal rat CMs. Knockdown of *Atg5* dramatically reduced reprogramming efficiency indicating autophagy is critical for the reprogramming process (Wang et al., 2020c). Overexpression of constitutively active AKT1 enhanced the reprogramming ability of GHMT (AGHMT) in MEFs, generating ∼50% beating cells after 3 weeks of culture vs. <1% generated by GHMT alone. AKT1 also enhanced GHMT-mediated reprogramming of CFs and TTFs, though generation of beating cells was much lower (<1%) (Zhou et al., 2015).

Inhibition of γ-secretase, which cleaves NOTCH to allow nuclear translocation, in both GHMT- and AGHMT-reprogrammed fibroblasts increased the percentage of cells expressing cTnT or α-actinin (Abad et al., 2017). Notably, γ-secretase inhibition did not significantly downregulate canonical NOTCH target genes, but NOTCH is known to disrupt the ability of MEF2C to bind target genes (Wilson-Rawls et al., 1999). Indeed, γ-secretase inhibition resulted in increased MEF2C binding to *Myh6, Tnnt2,* and *Actc1* promoters (Abad et al., 2017). Addition of ZNF281 to AGHMT increased the percentage of αMHC-GFP/cTnT positive TTFs by 10-fold compared to AGHMT alone and corresponded to repressed inflammatory signaling via TNFα and NF-κB pathways (Zhou et al., 2017). Inhibition of cyclooxygenase-2 (COX-2) in GHMT- or GMT-reprogrammed postnatal or adult TTFs increased the percentage of cells expressing both αMHC-GFP and cTnT by 3- to 4-fold (Muraoka et al., 2019). Stimulation of cells with prostaglandin E2 (PGE2), activation of prostaglandin E receptor 4 (EP4), activation of PKA signaling, or administration of interleukin (IL)-1β, but not IL-6 or monocyte chemoattractant protein-1 (MCP-1), counteracted the effects of COX-2 inhibition. Notably, COX-2 inhibition did not improve reprogramming efficiency in MEFs, likely because expression of *Ptgs2* (COX-2) was much lower in MEFs than postnatal or adult TTFs, underscoring that physiological differences between fibroblast origins impact the ease of reprogramming (Muraoka et al., 2019).

Liu et al. utilized single cell RNA sequencing (scRNA-seq) following delivery of polycistronic M-G-T to identify additional barriers to cardiac reprogramming. They observed significant downregulation of genes involved in mRNA processing and splicing. Further analysis revealed that knockdown of the splicing factor *Ptbp1* led to a ∼5-fold increase in the percentage of cells expressing both αMHC-GFP and cTnT vs. non-targeting short hairpin RNA (shRNA) control, and a concomitant transcriptomic shift toward the CM lineage. *Ptbp1* depletion resulted in significantly more alternative splicing events, the majority of which were exon skipping events (Liu et al., 2017). Similarly, knockdown of *Zrsr1*, a component of the U2 spliceosome complex improved reprogramming by polycistronic M-G-T in MEFs and CFs whereas knockdown of additional U2 spliceosome complex members *Sf3a1* and *Sf3b1* instead suppressed reprogramming efficiency (Zhou et al., 2018). These data identify RNA splicing as a novel regulator of cardiac reprogramming, though understanding precisely how altered splicing events contribute to the reprogramming process requires further investigation.

Mechanistic understanding of how these diverse signaling pathways influence the reprogramming process remains limited. Treatment with IGF1 mimicked AKT1 overexpression indicating insulin signaling activates AKT1 to drive reprogramming. In contrast, inhibition of PI3K, an upstream activator of AKT1, reduced reprogramming efficiency. AKT1 overexpression in reprogrammed cells was not associated with altered proliferation or apoptosis (Zhou et al., 2015). Inhibition of mTORC1 with rapamycin impaired reprogramming as did overexpression of Foxo3a. However, GSK3 inhibition did not affect reprogramming efficiency indicating that the downstream effectors of AKT1 are mTORC1 and Foxo3a but not GSK3. In contrast, Wang et al. observed enhanced reprogramming efficiency following rapamycin treatment, which they attributed to increased autophagy due to mTORC1 inhibition (Wang et al., 2020c). Thus, mTORC1 may exert dual roles on the reprogramming process; suppression of autophagy impairs the ability of the reprogramming cell to erase fibroblast identity by degrading and recycling fibrotic proteins whereas activation of protein translation may promote the ability of the reprogramming cell to acquire the CM identity via expression of cardiac proteins. Curiously, while knockdown of *Atg5* suppressed autophagy in reprogramming cells and impaired reprogramming efficiency, knockdown of *Beclin1*, a core component of the autophagy initiation complex, did not suppress baseline autophagy and potently increased reprogramming efficiency (Wang et al., 2020c). Thus, the precise regulation of autophagy during cardiac reprogramming requires further investigation.

Hashimoto et al. performed extensive chromatin immunoprecipitation followed by next generation sequencing (ChIP-seq) experiments in GMT, GHMT, and AGHMT-reprogrammed MEFs and revealed that inclusion of HAND2 and AKT1 increased the number of sites occupied by more than one reprogramming factor (50% co-occupancy in AGHMT, 46% in GHMT, and 33% in GMT) (Hashimoto et al., 2019). Moreover, cardiac enhancers enriched by Histone H3 acetylation at lysine 27 (H3K27ac), a mark of transcriptional activation, were highly enriched with MEF2 binding motifs. Inclusion of HAND2 and AKT1 to GMT promoted occupancy of these binding sites by multiple TFs suggesting cooperativity between MEF2C and other reprogramming factors to bind cardiac enhancer loci. TF enrichment at non-cardiac genes including the *Egfr* locus were also enhanced by AGHMT compared to GMT or GHMT. This enrichment corresponded to diminished H3K27ac signal and suppressed gene expression, suggesting silencing of EGFR signaling may promote cardiac reprogramming. Indeed, pharmacological or genetic inhibition of EGFR signaling increased AGHMT-mediated reprogramming efficiencies in MEFs, adult CFs, and adult TTFs (Hashimoto et al., 2019). EGFR signaling also results in the activation of pro-inflammatory signaling via activation of the JAK-STAT pathway, which is known to impair the reprogramming process (Efe et al., 2011; Jayawardena et al., 2012; Testa et al., 2020). Pharmacological inhibition of JAK2 enhanced reprogramming efficiency,

similar to EGFR inhibition (Hashimoto et al., 2019). Further investigation is required to understand mechanistically how crosstalk between these diverse signaling pathways influences cardiac reprogramming. Moreover, while AKT1 facilitates enhanced TF cooperativity to bind and activate cardiac genes and repress non-cardiac genes, it is unclear what signaling downstream of mTORC1/Foxo3a mediate GHMT recruitment to target gene binding sites (**Figure 3**).

## Epigenetic Repatterning in Cardiac Reprogramming

Global changes in activating and silencing epigenetic marks are well-established hallmarks of cardiomyogenesis. Marks associated with transcriptional repression including trimethylation of Lysine 27 on Histone H3 (H3K27me3) are often found within cardiac gene promoters and enhancers in pluripotent stem cells. Upon differentiation to cardiac progenitors and CMs, repressive marks are removed, and marks associated with transcriptional activation including H3K27ac and trimethylation of Histone H3 Lysine 4 (H3K4me3) are deposited at these promoters instead (Paige et al., 2012; Wamstad et al., 2012). Similarly, cardiac genes contain high levels of DNA methylation and H3K27me3 in fibroblasts, but upon reprogramming, DNA methylation and H3K27me3 are removed, followed by deposition of H3K4me3 (Ieda et al., 2010; Efe et al., 2011; Fu et al., 2013; Wang et al., 2014; Cao et al., 2016; Liu et al., 2016; Dal-Pra et al., 2017; Riching et al., 2021). In contrast, fibrotic genes contain high levels of H3K4me3 in fibroblasts. As reprogramming progresses, H3K4 is demethylated and these genes accumulate H3K27me3, albeit at a slower rate than the repatterning observed at cardiac genes (Fu et al., 2013; Cao et al., 2016; Liu et al., 2016).

Knockdown of polycomb repressive complex 1 component *Bmi1* facilitated removal of the transcriptionally repressive mark Histone H2A Lysine 119 ubiquitination (H2AK119ub) at cardiac genes and corresponded to increased H3K4me3 levels, increased expression, and increased reprogramming efficiency by polycistronic M-G-T (Zhou et al., 2016). Furthermore, 24 h pretreatment of MEFs or CFs with the Bmi1 inhibitor PTC-209 repressed STAT3-, IL-6-, and ERK1/2-mediated inflammatory signaling and resulted in a ∼25% increase in the number of αMHC-GFP positive cells generated by the CRFVPT small molecule combination (Testa et al., 2020). Targeted depletion of additional epigenetic regulators including lysine-specific methyltransferases *Kmt2a*, *Kmt2b*, and *Kmt2e* via shRNA delivery impaired the reprogramming process whereas depletion of chromatin remodeler complex and cohesion complex subunits *Ruvbl1/Bcor* and *Stag2*, respectively, enhanced reprogramming by polycistronic M-G-T (Zhou et al., 2018). HDAC inhibition alone or in conjunction with WNT inhibition and RA stimulation improved reprogramming by GMT, which coincided with elevated global H3K27ac levels in rat CFs (Singh et al., 2020). Further, overexpression of HDAC1 counteracted the effects of HDAC inhibition, indicating that HDACs antagonize reprogramming by GMT (**Figure 3**).

Changes in the epigenetic landscape are controlled by balancing enzymatic activities of epigenetic writers, erasers, and readers. H3K27me3 is deposited by enhancer of zeste homolog 1 and 2 (EZH1, EZH2) and removed by ubiquitously transcribed tetratricopeptide repeat protein X-linked transcript (UTX, also known as lysine demethylase 6A, KDM6A) or Jumonji domain-containing protein D3 (JMJD3, also known as KDM6B) (Hyun et al., 2017). Pharmacological inhibition of EZH2 methyltransferase activity approximately doubled the number of spontaneously beating iCMs reprogrammed by $MM_3$-GHT in MEFs (Hirai and Kikyo, 2014). Overexpression of miR-1, miR-133, miR-208, and miR-499 downregulated expression of *Ezh2* but upregulated expression of *Kdm6a* in neonatal CFs (Dal-Pra et al., 2017). Moreover, double knockdown of *Kdm6a* and *Kdm6b* prevented upregulation of *Gata4, Mef2c*, and *Tbx5* mRNA expression by miR combination, thereby impairing the reprogramming process (Dal-Pra et al., 2017). In agreement with Dal-Pra et al., our recent study indicated that *Kdm6b* knockdown also significantly impaired reprogramming of MEFs by GHMT + miR-1, miR-133, and TGF-β inhibition (Riching et al., 2021). We further demonstrated that activation of TGF-β signaling prevents removal of H3K27me3 and that the downstream TGF-β effector SMAD2 competes with GATA4 to bind and recruit JMJD3 to cardiac gene loci to facilitate removal of H3K27me3 (**Figure 3**). Moreover, JMJD3 enhances the interactions between GATA4 and SWI/SNF component BRG1, thereby promoting activation of cardiac gene expression independent of H3K27 demethylase activity. These data establish a novel mechanism by which inhibition of TGF-β signaling dramatically enhances epigenetic repatterning, thereby enhancing cardiac reprogramming efficiency (Riching et al., 2021). The TGF-β pathway was also recently shown to alter the occupancy of BRD4 and RNA pol II at super enhancers in CFs (Stratton et al., 2019); thus it is likely that downstream effectors of signaling pathways including the TGF-β pathway are key to driving epigenetic changes to promote or inhibit cellular differentiation. Elucidating the broad epigenetic changes in response to altered cellular signaling may therefore lead to further improvement in cardiac reprogramming.

## *In vivo* Reprogramming

The ability to reprogram CFs *in vitro* led to determining if reprogramming CFs in the heart post-MI would restore heart function. Co-injection of retroviral particles containing GMT alongside DsRed or GFP into the infarct of immunocompromised mice resulted in activation of αMHC-GFP and α-actinin expression in DsRed or GFP positive cells (Ieda et al., 2010; Inagawa et al., 2012) and increased expression of cardiac genes in cells that took up viral particles (Chen et al., 2012). Moreover, GMT injected mice and rats showed significantly higher EF and 50–75% reduced fibrosis compared to control injections (Mathison et al., 2012, 2014; Qian et al., 2012). Notably, injection of Thymosin β4 (Qian et al., 2012) or VEGF (Mathison et al., 2012, 2014, 2017) further improved these parameters compared to GMT alone. Injection of polycistronic GMT (M-G-T) doubled the number of iCMs generated which correlated to higher EF and fractional shortening (FS) parameters and lower fibrotic area compared to individual G/M/T viral particles (Ma et al., 2015). SeV delivery of polycistronic GMT and retroviral delivery of GMT both improved EF and FS

and reduced fibrosis vs. GFP control, but SeV GMT delivery also slightly improved FS over retroviral GMT (Miyamoto et al., 2018). Furthermore, labeling CFs with TdTomato driven by *Tcf21*-Cre indicated that SeV-GMT resulted in triple the number of cTnT/TdTomato positive cells compared to retroviral GMT (Miyamoto et al., 2018). Dual inhibition of TGF-β and WNT signaling further enhanced reprogramming by GMT; 12 weeks post-MI, EF in mice injected with GMT and TGF-β/WNT inhibitors, GMT alone, inhibitors alone, or DsRed was ∼35, ∼30, ∼22, or 20%, respectively. Labeling CFs with YFP driven by *Postn*-Cre indicated GMT + TGF-β/WNT inhibition resulted in ∼7 times as many YFP/cTnT double positive cells as GMT alone. Moreover, RNA-seq analysis performed on isolated YFP/cTnT double positive cells indicated that GMT overexpression alongside dual inhibition of TGF-β and WNT generated more mature iCMs that clustered closer to adult CMs by principle component analysis than those generated by GMT alone (Mohamed et al., 2017). Injection of *Beclin1* haploinsufficient mice with retroviral polycistronic M-G-T resulted in significantly improved heart function and reduced fibrosis compared to wildtype animals, though both groups demonstrated improved heart function and reduced fibrosis to mice injected with DsRed control (Wang et al., 2020c).

Addition of HAND2 to GMT likewise significantly improved heart function post-MI. Mice injected with GHMT had double the FS and 70% higher EF than mice injected with GFP 3 weeks post-MI. EF continued to improve in GHMT-injected animals by 6 and 12 weeks post-MI (EF = 57% at week 12), but slightly worsened in GFP injected mice (EF = 29% at week 12). Fibrotic area was reduced ∼50% in animals injected with GHMT compared to those injected with GFP (Song et al., 2012). Notably, functional parameters in GHMT-injected animals did not reach levels comparable to those in sham or unoperated mice indicating that further optimization of *in vivo* reprogramming is required to fully regenerate the heart post-MI. Regardless, the authors comment that the level of regeneration achieved in this study seems greater than expected based on the *in vitro* reprogramming efficiency of GHMT and speculate that the native environment of the intact heart may provide additional biochemical and mechanical cues that promote reprogramming *in vivo*.

*In vivo* reprogramming was also achieved by delivery of miR-1, miR-133, miR-208, and miR-499. Following coronary artery ligation, miR delivery generated 1–12% cTnT/*Fsp1*-tdTomato double positive cells (Jayawardena et al., 2012, 2015). *Fsp1*-TdTomato specifically labeled non-myocytes in the heart, the majority of which were CFs. Notably, ∼4% of cells in mice injected with negmiR control also expressed cTnT/*Fsp1*-tdTomato suggesting a small degree of promoter leakiness. Injection of miR combination blunted worsening of cardiac function post-MI. After 3 months, animals injected with miR combination had 50% higher FS than those injected with negmiR control (30% vs. 20%). Fibrotic area was also reduced 60% by miR combination (Jayawardena et al., 2015).

Finally, administration of small molecules CRFVPT + rolipram (CRFVPTM) post-MI reduced fibrotic area by >50% and significantly improved EF and FS vs. vehicle control (Huang et al., 2018). Labeling non-myocytes with tdTomato driven by *Fsp1*-Cre indicated that CRFVPTM generated 0.78% cTnT/tdTomato double positive cells and 1.02% MEF2C/tdTomato double positive cells. No double positive cells were generated by vehicle control. The authors noted that some compound dosing strategies, particularly those with short administration intervals induced significant weight loss indicating compound toxicity (Huang et al., 2018). Nevertheless, longer intervals between compound administration over longer periods of time did not cause noticeable toxicity suggesting small molecule delivery may be a promising therapeutic avenue to reprogram CFs to regenerate the heart. Restoration of heart function by various *in vivo* reprogramming strategies is shown in **Tables 1**–**3**. Collectively, these studies demonstrate that cardiac reprogramming reduces fibrosis and prevents worsening of cardiac function following MI. Additionally, some studies reported improved cardiac functional parameters following MI, though incomplete, possibly due to relatively low reprogramming efficiency. Thus, these studies offer a proof of concept for regenerative therapies post-MI.

## Translation to Human IHD

Although numerous strategies have greatly increased the efficiency of reprogramming murine fibroblasts in recent years, the efficiency of reprogramming human fibroblasts remains low. The GMT core TF cocktail, which could induce expression of the αMHC-mCherry reporter in up to ∼10% of murine fibroblasts, could not induce reporter activity in human ESC-differentiated fibroblasts. However, addition of ESSRG and MESP1 could activate expression of the αMHC-mCherry reporter and cTnT. Inclusion of MYOCD and ZFPM2 further enhanced expression in ESC-derived fibroblasts and could drive expression of these markers in human dermal fibroblasts (HDFs) and human CFs (HCFs) (Fu et al., 2013). Dual inhibition of TGF-β/WNT signaling in immortalized HCFs transduced with GMT + ESSRG, MYOCD, ZFPM2, and MESP1 (7F) resulted in spontaneous calcium transients in >50% of cells after 4 weeks in culture whereas 7F expression alone generated calcium transients in <5% of reprogrammed cells (Mohamed et al., 2017). GMT + MESP1 and MYOCD (GMTMM) induced expression of cTnT and α-actinin in ∼5–6% of HCFs and ∼1% of these cells exhibited calcium transients (Wada et al., 2013). Though spontaneously beating cells could not be identified in reprogrammed human CFs, co-culture with rat CMs resulted in ∼5% of reprogrammed cells to synchronously contract. Addition of miR-133 to GMTMM increased the percentage of cTnT positive cells by 3- to 10-fold vs. GMTMM alone (Muraoka et al., 2014). Overexpression of GHT, MYOCD, miR-1, and miR-133 induced cTnT or tropomyosin expression in >35% of human foreskin fibroblasts (HFFs) after 4 weeks. This combination of reprogramming factors also induced expression of cTnT in HCFs and HDFs, albeit at lower efficiencies. Additionally, after 11 weeks in culture, rare beating cells were observed in reprogrammed HCFs, but not in reprogrammed HFFs or HDFs (Nam et al., 2013). GHMT + MYOCD or GMT + miR-590 both induced expression of cTnT in ∼5% of HCFs (Singh et al., 2016). Dual inhibition of HDACs and WNT alongside administration of RA further improved

reprogramming by GHMT, MYOCD, and miR-590 compared to vehicle control (25% vs. 5.7% cTnT positive cells) (Singh et al., 2020). Though neither reprogramming condition generated spontaneously beating cells, ∼5% of reprogrammed cells treated with these compounds synchronously contracted after 4 weeks of coculture with neonatal rat CMs. SeV delivery of GMTMM + miR-133 induced expression of cTnT in ∼15% of HCFs after 10 days in culture (Miyamoto et al., 2018). Using a nuclease-dead Cas9 (dCas9) fused to the VP64 transcriptional activator (dCas9-VP64) alongside delivery of sgRNAs targeting *GATA4*, *HAND2*, *MEF2C*, *TBX5*, and *MEIS1* loci, Wang et al. demonstrated robust activation of endogenous TF expression resulting in cTnT expression in ∼9% of HFFs (Wang et al., 2020a).

Though less efficient than other methods, delivery of polycistronic M-G-T + miR-133 to ESC-derived fibroblasts generated ∼2.5% cTnT positive cells (Zhou et al., 2019). Zhou et al. then utilized puromycin selection following M-G-T + miR-133 transduction in ESC-derived fibroblasts and performed scRNA-seq to identify barriers to human reprogramming. This analysis suggested that high expression level of reprogramming factors correlated to more complete reprogramming and cell cycle exit whereas lower expression of reprogramming factors resulted in reversion back to a fibroblast state. The rate at which human fibroblasts reprogram was noted to be much slower than murine fibroblasts. By day 3, GMT/miR-133 induced differential expression of only 1/3rd the number of genes in human fibroblasts compared to murine fibroblasts (Liu et al., 2017; Zhou et al., 2019). Moreover, delivery of reprogramming factors generated an innate immune response, which was crucial to the reprogramming process. Knockdown of *TLR3, NFKB1,* or *PTGS2* all lowered the percentage of cTnT positive cells, in part by increasing DNA methylation at cardiac genes (Zhou et al., 2019). Intriguingly, inhibition of COX-2 (*PTGS2)* promoted reprogramming efficiency in mouse dermal fibroblasts (Muraoka et al., 2019) suggesting that inflammatory signaling may have vastly different effects on reprogramming efficiencies in different species.

Non-GMT or GHMT-based methods have also successfully generated iCPCs from human fibroblasts. Overexpression of E26 transformation-specific transcription factor 2 (ETS2) and MESP1 followed by treatment with Activin A and BMP4 generated CPCs marked by NKX2.5 expression from HDFs, which progressed through cardiac differentiation to CM-like cells, marked by sarcomere proteins including α-actinin and α-MHC (Islas et al., 2012). Finally, treatment with CHIR99021, BIX01294 (H3K9 methyltransferase inhibitor), A-83-01 (TGF-β inhibitor), AS8351 (H3K4 demethylase inhibitor), SC1 (ERK1 inhibitor), OAC2 (OCT4 activator), Y27632 (ROCK inhibitor), SU16F (PDGFRβ inhibitor), and JNJ10198409 (PDGFRβ and PDGFRα inhibitor) (9C) could also induce differentiation of HFFs or human fetal lung fibroblasts (HLFs) to iCPCs. Cao et al. observed that ∼6.6% of HFFs or HLFs treated with 9C expressed cTnT by day 30, with beating clusters of cells appearing starting at day 20 (Cao et al., 2016). Fibroblasts treated with 9C did not upregulate pluripotency markers but did express mesodermal/cardiac progenitor markers including *T* (Brachyury), *MESP1*, *GATA4*, *NKX2-5*, and *KDR*. Furthermore, H3K4me3 was lost at fibrotic genes and gained at cardiac genes whereas H3K27me3 was lost at cardiac genes and gained at fibrotic genes and 9C treatment was associated with global decondensation of chromatin (Cao et al., 2016). Thus, despite relatively lower efficiencies compared to rodent reprogramming and only rare generation of beating cells, these studies, summarized in **Table 4**, demonstrate that human fibroblasts are capable of being reprogrammed into iCMs.

## PERSPECTIVES

Though the development of infarct revascularization techniques dramatically reduced infarct size, which coincided with substantial reduction in in-hospital mortality and improved patient outcomes post-MI, mortality rates post-MI remain high. Identifying novel targetable pathways to blunt reperfusion injury could further reduce infarct size and post-MI mortality. Additionally, significant progress has been made over the last two decades in identifying strategies to regenerate the myocardium following ischemic injury and elucidating mechanisms to enhance these strategies. Moreover, both induction of CM proliferation and direct fibroblast reprogramming have resulted in partial restoration of heart function and reduced fibrotic area in pre-clinical animal models of MI (**Figure 1**). However, significant challenges must be overcome before these strategies can be translated into novel therapies for human heart regeneration.

The majority of studies reviewed above utilized adenoviral, lentiviral, or retroviral delivery of genetic factors that induce CM proliferation or fibroblast reprogramming, which have been previously linked to carcinogenesis (Escors and Breckpot, 2010) and the development lethal immune reactions in human patients (Sibbald, 2001). The Giacca group utilized intramyocardial AAV-delivery of miR-199a-1 to induce CM proliferation in both rodent and porcine MI models (Eulalio et al., 2012; Gabisonia et al., 2019). In contrast to adeno-, retro-, and lentiviral infection, AAV delivery has been used in hundreds of clinical trials to date with no evidence of tumor formation in >7 years of patient follow up (Colella et al., 2018). On the other hand, delivery of AAVs that display tropism for the heart including AAV6 and AAV9 are also well-established to infect other organs including the brain, lung, liver, and skeletal muscle (Wu et al., 2006; Castle et al., 2016; Naso et al., 2017). Moreover, expression of cargo is long lasting while inducing cardiac regeneration may only require transient expression (Zacchigna et al., 2014). Thus, delivery of modified mRNAs has also been explored as a therapeutic avenue for gene therapy. Lesizza et al. demonstrated that a single injection of miR-199a-3p or miR-590-3p mimics improved survival in mice post-MI coinciding with improved ventricular function, reduced scar size, and the induction of CM proliferation (Lesizza et al., 2017).

Strong expression of pro-proliferative gene cargo such as CDK/Cyclin proteins in non-myocytes may potentially trigger expansion of these cells, leading to activation of fibrosis or uncontrolled vasculogenesis, negatively affecting heart function. Similarly, inducing uncontrolled expansion of CMs via NRG1 overexpression, *Salv* KO, constitutive YAP activation, or Cyclin A2 overexpression induced CM hyperplasia and cardiomegaly in

**TABLE 4 |** Reprogramming efficiencies in human fibroblasts.

| Reprogramming strategy | | Fibroblast origin | | | Efficiency | | Study |
|---|---|---|---|---|---|---|---|
| **Core factors** | **Additional factors** | **Embryonic** | **Dermal** | **Cardiac** | **Cardiac marker expression** | **Spontaneously beating cells** | **Authors** |
| GMT | +ESSRG, MESP1, MyoCD, and ZFPM2 | X | X | X | 13% cTnT/αMHC-GFP$^+$ (ESC-fibroblasts); 3.7% cTnT$^+$ (HDFs); 1.8% cTnT$^+$ (HCFs) | Not detected | Fu et al., 2013 |
| | +MESP1 and MyoCD | | | X | 5.5% α-actinin$^+$, 5.9% cTnT$^+$ | Not detected | Wada et al., 2013 |
| | +MESP1, MyoCD, and miR-133 | | | X | 23–27% cTnT$^+$ | Not discussed | Muraoka et al., 2014 |
| | +ESSRG, MESP1, MyoCD, ZFPM2, and dual TGF-β/WNT inhibition | | | X | 12.5% TNT-GCaMP5$^+$; >50% of cells generated calcium transients | Not discussed | Mohamed et al., 2017 |
| | Sendai viral delivery +MESP1, MyoCD, and miR-133 | | | X | 15% cTnT$^+$ | Not detected | Miyamoto et al., 2018 |
| | +miR-133 | X | | X | 2.5% cTnT$^+$ (ESC-fibroblasts) | Not detected | Zhou et al., 2019 |
| GHMT | +MyoCD or +miR-590 | | | X | 5% cTnT$^+$ | Not discussed | Singh et al., 2016 |
| | +MyoCD, miR-590, HDAC/WNT inhibition, and retinoic acid | | | X | 25% cTnT$^+$ | Not detected | Singh et al., 2020 |
| | CRISPRa targeting GHMT + MEIS1 | | X | | 8.7% cTnT$^+$ | Not discussed | Wang et al., 2020a |
| GHT | +MyoCD, miR-1, and miR-133 | | X | X | 35% cTnT$^+$ (HFFs); 13% cTnT$^+$ (HCFs); 9.5% cTnT$^+$ (HDFs) | Rare after ∼11 weeks in culture (HCFs) | Nam et al., 2013 |
| ETS2 and MESP1 | +Activin A and BMP4 | | X | | 13.7% αMHC-GFP+ | Not discussed | Islas et al., 2012 |
| Small Molecules | CHIR99021, BIX01294, A83-01, AS8351, SC1, OAC2, Y27632, SU16F, and JNJ10198409 | X | X | | 6.6% cTnT$^+$ | ∼0.44% of total cells, 97% of αMHC-GFP$^+$ cells | Cao et al., 2016 |

embryonic and neonatal animals, resulting in cardiac dysfunction with potentially lethal consequences (Chaudhry et al., 2004; Heallen et al., 2011; Von Gise et al., 2012; Gemberling et al., 2015). Unlike viral delivery, the gene dosage of cargo can also be more carefully controlled via modified mRNA delivery, which may mitigate deleterious effects of strong expression, especially in non-target cells (Sultana et al., 2017).

Additional consideration should also be given to the maturation state of CMs generated by these regenerative strategies. While *in vivo* regeneration in rodent models has not been associated with the development of cardiac arrhythmia thus far, Gabisonia et al. demonstrated that the majority of pigs (7/10) that were administered AAV6-miR-199a-1 died of sudden death induced by tachyarrhythmia events/ventricular fibrillation 7 to 8 weeks after injection (Gabisonia et al., 2019). It is unclear if the cause of these arrhythmogenic phenotypes are a result of poor differentiation of newly proliferated CMs within the infarct leading to reentry currents or if the opposite strand of miR-199-3p, miR-199-5p, which has known deleterious consequences in CMs (Li et al., 2017), induces cardiac dysfunction. Understanding the long-term consequences of novel cardiac regeneration strategies, particularly in large animal pre-clinical studies is a required first step toward clinical translation. Overcoming these clinical barriers will undoubtedly begin a new era in the treatment of human heart disease.

## DATA AVAILABILITY STATEMENT

The original contributions presented in the study are included in the article/supplementary material, further inquiries can be directed to the corresponding author/s.

## AUTHOR CONTRIBUTIONS

AR and KS co-wrote the manuscript. All authors contributed to the article and approved the submitted version.

## FUNDING

AR was supported by predoctoral fellowships from the University of Colorado Consortium for Fibrosis Research & Translation, Colorado Clinical & Translational Sciences Institute (TL1 TR001081), and the American Heart Association (18PRE34030030). KS was supported by funds from the Boettcher Foundation, American Heart Association, University

of Colorado Department of Medicine Outstanding Early Career Scholar Program, Gates Frontiers Fund, and National Institutes of Health HL133230. **Figures 1–3** were generated using Biorender.com.

## ACKNOWLEDGMENTS

The authors thank Walter Knight for critical reading of the manuscript.

## REFERENCES

(Gissi), G.I.P.L.S.D.S.N.I.M. (1986). Effectiveness of intravenous thrombolytic treatment in acute myocardial infarction. Gruppo Italiano per lo Studio della Streptochinasi nell'Infarto Miocardico (GISSI). *Lancet* 1, 397–402.

(Isis-2), S.I.S.O.I.S.C.G. (1988). Randomised trial of intravenous streptokinase, oral aspirin, both, or neither among 17,187 cases of suspected acute myocardial infarction: ISIS-2. ISIS-2 (Second International Study of Infarct Survival) Collaborative Group. *Lancet* 2, 349–360. doi: 10.1016/S0140-6736(88)92833-4

Abad, M., Hashimoto, H., Zhou, H., Morales, M. G., Chen, B., Bassel-Duby, R., et al. (2017). Notch inhibition enhances cardiac reprogramming by increasing MEF2C transcriptional activity. *Stem Cell Rep.* 8, 548–560. doi: 10.1016/j.stemcr.2017.01.025

Addis, R. C., Ifkovits, J. L., Pinto, F., Kellam, L. D., Esteso, P., Rentschler, S., et al. (2013). Optimization of direct fibroblast reprogramming to cardiomyocytes using calcium activity as a functional measure of success. *J. Mol. Cell. Cardiol.* 60, 97–106. doi: 10.1016/j.yjmcc.2013.04.004

Aguirre, A., Montserrat, N., Zacchigna, S., Nivet, E., Hishida, T., Krause, M. N., et al. (2014). *In vivo* activation of a conserved microRNA program induces mammalian heart regeneration. *Cell Stem Cell* 15, 589–604. doi: 10.1016/j.stem.2014.10.003

Al Shammeri, O., and Garcia, L. (2013). Thrombolysis in the age of primary percutaneous coronary intervention: mini-review and meta-analysis of early PCI. *Int. J. Health Sci.* 7, 91–100. doi: 10.12816/0006026

Anand, I. (2018). Stable but progressive nature of heart failure: considerations for primary care physicians. *Am. J. Cardiovasc. Drugs* 18, 333–345. doi: 10.1007/s40256-018-0277-0

Bangalore, S., Makani, H., Radford, M., Thakur, K., Toklu, B., Katz, S. D., et al. (2014). Clinical outcomes with beta-blockers for myocardial infarction: a meta-analysis of randomized trials. *Am. J. Med.* 127, 939–953. doi: 10.1016/j.amjmed.2014.05.032

Bassat, E., Mutlak, Y. E., Genzelinakh, A., Shadrin, I. Y., Baruch Umansky, K., Yifa, O., et al. (2017). The extracellular matrix protein agrin promotes heart regeneration in mice. *Nature* 547, 179–184. doi: 10.1038/nature22978

Benjamin, E. J., Blaha, M. J., Chiuve, S. E., Cushman, M., Das, S. R., Deo, R., et al. (2017). Heart disease and stroke statistics-2017 Update: a report from the American Heart Association. *Circulation* 135, e146–e603. doi: 10.1161/CIR.0000000000000485

Bergmann, O., Bhardwaj, R. D., Bernard, S., Zdunek, S., Barnabe-Heider, F., Walsh, S., et al. (2009). Evidence for cardiomyocyte renewal in humans. *Science* 324, 98–102. doi: 10.1126/science.1164680

Bergmann, O., Zdunek, S., Felker, A., Salehpour, M., Alkass, K., Bernard, S., et al. (2015). Dynamics of cell generation and turnover in the human heart. *Cell* 161, 1566–1575. doi: 10.1016/j.cell.2015.05.026

Bersell, K., Arab, S., Haring, B., and Kuhn, B. (2009). Neuregulin1/ErbB4 signaling induces cardiomyocyte proliferation and repair of heart injury. *Cell* 138, 257–270. doi: 10.1016/j.cell.2009.04.060

Boucek, R. J., and Murphy, W. P. Jr. (1960). Segmental perfusion of the coronary arteries with fibrinolysin in man following a myocardial infarction. *Am. J. Cardiol.* 6, 525–533. doi: 10.1016/0002-9149(60)90348-9

Braunwald, E. (2012). The treatment of acute myocardial infarction: the past, the present, and the future. *Eur. Heart J. Acute Cardiovasc. Care* 1, 9–12. doi: 10.1177/2048872612438026

Cao, N., Huang, Y., Zheng, J., Spencer, C. I., Zhang, Y., Fu, J. D., et al. (2016). Conversion of human fibroblasts into functional cardiomyocytes by small molecules. *Science* 352, 1216–1220. doi: 10.1126/science.aaf1502

Castle, M. J., Turunen, H. T., Vandenberghe, L. H., and Wolfe, J. H. (2016). Controlling AAV tropism in the nervous system with natural and engineered capsids. *Methods Mol. Biol.* 1382, 133–149. doi: 10.1007/978-1-4939-3271-9_10

Chaudhry, H. W., Dashoush, N. H., Tang, H., Zhang, L., Wang, X., Wu, E. X., et al. (2004). Cyclin A2 mediates cardiomyocyte mitosis in the postmitotic myocardium. *J. Biol. Chem.* 279, 35858–35866. doi: 10.1074/jbc.M404975200

Chen, J. X., Krane, M., Deutsch, M. A., Wang, L., Rav-Acha, M., Gregoire, S., et al. (2012). Inefficient reprogramming of fibroblasts into cardiomyocytes using Gata4, Mef2c, and Tbx5. *Circ. Res.* 111, 50–55. doi: 10.1161/CIRCRESAHA.112.270264

Chen, Z., Xie, J., Hao, H., Lin, H., Wang, L., Zhang, Y., et al. (2017). Ablation of periostin inhibits post-infarction myocardial regeneration in neonatal mice mediated by the phosphatidylinositol 3 kinase/glycogen synthase kinase 3beta/cyclin D1 signalling pathway. *Cardiovasc. Res.* 113, 620–632. doi: 10.1093/cvr/cvx001

Chesebro, J. H., Knatterud, G., Roberts, R., Borer, J., Cohen, L. S., Dalen, J., et al. (1987). Thrombolysis in Myocardial Infarction (TIMI) trial, phase i: a comparison between intravenous tissue plasminogen activator and intravenous streptokinase. Clinical findings through hospital discharge. *Circulation* 76, 142–154. doi: 10.1161/01.CIR.76.1.142

Choi, J., Costa, M. L., Mermelstein, C. S., Chagas, C., Holtzer, S., and Holtzer, H. (1990). MyoD converts primary dermal fibroblasts, chondroblasts, smooth muscle, and retinal pigmented epithelial cells into striated mononucleated myoblasts and multinucleated myotubes. *Proc. Natl. Acad. Sci. U.S.A.* 87, 7988–7992. doi: 10.1073/pnas.87.20.7988

Christoforou, N., Chellappan, M., Adler, A. F., Kirkton, R. D., Wu, T., Addis, R. C., et al. (2013). Transcription factors MYOCD, SRF, Mesp1 and SMARCD3 enhance the cardio-inducing effect of GATA4, TBX5, and MEF2C during direct cellular reprogramming. *PLoS ONE* 8:e63577. doi: 10.1371/journal.pone.0063577

Colella, P., Ronzitti, G., and Mingozzi, F. (2018). Emerging Issues in AAV-mediated *in vivo* gene therapy. *Mol. Ther. Methods Clin. Dev.* 8, 87–104. doi: 10.1016/j.omtm.2017.11.007

Dal-Pra, S., Hodgkinson, C. P., Mirotsou, M., Kirste, I., and Dzau, V. J. (2017). Demethylation of H3K27 is essential for the induction of direct cardiac reprogramming by miR combo. *Circ. Res.* 120, 1403–1413. doi: 10.1161/CIRCRESAHA.116.308741

David, S. W., Khan, Z. A., Patel, N. C., Metzger, D. C., Wood, F. O., Wasserman, H. S., et al. (2019). Evaluation of intracoronary hyperoxemic oxygen therapy in acute anterior myocardial infarction: the IC-HOT study. *Catheter. Cardiovasc. Interv.* 93, 882–890. doi: 10.1002/ccd.27905

Davis, J., and Molkentin, J. D. (2014). Myofibroblasts: trust your heart and let fate decide. *J. Mol. Cell. Cardiol.* 70, 9–18. doi: 10.1016/j.yjmcc.2013.10.019

Davis, R. L., Weintraub, H., and Lassar, A. B. (1987). Expression of a single transfected cDNA converts fibroblasts to myoblasts. *Cell* 51, 987–1000. doi: 10.1016/0092-8674(87)90585-X

Derks, W., and Bergmann, O. (2020). Polyploidy in cardiomyocytes: roadblock to heart regeneration? *Circ. Res.* 126, 552–565. doi: 10.1161/CIRCRESAHA.119.315408

Efe, J. A., Hilcove, S., Kim, J., Zhou, H., Ouyang, K., Wang, G., et al. (2011). Conversion of mouse fibroblasts into cardiomyocytes using a direct reprogramming strategy. *Nat. Cell Biol.* 13, 215–222. doi: 10.1038/ncb2164

Engel, F. B., Hsieh, P. C., Lee, R. T., and Keating, M. T. (2006). FGF1/p38 MAP kinase inhibitor therapy induces cardiomyocyte mitosis, reduces scarring, and rescues function after myocardial infarction. *Proc. Natl. Acad. Sci. U.S.A.* 103, 15546–15551. doi: 10.1073/pnas.0607382103

Engel, F. B., Schebesta, M., Duong, M. T., Lu, G., Ren, S., Madwed, J. B., et al. (2005). p38 MAP kinase inhibition enables proliferation of adult mammalian cardiomyocytes. *Genes Dev.* 19, 1175–1187. doi: 10.1101/gad.1306705

Escors, D., and Breckpot, K. (2010). Lentiviral vectors in gene therapy: their current status and future potential. *Arch. Immunol. Ther. Exp.* 58, 107–119. doi: 10.1007/s00005-010-0063-4

Eulalio, A., Mano, M., Dal Ferro, M., Zentilin, L., Sinagra, G., Zacchigna, S., et al. (2012). Functional screening identifies miRNAs inducing cardiac regeneration. *Nature* 492, 376–381. doi: 10.1038/nature11739

Finn, A. V., Nakazawa, G., Joner, M., Kolodgie, F. D., Mont, E. K., Gold, H. K., et al. (2007). Vascular responses to drug eluting stents: importance of delayed healing. *Arterioscler. Thromb. Vasc. Biol.* 27, 1500–1510. doi: 10.1161/ATVBAHA.107.144220

Formiga, F. R., Pelacho, B., Garbayo, E., Imbuluzqueta, I., Diaz-Herraez, P., Abizanda, G., et al. (2014). Controlled delivery of fibroblast growth factor-1 and neuregulin-1 from biodegradable microparticles promotes cardiac repair in a rat myocardial infarction model through activation of endogenous regeneration. *J. Control. Release* 173, 132–139. doi: 10.1016/j.jconrel.2013.10.034

Frohlich, G. M., Meier, P., White, S. K., Yellon, D. M., and Hausenloy, D. J. (2013). Myocardial reperfusion injury: looking beyond primary PCI. *Eur. Heart J.* 34, 1714–1722. doi: 10.1093/eurheartj/eht090

Fu, J. D., Stone, N. R., Liu, L., Spencer, C. I., Qian, L., Hayashi, Y., et al. (2013). Direct reprogramming of human fibroblasts toward a cardiomyocyte-like state. *Stem Cell Rep.* 1, 235–247. doi: 10.1016/j.stemcr.2013.07.005

Fu, Y., Huang, C., Xu, X., Gu, H., Ye, Y., Jiang, C., et al. (2015). Direct reprogramming of mouse fibroblasts into cardiomyocytes with chemical cocktails. *Cell Res.* 25, 1013–1024. doi: 10.1038/cr.2015.99

Gabisonia, K., Prosdocimo, G., Aquaro, G. D., Carlucci, L., Zentilin, L., Secco, I., et al. (2019). MicroRNA therapy stimulates uncontrolled cardiac repair after myocardial infarction in pigs. *Nature* 569, 418–422. doi: 10.1038/s41586-019-1191-6

Gao, R., Zhang, J., Cheng, L., Wu, X., Dong, W., Yang, X., et al. (2010). A Phase II, randomized, double-blind, multicenter, based on standard therapy, placebo-controlled study of the efficacy and safety of recombinant human neuregulin-1 in patients with chronic heart failure. *J. Am. Coll. Cardiol.* 55, 1907–1914. doi: 10.1016/j.jacc.2009.12.044

Garbayo, E., Gavira, J. J., De Yebenes, M. G., Pelacho, B., Abizanda, G., Lana, H., et al. (2016). Catheter-based intramyocardial injection of FGF1 or NRG1-loaded MPs improves cardiac function in a preclinical model of ischemia-reperfusion. *Sci. Rep.* 6:25932. doi: 10.1038/srep25932

Gemberling, M., Karra, R., Dickson, A. L., and Poss, K. D. (2015). Nrg1 is an injury-induced cardiomyocyte mitogen for the endogenous heart regeneration program in zebrafish. *Elife* 4:e05871. doi: 10.7554/eLife.05871.015

Ginks, W. R., Sybers, H. D., Maroko, P. R., Covell, J. W., Sobel, B. E., and Ross, J. Jr. (1972). Coronary artery reperfusion. II. Reduction of myocardial infarct size at 1 week after the coronary occlusion. *J. Clin. Invest.* 51, 2717–2723. doi: 10.1172/JCI107091

Goetz, R. H., Rohman, M., Haller, J. D., Dee, R., and Rosenak, S. S. (1961). Internal mammary-coronary artery anastomosis. A nonsuture method employing tantalum rings. *J. Thorac. Cardiovasc. Surg.* 41, 378–386. doi: 10.1016/S0022-5223(20)31701-3

Gold, M. R., Van Veldhuisen, D. J., Hauptman, P. J., Borggrefe, M., Kubo, S. H., Lieberman, R. A., et al. (2016). Vagus nerve stimulation for the treatment of heart failure: the INOVATE-HF trial. *J. Am. Coll. Cardiol.* 68, 149–158. doi: 10.1016/j.jacc.2016.03.525

Gonzalez-Rosa, J. M., Burns, C. E., and Burns, C. G. (2017). Zebrafish heart regeneration: 15 years of discoveries. *Regeneration* 4, 105–123. doi: 10.1002/reg2.83

Gonzalez-Rosa, J. M., Martin, V., Peralta, M., Torres, M., and Mercader, N. (2011). Extensive scar formation and regression during heart regeneration after cryoinjury in zebrafish. *Development* 138, 1663–1674. doi: 10.1242/dev.060897

Green, G. E., Stertzer, S. H., and Reppert, E. H. (1968). Coronary arterial bypass grafts. *Ann. Thorac. Surg.* 5, 443–450. doi: 10.1016/S0003-4975(10)66377-1

Gruntzig, A. (1978). Transluminal dilatation of coronary-artery stenosis. *Lancet* 1:263. doi: 10.1016/S0140-6736(78)90500-7

Hashimoto, H., Olson, E. N., and Bassel-Duby, R. (2018). Therapeutic approaches for cardiac regeneration and repair. *Nat. Rev. Cardiol.* 15, 585–600. doi: 10.1038/s41569-018-0036-6

Hashimoto, H., Wang, Z., Garry, G. A., Malladi, V. S., Botten, G. A., Ye, W., et al. (2019). Cardiac reprogramming factors synergistically activate genomewide cardiogenic stage-specific enhancers. *Cell Stem Cell* 25, 69–86.e65. doi: 10.1016/j.stem.2019.03.022

Hassink, R. J., Pasumarthi, K. B., Nakajima, H., Rubart, M., Soonpaa, M. H., De La Riviere, A. B., et al. (2008). Cardiomyocyte cell cycle activation improves cardiac function after myocardial infarction. *Cardiovasc. Res.* 78, 18–25. doi: 10.1093/cvr/cvm101

Heallen, T., Morikawa, Y., Leach, J., Tao, G., Willerson, J. T., Johnson, R. L., et al. (2013). Hippo signaling impedes adult heart regeneration. *Development* 140, 4683–4690. doi: 10.1242/dev.102798

Heallen, T., Zhang, M., Wang, J., Bonilla-Claudio, M., Klysik, E., Johnson, R. L., et al. (2011). Hippo pathway inhibits Wnt signaling to restrain cardiomyocyte proliferation and heart size. *Science* 332, 458–461. doi: 10.1126/science.1199010

Hirai, H., Katoku-Kikyo, N., Keirstead, S. A., and Kikyo, N. (2013). Accelerated direct reprogramming of fibroblasts into cardiomyocyte-like cells with the MyoD transactivation domain. *Cardiovasc. Res.* 100, 105–113. doi: 10.1093/cvr/cvt167

Hirai, H., and Kikyo, N. (2014). Inhibitors of suppressive histone modification promote direct reprogramming of fibroblasts to cardiomyocyte-like cells. *Cardiovasc. Res.* 102, 188–190. doi: 10.1093/cvr/cvu023

Hou, P., Li, Y., Zhang, X., Liu, C., Guan, J., Li, H., et al. (2013). Pluripotent stem cells induced from mouse somatic cells by small-molecule compounds. *Science* 341, 651–654. doi: 10.1126/science.1239278

Hsieh, P. C., Segers, V. F., Davis, M. E., Macgillivray, C., Gannon, J., Molkentin, J. D., et al. (2007). Evidence from a genetic fate-mapping study that stem cells refresh adult mammalian cardiomyocytes after injury. *Nat. Med.* 13, 970–974. doi: 10.1038/nm1618

Huang, C., Tu, W., Fu, Y., Wang, J., and Xie, X. (2018). Chemical-induced cardiac reprogramming *in vivo*. *Cell Res.* 28, 686–689. doi: 10.1038/s41422-018-0036-4

Huang, P., He, Z., Ji, S., Sun, H., Xiang, D., Liu, C., et al. (2011). Induction of functional hepatocyte-like cells from mouse fibroblasts by defined factors. *Nature* 475, 386–389. doi: 10.1038/nature10116

Humeres, C., and Frangogiannis, N. G. (2019). Fibroblasts in the infarcted, remodeling, and failing heart. *JACC Basic Transl Sci.* 4, 449–467. doi: 10.1016/j.jacbts.2019.02.006

Hyun, K., Jeon, J., Park, K., and Kim, J. (2017). Writing, erasing and reading histone lysine methylations. *Exp. Mol. Med.* 49:e324. doi: 10.1038/emm.2017.11

Ieda, M., Fu, J. D., Delgado-Olguin, P., Vedantham, V., Hayashi, Y., Bruneau, B. G., et al. (2010). Direct reprogramming of fibroblasts into functional cardiomyocytes by defined factors. *Cell* 142, 375–386. doi: 10.1016/j.cell.2010.07.002

Ifkovits, J. L., Addis, R. C., Epstein, J. A., and Gearhart, J. D. (2014). Inhibition of TGFbeta signaling increases direct conversion of fibroblasts to induced cardiomyocytes. *PLoS ONE* 9:e89678. doi: 10.1371/journal.pone.0089678

Inagawa, K., Miyamoto, K., Yamakawa, H., Muraoka, N., Sadahiro, T., Umei, T., et al. (2012). Induction of cardiomyocyte-like cells in infarct hearts by gene transfer of Gata4, Mef2c, and Tbx5. *Circ. Res.* 111, 1147–1156. doi: 10.1161/CIRCRESAHA.112.271148

Islas, J. F., Liu, Y., Weng, K. C., Robertson, M. J., Zhang, S., Prejusa, A., et al. (2012). Transcription factors ETS2 and MESP1 transdifferentiate human dermal fibroblasts into cardiac progenitors. *Proc. Natl. Acad. Sci. U.S.A.* 109, 13016–13021. doi: 10.1073/pnas.1120299109

Jayawardena, T. M., Egemnazarov, B., Finch, E. A., Zhang, L., Payne, J. A., Pandya, K., et al. (2012). MicroRNA-mediated *in vitro* and *in vivo* direct reprogramming of cardiac fibroblasts to cardiomyocytes. *Circ. Res.* 110, 1465–1473. doi: 10.1161/CIRCRESAHA.112.269035

Jayawardena, T. M., Finch, E. A., Zhang, L., Zhang, H., Hodgkinson, C. P., Pratt, R. E., et al. (2015). MicroRNA induced cardiac reprogramming *in vivo*: evidence for mature cardiac myocytes and improved cardiac function. *Circ. Res.* 116, 418–424. doi: 10.1161/CIRCRESAHA.116.304510

Jones, N. R., Roalfe, A. K., Adoki, I., Hobbs, F. D. R., and Taylor, C. J. (2019). Survival of patients with chronic heart failure in the community: a systematic review and meta-analysis. *Eur. J. Heart Fail.* 21, 1306–1325. doi: 10.1002/ejhf.1594

Jopling, C., Sleep, E., Raya, M., Marti, M., Raya, A., and Izpisua Belmonte, J. C. (2010). Zebrafish heart regeneration occurs by cardiomyocyte dedifferentiation and proliferation. *Nature* 464, 606–609. doi: 10.1038/nature08899

Keeley, E. C., Boura, J. A., and Grines, C. L. (2003). Primary angioplasty versus intravenous thrombolytic therapy for acute myocardial infarction: a quantitative review of 23 randomised trials. *Lancet* 361, 13–20. doi: 10.1016/S0140-6736(03)12113-7

Kikuchi, K., Holdway, J. E., Major, R. J., Blum, N., Dahn, R. D., Begemann, G., et al. (2011). Retinoic acid production by endocardium and epicardium is an injury response essential for zebrafish heart regeneration. *Dev. Cell* 20, 397–404. doi: 10.1016/j.devcel.2011.01.010

Kikuchi, K., Holdway, J. E., Werdich, A. A., Anderson, R. M., Fang, Y., Egnaczyk, G. F., et al. (2010). Primary contribution to zebrafish heart regeneration by gata4(+) cardiomyocytes. *Nature* 464, 601–605. doi: 10.1038/nature08804

Kikuchi, K., and Poss, K. D. (2012). Cardiac regenerative capacity and mechanisms. *Annu. Rev. Cell Dev. Biol.* 28, 719–741. doi: 10.1146/annurev-cellbio-101011-155739

Kimura, W., Xiao, F., Canseco, D. C., Muralidhar, S., Thet, S., Zhang, H. M., et al. (2015). Hypoxia fate mapping identifies cycling cardiomyocytes in the adult heart. *Nature* 523, 226–230. doi: 10.1038/nature14582

Klose, K., Gossen, M., and Stamm, C. (2019). Turning fibroblasts into cardiomyocytes: technological review of cardiac transdifferentiation strategies. *FASEB J.* 33, 49–70. doi: 10.1096/fj.201800712R

Kuhn, B., Del Monte, F., Hajjar, R. J., Chang, Y. S., Lebeche, D., Arab, S., et al. (2007). Periostin induces proliferation of differentiated cardiomyocytes and promotes cardiac repair. *Nat. Med.* 13, 962–969. doi: 10.1038/nm1619

Laflamme, M. A., and Murry, C. E. (2011). Heart regeneration. *Nature* 473, 326–335. doi: 10.1038/nature10147

Leach, J. P., Heallen, T., Zhang, M., Rahmani, M., Morikawa, Y., Hill, M. C., et al. (2017). Hippo pathway deficiency reverses systolic heart failure after infarction. *Nature* 550, 260–264. doi: 10.1038/nature24045

Lesizza, P., Prosdocimo, G., Martinelli, V., Sinagra, G., Zacchigna, S., and Giacca, M. (2017). Single-dose intracardiac injection of pro-regenerative MicroRNAs improves cardiac function after myocardial infarction. *Circ. Res.* 120, 1298–1304. doi: 10.1161/CIRCRESAHA.116.309589

Levy, D., Kenchaiah, S., Larson, M. G., Benjamin, E. J., Kupka, M. J., Ho, K. K., et al. (2002). Long-term trends in the incidence of and survival with heart failure. *N. Engl. J. Med.* 347, 1397–1402. doi: 10.1056/NEJMoa020265

Li, F., Wang, X., Capasso, J. M., and Gerdes, A. M. (1996). Rapid transition of cardiac myocytes from hyperplasia to hypertrophy during postnatal development. *J. Mol. Cell. Cardiol.* 28, 1737–1746. doi: 10.1006/jmcc.1996.0163

Li, M., Zheng, C., Sato, T., Kawada, T., Sugimachi, M., and Sunagawa, K. (2004). Vagal nerve stimulation markedly improves long-term survival after chronic heart failure in rats. *Circulation* 109, 120–124. doi: 10.1161/01.CIR.0000105721.71640.DA

Li, Y., He, L., Huang, X., Bhaloo, S. I., Zhao, H., Zhang, S., et al. (2018). Genetic lineage tracing of nonmyocyte population by dual recombinases. *Circulation* 138, 793–805. doi: 10.1161/CIRCULATIONAHA.118.034250

Li, Z., Song, Y., Liu, L., Hou, N., An, X., Zhan, D., et al. (2017). miR-199a impairs autophagy and induces cardiac hypertrophy through mTOR activation. *Cell Death Differ.* 24, 1205–1213. doi: 10.1038/cdd.2015.95

Liu, Z., Chen, O., Zheng, M., Wang, L., Zhou, Y., Yin, C., et al. (2016). Re-patterning of H3K27me3, H3K4me3 and DNA methylation during fibroblast conversion into induced cardiomyocytes. *Stem Cell Res.* 16, 507–518. doi: 10.1016/j.scr.2016.02.037

Liu, Z., Wang, L., Welch, J. D., Ma, H., Zhou, Y., Vaseghi, H. R., et al. (2017). Single-cell transcriptomics reconstructs fate conversion from fibroblast to cardiomyocyte. *Nature* 551, 100–104. doi: 10.1038/nature24454

Liu, Z., Yue, S., Chen, X., Kubin, T., and Braun, T. (2010). Regulation of cardiomyocyte polyploidy and multinucleation by CyclinG1. *Circ. Res.* 106, 1498–1506. doi: 10.1161/CIRCRESAHA.109.211888

Lopez-Muneta, L., Miranda-Arrubla, J., and Carvajal-Vergara, X. (2020). The future of direct cardiac reprogramming: any GMT cocktail variety? *Int. J. Mol. Sci.* 21:7950. doi: 10.3390/ijms21217950

Lorts, A., Schwanekamp, J. A., Elrod, J. W., Sargent, M. A., and Molkentin, J. D. (2009). Genetic manipulation of periostin expression in the heart does not affect myocyte content, cell cycle activity, or cardiac repair. *Circ. Res.* 104, e1–e7. doi: 10.1161/CIRCRESAHA.108.188649

Ma, H., Wang, L., Yin, C., Liu, J., and Qian, L. (2015). *In vivo* cardiac reprogramming using an optimal single polycistronic construct. *Cardiovasc. Res.* 108, 217–219. doi: 10.1093/cvr/cvv223

Mahmoud, A. I., O'meara, C. C., Gemberling, M., Zhao, L., Bryant, D. M., Zheng, R., et al. (2015). Nerves regulate cardiomyocyte proliferation and heart regeneration. *Dev. Cell* 34, 387–399. doi: 10.1016/j.devcel.2015.06.017

Mathison, M., Gersch, R. P., Nasser, A., Lilo, S., Korman, M., Fourman, M., et al. (2012). *In vivo* cardiac cellular reprogramming efficacy is enhanced by angiogenic preconditioning of the infarcted myocardium with vascular endothelial growth factor. *J. Am. Heart Assoc.* 1:e005652. doi: 10.1161/JAHA.112.005652

Mathison, M., Singh, V. P., Chiuchiolo, M. J., Sanagasetti, D., Mao, Y., Patel, V. B., et al. (2017). *In situ* reprogramming to transdifferentiate fibroblasts into cardiomyocytes using adenoviral vectors: implications for clinical myocardial regeneration. *J. Thorac. Cardiovasc. Surg.* 153, 329–339 e323. doi: 10.1016/j.jtcvs.2016.09.041

Mathison, M., Singh, V. P., Gersch, R. P., Ramirez, M. O., Cooney, A., Kaminsky, S. M., et al. (2014). "Triplet" polycistronic vectors encoding Gata4, Mef2c, and Tbx5 enhances postinfarct ventricular functional improvement compared with singlet vectors. *J. Thorac. Cardiovasc. Surg.* 148, 1656–1664 e1652. doi: 10.1016/j.jtcvs.2014.03.033

Melly, L., Torregrossa, G., Lee, T., Jansens, J. L., and Puskas, J. D. (2018). Fifty years of coronary artery bypass grafting. *J. Thorac. Dis.* 10, 1960–1967. doi: 10.21037/jtd.2018.02.43

Menasche, P. (2020). Cell therapy with human esc-derived cardiac cells: clinical perspectives. *Front. Bioeng. Biotechnol.* 8:601560. doi: 10.3389/fbioe.2020.601560

Miyamoto, K., Akiyama, M., Tamura, F., Isomi, M., Yamakawa, H., Sadahiro, T., et al. (2018). Direct *in vivo* reprogramming with sendai virus vectors improves cardiac function after myocardial infarction. *Cell Stem Cell* 22, 91–103 e105. doi: 10.1016/j.stem.2017.11.010

Mohamed, T. M., Stone, N. R., Berry, E. C., Radzinsky, E., Huang, Y., Pratt, K., et al. (2017). Chemical enhancement of *in vitro* and *in vivo* direct cardiac reprogramming. *Circulation* 135, 978–995. doi: 10.1161/CIRCULATIONAHA.116.024692

Mohamed, T. M. A., Ang, Y. S., Radzinsky, E., Zhou, P., Huang, Y., Elfenbein, A., et al. (2018). Regulation of cell cycle to stimulate adult cardiomyocyte proliferation and cardiac regeneration. *Cell* 173, 104–116 e112. doi: 10.1016/j.cell.2018.02.014

Muraoka, N., Nara, K., Tamura, F., Kojima, H., Yamakawa, H., Sadahiro, T., et al. (2019). Role of cyclooxygenase-2-mediated prostaglandin E2-prostaglandin E receptor 4 signaling in cardiac reprogramming. *Nat. Commun.* 10:674. doi: 10.1038/s41467-019-08626-y

Muraoka, N., Yamakawa, H., Miyamoto, K., Sadahiro, T., Umei, T., Isomi, M., et al. (2014). MiR-133 promotes cardiac reprogramming by directly repressing Snai1 and silencing fibroblast signatures. *EMBO J.* 33, 1565–1581. doi: 10.15252/embj.201387605

Nag, A. C. (1980). Study of non-muscle cells of the adult mammalian heart: a fine structural analysis and distribution. *Cytobios* 28, 41–61.

Nakada, Y., Canseco, D. C., Thet, S., Abdisalaam, S., Asaithamby, A., Santos, C. X., et al. (2017). Hypoxia induces heart regeneration in adult mice. *Nature* 541, 222–227. doi: 10.1038/nature20173

Nam, Y. J., Lubczyk, C., Bhakta, M., Zang, T., Fernandez-Perez, A., Mcanally, J., et al. (2014). Induction of diverse cardiac cell types by reprogramming fibroblasts with cardiac transcription factors. *Development* 141, 4267–4278. doi: 10.1242/dev.114025

Nam, Y. J., Song, K., Luo, X., Daniel, E., Lambeth, K., West, K., et al. (2013). Reprogramming of human fibroblasts toward a cardiac fate. *Proc. Natl. Acad. Sci. U.S.A.* 110, 5588–5593. doi: 10.1073/pnas.1301019110

Naqvi, N., Li, M., Calvert, J. W., Tejada, T., Lambert, J. P., Wu, J., et al. (2014). A proliferative burst during preadolescence establishes the final cardiomyocyte number. *Cell* 157, 795–807. doi: 10.1016/j.cell.2014.03.035

Naso, M. F., Tomkowicz, B., Perry, W. L. III., and Strohl, W. R. (2017). Adeno-Associated Virus (AAV) as a vector for gene therapy. *BioDrugs* 31, 317–334. doi: 10.1007/s40259-017-0234-5

O'gara, P. T., Kushner, F. G., Ascheim, D. D., Casey, D. E. Jr., Chung, M. K., De Lemos, J. A., et al. (2013). 2013 ACCF/AHA guideline for the management of ST-elevation myocardial infarction: executive summary: a report of the American College of Cardiology Foundation/American Heart Association Task Force on Practice Guidelines. *J. Am. Coll. Cardiol.* 61, 485–510. doi: 10.1016/j.jacc.2012.11.018

Paige, S. L., Thomas, S., Stoick-Cooper, C. L., Wang, H., Maves, L., Sandstrom, R., et al. (2012). A temporal chromatin signature in human embryonic

stem cells identifies regulators of cardiac development. *Cell* 151, 221–232. doi: 10.1016/j.cell.2012.08.027

Pasumarthi, K. B., Nakajima, H., Nakajima, H. O., Soonpaa, M. H., and Field, L. J. (2005). Targeted expression of cyclin D2 results in cardiomyocyte DNA synthesis and infarct regression in transgenic mice. *Circ. Res.* 96, 110–118. doi: 10.1161/01.RES.0000152326.91223.4F

Pinto, A. R., Ilinykh, A., Ivey, M. J., Kuwabara, J. T., D'antoni, M. L., Debuque, R., et al. (2016). Revisiting cardiac cellular composition. *Circ. Res.* 118, 400–409. doi: 10.1161/CIRCRESAHA.115.307778

Porrello, E. R., Johnson, B. A., Aurora, A. B., Simpson, E., Nam, Y. J., Matkovich, S. J., et al. (2011a). MiR-15 family regulates postnatal mitotic arrest of cardiomyocytes. *Circ. Res.* 109, 670–679. doi: 10.1161/CIRCRESAHA.111.248880

Porrello, E. R., Mahmoud, A. I., Simpson, E., Hill, J. A., Richardson, J. A., Olson, E. N., et al. (2011b). Transient regenerative potential of the neonatal mouse heart. *Science* 331, 1078–1080. doi: 10.1126/science.1200708

Porrello, E. R., Mahmoud, A. I., Simpson, E., Johnson, B. A., Grinsfelder, D., Canseco, D., et al. (2013). Regulation of neonatal and adult mammalian heart regeneration by the miR-15 family. *Proc. Natl. Acad. Sci. U.S.A.* 110, 187–192. doi: 10.1073/pnas.1208863110

Porrello, E. R., and Olson, E. N. (2014). A neonatal blueprint for cardiac regeneration. *Stem Cell Res.* 13, 556–570. doi: 10.1016/j.scr.2014.06.003

Poss, K. D., Wilson, L. G., and Keating, M. T. (2002). Heart regeneration in zebrafish. *Science* 298, 2188–2190. doi: 10.1126/science.1077857

Protze, S., Khattak, S., Poulet, C., Lindemann, D., Tanaka, E. M., and Ravens, U. (2012). A new approach to transcription factor screening for reprogramming of fibroblasts to cardiomyocyte-like cells. *J. Mol. Cell. Cardiol.* 53, 323–332. doi: 10.1016/j.yjmcc.2012.04.010

Puente, B. N., Kimura, W., Muralidhar, S. A., Moon, J., Amatruda, J. F., Phelps, K. L., et al. (2014). The oxygen-rich postnatal environment induces cardiomyocyte cell-cycle arrest through DNA damage response. *Cell* 157, 565–579. doi: 10.1016/j.cell.2014.03.032

Qian, L., Huang, Y., Spencer, C. I., Foley, A., Vedantham, V., Liu, L., et al. (2012). *In vivo* reprogramming of murine cardiac fibroblasts into induced cardiomyocytes. *Nature* 485, 593–598. doi: 10.1038/nature11044

Raya, A., Koth, C. M., Buscher, D., Kawakami, Y., Itoh, T., Raya, R. M., et al. (2003). Activation of Notch signaling pathway precedes heart regeneration in zebrafish. *Proc Natl Acad Sci U.S.A.* 100(Suppl. 1), 11889–11895. doi: 10.1073/pnas.1834204100

Reuter, S., Soonpaa, M. H., Firulli, A. B., Chang, A. N., and Field, L. J. (2014). Recombinant neuregulin 1 does not activate cardiomyocyte DNA synthesis in normal or infarcted adult mice. *PLoS ONE* 9:e115871. doi: 10.1371/journal.pone.0115871

Riching, A. S., Danis, E., Zhao, Y., Cao, Y., Chi, C., Bagchi, R. A., et al. (2021). Suppression of canonical TGF-? signaling enables GATA4 to interact with H3K27me3 demethylase JMJD3 to promote cardiomyogenesis. *J. Mol. Cell. Cardiol.* 153, 44–59. doi: 10.1016/j.yjmcc.2020.12.005

Riching, A. S., Zhao, Y., Cao, Y., Londono, P., Xu, H., and Song, K. (2018). Suppression of pro-fibrotic signaling potentiates factor-mediated reprogramming of mouse embryonic fibroblasts into induced cardiomyocytes. *J. Vis. Exp.* e57687. doi: 10.3791/57687

Roth, G. A., Johnson, C., Abajobir, A., Abd-Allah, F., Abera, S. F., Abyu, G., et al. (2017). Global, regional, and national burden of cardiovascular diseases for 10 causes, 1990 to 2015. *J. Am. Coll. Cardiol.* 70, 1–25. doi: 10.1016/j.jacc.2017.04.052

Ruel, M., Falk, V., Farkouh, M. E., Freemantle, N., Gaudino, M. F., Glineur, D., et al. (2018). Myocardial revascularization trials. *Circulation* 138, 2943–2951. doi: 10.1161/CIRCULATIONAHA.118.035970

Sadek, H., and Olson, E. N. (2020). Toward the goal of human heart regeneration. *Cell Stem Cell* 26, 7–16. doi: 10.1016/j.stem.2019.12.004

Sdek, P., Zhao, P., Wang, Y., Huang, C. J., Ko, C. Y., Butler, P. C., et al. (2011). Rb and p130 control cell cycle gene silencing to maintain the postmitotic phenotype in cardiac myocytes. *J. Cell Biol.* 194, 407–423. doi: 10.1083/jcb.201012049

Senyo, S. E., Steinhauser, M. L., Pizzimenti, C. L., Yang, V. K., Cai, L., Wang, M., et al. (2013). Mammalian heart renewal by pre-existing cardiomyocytes. *Nature* 493, 433–436. doi: 10.1038/nature11682

Shapiro, S. D., Ranjan, A. K., Kawase, Y., Cheng, R. K., Kara, R. J., Bhattacharya, R., et al. (2014). Cyclin A2 induces cardiac regeneration after myocardial infarction through cytokinesis of adult cardiomyocytes. *Sci. Transl. Med.* 6:224ra227. doi: 10.1126/scitranslmed.3007668

Sibbald, B. (2001). Death but one unintended consequence of gene-therapy trial. *CMAJ* 164:1612.

Singh, V. P., Mathison, M., Patel, V., Sanagasetti, D., Gibson, B. W., Yang, J., et al. (2016). MiR-590 promotes transdifferentiation of porcine and human fibroblasts toward a cardiomyocyte-like fate by directly repressing specificity protein 1. *J. Am. Heart Assoc.* 5:e003922. doi: 10.1161/JAHA.116.003922

Singh, V. P., Pinnamaneni, J. P., Pugazenthi, A., Sanagasetti, D., Mathison, M., Wang, K., et al. (2020). Enhanced generation of induced cardiomyocytes using a small-molecule cocktail to overcome barriers to cardiac cellular reprogramming. *J. Am. Heart Assoc.* 9:e015686. doi: 10.1161/JAHA.119.015686

Song, K., Nam, Y. J., Luo, X., Qi, X., Tan, W., Huang, G. N., et al. (2012). Heart repair by reprogramming non-myocytes with cardiac transcription factors. *Nature* 485, 599–604. doi: 10.1038/nature11139

Stone, G. W., Martin, J. L., De Boer, M. J., Margheri, M., Bramucci, E., Blankenship, J. C., et al. (2009). Effect of supersaturated oxygen delivery on infarct size after percutaneous coronary intervention in acute myocardial infarction. *Circ. Cardiovasc. Interv.* 2, 366–375. doi: 10.1161/CIRCINTERVENTIONS.108.840066

Stratton, M. S., Bagchi, R. A., Felisbino, M. B., Hirsch, R. A., Smith, H. E., Riching, A. S., et al. (2019). Dynamic chromatin targeting of BRD4 stimulates cardiac fibroblast activation. *Circ. Res.* 125, 662–677. doi: 10.1161/CIRCRESAHA.119.315125

Sultana, N., Magadum, A., Hadas, Y., Kondrat, J., Singh, N., Youssef, E., et al. (2017). Optimizing cardiac delivery of modified mRNA. *Mol. Ther.* 25, 1306–1315. doi: 10.1016/j.ymthe.2017.03.016

Takahashi, K., Tanabe, K., Ohnuki, M., Narita, M., Ichisaka, T., Tomoda, K., et al. (2007). Induction of pluripotent stem cells from adult human fibroblasts by defined factors. *Cell* 131, 861–872. doi: 10.1016/j.cell.2007.11.019

Takahashi, K., and Yamanaka, S. (2006). Induction of pluripotent stem cells from mouse embryonic and adult fibroblast cultures by defined factors. *Cell* 126, 663–676. doi: 10.1016/j.cell.2006.07.024

Tallquist, M. D., and Molkentin, J. D. (2017). Redefining the identity of cardiac fibroblasts. *Nat. Rev. Cardiol.* 14, 484–491. doi: 10.1038/nrcardio.2017.57

Tang, Y., Nyengaard, J. R., Andersen, J. B., Baandrup, U., and Gundersen, H. J. (2009). The application of stereological methods for estimating structural parameters in the human heart. *Anat. Rec.* 292, 1630–1647. doi: 10.1002/ar.20952

Tao, G., Kahr, P. C., Morikawa, Y., Zhang, M., Rahmani, M., Heallen, T. R., et al. (2016). Pitx2 promotes heart repair by activating the antioxidant response after cardiac injury. *Nature* 534, 119–123. doi: 10.1038/nature17959

Testa, G., Russo, M., Di Benedetto, G., Barbato, M., Parisi, S., Pirozzi, F., et al. (2020). Bmi1 inhibitor PTC-209 promotes chemically-induced direct cardiac reprogramming of cardiac fibroblasts into cardiomyocytes. *Sci. Rep.* 10:7129. doi: 10.1038/s41598-020-63992-8

Tillett, W. S., and Garner, R. L. (1933). The fibrinolytic activity of hemolytic streptococci. *J. Exp. Med.* 58, 485–502. doi: 10.1084/jem.58.4.485

Travers, J. G., Kamal, F. A., Robbins, J., Yutzey, K. E., and Blaxall, B. C. (2016). Cardiac fibrosis: the fibroblast awakens. *Circ. Res.* 118, 1021–1040. doi: 10.1161/CIRCRESAHA.115.306565

Umei, T. C., Yamakawa, H., Muraoka, N., Sadahiro, T., Isomi, M., Haginiwa, S., et al. (2017). Single-construct polycistronic doxycycline-inducible vectors improve direct cardiac reprogramming and can be used to identify the critical timing of transgene expression. *Int. J. Mol. Sci.* 18:1805. doi: 10.3390/ijms18081805

Vierbuchen, T., Ostermeier, A., Pang, Z. P., Kokubu, Y., Sudhof, T. C., and Wernig, M. (2010). Direct conversion of fibroblasts to functional neurons by defined factors. *Nature* 463, 1035–1041. doi: 10.1038/nature08797

Von Gise, A., Lin, Z., Schlegelmilch, K., Honor, L. B., Pan, G. M., Buck, J. N., et al. (2012). YAP1, the nuclear target of Hippo signaling, stimulates heart growth through cardiomyocyte proliferation but not hypertrophy. *Proc. Natl. Acad. Sci. U.S.A.* 109, 2394–2399. doi: 10.1073/pnas.1116136109

Wada, R., Muraoka, N., Inagawa, K., Yamakawa, H., Miyamoto, K., Sadahiro, T., et al. (2013). Induction of human cardiomyocyte-like cells from

fibroblasts by defined factors. *Proc. Natl. Acad. Sci. U.S.A.* 110, 12667–12672. doi: 10.1073/pnas.1304053110

Wamstad, J. A., Alexander, J. M., Truty, R. M., Shrikumar, A., Li, F., Eilertson, K. E., et al. (2012). Dynamic and coordinated epigenetic regulation of developmental transitions in the cardiac lineage. *Cell* 151, 206–220. doi: 10.1016/j.cell.2012.07.035

Wang, H., Cao, N., Spencer, C. I., Nie, B., Ma, T., Xu, T., et al. (2014). Small molecules enable cardiac reprogramming of mouse fibroblasts with a single factor, Oct4. *Cell Rep.* 6, 951–960. doi: 10.1016/j.celrep.2014.01.038

Wang, J., Jiang, X., Zhao, L., Zuo, S., Chen, X., Zhang, L., et al. (2020a). Lineage reprogramming of fibroblasts into induced cardiac progenitor cells by CRISPR/Cas9-based transcriptional activators. *Acta Pharm. Sin. B* 10, 313–326. doi: 10.1016/j.apsb.2019.09.003

Wang, J., Panakova, D., Kikuchi, K., Holdway, J. E., Gemberling, M., Burris, J. S., et al. (2011). The regenerative capacity of zebrafish reverses cardiac failure caused by genetic cardiomyocyte depletion. *Development* 138, 3421–3430. doi: 10.1242/dev.068601

Wang, L., Huang, P., Near, D., Ravi, K., Xu, Y., Liu, J., et al. (2020b). Isoform specific effects of Mef2C during direct cardiac reprogramming. *Cells* 9:268. doi: 10.3390/cells9020268

Wang, L., Liu, Z., Yin, C., Asfour, H., Chen, O., Li, Y., et al. (2015a). Stoichiometry of Gata4, Mef2c, and Tbx5 influences the efficiency and quality of induced cardiac myocyte reprogramming. *Circ. Res.* 116, 237–244. doi: 10.1161/CIRCRESAHA.116.305547

Wang, L., Liu, Z., Yin, C., Zhou, Y., Liu, J., and Qian, L. (2015b). Improved generation of induced cardiomyocytes using a polycistronic construct expressing optimal ratio of Gata4, Mef2c and Tbx5. *J. Vis. Exp.* e53426. doi: 10.3791/53426

Wang, L., Ma, H., Huang, P., Xie, Y., Near, D., Wang, H., et al. (2020c). Down-regulation of Beclin1 promotes direct cardiac reprogramming. *Sci. Transl. Med.* 12:eaay7856. doi: 10.1126/scitranslmed.aay7856

Weintraub, W. S., Mandel, L., and Weiss, S. A. (2013). Antiplatelet therapy in patients undergoing percutaneous coronary intervention: economic considerations. *Pharmacoeconomics* 31, 959–970. doi: 10.1007/s40273-013-0088-8

White, I. A., Gordon, J., Balkan, W., and Hare, J. M. (2015). Sympathetic reinnervation is required for mammalian cardiac regeneration. *Circ. Res.* 117, 990–994. doi: 10.1161/CIRCRESAHA.115.307465

Wilson-Rawls, J., Molkentin, J. D., Black, B. L., and Olson, E. N. (1999). Activated notch inhibits myogenic activity of the MADS-Box transcription factor myocyte enhancer factor 2C. *Mol. Cell. Biol.* 19, 2853–2862. doi: 10.1128/MCB.19.4.2853

Wu, Z., Asokan, A., and Samulski, R. J. (2006). Adeno-associated virus serotypes: vector toolkit for human gene therapy. *Mol. Ther.* 14, 316–327. doi: 10.1016/j.ymthe.2006.05.009

Xin, M., Kim, Y., Sutherland, L. B., Murakami, M., Qi, X., Mcanally, J., et al. (2013). Hippo pathway effector Yap promotes cardiac regeneration. *Proc. Natl. Acad. Sci. U.S.A.* 110, 13839–13844. doi: 10.1073/pnas.1313192110

Yamakawa, H., Muraoka, N., Miyamoto, K., Sadahiro, T., Isomi, M., Haginiwa, S., et al. (2015). Fibroblast growth factors and vascular endothelial growth factor promote cardiac reprogramming under defined conditions. *Stem Cell Rep.* 5, 1128–1142. doi: 10.1016/j.stemcr.2015.10.019

Ye, L., D'agostino, G., Loo, S. J., Wang, C. X., Su, L. P., Tan, S. H., et al. (2018). Early regenerative capacity in the porcine heart. *Circulation* 138, 2798–2808. doi: 10.1161/CIRCULATIONAHA.117.031542

Yellon, D. M., and Hausenloy, D. J. (2007). Myocardial reperfusion injury. *N. Engl. J. Med.* 357, 1121–1135. doi: 10.1056/NEJMra071667

Zacchigna, S., Zentilin, L., and Giacca, M. (2014). Adeno-associated virus vectors as therapeutic and investigational tools in the cardiovascular system. *Circ. Res.* 114, 1827–1846. doi: 10.1161/CIRCRESAHA.114.302331

Zhang, Z., and Nam, Y. J. (2020). Assessing cardiac reprogramming using high content imaging analysis. *J. Vis. Exp.* e61859. doi: 10.3791/61859

Zhang, Z., Zhang, A. D., Kim, L. J., and Nam, Y. J. (2019a). Ensuring expression of four core cardiogenic transcription factors enhances cardiac reprogramming. *Sci. Rep.* 9:6362. doi: 10.1038/s41598-019-42945-w

Zhang, Z., Zhang, W., and Nam, Y. J. (2019b). Stoichiometric optimization of Gata4, Hand2, Mef2c, and Tbx5 expression for contractile cardiomyocyte reprogramming. *Sci. Rep.* 9:14970. doi: 10.1038/s41598-019-51536-8

Zhao, L., Borikova, A. L., Ben-Yair, R., Guner-Ataman, B., Macrae, C. A., Lee, R. T., et al. (2014). Notch signaling regulates cardiomyocyte proliferation during zebrafish heart regeneration. *Proc. Natl. Acad. Sci. U.S.A.* 111, 1403–1408. doi: 10.1073/pnas.1311705111

Zhao, Y., Londono, P., Cao, Y., Sharpe, E. J., Proenza, C., O'rourke, R., et al. (2015). High-efficiency reprogramming of fibroblasts into cardiomyocytes requires suppression of pro-fibrotic signalling. *Nat. Commun.* 6:8243. doi: 10.1038/ncomms9243

Zhao, Y. Y., Sawyer, D. R., Baliga, R. R., Opel, D. J., Han, X., Marchionni, M. A., et al. (1998). Neuregulins promote survival and growth of cardiac myocytes. Persistence of ErbB2 and ErbB4 expression in neonatal and adult ventricular myocytes. *J. Biol. Chem.* 273, 10261–10269. doi: 10.1074/jbc.273.17.10261

Zhou, H., Dickson, M. E., Kim, M. S., Bassel-Duby, R., and Olson, E. N. (2015). Akt1/protein kinase B enhances transcriptional reprogramming of fibroblasts to functional cardiomyocytes. *Proc. Natl. Acad. Sci. U.S.A.* 112, 11864–11869. doi: 10.1073/pnas.1516237112

Zhou, H., Morales, M. G., Hashimoto, H., Dickson, M. E., Song, K., Ye, W., et al. (2017). ZNF281 enhances cardiac reprogramming by modulating cardiac and inflammatory gene expression. *Genes Dev.* 31, 1770–1783. doi: 10.1101/gad.305482.117

Zhou, Y., Alimohamadi, S., Wang, L., Liu, Z., Wall, J. B., Yin, C., et al. (2018). A loss of function screen of epigenetic modifiers and splicing factors during early stage of cardiac reprogramming. *Stem Cells Int.* 2018:3814747. doi: 10.1155/2018/3814747

Zhou, Y., Liu, Z., Welch, J. D., Gao, X., Wang, L., Garbutt, T., et al. (2019). Single-cell transcriptomic analyses of cell fate transitions during human cardiac reprogramming. *Cell Stem Cell* 25, 149–164 e149. doi: 10.1016/j.stem.2019.05.020

Zhou, Y., Wang, L., Vaseghi, H. R., Liu, Z., Lu, R., Alimohamadi, S., et al. (2016). Bmi1 is a key epigenetic barrier to direct cardiac reprogramming. *Cell Stem Cell* 18, 382–395. doi: 10.1016/j.stem.2016.02.003

Zhu, M. M., Feit, A., Chadow, H., Alam, M., Kwan, T., and Clark, L. T. (2001). Primary stent implantation compared with primary balloon angioplasty for acute myocardial infarction: a meta-analysis of randomized clinical trials. *Am. J. Cardiol.* 88, 297–301. doi: 10.1016/S0002-9149(01)01645-9

**Conflict of Interest:** The authors declare that the research was conducted in the absence of any commercial or financial relationships that could be construed as a potential conflict of interest.

frontiers in Bioengineering and Biotechnology

REVIEW
published: 25 March 2021
doi: 10.3389/fbioe.2021.599928

# Cardiac Fibroblasts and Myocardial Regeneration

*Wangping Chen[1,2], Weihua Bian[1], Yang Zhou[1] and Jianyi Zhang[1]**

*[1] Department of Biomedical Engineering, School of Medicine and School of Engineering, University of Alabama at Birmingham, Birmingham, AL, United States, [2] Department of Cardiovascular Surgery, The Second Xiangya Hospital, Central South University, Changsha, China*

The billions of cardiomyocytes lost to acute myocardial infarction (MI) cannot be replaced by the limited regenerative capacity of adult mammalian hearts, and despite decades of research, there are still no clinically effective therapies for remuscularizing and restoring damaged myocardial tissue. Although the majority of the cardiac mass is composed of cardiomyocytes, cardiac fibroblasts (CFs) are one type of most numerous cells in the heart and the primary drivers of fibrosis, which prevents ventricular rupture immediately after MI but the fibrotic scar expansion and LV dilatation can eventually lead to heart failure. However, embryonic CFs produce cytokines that can activate proliferation in cultured cardiomyocytes, and the structural proteins produced by CFs may regulate cardiomyocyte cell-cycle activity by modulating the stiffness of the extracellular matrix (ECM). CFs can also be used to generate induced-pluripotent stem cells and induced cardiac progenitor cells, both of which can differentiate into cardiomyocytes and vascular cells, but cardiomyocytes appear to be more readily differentiated from iPSCs that have been reprogrammed from CFs than from other cell types. Furthermore, the results from recent studies suggest that cultured CFs, as well as the CFs present in infarcted hearts, can be reprogrammed directly into cardiomyocytes. This finding is very exciting as should we be able to successfully increase the efficiency of this reprogramming, we could remuscularize the injured ventricle and restore the LV function without need the transplantation of cells or cell products. This review summarizes the role of CFs in the innate response to MI and how their phenotypic plasticity and involvement in ECM production might be manipulated to improve cardiac performance in injured hearts.

**Keywords: cardiac fibroblast, myocardial infarction, extracellular matrix, stem cells, reprogramming**

OPEN ACCESS

***Edited by:***
*Diego Mantovani, Laval University, Canada*

***Reviewed by:***
*Xing Fu, Louisiana State University Agricultural Center, United States*
*Bryan Brown, University of Pittsburgh, United States*

***Correspondence:**
*Jianyi Zhang*
*jayzhang@uab.edu*

***Specialty section:***
*This article was submitted to Tissue Engineering and Regenerative Medicine, a section of the journal Frontiers in Bioengineering and Biotechnology*

***Received:*** *28 August 2020*
***Accepted:*** *05 March 2021*
***Published:*** *25 March 2021*

***Citation:***
*Chen W, Bian W, Zhou Y and Zhang J (2021) Cardiac Fibroblasts and Myocardial Regeneration. Front. Bioeng. Biotechnol. 9:599928. doi: 10.3389/fbioe.2021.599928*

## INTRODUCTION

The limited regenerative ability of adult mammalian hearts (Porrello et al., 2011) cannot replace the millions of cardiomyocytes that are lost to myocardial infarction (MI) (Prabhu and Frangogiannis, 2016). Instead, the damaged tissue is remodeled and replaced by non-contractile scar tissue, which impedes cardiac function and can eventually lead to catastrophic heart failure (HF) (Wang and Guan, 2010). HF is among the leading causes of hospitalization and death worldwide (Cahill et al., 2017) and is likely to become even more prevalent in response to lifestyle changes and the overall aging of the population. Currently, the available treatment options are generally

limited to pharmacological therapies and surgical interventions such as stents and coronary artery bypass graft surgery, which can delay disease progression but fail to increase the number of functional cardiomyocytes and, consequently, do not address the root cause of the decline in cardiac performance (Lin and Pu, 2014). Thus, the development of novel strategies for replacing the myocardial scar with active contractile tissue is perhaps the fundamental goal of cardiovascular research (Carvalho and de Carvalho, 2010).

Although the majority of the cardiac mass is composed of cardiomyocytes (Zhou and Pu, 2016), cardiac fibroblasts (CFs) are one type of the most numerous cells in the heart (Sadoshima and Weiss, 2014). Their exact proportion varies depending on species and age, and measurements can also be influenced by the techniques and marker(s) used for identification (Zak, 1974; Nag, 1980; Banerjee et al., 2007), because CFs can assume a variety of phenotypes and descend from numerous developmental origins (Sadoshima and Weiss, 2014). Nevertheless, CFs can be broadly defined as mesenchymal cells that reside in the cardiac interstitium (Souders et al., 2009), and they are the primary drivers of remodeling in response to both physiological and pathological conditions (Sadoshima and Weiss, 2014). Thus, they serve a critical role in the immediate aftermath of MI by producing the scar tissue required to maintain the structural integrity of the chamber walls and prevent rupture, but the scar also impedes contractile performance, disrupts electromechanical coupling (which can generate arrhythmias), and induces mechanical stress that can lead to additional cardiomyocyte toxicity and infarct expansion.

The healing process after MI can be divided into three distinct but overlapping stages–inflammation, proliferation, and maturity–and each stage is associated with a different CF phenotype (Frangogiannis, 2006; **Figure 1**). The inflammatory phenotype is characterized by the secretion of cytokines and chemotactic factors that promote the infiltration of neutrophils and monocytes (Sandanger et al., 2013; Shinde and Frangogiannis, 2014), which clear cellular debris, and by the production of matrix metalloproteinases (MMPs), which initiate remodeling by degrading the existing extracellular matrix (ECM). In the proliferative stage, CFs transform into myofibroblasts, which express the contractile protein α-smooth muscle actin (α-SMA), vigorously proliferate, and become the dominant effector molecules of the repair process by secreting both anti-inflammatory and pro-angiogenic molecules, and by generating the new ECM (Shinde and Frangogiannis, 2014; Ma et al., 2017). Unlike fibroblasts, myofibroblasts are specialized cells that possess a more contractile and synthetic phenotype than fibroblasts. The lineage tracing of Periostin+ myofibroblasts did not show expression of the endothelial cell marker CD31 after MI (Kanisicak et al., 2016), suggesting the limited plasticity of myofibroblasts to transdifferentiate to other cardiac cell. CFs continue to produce anti-inflammatory cytokines (e.g., interleukin 10) and pro-fibrotic factors (e.g., transforming growth factor β1) during the early maturation stage (Chen and Frangogiannis, 2013), and then the number of myofibroblasts declines as the cells transition to a phenotype that promotes scar maturation and maintains homeostasis in the remodeled myocardium (Ma et al., 2017). More recently, Fu et al. (2018) dissected the dynamic states of CFs during post-myocardial infarction remodeling by lineage tracing of cells expressing *Tcf21*, *Postn* and *Acta2* genes. Consistently, they identified proliferating activated fibroblasts early at post-MI day 2–4 and the α-SMA+ myofibroblasts at day 3–7 after injury. They also discovered a new differentiated state of fibroblasts in the mature scar beyond 10 days after injury. These CFs, termed as matrifibrocytes, highly express bone and cartilage-related ECM genes like *Chad*, *Cilp2* and *Comp*, which are common gene signatures of chondrocytes and osteoblasts, making CFs more specialized to support mature scar. Importantly, deletion of these cells in the scar impaired the cardiac function, suggesting an indispensable role of matrifibrocytes in the homeostasis of scarred hearts.

While both the immediate benefits and long-term, often detrimental, effects of CFs on cardiac performance after an infarct event are well established, efforts to improve myocardial recovery via CF-based therapies have also become a prominent field of research. The remainder of this review focuses on how the role of CFs in ECM production might be exploited to limit infarct size and manipulate cardiomyocyte activity and proliferation, as well as the reprogramming of CFs into pluripotent cells or, perhaps, directly into cardiomyocytes (**Figure 2**).

## CF-DERIVED EXTRACELLULAR MATRIX IN MYOCARDIAL REPAIR

Cardiac fibroblasts produce growth factors and other signaling molecules that directly regulate cardiomyocyte function (Torre-Amione et al., 1996; Long, 2001; Baudino et al., 2008), while also controlling the synthesis and degradation of the ECM (Baxter et al., 2008; Snider et al., 2009; Souders et al., 2009). The cardiac ECM was once believed to function primarily as an inert scaffold but is now known to be an ever-changing and plastic microenvironment that has a vital role in cardiac function and regeneration. The mammalian cardiac ECM consists of structural components such as collagens, fibronectin, tenascin, elastin, laminins, proteoglycans, and glycosaminoglycans (Lockhart et al., 2011), as well as dynamic, non-structural (i.e., matricellular) proteins that participate in critical signal transduction pathways (Rienks et al., 2014; Frangogiannis, 2017), some of which appear to regulate cardiomyocyte proliferation. Embryonic CFs produce fibronectin and heparin-binding EGF-like growth factor, which activate proliferation in cultured mouse cardiomyocytes via β1-integrin signaling (Ieda et al., 2009), while neonatal rat ventricular cells were significantly more proliferative when cultured with fetal cardiac ECM than with either neonatal or adult cardiac ECM, and the increase corresponded with 6- to 7-fold higher measures of fibronectin and periostin (Williams et al., 2014). Periostin is secreted by CFs after MI or pressure overload injury (Shimazaki et al., 2008) and has been shown to improve infarct size and cardiac function in infarcted rat hearts by activating integrin- and phosphatidylinositol-3 kinase (PI3K) signaling, which subsequently induces cardiomyocyte cell-cycle re-entry (Kuhn et al., 2007), while periostin deficiencies

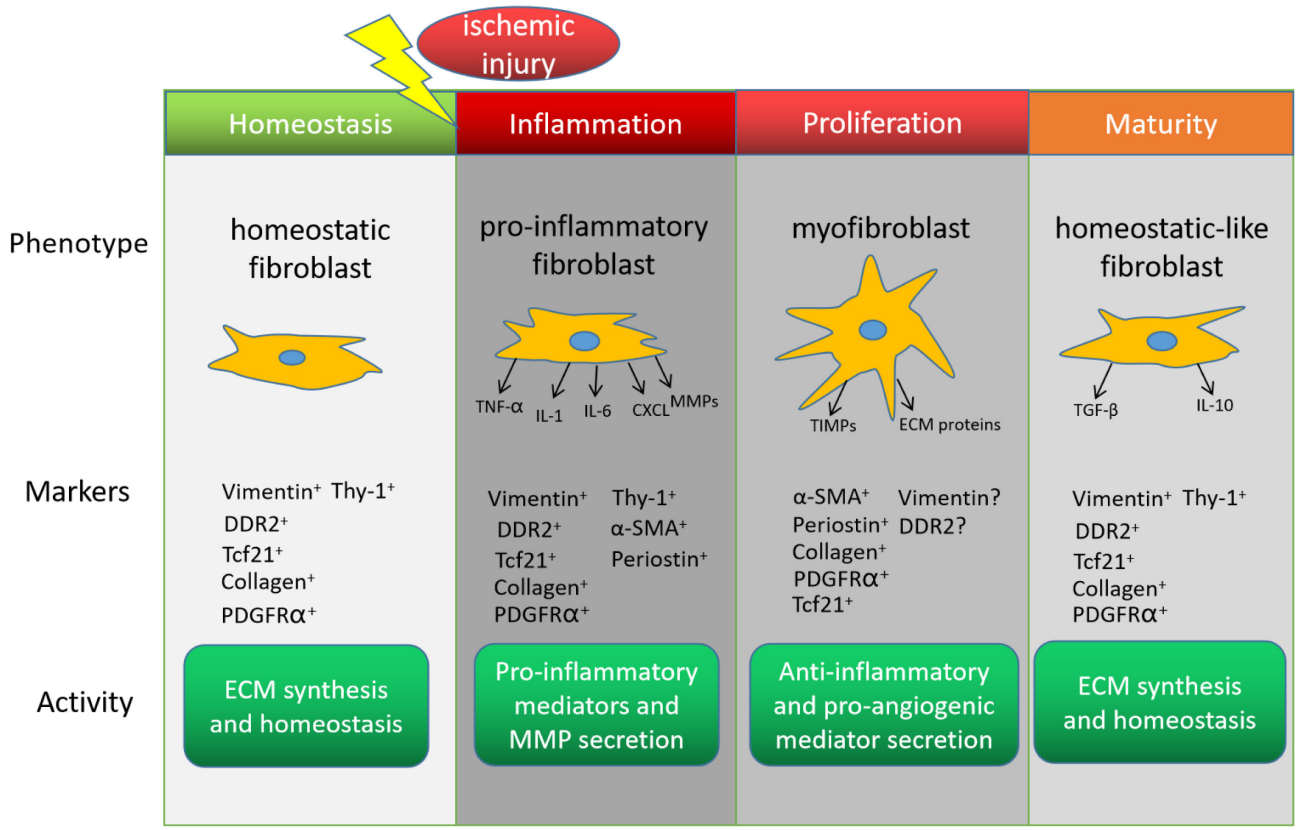


**FIGURE 1 |** Cardiac fibroblasts (CFs) in the endogenous response to myocardial infarction. The phenotype, marker expression, and activity of CFs change during recovery from myocardial infarction. DDR2, discoidin domain receptor tyrosine kinase 2; Tcf21, transcription factor 21; PDGFRα, platelet-derived growth factor receptor α; α-SMA, α smooth-muscle actin; TNF-α, tumor necrosis factor α; IL, interleukin; CXCL, C-X-C motif ligand; MMP, matrix metalloproteinase; ECM, extracellular matrix; TIMP, tissue inhibitors of metalloproteinase; TGF-β, transforming growth factor β.

inhibited myocardial regeneration after MI in neonatal mice (Chen et al., 2017).

The structural ECM components produced by CFs can also modulate cardiac regeneration by altering ECM stiffness (Yahalom-Ronen et al., 2015). Stiffness of the ECM increases with the deposition and crosslinking of collagen, elastin, and laminin (Notari et al., 2018; Frangogiannis, 2019), and ECM stiffness and maturation induce cell-cycle arrest in neonatal rat and mouse cardiomyocytes, whereas more compliant ECM (i.e., ECM that can accommodate greater blood volume with smaller increases in pressure) promotes cardiomyocyte proliferation and cytokinesis (Yahalom-Ronen et al., 2015). Furthermore, the regenerative capacity of neonatal mouse hearts in response to apical resection is greatest on the first day after birth (P1) and declines rapidly thereafter (Porrello et al., 2011; Lam and Sadek, 2018; Notari et al., 2018), and analyses of the transcriptomes of P1 and P2 mice identified significant differences in the expression of ECM and cytoskeletal genes that contribute to ECM stiffness. Notably, cardiac regenerative capacity can be restored in mice by pharmacologically reducing stiffness on P3 (Notari et al., 2018), and the composition and stiffness of the ECM may also influence the myogenic differentiation of stem and bone-marrow–derived cells (Engler et al., 2006; Zhang et al., 2009; Wang et al., 2010; Hastings et al., 2015). Increases in cardiomyocyte cell-cycle activity have also been observed in patients after implantation of a left-ventricular assist device, which can mimic increases in myocardial compliance by reducing the hemodynamic load (i.e., mechanical unloading) (Canseco et al., 2015).

The role of the ECM in cardiac function and cardiomyocyte cell-cycle activity also has important implications for the use of CFs in cardiac tissue engineering, particularly for the development of thicker and vascularized constructs (Shimizu et al., 2006; Novosel et al., 2011; Haraguchi et al., 2012). Both the functional and biochemical properties of engineered cardiac tissues composed of CFs, cardiomyocytes, and a biorubber scaffold improved when the two cell populations were added sequentially (CFs first, then cardiomyocytes) rather than simultaneously (Radisic et al., 2006), and the structural support provided by dermal fibroblasts improved cell-cell interactions and the synchronous beating of cardiomyocytes in injectable beating mini heart tissues (Guerzoni et al., 2019). CFs have also been combined with cardiomyocytes and endothelial cells to produce native-like three-dimensional (3D) cardiac tissue with oriented structures and a vascular network, which is crucial for cell survival after transplantation (Tsukamoto et al., 2020), and the ECM produced by CFs has been used as a transfer medium to

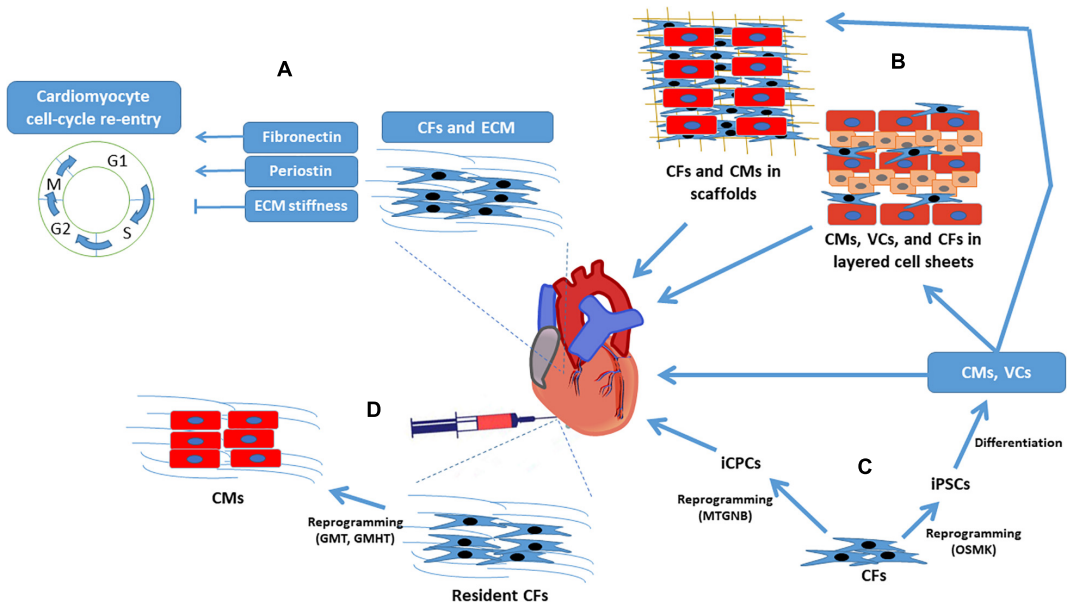


**FIGURE 2 |** Cardiac fibroblasts for regenerative myocardial therapy. Clockwise from top left: **(A)** CFs secrete cytokines that directly regulate cardiomyocyte cell-cycle activity, and the structural proteins produced by CFs influence cardiomyocyte proliferation by modulating ECM stiffness. **(B)** CFs have a supportive role in engineered myocardial tissues and **(C)** can be reprogrammed into iPSCs or iCPCs; iPSCs are differentiated into cardiomyocytes, endothelial cells, and smooth-muscle cells before administration to infarcted hearts or assembly into engineered myocardial tissues, whereas iCPCs spontaneously differentiate into cardiac cells after delivery to the heart. **(D)** CFs can also be reprogrammed directly into cardiomyocyte-like cells both *in-vitro* and *in-vivo*. CF, cardiac fibroblast; CM, cardiomyocyte; ECM, extracellular matrix; GHMT, Gata4, Hand, Mef2c, Tbx5; GMT, Gata4, Mef2c, Tbx5; iCPC, induced cardiac progenitor cell; iPSC, induced pluripotent stem cell; MTGNB, Mesp1, Tbx5, Gata4, Nkx2.5, Baf60c; OSMK, Oct4, Sox2, c-Myc, Klf4; VC, vascular cell.

improve the retention of transplanted mesenchymal stem cells in ischemic myocardium (Schmuck et al., 2014).

## CFs AS A SOURCE OF INDUCED-PLURIPOTENT CELLS

Because CFs are available in large numbers and phenotypically plastic, they are particularly useful for cell therapy and tissue engineering. The most common strategies involve reprogramming the cells into either induced pluripotent stem cells (iPSCs) or cardiac progenitor cells (iCPCs). iPSCs have an unlimited capacity for self-renewal and can differentiate into cells of any lineage, but have also been associated with tumorigenesis; thus, they are typically differentiated into cardiomyocytes and other cardiac-lineage cells before administration to infarcted hearts or assembly into engineered myocardial tissues. iPSCs were first generated via the overexpression of four transcription factors (Oct4, Sox2, Klf4, and c-Myc) in mouse and human dermal fibroblasts (Takahashi and Yamanaka, 2006; Takahashi et al., 2007), and have also been generated from endothelial cells (Lagarkova et al., 2010), hair-follicle cells (Illing et al., 2013), keratinocytes (Aasen et al., 2008) and peripheral blood cells (Okita et al., 2013). However, cardiomyocytes appear to be more readily differentiated from iPSCs that have been reprogrammed from human CFs (hciPSCs) than from other cell types: the purity of hciPSC-derived cardiomyocytes (hciPSC-CMs) exceeded 92% without any subsequent selection procedures, whereas iPSCs reprogrammed from human dermal FBs (hdiPSCs) or blood mononuclear cells ($h_{BMC}$iPSCs) yielded cardiomyocyte populations that were only 60–85% pure (Ye et al., 2013; Zhang et al., 2015). This difference in differentiation efficiency can likely be attributed to the presence of epigenetic factors that the iPSCs retained from their tissues of origin (Kim et al., 2010; Noguchi et al., 2018; Toubiana et al., 2019). Furthermore, the $Ca^{2+}$-handling profile of the hciPSC-CMs was more cardiac-like than the profiles of cardiomyocytes differentiated from hdiPSCs or $h_{BMC}$iPSCs, and when sheets of hciPSC-CMs were transplanted into infarcted mouse hearts, the rate of engraftment was exceptionally high (>30%) 28 days later; the treatment was also associated with significant improvements in cardiac contractile function. It is also interesting to notice that, as an unwanted limit of current cardiac differentiation protocol, non-cardiomyocytes cardiac cells (NMCCs) also emerge during iPSC differentiation and easily to be transdifferentiated into myofibroblast cells. We found that the inhibition of myofibroblast cells derived from NMCCs could improve the efficacy of cardiac cell therapy (Gao et al., 2018).

Cardiac progenitor cells (iCPCs) are also highly proliferative and multipotent, but their intrinsic capacity for differentiation is restricted to the cardiac mesoderm lineage (Masino et al., 2004), and they can be delivered directly to the heart. Mouse CFs were first stably reprogrammed into iCPCs via the overexpression of five (Mesp1, Tbx5, Gata4, Nkx2.5, and Baf60c), or as many as eleven (Mesp1, Mesp2, Gata4, Gata6, Baf60c, SRF, Isl1, Nkx2.5, Irx4, Tbx5, and Tbx20), cardiac transcription factors (Lalit

et al., 2016), and the yield of iCPCs was further increased by including 6-bromoindirubin-30-oxime (a canonical Wnt activator) and leukemia inhibitory factor (LIF; a JAK/STAT activator) during the reprogramming process. Both *in-vitro* and *in-vivo* studies confirmed that the iCPCs could differentiate into cardiomyocytes, endothelial cells (ECs), and smooth-muscle cells (SMCs), and iCPC transplantation significantly improved cardiac function and survival in a mouse MI model with no evidence of tumor formation. iCPCs also repopulated ECM scaffolds and differentiated into cardiomyocytes, ECs, and SMCs when injected through an aortic cannula into decellularized whole mouse hearts (Alexanian et al., 2020). Thus, both iPSCs and iCPCs dedifferentiated from CFs may provide a readily available, safe, and scalable source of contractile and vascular cells for regenerative myocardial therapies.

## REPROGRAMMING CFs INTO INDUCED CARDIOMYOCYTES

Cardiac fibroblasts can also be directly reprogrammed into cardiomyocyte-like cells [induced cardiomyocytes (iCMs)] without first passing through an intermediate iPSC stage; however, the technique is quite new, so the optimal reprogramming protocol has yet to be identified and may vary depending upon how the cells will be used after reprogramming. iCMs were first generated in 2010 via the overexpression of three developmental transcription factors (Gata4, Mef2c, and Tbx5; i.e., the GMT protocol) in CFs: the reprogrammed cells expressed cardiomyocyte-specific markers, contracted spontaneously, and displayed cardiomyocyte-like electrophysiological properties and global gene-expression profiles (Ieda et al., 2010). Subsequent work demonstrated that the efficiency of the GMT protocol could be improved significantly by combining relatively high levels of Mef2c with lower levels of Gata4, and Tbx5 (Wang et al., 2015), or by adding Hand2 to the list of transduced genes (the GHMT protocol) (Song et al., 2012), and the activity of a transgenic, cardiomyocyte-specific troponin T promoter-reporter construct was more prevalent when iCMs were generated from mouse CFs by adding Nkx2.5 to the GHMT reprogramming protocol than via any other published combination of transcription factors (Addis et al., 2013). The expression of mature cardiomyocyte markers also varied depending on the relative proportions of Gata4, Mef2c, and Tbx5 (Wang et al., 2015), while the overall profile of cardiac-gene expression could be broadened by using a reprogramming cocktail composed of Tbx5, Mef2c, and Myocd (Protze et al., 2012).

Researchers are also investigating the mechanisms and signaling pathways that contribute to CF-iCM reprogramming by including small molecules in the established protocols. Adding Akt1 (protein kinase B) to the GHMT protocol dramatically increased spontaneous beating in reprogrammed iCMs and produced cells that were polynucleated, hypertrophic, and responsive to β-adrenoreceptor modulation, which suggests a more mature cardiomyocyte phenotype; furthermore, the role of Akt in iCM reprogramming appeared to be regulated upstream by insulin-like growth factor 1 (IGF1) and PI3K and facilitated downstream by target of rapamycin complex 1 (mTORC1) and forkhead box o3a (Foxo3a) (Zhou H. et al., 2015). A83-01, a selective inhibitor of TGF-β signaling, also increased spontaneous beating and the expression of cardiac genes such as *Actc1*, *Myh6,* and *Ryr2*, in GHMT-reprogrammed iCMs (Zhao Y. et al., 2015), which suggests that pro-fibrotic signaling pathways impede CF-iCM reprogramming, and the efficiency of GMT-reprogramming increased when Bmi1 activity was inhibited with shRNA during an early stage of the protocol (Zhou et al., 2016), which confirms that epigenetic factors could be key obstacles to CF-iCM reprogramming. MicroRNAs can also contribute to CF-iCM reprogramming, as evidenced by reports that pairing miR-133 overexpression with the GMT protocol significantly increased functional iCM yield by suppressing Snai1 (Muraoka et al., 2014), and that even in the absence of transcription factors, a combination of miR-1, miR-133, miR-208, and miR-499 induced mouse CFs to express cardiomyocyte-specific genes, beat spontaneously, and display cardiomyocyte-like organization of the sarcomere (Jayawardena et al., 2012).

## *In-situ* iCM REPROGRAMMING

When lentiviruses encoding the same set of four microRNAs (miR-1, -133, -208, and -499) were administered directly to the hearts of mice after MI, the treatment appeared to reprogram resident CFs into iCMs and was associated with increases in ejection fraction and lower measures of fibrosis (Jayawardena et al., 2015), which suggests that the vast pool of CFs could serve as an endogenous source of new cardiomyocytes for regenerative therapy. Genetic lineage-tracing studies have shown that GMT retroviruses also reprogram resident mouse CFs into iCMs when injected immediately after coronary artery ligation: the reprogrammed CFs formed sarcomeres, displayed a cardiomyocyte-like gene expression profile, and were bi-nuclear and electrically coupled to endogenous cardiomyocytes, and the treatment was associated with significant improvements in measures of cardiac ejection fraction, stroke volume, and infarct size (Qian et al., 2012). Retroviral delivery of GHMT also converted resident CFs into iCMs and improved recovery from myocardial injury in mice–measures of ejection fraction increased 2-fold while infarct sizes declined by 50%–and the efficiency of CF-to-iCM reprogramming was greater than in animals treated with GMT alone (Song et al., 2012). *In-situ* GMT reprogramming of CFs into iCMs has also been performed with Sendai virus (Miyamoto et al., 2018) and adenovirus (Mathison et al., 2017), which are more suitable than lenti- or retroviruses for clinical applications, because the vectors are not integrated into the host genome and are unlikely to cause insertional mutagenesis; both approaches significantly improved recovery from myocardial injury in rodents, and reprogramming efficiency was greater when performed with the Sendai virus than with integrating retroviruses.

Observations from at least two studies (Qian et al., 2012; Song et al., 2012) suggest that the efficiency of iCM reprogramming, as well as the maturity of the reprogrammed cells, is greater when performed *in-situ* after MI than in culture, which

suggests that properties of the infarcted heart can enhance iCM reprogramming. Whether the inflammatory signaling from neutrophils and macrophages (Prabhu and Frangogiannis, 2016) contribute to this enhancement has yet to be determined, and the results from studies of inflammation in direct reprogramming have been somewhat contradictory: the anti-inflammatory drug diclofenac promoted cardiac reprogramming in postnatal and adult fibroblasts (Muraoka et al., 2019), whereas shRNA-mediated knockdown of the pro-inflammatory regulators TLR3, NFKB1, and COX2 impeded the cardiac reprogramming of human fibroblasts (Zhou et al., 2019). Necrotic cardiomyocytes also release damage signals [i.e., damage-associated molecular patterns (DAMPs)] that activate CFs after MI, and measures of cardiac function and scar size in infarcted mouse hearts were significantly better after co-treatment with GMT and thymosin β4, which activates fibroblasts and promotes angiogenesis, than after treatment with GMT alone (Qian et al., 2012). Additional clues about how the environment of the infarcted myocardium may influence iCM reprogramming can be inferred from observations in cultured cells: the conversion rate of iCMs improved, and was accompanied by increases in MMP3 expression, when the cells were suspended in a 3D hydrogel that mimicked cardiac ECM (Li et al., 2016), and both the quantity and maturity of iCMs increased when reprogramming was conducted on microgrooved substrate (Sia et al., 2016). Mechanical properties of the damaged myocardium could also contribute to iCM reprogramming, because the stiffness of the scarred region likely changes in response to collagen deposition (Voorhees et al., 2015), and the maturation of iPSC-CMs can be improved by manipulating the stiffness of the culture substrate (Ribeiro et al., 2015).

## CONCLUSION AND PERSPECTIVES

Cardiac fibroblast are key players in every stage of recovery from myocardial injury, and their roles in both beneficial and maladaptive fibrosis have been well established; however, more recent investigations have begun to evaluate whether their phenotypic plasticity and involvement in ECM production can be manipulated to promote myocardial regeneration. CFs could be targeted directly to promote the proliferation of endogenous cardiomyocytes by upregulating the production of matricellular ECM proteins that activate the cardiomyocyte cell-cycle or by altering structural components to reduce ECM stiffness. CFs are one type of most numerous cells in the heart, and the epigenetic profile of iPSCs generated from CFs, rather than other cell types, appears to be more favorable for differentiation into cardiac-lineage cells, which suggests that CFs could be an abundant source of cardiomyocytes for cell-based therapy and tissue engineering. iCPCs reprogrammed from CFs can differentiate into cardiomyocytes, ECs, and SMCs after transplantation into infarcted hearts and have been associated with improvements in cardiac function and survival with no evidence of tumorigenesis, while a number of protocols have been developed for reprogramming CFs directly into iCMs both *in vitro* and *in situ*, which could enable a promising therapeutic strategy to repopulate the myocardial scar with cardiomyocytes while avoiding the need for transplanted cells. However, the optimal combination of transcription factors and/or microRNAs for CF-iCM reprogramming has yet to be identified, and ongoing investigations into potential tumorigenicity of iPSC-CMs and the mechanisms that regulate both the generation of iCPCs and their differentiation into functional cardiac cells are required to facilitate the translation of these technologies to the clinic.

Certainly, challenges remain in our understanding of CF's functions and plasticity as well as how the knowledge can be utilized to achieve heart regeneration. Although increasing evidence has shown that CFs and ECM significantly contribute to homeostasis and recovery after injury, the complexity of their crosstalk with cardiomyocytes and other cells remains largely unknown. Additionally, it is still unclear how the *in vivo* environment with changed ECM compositions influences fibroblast plasticity and integration of transplanted cardiomyocytes. It is also interesting to investigate whether *in situ* cardiac reprogramming will affect CF dynamics and ECM production, which might lead to synergetic benefit for heart tissue repair. Finally, most of the current findings are mainly from mouse studies. It is necessary and important to expand our understanding of cardiac fibroblasts in terms of their characteristics, behaviors, and functions in large animals and humans.

## AUTHOR CONTRIBUTIONS

WC and JZ wrote the manuscript. JZ, YZ, and WB made the revision. JZ supervised the entire manuscript preparation process and figures design and creation. All authors approved the submission and publication of the manuscript.

## FUNDING

This work was supported by the following funding sources: NIH RO1s, HL114120, HL 131017, HL 149137, NIH UO1 HL134764 to JZ, and NIH R01HL153220 to YZ.

## ACKNOWLEDGMENTS

The authors would like to thank W. Kevin Meisner, Ph.D., ELS, for editorial assistance.

## REFERENCES


Aasen, T., Raya, A., Barrero, M. J., Garreta, E., Consiglio, A., Gonzalez, F., et al. (2008). Efficient and rapid generation of induced pluripotent stem cells from human keratinocytes. *Nat. Biotechnol.* 26, 1276–1284.

Addis, R. C., Ifkovits, J. L., Pinto, F., Kellam, L. D., Esteso, P., Rentschler, S., et al. (2013). Optimization of direct fibroblast reprogramming to cardiomyocytes using calcium activity as a functional measure of success. *J. Mol. Cell Cardiol.* 60, 97–106. doi: 10.1016/j.yjmcc.2013.04.004

Alexanian, R. A., Mahapatra, K., Lang, D., Vaidyanathan, R., Markandeya, Y. S., Gill, R. K., et al. (2020). Induced cardiac progenitor cells repopulate decellularized mouse heart scaffolds and differentiate to generate cardiac tissue. *Biochim. Biophys. Acta Mol. Cell. Res.* 1867:118559. doi: 10.1016/j.bbamcr.2019.118559

Banerjee, I., Fuseler, J. W., Price, R. L., Borg, T. K., and Baudino, T. A. (2007). Determination of cell types and numbers during cardiac development in the neonatal and adult rat and mouse. *Am. J. Physiol. Heart Circ. Physiol.* 293, H1883–H1891.

Baudino, T. A., McFadden, A., Fix, C., Hastings, J., Price, R., and Borg, T. K. (2008). Cell patterning: interaction of cardiac myocytes and fibroblasts in three-dimensional culture. *Microsc. Microanal.* 14, 117–125. doi: 10.1017/s1431927608080021

Baxter, S. C., Morales, M. O., and Goldsmith, E. C. (2008). Adaptive changes in cardiac fibroblast morphology and collagen organization as a result of mechanical environment. *Cell Biochem. Biophys.* 51, 33–44. doi: 10.1007/s12013-008-9013-8

Cahill, T. J., Choudhury, R. P., and Riley, P. R. (2017). Heart regeneration and repair after myocardial infarction: translational opportunities for novel therapeutics. *Nat. Rev. Drug. Discov.* 16, 699–717. doi: 10.1038/nrd.2017.106

Canseco, D. C., Kimura, W., Garg, S., Mukherjee, S., Bhattacharya, S., Abdisalaam, S., et al. (2015). Human ventricular unloading induces cardiomyocyte proliferation. *J. Am. Coll. Cardiol.* 65, 892–900. doi: 10.1016/j.jacc.2014.12.027

Carvalho, A. B., and de Carvalho, A. C. (2010). Heart regeneration: Past, present and future. *World J. Cardiol.* 2, 107–111. doi: 10.4330/wjc.v2.i5.107

Chen, W., and Frangogiannis, N. G. (2013). Fibroblasts in post-infarction inflammation and cardiac repair. *Biochim. Biophys. Acta* 1833, 945–953. doi: 10.1016/j.bbamcr.2012.08.023

Chen, Z., Xie, J., Hao, H., Lin, H., Wang, L., Zhang, Y., et al. (2017). Ablation of periostin inhibits post-infarction myocardial regeneration in neonatal mice mediated by the phosphatidylinositol 3 kinase/glycogen synthase kinase 3beta/cyclin D1 signalling pathway. *Cardiovasc. Res.* 113, 620–632. doi: 10.1093/cvr/cvx001

Engler, A. J., Sen, S., Sweeney, H. L., and Discher, D. E. (2006). Matrix elasticity directs stem cell lineage specification. *Cell* 126, 677–689. doi: 10.1016/j.cell.2006.06.044

Frangogiannis, N. G. (2006). The mechanistic basis of infarct healing. *Antioxid. Redox Signal.* 8, 1907–1939. doi: 10.1089/ars.2006.8.1907

Frangogiannis, N. G. (2017). The extracellular matrix in myocardial injury, repair, and remodeling. *J. Clin. Invest.* 127, 1600–1612. doi: 10.1172/jci87491

Frangogiannis, N. G. (2019). The extracellular matrix in ischemic and nonischemic heart failure. *Circ. Res.* 125, 117–146. doi: 10.1161/circresaha.119.311148

Fu, X., Khalil, H., Kanisicak, O., Boyer, J. G., Vagnozzi, R. J., Maliken, B. D., et al. (2018). Specialized fibroblast differentiated states underlie scar formation in the infarcted mouse heart. *J. Clin. Invest.* 128, 2127–2143. doi: 10.1172/jci98215

Gao, L., Yang, L., Wang, L., Geng, Z., Wei, Y., Gourley, G., et al. (2018). Relationship between the efficacy of cardiac cell therapy and the inhibition of differentiation of human iPSC-derived nonmyocyte cardiac cells into myofibroblast-like cells. *Circ. Res.* 123, 1313–1325. doi: 10.1161/circresaha.118.313094

Guerzoni, L. P. B., Tsukamoto, Y., Gehlen, D. B., Rommel, D., Haraszti, T., Akashi, M., et al. (2019). A layer-by-layer single-cell coating technique to produce injectable beating mini heart tissues via microfluidics. *Biomacromolecules* 20, 3746–3754. doi: 10.1021/acs.biomac.9b00786

Haraguchi, Y., Shimizu, T., Sasagawa, T., Sekine, H., Sakaguchi, K., Kikuchi, T., et al. (2012). Fabrication of functional three-dimensional tissues by stacking cell sheets in vitro. *Nat. Protoc.* 7, 850–858. doi: 10.1038/nprot.2012.027

Hastings, C. L., Roche, E. T., Ruiz-Hernandez, E., Schenke-Layland, K., Walsh, C. J., and Duffy, G. P. (2015). Drug and cell delivery for cardiac regeneration. *Adv. Drug Deliv. Rev.* 84, 85–106. doi: 10.1016/j.addr.2014.08.006

Ieda, M., Fu, J. D., Delgado-Olguin, P., Vedantham, V., Hayashi, Y., Bruneau, B. G., et al. (2010). Direct reprogramming of fibroblasts into functional cardiomyocytes by defined factors. *Cell* 142, 375–386. doi: 10.1016/j.cell.2010.07.002

Ieda, M., Tsuchihashi, T., Ivey, K. N., Ross, R. S., Hong, T. T., Shaw, R. M., et al. (2009). Cardiac fibroblasts regulate myocardial proliferation through beta1 integrin signaling. *Dev. Cell* 16, 233–244. doi: 10.1016/j.devcel.2008.12.007

Illing, A., Stockmann, M., Swamy Telugu, N., Linta, L., Russell, R., Muller, M., et al. (2013). Definitive endoderm formation from plucked human hair-derived induced pluripotent stem cells and SK channel regulation. *Stem. Cells Int.* 2013:360573.

Jayawardena, T. M., Egemnazarov, B., Finch, E. A., Zhang, L., Payne, J. A., Pandya, K., et al. (2012). MicroRNA-mediated in vitro and in vivo direct reprogramming of cardiac fibroblasts to cardiomyocytes. *Circ. Res.* 110, 1465–1473. doi: 10.1161/circresaha.112.269035

Jayawardena, T. M., Finch, E. A., Zhang, L., Zhang, H., Hodgkinson, C. P., Pratt, R. E., et al. (2015). MicroRNA induced cardiac reprogramming in vivo: evidence for mature cardiac myocytes and improved cardiac function. *Circ. Res.* 116, 418–424. doi: 10.1161/circresaha.116.304510

Kanisicak, O., Khalil, H., Ivey, M. J., Karch, J., Maliken, B. D., Correll, R. N., et al. (2016). Genetic lineage tracing defines myofibroblast origin and function in the injured heart. *Nat. Commun.* 7:12260.

Kim, K., Doi, A., Wen, B., Ng, K., Zhao, R., Cahan, P., et al. (2010). Epigenetic memory in induced pluripotent stem cells. *Nature* 467, 285–290.

Kuhn, B., del Monte, F., Hajjar, R. J., Chang, Y. S., Lebeche, D., Arab, S., et al. (2007). Periostin induces proliferation of differentiated cardiomyocytes and promotes cardiac repair. *Nat. Med.* 13, 962–969. doi: 10.1038/nm1619

Lagarkova, M. A., Shutova, M. V., Bogomazova, A. N., Vassina, E. M., Glazov, E. A., Zhang, P., et al. (2010). Induction of pluripotency in human endothelial cells resets epigenetic profile on genome scale. *Cell Cycle* 9, 937–946. doi: 10.4161/cc.9.5.10869

Lalit, P. A., Salick, M. R., Nelson, D. O., Squirrell, J. M., Shafer, C. M., Patel, N. G., et al. (2016). Lineage reprogramming of fibroblasts into proliferative induced cardiac progenitor cells by defined factors. *Cell Stem Cell* 18, 354–367. doi: 10.1016/j.stem.2015.12.001

Lam, N. T., and Sadek, H. A. (2018). Neonatal heart regeneration: comprehensive literature review. *Circulation* 138, 412–423. doi: 10.1161/circulationaha.118.033648

Li, Y., Dal-Pra, S., Mirotsou, M., Jayawardena, T. M., Hodgkinson, C. P., Bursac, N., et al. (2016). Tissue-engineered 3-dimensional (3D) microenvironment enhances the direct reprogramming of fibroblasts into cardiomyocytes by microRNAs. *Sci. Rep.* 6:38815.

Lin, Z., and Pu, W. T. (2014). Strategies for cardiac regeneration and repair. *Sci. Transl. Med.* 6, 239rv1.

Lockhart, M., Wirrig, E., Phelps, A., and Wessels, A. (2011). Extracellular matrix and heart development. *Birth Defects Res. A Clin. Mol. Teratol.* 91, 535–550.

Long, C. S. (2001). The role of interleukin-1 in the failing heart. *Heart Fail. Rev.* 6, 81–94.

Ma, Y., Iyer, R. P., Jung, M., Czubryt, M. P., and Lindsey, M. L. (2017). Cardiac fibroblast activation post-myocardial infarction: current knowledge gaps. *Trends Pharmacol. Sci.* 38, 448–458. doi: 10.1016/j.tips.2017.03.001

Masino, A. M., Gallardo, T. D., Wilcox, C. A., Olson, E. N., Williams, R. S., and Garry, D. J. (2004). Transcriptional regulation of cardiac progenitor cell populations. *Circ. Res.* 95, 389–397. doi: 10.1161/01.res.0000138302.02691.be

Mathison, M., Singh, V. P., Chiuchiolo, M. J., Sanagasetti, D., Mao, Y., Patel, V. B., et al. (2017). In situ reprogramming to transdifferentiate fibroblasts into cardiomyocytes using adenoviral vectors: implications for clinical myocardial regeneration. *J. Thorac. Cardiovasc. Surg.* 153, 329–339e3.

Miyamoto, K., Akiyama, M., Tamura, F., Isomi, M., Yamakawa, H., Sadahiro, T., et al. (2018). Direct in vivo reprogramming with sendai virus vectors improves cardiac function after myocardial infarction. *Cell Stem Cell* 22, 91–103.e5.

Muraoka, N., Nara, K., Tamura, F., Kojima, H., Yamakawa, H., Sadahiro, T., et al. (2019). Role of cyclooxygenase-2-mediated prostaglandin E2-prostaglandin E receptor 4 signaling in cardiac reprogramming. *Nat. Commun.* 10:674.

Muraoka, N., Yamakawa, H., Miyamoto, K., Sadahiro, T., Umei, T., Isomi, M., et al. (2014). MiR-133 promotes cardiac reprogramming by directly repressing Snai1 and silencing fibroblast signatures. *EMBO J.* 33, 1565–1581. doi: 10.15252/embj.201387605

Nag, A. C. (1980). Study of non-muscle cells of the adult mammalian heart: a fine structural analysis and distribution. *Cytobios* 28, 41–61.

Noguchi, H., Miyagi-Shiohira, C., and Nakashima, Y. (2018). Induced tissue-specific stem cells and epigenetic memory in induced pluripotent stem cells. *Int. J. Mol. Sci.* 19:930. doi: 10.3390/ijms19040930

Notari, M., Ventura-Rubio, A., Bedford-Guaus, S. J., Jorba, I., Mulero, L., Navajas, D., et al. (2018). The local microenvironment limits the regenerative potential of the mouse neonatal heart. *Sci. Adv.* 4:eaao5553. doi: 10.1126/sciadv.aao5553

Novosel, E. C., Kleinhans, C., and Kluger, P. J. (2011). Vascularization is the key challenge in tissue engineering. *Adv. Drug Deliv. Rev.* 63, 300–311. doi: 10.1016/j.addr.2011.03.004

Okita, K., Yamakawa, T., Matsumura, Y., Sato, Y., Amano, N., Watanabe, A., et al. (2013). An efficient nonviral method to generate integration-free human-induced pluripotent stem cells from cord blood and peripheral blood cells. *Stem Cells* 31, 458–466. doi: 10.1002/stem.1293

Porrello, E. R., Mahmoud, A. I., Simpson, E., Hill, J. A., Richardson, J. A., Olson, E. N., et al. (2011). Transient regenerative potential of the neonatal mouse heart. *Science* 331, 1078–1080. doi: 10.1126/science.1200708

Prabhu, S. D., and Frangogiannis, N. G. (2016). The biological basis for cardiac repair after myocardial infarction: from inflammation to fibrosis. *Circ. Res.* 119, 91–112. doi: 10.1161/circresaha.116.303577

Protze, S., Khattak, S., Poulet, C., Lindemann, D., Tanaka, E. M., and Ravens, U. (2012). A new approach to transcription factor screening for reprogramming of fibroblasts to cardiomyocyte-like cells. *J. Mol. Cell Cardiol.* 53, 323–332. doi: 10.1016/j.yjmcc.2012.04.010

Qian, L., Huang, Y., Spencer, C. I., Foley, A., Vedantham, V., Liu, L., et al. (2012). In vivo reprogramming of murine cardiac fibroblasts into induced cardiomyocytes. *Nature* 485, 593–598. doi: 10.1038/nature11044

Radisic, M., Park, H., Chen, F., Salazar-Lazzaro, J. E., Wang, Y., Dennis, R., et al. (2006). Biomimetic approach to cardiac tissue engineering: oxygen carriers and channeled scaffolds. *Tissue Eng.* 12, 2077–2091. doi: 10.1089/ten.2006.12.2077

Ribeiro, A. J., Ang, Y. S., Fu, J. D., Rivas, R. N., Mohamed, T. M., Higgs, G. C., et al. (2015). Contractility of single cardiomyocytes differentiated from pluripotent stem cells depends on physiological shape and substrate stiffness. *Proc. Natl. Acad. Sci. U.S.A.* 112, 12705–12710. doi: 10.1073/pnas.1508073112

Rienks, M., Papageorgiou, A. P., Frangogiannis, N. G., and Heymans, S. (2014). Myocardial extracellular matrix: an ever-changing and diverse entity. *Circ. Res.* 114, 872–888. doi: 10.1161/circresaha.114.302533

Sadoshima, J., and Weiss, J. N. (2014). Cardiac fibroblasts: the good, the bad, the ugly, the beautiful. *J. Mol. Cell. Cardiol.* 70:1. doi: 10.1016/j.yjmcc.2014.03.009

Sandanger, O., Ranheim, T., Vinge, L. E., Bliksoen, M., Alfsnes, K., Finsen, A. V., et al. (2013). The NLRP3 inflammasome is up-regulated in cardiac fibroblasts and mediates myocardial ischaemia-reperfusion injury. *Cardiovasc. Res.* 99, 164–174. doi: 10.1093/cvr/cvt091

Schmuck, E. G., Mulligan, J. D., Ertel, R. L., Kouris, N. A., Ogle, B. M., Raval, A. N., et al. (2014). Cardiac fibroblast-derived 3D extracellular matrix seeded with mesenchymal stem cells as a novel device to transfer cells to the ischemic myocardium. *Cardiovasc. Eng. Technol.* 5, 119–131. doi: 10.1007/s13239-013-0167-1

Shimazaki, M., Nakamura, K., Kii, I., Kashima, T., Amizuka, N., Li, M., et al. (2008). Periostin is essential for cardiac healing after acute myocardial infarction. *J. Exp. Med.* 205, 295–303.

Shimizu, T., Sekine, H., Yang, J., Isoi, Y., Yamato, M., Kikuchi, A., et al. (2006). Polysurgery of cell sheet grafts overcomes diffusion limits to produce thick, vascularized myocardial tissues. *FASEB. J.* 20, 708–710. doi: 10.1096/fj.05-4715fje

Shinde, A. V., and Frangogiannis, N. G. (2014). Fibroblasts in myocardial infarction: a role in inflammation and repair. *J. Mol. Cell Cardiol.* 70, 74–82. doi: 10.1016/j.yjmcc.2013.11.015

Sia, J., Yu, P., Srivastava, D., and Li, S. (2016). Effect of biophysical cues on reprogramming to cardiomyocytes. *Biomaterials* 103, 1–11. doi: 10.1016/j.biomaterials.2016.06.034

Snider, P., Standley, K. N., Wang, J., Azhar, M., Doetschman, T., and Conway, S. J. (2009). Origin of cardiac fibroblasts and the role of periostin. *Circ. Res.* 105, 934–947. doi: 10.1161/circresaha.109.201400

Song, K., Nam, Y. J., Luo, X., Qi, X., Tan, W., Huang, G. N., et al. (2012). Heart repair by reprogramming non-myocytes with cardiac transcription factors. *Nature* 485, 599–604. doi: 10.1038/nature11139

Souders, C. A., Bowers, S. L., and Baudino, T. A. (2009). Cardiac fibroblast: the renaissance cell. *Circ. Res.* 105, 1164–1176. doi: 10.1161/circresaha.109.209809

Takahashi, K., Tanabe, K., Ohnuki, M., Narita, M., Ichisaka, T., Tomoda, K., et al. (2007). Induction of pluripotent stem cells from adult human fibroblasts by defined factors. *Cell* 131, 861–872. doi: 10.1016/j.cell.2007.11.019

Takahashi, K., and Yamanaka, S. (2006). Induction of pluripotent stem cells from mouse embryonic and adult fibroblast cultures by defined factors. *Cell* 126, 663–676. doi: 10.1016/j.cell.2006.07.024

Torre-Amione, G., Kapadia, S., Benedict, C., Oral, H., Young, J. B., and Mann, D. L. (1996). Proinflammatory cytokine levels in patients with depressed left ventricular ejection fraction: a report from the Studies of Left Ventricular Dysfunction (SOLVD). *J. Am. Coll. Cardiol.* 27, 1201–1206. doi: 10.1016/0735-1097(95)00589-7

Toubiana, S., Gagliardi, M., Papa, M., Manco, R., Tzukerman, M., Matarazzo, M. R., et al. (2019). Persistent epigenetic memory impedes rescue of the telomeric phenotype in human ICF iPSCs following DNMT3B correction. *eLife* 8:e47859.

Tsukamoto, Y., Akagi, T., and Akashi, M. (2020). Vascularized cardiac tissue construction with orientation by layer-by-layer method and 3D printer. *Sci. Rep.* 10:5484.

Voorhees, A. P., DeLeon-Pennell, K. Y., Ma, Y., Halade, G. V., Yabluchanskiy, A., Iyer, R. P., et al. (2015). Building a better infarct: modulation of collagen cross-linking to increase infarct stiffness and reduce left ventricular dilation post-myocardial infarction. *J. Mol. Cell Cardiol.* 85, 229–239. doi: 10.1016/j.yjmcc.2015.06.006

Wang, F., and Guan, J. (2010). Cellular cardiomyoplasty and cardiac tissue engineering for myocardial therapy. *Adv. Drug. Deliv. Rev.* 62, 784–797. doi: 10.1016/j.addr.2010.03.001

Wang, L., Liu, Z., Yin, C., Asfour, H., Chen, O., Li, Y., et al. (2015). Stoichiometry of Gata4, Mef2c, and Tbx5 influences the efficiency and quality of induced cardiac myocyte reprogramming. *Circ. Res.* 116, 237–244. doi: 10.1161/circresaha.116.305547

Wang, L. S., Boulaire, J., Chan, P. P., Chung, J. E., and Kurisawa, M. (2010). The role of stiffness of gelatin-hydroxyphenylpropionic acid hydrogels formed by enzyme-mediated crosslinking on the differentiation of human mesenchymal stem cell. *Biomaterials* 31, 8608–8616. doi: 10.1016/j.biomaterials.2010.07.075

Williams, C., Quinn, K. P., Georgakoudi, I., and Black, L. D. III (2014). Young developmental age cardiac extracellular matrix promotes the expansion of neonatal cardiomyocytes in vitro. *Acta Biomater.* 10, 194–204. doi: 10.1016/j.actbio.2013.08.037

Yahalom-Ronen, Y., Rajchman, D., Sarig, R., Geiger, B., and Tzahor, E. (2015). Reduced matrix rigidity promotes neonatal cardiomyocyte dedifferentiation, proliferation and clonal expansion. *eLife* 4:e07455.

Ye, L., Zhang, S., Greder, L., Dutton, J., Keirstead, S. A., Lepley, M., et al. (2013). Effective cardiac myocyte differentiation of human induced pluripotent stem cells requires VEGF. *PLoS One* 8:e53764. doi: 10.1371/journal.pone.0053764

Zak, R. (1974). Development and proliferative capacity of cardiac muscle cells. *Circ. Res.* 35(Suppl. II), 17–26.

Zhang, L., Guo, J., Zhang, P., Xiong, Q., Wu, S. C., Xia, L., et al. (2015). Derivation and high engraftment of patient-specific cardiomyocyte sheet using induced pluripotent stem cells generated from adult cardiac fibroblast. *Circ. Heart Fail.* 8, 156–166. doi: 10.1161/circheartfailure.114.001317

Zhang, S., Sun, A., Liang, Y., Chen, Q., Zhang, C., Wang, K., et al. (2009). A role of myocardial stiffness in cell-based cardiac repair: a hypothesis. *J. Cell Mol. Med.* 13, 660–663. doi: 10.1111/j.1582-4934.2009.00710.x

Zhou, H., Dickson, M. E., Kim, M. S., Bassel-Duby, R., and Olson, E. N. (2015). Akt1/protein kinase B enhances transcriptional reprogramming of fibroblasts to functional cardiomyocytes. *Proc. Natl. Acad. Sci. U.S.A.* 112, 11864–11869. doi: 10.1073/pnas.1516237112

Zhao, Y., Londono, P., Cao, Y., Sharpe, E. J., Proenza, C., O'Rourke, R., et al. (2015). High-efficiency reprogramming of fibroblasts into cardiomyocytes requires suppression of pro-fibrotic signalling. *Nat. Commun.* 6:8243.

Zhou, P., and Pu, W. T. (2016). Recounting cardiac cellular composition. *Circ. Res.* 118, 368–370. doi: 10.1161/circresaha.116.308139

Zhou, Y., Liu, Z., Welch, J. D., Gao, X., Wang, L., Garbutt, T., et al. (2019). Single-cell transcriptomic analyses of cell fate transitions during human cardiac reprogramming. *Cell Stem Cell* 25, 149–164.e9.

Zhou, Y., Wang, L., Vaseghi, H. R., Liu, Z., Lu, R., Alimohamadi, S., et al. (2016). Bmi1 is a key epigenetic barrier to direct cardiac reprogramming. *Cell Stem Cell* 18, 382–395. doi: 10.1016/j.stem.2016.02.003

**Conflict of Interest:** The authors declare that the research was conducted in the absence of any commercial or financial relationships that could be construed as a potential conflict of interest.

frontiers in Bioengineering and Biotechnology

REVIEW
published: 12 April 2021
doi: 10.3389/fbioe.2021.637048

# Review on the Vascularization of Organoids and Organoids-on-a-Chip

*Xingli Zhao[1†], Zilu Xu[1†], Lang Xiao[1], Tuo Shi[1], Haoran Xiao[1], Yeqin Wang[1], Yanzhao Li[1], Fangchao Xue[1] and Wen Zeng[1,2,3]**

[1] Department of Cell Biology, Third Military Medical University, Chongqing, China, [2] State Key Laboratory of Trauma, Burn and Combined Injury, Chongqing, China, [3] Department of Neurology, Southwest Hospital, Third Military Medical University, Chongqing, China

The use of human cells for the construction of 3D organ models *in vitro* based on cell self-assembly and engineering design has recently increased in popularity in the field of biological science. Although the organoids are able to simulate the structures and functions of organs *in vitro*, the 3D models have difficulty in forming a complex vascular network that can recreate the interaction between tissue and vascular systems. Therefore, organoids are unable to survive, due to the lack of oxygen and nutrients, as well as the accumulation of metabolic waste. Organoids-on-a-chip provides a more controllable and favorable design platform for co-culture of different cells and tissue types in organoid systems, overcoming some of the limitations present in organoid culture. However, the majority of them has vascular networks that are not adequately elaborate to simulate signal communications between bionic microenvironment (e.g., fluid shear force) and multiple organs. Here, we will review the technological progress of the vascularization in organoids and organoids-on-a-chip and the development of intravital 3D and 4D bioprinting as a new way for vascularization, which can aid in further study on tissue or organ development, disease research and regenerative medicine.

**Keywords: organoid, organiods-on-a-chip, vascularization, advanced printing methods, micro-environment**

OPEN ACCESS

***Edited by:***
*Philippe Menasché, Assistance Publique Hopitaux De Paris, France*

***Reviewed by:***
*Daniel John Kelly, Trinity College Dublin, Ireland*
*Ngan F. Huang, Stanford University, United States*

****Correspondence:***
*Wen Zeng*
*zengw0105@163.com*

*† These authors have contributed equally to this work*

***Specialty section:***
*This article was submitted to Tissue Engineering and Regenerative Medicine, a section of the journal Frontiers in Bioengineering and Biotechnology*

***Received:*** *02 December 2020*
***Accepted:*** *04 March 2021*
***Published:*** *12 April 2021*

***Citation:***
*Zhao X, Xu Z, Xiao L, Shi T, Xiao H, Wang Y, Li Y, Xue F and Zeng W (2021) Review on the Vascularization of Organoids and Organoids-on-a-Chip. Front. Bioeng. Biotechnol. 9:637048. doi: 10.3389/fbioe.2021.637048*

## INTRODUCTION

Recent years have seen wide development of organoids and organoids-on-a-chip, as they are important in the imitation of the structure and function of human organs. At present, vascularization attempts of organoids and organoids-on-a-chip have attracted attention. Thick organ tissue requires an abundant network of micro-vascular vessels to provide oxygen and nutrients, as well as handle the discharge of metabolic waste. Specifically for organoids-on-a-chip, vascularization helps us observe the bio-chemical reactions and transport of substances in vascular tissue. In recent years, the literature has focused on the *in vitro* regeneration of angiogenesis. At the same time, the micro-flow control system successfully simulates the precise regulation of the tissue micro-environment in many aspects and provides biochemical and mechanical shear force as a method for *in vitro* vascular network construction. Therefore, we aim to establish a macro-micro bridge by reviewing the current research on micro-flow control technology, providing ideas for the precise regulation of the complex tissue structure model of *in vitro* organ reshaping and exploring

the interaction of vascularization in various tissues. These concepts are of great significance to the next generation of vascular tissue engineering and the development of regenerative medicine.

## VASCULARIZATION OF ORGANOIDS

For the organoids having been constructed, the mainly limitation of achieving completely functional organoids like *in vivo* is the lack of rational tissue size. The main cause of growth arrest or cell death of all organoids in tissue engineering is the lack of adequate oxygen and nutrient supply. The maturation of organoids is influenced by the limitation of nutritional supply (Lancaster and Knoblich, 2014). The transport of oxygen and nutrients *in vivo* to tissue cells through diffusion is limited within a few hundred microns of capillaries (Yin et al., 2016). Additionally, the removal of cellular metabolic waste is also essential for the survival of cells (Muschler et al., 2004). Therefore, it is necessary for the successful development of organoids to remodel functional vessel networks for most organs with high metabolism, such as the heart, liver, kidney, and brain (Auger et al., 2013).

The approaches for organoid vascularization can be sorted into two categories: *in vitro* and *in vivo* vascularization. *In vitro* vascularization is obtained by co-culture with vascular cells or tissue engineering (Mansour et al., 2018). The strategies for *in vitro* vascularization can be sorted into templating and self-organizing methods (Nashimoto et al., 2017). Templating methods include hydrogel molding by needles, sacrificial molding, assembly of patterned hydrogel slabs and bio-printing (Nashimoto et al., 2017). Endothelial cells are co-cultured with supporting cells in the self-organizing method (Nashimoto et al., 2017) and neo-angiogenesis is induced by angiogenic growth factors, which can also promote cell self-assembly by gradient (Yin et al., 2016). *In vivo* vascularization is achieved by transplanting organoid models built *in vitro* into a host. The following paragraphs illustrate representative studies for each type of organoid vascularization approach.

### Vascularization *in vitro*

#### Templating Method

This method has been applied into different strategies of realizing vascularization of heart tissue.

The first strategy is printing the endothelial cells (ECs) without the parenchymal tissue. This method is enabled with the use of a composite bio-ink encapsulating ECs (Zhang Y. S. et al., 2016) (**Figure 1A**). A micro-fibrous scaffold can be bio-printed using this bio-ink, ECs can be directly bio-printed within scaffolds and then gradually migrate toward the periphery of the microfibers to form a layer of confluent endothelium. Along with controlled anisotropy (achieved by capability of their technique to bioprint 3D microfibrous scaffolds with anisotropic arrangements), cardiomyocytes are seeded into the interstitial space of the endothelialized scaffold to generate an aligned myocardium layer capable of spontaneous and synchronous contraction.

The second strategy is printing ECs along with surrounding tissues followed by external perfusion of ECs. A technique for hydrogel construct vascularization that confirmed endothelial monolayer formation within the fabricated channels has been reported by Bertassoni et al. (2014). They described a 3D micro-molding technique that utilized bio-printed agarose template fibers to fabricate micro-channel networks with various architectural features within photo-cross-linkable hydrogel constructs and successfully embed micro-channels inside hydrogels. The bio-printed templates can then be easily removed to form fully perfusable networks without any template dissolution. A method for bio-printing 3D cell-laden, vascularized tissues that exceed 1cm in thickness and can be perfused on a chip for long time periods (>6 weeks) can be used to improve perfusion (**Figure 1B**). A technique for integrated parenchyma, stroma and endothelium into a single thick tissue by co-printing multiple inks composed of hMSCs (human mesenchymal stem cells) and human neonatal dermal fibroblasts (hNDFs) within a customized extracellular matrix alongside embedded vasculature, which was subsequently lined with HUVECs (human umbilical vein endothelial cells) has been reported by Kolesky et al. (2016). The vascularized tissues were then perfused with growth factors. Miller et al. (2012) reported a general approach for rapid construction of such networks. They printed rigid 3D filament networks of carbohydrate glass and used them as a cyto-compatible sacrificial template in engineered tissues to generate cylindrical networks that could be lined with ECs and perfused with blood under high-pressure pulsatile flow. This simple vascular casting approach is compatible with a wide variety of cell types, synthetic and natural extracellular matrices and cross-linking strategies.

The third is printing a full, thick, vascularized tissue in one step. Noor et al. (2019) reported 3D printing techniques using personalized hydrogel as a bio-ink and printing a full, thick, vascularized tissue in one step (**Figure 1C**). Omentum tissue was isolated from the patient and cells were separated from the matrix. The matrix was processed into a personalized, thermo-responsive hydrogel. The cells were reprogrammed and encapsulated within the hydrogel to generate the bio-inks used for printing. The bio-inks were then used to print vascularized tissues. It was demonstrated that the personalized hydrogel can be used to print volumetric, freestanding, cellular structures, including whole hearts and their major blood vessels.

#### Self-Organizing Method

The advantage of templating is that it is usable immediately after manufacture (Nashimoto et al., 2017). However, the non-dynamic of vessel structure hinders the functional vessel formation, therefore, cells cannot dynamically adapt to the environment of the surrounding tissue, during co-culturing (Nashimoto et al., 2017). By contrast, *in vitro* vascular network established by the self-organizing method resembles angiogenesis, morphology and permeability *in vivo* more closely (Nashimoto et al., 2017).

Nashimoto et al. (2017) used a microfluidic device to induce angiogenic sprouts in a human lung fibroblast (hLFs) spheroid, which led to perfusable self-assembled vascular networks

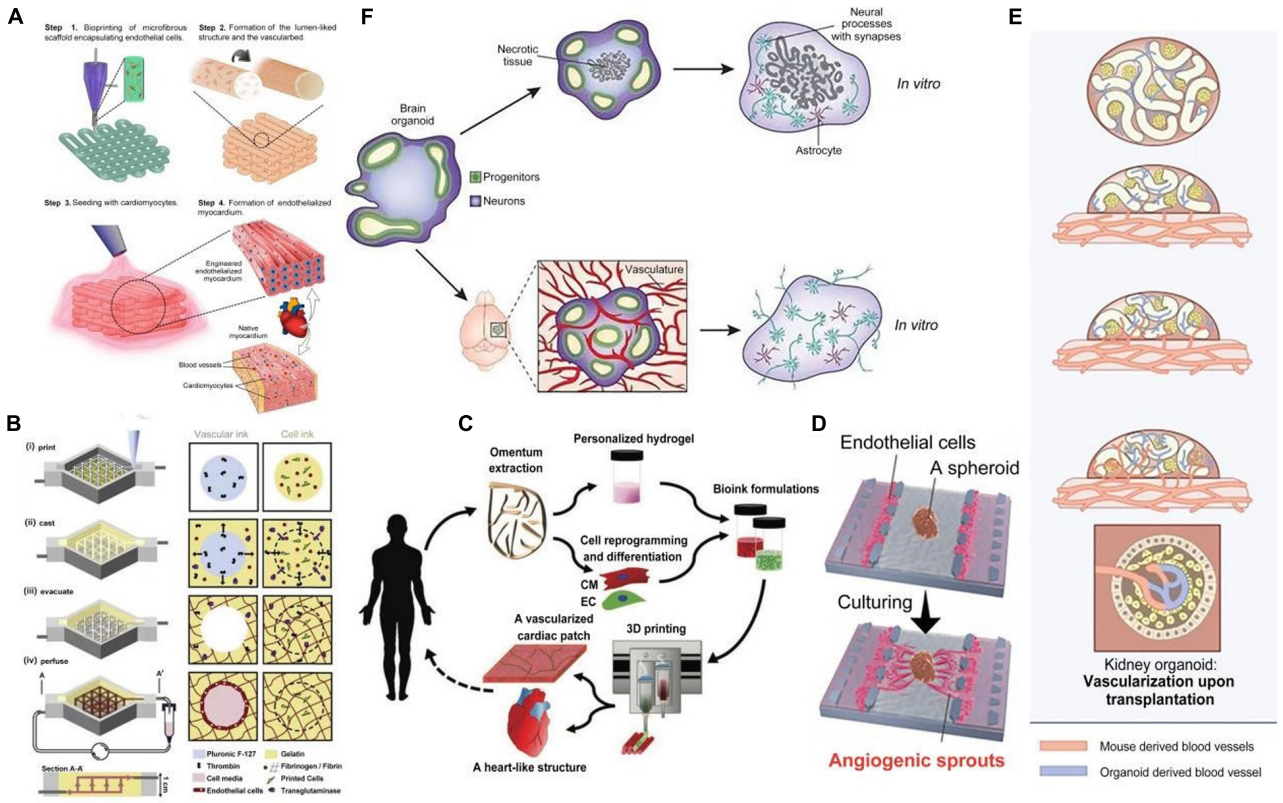


**FIGURE 1 |** Vascularization of organoids in various methods. **(A)** The procedure of endothelialized myocardium fabrication using the 3D bio-printing strategy. **(B)** Schematic illustration of the tissue manufacturing process. **(C)** Concept schematic of printing a full, thick vascularized tissue in one step. **(D)** Overview of microfluidic device use for angiogenic sprout inducing in a human lung fibroblast (hLFs) spheroid. Reprinted with permission from Nashimoto et al. (2017). **(E)** Upon transplantation, host-derived vascular networks invaded the hPSC-derived kidney organoids and connected to the organoid-derived plexus. **(F)** Brain organoids grown *in vitro* and transplanted into the mouse cortex.

(**Figure 1D**). The spheroid was prepared from co-cultured HUVECs and hLFs, in which vessel-like structures would form. The spheroid was then introduced to the spheroid well in the microfluidic device and HUVECs were seeded in the left and right channels of that well. The soluble angiogenic factors secreted by HLFs induced the formation of angiogenic sprouts toward the spheroid. These angiogenic sprouts grew into the perfusable vascular networks supporting active transport, which could anastomose to the previous vessel-like structures in the spheroid. Additionally, these vascular networks could transport nutrients and oxygen to cells in the spheroid and dispose of the metabolic product, which is similar to the *in vivo* physiological functions. The perfusable vessel model constructed by this approach subsequently led to culturing conditions the in spheroid that were more beneficial, which provides an effective model for long-term *in vitro* tissue culture.

A strategy for vascularization of brain organoids includes inducing the formation of blood vessel-like structures by vascular endothelial growth factor (VEGF) *in vitro*. Ham et al. (2020) applied this strategy for *in vitro* the formation of blood vessel-like structures in cerebral organoids. The results indicated that VEGF enhanced the differentiation of vascular ECs without reducing neuronal markers in the embryonic bodies (EBs), which then successfully developed into cerebral organoids with open-circle vascular structures expressing characteristic of the blood–brain barrier (BBB). Therefore, VEGF treatment can be used to generate vessel-like structures with mature BBB characteristics in cerebral organoids *in vitro*.

Another strategy for brain organoid vascularization involves achieving revascularization from the outside surrounding matrix. Pham et al. (2018) modeled the developmental peri-neural vascular plexus by coating the whole-brain organoid with Matrigel-embedded ECs. They achieved revascularization from the outside surrounding matrix, as opposed to direct injection into the center of the organoid. Induced pluripotent stem cells (iPSCs) were grown into whole-brain organoids. Simultaneously, iPSCs from the same body were differentiated into ECs. The organoid was then re-embedded in Matrigel with 250.000 ECs. Coating of brain organoids with ECs led to robust vascularization of the organoid. Vascularized organoids were grown *in vitro* and then transplanted into immunodeficient mice, to found that blood vessels did not stay on the periphery of the organoid but instead penetrated its center *in vivo*.

The approaches of vascularization *in vitro* can fully control over the growth of vascular network and immediate functionality. However, it still needs to be improved to be more viable and

changeable because of the incapability to adapt to the real-time change of organoids.

## Vascularization *in vivo*

Though current progress in microfluidic technology has demonstrated the feasibility of tissue angiogenesis, these methods will disturb the self-organizing structure in organoids (Lancaster, 2018). So far, transplanting organoids into hosts has been the only way to achieve tissue vascularization with complete function (Grebenyuk and Ranga, 2019). When the organoid is transplanted into hosts, the vascularization process mimics the native angiogenesis that occurs in the human body (Lancaster, 2018). Thus, *in vivo* vascularization by transplantation will develop organoids with complete function more efficiently and be more beneficial to the survival of organoids.

Van den Berg et al. (2018) used the approach of transplantation and described the vascularization of kidney organoids (**Figure 1E**). Human pluripotent stem cell (hPSC)-derived kidney organoids were transplanted under the kidney capsule of host mice. Then they observed that the host-derived vascular networks invaded the developing glomerular structures in the organoids and actively connected to the human-derived plexus. In addition, they confirmed that the organoids in hosts performed more integrated process of development and maturation, in comparison with the non-transplanted organoids. However, unsolved defects still exist in vascular networks generated in hosts, for instance the functional maturity of blood vessels in kidney organoids is not on part with that of kidneys in human (Koning et al., 2020).

Takebe et al. (2014) used the same approach to develop vascularized liver organoids. They cultivated human iPSCs-derived hepatic endoderm cells (iPSCs-HEs), HUVECs and hMSCs, which self-organized to liver buds (iPSCs-LBs). Then they transplanted the iPSCs-LBs under the cranial window in mice. Results showed that human-derived vessels connected to the host vessels and formed unobstructed conduits which could deliver nutrients and oxygen (Takebe et al., 2013). This work shows that transplantation of *in vitro* cultured iPSCs-LBs into a host could develop vascularized liver organoids with functional tissue architecture (Takebe et al., 2013).

Mansour et al. (2018) reported on the generation of vascularized brain organoids after transplantation into the mouse brain, at the Society for Neuroscience Meeting 2017. This research focused on the issue of vascularization by transplanting cerebral organoids onto a vascular bed in the cortex of an adult mouse. They showed that intra-cerebral transplantation of brain organoids in mice resulted in impressive growth of blood vessels into the human tissue, with clear benefits for cell survival and maturation compared with organoids kept *in vitro* (**Figure 1F**).

Currently, the main challenge of achieving completely functionalized organoid is achieving spontaneous perfusing capability of blood vessels. The approaches of vascularizing organoids both *in vitro* and *in vivo* have not achieved this goal. Future researches of vascularized organoids will focus on the angiogenesis principles to induce viable and functional vasculature. With the advance of tissue engineering technologies and the improvement of existing approaches, the barriers of vascularizing organoids will be cleared up, which will promote the substantial production of implantable organoids with fully functionalized vessels.

# VASCULARIZATION OF ORGANOIDS-ON-A-CHIP

## The Importance of Organoids-on-a-Chip

Traditional *in vitro* cell culture techniques frequently use culture bottles, culture dishes, etc. as a living environment for cells. This 2D culture method lacks the complex living environment the cells grow in *in vivo* and cannot stimulate the cells by specific physical and chemical factors, such as biochemic concentration gradient, fluid shear force and mechanical stress. Through this method, the cells cannot achieve the level of self-assembly and truly restore the specific physiological function of the organ prototype (Bhatia and Ingber, 2014).

The gold standard for biological testing and animal models also has certain defects. Due to differences in biological metabolism and immune function between animals and humans, there still remains uncertainty such as medical diagnoses (Bhushan et al., 2013). Therefore, development of an effective model that simulates the human body is particularly important.

Organoids-on-a-chip is an effective alternative solution. During the construction of organoids-on-a-chip, it is necessary to consider the anatomical structure of the target organ and restore its basic physiological and characteristic structure. In this way, we are able to design the 3D mechanical and biochemical environment that corresponds to the target organ, according to the growth characteristics of the cell and use micro-processing technology (such as soft lithology) to construct the model necessary for cell growth (Park et al., 2019). The model is widely used in the study of organ function (Occhetta et al., 2018), disease modeling (Mazio et al., 2018) and pharmacological modeling (Sung et al., 2014). Blood vessels are important in connecting organs and realizing material exchange between organs. Additionally, micro-vascular networks maintain metabolism and the stability of the tissue micro-environment. The vascularization of organoids-on-a-chip provides us with a good platform to explore the physiological barrier role of blood vessels (Tarbell, 2010), the pathological study of blood vessels by blood flow shear force (Zheng et al., 2012), vascular regeneration (Zheng et al., 2012) and substance transport between tissues (Skardal et al., 2017).

## Regulation in Micro-Environment

Micro-environment conditions determine the growth and development of cells in organoids-on-a-chip, among which micro-flow models, embedded hydrogels and fluid shear forces are important conditions that affect the vascularization of organ chips.

In micro-flow models, cell adhesion of biomass formed by polymers, such as polydimethylsiloxane (PDMS), is mostly poor. Cell adhesion is promoted by coating its surface with a layer of

fibrin or hydrogel material (Taylor et al., 2005; Park et al., 2006). In addition, the size of channel has an important effect on the growth of vascular ECs. ECs extend in all directions in channels of 250–500 μm. Reduction of the inner diameter of the channels, causes almost all ECs to extend along the axial direction of the flow path, especially in the channels ranging from 10–20 μm (Greca et al., 2018), which are similar to the size of capillaries (i.e., less than 10 μm) *in vivo*. However, due to the accuracy of the manufacturing process, the formation of micro-vessels *in vitro* is usually greater than 50 μm (Haase and Kamm, 2017). The construction of small lumen plays an important role in the simulation of blood microcirculation.

The properties of hydrogels have a noteworthy influence on the formation process and function of microvascular networks. In hard hydrogels, the resulting microvascular network tends to have smaller channel diameters, thus limiting the migration of ECs (Chung et al., 2009). On the other hand, although the hydrogel itself has pores, they are mostly nanoscale, which makes nutrient and cell metabolic waste hard to discharge inside the hydrogel, hinders the function of cells and is not conducive to the fusion of body tissue. Ying et al. (2020) Developed macro-micro-nano-porous cell-laden gelatin methacryloyl (GelMA) hydrogel constructs by 3D extrusion bio-printing technology. Because hydrogels have better permeability than PDMS, plastics, silicon and many other substrate materials. HeYong team (Nie et al., 2018) develops some new methods in manufacturing micro-flow control chip based on a twice cross-linking hydrogel bulk. Hydrogel chips with good mechanical and biological properties were developed through cross-linking the commonly used alginate, gelatin and GelMA. The chip was very similar to natural extracellular matrix (ECM) in both water content and cytokine diffusivity and can be made into vascular chips in order to simulate disease models of blood vessels. The addition of specific acellular extracellular matrix into hydrogels as bio-inks has been reported to also promote angiogenesis (Zheng et al., 2020). Hydrogels with high biocompatibility are mature platforms for 3D cell culture. Appropriate hardness and pores are conducive to the growth of microvessels in hydrogels and the diffusion of various pro-vascular growth factors in hydrogels.

Mechanical stress affects the shape and function of the resulting blood vessels. Hemodynamic disorders are also easy to cause thrombus and atherosclerosis and induce inflammation. In increasingly fast blood flow, the vascular barrier function is the same as the one in the human body. Additionally, cyclic adenosine monophosphate (cAMP) in vascular ECs increases, under fast blood flow, improving the selectivity of the vascular barrier and the proliferation of ECs (Price et al., 2010). These findings provide good starting ground for building artificial blood vessels *in vitro*. Moreover, Vickerman's studies have found that high vascular shear force is important for the formation of new blood vessels (Vickerman et al., 2008; Vickerman and Kamm, 2012). Appropriate blood flow is essential to simulate organ function when constructing organ microarray. The existing problem is that vascular ECs are difficult to arrange evenly and neatly in the constructed vascular lumen. This phenomenon is more prominent in the complex vascular network structure. The perfusion blood shear force can cause damage to the vascular ECs attached to the lumen and mediate the occurrence of subsequent vascular diseases. On the other hand, blood vessels themselves have tension, and the dilation of blood vessels has a great influence on the growth of ECs, but these have been ignored in most of the construction of vascularized organ chips. At the same time, it also puts forward higher requirements for the selection of vascular construction materials.

## Application of Vascularization in Organoids-on-a-Chip

Development of organoids-on-a-chip has recently been seen significant growth. Several functions in the target organs have been successfully reproduced, many of which are closely related to the vascularization of organoids-on-a-chip. Functional microvascular structure provides a model for the study of complex vascular phenomena *in vitro*.

### Lung-on-a-Chip

Lung-on-a-chip was the first organoids-on-a-chip to be developed (Huh et al., 2007, 2010, 2012) (**Figure 2A**). A porous PDMS membrane covers the middle area of the chip. The alveolar epithelial cells are attached to the upper surface of the membrane in a gas channel and the vascular ECs are attached to the lower surface of the membrane in a blood channel. Two side channels connected to the vacuum pump on both left and right sides of the channel cause the PDMS membrane to deform under vacuum conditions to simulate the expansion and contraction of the alveolar wall during breathing. This model is a good simulation of the alveolar-capillary barrier. The micro-porous pathways of this model can be used to simulate pulmonary edema (Huh et al., 2012), as well as chronic obstructive pulmonary disease (COPD) (Benam et al., 2016) caused by viral or bacterial infections. The lung-on-a-chip has been used to explore disease models between vascular ECs and alveolar epithelial cells and findings have revealed that periodic respiratory rhythms play an important role in the development of lung diseases.

### Kidney-on-a-Chip

Early studies using kidney-on-a-chip have simulated glomerulus, proximal convoluted tubule and proximal convoluted tubule in the structure of kidney units, achieving blood filtration and re-absorption of initial urine (Weinberg et al., 2008). Furthermore, the introduction of fluid shear force has been reported to improve the re-absorption capacity of albumin and glucose of kidney-on-a-chip (Duan et al., 2008; Jang and Suh, 2010). Mu et al. (2013) stitched together two hydrogels through hydrogel bonding technology, forming two parallel 3D micro-vein networks. Madin-Darby Canine Kidney (MDCK) cells and HUVEC cells were cultured in these networks respectively, so that the formation of the kidney hydrogel chip simulated the passive diffusion of kidney units. This was an effective way to increase the diversity and complexity of kidney-on-a-chip. The majority of previous studies have focused on renal tubular epithelial cells, however, the re-emergence of the function of the kidney filter barrier is gradually gaining popularity using the combination of stem cell technology and regenerative medicine. On both sides of the porous PDMS, hiPS-cell-derived podocytes and primary

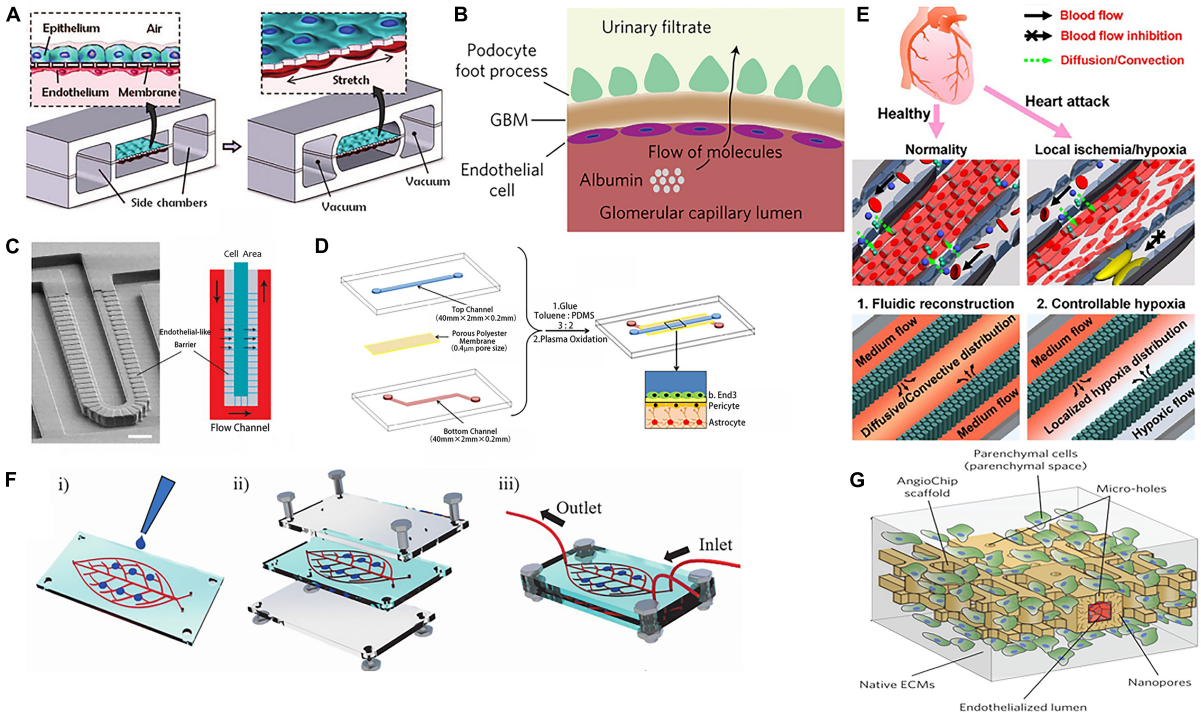


**FIGURE 2 |** Vascularization of organoids using various methods. **(A)** The alveolar epithelial cells and the vascular endothelial cells with flexible PDMS membrane form an alveolar-capillary barrier. Adapted from Huh et al. (2010). Reprinted with permission from AAAS. **(B)** Schematic representation of glomerular capillary wall with podocytes and endothelial cells that form a filtration barrier. **(C)** SEM micrograph and structure diagram of microfluidic chip simulates the hepatic sinusoid model. **(D)** Endothelial cells, pericytes, and astrocytes construct the blood–brain barrier (BBB). **(E)** The microfluidic device for studying controllable myocardial hypoxia and for myocardial fluidic microenvironment mimicking. **(F)** Human-on-leaf-chip simulates the complex vascular network structure of the human body. **(G)** AngioChip with branching interconnected lumen composed of POMaC and biological components.

human glomerular ECs are attached, simulating the urinary and capillary compartments of the glomerulus respectively. The high retention rate of albumin and the high permeability of inulin prove the successful construction of kidney filter barrier *in vitro* (Musah et al., 2017) (**Figure 2B**). These findings can be used in the exploration of the physiological and pathological function of the kidneys.

## Blood–Brain Barrier-on-a-Chip

The BBB is a highly selective barrier structure that separates the brain and central nervous system from blood circulation. The BBB is a network of interacting blood vessels, pericytes and astrocytes that provides oxygen and nutrients to the brain. It is very important to maintain the physiological activities of the central nervous system and the homeostasis of the microenvironment in the brain. It also has a guiding significance for how drugs act on the central system through the BBB. Wang et al. (2016) Further establish BBB model by co-culture of cerebral microvascular ECs and rat primary astrocytes on both sides of the porous membrane (**Figure 2D**). The results show that the activity of the cells are still in good condition for 21 days after construction. Each side of the BBB forms a monolayer of cells, simulating the BBB permeability to a certain extent. In the following research, key elements such as the inclusion of more types of brain cells, extracellular matrix and mechanical fluid conditions will be the direction for the functions of brain research. The BBB-on-a-chip can be constructed in many ways, but the vascular bed in the brain vessels is much tighter than the blood vessels in other peripheral organs. It requires us to use some special indicators to evaluate its function, such as TEER, small molecule permeability test, etc. (Oddo et al., 2019). The development of BBB chips provides an innovative approach for brain-related research, including modeling of neurodegenerative diseases and high-throughput drug screening.

Other single-organ chips such as liver chip (Lee et al., 2007; Kang et al., 2015) (**Figure 2C**), heart chip (Grosberg et al., 2011; Ren et al., 2013; Shao et al., 2016) (**Figure 2E**) and so on have also attracted attention with significant development. Several studies on organoids-on-a-chip have also focused in the observation of the drug responses in tissues and in the detection of the toxic and side-effects of target drugs on tissue chips *in vitro*. With the development of organoids-on-a-chip technology, the "multi-organ chip" (Oleaga et al., 2016), which contains more than ten kinds of organs, is gaining popularity. The chip channels provide a platform for the connection between the organs on the chip, which can be used to construct the ADME model to detect the interaction of drug effects between multiple tissues (Oleaga et al., 2016; Skardal et al., 2017) and the effect of tumor-on-a-chip on other tissue chips (Skardal et al., 2016; Greca et al., 2018).

Cells and organs establish contact with the peripheral circulatory system by secreting soluble factors and extracellular vesicles. A microfluidic system is used to connect different organoids-on-a-chip to simulate blood perfusion *in vivo* and regulate the culture environment. Vascularization between organs is an important aspect to be realized, as a bridge for intra-organ communication. At the same time, organoids-on-a-chip mostly uses parallel channels (Biselli et al., 2017; Chung et al., 2017) and seldom connects with each other through the vascular structure. This structure is quite different from the multi-stage complex vascular network *in vivo*, which makes providing a real physiological micro-environment (e.g., shear force stimulation) and simulating multi-organ signal communication conduction difficult. Therefore, the emergence of a bio-mimetic vascular leaf chip addresses those limitations (Mao et al., 2020) (**Figure 2F**). Through artificially edited digital models, photolithography is used to form an embedded multi-scale vascular network chamber, in which vascular ECs are growing. This model reconstructs complex physiological features, similar to those of the blood circulation system in the human body. The 3D vascularized organs in the larger chambers on the chip communicate with each other through the vascular network. It was found that pancreatic tumor cells tended to migrate to bone tissue and interact with bone MSCs. Milica Radisic's team simulated the vascular network system with poly(octamethylene maleate (anhydride) citrate) (POMaC), which contains microns and nanoscale micro-pores. And they successfully constructed functional and vascularized liver and heart tissue (Zhang B. et al., 2016) (**Figure 2G**). In the case of multi-organ devices, simple diffusion or convection of soluble factors between different regions on the chip can be realized by means of inter-organ communication through vascularization. The monitoring of each factor in this process can be more conducive to our cognition of some physiological and pathological processes and impose intervention conditions from them. The main challenge in establishing inter-organ linkages is to develop and optimize the medium formulation for each organ. At the same time, reducing the effects of unnecessary metabolic waste from the previous organ on the blood vessels and the next organ also needs to be addressed.

## ADVANCED PRINTING METHODS

The cutting-edge vascular printing methods that are presently available include extruded 3D printing and the improvement of printing materials and printing methods based on extruded 3D and 4D printing based on projection light-curing printing. At the same time, new applications of extruded 3D printing emerge in the construction of vascularized tissue, vascular-like structure and vascular network structure.

Professor Ali Khademhosseini's team developed GelMA-based vascularized skin using 3D printing by using GelMA/alginate saline gel containing HUVECs on a porous polyester membrane with a pore diameter of 0.4 μm. This structure is beneficial to the interaction between dermal fibroblasts and ECs and promotes the diffusion of nutrients to form an internal vascular network (Barros et al., 2020). Songwan Jin's team implemented 3D printing to develop multi-scale hepatic lobules with highly vascularized structure. The hepatic lobular vascular system was realized through the use of coaxial nozzles and sacrificial materials, leading to the adjacent ECs at the lumen or surface to form a cell layer, thus realizing the connection of ECs between the lumen and the surface. Vascular-like structures include trachea, gastrointestinal tract, renal tubule and urinary catheter, which are distributed all over the body and the diameter of the tube ranges from micron to centimeter (Kang et al., 2020). The mechanical strength of micro-tubules constructed by coaxial printing can be improved, through the construction of a new type of mixed high-strength hydrogel 3D printing ink (Liang et al., 2020). The construction of the entire vascular network including macro-vessels and capillaries is based on the hydrogel and the secondary cross-linking encapsulation method of hydrogel has been proposed according to the cross-linking characteristics of the hydrogel. A variety of vascular models with physiological significance can be constructed, such as bifurcated vascular network, spiral vessels and vascular stenosis (Greca et al., 2018).

In addition to extruded 3D printing, new conceptual printing methods, such as 4D biological printing, combine "time" as the fourth dimension with 3D printing to simulate the complex dynamics of natural tissue (**Figure 3**). The 4D printing method is based on projection light-curing printing. Compared with the

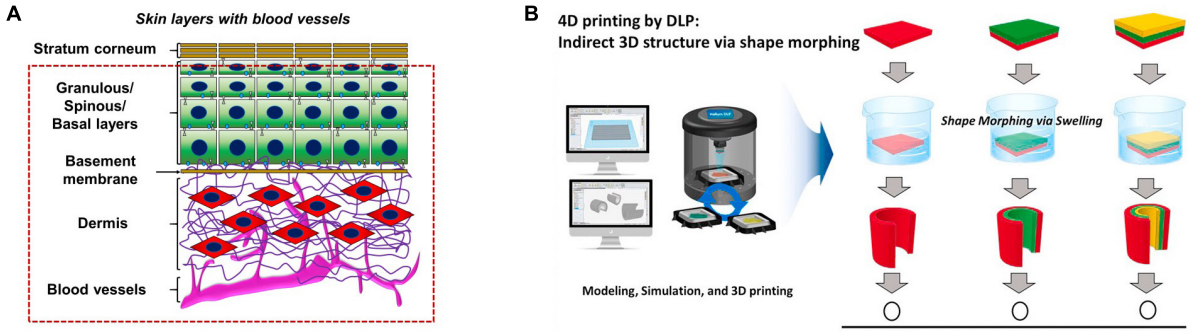


**FIGURE 3 |** New conceptual printing methods. **(A)** Layered printing to achieve vascularized skin. **(B)** The advantage of digital light processing 4D printing is that on the basis of digital light processing 3D printing, one material is used to manufacture structures with multiple curvatures. Reprinted with the permission from Elsevier (Kim et al., 2020; Su et al., 2020). With the permission from Elsevier. Reprinted from Barros et al. (2020) and Kim et al. (2020).

traditional light-curing printing, it can greatly reduce the printing time, while replacing multiple groups of material components (Kim et al., 2020). Future improvements include printing of microfluidic channels directly on curved surfaces such as the skin, allowing real-time detection of body fluids and bodily functions (Su et al., 2020).

## CONCLUSION

Developing tissue in organoids requires interaction of a vascular network within the appropriate diffusion distance to enable the exchange of oxygen, nutrients and metabolic substances. Consequently, the phenomenon of grow arrest in organoids can be attributed to the lack of vascularization. According to the categories of organoid vascularization approaches, both *in vitro* and *in vivo*, we respectively demonstrate these methods by commenting on past literature. We discussed the advantages and disadvantages of these approaches and draw a conclusion that only the method of transplantation *in vivo* can lead to angiogenesis similar to that in human. However, none of these methods have achieved a vessel network standard in organoids, the same as that *in vivo*.

The micro-flow control device provides a good platform for building vascular chips *in vitro*, regarding organoids-on-a-chip. By regulating micro-flow control models, hydrogels, fluid shear forces, etc., we can have a clearer understanding of the interaction of blood between vessels and tissues. At present, the technology of vascular regeneration has matured, nevertheless, It requires further improvement of its long term application that maintains good functional activity and simulation of relative changes in the high-volume micro-flow control chip. Simultaneously, the successful realization of vascularization in organoids-on-a-chip can also provide ideas for the realization of organoid vascularization.

## FUTURE DIRECTIONS

Organoids and organoids-on-a-chip are important means for 3D culture *in vitro*. They overcome many shortcomings of traditional 2D culture and are better in restoring the specific function of organs.

The largest obstacle for organoid maturation is the lack of functional vascularization, this leads to the lack of rational tissue size. The field of organoid vascularization has only recently started developing. And many challenges are on the way of realizing fully functional and spontaneous perfusing capability vascularization. Finding methods of constructing functional vessels in organoids with perfusing capability same as that in humans is the focus of future studies. The strategy based on the developmental principles of vasculature should receive more attention. The engineered vascular tissue should be highly consistent with the vascular development process *in vivo,* both in time and space, in order to form a vascular network with the same functionality. Additionally, new bioengineering approaches are needed to provide long-term cultivation of the organs and efficient mass transfer, while supplying biochemical and physical cues for maturation. For the printing method, advanced technologies to precisely print small-diameter blood vessels should be developed. Establishing a mature system of transplantation methods and cytokine induction is essential for *in vivo* vascularization. With the progress of micro-fabrication technologies and the improvement of previous methods, new methods will emerge in organoid vascularization. The combination of multiple methods may replace the single technical strategy to vascularize organoids. Organoids with fully functional vessels will become real substitute organ models to serve for various fields.

Challenges and problems still exist in the vascularization of organoids-on-a-chip. Due to the limited size of the chip, the implant is embedded on the chip and does not allow adequate space for the formation of a complex network of blood vessels, which may be considered for the expansion of the chip. HUVECs are mostly used as the EC phenotype. However, organ-specific vascular ECs or pluripotent stem cell are recommended for a more realistic restoration of the target organ. In addition, co-cultured cells also have a significant effect on blood vessel growth (Norotte et al., 2009). At present, many vascular organoids-on-a-chip do not apply pericytes to the vascular network, ignoring the important role of the pericytes in regulating and maintaining the growth of blood vessels (Orekhov et al., 2014). In research on therapeutic applications, we can use patient-specific ECs (and support cells) to avoid immune rejection of such implants. This also allows for a more accurate reflection of the function of a particular part. The biggest challenge today remains the precise simulation of the internal environment, such as the shape of the micro-flow model, hydrogel properties, the chemical gradient of cytokines and mechanical stress, which all affect the vascularization of organoids-on-a-chip. Combining organoids-on-a-chip with electronic components will also be a trend. To detect the output, studies have investigated electronic components loaded into organoids-on-a-chip, such as 3D multiwell–multielectrode devices (Eichler et al., 2015), that detect hydrogel and cellular impedances to improve detection of cell toxicity and drug reactions. This also provides an intuitive method for *in vitro* indicator observation. The combination of sensors and organoids-on-a-chip will see further study, however, requirements for the accuracy of sensors increase. For vascularized multi-organoids-on-a-chip, blood vessels acting as a path to connect tissues and loading sensors on the blood vessels can help monitor the overall situation of the chip. The development of non-destructive and real-time methods to characterize the vascular networks in organs on a chip will be the key to the development of the next generation of vascularized organoids-on-a-chip. In addition, further optimization should be made in culture conditions (such as medium composition) to support specific organs and develop vascular networks. The development of a universal medium to ensure that all organs receive essential nutrients and minimize unnecessary toxic reactions is an unresolved issue in the development of a multi-organoids-on-a-chip model.

## AUTHOR CONTRIBUTIONS

WZ directed the completion of this article. XZ and ZX wrote the main content of this article. TS, HX, and LX collected the information and created pictures for this article. YL, FX, and YW provided advice for this article. All authors contributed to the article and approved the submitted version.

## FUNDING

This work was supported by the National Key Research and Development Plan Young Scientists Program (No: 2017YFA0106000); The National Science Fund for Outstanding Young Scholars (No. 31822021); National Science Foundation of China (No: 31771057); and the National Key Research and Development Plan (No. 2016YFC1101100).

## REFERENCES

Auger, F. A., Gibot, L., and Lacroix, D. (2013). The pivotal role of vascularization in tissue engineering. *Annu. Rev. Biomed. Eng.* 15, 177–200. doi: 10.1146/annurev-bioeng-071812-152428

Barros, N., Kim, H., Goudie, M. J., Lee, K., Bandaru, P., Banton, E. A., et al. (2020). Biofabrication of endothelial cell, dermal fibroblast, and multilayered keratinocyte layers for skin tissue engineering. *Biofabrication* doi: 10.1088/1758-5090/aba503

Benam, K. H., Villenave, R., Lucchesi, C., Varone, A., Hubeau, C., Lee, H. H., et al. (2016). Small airway-on-a-chip enables analysis of human lung inflammation and drug responses in vitro. *Nat. Methods* 13, 151–157. doi: 10.1038/nmeth.3697

Bertassoni, L. E., Cecconi, M., Manoharan, V., Nikkhah, M., Hjortnaes, J., Cristino, A. L., et al. (2014). Hydrogel bioprinted microchannel networks for vascularization of tissue engineering constructs. *Lab Chip* 14, 2202–2211. doi: 10.1039/C4LC00030G

Bhatia, S. N., and Ingber, D. E. (2014). Microfluidic organs-on-chips. *Nat. Biotechnol.* 32, 760–772. doi: 10.1038/nbt.2989

Bhushan, A., Senutovitch, N., Bale, S. S., McCarty, W. J., Hegde, M., Jindal, R., et al. (2013). Towards a three-dimensional microfluidic liver platform for predicting drug efficacy and toxicity in humans. *Stem Cell Res. Ther.* 4(Suppl. 1):S16. doi: 10.1186/scrt377

Biselli, E., Agliari, E., Barra, A., Bertani, F. R., Gerardino, A., De Ninno, A., et al. (2017). Organs on chip approach: a tool to evaluate cancer -immune cells interactions. *Sci. Rep.* 7:12737. doi: 10.1038/s41598-017-13070-3

Chung, M., Ahn, J., Son, K., Kim, S., and Jeon, N. L. (2017). Biomimetic model of tumor microenvironment on microfluidic platform. *Adv. Healthc. Mater.* 6:1700196. doi: 10.1002/adhm.201700196

Chung, S., Sudo, R., Mack, P. J., Wan, C., Vickerman, V., Kamm, R. D., et al. (2009). Cell migration into scaffolds under co-culture conditions in a microfluidic platform. *Lab Chip* 9, 269–275. doi: 10.1039/B807585A

Duan, Y., Gotoh, N., Yan, Q., Du, Z., Weinstein, A. M., Wang, T., et al. (2008). Shear-induced reorganization of renal proximal tubule cell actin cytoskeleton and apical junctional complexes. *Proc. Natl. Acad. Sci. U.S.A.* 105, 11418–11423. doi: 10.1073/pnas.0804954105

Eichler, M., Jahnke, H. G., Krinke, D., Muller, A., Schmidt, S., Azendorf, R., et al. (2015). A novel 96-well multielectrode array based impedimetric monitoring platform for comparative drug efficacy analysis on 2D and 3D brain tumor cultures. *Biosens. Bioelectron.* 67, 582–589. doi: 10.1016/j.bios.2014.09.049

Grebenyuk, S., and Ranga, A. (2019). Engineering organoid vascularization. *Front. Bioeng. Biotechnol.* 7:39. doi: 10.3389/fbioe.2019.00039

Greca, L. G., Lehtonen, J., Tardy, B. L., Guo, J., and Rojas, O. J. (2018). Biofabrication of multifunctional nanocellulosic 3D structures: a facile and customizable route. *Mater. Horizons* 5, 408–415. doi: 10.1039/C7MH01139C

Grosberg, A., Alford, P. W., McCain, M. L., and Parker, K. K. (2011). Ensembles of engineered cardiac tissues for physiological and pharmacological study: heart on a chip. *Lab Chip* 11, 4165–4173. doi: 10.1039/c1lc20557a

Haase, K., and Kamm, R. D. (2017). Advances in on-chip vascularization. *Regen. Med.* 12, 285–302. doi: 10.2217/rme-2016-0152

Ham, O., Jin, Y. B., Kim, J., and Lee, M. O. (2020). Blood vessel formation in cerebral organoids formed from human embryonic stem cells. *Biochem. Biophys. Res. Commun.* 521, 84–90. doi: 10.1016/j.bbrc.2019.10.079

Huh, D., Fujioka, H., Tung, Y. C., Futai, N., Paine, R., Grotberg, J. B., et al. (2007). Acoustically detectable cellular-level lung injury induced by fluid mechanical stresses in microfluidic airway systems. *Proc. Natl. Acad. Sci. U.S.A.* 104, 18886–18891. doi: 10.1073/pnas.0610868104

Huh, D., Leslie, D. C., Matthews, B. D., Fraser, J. P., Jurek, S., Hamilton, G. A., et al. (2012). A human disease model of drug toxicity–induced pulmonary edema in a Lung-on-a-Chip microdevice. *Sci. Transl. Med.* 4:159ra147. doi: 10.1126/scitranslmed.3004249

Huh, D., Matthews, B. D., Mammoto, A., Montoya-Zavala, M., Hsin, H. Y., Ingber, D. E., et al. (2010). Reconstituting organ-level lung functions on a chip. *Science* 328, 1662–1668. doi: 10.1126/science.1188302

Jang, K. J., and Suh, K. Y. (2010). A multi-layer microfluidic device for efficient culture and analysis of renal tubular cells. *Lab Chip* 10, 36–42. doi: 10.1039/b907515a

Kang, D., Hong, G., An, S., Jang, I., Yun, W., Shim, J., et al. (2020). Bioprinting of multiscaled hepatic lobules within a highly vascularized construct. *Small* 16:1905505. doi: 10.1002/smll.201905505

Kang, Y. B. A., Sodunke, T. R., Lamontagne, J., Cirillo, J., Rajiv, C., Bouchard, M. J., et al. (2015). Liver sinusoid on a chip: long-term layered co-culture of primary rat hepatocytes and endothelial cells in microfluidic platforms. *Biotechnol. Bioeng.* 112, 2571–2582. doi: 10.1002/bit.25659

Kim, S. H., Seo, Y. B., Yeon, Y. K., Lee, Y. J., Park, H. S., Sultan, M. T., et al. (2020). 4D-bioprinted silk hydrogels for tissue engineering. *Biomaterials* 260:120281. doi: 10.1016/j.biomaterials.2020.120281

Kolesky, D. B., Homan, K. A., Skylar-Scott, M. A., and Lewis, J. A. (2016). Three-dimensional bioprinting of thick vascularized tissues. *Proc. Natl. Acad. Sci. U.S.A.* 113, 3179–3184. doi: 10.1073/pnas.1521342113

Koning, M., van den Berg, C. W., and Rabelink, T. J. (2020). Stem cell-derived kidney organoids: engineering the vasculature. *Cell. Mol. Life Sci.* 77, 2257–2273. doi: 10.1007/s00018-019-03401-0

Lancaster, M. A. (2018). Brain organoids get vascularized. *Nat. Biotechnol.* 36, 407–408. doi: 10.1038/nbt.4133

Lancaster, M. A., and Knoblich, J. A. (2014). Organogenesis in a dish: modeling development and disease using organoid technologies. *Science* 345:1247125. doi: 10.1126/science.1247125

Lee, P. J., Hung, P. J., and Lee, L. P. (2007). An artificial liver sinusoid with a microfluidic endothelial-like barrier for primary hepatocyte culture. *Biotechnol Bioeng* 97, 1340–1346. doi: 10.1002/bit.21360

Liang, Q., Gao, F., Zeng, Z., Yang, J., Wu, M., Gao, C., et al. (2020). Coaxial scale-up printing of diameter-tunable biohybrid hydrogel microtubes with high strength, perfusability, and endothelialization. *Adv. Funct. Mater.* 43:2001485. doi: 10.1002/adfm.202001485

Mansour, A. A., Gonçalves, J. T., Bloyd, C. W., Li, H., Fernandes, S., Quang, D., et al. (2018). An in vivo model of functional and vascularized human brain organoids. *Nat. Biotechnol.* 36, 432–441. doi: 10.1038/nbt.4127

Mao, M., Bei, H. P., Lam, C. H., Chen, P., Wang, S., Chen, Y., et al. (2020). Human-on-leaf-chip: a biomimetic vascular system integrated with chamber-specific organs. *Small* 16:e2000546. doi: 10.1002/smll.202000546

Mazio, C., Casale, C., Imparato, G., Urciuolo, F., and Netti, P. A. (2018). Recapitulating spatiotemporal tumor heterogeneity in vitro through engineered breast cancer microtissues. *Acta Biomater.* 73, 236–249. doi: 10.1016/j.actbio.2018.04.028

Miller, J. S., Stevens, K. R., Yang, M. T., Baker, B. M., Nguyen, D. H., Cohen, D. M., et al. (2012). Rapid casting of patterned vascular networks for perfusable engineered three-dimensional tissues. *Nat. Mater.* 11, 768–774. doi: 10.1038/nmat3357

Mu, X., Zheng, W., Xiao, L., Zhang, W., and Jiang, X. (2013). Engineering a 3D vascular network in hydrogel for mimicking a nephron. *Lab Chip* 13:1612. doi: 10.1039/c3lc41342j

Musah, S., Mammoto, A., Ferrante, T. C., Jeanty, S., Hirano-Kobayashi, M., Mammoto, T., et al. (2017). Mature induced-pluripotent-stem-cell-derived

human podocytes reconstitute kidney glomerular-capillary-wall function on a chip. *Nat. Biomed. Eng.* 1:0069. doi: 10.1038/s41551-017-0069

Muschler, G. F., Nakamoto, C., and Griffith, L. G. (2004). Engineering principles of clinical cell-based tissue engineering. *J. Bone Joint Surg. Am.* 86, 1541–1558. doi: 10.2106/00004623-200407000-00029

Nashimoto, Y., Hayashi, T., Kunita, I., Nakamasu, A., Torisawa, Y., Nakayama, M., et al. (2017). Integrating perfusable vascular networks with a three-dimensional tissue in a microfluidic device. *Integr. Biol.* 9, 506–518. doi: 10.1039/C7IB00024C

Nie, J., Gao, Q., Wang, Y., Zeng, J., Zhao, H., Sun, Y., et al. (2018). Vessel-on-a-chip with hydrogel-based microfluidics. *Small* 14:e1802368. doi: 10.1002/smll.201802368

Noor, N., Shapira, A., Edri, R., Gal, I., Wertheim, L., Dvir, T., et al. (2019). 3D printing of personalized thick and perfusable cardiac patches and hearts. *Adv. Sci.* 6:1900344. doi: 10.1002/advs.201900344

Norotte, C., Marga, F. S., Niklason, L. E., and Forgacs, G. (2009). Scaffold-free vascular tissue engineering using bioprinting. *Biomaterials* 30, 5910–5917. doi: 10.1016/j.biomaterials.2009.06.034

Occhetta, P., Isu, G., Lemme, M., Conficconi, C., Oertle, P., Räz, C., et al. (2018). A three-dimensionalin vitro dynamic micro-tissue model of cardiac scar formation. *Integr. Biol.* 10, 174–183. doi: 10.1039/C7IB00199A

Oddo, A., Peng, B., Tong, Z., Wei, Y., Tong, W. Y., Thissen, H., et al. (2019). Advances in microfluidic blood–brain barrier (BBB) models. *Trends Biotechnol.* 37, 1295–1314. doi: 10.1016/j.tibtech.2019.04.006

Oleaga, C., Bernabini, C., Smith, A. S., Srinivasan, B., Jackson, M., Mclamb, W., et al. (2016). Multi-Organ toxicity demonstration in a functional human in vitro system composed of four organs. *Sci. Rep.* 6:20030. doi: 10.1038/srep20030

Orekhov, A. N., Bobryshev, Y. V., and Chistiakov, D. A. (2014). The complexity of cell composition of the intima of large arteries: focus on pericyte-like cells. *Cardiovasc. Res.* 103, 438–451. doi: 10.1093/cvr/cvu168

Park, J. W., Vahidi, B., Taylor, A. M., Rhee, S. W., and Jeon, N. L. (2006). Microfluidic culture platform for neuroscience research. *Nat. Protoc.* 1, 2128–2136. doi: 10.1038/nprot.2006.316

Park, S. E., Georgescu, A., and Huh, D. (2019). Organoids-on-a-chip. *Science* 364, 960–965. doi: 10.1126/science.aaw7894

Pham, M. T., Pollock, K. M., Rose, M. D., Cary, W. A., Stewart, H. R., Zhou, P., et al. (2018). Generation of human vascularized brain organoids. *Neuroreport* 29, 588–593. doi: 10.1097/WNR.0000000000001014

Price, G. M., Wong, K. H. K., Truslow, J. G., Leung, A. D., Acharya, C., Tien, J., et al. (2010). Effect of mechanical factors on the function of engineered human blood microvessels in microfluidic collagen gels. *Biomaterials* 31, 6182–6189. doi: 10.1016/j.biomaterials.2010.04.041

Ren, L., Liu, W., Wang, Y., Wang, J., Tu, Q., Xu, J., et al. (2013). Investigation of Hypoxia-Induced myocardial injury dynamics in a tissue interface mimicking microfluidic device. *Anal. Chem.* 85, 235–244. doi: 10.1021/ac3025812

Shao, X., Gao, D., Chen, Y., Jin, F., Hu, G., Jiang, Y., et al. (2016). Development of a blood-brain barrier model in a membrane-based microchip for characterization of drug permeability and cytotoxicity for drug screening. *Anal. Chim. Acta* 934, 186–193. doi: 10.1016/j.aca.2016.06.028

Skardal, A., Devarasetty, M., Forsythe, S., Atala, A., and Soker, S. (2016). A reductionist metastasis-on-a-chip platform for in vitro tumor progression modeling and drug screening. *Biotechnol. Bioeng.* 113, 2020–2032. doi: 10.1002/bit.25950

Skardal, A., Murphy, S. V., Devarasetty, M., Mead, I., Kang, H., Seol, Y. J., et al. (2017). Multi-tissue interactions in an integrated three-tissue organ-on-a-chip platform. *Sci. Rep.* 7:8837. doi: 10.1038/s41598-017-08879-x

Su, R., Wen, J., Su, Q., Wiederoder, M. S., Koester, S. J., Uzarski, J. R., et al. (2020). 3D printed self-supporting elastomeric structures for multifunctional microfluidics. *Sci. Adv.* 6:eabc9846. doi: 10.1126/sciadv.abc9846

Sung, J. H., Srinivasan, B., Esch, M. B., McLamb, W. T., Bernabini, C., Shuler, M. L., et al. (2014). Using physiologically-based pharmacokinetic-guided "body-on-a-chip" systems to predict mammalian response to drug and chemical exposure. *Exp. Biol. Med.* 239, 1225–1239. doi: 10.1177/1535370214529397

Takebe, T., Sekine, K., Enomura, M., Koike, H., Kimura, M., Ogaeri, T., et al. (2013). Vascularized and functional human liver from an iPSC-derived organ bud transplant. *Nature* 499, 481–484. doi: 10.1038/nature12271

Takebe, T., Zhang, R.-R., Koike, H., Kimura, M., Yoshizawa, E., Enomura, M., et al. (2014). Generation of a vascularized and functional human liver from an iPSC-derived organ bud transplant. *Nat. Protoc.* 9, 396–409. doi: 10.1038/nprot.2014.020

Tarbell, J. M. (2010). Shear stress and the endothelial transport barrier. *Cardiovasc. Res.* 87, 320–330. doi: 10.1093/cvr/cvq146

Taylor, A. M., Blurton-Jones, M., Rhee, S. W., Cribbs, D. H., Cotman, C. W., Jeon, N. L., et al. (2005). A microfluidic culture platform for CNS axonal injury, regeneration and transport. *Nat. Methods* 2, 599–605. doi: 10.1038/nmeth777

Van den Berg, C. W., Ritsma, L., Avramut, M. C., Wiersma, L. E., van den Berg, B. M., Leuning, D. G., et al. (2018). Renal subcapsular transplantation of PSC-Derived kidney organoids induces neo-vasculogenesis and significant glomerular and tubular maturation in vivo. *Stem Cell Rep.* 10, 751–765. doi: 10.1016/j.stemcr.2018.01.041

Vickerman, V., Blundo, J., Chung, S., and Kamm, R. (2008). Design, fabrication and implementation of a novel multi-parameter control microfluidic platform for three-dimensional cell culture and real-time imaging. *Lab Chip* 8:1468. doi: 10.1039/b802395f

Vickerman, V., and Kamm, R. D. (2012). Mechanism of a flow-gated angiogenesis switch: early signaling events at cell-matrix and cell-cell junctions. *Integr. Biol.* 4, 863–874. doi: 10.1039/c2ib00184e

Wang, J. D., Khafagy, E., Khanafer, K., Takayama, S., and ElSayed, M. E. H. (2016). Organization of endothelial cells, pericytes, and astrocytes into a 3D microfluidicin vitro model of the blood–brain barrier. *Mol. Pharm.* 13, 895–906. doi: 10.1021/acs.molpharmaceut.5b00805

Weinberg, E., Kaazempur-Mofrad, M., and Borenstein, J. (2008). Concept and computational design for a bioartificial nephron-on-a-chip. *Int. J. Artif. Organs* 31, 508–514. doi: 10.1177/039139880803100606

Yin, X., Mead, B. E., Safaee, H., Langer, R., Karp, J. M., and Levy, O. (2016). Engineering stem cell organoids. *Cell Stem Cell* 18, 25–38. doi: 10.1016/j.stem.2015.12.005

Ying, G., Jiang, N., Parra Cantu, C., Tang, G., Zhang, J., Wang, H., et al. (2020). Bioprinted injectable hierarchically porous gelatin methacryloyl hydrogel constructs with shape-memory properties. *Adv. Func. Mater.* 30:2003740. doi: 10.1002/adfm.202003740

Zhang, B., Montgomery, M., Chamberlain, M. D., Ogawa, S., Korolj, A., Pahnke, A., et al. (2016). Biodegradable scaffold with built-in vasculature for organ-on-a-chip engineering and direct surgical anastomosis. *Nat. Mater.* 15, 669–678. doi: 10.1038/nmat4570

Zhang, Y. S., Arneri, A., Bersini, S., Shin, S.-R., Zhu, K., Goli-Malekabadi, Z., et al. (2016). Bioprinting 3D microfibrous scaffolds for engineering endothelialized myocardium and heart-on-a-chip. *Biomaterials* 110, 45–59. doi: 10.1016/j.biomaterials.2016.09.003

Zheng, D.-W., Hong, S., Zhang, Q.-L., Dong, X., Pan, P., Song, W.-F., et al. (2020). Controllable gelation of artificial extracellular matrix for altering mass transport and improving cancer therapies. *Nat. Commun.* 11:4907. doi: 10.1038/s41467-020-18493-7

Zheng, Y., Chen, J., Craven, M., Choi, N. W., Totorica, S., Diaz-Santana, A., et al. (2012). In vitro microvessels for the study of angiogenesis and thrombosis. *Proc. Natl. Acad. Sci.U.S.A.* 109, 9342–9347. doi: 10.1073/pnas.1201240109

**Conflict of Interest:** The authors declare that the research was conducted in the absence of any commercial or financial relationships that could be construed as a potential conflict of interest.

frontiers in Bioengineering and Biotechnology

MINI REVIEW
published: 20 April 2021
doi: 10.3389/fbioe.2021.673212

# Engineering Cardiovascular Tissue Chips for Disease Modeling and Drug Screening Applications

*Alex H. P. Chan*[1,2,3] *and Ngan F. Huang*[1,2,3]*

[1] Department of Cardiothoracic Surgery, Stanford University, Stanford, CA, United States, [2] Stanford Cardiovascular Institute, Stanford University, Stanford, CA, United States, [3] Veterans Affairs Palo Alto Health Care System, Palo Alto, CA, United States

In recent years, the cost of drug discovery and development have been progressively increasing, but the number of drugs approved for treatment of cardiovascular diseases (CVDs) has been limited. Current *in vitro* models for drug development do not sufficiently ensure safety and efficacy, owing to their lack of physiological relevance. On the other hand, preclinical animal models are extremely costly and present problems of inaccuracy due to species differences. To address these limitations, tissue chips offer the opportunity to emulate physiological and pathological tissue processes in a biomimetic *in vitro* platform. Tissue chips enable *in vitro* modeling of CVDs to give mechanistic insights, and they can also be a powerful approach for drug screening applications. Here, we review recent advances in CVD modeling using tissue chips and their applications in drug screening.

**Keywords: cardiovascular, tissue chip, disease modeling, bioengineering (general), iPSC**

OPEN ACCESS

***Edited by:***
*Jianyi Zhang,*
*University of Alabama at Birmingham, United States*

***Reviewed by:***
*Wuqiang Zhu,*
*Mayo Clinic Arizona, United States*
*Vahid Serpooshan,*
*Emory University, United States*

***Correspondence:**
*Ngan F. Huang*
*ngantina@stanford.edu*
*orcid.org/0000-0003-2298-6790*

***Specialty section:***
*This article was submitted to Tissue Engineering and Regenerative Medicine, a section of the journal Frontiers in Bioengineering and Biotechnology*

***Received:*** *27 February 2021*
***Accepted:*** *26 March 2021*
***Published:*** *20 April 2021*

***Citation:***
*Chan AHP and Huang NF (2021) Engineering Cardiovascular Tissue Chips for Disease Modeling and Drug Screening Applications. Front. Bioeng. Biotechnol. 9:673212. doi: 10.3389/fbioe.2021.673212*

## INTRODUCTION

Cardiovascular disease (CVD) is the leading cause of death worldwide (Virani Salim et al., 2020). In the United States alone, nearly half of the population is expected to have some kind of CVD by 2035 (Virani et al., 2021). Despite its prevalence, the number of new drugs aimed to treat CVD has been declining over the last decade (Van Norman, 2020). For example, in a list of Food and Drug Administration (FDA) approved drugs in 2020, there were no new drug approved for the treatment of CVD, which encompass more than half of all CVDs (U.S. Food and Drug Administraion (FDA), 2020). Only one drug was approved in 2019 for cardiomyopathy (Berk et al., 2020), and one drug approved in 2020 for hypercholesterolemia (Markham, 2020). One contributing factor to the low number of approved drugs is cardiotoxicity. Current methods of cardiotoxicity screening *in vitro* rely heavily on the use of cell lines that express cardiac specific ion channels, whereby the drugs interactions with the ion channels are directly observed for evaluation. Following these *in vitro* assays, drug candidates undergo further cardiotoxicity testing *in vivo* before entering clinical trials. Even with stringent preclinical testing, cardiotoxicity remains the second most common reason for drug recall from market, behind hepatic toxicity (Siramshetty et al., 2016). Taken together, there remains a huge unmet need for accurate, efficient, and reliable methods for drug screening.

To address the limitation of existing *in vitro* cardiotoxicity and drug screening efforts that use overly simplified *in vitro* platforms, cardiovascular tissue chips are micro-to-miniature culture

systems that intend to better mimic the complex structure and function of the myocardium or vasculature. The tissue chips incorporate features such as three-dimensionality, multi-cellular interactions, tissue perfusion, hemodynamic shear stress, pulsatile flow, and cyclic stretch to better resemble the native environment. Additionally, the use of primary human cells or specific induced pluripotent stem cell derivatives into cardiovascular tissue chips enable more precise testing of patient-specific responses. Accordingly, cardiovascular tissue chips can complement the current developmental pipeline for drug discovery. In this focused review, we will describe the various strategies by which cardiovascular tissue chips have been developed for disease modeling or drug screening applications, and then discuss emerging areas in this field.

## DESIGN CONSIDERATIONS OF CARDIOVASCULAR TISSUE CHIPS

Numerous design considerations are necessary for replicating physiologically relevant microenvironments. Here we will discuss the considerations of cell sources, multi-cellular interactions, three dimensionality, and mechanical cues. Techniques for fabricating cardiovascular tissue chips, such as photolithography, micromolding, *and* three dimensional (3D) bioprinting are described in detail elsewhere (Zhang et al., 2018; Pradhan et al., 2020). Depending on the complexity of tissue chip and application, researchers may employ multiple manufacturing methods to produce the desired outcome.

### Cell Source

Cardiomyocytes (CMs), the contractile cells of the myocardium, are generally considered to be non-proliferative in the post-natal state and cannot be expanded *in vitro*. Although other cardiovascular lineages like endothelial cells (EC) and smooth muscle cells (SMC) can be expanded *in vitro*, primary human cells have limited doubling times. As an alternative cell source for tissue chips, human induced pluripotent stem cells (iPSC) are ideal because they are a theoretically infinite source of cardiovascular cells. When coupled with robust differentiation methods for CMs and vascular lineages (Rufaihah et al., 2011; Lian et al., 2012, 2014; Burridge et al., 2014a), the ability to generate millions to billions of cardiovascular lineages has no longer become a bottleneck in engineering scalable tissues (Huang et al., 2018). However, a current limitation of iPSC derivatives is the immature phenotype of iPSC-derived CMs that do not resemble that of an adult heart (Koivumäki et al., 2018). To address this limitation, electrical and mechanical stimulation (Ronaldson-Bouchard et al., 2019) or spatially organized biomaterials (Ribeiro et al., 2015; Wanjare et al., 2017) have been shown to enhance the maturity of iPSC-derived CMs. Owing to the advantages of iPSCs, many tissue chips utilize iPSC derivatives for disease modeling or drug screening efforts.

### Multi-Cellular Interactions

The myocardium consists of several different cell types, including CMs, ECs, fibroblasts, and pacemaker cells (Wanjare and Huang, 2017; Zamani et al., 2018). Blood vessels are composed of a luminal layer of endothelium, a medial layer of SMCs, and an adventitial layer of fibroblasts. In both the myocardium and vasculature, intercellular communication via cell-cell contact or paracrine signaling plays an important role in maintaining tissue function or cell survival (Narmoneva et al., 2004; Burridge et al., 2014b). Tissue chips have been developed to incorporate multi-cellular interactions between vascular SMCs and ECs using parallel channels separated by a porous membrane to mimic the internal elastic lamina that physiologically separates these two cell types (Van Engeland et al., 2018). Shear stress of 1–1.5 Pa was applied to the EC by flow of media, and cyclic radial strain of 5–8% was provided by two channels flanking the cell containing channel connected to vacuum. Using this dynamic culturing device, the authors demonstrated biomimetic cellular responses, namely in SMCs aligning perpendicular to the direction of shear stress. This work highlights the importance of multicellular interactions and mechanical cues in conferring physiological vascular responses using tissue chips. However, advancements in the field will enable the inclusion of more cell types within a tissue chip, which should better reflect the complex multi-cellular makeup of cardiovascular tissues.

### Three-Dimensionality

The culture dimensionality of the substrate can also influence cardiovascular function and phenotype. For example, rat neonatal CMs grown in a 3D fibrinogen/Matrigel patch for 3 weeks showed more electrochemically coupled CMs with mature sarcomere structure and well-formed *t*-tubules and *z*-disks, compared to cells in two-dimensional (2D) monolayers (Bian et al., 2014). Similar findings have also been reported using human embryonic stem cell-derived CMs embedded in 3D fibrin hydrogel, compared to 2D monolayered cells (Zhang et al., 2013). Besides regulating cell function, 3D culture can also modulate cardiovascular differentiation of iPSCs. We previously showed that endothelial differentiation of iPSCs within porous 3D polycaprolactone scaffolds significantly increased endothelial differentiation and subsequent vascular-like network formation, compared to on 2D polymer films (Kim et al., 2017). Tissue chips have also incorporated 3D culture to better mimic the spatial dimensionality of native tissues. For example, Zhang et al. (2020) developed arteriole-sized tissue engineered vascular grafts in the shape of hollow conduits in the presence of physiological shear stress (**Figure 1A**). For over 4 weeks, the authors demonstrated that the vascular grafts possessed mechanical strength, vasoactivity, and nitric oxide production. This body of work suggests distinctive differences in cellular response between 2D and 3D culture, and therefore the incorporation of 3D culture within tissue chips better reflect physiological spatial dimensions.

### External Mechanical Cues

The myocardium and vasculature are physiologically subjected to external mechanical cues, including mechanical stretch resulting from pulsatile flow and hemodynamic shear stress within blood vessels (Huang et al., 2007). Unlike tissue culture dishes that lack dynamic stimulation, tissue chips can incorporate externally applied stimuli to better resemble the physiological

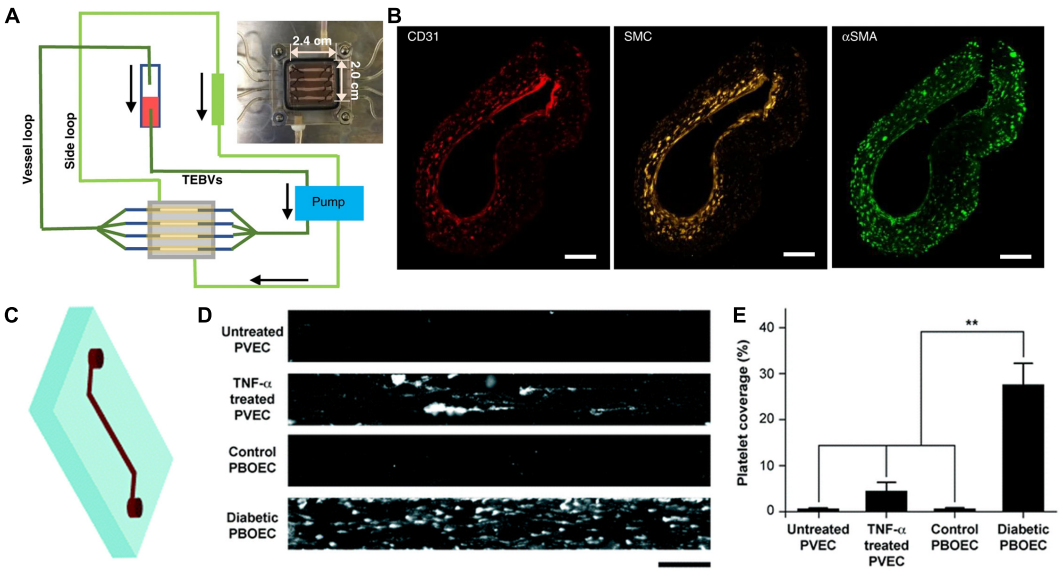


**FIGURE 1 |** Application of tissue chips for cardiovascular disease modeling. **(A)** Schematic of tissue chip composed of perfused tissue-engineered blood vessels for modeling vascular disease. **(B)** Immunofluorescence staining of a three-layered vascular graft comprising CD31-expressing endothelial cells, smooth muscle cells (cell tracker yellow), and smooth muscle actin (αSMA)-expressing fibroblasts. Reproduced with permission from Zhang et al. (2020). Copyright 2020 authors licensed under a CC BY 4.0 (https://creativecommons.org/licenses/by/4.0/; Zhang et al., 2020). **(C)** Schematic of vessel chip. **(D)** Adhesion of fluorescently tagged platelets onto vessel chips seeded with porcine primary vein endothelial cell (PVEC) with or without TNF-α induction, or porcine blood outgrowth endothelial cells (PBOEC) from healthy or diabetic donors. **(E)** Quantification of platelet area coverage inside vessel chip after perfusion of blood (** indicates $p < 0.005$). Adapted from Mathur et al. (2019) with permission from the Centre National de la Recherche Scientifique (CNRS) and The Royal Society of Chemistry.

cardiovascular environment. For example, a tissue chip was developed that incorporated shear stress and radial mechanical strain (Jin et al., 2020). The authors applied cyclic radial strain to up 18% to their tissue chip by utilizing a dual chamber design, in which the top chamber was filled with media and human umbilical vein endothelial cells (HUVECs) were seeded on an elastic polydimethylsiloxane (PDMS) membrane connecting to the bottom chamber. Negative pressure was employed to modulate the degree of radial strain on the membrane. An electrochemical sensor made of conductive carbon nanotubes was also incorporated into the PDMS membrane to monitor mechanotransduction in real time as the HUVECs respond to the cyclic radial strain. This system was shown to recapitulate nitric oxide production and reactive oxygen species production in response to hypertensive (18%) radial strain. In another study that combined both mechanical stretch and shear stress in their tissue chip system, a 3D printed sacrificial mold embedded in a gelatin-based solution formed ∼600 μm-wide microchannels (Shimizu et al., 2020) that were endothelialized with HUVECs and perfused with media. Periodic cyclic stretch of 10% was applied to the microchannel, concomitant with 2 dyn/cm$^2$ shear stress. This work demonstrated that the combination of shear stress and cyclic strain led to improved cytoskeletal assembly of F-actin along the direction of flow, compared to cells induced with shear stress alone or cells under static culture conditions, suggesting that shear stress and cyclic strain are necessary for physiological endothelial response. Together, these studies illustrate the importance of incorporating mechanical cues into the design of tissue chips for mimicking physiological cellular response.

## APPLICATIONS OF TISSUE CHIPS FOR CARDIOVASCULAR DISEASE MODELING AND DRUG SCREENING

### Cardiac Tissue Chips

Myocardial infarction (MI) and reperfusion injury that often follows is the most common morbidity amongst CVDs (Virani et al., 2021). Using tissue chips that contain PDMS pillars, CMs were incorporated into hydrogel and undergoes compaction such that a myocardial construct forms around the pillars. These myocardial constructs were then subjected to anoxic conditions (0% $O_2$) for 6 h to model MI, whereby nutrients were also depleted from the culture media (Chen and Vunjak-Novakovic, 2019). Then to emulate reperfusion injury, the media was replaced with nutrient rich media and constructs returned to normoxic conditions (20% $O_2$). This method showed distinct differences by the increased cell death during ischemia and mitochondrial membrane permeability during reperfusion. Another approach to model MI utilizes oxygen diffusion gradient through spherical cardiac organoids (300 μm diameter) were cultured under hypoxic condition (10% $O_2$) for 10 days to mimic clinically relevant hallmarks of a post-MI heart: infarcted, border, and remote zones (Richards et al., 2020). Molecular changes were also observed in the metabolic shifts, calcium handling, fibrotic

response, and transcriptomic changes that were similar to *in vivo* responses to MI.

Heart failure is one of the most prominent CVDs (Virani et al., 2021) with limited strategies for surgical intervention (Bowen et al., 2020). To model heart failure using tissue chips, a gas chamber and a bioreactor were employed to recapitulate the mechanical cues of cardiac fibrosis using cardiac fibroblasts (Kong et al., 2019). The study showed that pathological strains of 15–20% induced significant increase fibroblast proliferation and collagen expression. The addition of transforming growth factor-β (TGF-β) further exacerbated the fibrotic response in the model. In another study, CMs and cardiac fibroblasts were combined into a hydrogel to form myofibers between two PDMS rods over a period of 14 days to induce maturation (Mastikhina et al., 2020). Contraction of the myofiber causes displacement of the PDMS rods which can be measured in real time. TGF-β was also used to induced fibrosis in this model, which resulted in increasing collagen and smooth muscle α-actin content as well as stiffness of the myofiber. Using this system, the authors also tested an anti-fibrotic drug, pirfenidone, to evaluate the tissue chip as a drug screening platform. The results showed a decrease of brain natriuretic peptide secretion and decreased stiffness, along with significant differences in transcriptional signature in cells between drug treatment and the control group (Mastikhina et al., 2020).

Most cardiac tissue chips focus on the ventricular function as it is the most common mode of heart failure associated with reduced ejection fraction. However, it is also important to consider effects on atrial functions for disease modeling, especially in the context of arrhythmia. One group produced a cardiac tissue with both atrial and ventricular on the ends of a cardiac tissue using the Biowire II platform (Zhao et al., 2019). This method involved iPSC differentiated into atrial and ventricular CMs and seeding on opposing ends of a microwell to form cardiac construct known as Biowire II. The authors reported that the two ends were distinct in terms of action potential, calcium transient and response to atrial specific drugs, with transition zone between two ends to exhibit mixed properties. Similar results were observed in a ring-shaped engineered heart tissue, in which human embryonic stem cell derived CMs were seeded on circular molds and matured on silicon passive stretcher (Goldfracht et al., 2020). Distinctive atrial engineered constructs mimicked atrial fibrillation and was able to respond in a predictable manner to known pharmacological interventions. Cell sheet technology have also contributed to arrhythmia modeling. Using a mixture of human iPSC-derived CMs and non-myocytes to make up tissue sheets of 5–6 cell layers, it was shown that cell heterogeneity was key in recapitulating torsade de pointes arrhythmia (Kawatou et al., 2017). Together, these studies highlight the feasibility and progress of tissue chips for modeling cardiac diseases and screening of therapeutic drug candidates.

## Vascular Tissue Chips

Vascular component of the cardiovascular system consists of arteries and veins to transport blood and nutrients to the body. Endothelial dysfunction is known to be the first stages of atherosclerosis, the most common CVD (Virani et al., 2021). ECs regulate the traffic of cells and nutrients into and out of blood vessels. One predictor of endothelial dysfunction is abnormal endothelial permeability (Gimbrone and García-Cardeña, 2016). Investigators developed an electrochemical assay for endothelial permeability in a microfluidic design (Wong et al., 2020), which bypasses the need for fluorescent tracers and imaging-based analysis. Another study employed tissue chips to study the abnormal endothelial permeability associated with sickle cell disease (Qiu et al., 2018). Using an agarose gelatin interpenetrating polymer network with PDMS adaptor layer, microvessels as small as 20 μm could be generated. The hallmarks of pathological endothelial permeability were further confirmed with gradation of tumor necrosis factor -α (TNF-α).

In addition, vascular chips are also useful for modeling aspects of atherosclerosis. Tissue engineered blood vessels (1 mm OD, 1 cm length) were fabricated in a perfusion system to model early-stage atherosclerosis (**Figures 1A,B**; Zhang et al., 2020). The size of the engineered blood vessel was significantly larger compared to microfluidic approaches, which allowed for assessment of macro-scale properties such as vasoconstriction. Exposure of enzyme modified low density lipoprotein or TNF-α via perfusion to the vascular grafts recapitulated key events in atherosclerosis, including monocyte adhesion and formation of foam cells.

Thrombosis is commonly associated with atherosclerosis, MI, and stroke (Virani et al., 2021). Thrombosis is extensively studied in animal models, but the exact mechanism for pathology is not fully understood. Attempts to recapitulate the hallmarks of clinically relevant features of thrombosis have led to use application of soft lithography and 3D printing for microfluidic devices. A prominent example used soft lithography to create microchannels within a collagen matrix (Zheng et al., 2012). These channels were endothelialized with HUVECs that remained non-thrombogenic under normal culture condition. However, but upon inflammatory stimulation, platelet aggregation occurred within 1 min of whole blood perfusion, and leukocytes migrated through the endothelium after 1 h. The major advantage of this technique over other approaches is the generation of 3D architecture such as bifurcations, which formed a 3D platelet fibrin web that is not observed in 2D models.

Three dimensional printing technology allows for further freedom and greater control to mimic 3D architecture of blood vessels. Zhang et al. (2016) used 3D printed sacrificial molds encapsulated with gelatin methacrylate (GelMA) hydrogel to form microchannels with bifurcation structures. The lumens of the micro channels were endothelialized with HUVECs, and fibroblasts were incorporated into GelMA to simulate perivascular cells. This method accurately modeled dissolution of non-fibrotic clots using thrombolytic therapeutics and showed the protective property of a healthy endothelium in preventing fibroblast infiltration to the clot. Stenosis was also modeled using a 3D printing method in conjunction with computational fluid dynamics to miniaturize blood vessel from computed tomography angiography, while keeping physiological relevant flow and sheer rates (Costa et al., 2017). This study showed potential for rapid modeling of patients with stenosed coronary

arteries to better inform healthcare providers of thrombotic risks in a personalized manner.

Tissue chips have also been employed to examine the function of ECs from diseased settings. Blood outgrowth ECs from healthy or type 1 diabetic pigs and used to endothelialize microchannels in a single-channel vascular chip (**Figure 1C**; Mathur et al., 2019). Microvessels from diabetic cells exhibited many of the hallmarks of endothelial dysfunction, including increased platelet adhesion (**Figures 1D,E**). This study points to patient-specific modeling of thrombosis as a predictive tool for diagnostics. Diabetic vasculopathy was modeled using a self-assembly method in which human iPSC- or embryonic stem cell-derived ECs formed microvascular organoids (Wimmer et al., 2019). The functional hallmark of basement membrane thickening was induced under diabetic conditions. Using this model, the authors elucidated signaling pathways leading to diabetic vasculopathy and identified potential drug targets. This study showed the potential of mechanistic studies through organoids culturing system and disease modeling.

Preclinical screening of a drug's thrombogenicity remains to be an unmet need given the complex and multifactorial process of thrombosis. Utilizing a vessel chip, Barrile et al. (2018) was able to demonstrate thrombogenic effects of a monoclonal antibody therapy in a simple two channel device. The device allowed for evaluation of endothelial activation, platelet adhesion and aggregation, fibrin clot formation and thrombin complexes at physiological concentrations of the monoclonal antibody therapeutic. More importantly, this study revealed mechanistic insights into the prothrombotic property of the antibody, in which modification of the fragment crystallizable domain resulted a decrease in platelet activation. This has significant implications for drug safety and development, as more complete physiological systems of screening are becoming increasingly more prevalent. Blood interactions assays are needed to elucidate mechanisms of thrombosis. However, given the large degree of biological variation among human whole blood, it is likely that differences in platelet activation and clot formation among donors will be observed.

## EMERGING DIRECTIONS FOR TISSUE CHIPS

An emerging direction of tissue chips is the down scaling of the technology to enable higher throughput analysis, while maintaining its superiority over conventional 2D cell culture assays. For example, muscle thin films were generated using $4 \times 10^5$ CMs in 50 replicates (Agarwal et al., 2013), which is much fewer in cells, compared to the cells ($7 \times 10^4$ CMs per sample) used in the Biowire II 3D cardiac constructs (Zhao et al., 2019). While muscle thin film technology reduced the three dimensionality of the model, the contractile forces generated were sufficient to reflect changes in a cardiotoxic drug dose.

Another emerging direction is the automation of data collection and analysis. Recent advances in tissue chip designs have led to the incorporation of sensors or imaging capabilities to increase throughput. Micro-cracked titanium gold thin films were incorporated into the muscle thin films as a flexible strain sensor to measure contractile force (Lind et al., 2017). This improvement enabled real-time continuous readout with minimal handling after cell seeding. Other methods of contractile force measurements have implemented video microscopy to measure the displacement of fixed elements in contact with cardiac constructs. In the Biowire II platform, each cardiac construct is attached to elastic wires on the ends of the well, such that the displacement of the elastic wires can be measured to calculate force generation (Zhao et al., 2019). Optical reporters have been incorporated into tissue chips. One example are voltage-sensitive probes that change in fluorescence intensity in response to voltage changes as a measure of CM action potential. This was successfully demonstrated using a 384-well platform, where individual wells were sampled using automated fluorescence microscopy and analysis (McKeithan et al., 2017). Although this study was conducted using 2D culture, it demonstrated compatibility with patient-specific iPSC-derived CMs and showed proarrhythmic effects of known drugs.

## FUTURE PERSPECTIVES AND CONCLUSION

In conclusion, cardiovascular tissue chips have been shown to be useful in modeling cardiac and vascular diseases, as well as in providing a physiologically relevant platform for drug screening. However, in the design of tissue chips, the balance between physiological fidelity and efficiency should be considered. Tissue chips that mimic multiple aspects of physiological or pathological states often entail complex designs, but complexity can adversely affect a tissue chip's scalability and adaptation to high-throughput systems. Therefore, this balance between complexity and scalability should be thoughtfully considered in the design of tissue chips.

Despite recent advances, tissue chips have not yet become the "gold standard" platform for CVD drug screening. Looking forward, patient-specific cells for personalized disease modeling will become increasingly more prevalent. Conversely, drug screens will utilize genetically diverse patient-derived cells to increase the confidence in the efficacy of a drug candidate. Although iPSC-derived CMs from patients with dilated cardiomyopathy (Shah et al., 2019), long QT syndrome (Sala et al., 2019), and Leopard syndrome (Carvajal-Vergara et al., 2010) have been generated, such disease-specific cells have not been fully integrated into tissue chip systems. In addition, genetic manipulation tools like clustered regularly interspaced short palindromic repeats (CRISPR) technology are expected to make major contributions in disease modeling and drug screening applications. Advancement in real-time sensor technologies will continue improve high throughput systems and lead to more comprehensive data readouts. Knowledge gaps in disease states such as neointimal hyperplasia, arterial calcification and atherosclerotic plaque rupture remain unexplored. Additionally, other systemic aspects involving multi-organ interaction

such as neurohormonal activation in heart failure should be incorporated for improved physiological relevance. Accordingly, interdisciplinary collaborations among the fields of stem cell biology, cardiology, vascular biology and bioengineering will likely advance our knowledge in these areas. The future is bright for tissue chip technology in transforming our approach to CVD modeling and drug screening applications.

## AUTHOR CONTRIBUTIONS

NH and AC performed literature analysis, analyzed the data, and interpreted the data. AC wrote the manuscript, with editorial feedback by NH. Both authors contributed to the article and approved the submitted version.

## FUNDING

This work was supported in part by grants to NH from the US National Institutes of Health (R01 HL127113 and R01 HL142718), the United States Department of Veterans Affairs (1I01BX002310 and 1I01BX004259), and the American Heart Association (20IPA35360085 and 20IPA35310731). AC was supported by a postdoctoral fellowship from the Tobacco Related Disease Research Program (T30FT0860). This publication was made possible by Grant Number U01FD005978 from the FDA/HHS, which supports the UCSF-Stanford Center of Excellence in Regulatory Science and Innovation totaling $99,528 with 100 percentage funded by the FDA/HHS. Its contents are solely the responsibility of the authors and do not necessarily represent the official views of the HHS or FDA.

## REFERENCES

Agarwal, A., Goss, J. A., Cho, A., Mccain, M. L., and Parker, K. K. (2013). Microfluidic heart on a chip for higher throughput pharmacological studies. *Lab. Chip.* 13, 3599–3608. doi: 10.1039/c3lc50350j

Barrile, R., Van Der Meer, A. D., Park, H., Fraser, J. P., Simic, D., Teng, F., et al. (2018). Organ-on-chip recapitulates thrombosis induced by an anti-CD154 monoclonal antibody: translational potential of advanced microengineered systems. *Clin. Pharmacol. Ther.* 104, 1240–1248. doi: 10.1002/cpt.1054

Berk, J., Damy, T., Drachman, B., Elliott, P., Gottlieb, S., Grogan, M., et al. (2020). Efficacy of tafamidis in transthyretin amyloid cardiomyopathy in the ATTR-ACT trial. *Heart Lung* 49, 209–210. doi: 10.1016/j.hrtlng.2020.02.009

Bian, W., Badie, N., Himel, H. D. T., and Bursac, N. (2014). Robust T-tubulation and maturation of cardiomyocytes using tissue-engineered epicardial mimetics. *Biomaterials* 35, 3819–3828. doi: 10.1016/j.biomaterials.2014.01.045

Bowen, R. E. S., Graetz, T. J., Emmert, D. A., and Avidan, M. S. (2020). Statistics of heart failure and mechanical circulatory support in 2020. *Ann. Transl. Med.* 8:827. doi: 10.21037/atm-20-1127

Burridge, P. W., Matsa, E., Shukla, P., Lin, Z. C., Churko, J. M., Ebert, A. D., et al. (2014a). Chemically defined generation of human cardiomyocytes. *Nat. Methods* 11, 855–860. doi: 10.1038/nmeth.2999

Burridge, P. W., Metzler, S. A., Nakayama, K. H., Abilez, O. J., Simmons, C. S., Bruce, M. A., et al. (2014b). Multi-cellular interactions sustain long-term contractility of human pluripotent stem cell-derived cardiomyocytes. *Am. J. Transl. Res.* 6, 724–735.

Carvajal-Vergara, X., Sevilla, A., D'souza, S. L., Ang, Y. S., Schaniel, C., Lee, D. F., et al. (2010). Patient-specific induced pluripotent stem-cell-derived models of LEOPARD syndrome. *Nature* 465, 808–812. doi: 10.1038/nature09005

Chen, T., and Vunjak-Novakovic, G. (2019). Human tissue-engineered model of myocardial ischemia-reperfusion injury. *Tissue Eng. Part A* 25, 711–724. doi: 10.1089/ten.TEA.2018.0212

Costa, P. F., Albers, H. J., Linssen, J. E. A., Middelkamp, H. H. T., Van Der Hout, L., Passier, R., et al. (2017). Mimicking arterial thrombosis in a 3D-printed microfluidic in vitro vascular model based on computed tomography angiography data. *Lab. Chip.* 17, 2785–2792. doi: 10.1039/c7lc00202e

Gimbrone, M. A. Jr., and García-Cardeña, G. (2016). Endothelial cell dysfunction and the pathobiology of atherosclerosis. *Circ. Res.* 118, 620–636. doi: 10.1161/circresaha.115.306301

Goldfracht, I., Protze, S., Shiti, A., Setter, N., Gruber, A., Shaheen, N., et al. (2020). Generating ring-shaped engineered heart tissues from ventricular and atrial human pluripotent stem cell-derived cardiomyocytes. *Nat. Commun.* 11:75. doi: 10.1038/s41467-019-13868-x

Huang, N. F., Lee, R. J., and Li, S. (2007). Chemical and physical regulation of stem cells and progenitor cells: potential for cardiovascular tissue engineering. *Tissue Eng.* 13, 1809–1823. doi: 10.1089/ten.2006.0096

Huang, N. F., Serpooshan, V., Morris, V. B., Sayed, N., Pardon, G., Abilez, O. J., et al. (2018). Big bottlenecks in cardiovascular tissue engineering. *Commun. Biol.* 1:199. doi: 10.1038/s42003-018-0202-8

Jin, Z. H., Liu, Y. L., Fan, W. T., and Huang, W. H. (2020). Integrating flexible electrochemical sensor into microfluidic chip for simulating and monitoring vascular mechanotransduction. *Small* 16:e1903204. doi: 10.1002/smll.201903204

Kawatou, M., Masumoto, H., Fukushima, H., Morinaga, G., Sakata, R., Ashihara, T., et al. (2017). Modelling torsade de pointes arrhythmias in vitro in 3D human iPS cell-engineered heart tissue. *Nat. Commun.* 8:1078. doi: 10.1038/s41467-017-01125-y

Kim, J. J., Hou, L., Yang, G., Mezak, N. P., Wanjare, M., Joubert, L. M., et al. (2017). Microfibrous scaffolds enhance endothelial differentiation and organization of induced pluripotent stem cells. *Cell Mol. Bioeng.* 10, 417–432. doi: 10.1039/c7bm00883j

Koivumäki, J. T., Naumenko, N., Tuomainen, T., Takalo, J., Oksanen, M., Puttonen, K. A., et al. (2018). Structural immaturity of human iPSC-derived cardiomyocytes: in silico investigation of effects on function and disease modeling. *Front. Physiol.* 9:80. doi: 10.3389/fphys.2018.00080

Kong, M., Lee, J., Yazdi, I. K., Miri, A. K., Lin, Y. D., Seo, J., et al. (2019). Cardiac fibrotic remodeling on a chip with dynamic mechanical stimulation. *Adv. Healthc. Mater* 8:e1801146. doi: 10.1002/adhm.201801146

Lian, X., Bao, X., Al-Ahmad, A., Liu, J., Wu, Y., Dong, W., et al. (2014). Efficient differentiation of human pluripotent stem cells to endothelial progenitors via small-molecule activation of WNT signaling. *Stem Cell Rep.* 3, 804–816. doi: 10.1016/j.stemcr.2014.09.005

Lian, X., Hsiao, C., Wilson, G., Zhu, K., Hazeltine, L. B., Azarin, S. M., et al. (2012). Robust cardiomyocyte differentiation from human pluripotent stem cells via temporal modulation of canonical Wnt signaling. *Proc. Natl. Acad. Sci. U.S.A.* 109, E1848–E1857. doi: 10.1073/pnas.1200250109

Lind, J. U., Yadid, M., Perkins, I., O'connor, B. B., Eweje, F., Chantre, C. O., et al. (2017). Cardiac microphysiological devices with flexible thin-film sensors for higher-throughput drug screening. *Lab. Chip.* 17, 3692–3703. doi: 10.1039/c7lc00740j

Markham, A. (2020). Bempedoic acid: first approval. *Drugs* 80, 747–753. doi: 10.1007/s40265-020-01308-w

Mastikhina, O., Moon, B. U., Williams, K., Hatkar, R., Gustafson, D., Mourad, O., et al. (2020). Human cardiac fibrosis-on-a-chip model recapitulates disease hallmarks and can serve as a platform for drug testing. *Biomaterials* 233:119741. doi: 10.1016/j.biomaterials.2019.119741

Mathur, T., Singh, K. A., Nk, R. P., Tsai, S. H., Hein, T. W., Gaharwar, A. K., et al. (2019). Organ-on-chips made of blood: endothelial progenitor cells from blood reconstitute vascular thromboinflammation in vessel-chips. *Lab. Chip.* 19, 2500–2511. doi: 10.1039/c9lc00469f

McKeithan, W. L., Savchenko, A., Yu, M. S., Cerignoli, F., Bruyneel, A. A. N., Price, J. H., et al. (2017). An automated platform for assessment of congenital and drug-induced arrhythmia with hiPSC-derived cardiomyocytes. *Front. Physiol.* 8:766. doi: 10.3389/fphys.2017.00766

Narmoneva, D. A., Vukmirovic, R., Davis, M. E., Kamm, R. D., and Lee, R. T. (2004). Endothelial cells promote cardiac myocyte survival and spatial

reorganization: implications for cardiac regeneration. *Circulation* 110, 962–968. doi: 10.1161/01.Cir.0000140667.37070.07

Pradhan, S., Banda, O. A., Farino, C. J., Sperduto, J. L., Keller, K. A., Taitano, R., et al. (2020). Biofabrication strategies and engineered in vitro systems for vascular mechanobiology. *Adv. Healthc. Mater.* 9:1901255. doi: 10.1002/adhm.201901255

Qiu, Y., Ahn, B., Sakurai, Y., Hansen, C. E., Tran, R., Mimche, P. N., et al. (2018). Microvasculature-on-a-chip for the long-term study of endothelial barrier dysfunction and microvascular obstruction in disease. *Nat. Biomed. Eng.* 2, 453–463. doi: 10.1038/s41551-018-0224-z

Ribeiro, A. J., Ang, Y. S., Fu, J. D., Rivas, R. N., Mohamed, T. M., Higgs, G. C., et al. (2015). Contractility of single cardiomyocytes differentiated from pluripotent stem cells depends on physiological shape and substrate stiffness. *Proc. Natl. Acad. Sci. U.S.A.* 112, 12705–12710. doi: 10.1073/pnas.1508073112

Richards, D. J., Li, Y., Kerr, C. M., Yao, J., Beeson, G. C., Coyle, R. C., et al. (2020). Human cardiac organoids for the modelling of myocardial infarction and drug cardiotoxicity. *Nat. Biomed. Eng.* 4, 446–462. doi: 10.1038/s41551-020-0539-4

Ronaldson-Bouchard, K., Yeager, K., Teles, D., Chen, T., Ma, S., Song, L., et al. (2019). Engineering of human cardiac muscle electromechanically matured to an adult-like phenotype. *Nat. Protoc.* 14, 2781–2817. doi: 10.1038/s41596-019-0189-8

Rufaihah, A. J., Huang, N. F., Jame, S., Lee, J. C., Nguyen, H. N., Byers, B., et al. (2011). Endothelial cells derived from human iPSCS increase capillary density and improve perfusion in a mouse model of peripheral arterial disease. *Arteriosc. Thromb. Vasc. Biol.* 31, e72–e79. doi: 10.1161/atvbaha.111.230938

Sala, L., Gnecchi, M., and Schwartz, P. J. (2019). Long QT syndrome modelling with cardiomyocytes derived from human-induced pluripotent stem cells. *Arrhythm Electrophysiol. Rev.* 8, 105–110. doi: 10.15420/aer.2019.1.1

Shah, D., Virtanen, L., Prajapati, C., Kiamehr, M., Gullmets, J., West, G., et al. (2019). Modeling of LMNA-related dilated cardiomyopathy using human induced pluripotent stem cells. *Cells* 8:594. doi: 10.3390/cells8060594

Shimizu, A., Goh, W. H., Itai, S., Hashimoto, M., Miura, S., and Onoe, H. (2020). ECM-based microchannel for culturing in vitro vascular tissues with simultaneous perfusion and stretch. *Lab. Chip.* 20, 1917–1927. doi: 10.1039/d0lc00254b

Siramshetty, V. B., Nickel, J., Omieczynski, C., Gohlke, B. O., Drwal, M. N., and Preissner, R. (2016). WITHDRAWN–a resource for withdrawn and discontinued drugs. *Nucleic Acids Res.* 44, D1080–D1086. doi: 10.1093/nar/gkv1192

U.S. Food and Drug Administraion (FDA) (2020). *Novel Drug Approvals for 2020*. Available online at: https://www.fda.gov/drugs/new-drugs-fda-cders-new-molecular-entities-and-new-therapeutic-biological-products/novel-drug-approvals-2020 (accessed August 2, 2021).

Van Engeland, N. C. A., Pollet, A., Den Toonder, J. M. J., Bouten, C. V. C., Stassen, O., and Sahlgren, C. M. (2018). A biomimetic microfluidic model to study signalling between endothelial and vascular smooth muscle cells under hemodynamic conditions. *Lab. Chip.* 18, 1607–1620. doi: 10.1039/c8lc00286j

Van Norman, G. A. (2020). Limitations of animal studies for predicting toxicity in clinical trials: Part 2: potential alternatives to the use of animals in preclinical trials. *JACC Basic Transl. Sci.* 5, 387–397. doi: 10.1016/j.jacbts.2020.03.010

Virani Salim, S., Alonso, A., Benjamin Emelia, J., Bittencourt Marcio, S., Callaway Clifton, W., Carson April, P., et al. (2020). Heart disease and stroke statistics—2020 update: a report from the american heart association. *Circulation* 141, e139–e596. doi: 10.1161/CIR.0000000000000757

Virani, S. S., Alonso, A., Aparicio, H. J., Benjamin, E. J., Bittencourt, M. S., Callaway, C. W., et al. (2021). Heart disease and stroke statistics-2021 update: a report from the american heart association. *Circulation* 143, e254–e743. doi: 10.1161/cir.0000000000000950

Wanjare, M., and Huang, N. F. (2017). Regulation of the microenvironment for cardiac tissue engineering. *Regen. Med.* 12, 187–201. doi: 10.2217/rme-2016-0132

Wanjare, M., Hou, L., Nakayama, K. H., Kim, J. J., Mezak, N. P., Abilez, O. J., et al. (2017). Anisotropic microfibrous scaffolds enhance the organization and function of cardiomyocytes derived from induced pluripotent stem cells. *Biomater. Sci.* 5, 1567–1578. doi: 10.1039/c7bm00323d

Wimmer, R. A., Leopoldi, A., Aichinger, M., Wick, N., Hantusch, B., Novatchkova, M., et al. (2019). Human blood vessel organoids as a model of diabetic vasculopathy. *Nature* 565, 505–510. doi: 10.1038/s41586-018-0858-8

Wong, J. F., Mohan, M. D., Young, E. W. K., and Simmons, C. A. (2020). Integrated electrochemical measurement of endothelial permeability in a 3D hydrogel-based microfluidic vascular model. *Biosens. Bioelectron.* 147:111757. doi: 10.1016/j.bios.2019.111757

Zamani, M., Karaca, E., and Huang, N. F. (2018). Multicellular interactions in 3D engineered myocardial tissue. *Front. Cardiovasc. Med.* 5:147. doi: 10.3389/fcvm.2018.00147

Zhang, B., Korolj, A., Lai, B. F. L., and Radisic, M. (2018). Advances in organ-on-a-chip engineering. *Nat. Rev. Mater.* 3, 257–278. doi: 10.1038/s41578-018-0034-7

Zhang, D., Shadrin, I. Y., Lam, J., Xian, H. Q., Snodgrass, H. R., and Bursac, N. (2013). Tissue-engineered cardiac patch for advanced functional maturation of human ESC-derived cardiomyocytes. *Biomaterials* 34, 5813–5820. doi: 10.1016/j.biomaterials.2013.04.026

Zhang, X., Bishawi, M., Zhang, G., Prasad, V., Salmon, E., Breithaupt, J. J., et al. (2020). Modeling early stage atherosclerosis in a primary human vascular microphysiological system. *Nat. Commun.* 11:5426. doi: 10.1038/s41467-020-19197-8

Zhang, Y. S., Davoudi, F., Walch, P., Manbachi, A., Luo, X., Dell'erba, V., et al. (2016). Bioprinted thrombosis-on-a-chip. *Lab. Chip.* 16, 4097–4105. doi: 10.1039/c6lc00380j

Zhao, Y., Rafatian, N., Feric, N. T., Cox, B. J., Aschar-Sobbi, R., Wang, E. Y., et al. (2019). A platform for generation of chamber-specific cardiac tissues and disease modeling. *Cell* 176, 913–927.e918. doi: 10.1016/j.cell.2018.11.042

Zheng, Y., Chen, J., Craven, M., Choi, N. W., Totorica, S., Diaz-Santana, A., et al. (2012). In vitro microvessels for the study of angiogenesis and thrombosis. *Proc. Natl. Acad. Sci. U.S.A.* 109, 9342–9347. doi: 10.1073/pnas.1201240109

**Conflict of Interest:** The authors declare that the research was conducted in the absence of any commercial or financial relationships that could be construed as a potential conflict of interest.

frontiers in Bioengineering and Biotechnology

MINI REVIEW
published: 29 April 2021
doi: 10.3389/fbioe.2021.673683

# Current Status and Limitations of Myocardial Infarction Large Animal Models in Cardiovascular Translational Research

*Hye Sook Shin*[1,2†], *Heather Hyeyoon Shin*[3†] *and Yasuhiro Shudo*[1,2*]

[1] Department of Cardiothoracic Surgery, Stanford University School of Medicine, Stanford, CA, United States, [2] Stanford Cardiovascular Institute, Stanford University School of Medicine, Stanford, CA, United States, [3] Department of Neurology and Neurological Sciences, Stanford University School of Medicine, Stanford, CA, United States

Establishing an appropriate disease model that mimics the complexities of human cardiovascular disease is critical for evaluating the clinical efficacy and translation success. The multifaceted and complex nature of human ischemic heart disease is difficult to recapitulate in animal models. This difficulty is often compounded by the methodological biases introduced in animal studies. Considerable variations across animal species, modifications made in surgical procedures, and inadequate randomization, sample size calculation, blinding, and heterogeneity of animal models used often produce preclinical cardiovascular research that looks promising but is irreproducible and not translatable. Moreover, many published papers are not transparent enough for other investigators to verify the feasibility of the studies and the therapeutics' efficacy. Unfortunately, successful translation of these innovative therapies in such a closed and biased research is difficult. This review discusses some challenges in current preclinical myocardial infarction research, focusing on the following three major inhibitors for its successful translation: Inappropriate disease model, frequent modifications to surgical procedures, and insufficient reporting transparency.

**Keywords: myocardial infarction, heart failure, large animal models, large animal surgery, preclinical, translational research, review**

OPEN ACCESS

***Edited by:***
*Vahid Serpooshan, Emory University, United States*

***Reviewed by:***
*Richard Jung, University of Ottawa Heart Institute, Canada*
*Nilesh Ghugre, Sunnybrook Research Institute (SRI), Canada*

***Correspondence:**
*Yasuhiro Shudo*
*yshudo@stanford.edu*

*[†] These authors have contributed equally to this work*

***Specialty section:***
*This article was submitted to Tissue Engineering and Regenerative Medicine, a section of the journal Frontiers in Bioengineering and Biotechnology*

***Received:*** *28 February 2021*
***Accepted:*** *06 April 2021*
***Published:*** *29 April 2021*

***Citation:***
*Shin H, Shin HH and Shudo Y (2021) Current Status and Limitations of Myocardial Infarction Large Animal Models in Cardiovascular Translational Research. Front. Bioeng. Biotechnol. 9:673683. doi: 10.3389/fbioe.2021.673683*

## INTRODUCTION

Cardiovascular diseases (CVDs) are devastating health problems worldwide; they accounted for 18.6 million deaths globally in 2019, which amounted to an increase of 17.1% since 2010 (Virani et al., 2021). Myocardial ischemia is the most prevalent cause of death within the spectrum of cardiovascular illnesses. Myocardial ischemia occurs when blood flow to the myocardium is obstructed by a partial or complete blockage of the coronary artery due to plaque buildup (atherosclerosis). Coronary artery narrowing and plaque rupture causes insufficient oxygen delivery to the myocardium, causing myocardial infarction (MI). The American Heart Association estimates that a new MI case is diagnosed every 40 s in the United States (Virani et al., 2021). Over the past several decades, the pathophysiological mechanisms driving these cardiovascular complications have extensively been studied in animal models, resulting in the development of numerous interventional and pharmacological treatments (Nicolini and Gherli, 2009).

Various therapeutic strategies have been proposed to mitigate the risk of myocardial infarction with cardioprotective effects in preclinical studies, but only a few have shown positive clinical study results (Bolli et al., 2004; Kloner, 2013). Ischemic remote, pre-, per-, or post-conditioning (i.e., a series of alternating intervals of brief ischemia and reperfusion) and pharmacological manipulation have been extensively studied over the last 30 years to treat acute myocardial infarction with many positive conclusions and discoveries of many pharmacological targets in preclinical settings (Heusch, 2015). However, most of the clinical outcomes remain mixed or statistically underpowered (Heusch, 2013; Kloner, 2013; Hausenloy and Yellon, 2016; Giustino and Dangas, 2017). For example, reperfusion therapy, often coupled with the administration of adjunctive therapies, has shown to reduce infarct size in animal models of acute myocardial infarction (AMI) and improve left ventricular function; however, it has failed to show similar effects in human AMI patients, potentially due to significant discrepancies between different preclinical animal models and clinical situations (Cannon, 2005; Dirksen et al., 2007; Miura and Miki, 2008; Trankle et al., 2016).

Several cardiac repair strategies have been recently developed with promising preclinical results but also with little translational success. One strategy is the direct injection of cells or biomimetic scaffolds made of polymers with cells, growth factors, or cytokines (Ungerleider and Christman, 2014). However, the grafted cells directly injected through a needle into the myocardium easily aggregate and undergo necrosis, and they are poorly localized on the myocardium of interest, thus limiting the efficacy of the therapy (Menasché, 2018). The tissue engineering using biomaterial scaffolds is limited due to their questionable immuno- or bio-compatibility and bio-functionality (Christman and Lee, 2006; Guo et al., 2020). As an alternative, scaffold-free stem cell sheet treatment has been developed with increased cell engraftment and survival on the host myocardium and promising therapeutic effects in animal studies (Shudo et al., 2011, 2013, 2014), but there are not yet many clinical studies to date (Miyagawa et al., 2017).

Despite the disagreement over the optimal cell type, cell counts, cell delivery methods, and unknown therapeutic mechanisms, stem cell therapies seem to demonstrate some degree of therapeutic improvements in terms of reduced ischemic injury size or improved left ventricular function in MI animal models in preclinical studies (Laflamme et al., 2007; Wang et al., 2009; Wolf et al., 2009; Shudo et al., 2011; Lu et al., 2012; Okura et al., 2012; Li et al., 2013; Chong et al., 2014; Zhao et al., 2014; Alestalo et al., 2015; Haller et al., 2015; Suzuki et al., 2016; Kim et al., 2017; Sharp et al., 2017; Lim et al., 2018; Crisostomo et al., 2019; Ishida et al., 2019; Romagnuolo et al., 2019; Sun et al., 2020). Nevertheless, the promising results of many preclinical studies on cell therapies have not been successfully replicated in randomized clinical trials (Janssens et al., 2006; Lunde et al., 2006; Penicka et al., 2007; Makkar et al., 2012; Perin et al., 2012; Gao et al., 2013; Quyyumi et al., 2017; Wollert et al., 2017). According to the review of articles on PubMed (preclinical) and ClinicalTrials.Gov (clinical research), no regenerative medicine was commercialized between 2008 and 2014, and only about 50 cell therapies and eight gene therapies moved onto the clinical phase, although there had been approximately 800 preclinical studies per year (Ungerleider and Christman, 2014). The frequent failure to translate the cardio-protective and regenerative therapeutics from the bench to the bedside has been attributed to the large gap between animal models and humans and inadequate preclinical study design (Bolli et al., 2004; Kloner and Rezkalla, 2004; Downey and Cohen, 2009; Hausenloy et al., 2010; Ludman et al., 2010; Heusch, 2017). There is a growing concern over the safety and efficacy of regenerative therapeutics, which many researchers have determined to be due to low internal and external validities in preclinical animal research (Ioannidis, 2005, 2016; Bracken, 2009; van der Worp et al., 2010; Hooijmans and Ritskes-Hoitinga, 2013; Steele et al., 2017; Pound and Ritskes-Hoitinga, 2018; Voelkl et al., 2018; Lüscher, 2019; Ferreira et al., 2020). This review addresses the issues prevalent in preclinical MI research, which hinder the successful therapeutic translation of promising treatment strategies. The review proceeds by discussing (1) the obstacles in building a representative animal model for MI studies, (2) factors limiting the scientific rigor in the MI study design, and (3) suggestions for improving the relevance of preclinical MI studies.

# REVIEW

## Suitability of Animal Models for Human MI

A major hurdle in clinical translation from bench to bedside for MI therapies is the difficulty in creating a representative disease model. Modeling MI induced heart failure (HF) that resembles human cardiac conditions is challenging because human MI develops as a result of the interplay of many causes over time and is often complicated by comorbidity and polypharmacy (Pound and Ritskes-Hoitinga, 2018). A wide range of comorbid health conditions, such as epilepsy, smoking, alcoholism, cancer, diabetes, and rheumatoid arthritis, are known to remarkably affect MI fatality (Quintana et al., 2018). The incidence of HF caused by MI is often age- and gender-biased, with higher rates in men than women and in the elderly than young adults (Savarese and Lund, 2017; Virani et al., 2021). Specific racial and ethnic populations, especially minority groups, are at a considerable risk of developing MI, which may lead to death (Graham, 2015, 2016; Virani et al., 2021). However, many animal studies have failed to reflect the heterogeneity observed in the patients with MI. The animal models currently used in the laboratory settings tend to be relatively homogeneous, young, and healthy, with no genetic predisposition or underlying medical conditions (van der Worp et al., 2010; Pound and Ritskes-Hoitinga, 2018). Many preclinical studies induce MI through direct ligation of coronary artery, which does not represent the natural pathophysiology of atherosclerosis that develops over life time in humans (Getz and Reardon, 2012; Gao et al., 2016; Lee et al., 2017). Different species are used to recapitulate the pathogenesis of MI with its own advantages and disadvantages. Small animal models (rodents) are widely used in MI studies for their practical benefits, such as small body size, easy pre-/post-care, low maintenance cost, shorter generation time, and well-defined genetics. However,

small animals have limitations in that their anatomy and cardiac kinetics are fundamentally different from those of humans. For example, rodent hearts function at very high heart rates (HRs), with their resting HR being more than five times higher than in humans. Their small body and organ sizes and short lifespan require expression of different genes related to action potential properties and contractile kinetics in ventricular cardiomyocytes (CMs) (Locher et al., 2009; Milani-Nejad and Janssen, 2014). For example, their ventricular CMs predominately express fast α-myosin heavy chain (MHC) (>94–100%), whereas human LV cardiomyocytes (CMs) predominately expresses slow β-MHC (>90–95%), thus resulting in differential cardiac contractile and kinetic responses to cardiac dysfunction (Milani-Nejad and Janssen, 2014). These differences in cardiac parameters may lead to different results of cell therapy experiments across different animal models. For example, Laflamme et al. (2007) observed frequent arrhythmias in non-human primates and pigs following transplantation of embryonic stem cell-derived cardiomyocytes, but not in rats, possibly because rats' high heart rate could mask arrhythmias (Chong et al., 2014; Romagnuolo et al., 2019).

Small animals' body and organ sizes make it even more challenging to mimic the natural pathophysiology of human atherosclerosis and thus MI. The gradual occlusion of the coronary artery can be established in animal models by using interventional operation using various materials, such as Ameroid Constrictors (Shudo et al., 2011; Potz et al., 2018; Ishida et al., 2019). However, small animals' heart is too small to correctly identify each vasculature, which is tricky to occlude using these materials. The most feasible way to induce MI in small animals is the permanent ligation of the coronary artery using a suture loop, but the etiology is different from that naturally occurring MI in humans in this case. Even though there have been attempts to model atherosclerosis in transgenic or high fat-fed rodents, rodents rarely develop atherosclerosis in coronary arteries but readily in the aortic root probably due to their rapid heart rate and blood flow and often in the absence of complications seen in human MI patients such as thrombosis (Getz and Reardon, 2012; Gao et al., 2016; Lee et al., 2017).

Besides, small animals' cardiac anatomy and physiology make it challenging to visualize and quantify the spatial distribution of blood flow and assess microvascular histomorphology following MI (Krueger et al., 2013; Liu et al., 2020). To overcome these technical difficulties, some new imaging technologies have been developed to improve spatial resolution, such as the Imaging Cryomicrotome (Krueger et al., 2013), micro-PET/CT hybrid systems (Gargiulo et al., 2012), and magnetic resonance (MR) tagging (Epstein et al., 2002; Thomas et al., 2004). Researchers must consider these fundamental differences in anatomy and cardiac kinetics across species when interpreting the animal study results as they give rise to different phenotypes between humans with genetic predispositions and transgenic animal models that recapitulate the diseases (Riehle and Bauersachs, 2019). Consideration of available options for post-operative evaluation must be made when choosing an animal model as well. Large animals, such as swine and sheep, which are anatomically and physiologically closer to the humans, are used to minimize these phenotypic differences between humans and animal models. In MI research, it is essential to correctly identify the perfusion and coronary collateral circulation systems in the animal of choice, as the variations in these structures across animals can significantly affect the early and progressive response to ischemia (Harken et al., 1981; Hill and Iaizzo, 2009). In this regard, swine and ovine models are preferred to smaller animals, such as rodents and canines, as their coronary arterial structure and scant collateral arteries resemble those of humans, which allows for the creation of predictable infarct size at a preferred location in the myocardium (Dixon and Spinale, 2009; Nguyen and Wu, 2015). Moreover, swine, sheep, and human myocardia share high degrees of similarities in cardiac kinetics (Milani-Nejad and Janssen, 2014) and healing characteristics following injury (Lelovas et al., 2014). A domestic sheep is ideal in size for clinical imaging modalities (such as MRI and CT) and medical devices (such as pacemakers and stents) designed for the humans (Ribitsch et al., 2020).

However, there are several disadvantages of using large animal models, which can eventually limit the reproducibility of the research. Some of the factors that discourage their use in research are the high cost required for performing the experiments, housing/maintenance and care, and lower acceptance as model animals by society (Freedman et al., 2015; Camacho et al., 2016; Spannbauer et al., 2019). The public's growing concern about the welfare of research animals, especially companion animals such as dogs and cats, has led to more stringent laws, policies, and guidelines, limiting their prevalent use in research (National Research Council (Us) Committee on Scientific and Humane Issues in the Use of Random Source Dogs and Cats in Research, 2009). Additionally, swine, especially the Yorkshire pigs, dramatically gain weight in adulthood, which complicates long-term follow-up and makes it an unsuitable model for chronic IHF studies (Schuleri et al., 2008; Tohyama and Kobayashi, 2019). Anesthetized swine of MI models often display high mortality rates due to fatal arrhythmia, such as ventricular fibrillation, during or shortly after the coronary artery occlusion or ischemia (Halkos et al., 2008; Lim et al., 2018), which may introduce sample size bias and confound experimental results. **Table 1** shows a comparative analysis of different animal models commonly used in MI studies.

No single animal model can sufficiently answer every question raised in the field of cardiovascular research. Different species as animal models for MI studies may vary in size, anatomical structure, and genetic and phenotypic expression, and have their own advantages and disadvantages. Because of the heterogeneity and multimorbidity observed in patients with MI, animal models in the preclinical studies are considered by some as too remote to be applicable in translational efforts. Some researchers emphasize the use of human-based research methods, such as the use of human-induced pluripotent stem cells (iPSCs), cardiac organoids, and cardiovascular "organs-on-chips" (Ribas et al., 2016; Pound and Ritskes-Hoitinga, 2018; Richards et al., 2020). However, it is undeniable that there is no adequate substitute for animal models that allow us to systematically examine how the entire body systems respond to a disease. The ideal approach to preclinical studies would be to use multiple, complementary animal models, and human-based models to

**TABLE 1 |** Comparison of central cardiovascular systems in small and large animals used in MI study.

| Animal | *Body weight (kg) | *HR (rpm) *BP (mmHg) | **Coronary anatomy | **Collaterals | ***Advantages/ Similarities to human | ***Disadvantages/ Dissimilarities to human |
|---|---|---|---|---|---|---|
| Mouse/Rat (Rodents) | **Mouse:** 0.02–0.063<br>**Rat:** 0.225–0.52 | **Mouse:**<br>• HR: 310–840<br>• SBP:113–160<br>• DBP: 81–11<br>**Rat:**<br>• RHR: 250–493<br>• SBP: 84–184<br>• DBP: 58–145 | • Distinct septal coronary artery coursing along the right interventricular septum and a left coronary artery<br>→ Result in different regionality of infarction compared with human and large animals | • Have collateral arteries<br>→ Vessel occlusion does not cause a complete cessation of circulation<br>• Mice – Collateral extent varies widely within the species primarily due to variation at a single genetic locus | • Transgenic models readily available (e.g., atherosclerosis model)<br>• Express proteins with similar functions and roles as those in humans<br>• Lower cost for maintenance<br>• Similar electrophysiological characteristics and calcium transport | • Most remote from human contractile function due to small size and short lifespan<br>• Visualization and histological assessment are difficult due to the small coronary arteries<br>• Hearts function at very high HRs<br>• Ventricular CMs predominately express fast α-MHC (>94–100%) |
| Rabbit | 1–6 | • HR: 130–300<br>• SBP: 90–130<br>• DBP: 60–90 | • Left dominance<br>• The LCx is larger and supplies a much greater portion of the myocardium than does LAD | • Have little innate coronary collateral flow | • Less expensive than other large animal models<br>• Transgenic models available<br>• Similar electrophysiological characteristics and calcium transport | • Their kinetics of cardiac contraction and relaxation are still very faster than those of humans<br>• Different and inconsistent coronary artery systems<br>• Not always considered as large animal<br>• Less reported studies than other species<br>• No tricuspid valve |
| Dog (Canine) | 7–16 | • HR: 70–160<br>• SBP: 95–136<br>• DBP: 43–66 | • Left dominance | • Variable and extensive preexisting collateral epicardial circulation which can supply as much as 40% of the blood flow after the occlusion of a coronary artery | • Similar electrophysiological characteristics and calcium transport<br>• Similar excitation-contraction coupling processes<br>• Similar ventricular activation sequence | • Difficult to obtain the necessary approval for using canines as an animal model<br>• Extensive collateral circulation in myocardium<br>→ Cannot create consistent degrees of MI<br>→ Different ischemic patterns than other large mammalians<br>→ Delivers blood flow preferentially to the epicardial tissue, thus at the greater vulnerability of the endocardium to necrosis and the phenomenon of the "wave front of cell death" |

*(Continued)*

**TABLE 1 |** Continued

| Animal | *Body weight (kg) | *HR (rpm)<br>*BP (mmHg) | **Coronary anatomy | **Collaterals | ***Advantages/ Similarities to human | ***Disadvantages/ Dissimilarities to human |
|---|---|---|---|---|---|---|
| Sheep (ovine) | 20–160 | • HR: 60–120<br>• SBP: ∼90–115<br>• DBP: ∼100 | • Left dominance | • Have little innate coronary collateral flow | • Scant collateral arteries, allowing to produce a predictable infarct size | • Costly experiment and maintenance<br>• High risk of arrhythmia, including fibrillation, with little provocation<br>• Dissimilar coronary anatomy<br>• Difficult to perform non-invasive due to thoracic and gastrointestinal anatomy<br>• High risk of arrhythmia, including fibrillation<br>• High risk of infection |
| Pig (swine/Porcine) | 200–300 | • HR: 50–116<br>• SBP: 135–150<br>• DBP: – | • Right dominance<br>• Like human, left coronary artery larger in diameter, and longer than the right coronary artery | • Scant innate collateral arteries, primarily localized to the mid myocardium and subendocardium (little collateral blood flow) | • Myocardial excitation-contraction coupling<br>• *In vivo* contractile and relaxation kinetics<br>• Similar coronary anatomy and gross anatomical structure to humans<br>• Similar cardiac output to humans<br>• Scant collateral arteries, allowing to produce a predictable infarct size<br>• Resistant to infections and relatively rapid healing after surgery | • Costly experiment and maintenance<br>• High risk of arrhythmia, including fibrillation, with little provocation<br>• Different ventricular activation sequence is different due to different distribution of Purkinje fibers<br>• Heart-to-body ratio decreases with aging<br>→ Gain weight dramatically in their adulthood, thus not suitable for long-term study<br>• Brief diastole makes them prone to coronary insufficiency and increase sensitivity and decrease specificity the effects of drugs or treatment |
| Miniature Pig (mini swine) | 32–68 | • HR: ∼ 56<br>• SBP: 122 ± 16<br>• DBP: 88 ± 10 | • Right dominance<br>• The posterior descending artery arise from right coronary artery | • Have little coronary collateral flow | • Similar heart-to-body weight ratio<br>• Similar coronary artery distribution<br>• Cardiac anatomy, metabolism, electrophysiology – comparable to man<br>• Relatively smaller body size than large pig, even at full sexual maturity<br>→ Offer experimental control and reproducibility due to manageable size | • Similar to large pig (above) |

*(Continued)*

**TABLE 1** | Continued

| Animal | *Body weight (kg) | *HR (rpm) *BP (mmHg) | **Coronary anatomy | **Collaterals | ***Advantages/ Similarities to human | ***Disadvantages/ Dissimilarities to human |
|---|---|---|---|---|---|---|
| Human | 50–86 | • HR: 60–100<br>• SBP: 115–135<br>• DBP: 60–80 | • Right dominance<br>• Left coronary artery larger in diameter and longer than the right coronary artery | • Minimal preexisting collaterals | | |

*Cardiovascular parameters (Body weight, HR, and BP) are retrieved from Stubhan et al. (2008); Bode et al. (2010), Gandolfi et al. (2011); Milani-Nejad and Janssen (2014).*

***The characteristics of coronary and collateral artery anatomy are adapted from Blair (1961); Spadaro et al. (1980), Weaver et al. (1986); Maxwell et al. (1987), Kamimura et al. (1996); Podesser et al. (1997), Hearse (2000); Kumar et al. (2005), Dixon and Spinale (2009); Lelovas et al. (2014).*

****Other characteristics are adapted from Harken et al. (1981); Khan (1984), Hearse (2000); Nunoya et al. (2007), Dixon and Spinale (2009); Milani-Nejad and Janssen (2014), Morrissey et al. (2017); Stricker-Krongrad et al. (2017), Tang et al. (2018).*

*SBP, systolic blood pressure; DBP, diastolic blood pressure; LCx, left circumflex coronary artery; LAD, left anterior descending coronary artery; CM, cardiomyocyte.*

utilize the advantages of strengths of each model and take preventive measures to minimize bias in the experimental design and data interpretation.

## Seeing What We Want to See: Biased Experiments in Animal Studies Decelerate Reliable Clinical Translations in MI Studies

A rapid technological advancement has dramatically improved our understanding of human heart diseases and therapeutic development; however, the translation of these findings has not been keeping up with this trend (Ioannidis, 2005, 2016). This review argues that two primary sources of this slow translation are: (1) the lack of transparency in experimental design and data assessment and (2) excessive variation in the protocols for animal surgeries; both of these factors may have resulted from the inherent technical difficulties in dealing with large animal models. Compared to small animals, a higher degree of financial, husbandry, and technical obstacles exist in large animal studies, which often limit the study scale and lead to self-justified modifications in the surgical protocols along with lack of internal validity. Studies involving large animal models are expensive and technically demanding as they require advanced surgical and anesthetic techniques and materials. However, most published papers do not report the precise and detailed protocols or visual representations needed for other researchers to reproduce the same animal model or verify the surgical procedure and experimental results. The difficulty in finding a verifiable open reference leads to poor experimental designs and varied animal survival rates; this introduces sampling bias, which is especially detrimental for small-scale studies involving large animal models.

Another source of bias is the flexibility in surgical procedures for creating MI in animals. For example, the most common method to induce acute MI is the permanent or catheter-assisted temporary coronary artery occlusion with the left anterior descending coronary artery (LAD) as the primary target vasculature. The mortality rate from LAD occlusion is relatively high, especially for large animals, as they are at a considerable risk of developing ventricular fibrillation following MI (de Jong et al., 2014; Mu et al., 2016; Lim et al., 2018). To avoid this occurrence, the left circumflex artery (LCx) is often used as an alternative target at the cost of inducing a smaller infarct at a different location (Hirano et al., 2017; Cremer et al., 2019). The substantial inconsistency in the occlusion site along these two coronary arteries further complicates the MI studies. Some segments of the LAD and LCx commonly targeted for occlusion are as follows and can be found in **Figure 1**:

- The LAD "distal to" the 1st diagonal branch (Kraitchman et al., 2003; Okura et al., 2012; Li et al., 2013; Sharp et al., 2017).
- The "Mid"-LAD "just beyond" the 1st diagonal branch (Lim et al., 2018).
- The "Mid-left" LAD "distal to" the 1st diagonal branch (de Jong et al., 2014).
- The LAD "beyond" the 1st diagonal branch (Wolf et al., 2009).
- The LAD "distal to" the 2nd diagonal branch (Rabbani et al., 2008; Wang et al., 2009; Mu et al., 2016; Rabbani et al., 2017).
- The "proximal" LCx (Timmers et al., 2011; Wang B. et al., 2017).
- The 1st "marginal" branch of the LCx (Gálvez-Montón et al., 2014).

Several other studies have not specified the exact location of occluded segments of the LAD (Wolf et al., 2009; Crisostomo et al., 2019) or LCx (van der Velden et al., 2004; Charles et al., 2020). Without appropriate visual representation, this inconsistent and vague language, such as "beyond" and "mid," leaves room for arbitrary interpretation and changes in the surgical procedures, potentially leading to varied experimental outcomes. One study determined the site(s) and number of ligatures based on the visual inspection of the LAD and LCx branches in each ovine, in order to produce a consistent anterolateral infarct size across different animals (Locatelli et al., 2011) while many studies have not reported the infarct size (Kraitchman et al., 2003; Zhao et al., 2014; Alestalo et al., 2015; Haller et al., 2015; Kim et al., 2017; Lim et al., 2018; Ishida et al., 2019).

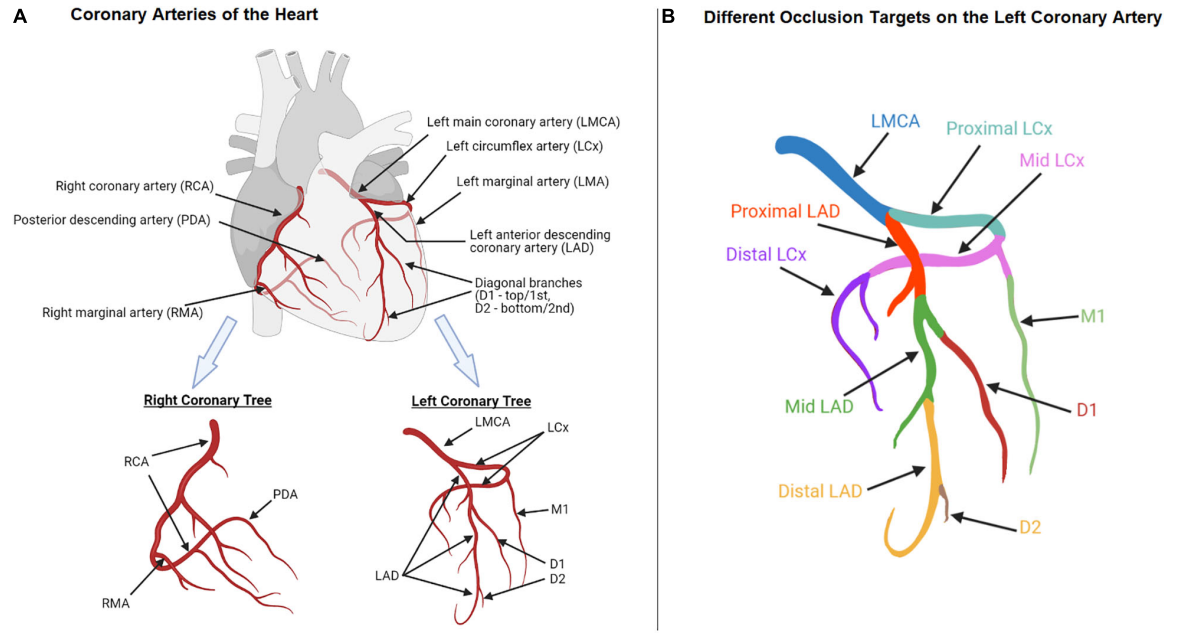


**FIGURE 1 |** Anatomy of coronary arteries of the heart **(A)** Left and right coronary trees; **(B)** Different occlusion targets (indicated in different colors) on the left coronary artery.

Additionally, different surgical procedures for inducing MI often create various degrees of ischemia via different pathogenic mechanisms thus generating different MI models (**Table 2**). For example, catheter-based occlusion is often used as a non-invasive way to induce MI, but there is a significant variation in the occlusion sites and durations followed by reperfusion across different studies (**Table 3**). Some studies using pig models have demonstrated that the longer occlusion duration resulted in bigger infarct sizes and more severe left ventricular dysfunction (Garcia-Dorado et al., 1987; Ghugre et al., 2013; Thomas et al., 2021). However, besides the occlusion site and duration, this inconsistent infarct size and ventricular remodeling were likely to be affected by the subsequent reperfusion. Myocardial reperfusion using thrombolytic therapy or primary percutaneous coronary intervention is a treatment option for human MI patients. However, it is known that the reperfusion of myocytes irreversibly injured by ischemia following coronary occlusion may accelerate the necrotic process, a phenomenon called "myocardial ischemia-reperfusion injury." This could consequently affect the infarct size and lead to adverse cardiac remodeling (Braunwald and Kloner, 1985; Yellon and Hausenloy, 2007; Hausenloy and Yellon, 2013; Acharya, 2020). All these situational specifics of a surgical procedure as part of MI preclinical study design (for example, method, site, and duration of coronary artery occlusion, and presence and duration of reperfusion following occlusion) potentially limit the generalizability and reproducibility of scientific results and likely contribute to the failure of subsequent clinical trials.

## Potential of Human-Based Models as an Alternative for Animal Models?

Whether small or large, animal models cannot fully recapitulate human CVD phenotypes, thus requiring new forms of human-based experimentation. The tissue engineering community has been developing *in vitro* and *in silico* CVD models for more physiologically and clinically relevant readouts of CVDs (Savoji et al., 2019). Human organs-on-chips are 3D microfluidic cell culture devices that mimic the physical and mechanical microenvironment of key organ systems and provide dynamic vascular perfusion *in vitro*, which is difficult to achieve in 2D cell culture (Ingber, 2018). This burgeoning biomimetic system can incorporate patient-specific cell models, allowing the study of pathophysiology and pharmacological responses unique to each patient (Ingber, 2020; Wu et al., 2020).

However, an organ-on-a-chip is still limited in that although it can capture distinct functional units of organ systems separately (e.g., heart vs. liver), it cannot link each unit via vascular channels (e.g., the hepatic portal system). "Multi" organ-on-a-chip device may allow combining several cellular models in a single chip; however, certain technical difficulties, such as selecting a co-culture medium required for incorporating multiple cell lineages and ensuring the correct sizing of each organ, need to be resolved (Bovard and Sandoz, 2020). However, this innovative *in vitro* model is still distant from a complete replacement of animal studies because they cannot mimic the complex nervous and immune systems of humans. Thus, investigators, particularly those concerned with cognition, behavior, immune responses, and pain management, still require animal studies to systematically monitor disease progression

**TABLE 2 |** Comparison of surgical procedures used to induce MI in large animal models.

| MI induction methods | Open-chest (or surgical-based) vs. Close-chest (or catheter based) | Advantages | Disadvantages | Studies |
|---|---|---|---|---|
| Coronary artery ligation | Open-chest | • Provides precise timing, location and extent of the coronary event due to direct visualization and observation of the procedure and targeted area of infarct | • Invasive procedure<br>– Increased mortality and complications<br>– Affects the whole balance of bodily function and modifies local and systemic immunological and inflammatory responses<br>• The site of ligation of the vessel varies (proximal, mid, or distal) in studies, resulting in various degree of ischemic injury and mortality rate<br>• The LAD occlusion often causes ventricular fibrillation and sudden death, especially in pigs (Muller et al., 1988) | LAD ligation (Krause et al., 2007; Wolf et al., 2009; Chen et al., 2014; de Jong et al., 2014; Zhao et al., 2014; Haller et al., 2015; Lim et al., 2018)<br>LCx ligation (van der Velden et al., 2004; Timmers et al., 2011; Gálvez-Montón et al., 2014; Wang L. et al., 2017; Charles et al., 2020) |
| Ameroid constrictor or hydraulic occluder | Open-chest or close-chest | • Gradual occlusion mimics chronic MI and enables the development of the collateral arterial supply | • May require invasive procedure | Sjaastad et al., 2000; Shudo et al., 2011; Potz et al., 2018; Ishida et al., 2019 |
| Cryoinjury | Open-chest | • Freezing-induced scar has similar cellular patterns of coagulation necrosis of MI – a suitable model used to demonstrate myocardial repair, heart regeneration and cellular remodeling using cellular therapies | • Invasive procedure<br>• The pathophysiology of freezing induced MI is different from other methods because acute cell death occurs following the cryoinjury without concomitant ischemia<br>• Several applications are necessary for large animal hearts and also due to rapid defrosting of cryoprobe, which makes it difficult to control the size of infarction<br>• Difficult to induce transmural infarction<br>• Less tested in large animals | Yang et al., 2010, 2012; Hirano et al., 2017 |
| Percutaneous intracoronary embolization using various insertion materials, followed by reperfusion | Close-chest | • Minimally invasive<br>• Resembles human course of atherosclerotic disease superimposed by thrombus formation during MI event<br>• Various embolic agents<br>– Sponge foam/sponge microspheres, coils, polystyrene microspheres, alcohol injection, balloon catheter<br>• Clinically relevant as myocardial reperfusion is performed in human MI by fibrinolytic therapy or Percutaneous Coronary Intervention (PCI)<br>• Timely reperfusion of the coronary artery after MI helps salvage the viable myocardium, limit infarct size, preserve LV systolic function and prevent the onset of heart failure | • Requires anticoagulant therapy to prevent blood clot formation during instrumentation<br>• Require anti-arrhythmic protocol to prevent arrhythmia and ventricular fibrillation<br>• Difficult to control the exact location, length and duration of the coronary artery occlusion and the overall volume of myocardial necrosis (Camacho et al., 2016)<br>• Requires advanced technical skills and highly trained personnel to manipulate the catheter for deployment of the material for embolization<br>• Inconsistent occlusion duration across studies<br>• Reperfusion of an ischemic area often results in myocardial cell necrosis (or called reperfusion injury)<br>• Just like coronary artery ligation, mortality rate can vary depending on the embolization sites (higher mortality at the proximal site) | Sponge foam/sponge microspheres (Dariolli et al., 2014; Sun et al., 2020)<br>Coils (Watanabe et al., 1998; Li et al., 2000; Makkar et al., 2005; Dib et al., 2006)<br>Polystyrene microspheres (Hanes et al., 2015; Suzuki et al., 2016)<br>Ethyl alcohol injection (Joudinaud et al., 2005; Rienzo et al., 2020)<br>Balloon catheter (Kraitchman et al., 2003; Price et al., 2006; Wang et al., 2009; Lu et al., 2012; Okura et al., 2012; Li et al., 2013; de Jong et al., 2014; Mu et al., 2016) |

*(Continued)*

**TABLE 2** | Continued

| MI induction methods | Open-chest (or surgical-based) vs. Close-chest (or catheter based) | Advantages | Disadvantages | Studies |
|---|---|---|---|---|
| Chemical reagent e.g., isoproterenol | Closed-chest Subcutaneously intraperitoneally, intravenously | • Non-invasive – can be injected subcutaneously intraperitoneally, or intravenously<br>• Low mortality rate | • Indirect method – unable to visualize the effects on the targeted area during the procedure<br>• Different methods of administration affect the drug metabolism and its conversion into inactive metabolites<br>• Less tested in large animals | Kim et al., 2014; Lim et al., 2014 |

*Comparison is adapted from Halim et al. (2018).*

and develop corresponding therapeutic interventions. Animal studies have been misinterpreted as poor predictors of clinical study outcomes. This may be true merely because animals and humans are inherently different, and the human body and pathogenesis of CVDs and other diseases are far too complicated to be replicated in other models. However, this inherent difficulty should not be used as an excuse to adopt a less rigorous but more convenient experimental design and data interpretation. Although new technological advances will allow us to adopt more disease-representative models, the clinical study outcomes will still largely depend on scientific rigor.

## DISCUSSION

Despite increasing knowledge about the etiologies of MI and relevant therapeutic strategies, the translational gap between basic science and clinical research is widening. Lack of experimental rigor and quality in preclinical research has been accused as the main cause of slow translation of "promising" preclinical results, and various issues regarding reproducibility have been raised across different biomedical and social science fields (Pound et al., 2004; Begley and Ioannidis, 2015).

In section "Suitability of Animal Models for Human MI," we discussed the importance of choosing a representative animal model in preclinical studies and considering the differences between different animal species and humans when interpreting experimental data. Some researchers believe that the limited opportunities to carry out studies based on large animal models prevent them from testing their hypothesis more rigorously and openly, justifying adjustments in an experimental design and biased interpretations of study outcomes. Yet, the discordance between animal-based preclinical and human-based clinical studies is often attributed for the failures of clinical trials for cardiovascular and other disease therapies (Pound et al., 2004; Perel et al., 2007). Some human-based preclinical models have been proposed as a complementary platform to overcome the limitations of using an animal model. However, they will not replace animal models entirely soon as discussed in section "Potential of Human-Based Models as an Alternative for Animal Models?" The difficulty of establishing the optimal animal model prompts a periodic systematic review or meta-analysis of animal studies (Sandercock and Roberts, 2002; Pound et al., 2004; Hooijmans and Ritskes-Hoitinga, 2013). However, a systematic review of studies with poor methodological quality is likely to produce additional animal studies of similarly poor quality. Instead, the preclinical, animal study quality must be scrutinized at the original study design process and journals' review process at the time of submission.

In section "Seeing What We Want to See: Biased Experiments in Animal Studies Decelerate Reliable Clinical Translations in MI Studies," we reviewed how the lack of standardized protocols and transparency in preclinical MI studies involving animal experiments could allow investigators too much flexibility in their study design and data assessment, depriving "promising" preclinical research results reproducibility and translational power. Investigators often adopt a disease model that is remote from what they intend to model and tend to report the desired results that are harmonious with their hypothesis alone (Baker, 2016). A standardized experimental method is critical for ensuring reproducibility, but the lack of overall methodological rigor in preclinical cardiovascular studies is prevalent, delaying the translational process; this issue has called for a set of improved reporting standards, more strict funding policies, and better instructions for peer reviewer (Hooijmans et al., 2010; Hirst and Altman, 2012; Henderson et al., 2013; Anon, 2013; Principles and Guidelines for Reporting Preclinical Research and National Institutes of Health (NIH), 2021).

Four elements of methodological quality of preclinical research that critically determine its translational power are randomization, sample size calculation, blinding, and heterogeneity of animals used (i.e., strains, ages, and sexes) (Henderson et al., 2013). A recently added critical element of heterogeneity of animal models is environmental factors, which suggests the benefit of multi-laboratory experiments (Richter et al., 2009; Voelkl et al., 2018). Ramirez et al. (2017) found that randomization was reported only in 21.8%, blinding in 32.7%, and sample size estimation in 2.3% of all preclinical cardiovascular studies published in five leading cardiovascular journals between July 2006 and June 2016 (Ramirez et al., 2017). Similar or worse results are found in the review of thirty-one systematic reviews of animal studies on treatments for various diseases (Hirst et al., 2014; van Luijk et al., 2014). Additionally, the quality of these study design elements has not improved in all disease-specific studies, except for stroke research

**TABLE 3 |** Variations in occlusion duration in catheter-based MI studies.

| Large animal model | MI induction method | Occlusion location | Occlusion duration | Mortality rate due to MI occlusion (during or shortly after MI induction) | Infarct size (Untreated group) | Study |
|---|---|---|---|---|---|---|
| Farm pigs | Cardiac catheterization (carotid sheath and coronary angioplasty balloon) | LAD beyond the first diagonal branch | 60 min | – | – | Kraitchman et al., 2003 |
| Young Yorkshire pigs | Percutaneous transluminal angiography (balloon occlusion) followed by reperfusion (after anticoagulation) | LAD distal to the second diagonal branch | 60 min | Four died within first 60 min after coronary occlusion due to ventricular fibrillation | 8.8 ± 2.1% | Wang et al., 2009 |
| Farm pigs | Balloon occlusion/reperfusion | LAD just distal to the second largest diagonal branch | 60 min | Six died within 3 days after MI | 5.3 ± 1.8% | Price et al., 2006 |
| Yorkshire-cross bred pigs | Balloon catheter occlusion-reperfusion | LAD just distal to the second diagonal branch | 60 min | Two died within the first 15 min of reperfusion due to ventricular arrhythmias | 9.8 ± 1.1 | Techiryan et al., 2018 |
| Yorkshire pigs | Angioplasty-induced coronary artery occlusion-reperfusion | Proximal LAD at the level of the first or second diagonal branch | 75 min | 17% developed fatal arrhythmias during ischemia | 8.1 ± 1.8% in Control | Halkos et al., 2008 |
| Chinese mini-pigs | Acute MI – percutaneous transluminal angiography (balloon occlusion) followed by reperfusion (after anticoagulation) | LAD distal to the second diagonal | 90 min | Four died due to ventricular fibrillation during occlusion procedure | 56% decreased after ILK-MSC treatment ($P < 0.001$) (<40% decrease after treatment of MSC alone) | Mu et al., 2016 |
| Landrace pigs | Moderate acute MI by inflation of an angioplasty balloon | Left circumflex artery occlusion (posterolateral infarct) | 90 min | Two died of ventricular fibrillation (VF) 1 day post-MI | 9.6 ± 1.3% | de Jong et al., 2014 |
| Yorkshire pigs | Percutaneous balloon dilation catheter | LAD distal to second diagonal branch | • 45 min<br>• 90 min | – | –<br>Result: More adverse remodeling in the 90-min groups than 45-min groups | Ghugre et al., 2013 |
| Yorkshire pigs | Occlusion-reperfusion | Mid LAD | • 60 min<br>• 90 min | – | – | Thomas et al., 2021 |

*(Continued)*

**TABLE 3 |** Continued

| Large animal model | MI induction method | Occlusion location | Occlusion duration | Mortality rate due to MI occlusion (during or shortly after MI induction) | Infarct size (Untreated group) | Study |
|---|---|---|---|---|---|---|
| Large white pigs | Occlusion-reperfusion | Mid LAD | • 30 min<br>• 45 min<br>• 60 min<br>• 90 min<br>• Permanent | One died from ventricular fibrillation during coronary occlusion<br>One from 30 min group and one from 60 min group died the night after the occlusion<br>One developed malignant hyperthermia | LV mass:<br>• 30 min: 0.46 (0.42)%<br>• 45 min: 2.85 (1.14)%<br>• 60 min: 9.74 (1.65)%<br>• 90 min: 8.93 (1.37)%<br>• Permanent: 3.17 (1.17)%<br>Transmural extension:<br>• 30 min: 14.6 (11.4)%<br>• 45 min: 42.1 (12.9)%<br>• 60 min: 87.4 (6.6)%<br>• 90 min: 96.2 (3.2)%<br>• Permanent: 100 (0)%<br>Result: Infarct size and the transmurality index correlated exponentially with the duration of the occlusion | Garcia-Dorado et al., 1987 |
| Ovine (Sheep) | Coronary artery ischemia–reperfusion<br>Coronary occlusion using a suture loop | Mid-second diagonal branch | 90 min | One died of ventricular fibrillation during the ischemic period | – | Dayan et al., 2016 |
| Coopworth ewes (Sheeps) | PTCA Balloon occlusion-reperfusion vs. Thrombogenic coil embolization (permanent) | Distal to the first diagonal branch but proximal to the second diagonal branch | 90 min (coil: 2 min) | Two died of arrhythmia within 4 min following reperfusion<br>Coil embolization group: Three died 30 min, 60 min, and between 6 and 12 h post-infarction | – Result: Restriction of coronary artery occlusion to 90 min results in infarction, but less LV dysfunction with reduced early remodeling, compared with permanent occlusion | Charles et al., 2000 |
| Sheep | Balloon occlusion-reperfusion | Mid-LAD | 90 min | Phase 3: 34/68 sheep died during infarct induction due to ventricular fibrillation refractory to defibrillation | 18.4 ± 1.5% | Houtgraaf et al., 2013 |

(Hirst et al., 2014). From 1997 to 2007, the number of cardiovascular papers and journals increased by 56.9 and 75.2%, respectively, yet 46% of original papers published in cardiovascular journals in the same period were poorly cited (with < = 5 citations in the 5 years following publication); however, 44% of cardiovascular journals had more than three-fourths of the journal's content poorly cited at 5 years (Ranasinghe et al., 2015). Interestingly, studies that employed randomization, blinding, or sample size estimation were equally cited in numbers as those that did not; however, studies that included both males and females were less frequently cited, suggesting that methodological rigor might have been overlooked by cardiovascular researchers (Ramirez et al., 2017). This suggests the need for strict enforcement of a comprehensive guideline and requirements by journals and funding institutions to ensure the rigor of animal studies and publication to the level of human-involving, clinical studies, which consequently promotes reproducibility and animal welfare (Hooijmans et al., 2010; Carbone and Austin, 2016).

It is almost always impossible to control every aspect of a scientific experiment and to perfectly mimic human pathophysiology in a disease model. Consequently, any experimental data are biased, and it is a matter of how biased they are and whether researchers are aware of and report those biases correctly. Additionally, the failure to reproduce or conflicting data is not always a vice but could be a valuable resource that potentially enriches biomedical research (Daugherty et al., 2016). However, in translational medicine, reproducibility is the ultimate goal, and this review article emphasizes there is much room for improvements in preclinical study design and animal models for MI research. Methodological rigors such as sample randomization, consistent surgical procedures, blind analyses, and greater sample statistical power are essential in animal models of human CVDs or other diseases. Along with following the correct procedures during research, transparent reporting of experimental protocols and results is equally essential to improve reproducibility, effectiveness, predictability, and safety of the clinical studies.

Considering the economic and emotional cost of a clinical trial and the exponentially growing number of published articles, it may be much more cost-effective from the standpoint of the entire population to maintain rigor and quality in the preclinical study level with good practice and additional cost than to see a series of "promising" preclinical study continuously failing in clinical trials (Freedman et al., 2015). However, probably most trained researchers may be well aware of these prerequisites of successful translation mentioned above. The root cause of the imbalance between the translational crisis and exponentially growing research in the cardiovascular field might be the competition for grants and positions (Baker, 2016). In this case, more opportunities for quality training and mentorship within research communities as well as a clear publication or funding guideline by journals and funding institutions are proposed (Begley and Ioannidis, 2015).

Yet, probably most trained researchers may be well aware of these prerequisites of successful translation. The root cause of the imbalance between the translational crisis and exponentially growing research in cardiovascular field might be the competition for grants and positions (Baker, 2016). In this case, more opportunities for quality training and mentorship within research communities in addition to a clear publication or funding guideline by journals and funding institutions are proposed (Begley and Ioannidis, 2015).

## AUTHOR CONTRIBUTIONS

HSy, HSe, and YS: conceptualization, writing—review and editing, and visualization. HSy and HSe: methodology, investigation, and writing—original draft preparation. HSy and YS: resources and project administration. YS: supervision and funding acquisition. All authors have read and agreed to the published version of the manuscript.

## FUNDING

This work was supported by Stanford Cardiovascular Institute (CVI) 2020 Seed Grant funded from Staford CVI and Gootter Foundation (YS).

## REFERENCES

Acharya, D. (2020). Unloading and reperfusion in myocardial infarction. *Circulation* 13:1.

Alestalo, K., Korpi, R., Mäkelä, J., Lehtonen, S., Mäkelä, T., Yannopoulos, F., et al. (2015). High number of transplanted stem cells improves myocardial recovery after AMI in a porcine model. *Scand. Cardiovasc. J.* 49, 82–94. doi: 10.3109/14017431.2015.1018311

Baker, M. (2016). 1,500 scientists lift the lid on reproducibility. *Nature* 533, 452–454. doi: 10.1038/533452a

Begley, C. G., and Ioannidis, J. P. A. (2015). Reproducibility in science: improving the standard for basic and preclinical research. *Circ. Res.* 116, 116–126. doi: 10.1161/circresaha.114.303819

Blair, E. (1961). Anatomy of the ventricular coronary arteries in the dog. *Circ. Res.* 9, 333–341. doi: 10.1161/01.res.9.2.333

Bode, G., Clausing, P., Gervais, F., Loegsted, J., Luft, J., Nogues, V., et al. (2010). The utility of the minipig as an animal model in regulatory toxicology. *J. Pharmacol. Toxicol. Methods* 62, 196–220. doi: 10.1016/j.vascn.2010.05.009

Bolli, R., Becker, L., Gross, G., Mentzer, R., Balshaw, D., Lathrop, D. A., et al. (2004). Myocardial protection at a crossroads: the need for translation into clinical therapy. *Circ. Res.* 95, 125–134. doi: 10.1161/01.res.0000137171.97172.d7

Bovard, D., and Sandoz, A. (2020). *How to build your multiorgan-on-a-chip system: a case study. Organ-on-a-chip*. Amsterdam: Elsevier, 463–506.

Bracken, M. B. (2009). Why animal studies are often poor predictors of human reactions to exposure. *J. R. Soc. Med.* 102, 120–122. doi: 10.1258/jrsm.2008.08k033

Braunwald, E., and Kloner, R. A. (1985). Myocardial reperfusion: a double-edged sword? *J. Clin. Invest.* 76, 1713–1719. doi: 10.1172/jci112160

Camacho, P., Fan, H., Liu, Z., and He, J.-Q. (2016). Large mammalian animal models of heart disease. *J. Cardiovasc. Dev. Dis.* 3:4.

Cannon, R. O. (2005). Mechanisms, management and future directions for reperfusion injury after acute myocardial infarction. *Nat. Clin. Pract. Cardiovasc. Med.* 2, 88–94. doi: 10.1038/ncpcardio0096

Carbone, L., and Austin, J. (2016). Pain and laboratory animals: publication practices for better data reproducibility and better animal welfare. *PLoS One* 11:e0155001. doi: 10.1371/journal.pone.0155001

Charles, C. J., Elliott, J. M., Nicholls, M. G., Rademaker, M. T., and Richards, M. (2000). Myocardial infarction with and without reperfusion in sheep: early cardiac and neurohumoral changes. *Clin. Sci.* 98, 703–711. doi: 10.1042/cs19990266

Charles, C. J., Li, R. R., Yeung, T., Mazlan, S. M. I., Lai, R. C., de Kleijn, D. P. V., et al. (2020). systemic mesenchymal stem cell-derived exosomes reduce myocardial infarct size: characterization with mri in a porcine model. *Front. Cardiovasc. Med.* 7:601990. doi: 10.3389/fcvm.2020.601990

Chen, C.-H., Chang, M.-Y., Wang, S.-S., and Hsieh, P. C. H. (2014). Injection of autologous bone marrow cells in hyaluronan hydrogel improves cardiac performance after infarction in pigs. *Am. J. Physiol. Heart Circ. Physiol.* 306, H1078–H1086.

Chong, J. J. H., Yang, X., Don, C. W., Minami, E., Liu, Y.-W., Weyers, J. J., et al. (2014). Human embryonic-stem-cell-derived cardiomyocytes regenerate non-human primate hearts. *Nature* 510, 273–277.

Christman, K. L., and Lee, R. J. (2006). Biomaterials for the treatment of myocardial infarction. *J. Am. Coll Cardiol.* 48, 907–913. doi: 10.1016/j.jacc.2006.06.005

Cremer, S., Schloss, M. J., Vinegoni, C., Zhang, S., Rohde, D., Feruglio, P. F., et al. (2019). A mouse model of recurrent myocardial infarction reports diminished emergency hematopoiesis and cardiac inflammation. *BioRxiv* 2019:4.

Crisostomo, V., Baez, C., Abad, J. L., Sanchez, B., Alvarez, V., Rosado, R., et al. (2019). Dose-dependent improvement of cardiac function in a swine model of acute myocardial infarction after intracoronary administration of allogeneic heart-derived cells. *Stem Cell Res. Ther.* 10:152.

Dariolli, R., Takimura, C. K., Campos, C. A., Lemos, P. A., and Krieger, J. E. (2014). Development of a closed-artery catheter-based myocardial infarction in pigs using sponge and lidocaine hydrochloride infusion to prevent irreversible ventricular fibrillation. *Physiol. Rep.* 2:8.

Daugherty, A., Hegele, R. A., Mackman, N., Rader, D. J., Schmidt, A. M., and Weber, C. (2016). Complying with the national institutes of health guidelines and principles for rigor and reproducibility: refutations. *Arterioscler. Thromb. Vasc. Biol.* 36, 1303–1304. doi: 10.1161/atvbaha.116.307906

Dayan, V., Sotelo, V., Delfina, V., Delgado, N., Rodriguez, C., Suanes, C., et al. (2016). Human mesenchymal stromal cells improve cardiac perfusion in an ovine immunocompetent animal model. *J. Invest. Surg.* 29, 218–225. doi: 10.3109/08941939.2015.1128997

de Jong, R., van Hout, G. P. J., Houtgraaf, J. H., Kazemi, K., Wallrapp, C., Lewis, A., et al. (2014). Intracoronary infusion of encapsulated glucagon-like peptide-1-eluting mesenchymal stem cells preserves left ventricular function in a porcine model of acute myocardial infarction. *Circ. Cardiovasc. Interv.* 7, 673–683. doi: 10.1161/circinterventions.114.001580

Dib, N., Diethrich, E. B., Campbell, A., Gahremanpour, A., McGarry, M., and Opie, S. R. A. (2006). percutaneous swine model of myocardial infarction. *J. Pharmacol. Toxicol. Methods* 53, 256–263.

Dirksen, M. T., Laarman, G. J., Simoons, M. L., and Duncker, D. J. G. M. (2007). Reperfusion injury in humans: a review of clinical trials on reperfusion injury inhibitory strategies. *Cardiovasc. Res.* 74, 343–355. doi: 10.1016/j.cardiores.2007.01.014

Dixon, J. A., and Spinale, F. G. (2009). Large animal models of heart failure: a critical link in the translation of basic science to clinical practice. *Circ. Heart Fail.* 2, 262–271. doi: 10.1161/circheartfailure.108.814459

Downey, J. M., and Cohen, M. V. (2009). Why do we still not have cardioprotective drugs? *Circ. J.* 73, 1171–1177. doi: 10.1253/circj.cj-09-0338

Epstein, F. H., Yang, Z., Gilson, W. D., Berr, S. S., Kramer, C. M., and French, B. A. M. R. (2002). tagging early after myocardial infarction in mice demonstrates contractile dysfunction in adjacent and remote regions. *Magn. Reson. Med.* 48, 399–403. doi: 10.1002/mrm.10210

Ferreira, G. S., Veening-Griffioen, D. H., Boon, W. P. C., Moors, E. H. M., and van Meer, P. J. K. (2020). Levelling the translational gap for animal to human efficacy data. *Animals* 10:7.

Freedman, L. P., Cockburn, I. M., and Simcoe, T. S. (2015). The economics of reproducibility in preclinical research. *PLoS Biol.* 13:e1002165. doi: 10.1371/journal.pbio.1002626

Gálvez-Montón, C., Prat-Vidal, C., Díaz-Güemes, I., Crisóstomo, V., Soler-Botija, C., Roura, S., et al. (2014). Comparison of two preclinical myocardial infarct models: coronary coil deployment versus surgical ligation. *J. Transl. Med.* 12:137. doi: 10.1186/1479-5876-12-137

Gandolfi, F., Vanelli, A., Pennarossa, G., Rahaman, M., Acocella, F., and Brevini, T. A. L. (2011). Large animal models for cardiac stem cell therapies. *Theriogenology* 75, 1416–1425. doi: 10.1016/j.theriogenology.2011.01.026

Gao, L. R., Pei, X. T., Ding, Q. A., Chen, Y., Zhang, N. K., Chen, H. Y., et al. (2013). A critical challenge: dosage-related efficacy and acute complication intracoronary injection of autologous bone marrow mesenchymal stem cells in acute myocardial infarction. *Int. J. Cardiol.* 168, 3191–3199. doi: 10.1016/j.ijcard.2013.04.112

Gao, M., Xin, G., Qiu, X., Wang, Y., and Liu, G. (2016). Establishment of a rat model with diet-induced coronary atherosclerosis. *J. Biomed. Res.* 31, 47–55.

Garcia-Dorado, D., Théroux, P., Elizaga, J., Galiñanes, M., Solares, J., Riesgo, M., et al. (1987). Myocardial reperfusion in the pig heart model: infarct size and duration of coronary occlusion. *Cardiovasc. Res.* 21, 537–544. doi: 10.1093/cvr/21.7.537

Gargiulo, S., Greco, A., Gramanzini, M., Petretta, M. P., Ferro, A., Larobina, M., et al. (2012). PET/CT imaging in mouse models of myocardial ischemia. *J. Biomed. Biotechnol.* 2012:541872.

Getz, G. S., and Reardon, C. A. (2012). Animal models of atherosclerosis. *Arterioscler. Thromb. Vasc. Biol.* 32, 1104–1115.

Ghugre, N. R., Pop, M., Barry, J., Connelly, K. A., and Wright, G. A. (2013). Quantitative magnetic resonance imaging can distinguish remodeling mechanisms after acute myocardial infarction based on the severity of ischemic insult. *Magn. Reson. Med.* 70, 1095–1105. doi: 10.1002/mrm.24531

Giustino, G., and Dangas, G. D. (2017). Ischemia-reperfusion injury and ischemic post-conditioning in acute myocardial infarction: Lost in translation. *Catheter. Cardiovasc. Interv.* 90, 1068–1069. doi: 10.1002/ccd.27436

Graham, G. (2015). Disparities in cardiovascular disease risk in the United States. *Curr. Cardiol. Rev.* 11, 238–245. doi: 10.2174/1573403x11666141122220003

Graham, G. (2016). Racial and ethnic differences in acute coronary syndrome and myocardial infarction within the united states: from demographics to outcomes. *Clin. Cardiol.* 39, 299–306. doi: 10.1002/clc.22524

Guo, R., Morimatsu, M., Feng, T., Lan, F., Chang, D., Wan, F., et al. (2020). Stem cell-derived cell sheet transplantation for heart tissue repair in myocardial infarction. *Stem Cell Res. Ther.* 11:19.

Halim, S. A. S. A., Ghafar, N. A., Jubri, Z., and Das, S. (2018). Induction of myocardial infarction in experimental animals: A review. *JCDR* 2018:12221.

Halkos, M. E., Zhao, Z.-Q., Kerendi, F., Wang, N.-P., Jiang, R., Schmarkey, L. S., et al. (2008). Intravenous infusion of mesenchymal stem cells enhances regional perfusion and improves ventricular function in a porcine model of myocardial infarction. *Basic Res. Cardiol.* 103, 525–536. doi: 10.1007/s00395-008-0741-0

Haller, C., Sobolewska, B., Schibilsky, D., Avci-Adali, M., Schlensak, C., Wendel, H.-P., et al. (2015). One-staged aptamer-based isolation and application of endothelial progenitor cells in a porcine myocardial infarction model. *Nucleic Acid Ther.* 25, 20–26. doi: 10.1089/nat.2014.0499

Hanes, D. W., Wong, M. L., Jenny Chang, C. W., Humphrey, S., Grayson, J. K., Boyd, W. D., et al. (2015). Embolization of the first diagonal branch of the left anterior descending coronary artery as a porcine model of chronic trans-mural myocardial infarction. *J. Transl. Med.* 13:187.

Harken, A. H., Simson, M. B., Haselgrove, J., Wetstein, L., Harden, W. R., and Barlow, C. H. (1981). Early ischemia after complete coronary ligation in the rabbit, dog, pig, and monkey. *Am. J. Physiol.* 241, H202–H210.

Hausenloy, D. J., and Yellon, D. M. (2013). Myocardial ischemia-reperfusion injury: a neglected therapeutic target. *J. Clin. Invest.* 123, 92–100. doi: 10.1172/jci62874

Hausenloy, D. J., and Yellon, D. M. (2016). Ischaemic conditioning and reperfusion injury. *Nat. Rev. Cardiol.* 13, 193–209. doi: 10.1038/nrcardio.2016.5

Hausenloy, D. J., Baxter, G., Bell, R., Bøtker, H. E., Davidson, S. M., Downey, J., et al. (2010). Translating novel strategies for cardioprotection: the Hatter Workshop Recommendations. *Basic Res. Cardiol.* 105, 677–686. doi: 10.1007/s00395-010-0121-4

Hearse, D. (2000). The elusive coypu: the importance of collateral flow and the search for an alternative to the dog. *Cardiovasc. Res.* 45, 215–219. doi: 10.1016/s0008-6363(99)00331-4

Henderson, V. C., Kimmelman, J., Fergusson, D., Grimshaw, J. M., and Hackam, D. G. (2013). Threats to validity in the design and conduct of preclinical efficacy studies: a systematic review of guidelines for in vivo animal experiments. *PLoS Med.* 10:e1001489. doi: 10.1371/journal.pmed.1001489

Heusch, G. (2013). Cardioprotection: chances and challenges of its translation to the clinic. *Lancet* 381, 166–175. doi: 10.1016/s0140-6736(12)60916-7

Heusch, G. (2015). Molecular basis of cardioprotection: signal transduction in ischemic pre-, post-, and remote conditioning. *Circ. Res.* 116, 674–699. doi: 10.1161/circresaha.116.305348

Heusch, G. (2017). Critical issues for the translation of cardioprotection. *Circ. Res.* 120, 1477–1486. doi: 10.1161/circresaha.117.310820

Hill, A. J., and Iaizzo, P. A. (2009). "Comparative Cardiac Anatomy," in *Handbook of cardiac anatomy, physiology, and devices*, ed. P. A. Iaizzo (Totowa, NJ: Humana Press), 87–108. doi: 10.1007/978-1-60327-372-5_6

Hirano, A., Fujita, J., Kanazawa, H., Kawaguchi, S., Handa, N., Yamada, Y., et al. (2017). Cryoinjury-induced acute myocardial infarction model and ameroid constrictor-induced ischemic heart disease model in adult micro-mini pigs for preclinical studies. *Transl. Med. Commun.* 2:1. doi: 10.1155/2014/571076

Hirst, A., and Altman, D. G. (2012). Are peer reviewers encouraged to use reporting guidelines? A survey of 116 health research journals. *PLoS One* 7:e35621. doi: 10.1371/journal.pone.0035621.g001

Hirst, J. A., Howick, J., Aronson, J. K., Roberts, N., Perera, R., Koshiaris, C., et al. (2014). The need for randomization in animal trials: an overview of systematic reviews. *PLoS One* 9:e98856. doi: 10.1371/journal.pone.0098856

Hooijmans, C. R., and Ritskes-Hoitinga, M. (2013). Progress in using systematic reviews of animal studies to improve translational research. *PLoS Med.* 10:e1001482. doi: 10.1371/journal.pmed.1001482

Hooijmans, C. R., Leenaars, M., and Ritskes-Hoitinga, M. A. (2010). gold standard publication checklist to improve the quality of animal studies, to fully integrate the Three Rs, and to make systematic reviews more feasible. *Altern. Lab. Anim.* 38, 167–182. doi: 10.1177/026119291003800208

Houtgraaf, J. H., de Jong, R., Kazemi, K., de Groot, D., van der Spoel, T. I. G., Arslan, F., et al. (2013). Intracoronary infusion of allogeneic mesenchymal precursor cells directly after experimental acute myocardial infarction reduces infarct size, abrogates adverse remodeling, and improves cardiac function. *Circ. Res.* 113, 153–166. doi: 10.1161/circresaha.112.300730

Ingber, D. E. (2018). Developmentally inspired human "organs on chips". *Development* 145:16.

Ingber, D. E. (2020). Is it time for reviewer 3 to request human organ chip experiments instead of animal validation studies? *Adv. Sci.* 7:2002030. doi: 10.1002/advs.202002030

Ioannidis, J. P. A. (2005). Why most published research findings are false. *PLoS Med.* 2:e124. doi: 10.1371/journal.pmed.0020124

Ioannidis, J. P. A. (2016). Why most clinical research is not useful. *PLoS Med.* 13:e1002049. doi: 10.1371/journal.pmed.1002049

Ishida, M., Miyagawa, S., Saito, A., Fukushima, S., Harada, A., Ito, E., et al. (2019). Transplantation of Human-induced Pluripotent Stem Cell-derived Cardiomyocytes Is Superior to Somatic Stem Cell Therapy for Restoring Cardiac Function and Oxygen Consumption in a Porcine Model of Myocardial Infarction. *Transplantation* 103, 291–298. doi: 10.1097/tp.0000000000002384

Janssens, S., Dubois, C., Bogaert, J., Theunissen, K., Deroose, C., Desmet, W., et al. (2006). Autologous bone marrow-derived stem-cell transfer in patients with ST-segment elevation myocardial infarction: double-blind, randomised controlled trial. *Lancet* 367, 113–121. doi: 10.1016/s0140-6736(05)67861-0

Joudinaud, T. M., Kegel, C. L., Gabster, A. A., Sanz, M. L., MacDonald, A., Propp, D., et al. (2005). An experimental method for the percutaneous induction of a posterolateral infarct and functional ischemic mitral regurgitation. *J. Heart Valve Dis.* 14, 460–466.

Kamimura, R., Suzuki, S., Nozaki, S., Sakamoto, H., Maruno, H., and Kawaida, H. (1996). Branching patterns in coronary artery and ischemic areas induced by coronary arterial occlusion in the CLAWN miniature pig. *Exp. Anim.* 45, 149–153. doi: 10.1538/expanim.45.149

Khan, M. A. (1984). Minipig: advantages and disadvantages as a model in toxicity testing. *J. Am. Coll Toxicol.* 3, 337–342. doi: 10.3109/10915818409104396

Kim, J.-H., Chung, H.-S., Antonisamy, P., Lee, S. R., and Bae, H. (2014). Cardioprotective effect of rhizomes of Acorus gramineus against isoproterenol-induced cardiac damage in pigs. *Cardiovasc. Toxicol.* 14, 183–192. doi: 10.1007/s12012-014-9243-5

Kim, M. C., Kim, Y. S., Kang, W. S., Lee, K. H., Cho, M., Hong, M. H., et al. (2017). Intramyocardial injection of stem cells in pig myocardial infarction model: the first trial in korea. *J. Korean. Med. Sci.* 32, 1708–1712. doi: 10.3346/jkms.2017.32.10.1708

Kloner, R. A. (2013). Current state of clinical translation of cardioprotective agents for acute myocardial infarction. *Circ. Res.* 113, 451–463. doi: 10.1161/circresaha.112.300627

Kloner, R. A., and Rezkalla, S. H. (2004). Cardiac protection during acute myocardial infarction: where do we stand in 2004? *J. Am. Coll. Cardiol.* 44, 276–286. doi: 10.1016/j.jacc.2004.03.068

Kraitchman, D. L., Heldman, A. W., Atalar, E., Amado, L. C., Martin, B. J., Pittenger, M. F., et al. (2003). In vivo magnetic resonance imaging of mesenchymal stem cells in myocardial infarction. *Circulation* 107, 2290–2293. doi: 10.1161/01.cir.0000070931.62772.4e

Krause, U., Harter, C., Seckinger, A., Wolf, D., Reinhard, A., Bea, F., et al. (2007). Intravenous delivery of autologous mesenchymal stem cells limits infarct size and improves left ventricular function in the infarcted porcine heart. *Stem Cells Dev.* 16, 31–37. doi: 10.1089/scd.2006.0089

Krueger, M. A., Huke, S. S., and Glenny, R. W. (2013). Visualizing regional myocardial blood flow in the mouse. *Circ. Res.* 112, e88–e97.

Kumar, D., Hacker, T. A., Buck, J., Whitesell, L. F., Kaji, E. H., Douglas, P. S., et al. (2005). Distinct mouse coronary anatomy and myocardial infarction consequent to ligation. *Coron. Artery Dis.* 16, 41–44. doi: 10.1097/00019501-200502000-00008

Laflamme, M. A., Chen, K. Y., Naumova, A. V., Muskheli, V., Fugate, J. A., Dupras, S. K., et al. (2007). Cardiomyocytes derived from human embryonic stem cells in pro-survival factors enhance function of infarcted rat hearts. *Nat. Biotechnol.* 25, 1015–1024. doi: 10.1038/nbt1327

Lee, Y. T., Lin, H. Y., Chan, Y. W. F., Li, K. H. C., To, O. T. L., Yan, B. P., et al. (2017). Mouse models of atherosclerosis: a historical perspective and recent advances. *Lipids Health Dis.* 16:12.

Lelovas, P. P., Kostomitsopoulos, N. G., and Xanthos, T. T. A. (2014). comparative anatomic and physiologic overview of the porcine heart. *J. Am. Assoc. Lab. Anim. Sci.* 53, 432–438.

Li, R. K., Weisel, R. D., Mickle, D. A., Jia, Z. Q., Kim, E. J., Sakai, T., et al. (2000). Autologous porcine heart cell transplantation improved heart function after a myocardial infarction. *J. Thorac. Cardiovasc. Surg.* 119, 62–68. doi: 10.1016/s0022-5223(00)70218-2

Li, X., Zhang, F., Song, G., Gu, W., Chen, M., Yang, B., et al. (2013). Intramyocardial injection of pig pluripotent stem cells improves left ventricular function and perfusion: A study in a porcine model of acute myocardial infarction. *PLoS One.* 8:e66688. doi: 10.1371/journal.pone.0066688

Lim, K. H., Cho, J. Y., Kim, B., Bae, B.-S., and Kim, J.-H. (2014). Red ginseng (Panax ginseng) decreases isoproterenol-induced cardiac injury via antioxidant properties in porcine. *J. Med. Food.* 17, 111–118. doi: 10.1089/jmf.2013.2768

Lim, M., Wang, W., Liang, L., Han, Z.-B., Li, Z., Geng, J., et al. (2018). Intravenous injection of allogeneic umbilical cord-derived multipotent mesenchymal stromal cells reduces the infarct area and ameliorates cardiac function in a porcine model of acute myocardial infarction. *Stem Cell Res. Ther.* 9:129.

Liu, X., Wang, Y., Tang, M., Liu, Y., Hu, L., and Gu, Y. (2020). Three-dimensional visualization of coronary microvasculature in rats with myocardial infarction. *Microvasc. Res.* 130:103990. doi: 10.1016/j.mvr.2020.103990

Locatelli, P., Olea, F. D., Mendiz, O., Salmo, F., Fazzi, L., Hnatiuk, A., et al. (2011). An ovine model of postinfarction dilated cardiomyopathy in animals with highly variable coronary anatomy. *ILAR J.* 52, E16–E21.

Locher, M. R., Razumova, M. V., Stelzer, J. E., Norman, H. S., Patel, J. R., and Moss, R. L. (2009). Determination of rate constants for turnover of myosin isoforms in rat myocardium: implications for in vivo contractile kinetics. *Am. J. Physiol. Heart Circ. Physiol.* 297, H247–H256.

Lu, M., Zhao, S., Liu, Q., Jiang, S., Song, P., Qian, H., et al. (2012). Transplantation with autologous mesenchymal stem cells after acute myocardial infarction

evaluated by magnetic resonance imaging: an experimental study. *J. Thorac. Imaging* 27, 125–135. doi: 10.1097/rti.0b013e31820446fa

Ludman, A. J., Yellon, D. M., and Hausenloy, D. J. (2010). Cardiac preconditioning for ischaemia: lost in translation. *Dis. Model Mech.* 3, 35–38. doi: 10.1242/dmm.003855

Lunde, K., Solheim, S., Aakhus, S., Arnesen, H., Abdelnoor, M., Egeland, T., et al. (2006). Intracoronary injection of mononuclear bone marrow cells in acute myocardial infarction. *N. Engl. J. Med.* 355, 1199–1209.

Lüscher, T. F. (2019). Back to square one. *Eur. Heart J.* 40, 1031–1033.

Makkar, R. R., Price, M. J., Lill, M., Frantzen, M., Takizawa, K., Kleisli, T., et al. (2005). Intramyocardial injection of allogenic bone marrow-derived mesenchymal stem cells without immunosuppression preserves cardiac function in a porcine model of myocardial infarction. *J. Cardiovasc. Pharmacol. Ther.* 10, 225–233. doi: 10.1177/107424840501000403

Makkar, R. R., Smith, R. R., Cheng, K., Malliaras, K., Thomson, L. E., Berman, D., et al. (2012). Intracoronary cardiosphere-derived cells for heart regeneration after myocardial infarction (CADUCEUS): a prospective, randomised phase 1 trial. *Lancet* 379, 895–904. doi: 10.1016/s0140-6736(12)60195-0

Maxwell, M. P., Hearse, D. J., and Yellon, D. M. (1987). Species variation in the coronary collateral circulation during regional myocardial ischaemia: a critical determinant of the rate of evolution and extent of myocardial infarction. *Cardiovasc. Res.* 21, 737–746. doi: 10.1093/cvr/21.10.737

Menasché, P. (2018). Cell therapy trials for heart regeneration - lessons learned and future directions. *Nat. Rev. Cardiol.* 15, 659–671. doi: 10.1038/s41569-018-0013-0

Milani-Nejad, N., and Janssen, P. M. L. (2014). Small and large animal models in cardiac contraction research: advantages and disadvantages. *Pharmacol. Ther.* 141, 235–249. doi: 10.1016/j.pharmthera.2013.10.007

Miura, T., and Miki, T. (2008). Limitation of myocardial infarct size in the clinical setting: current status and challenges in translating animal experiments into clinical therapy. *Basic Res. Cardiol.* 103, 501–513. doi: 10.1007/s00395-008-0743-y

Miyagawa, S., Domae, K., Yoshikawa, Y., Fukushima, S., Nakamura, T., Saito, A., et al. (2017). Phase I Clinical Trial of Autologous Stem Cell-Sheet Transplantation Therapy for Treating Cardiomyopathy. *J Am. Heart Assoc.* 6:4.

Morrissey, P. J., Murphy, K. R., Daley, J. M., Schofield, L., Turan, N. N., Arunachalam, K., et al. (2017). A novel method of standardized myocardial infarction in aged rabbits. *Am. J. Physiol. Heart Circ. Physiol.* 312, H959–H967.

Mu, D., Zhang, X.-L., Xie, J., Yuan, H.-H., Wang, K., Huang, W., et al. (2016). Intracoronary Transplantation of Mesenchymal Stem Cells with Overexpressed Integrin-Linked Kinase Improves Cardiac Function in Porcine Myocardial Infarction. *Sci. Rep.* 6:19155.

Muller, C. A., Opie, L. H., Hamm, C. W., Peisach, M., Pineda, C. A., and Thandroyen, F. T. (1988). Verapamil and tiapamil in prevention of ventricular fibrillation in pigs with coronary ligation. Comparative effects on left ventricular function. *Circulation* 78, 227–232. doi: 10.1161/01.cir.78.1.227

National Research Council (Us) Committee on Scientific and Humane Issues in the Use of Random Source Dogs and Cats in Research (2009). *Use of Dogs and Cats in Research: Public Perception and Evolution of Laws and Guidelines - Scientific and Humane Issues in the Use of Random Source Dogs and Cats in Research - NCBI Bookshelf*. Washington, DC: National Research Council.

Nguyen, P. K., and Wu, J. C. (2015). Large animal models of ischemic cardiomyopathy: are they enough to bridge the translational gap? *J. Nucl. Cardiol.* 22, 666–672. doi: 10.1007/s12350-015-0078-7

Nicolini, F., and Gherli, T. (2009). Alternatives to transplantation in the surgical therapy for heart failure. *Eur. J. Cardiothorac. Surg.* 35, 214–228. doi: 10.1016/j.ejcts.2008.11.003

Anon, J. (2013). Announcement: Reducing our irreproducibility. *Nature* 496, 398–398. doi: 10.1038/496398a

Nunoya, T., Shibuya, K., Saitoh, T., Yazawa, H., Nakamura, K., Baba, Y., et al. (2007). Use of Miniature Pig for Biomedical Research, with Reference to Toxicologic Studies. *J. Toxicol. Pathol.* 20, 125–132. doi: 10.1293/tox.20.125

Okura, H., Saga, A., Soeda, M., Miyagawa, S., Sawa, Y., Daimon, T., et al. (2012). Intracoronary artery transplantation of cardiomyoblast-like cells from human adipose tissue-derived multi-lineage progenitor cells improve left ventricular dysfunction and survival in a swine model of chronic myocardial infarction. *Biochem. Biophys. Res. Commun.* 425, 859–865. doi: 10.1016/j.bbrc.2012.08.004

Penicka, M., Horak, J., Kobylka, P., Pytlik, R., Kozak, T., Belohlavek, O., et al. (2007). Intracoronary injection of autologous bone marrow-derived mononuclear cells in patients with large anterior acute myocardial infarction: a prematurely terminated randomized study. *J. Am. Coll. Cardiol.* 49, 2373–2374. doi: 10.1016/j.jacc.2007.04.009

Perel, P., Roberts, I., Sena, E., Wheble, P., Briscoe, C., Sandercock, P., et al. (2007). Comparison of treatment effects between animal experiments and clinical trials: systematic review. *BMJ* 334:197. doi: 10.1136/bmj.39048.407928.be

Perin, E. C., Willerson, J. T., Pepine, C. J., Henry, T. D., Ellis, S. G., Zhao, D. X. M., et al. (2012). Effect of transendocardial delivery of autologous bone marrow mononuclear cells on functional capacity, left ventricular function, and perfusion in chronic heart failure: the FOCUS-CCTRN trial. *JAMA* 307, 1717–1726.

Podesser, B., Wollenek, G., Seitelberger, R., Siegel, H., Wolner, E., Firbas, W., et al. (1997). Epicardial branches of the coronary arteries and their distribution in the rabbit heart: The rabbit heart as a model of regional ischemia. *Anatomical. Record* 1997:1.

Potz, B. A., Scrimgeour, L. A., Pavlov, V. I., Sodha, N. R., Abid, M. R., and Sellke, F. W. (2018). Extracellular vesicle injection improves myocardial function and increases angiogenesis in a swine model of chronic ischemia. *J. Am. Heart Assoc.* 7:12.

Pound, P., and Ritskes-Hoitinga, M. (2018). Is it possible to overcome issues of external validity in preclinical animal research? Why most animal models are bound to fail. *J. Transl. Med.* 16:304.

Pound, P., Ebrahim, S., Sandercock, P., Bracken, M. B., and Roberts, I. (2004). Reviewing Animal Trials Systematically (RATS) Group. Where is the evidence that animal research benefits humans? *BMJ* 328, 514–517. doi: 10.1136/bmj.328.7438.514

Price, M. J., Chou, C.-C., Frantzen, M., Miyamoto, T., Kar, S., Lee, S., et al. (2006). Intravenous mesenchymal stem cell therapy early after reperfused acute myocardial infarction improves left ventricular function and alters electrophysiologic properties. *Int. J. Cardiol.* 111, 231–239. doi: 10.1016/j.ijcard.2005.07.036

Principles and Guidelines for Reporting Preclinical Research and National Institutes of Health (NIH) (2021). Available online at: https://www.nih.gov/research-training/rigor-reproducibility/principles-guidelines-reporting-preclinical-research (acceessed date 28, March 2021)

Quintana, H. K., Janszky, I., Kanar, A., Gigante, B., Druid, H., Ahlbom, A., et al. (2018). Comorbidities in relation to fatality of first myocardial infarction. *Cardiovasc. Pathol.* 32, 32–37. doi: 10.1016/j.carpath.2017.11.002

Quyyumi, A. A., Vasquez, A., Kereiakes, D. J., Klapholz, M., Schaer, G. L., Abdel-Latif, A., et al. (2017). PreSERVE-AMI: A Randomized, Double-Blind, Placebo-Controlled Clinical Trial of Intracoronary Administration of Autologous CD34+ Cells in Patients With Left Ventricular Dysfunction Post STEMI. *Circ. Res.* 120, 324–331. doi: 10.1161/circresaha.115.308165

Rabbani, S., Ahmadi, H., Fayazzadeh, E., Sahebjam, M., Boroumand, M. A., Sotudeh, M., et al. (2008). Development of an ovine model of myocardial infarction. *ANZ J. Surg.* 78, 78–81. doi: 10.1111/j.1445-2197.2007.04359.x

Rabbani, S., Soleimani, M., Sahebjam, M., Imani, M., Nassiri, S. M., Atashi, A., et al. (2017). Effects of endothelial and mesenchymal stem cells on improving myocardial function in a sheep animal model. *J. Tehran. Heart Cent.* 12, 65–71.

Ramirez, F. D., Motazedian, P., Jung, R. G., Di Santo, P., MacDonald, Z. D., Moreland, R., et al. (2017). Methodological rigor in preclinical cardiovascular studies: targets to enhance reproducibility and promote research translation. *Circ. Res.* 120, 1916–1926. doi: 10.1161/circresaha.117.310628

Ranasinghe, I., Shojaee, A., Bikdeli, B., Gupta, A., Chen, R., Ross, J. S., et al. (2015). Poorly cited articles in peer-reviewed cardiovascular journals from 1997 to 2007: analysis of 5-year citation rates. *Circulation* 131, 1755–1762. doi: 10.1161/circulationaha.114.015080

Ribas, J., Sadeghi, H., Manbachi, A., Leijten, J., Brinegar, K., Zhang, Y. S., et al. (2016). Cardiovascular Organ-on-a-Chip Platforms for Drug Discovery and Development. *Appl. Vitro Toxicol.* 2, 82–96. doi: 10.1089/aivt.2016.0002

Ribitsch, I., Baptista, P. M., Lange-Consiglio, A., Melotti, L., Patruno, M., Jenner, F., et al. (2020). Large animal models in regenerative medicine and tissue

engineering: to do or not to do. *Front. Bioeng. Biotechnol.* 8:972. doi: 10.3389/fbioe.2020.00972

Richards, D. J., Li, Y., Kerr, C. M., Yao, J., Beeson, G. C., Coyle, R. C., et al. (2020). Human cardiac organoids for the modelling of myocardial infarction and drug cardiotoxicity. *Nat. Biomed. Eng.* 4, 446–462. doi: 10.1038/s41551-020-0539-4

Richter, S. H., Garner, J. P., and Würbel, H. (2009). Environmental standardization: cure or cause of poor reproducibility in animal experiments? *Nat. Methods* 6, 257–261. doi: 10.1038/nmeth.1312

Riehle, C., and Bauersachs, J. (2019). Small animal models of heart failure. *Cardiovasc. Res.* 115, 1838–1849. doi: 10.1093/cvr/cvz161

Rienzo, M., Imbault, J., El Boustani, Y., Beurton, A., Carlos Sampedrano, C., Pasdois, P., et al. (2020). A total closed chest sheep model of cardiogenic shock by percutaneous intracoronary ethanol injection. *Sci. Rep.* 10:12417.

Romagnuolo, R., Masoudpour, H., Porta-Sánchez, A., Qiang, B., Barry, J., Laskary, A., et al. (2019). Human Embryonic Stem Cell-Derived Cardiomyocytes Regenerate the Infarcted Pig Heart but Induce Ventricular Tachyarrhythmias. *Stem Cell Rep.* 12, 967–981. doi: 10.1016/j.stemcr.2019.04.005

Sandercock, P., and Roberts, I. (2002). Systematic reviews of animal experiments. *Lancet* 360:586. doi: 10.1016/s0140-6736(02)09812-4

Savarese, G., and Lund, L. H. (2017). Global public health burden of heart failure. *Card Fail Rev.* 3, 7–11.

Savoji, H., Mohammadi, M. H., Rafatian, N., Toroghi, M. K., Wang, E. Y., Zhao, Y., et al. (2019). Cardiovascular disease models: A game changing paradigm in drug discovery and screening. *Biomaterials* 198, 3–26. doi: 10.1016/j.biomaterials.2018.09.036

Schuleri, K. H., Boyle, A. J., Centola, M., Amado, L. C., Evers, R., Zimmet, J. M., et al. (2008). The adult Göttingen minipig as a model for chronic heart failure after myocardial infarction: focus on cardiovascular imaging and regenerative therapies. *Comp. Med.* 58, 568–579.

Sharp, T. E., Schena, G. J., Hobby, A. R., Starosta, T., Berretta, R. M., Wallner, M., et al. (2017). Cortical bone stem cell therapy preserves cardiac structure and function after myocardial infarction. *Circ. Res.* 121, 1263–1278. doi: 10.1161/circresaha.117.311174

Shudo, Y., Cohen, J. E., Macarthur, J. W., Atluri, P., Hsiao, P. F., Yang, E. C., et al. (2013). Spatially oriented, temporally sequential smooth muscle cell-endothelial progenitor cell bi-level cell sheet neovascularizes ischemic myocardium. *Circulation* 128(11 Suppl. 1), S59–S68.

Shudo, Y., Miyagawa, S., Fukushima, S., Saito, A., Shimizu, T., Okano, T., et al. (2011). Novel regenerative therapy using cell-sheet covered with omentum flap delivers a huge number of cells in a porcine myocardial infarction model. *J. Thorac. Cardiovasc. Surg.* 142, 1188–1196. doi: 10.1016/j.jtcvs.2011.07.002

Shudo, Y., Miyagawa, S., Ohkura, H., Fukushima, S., Saito, A., Shiozaki, M., et al. (2014). Addition of mesenchymal stem cells enhances the therapeutic effects of skeletal myoblast cell-sheet transplantation in a rat ischemic cardiomyopathy model. *Tissue Eng. Part A.* 20, 728–739.

Sjaastad, I., Grund, F., and Ilebekk, A. (2000). Effects on infarct size and on arrhythmias by controlling reflow after myocardial ischaemia in pigs. *Acta Physiol. Scand.* 169, 195–201. doi: 10.1046/j.1365-201x.2000.00735.x

Spadaro, J., Fishbein, M. C., Hare, C., Pfeffer, M. A., and Maroko, P. R. (1980). Characterization of myocardial infarcts in the rat. *Arch. Pathol. Lab. Med.* 104, 179–183.

Spannbauer, A., Traxler, D., Zlabinger, K., Gugerell, A., Winkler, J., Mester-Tonczar, J., et al. (2019). Large animal models of heart failure with reduced ejection fraction (hfref). *Front. Cardiovasc. Med.* 6:117. doi: 10.3389/fcvm.2019.00117

Steele, A. N., MacArthur, J. W., and Woo, Y. J. (2017). Stem cell therapy: healing or hype? why stem cell delivery doesn't work. *Circ. Res.* 120, 1868–1870. doi: 10.1161/circresaha.117.310584

Stricker-Krongrad, A., Shoemake, C., Brocksmith, D., Liu, J., Hamlin, R., and Bouchard, G. (2017). Comparative cardiovascular physiology and pathology in selected lineages of minipigs. *Toxicol. Res. Appl.* 1:239784731769636. doi: 10.1177/2397847317696367

Stubhan, M., Markert, M., Mayer, K., Trautmann, T., Klumpp, A., Henke, J., et al. (2008). Evaluation of cardiovascular and ECG parameters in the normal, freely moving Göttingen Minipig. *J. Pharmacol. Toxicol. Methods* 57, 202–211. doi: 10.1016/j.vascn.2008.02.001

Sun, S., Jiang, Y., Zhen, Z., Lai, W.-H., Liao, S., and Tse, H.-F. (2020). Establishing a Swine Model of Post-myocardial Infarction Heart Failure for Stem Cell Treatment. *J. Vis. Exp.* 2020:159.

Suzuki, G., Young, R. F., Leiker, M. M., and Suzuki, T. (2016). Heart-Derived Stem Cells in Miniature Swine with Coronary Microembolization: Novel Ischemic Cardiomyopathy Model to Assess the Efficacy of Cell-Based Therapy. *Stem Cells Int.* 2016: 6940195.

Tang, Y.-P., Liu, Y., Fan, Y.-J., Zhao, Y.-Y., Feng, J.-Q., and Liu, Y. (2018). To develop a novel animal model of myocardial infarction: A research imperative. *Anim. Models Exp. Med.* 1, 36–39. doi: 10.1002/ame2.12010

Techiryan, G., Weil, B. R., Palka, B. A., and Canty, J. M. (2018). Effect of intracoronary metformin on myocardial infarct size in swine. *Circ. Res.* 123, 986–995. doi: 10.1161/circresaha.118.313341

Thomas, D., Ferrari, V. A., Janik, M., Kim, D. H., Pickup, S., Glickson, J. D., et al. (2004). Quantitative assessment of regional myocardial function in a rat model of myocardial infarction using tagged MRI. *MAGMA* 17, 179–187. doi: 10.1007/s10334-004-0051-y

Thomas, R., Thai, K., Barry, J., Wright, G. A., Strauss, B. H., and Ghugre, N. R. (2021). T2-based area-at-risk and edema are influenced by ischemic duration in acute myocardial infarction. *Magn. Reson. Imaging* 79, 1–4. doi: 10.1016/j.mri.2021.02.011

Timmers, L., Lim, S. K., Hoefer, I. E., Arslan, F., Lai, R. C., van Oorschot, A. A. M., et al. (2011). Human mesenchymal stem cell-conditioned medium improves cardiac function following myocardial infarction. *Stem Cell Res.* 6, 206–214.

Tohyama, S., and Kobayashi, E. (2019). Age-Appropriateness of Porcine Models Used for Cell Transplantation. *Cell Trans.* 28, 224–228.

Trankle, C., Thurber, C. J., Toldo, S., and Abbate, A. (2016). Mitochondrial membrane permeability inhibitors in acute myocardial infarction: still awaiting translation. *JACC Basic Transl. Sci.* 1, 524–535.

Ungerleider, J. L., and Christman, K. L. (2014). Concise review: injectable biomaterials for the treatment of myocardial infarction and peripheral artery disease: translational challenges and progress. *Stem Cells Transl. Med.* 3, 1090–1099.

van der Velden, J., Merkus, D., Klarenbeek, B. R., James, A. T., Boontje, N. M., Dekkers, D. H. W., et al. (2004). Alterations in myofilament function contribute to left ventricular dysfunction in pigs early after myocardial infarction. *Circ. Res.* 95, e85–e95.

van der Worp, H. B., Howells, D. W., Sena, E. S., Porritt, M. J., Rewell, S., O'Collins, V., et al. (2010). Can animal models of disease reliably inform human studies? *PLoS Med.* 7:e1000245. doi: 10.1371/journal.pmed.1000245

van Luijk, J., Bakker, B., Rovers, M. M., Ritskes-Hoitinga, M., de Vries, R. B. M., and Leenaars, M. (2014). Systematic reviews of animal studies; missing link in translational research? *PLoS One* 9:e89981. doi: 10.1371/journal.pone.0089981

Virani, S. S., Alonso, A., Aparicio, H. J., Benjamin, E. J., Bittencourt, M. S., Callaway, C. W., et al. (2021). Heart Disease and Stroke Statistics-2021 Update: A Report From the American Heart Association. *Circulation* 143, e254–e743.

Voelkl, B., Vogt, L., Sena, E. S., and Würbel, H. (2018). Reproducibility of preclinical animal research improves with heterogeneity of study samples. *PLoS Biol.* 16:e2003693. doi: 10.1371/journal.pbio.2003693

Wang, B., Zhang, L., Cao, H., Yang, J., Wu, M., Ma, Y., et al. (2017). Myoblast transplantation improves cardiac function after myocardial infarction through attenuating inflammatory responses. *Oncotarget* 8, 68780–68794.

Wang, L., Tao, T., Su, W., Yu, H., Yu, Y., and Qin, J. A. (2017). disease model of diabetic nephropathy in a glomerulus-on-a-chip microdevice. *Lab. Chip.* 17, 1749–1760.

Wang, X., Jameel, M. N., Li, Q., Mansoor, A., Qiang, X., Swingen, C., et al. (2009). Stem cells for myocardial repair with use of a transarterial catheter. *Circulation* 120(11 Suppl.), S238–S246.

Watanabe, E., Smith, D. M., Delcarpio, J. B., Sun, J., Smart, F. W., Van Meter, C. H., et al. (1998). Cardiomyocyte transplantation in a porcine myocardial infarction model. *Cell Trans.* 7, 239–246.

Weaver, M. E., Pantely, G. A., Bristow, J. D., and Ladley, H. D. A. (1986). quantitative study of the anatomy and distribution of coronary arteries in swine in comparison with other animals and man. *Cardiovasc. Res.* 20, 907–917.

Wolf, D., Reinhard, A., Seckinger, A., Katus, H. A., Kuecherer, H., and Hansen, A. (2009). Dose-dependent effects of intravenous allogeneic mesenchymal stem cells in the infarcted porcine heart. *Stem Cells Dev.* 18, 321–329.

Wollert, K. C., Meyer, G. P., Müller-Ehmsen, J., Tschöpe, C., Bonarjee, V., Larsen, A. I., et al. (2017). Intracoronary autologous bone marrow cell transfer after myocardial infarction: the BOOST-2 randomised placebo-controlled clinical trial. *Eur. Heart J.* 38, 2936–2943.

Wu, Q., Liu, J., Wang, X., Feng, L., Wu, J., Zhu, X., et al. (2020). Organ-on-a-chip: recent breakthroughs and future prospects. *Biomed. Eng. Online* 19:9.

Yang, Y., Gruwel, M. L., Dreessen de Gervai, P., Sun, J., Jilkina, O., and Gussakovsky, E. (2012). MRI study of cryoinjury infarction in pig hearts: i. Effects of intrapericardial delivery of bFGF/VEGF embedded in alginate beads. *NMR Biomed.* 25, 177–188.

Yang, Y., Sun, J., Gervai, P., Gruwel, M. L., Jilkina, O., Gussakovsky, E., et al. (2010). Characterization of cryoinjury-induced infarction with manganese-and gadolinium-enhanced MRI and optical spectroscopy in pig hearts. *Magn. Reson. Imag.* 28, 753–766.

Yellon, D. M., and Hausenloy, D. J. (2007). Myocardial reperfusion injury. *N. Engl. J. Med.* 357, 1121–1135.

Zhao, J.-J., Liu, X.-C., Kong, F., Qi, T.-G., Cheng, G.-H., Wang, J., et al. (2014). Bone marrow mesenchymal stem cells improve myocardial function in a swine model of acute myocardial infarction. *Mol. Med. Rep.* 10, 1448–1454.

**Conflict of Interest:** The authors declare that the research was conducted in the absence of any commercial or financial relationships that could be construed as a potential conflict of interest.

frontiers in Bioengineering and Biotechnology

MINI REVIEW
published: 01 June 2021
doi: 10.3389/fbioe.2021.674172

# The Expanding Armamentarium of Innovative Bioengineered Strategies to Augment Cardiovascular Repair and Regeneration

*Stefan Elde*[1], *Hanjay Wang*[1,2] *and Y. Joseph Woo*[1,2,3]*

[1] Department of Cardiothoracic Surgery, Stanford University, Stanford, CA, United States, [2] Stanford Cardiovascular Institute, Stanford University, Stanford, CA, United States, [3] Department of Bioengineering, Stanford University, Stanford, CA, United States

Cardiovascular disease remains the leading cause of death worldwide. While clinical trials of cell therapy have demonstrated largely neutral results, recent investigations into the mechanisms of natural myocardial regeneration have demonstrated promising new intersections between molecular, cellular, tissue, biomaterial, and biomechanical engineering solutions. New insight into the crucial role of inflammation in natural regenerative processes may explain why previous efforts have yielded only modest degrees of regeneration. Furthermore, the new understanding of the interdependent relationship of inflammation and myocardial regeneration have catalyzed the emergence of promising new areas of investigation at the intersection of many fields.

**Keywords: regeneration, heart regeneration, cardiac regeneration, myocardial regeneration, bioengineering, cell sheet and tissue engineering, hydrogel, inflammation**

OPEN ACCESS

***Edited by:***
*Vahid Serpooshan, Emory University, United States*

***Reviewed by:***
*Morteza Mahmoudi, Michigan State University, United States*
*Marie-noelle Giraud, Université de Fribourg, Switzerland*

***Correspondence:**
*Y. Joseph Woo*
*joswoo@stanford.edu*

***Specialty section:***
*This article was submitted to Tissue Engineering and Regenerative Medicine, a section of the journal Frontiers in Bioengineering and Biotechnology*

***Received:*** *28 February 2021*
***Accepted:*** *13 April 2021*
***Published:*** *01 June 2021*

***Citation:***
*Elde S, Wang H and Woo YJ (2021) The Expanding Armamentarium of Innovative Bioengineered Strategies to Augment Cardiovascular Repair and Regeneration. Front. Bioeng. Biotechnol. 9:674172. doi: 10.3389/fbioe.2021.674172*

## INTRODUCTION

Cardiovascular disease is responsible for 17.6 million deaths worldwide every year, and the cost of treating these patients is expected to double over the next two decades (Heidenreich et al., 2011; Benjamin et al., 2019). Significant advancements in revascularization strategies after myocardial infarction (MI) such as coronary artery bypass grafting (CABG) and percutaneous coronary intervention (PCI) have considerably improved outcomes, but do not address microvascular perfusion deficits that result in adverse ventricular remodeling despite successful macrorevascularization (Araszkiewicz et al., 2006). This unmet clinical need has stimulated a significant interest in bioengineering strategies including molecular and cellular, tissue, biomaterial, and biomechanical engineering. In this mini review, we will briefly discuss current strategies, challenges, and future directions.

Given the exponential expansion of new techniques that fall under the broad definition of bioengineering, for the purpose of this article we find it useful to define the scope of *bioengineered strategies* that will be covered in this review.

### Molecular and Cellular Bioengineering

Application of engineering principles at the molecular and cellular levels such as the development of novel cytokines, targeted delivery of intracellular cargo, modulation of gene expression, and cross-species photosynthetic oxygen production.

### Tissue Engineering

Engineered solutions to recapitulate viable myocardium from myocardial patches, cell sheets, and engineered extracellular matrices embedded with various cell types.

### Biomaterial Engineering

Engineering strategies involving hydrogels, cellular scaffolds, or other insoluble substrates that are either impregnated with progenitor cells, growth factors, cytokines, or possess other proangiogenic stimulatory cues.

### Biomechanical Engineering

Engineered substrates that mimic the anisotropic properties of native myocardium and thereby promote the proper alignment of myocardial fibers.

## MOLECULAR AND CELLULAR BIOENGINEERING

Molecular bioengineering techniques to develop novel analogs of endogenous cytokines are a powerful tool to modulate the activation and suppression of specific pathways relevant to the regenerative response (**Table 1**). Following significant insult such as MI, an influx of inflammatory cytokines triggers an acute inflammatory response and migration of macrophages, fibroblasts, and T cells to the infarct zone. Remodeling of the extracellular matrix (ECM) and secretion of potent chemo attractants such as stromal cell-derived factor 1 (SDF-1α) recruit endothelial progenitor cells (EPCs) to the border zone to initiate angiogenesis and myocardial regeneration in rodents (Ingason et al., 2018). The pro-angiogenic properties of SDF-1α and its conservation across many species made it an appealing target for inducing natural myocardial angiogenesis and regeneration. For these reasons, Hiesinger et al. (2011) used molecular modeling to create a synthetic Engineered SDF-1α Analog (ESA) that demonstrated enhanced stability and efficiency in microrevascularization in a murine ischemic cardiomyopathy model. ESA was subsequently shown to improve angiogenesis and perfusion in a rat hindlimb ischemia model (Edwards et al., 2016) and an ovine MI model (MacArthur et al., 2013a).

Direct intramyocardial injection of cytokines or growth factors has proven to be inefficient due to their susceptibility to rapid degradation and diffusion away from the target site. To address these challenges, one group developed a shear thinning hydrogel to serve as the vehicle for cytokine or stem cell delivery via a catheter and returns to its gel form post-injection, named Shear-Thinning Hydrogels for Injectable Encapsulation and Long-Term Delivery (SHIELD) (Mulyasasmita et al., 2014; Cai et al., 2015). Using this novel hydrogel to encapsulate another bioengineered analog of a potent proangiogenic and antiapoptotic cytokine, dimeric fragment of hepatocyte growth factor (HGFdf), resulted in sustained HGFdf release and improved ventricular function with evidence of enhanced angiogenesis in a mouse model (Steele et al., 2020). Combining multiple engineered cytokines, specifically ESA + HGFdf, has also proven effective at reducing scar size and improving angiogenesis after MI in both a small animal model and in sheep (**Figure 1**; Steele et al., 2020).

The success of these efforts to engineer biologically active, shelf-stable, pro-angiogenic small molecules suggests that *in vivo* modulation of the pathways that govern natural regenerative pathways may be possible in the near future. For example, a recent study from Schoger et al. (2020) demonstrated the feasibility of using CRISP/Cas9 gene editing *in vivo* to modify cardiomyocyte (CM) gene expression in a mouse model. Neonatal mice, piglets, and rats all exhibit the capacity for natural myocardial regeneration after myocardial infarction, which is an encouraging sign that these strategies may be translatable to humans pending further study (Wang et al., 2020b).

Complex processes such as the transient ability of neonatal mammals to regenerate injured myocardium are rarely regulated by a single gene or pathway. Accordingly, myocardial regeneration in mammals is a highly regulated process that depends on a symphony of mediators (Desgres and Menasché, 2019). For this reason, one limitation of molecular engineering techniques is that activating a single pathway *in absentia* a coordinated cellular response may result in incomplete or partial activation of the regenerative response. A related challenge of modulating CM developmental pathways via bioengineered small molecules is balancing the specificity of the effectors to mitigate undesirable off-target effects, while attempting to also activate the necessary ancillary or supportive pathways required for regeneration.

For decades, stem cells appeared to be the intuitive solution to the puzzle of myocardial regeneration. However, there is strong evidence to suggest that the mild therapeutic benefit of cell therapy for treatment of ischemic heart disease is actually due to an acute sterile inflammatory response (Vagnozzi et al., 2020). In this study by Vagnozzi et al. (2020), killed cardiac progenitor cells induced an inflammatory response that attenuated fibrosis and rescued ventricular function. Although an acellular inflammatory agent, Zymosan, had a similar effect, it appeared as though cellular debris such as the micro-RNA (miRNA) contained within exosomes may provide a potentially intervenable entry point into the regulatory mechanisms of regeneration. To address this, multiple groups have turned to exosomes from induced pluripotent stem cells (iPSC) that have transdifferentiated into CMs. Exosomes are an appealing vehicle for delivery of a balanced milieu of endogenous miRNA, peptides, and other small molecules to provide the environmental cues to the resident cells of the myocardium. A recent study found that injection of exosomes derived from induced CMs both reduced apoptosis and fibrosis while also upregulating autophagy of cellular debris in the infarcted territory, a necessary prelude to full scale microrevascularization (Santoso et al., 2020). Similar effects have been demonstrated with extra cellular vesicles (EVs), which contain exosomes and a variety of small signaling molecules (Menasché, 2018).

Recent discoveries resulting from innovative approaches in cellular engineering have the potential to create entirely new fields of research. One example of innovative cellular engineering is from Cohen et al. (2017), who demonstrated that administering cyanobacteria into the ischemic rodent heart significantly

**TABLE 1 |** *In vivo* molecular and cellular engineering approaches to myocardial regeneration.

| Author, year of publication | Model | Therapy | Delivery route | Dose | Outcomes |
|---|---|---|---|---|---|
| Ingason et al., 2018 | P1 mouse, apical resection | N/A | N/A | N/A | Regeneration in neonatal mice, proof of concept |
| Hiesinger et al., 2011 | Mouse, LAD ligation | ESA | Intramyocardial injection | 6 μg/kg ESA | Increased EF, CO, SV, fractional area change |
| Edwards et al., 2016 | Rat, hind limb ischemia | ESA | Quadricep injection | 6 μg/kg ESA | Increased perfusion ratio by doppler/Increased capillary density/Increased VEGF MRNA |
| MacArthur et al., 2013a | Sheep, LAD ligation | ESA | Intramyocardial injection | 6 μg/kg ESA | Improved ventricular function<br>Increased EPC chemotaxis<br>Increased capillary and arteriolar density<br>Decreased infarct size<br>Increased maximal principle strain<br>Steeper slope of end systolic pressure volume relationship |
| Mulyasasmita et al., 2014 | Mouse, hindlimb ischemia | hiPSC-ECs VEGF | Protein-polyethylene glycol hydrogel | $5 \times 10^5$ cells 3 μg VEGF | Reduced inflammation<br>Increased muscle regeneration |
| Cai et al., 2015 | Mouse, subcutaneous injection | hASC | Protein polyethylene glycol hydrogel | $5 \times 10^5$ cells | Improved cell survival and retention |
| Steele et al., 2020 | Mouse, LAD ligation<br>Sheep, LAD ligation | ESA<br>HGFdf | Hyaluronic acid hydrogel with PEG-PLA nanoparticles | ESA 25 μg 16 μg HGFdf | Reduction in scar size<br>Increased density of borderzone arterioles<br>Improved ventricular function and geometry |
| Schoger et al., 2020 | Mouse | CRISPR-mediated gene activation | Adeno-associated virus serotype 9 | N/A | Proof of concept, enhanced gene expression of *mef2d* and *Klf15* |
| Wang et al., 2020b | P1 Rat, LAD ligation | N/A | N/A | N/A | Regeneration in neonatal rats, proof of concept |
| Vagnozzi et al., 2020 | Mouse, LAD ligation | MNCs<br>CPCs<br>Zymosan | Intramyocardial injection | 150,000 MNCs or CPCs<br>10–20 μg zymosan | Inflammation stimulates improved ventricular performance |
| Santoso et al., 2020 | Mouse, LAD ligation | Induced cardiomyocyte exosomes | Intramyocardial injection | $4 \times 10^8$ exosomes | Preserved ventricular performance<br>Increased cardiomyocyte viability |
| Cohen et al., 2017 | Rat, LAD ligation | Cyanobacteria | Intramyocardial injection | $1 \times 10^6$ *Synechococcus elongatus* cells | Improved tissue oxygenation<br>60% increase in cardiac output vs. control<br>Improved EF 4-weeks post MI |
| Schenck et al., 2015 | Mouse, full thickness skin defect | Microalgae (*Chlamydomonas reinhardtii*) | *Integra matrix double layer scaffold | $1 \times 10^4$ *C. reinhardtii* cells | Chimeric tissues of *C. reinhardtii* and mouse cells<br>Viable algae at 5 days |
| Chávez et al., 2016 | Mouse, full thickness skin defect | Genetically modified (+VEGF) microalgae (*Chlamydomonas reinhardtii*) HUVECS | *Integra dermal regeneration template | Variable | No significant adverse immune response<br>Successful expression of VEGF via *C. reinhardtii* |

*Summary of in vivo studies investigating molecular and cellular engineering solutions for myocardial regeneration or treatment of ischemic heart disease. Note that the outcomes column is an abbreviated summary of the findings relevant to the focus of this review and is not intended to summarize the study as a whole. Left anterior descending coronary artery (LAD), engineered stromal cell-derived factor-1a (ESA), ejection fraction% (EF), cardiac output (CO), stroke volume (SV), vascular endothelial growth factor (VEGF), end diastolic volume (EDV), end systolic volume (ESV), endothelial progenitor cell (EPC), human induced pluripotent stem cells (hiPSC), human adipose-derived stem cell (hASC), poly(ethylene glycol)-block-poly(lactic acid) (PEG-PLA), dimeric fragment of hepatocyte growth factor (HGFdf), bone marrow mononuclear cells (MNCs), cardiac mesenchymal cells/cardiac progenitor cells (CPCs), human umbilical vein endothelial cells (HUVECS), *Integra Life Science Corporation, Plainsboro, NJ, United States.*

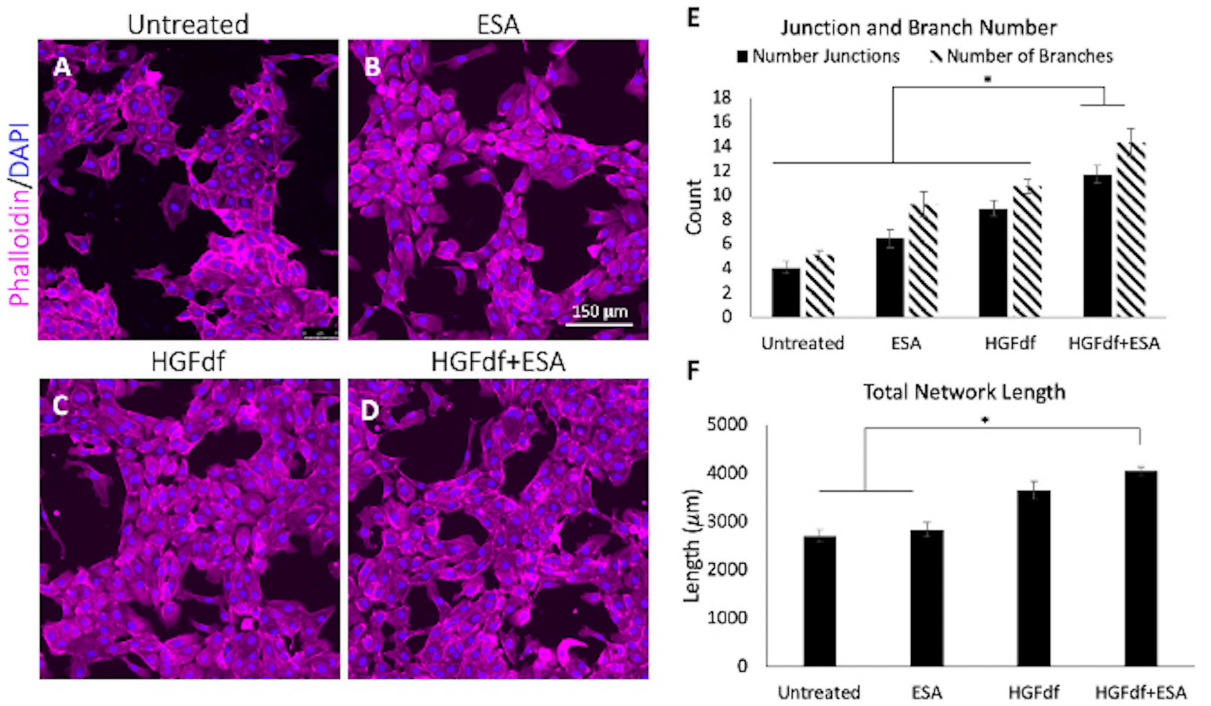


**FIGURE 1 |** Assessment of *in vitro* angiogenesis. Human umbilical cord vein endothelial cells were treated with **(A)** untreated, **(B)** engineered stromal cell-derived factor 1α(ESA), **(C)** engineered dimeric fragment of hepatocyte growth factor (HGFdf) or **(D)** a combination of HGFdf and ESA. The extent of network formation **(E,F)** was evaluated in all groups. Pairwise student *t*-test with Bonferroni's correction, $^*p < 0.05$ (Steele et al., 2020).

improves oxygen delivery and ventricular performance after MI. This concept has been reproduced by other groups that have shown the ability of other photosynthetic bacteria to attenuate the murine fibroblast response to hypoxia, and to switch ischemic rat CMs from anaerobic to aerobic metabolism (Hopfner et al., 2014; Haraguchi et al., 2017). Studies to optimize the stability of photosynthetic bacteria *in vivo* by introducing them via scaffolds or fibrin based hydrogels have successfully reduced cell scattering and proven effective in wound healing assays (Schenck et al., 2015; Chávez et al., 2016; Wang et al., 2019b). Furthermore, the genetic adaptability of cyanobacteria allows for essentially limitless creativity in modifying or augmenting gene expression, such as enhancing expression of angiogenic growth factors like vascular endothelial growth factor (VEGF) (Chávez et al., 2016). These findings have widespread implications for fields such as tissue engineering, organ preservation and transplantation, wound healing, diabetic complications, and neurovascular disease (Wang et al., 2019b).

## TISSUE ENGINEERED SOLUTIONS

Engineered cardiac muscle patches are an emerging potential therapy to address the microvascular perfusion deficit following ischemic insult, e.g., after (MI) (**Table 2**). Patches (also referred to in the literature as scaffolds) may be comprised of reconstituted synthetic materials such as polymers or metals, or as naturally occurring materials such as collagen, chitosan, or alginate, among many others (Cui et al., 2016). Typically, these constructs are applied directly to the epicardium, providing mechanical support to attenuate adverse myocardial remodeling such as wall thinning and fibrosis (Serpooshan et al., 2013). In addition to mechanical reinforcement of the myocardium, patches may also be engineered to serve as a cellular substrate (i.e., engineered ECM) to recruit and retain cell types involved in native myocardial regeneration and angiogenesis (Serpooshan et al., 2013). Building on these techniques, scaffolds can serve as vehicles to deliver therapeutic cytokines, growth factors, proteins, and stem cells to the affected areas (Naveed et al., 2018).

While cardiac patches embedded with pro-angiogenic cell types such as mesenchymal stem cells (MSCs), induced pluripotent stem cells (iPSCs), CMs derived from iPSCs, skeletal myoblasts, and cells derived from bone marrow continue to be investigated (Bw and Me, 2019), select trials in humans have had shown variable results (Chachques et al., 2008; Steele et al., 2017; Menasché et al., 2018). Specifically, engineering living patches introduces issues such as potential immunogenicity or tumorigenicity, transportation and storage logistics, and quality control concerns. Given these valid concerns, there has been a recent resurgence of interest in acellular approaches.

Combining many of the aforementioned techniques, one group recently developed a shelf-stable cardiac patch using decellularized porcine ECM embedded with polylactic-co-glycolic acid (PLGA) microparticles containing growth factors from cardiac stromal cells in a porcine model. By recapitulating native paracrine signaling while avoiding the

inherent challenges of stem cell engraftment, this novel artificial cardiac patch preserved ejection fraction (EF), reduced pathologic remodeling, increased residual viable myocardial tissue, promoted angiogenesis, and may be stored for up to 28 days (Huang et al., 2020).

In contrast to engineering synthetic substrates to provide mechanical support to the infarcted myocardium while simultaneously stimulating angiogenesis, several groups have focused on repurposing nature's preexisting efficiencies. Shudo et al. (2013) engineered a scaffold-free bilevel cell sheet comprised of EPCs and smooth muscle cells (SMCs) from the thoracic aorta which was applied to ischemic myocardium in a rat model. Fate-Tracking assays showed evidence of migration of the EPC/SMCs into the myocardium followed by a transition into mature and

**TABLE 2 |** *In vivo* tissue engineering approaches to myocardial regeneration.

| Author, year of publication | Model | Therapy | Delivery route | Scaffold | Dose | Outcomes |
|---|---|---|---|---|---|---|
| Serpooshan et al., 2013 | Mouse, LAD ligation | Mechanical support of ischemic myocardium | Grafted onto ischemic epicardium | Acellular 3D collagen (type I) patch with elastic moduli 2–10 kPa | N/A | Improved EF and FS<br>Enhanced neo-angiogenesis<br>Diminished fibrosis<br>Migration of native cardiac cells into patch |
| Chachques et al., 2008 | Human, ischemic cardiomyopathy | Autologous BMCs | Intramyocardial injection during CABG ± BMC seed collagen matrix | *CE Mark collagen kit | 250 ± 28 million cells | Safe and feasible<br>No difference in arrhythmias<br>Attenuated adverse ventricular remodeling |
| Menasché et al., 2018 | Human, ischemic cardiomyopathy | hESC derived cardiac progenitor cells | Epicardial patch during CABG | Fibrin patch | 5–10 million cells | Safe and feasible<br>No difference in frequency of tumors or arrhythmias<br>50% alloimmunization |
| Huang et al., 2020 | Rat, LAD ligation<br>Pig, LAD ligation | Synthetic cardiac stromal cells | Epicardial patch | Decellularized porcine ECM + synthetic cardiac stromal cells | $2 \times 10^6$ cells | Improved EF and FS at 7 days (pig) and 3 weeks (rat)<br>Reduced infarct size<br>Increased capillary density<br>Increased cardiomyocyte cell cycle activity |
| Shudo et al., 2013 | Rat, LAD ligation | Aortic SMC and EPCs | Epicardial cell sheet | Bi-level cell sheet | $1.3 \times 10^6$ SMCs<br>$1.3 \times 10^6$ EPCs | Enhanced capillary density and functional microvasculature<br>Migration of EPCs and SMCs into native myocardium<br>Reduced adverse ventricular remodeling<br>Improved EF and FS at 4 weeks post injury |
| Shudo et al., 2017 | Rat, LAD ligation | Bone marrow derived SMC and EPCs | Epicardial cell sheet | Bi-level cell sheet | $1.5 \times 10^5/cm^2$ EPCs<br>$1.5 \times 10^5/cm^2$ SMCs | Improved EF<br>Enhanced neovascularization<br>Reduced adverse ventricular remodeling |
| von Bornstädt et al., 2018 | Rat, femoral artery interposition graft | Human aortic SMCs and skin fibroblasts | Interposition graft | Bi-level cell sheet conduit | $1.5 \times 10^5/cm^2$ SMCs | Rapid conduit maturation (2 weeks)<br>Responsive to vasoactive agents<br>100% patency at 8 weeks<br>Similar histological structure to native arteries |

*Summary of in vivo studies investigating tissue engineering solutions for myocardial regeneration or treatment of ischemic heart disease. Note that the outcomes column is an abbreviated summary of the findings relevant to the focus of this review and is not intended to summarize the study as a whole. Left anterior descending coronary artery (LAD), ejection fraction% (EF), fractional shortening% (FS), bone marrow cells (BMC), coronary artery bypass grafting (CABG), *Pangen 2; Urgo Laboratory, Chenove, France, human embryonic stem cells (hESC), endothelial progenitor cells (EPC), smooth muscle cells (SMC).*

functional microvasculature (Shudo et al., 2013). Similarly, the same group found that ECM rich in fibronectin may help guide MSCs toward a SMC fate, suggesting that an MSC/ECM cell sheet may provide therapeutic benefit. Combining these two findings, they were able to develop a sheet derived entirely from bone marrow which enhances neovascularization, limits adverse remodeling, and improves ventricular function (Shudo et al., 2017). Collectively, these findings also have potential for clinical translation as vascular conduits, demonstrated by using tubularized cell sheets in a rat femoral artery interposition graft model (von Bornstädt et al., 2018). Importantly, the mechanical properties and specifically the stiffness of cell sheets can be easily modified by titrating the collagen content during incubation (Zhu et al., 2020).

## BIOMATERIAL ENGINEERED SOLUTIONS

In an effort to address the challenges of low cell retention and engraftment in techniques that utilize stem cells to repair injured myocardium (Laflamme et al., 2007; Terrovitis et al., 2010), injectable hydrogels have gained traction as a possible solution given their mechanical properties and 3D structure that may protect the fragile stem cells from membranous injury, host rejection, and cell death (Aguado et al., 2012; Dhingra et al., 2013) (**Table 3**). While injectable, shear-thinning hydrogels provide relative protection, optimizing the physical characteristics of the gel, both *ex vivo* during production and *in vivo* after injection, depends on the crosslinking strategy. As discussed above, SHIELD hydrogels were engineered to provide weak *ex vivo* interactions making injection possible, followed by significantly stronger crosslinking once exposed to temperatures above 34°C to maintain hydrogel integrity *in vivo* (Cai et al., 2015). There is ongoing debate regarding the optimal hydrogel stiffness, and this may vary depending on whether the intent is to provide mechanical support to the ventricular wall with or without stem cell transplantation or other cell therapies. Some studies suggest that intermediate stiffness gels (200–400 Pa) could promote the angiogenic potential of engrafted MSCs (Cai et al., 2016), while supraphysiologic gel stiffness may be optimal if the intent is purely mechanical support of the infarcted myocardial territory.

While mechanical support of the ischemic ventricular wall may facilitate later neovascularization, integration of biologically active substrates within the hydrogel may further augment angiogenesis and myocardial repair. One such example is Neuregulin (NRG), an epidermal growth factor with a critical role in CM development which has demonstrated utility in cardiomyopathy animal models. Analogous to the challenges of injectable therapies such as

**TABLE 3 |** *In vivo* biomaterial engineering approaches to myocardial regeneration.

| Author, year of publication | Model | Therapy | Delivery route | Scaffold (if applicable) | Dose | Outcomes |
|---|---|---|---|---|---|---|
| Laflamme et al., 2007 | Rat, LAD ligation | Human embryonic stem cell derived cardiomyocytes + pro-survival factors | Intramyocardial injection | N/A | $10 \times 10^6$ human embryonic stem cells | Limited adverse ventricular remodeling<br>Preserved EF<br>Partial remuscularization of infarct zone |
| Dhingra et al., 2013 | Rat, LAD ligation | Allogeneic MSCs + Prostaglandin E2 | Intramyocardial injection/hydrogel | Biodegradable hydrogel impregnated with prostaglandin E2 | $3 \times 10^6$ cells | Improved MSC survival/immunoprivilege<br>Improved ventricular FS and attenuated adverse remodeling |
| Cai et al., 2016 | Mouse, subcutaneous injection | hASCs + hydrogel | Intramyocardial injection/hydrogel | SHIELD hydrogel, 200–400 Pa | $5 \times 10^5$ cells | Enhanced cell retention |
| Cohen et al., 2014 | Mouse, LAD ligation | NRG + hydrogel | Intramyocardial injection/hydrogel | Biodegradable hydrogel impregnated with NRG | 2.5 μg NRG<br>$3.33 \times 10^5$/mL rat cardiomyocytes | Enhanced EF<br>Increased myocardial thickness at infarct border zone |
| Cohen et al., 2020 | Sheep, LAD ligation | NRG + hydrogel | Intramyocardial injection/hydrogel | Biodegradable hydrogel impregnated with NRG | 100 μg NRG | Enhanced EF and contractility at 8 weeks<br>Reduced infarct size |
| Purcell et al., 2012 | Mouse, LAD ligation | rSDF-1α + hydrogel | Intramyocardial/hydrogel | Hyaluronic acid hydrogel | 200 ng rSDF-1α | Enhanced BMC chemotaxis to remodeling myocardium |

*Summary of in vivo studies investigating biomaterial engineering solutions for myocardial regeneration or treatment of ischemic heart disease. Note that the outcomes column is an abbreviated summary of the findings relevant to the focus of this review and is not intended to summarize the study as a whole. Left anterior descending coronary artery (LAD), ejection fraction% (EF), mesenchymal stem cells (MSC), fractional shortening% (FS), human adipose-derived stem cell (hASC), shear-thinning hydrogel for injectable encapsulation and long-term delivery (SHIELD), polyethylene glycol (PEG), neuregulin (NRG), recombinant stromal cell derived-factor-1a (rSDF-1α), bone marrow-derived cells (BMC).*

stem cells or other biologically active substances, recurrent infusions and off-target exposure preclude the clinical translation of an otherwise promising therapy. To address this, hydrogels encapsulating NRG were engineered to deliver a localized and sustained therapeutic dose while simultaneously providing mechanical support to the ischemic myocardium. This construct stimulated CM mitotic activity, reduced LV dilation, decreased infarct scar size, and enhanced ventricular function in mice and later in sheep 8 weeks post-MI (Cohen et al., 2014, 2020).

Utilizing the sustained, localized delivery of biologically active products via a hydrogel vehicle, similar approaches have shown promise with engrafted stem cells. A limitation of earlier technologies may have been that transplanted stem cells lose their immune privilege and are ultimately rejected upon prolonged interactions with the host myocardium (Dhingra et al., 2013). However, when hydrogels seeded with rat MSCs were treated with prostaglandin E2, which stimulates secretion of the cytokines CCL12 and CCL5, they retained their immune privilege and improved cardiac function in rats (Dhingra et al., 2013). These results stimulated interest in encapsulation of cytokines and exosomal cargo within the hydrogels, given the simplified production and scalability of this approach compared to using MSCs. Examples of cytokines and growth factors that have shown promise when integrated into hydrogels include stromal cell-derived factor-1 alpha (SDF-1α) (Purcell et al., 2012), insulin-like growth factor-1 (IGF-1), hepatocyte growth factor (HGFdf), and many others (Ferrini et al., 2019).

## BIOMECHANICAL ENGINEERING

In healthy myocardium CMs use the ECM as an anchor for actomyosin to generate contractile force. In addition to the rapidly expanding library of small molecules that influence CM development and response after insult, mechanical cues also influence cell shape, protein expression, and differentiation (Engler et al., 2008) (**Table 4**). Engineered matrices that are too soft will provide inadequate resistance for the myosin power stroke, leading to inefficient myocardial contraction. Conversely, matrices that are too stiff lead to intracellular strain on protein structure and earlier loss of contractility when cultured with CMs. Unsurprisingly, it appears as though the optimal stiffness of engineered ECM is that which mimics *in vivo* ECM (Engler et al., 2008). This has implications for engineering solutions for myocardial regeneration and also provides insight into the mechanical dysfunction seen in pathologic states such as pathologic fibrosis following ischemic injury. This prompted investigation of the effect of proangiogenic peptides such as

**TABLE 4 |** *In vivo* biomechanical engineering approaches to myocardial regeneration.

| Author, year of publication | Model | Therapy | Delivery Route | Scaffold (if applicable) | Dose | Outcomes |
|---|---|---|---|---|---|---|
| Hiesinger et al., 2012 | Mouse, LAD ligation | SDF-1α | Intramyocardial injection | N/A | 6 μg/kg | SDF-1α treated peri-infarct myocardium with similar elasticity to normal ventricle<br>SDF-1α treatment stiffened scarred ventricle |
| MacArthur et al., 2013b | Rat, LAD ligation | ESA | Intramyocardial injection | N/A | 6 μg/kg | Enhanced EF and improved CO<br>Reduced adverse remodeling<br>Improved elasticity |
| Trubelja et al., 2014 | Rat, LAD ligation | ESA | Intramyocardial injection | N/A | 6 μg/kg | Increased relaxation rate and decreased transition strain |
| Wang et al., 2019a | Rat, LAD ligation | ESA | Intramyocardial injection | N/A | 6 μg/kg | Greater wall thickness<br>Reduced LVEDD<br>Enhanced EF<br>Reduced infarct size<br>Preserved biaxial mechanical properties of left ventricle |
| Wang et al., 2020a | P1 mouse, LAD ligation | N/A | N/A | N/A | N/A | Natural myocardial regeneration in P1 mice results in similar biomechanical properties as the native myocardium |
| Notari et al., 2018 | P3 mouse, apical resection | Local modification of ECM stiffness (BAPN, LOX inhibitor) | Oral administration | N/A | 1 mg/mL | Decreasing stiffness of ECM results in extended window for natural regeneration in neonatal mice |
| Yu et al., 2018 | Zebrafish, cryoinjury | N/A | N/A | N/A | N/A | Regenerating myocardium requires biomechanical stimulation |

*Summary of in vivo studies investigating biomechanical engineering solutions for myocardial regeneration or treatment of ischemic heart disease. Note that the outcomes column is an abbreviated summary of the findings relevant to the focus of this review and is not intended to summarize the study as a whole. Stromal cell-derived factor-1α, engineered stromal cell–derived factor-1a analog (ESA), ejection fraction% (EF), cardiac output (CO), left ventricular end-diastolic dimension (LVEDD), 3-aminopropionitrile (BAPN, an inhibitor of the LOX ECM crosslinking enzyme), extracellular matrix (ECM).*

SDF-1α with respect to their mechanical effects on the injured myocardium. SDF-1α administration after MI appears to increase the elasticity of the border zone and strengthens the fibrotic myocardium, which may provide a mechanical advantage to CMs and attenuate adverse remodeling (Hiesinger et al., 2012). In addition to naturally occurring small molecules such as SDF-1α, engineered analogs such as ESA have demonstrated the ability to preserve biaxial mechanical properties of the native myocardium, improve myocardial relaxation, reduce infarct size, reduce ventricular thinning, and improve ventricular function (MacArthur et al., 2013b; Trubelja et al., 2014; Wang et al., 2019a).

While biomechanical approaches to emulate the properties of native myocardium have shown promise and should continue to be investigated, naturally regenerated myocardium in a neonatal mouse MI model successfully replicates the mechanical properties of native uninjured myocardium (Wang et al., 2020a). Furthermore, studies in zebrafish have demonstrated that naturally regenerating myocardium is dependent on biomechanical stimulation, i.e., strain, to recover ventricular function after cryoinjury. Collectively, this evidence suggests that biomechanical cues such as ECM stiffness play an important role in the coordination of the regenerative response (Notari et al., 2018; Yu et al., 2018).

## LIMITATIONS OF CURRENT TECHNIQUES

The most challenging limitation to molecular and cellular engineering solutions are that profibrotic, inflammatory, and natural regenerative pathways have complex networks of built-in checks and balances which are difficult to precisely modulate. For example, in reference to regeneration, Berry et al. (2019) describe a "Goldilocks zone" of innate immune signaling, outside of which attempts at cellular reprogramming may be impaired. Additionally, because most molecular and cellular engineering solutions focus on endogenous pathways, the primary safety concerns relate to the potential for non-specific off-target effects. The principal safety concern of cell therapy and tissue engineering are rejection and the inherent potential for uncontrolled proliferation of pluripotent cells. Because exosomes are acellular, they are less immunogenic and have fewer safety concerns than transplantation of allogeneic progenitor cells (Gallet et al., 2017). Additionally, optimizing the delivery substrate without sacrificing cell retention remains a challenge. Direct application of a myocardial patch or hydrogel via a surgical operation are being replaced with catheter-injectable hydrogels, which should improve the safety profile from a periprocedural complication perspective (Steele et al., 2020). Although the chief concern with biomaterials is biocompatibility, most scaffolds and hydrogels in the current era are constructed from immunologically inert materials such as decellularized ECM, alginate, collagen, hyaluronan, fibrin, or insoluble polymers and appear to be safe (Seif-Naraghi et al., 2013; Cai et al., 2015).

## CONCLUSION

Despite significant advancements in our understanding and treatment of ischemic heart disease, the global burden and cost of treating these patients continues to increase. Bioengineering strategies to address the unmet need for paradigm-shifting therapies for ischemic heart disease have shown significant potential for clinical translation and are already being tested in large animal models. New insight into the potential therapeutic mechanism of cell therapy trials have lent credence to the theory of inflammation playing a central role in the natural regenerative pathways, which have informed future directions of this important research. It has become clear that successful translation of bioengineering solutions to treating ischemic heart disease will require an intricate and coordinated series of biologic and mechanical cues to replicate the robust myocardial regenerative pathways that occur naturally in neonatal mammals.

## AUTHOR CONTRIBUTIONS

YJW and HW conceptualized the manuscript. SE wrote the manuscript. YJW and HW revised the manuscript. All the authors contributed to the article and approved the submitted version.

## FUNDING

Funded in part by National Institutes of Health (5R01HL089315, YJW) and the American Heart Association (18POST33990223, HW).

## REFERENCES

Aguado, B. A., Mulyasasmita, W., Su, J., Lampe, K. J., and Heilshorn, S. C. (2012). Improving viability of stem cells during syringe needle flow through the design of hydrogel cell carriers. *Tissue Eng. Part A* 18, 806–815. doi: 10.1089/ten.tea.2011.0391

Araszkiewicz, A., Grajek, S., Lesiak, M., Prech, M., Pyda, M., Janus, M., et al. (2006). Effect of impaired myocardial reperfusion on left ventricular remodeling in patients with anterior wall acute myocardial infarction treated with primary coronary intervention. *Am. J. Cardiol.* 98, 725–728. doi: 10.1016/j.amjcard.2006.04.009

Benjamin, E. J., Muntner, P., Alonso, A., Bittencourt, M. S., Callaway, C. W., Carson, A. P., et al. (2019). Heart disease and stroke statistics—2019 update: a report from the American Heart Association. *Circulation* 139, e56–e528. doi: 10.1161/CIR.0000000000000659

Berry, J. L., Zhu, W., Tang, Y. L., Krishnamurthy, P., Ge, Y., Cooke, J. P., et al. (2019). Convergences of life sciences and engineering in understanding and treating heart failure. *Circulation Res.* 124, 161–169. doi: 10.1161/CIRCRESAHA.118.314216

Bw, S., and Me, D. (2019). Therapeutic cardiac patches for repairing the myocardium. *Adv. Exp. Med. Biol.* 1144, 1–24. doi: 10.1007/5584_2018_309

Cai, L., Dewi, R. E., Goldstone, A. B., Cohen, J. E., Steele, A. N., Woo, Y. J., et al. (2016). Regulating stem cell secretome using injectable hydrogels with in situ network formation. *Adv. Healthc. Mater.* 5, 2758–2764. doi: 10.1002/adhm.201600497

Cai, L., Dewi, R. E., and Heilshorn, S. C. (2015). Injectable hydrogels with in situ double network formation enhance retention of transplanted stem cells. *Adv. Funct. Mater.* 25, 1344–1351. doi: 10.1002/adfm.201403631

Chachques, J. C., Trainini, J. C., Lago, N., Cortes-Morichetti, M., Schussler, O., and Carpentier, A. (2008). Myocardial assistance by grafting a new bioartificial upgraded myocardium (MAGNUM Trial): clinical feasibility study. *Ann. Thoracic Surg.* 85, 901–908. doi: 10.1016/j.athoracsur.2007.10.052

Chávez, M. N., Schenck, T. L., Hopfner, U., Centeno-Cerdas, C., Somlai-Schweiger, I., Schwarz, C., et al. (2016). Towards autotrophic tissue engineering: photosynthetic gene therapy for regeneration. *Biomaterials* 75, 25–36. doi: 10.1016/j.biomaterials.2015.10.014

Cohen, J. E., Goldstone, A. B., Paulsen, M. J., Shudo, Y., Steele, A. N., Edwards, B. B., et al. (2017). An innovative biologic system for photon-powered myocardium in the ischemic heart. *Sci. Adv.* 3:e1603078. doi: 10.1126/sciadv.1603078

Cohen, J. E., Goldstone, A. B., Wang, H., Purcell, B. P., Shudo, Y., MacArthur, J. W., et al. (2020). A bioengineered neuregulin-hydrogel therapy reduces scar size and enhances post-infarct ventricular contractility in an ovine large animal model. *J. Cardiovasc. Dev. Dis.* 7:53. doi: 10.3390/jcdd7040053

Cohen, J. E., Purcell, B. P., MacArthur, J. W., Mu, A., Shudo, Y., Patel, J. B., et al. (2014). A Bioengineered hydrogel system enables targeted and sustained intramyocardial delivery of neuregulin, activating the cardiomyocyte cell cycle and enhancing ventricular function in a murine model of ischemic cardiomyopathy. *Circ. Heart Fail* 7, 619–626. doi: 10.1161/CIRCHEARTFAILURE.113.001273

Cui, Z., Yang, B., and Li, R.-K. (2016). Application of biomaterials in cardiac repair and regeneration. *Engineering* 2, 141–148. doi: 10.1016/J.ENG.2016.01.028

Desgres, M., and Menasché, P. (2019). Clinical translation of pluripotent stem cell therapies: challenges and considerations. *Cell. Stem Cell* 25, 594–606. doi: 10.1016/j.stem.2019.10.001

Dhingra, S., Li, P., Huang, X.-P., Guo, J., Wu, J., Mihic, A., et al. (2013). Preserving prostaglandin E2 level prevents rejection of implanted allogeneic mesenchymal stem cells and restores postinfarction ventricular function. *Circulation* 128, S69–S78. doi: 10.1161/CIRCULATIONAHA.112.000324

Edwards, B. B., Fairman, A. S., Cohen, J. E., MacArthur, J. W., Goldstone, A. B., Woo, J. B., et al. (2016). Biochemically engineered stromal cell-derived factor 1-alpha analog increases perfusion in the ischemic hind limb. *J. Vasc. Surg.* 64, 1093–1099. doi: 10.1016/j.jvs.2015.06.140

Engler, A. J., Carag-Krieger, C., Johnson, C. P., Raab, M., Tang, H.-Y., Speicher, D. W., et al. (2008). Embryonic cardiomyocytes beat best on a matrix with heart-like elasticity: scar-like rigidity inhibits beating. *J. Cell Sci.* 121, 3794–3802. doi: 10.1242/jcs.029678

Ferrini, A., Stevens, M. M., Sattler, S., and Rosenthal, N. (2019). Toward regeneration of the heart: bioengineering strategies for immunomodulation. *Front. Cardiovasc. Med.* 6:26. doi: 10.3389/fcvm.2019.00026

Gallet, R., Dawkins, J., Valle, J., Simsolo, E., de Couto, G., Middleton, R., et al. (2017). Exosomes secreted by cardiosphere-derived cells reduce scarring, attenuate adverse remodelling, and improve function in acute and chronic porcine myocardial infarction. *Eur. Heart J.* 38, 201–211. doi: 10.1093/eurheartj/ehw240

Haraguchi, Y., Kagawa, Y., Sakaguchi, K., Matsuura, K., Shimizu, T., and Okano, T. (2017). Thicker three-dimensional tissue from a "symbiotic recycling system" combining mammalian cells and algae. *Sci. Rep.* 7:41594. doi: 10.1038/srep41594

Heidenreich, P. A., Trogdon, J. G., Khavjou, O. A., Butler, J., Dracup, K., Ezekowitz, M. D., et al. (2011). Forecasting the future of cardiovascular disease in the United States: a policy statement from the American Heart Association. *Circulation* 123, 933–944. doi: 10.1161/CIR.0b013e31820a55f5

Hiesinger, W., Brukman, M. J., McCormick, R. C., Fitzpatrick, J. R., Frederick, J. R., Yang, E. C., et al. (2012). Myocardial tissue elastic properties determined by atomic force microscopy after stromal cell-derived factor 1α angiogenic therapy for acute myocardial infarction in a murine model. *J. Thorac. Cardiovasc. Surg.* 143, 962–966. doi: 10.1016/j.jtcvs.2011.12.028

Hiesinger, W., Perez-Aguilar, J. M., Atluri, P., Marotta, N. A., Frederick, J. R., Fitzpatrick, J. R., et al. (2011). Computational protein design to re-engineer stromal cell-derived factor-1α (SDF) generates an effective and translatable angiogenic polypeptide analog. *Circulation* 124, S18–S26. doi: 10.1161/CIRCULATIONAHA.110.009431

Hopfner, U., Schenck, T.-L., Chávez, M.-N., Machens, H.-G., Bohne, A.-V., Nickelsen, J., et al. (2014). Development of photosynthetic biomaterials for in vitro tissue engineering. *Acta Biomater.* 10, 2712–2717. doi: 10.1016/j.actbio.2013.12.055

Huang, K., Ozpinar, E. W., Su, T., Tang, J., Shen, D., Qiao, L., et al. (2020). An off-the-shelf artificial cardiac patch improves cardiac repair after myocardial infarction in rats and pigs. *Sci. Transl. Med.* 12:eaat9683. doi: 10.1126/scitranslmed.aat9683

Ingason, A. B., Goldstone, A. B., Paulsen, M. J., Thakore, A. D., Truong, V. N., Edwards, B. B., et al. (2018). Angiogenesis precedes cardiomyocyte migration in regenerating mammalian hearts. *J. Thorac. Cardiovasc. Surg.* 155, 1118.e1–1127.e1. doi: 10.1016/j.jtcvs.2017.08.127

Laflamme, M. A., Chen, K. Y., Naumova, A. V., Muskheli, V., Fugate, J. A., Dupras, S. K., et al. (2007). Cardiomyocytes derived from human embryonic stem cells in pro-survival factors enhance function of infarcted rat hearts. *Nat. Biotechnol.* 25, 1015–1024. doi: 10.1038/nbt1327

MacArthur, J. W., Cohen, J. E., McGarvey, J. R., Shudo, Y., Patel, J. B., Trubelja, A., et al. (2013a). Preclinical evaluation of the engineered stem cell chemokine stromal cell-derived factor 1α analog in a translational ovine myocardial infarction model. *Circ. Res.* 114, 650–659. doi: 10.1161/circresaha.114.302884

MacArthur, J. W., Trubelja, A., Shudo, Y., Hsiao, P., Fairman, A. S., Yang, E., et al. (2013b). Mathematically engineered stromal cell-derived factor-1α stem cell cytokine analog enhances mechanical properties of infarcted myocardium. *J. Thorac. Cardiovasc. Surg.* 145, 278–284. doi: 10.1016/j.jtcvs.2012.09.080

Menasché, P. (2018). Cell therapy trials for heart regeneration — lessons learned and future directions. *Nat. Rev. Cardiol.* 15, 659–671. doi: 10.1038/s41569-018-0013-0

Menasché, P., Vanneaux, V., Hagège, A., Bel, A., Cholley, B., Parouchev, A., et al. (2018). Transplantation of human embryonic stem cell–derived cardiovascular progenitors for severe ischemic left ventricular dysfunction. *J. Am. College Cardiol.* 71, 429–438. doi: 10.1016/j.jacc.2017.11.047

Mulyasasmita, W., Cai, L., Dewi, R. E., Jha, A., Ullmann, S. D., Luong, R. H., et al. (2014). Avidity-controlled hydrogels for injectable co-delivery of induced pluripotent stem cell-derived endothelial cells and growth factors. *J. Control Release* 191, 71–81. doi: 10.1016/j.jconrel.2014.05.015

Naveed, M., Han, L., Khan, G. J., Yasmeen, S., Mikrani, R., Abbas, M., et al. (2018). Cardio-supportive devices (VRD & DCC device) and patches for advanced heart failure: a review, summary of state of the art and future directions. *Biomed. Pharmacother.* 102, 41–54. doi: 10.1016/j.biopha.2018.03.049

Notari, M., Ventura-Rubio, A., Bedford-Guaus, S. J., Jorba, I., Mulero, L., Navajas, D., et al. (2018). The local microenvironment limits the regenerative potential of the mouse neonatal heart. *Sci. Adv.* 4:eaao5553. doi: 10.1126/sciadv.aao5553

Purcell, B. P., Elser, J. A., Mu, A., Margulies, K. B., and Burdick, J. A. (2012). Synergistic effects of SDF-1α chemokine and hyaluronic acid release from degradable hydrogels on directing bone marrow derived cell homing to the myocardium. *Biomaterials* 33, 7849–7857. doi: 10.1016/j.biomaterials.2012.07.005

Santoso, M. R., Ikeda, G., Tada, Y., Jung, J., Vaskova, E., Sierra, R. G., et al. (2020). Exosomes from induced pluripotent stem cell–derived cardiomyocytes promote autophagy for myocardial repair. *J. Am. Heart Assoc.* 9:e014345. doi: 10.1161/JAHA.119.014345

Schenck, T. L., Hopfner, U., Chávez, M. N., Machens, H.-G., Somlai-Schweiger, I., Giunta, R. E., et al. (2015). Photosynthetic biomaterials: a pathway towards autotrophic tissue engineering. *Acta Biomater.* 15, 39–47. doi: 10.1016/j.actbio.2014.12.012

Schoger, E., Carroll, K. J., Iyer, L. M., McAnally, J. R., Tan, W., Liu, N., et al. (2020). CRISPR-mediated activation of endogenous gene expression in the postnatal heart. *Circ. Res.* 126, 6–24. doi: 10.1161/CIRCRESAHA.118.314522

Seif-Naraghi, S. B., Singelyn, J. M., Salvatore, M. A., Osborn, K. G., Wang, J. J., Sampat, U., et al. (2013). Safety and efficacy of an injectable extracellular matrix hydrogel for treating myocardial infarction. *Sci. Transl. Med.* 5:173ra25. doi: 10.1126/scitranslmed.3005503

Serpooshan, V., Zhao, M., Metzler, S. A., Wei, K., Shah, P. B., Wang, A., et al. (2013). The effect of bioengineered acellular collagen patch on cardiac remodeling and ventricular function post myocardial infarction. *Biomaterials* 34, 9048–9055. doi: 10.1016/j.biomaterials.2013.08.017

Shudo, Y., Cohen, J. E., MacArthur, J. W., Atluri, P., Hsiao, P. F., Yang, E. C., et al. (2013). Spatially oriented, temporally sequential smooth muscle cell-endothelial progenitor Cell Bi-Level cell sheet neovascularizes ischemic myocardium. *Circulation* 128, S59–S68. doi: 10.1161/CIRCULATIONAHA.112.000293

Shudo, Y., Goldstone, A. B., Cohen, J. E., Patel, J. B., Hopkins, M. S., Steele, A. N., et al. (2017). Layered smooth muscle cell-endothelial progenitor cell sheets derived from the bone marrow augment post-infarction ventricular function. *J. Thorac. Cardiovasc. Surg.* 154, 955–963. doi: 10.1016/j.jtcvs.2017.04.081

Steele, A. N., MacArthur, J., and Woo, Y. J. (2017). Stem cell therapy: healing or hype? Why stem cell delivery doesn't work. *Circ. Res.* 120, 1868–1870. doi: 10.1161/CIRCRESAHA.117.310584

Steele, A. N., Paulsen, M. J., Wang, H., Stapleton, L. M., Lucian, H. J., Eskandari, A., et al. (2020). Multi-phase catheter-injectable hydrogel enables dual-stage protein-engineered cytokine release to mitigate adverse left ventricular remodeling following myocardial infarction in a small animal model and a large animal model. *Cytokine* 127:154974. doi: 10.1016/j.cyto.2019.154974

Terrovitis, J. V., Smith, R. R., and Marbán, E. (2010). Assessment and optimization of cell engraftment after transplantation into the heart. *Circ. Res.* 106, 479–494. doi: 10.1161/CIRCRESAHA.109.208991

Trubelja, A., MacArthur, J. W., Sarver, J. J., Cohen, J. E., Hung, G., Shudo, Y., et al. (2014). Bioengineered stromal cell-derived factor-1α analogue delivered as an angiogenic therapy significantly restores viscoelastic material properties of infarcted cardiac muscle. *J. Biomech. Eng.* 136, 0845011–0845015. doi: 10.1115/1.4027731

Vagnozzi, R. J., Maillet, M., Sargent, M. A., Khalil, H., Johansen, A. K. Z., Schwanekamp, J. A., et al. (2020). An acute immune response underlies the benefit of cardiac stem cell therapy. *Nature* 577, 405–409. doi: 10.1038/s41586-019-1802-2

von Bornstädt, D., Wang, H., Paulsen, M. J., Goldstone, A. B., Eskandari, A., Thakore, A., et al. (2018). Rapid self-assembly of bioengineered cardiovascular bypass grafts from scaffold-stabilized, tubular bi-level cell sheets. *Circulation* 138, 2130–2144. doi: 10.1161/CIRCULATIONAHA.118.035231

Wang, H., Bennett-Kennett, R., Paulsen, M. J., Hironaka, C. E., Thakore, A. D., Farry, J. M., et al. (2020a). Multiaxial lenticular stress-strain relationship of native myocardium is preserved by infarct-induced natural heart regeneration in neonatal mice. *Sci. Rep.* 10:7319. doi: 10.1038/s41598-020-63324-w

Wang, H., Paulsen, M. J., Hironaka, C. E., Shin, H. S., Farry, J. M., Thakore, A. D., et al. (2020b). Natural heart regeneration in a neonatal rat myocardial infarction model. *Cells* 9:229. doi: 10.3390/cells9010229

Wang, H., Wisneski, A., Paulsen, M. J., Imbrie-Moore, A., Wang, Z., Xuan, Y., et al. (2019a). Bioengineered analog of stromal cell-derived factor 1α preserves the biaxial mechanical properties of native myocardium after infarction. *J. Mech. Behav. Biomed. Mater.* 96, 165–171. doi: 10.1016/j.jmbbm.2019.04.014

Wang, H., Wu, M. A., and Woo, Y. J. (2019b). Photosynthetic symbiotic therapy. *Aging* 11, 843–844. doi: 10.18632/aging.101796

Yu, J. K., Sarathchandra, P., Chester, A., Yacoub, M., Brand, T., and Butcher, J. T. (2018). Cardiac regeneration following cryoinjury in the adult zebrafish targets a maturation-specific biomechanical remodeling program. *Sci. Rep.* 8:15661. doi: 10.1038/s41598-018-33994-8

Zhu, Y., Thakore, A. D., Farry, J. M., Jung, J., Anilkumar, S., Wang, H., et al. (2020). Collagen-supplemented incubation rapidly augments mechanical property of fibroblast cell sheets. *Tissue Eng. Part A*. 27, 328–335. doi: 10.1089/ten.tea.2020.0128

**Conflict of Interest:** The authors declare that the research was conducted in the absence of any commercial or financial relationships that could be construed as a potential conflict of interest.

frontiers in Bioengineering and Biotechnology

REVIEW
published: 03 June 2021
doi: 10.3389/fbioe.2021.681705

# Bioengineering Technologies for Cardiac Regenerative Medicine

*Mira Chingale[1], Dashuai Zhu[1,2], Ke Cheng[1,2]* and Ke Huang[1,2]**

[1] *Department of Molecular Biomedical Sciences and Comparative Medicine Institute, North Carolina State University, Raleigh, NC, United States,* [2] *Joint Department of Biomedical Engineering, University of North Carolina at Chapel Hill, North Carolina State University, Raleigh, NC, United States*

Cardiac regenerative medicine faces big challenges such as a lack of adult cardiac stem cells, low turnover of mature cardiomyocytes, and difficulty in therapeutic delivery to the injured heart. The interaction of bioengineering and cardiac regenerative medicine offers innovative solutions to this field. For example, cell reprogramming technology has been applied by both direct and indirect routes to generate patient-specific cardiomyocytes. Various viral and non-viral vectors have been utilized for gene editing to intervene gene expression patterns during the cardiac remodeling process. Cell-derived protein factors, exosomes, and miRNAs have been isolated and delivered through engineered particles to overcome many innate limitations of live cell therapy. Protein decoration, antibody modification, and platelet membranes have been used for targeting and precision medicine. Cardiac patches have been used for transferring therapeutics with better retention and integration. Other technologies such as 3D printing and 3D culture have been used to create replaceable cardiac tissue. In this review, we discuss recent advancements in bioengineering and biotechnologies for cardiac regenerative medicine.

**Keywords: bioengineering, cardiac repair, cell reprogramming, exosome, cardiac patch, targeting**

OPEN ACCESS

***Edited by:***
*Jianyi Zhang,*
*University of Alabama at Birmingham, United States*

***Reviewed by:***
*Lei Ye,*
*National Heart Centre Singapore, Singapore*
*Zhen Ma,*
*Syracuse University, United States*
*Shijun Hu,*
*Soochow University, China*

****Correspondence:***
*Ke Cheng*
*ke_cheng@ncsu.edu*
*Ke Huang*
*khuang7@ncsu.edu*

***Specialty section:***
*This article was submitted to Tissue Engineering and Regenerative Medicine, a section of the journal Frontiers in Bioengineering and Biotechnology*

***Received:*** *17 March 2021*
***Accepted:*** *12 April 2021*
***Published:*** *03 June 2021*

***Citation:***
*Chingale M, Zhu D, Cheng K and Huang K (2021) Bioengineering Technologies for Cardiac Regenerative Medicine. Front. Bioeng. Biotechnol. 9:681705. doi: 10.3389/fbioe.2021.681705*

## INTRODUCTION

Cardiovascular disease (CVD) is the leading cause of death in both developed and developing countries. According to the World Health Organization (WHO), 17.9 million people across the globe (31%) die due to CVD, of which 85% die from myocardial infarction (MI) (World Health Organization, 2021). In adult hearts post-MI, injured heart muscle cells are replaced by fibrotic tissue. During this maladaptive remodeling process, activated cardiac fibroblasts turn into myofibroblasts, causing stiffness and fibrosis, which is, in turn, associated with poor prognosis and heart failure. Though cardiac fibroblasts provide structural integrity to the heart after MI, it also causes a non-contracting scar. Such events hamper cardiac perfusion and pumping capacity and leads to cardiac remodeling further toward depravation to cardiac dysfunction, myocardium loss, and, eventually, heart failure (Xin et al., 2013; Saparov et al., 2017; Tallquist and Molkentin, 2017; Bo et al., 2020; Nelson and Brunt, 2021).

Conventional treatments for MI include coronary artery bypass, coronary reperfusion therapy, and fibrinolytic therapy, which are mainly for acute symptom relief rather than to promote repair and regeneration of the damaged myocardium (Awada et al., 2015). A heart transplant or a left ventricular assist device (LVAD) (Rose et al., 2001) is the final treatment option for heart failure patients. However, prognosis varies due to the complexity of the required highly invasive transplant surgery and its subsequent acute/chronic immune rejections (White and Chew, 2008;

Wilhelm, 2015). Although pharmacological treatments of β-blockers and angiotensin-converting enzyme (ACE) inhibitors (Packer et al., 2001; McMurray et al., 2014) are beneficial to MI patients, these existing approaches make it necessary to explore new methods of treatment that aim at regenerating the infarcted myocardium as well as becoming implementable in the clinical practices (Raziyeva et al., 2020).

Biomedical engineering seeks to close the gap between engineering and medicine by combining the design and problem-solving skills of engineering with medical and biological sciences. Biomedical engineering hopes to advance health care treatment, including diagnosis, monitoring, and therapy. It has been transforming the cardiac regenerative approaches into potential treatments for CVD (Lee and Walsh, 2016). Treatments for ischemic/reperfusion-damaged or infarcted myocardium have been designed by using multifarious biotechnologies based on the purpose of treatment. With the idea of using autologous cells for cardiac treatment, patient-specific cardiomyocytes (CMs) were generated through cell reprogramming technologies (Wang et al., 2021). To improve the regenerative capability of CMs, various viral and non-viral vectors have been used for gene editing to intervene with gene expression during cardiac remodeling process after MI (Rincon et al., 2015; Kohama et al., 2020). To overcome the retention, fragile, tumorigenicity, and immunogenicity limitations of cell therapy (Tang et al., 2018c), cell-derived protein factors, exosomes, and miRNAs have been isolated and delivered through micro- (Huang et al., 2020) or nanosized particles (Su et al., 2018b). For better targeting, scientists have used proteins, antibodies, and platelet membranes to decorate their therapeutics. For better retention and integration, cardiac patches have been designed by transfer therapeutics in vehicles made of various biomaterials (Mei and Cheng, 2020). Additionally, 3D printing (Maiullari et al., 2018) and 3D culture (Jackman et al., 2018) technologies were utilized to create replaceable cardiac tissue (**Figure 1** and **Table 1**). In this review, we will discuss current biotechnologies for cardiac repair.

## CELL REPROGRAMMING

Cell reprogramming is a powerful tool that converts the somatic cell lineage into pluripotent stem cells (iPSCs) (Rao and Malik, 2012), CMs (Fu et al., 2015) or endothelial cells (ECs) (Lee C. S. et al., 2017). Generally, this tool is used both *in vitro* and *in vivo* for cardiac injury site repair (Patel et al., 2016), cardiac disease modeling, or drug screening (Ebert et al., 2012; Chen and Vunjak-Novakovic, 2018). In the process of changing cell fate, an intermediary pluripotent state is key to differentiate direct and indirect reprogramming (Wang et al., 2021).

### Indirect Cell Reprogramming

Indirect cell reprogramming from adult somatic cells to iPSC-derived CMs (iPSC-CMs) is a well-established process (Tai et al., 2018). iPSCs from multiple origins are now commercially available. This reprogramming method is widely used not only due to the difficulty of culturing human primary CMs *in vitro* but also because they contain patient-specific genomic information and could be used for autologous cardiac regenerative medicine (Martins et al., 2014). Commonly, adult fibroblasts are reprogrammed into iPSCs through the activation of alkaline phosphatase, silencing of somatic-specific expression, expression of SSEA1, and progressive silencing of exogenous genes with upregulation of Oct4 and Nanog (Teshigawara et al., 2017). However, these CMs are closer to an immature stage in terms of marker expression, ultrastructural features, metabolic signature, and electrophysiological properties (Tang, 2020). First, the origin of somatic cells is a determinant of iPSC-CM maturation (Pianezzi et al., 2020). Comparison of iPSC-CMs derived from cardiac-derived mesenchymal progenitor cells (CPCs), bone marrow-derived mesenchymal stem cells (BMCs), and human dermal fibroblasts (HDFs) that comes from the same patient showed the cardiac somatic cell's enhanced capacity for cardiac re-differentiation due to upregulated cardiac genes (*MYH6, TNNI3, KCNQ1, KCNE1*) (Altomare et al., 2016; Pianezzi et al., 2020). Additionally, the application of iPSC-CMs is highly affected by the purification process because tumors can form during *in vitro* culture of iPSCs that increase the malignant risks to *in vivo* application (Tohyama et al., 2013). To overcome the purification obstacles, a distinct metabolic flow technology has been designed to enable large-scale purification through glucose depletion and lactate supplementation because the mature iPSC-CMs have a higher oxygen consumption rate with increased mitochondrial maturity (Tohyama et al., 2013; Tang, 2020).

### Direct Cell Reprogramming

Direct cell reprograming is a process of transforming of somatic cells to a desired cell fate without a pluripotent or multipotent state (Wang et al., 2021). Ideally, direct cell reprogramming is more suitable for *in vivo* cardiac tissue repair by generating reprogrammed cells *in situ* in the diseased heart (Wang et al., 2021); however, it is still challenging to perform it *in vivo* due to the low transforming efficiency. For example, direct reprogramming of transcriptional factors like Gata4, Oct4, Tbx5, Sox2, and Klf4 were delivered directly into the damaged heart to initiate regeneration (Ieda et al., 2010; Chen et al., 2017; Hashimoto et al., 2018). Six core transcriptional factors Gata4, Hand2, Mef2c, Mesp1, Nkx2.5, and Tbx5 were examined for their cardiac linage reprograming capability (Li et al., 2015; Wang et al., 2015). Retroviruses were used to express these transcription factors in fibroblasts that were derived from adult mice (Pasumarthi and Field, 2002; Ieda et al., 2010; Song et al., 2012). Another study reported *in vitro* formation of CMs from fibroblasts by expressing transcriptional factors Gata4, Mef2c, and Tbx5 (GMT) and thereby functionally repopulating the scar (Qian et al., 2012; Wang et al., 2015). Although direct cell reprogramming bypasses early developmental stages (Barreto et al., 2019) such as the cardiac progenitor stages, the tumorigenic risks may not lower than indirect reprogramming because the small molecules cannot be guaranteed, which can also produce iPSCs (Chen et al., 2017). Most importantly, the fate of transduced cells *in vivo* is still debated, although single-cell transcriptomics have been done to discover the mechanism of the fate conversion from fibroblast to CMs

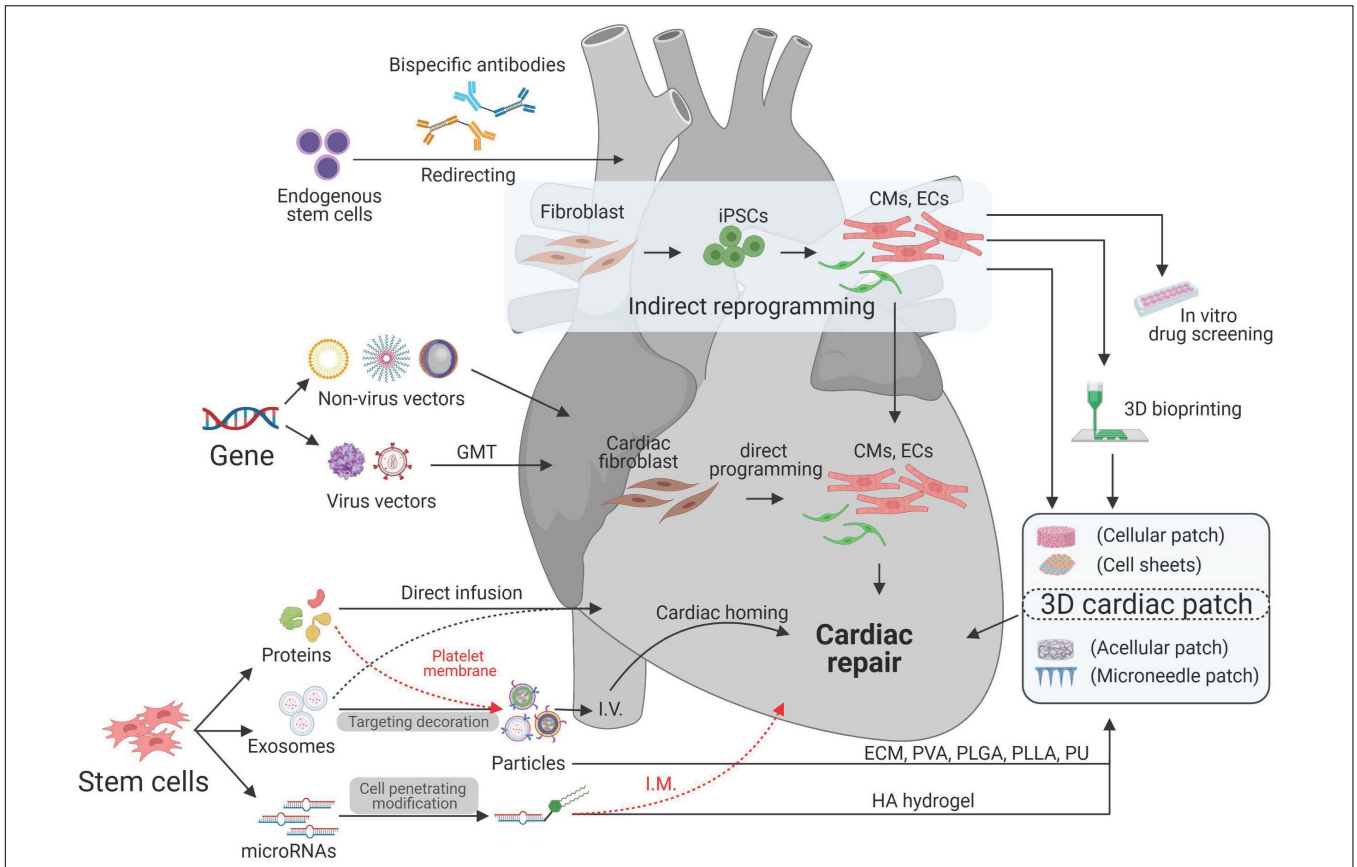


**FIGURE 1 |** Bioengineering and biotechnologies for cardiac repair.

(Liu et al., 2017). Additionally, miRNAs have the ability to regulate various signaling pathways at the same time, which makes them a promising alternative (Sandmaier and Telugu, 2015). Researchers provided evidence that direct administration of miRNAs through lipid-based transfection at the target site successfully converted fibroblasts into cardiomyocytes *in vivo* (Elmén et al., 2008; Sridharan and Plath, 2011). Cardiac reprogramming through miRNAs (miR-1 miR-133, miR208, and miR499) was enhanced when combined with JAK inhibitor I treatment (Jayawardena et al., 2012).

## GENE EDITING

Many genes are essential for CM proliferation and cardiac repair. For example, ERBB2 has been reported triggering mammalian heart regeneration by promoting cardiomyocyte dedifferentiation and proliferation through YAP activation and EMT (epithelial–mesenchymal transition)-like processes (D'Uva et al., 2015; Aharonov et al., 2020). Cyclin A2 or CCNA2, a gene normally silenced after birth, has been demonstrated as a key cell cycle regulatory gene to induce cardiac repair by mediating both the G1–S and G2–M transitions of the cell cycle (Shapiro et al., 2014). So, an efficient delivery of the desired gene to heart is important for cardiac gene therapy.

### Non-viral Gene Delivery

In cardiac gene therapy, efficient delivery of the desired gene to target tissue is important. Non-viral gene delivery methods, such as needle or jet injection, hydrodynamic gene transfer, electroporation, and cationic lipids make use of natural or synthetic compounds or physical forces to deliver the gene of interest to the target site. It is an important technology for tissue engineering with many features, including low toxicity, easy modification, high productivity, and cell specificity (Wu et al., 2018). A needleless liquid jet methodology using a jet device with micro jets has been used to expand or generate cell pores for cardiac gene delivery. However, it is not suitable for cardiac applications due to the jet's piercing with high force (Fargnoli et al., 2017). Additionally, hydrophilic naked DNA could be consumed by cells (Al-Dosari and Gao, 2009); however, only a small percentage of target cells express the delivered genes, thus, making them inefficient.

### Viral Gene Delivery

Recombinant viral vectors such as adenoviruses, lentiviruses, and adeno-associated viruses are generally used for gene delivery (Wolfram and Donahue, 2013). Adenoviral gene delivery systems have been extensively used in gene-based therapies and cell-based therapies. Adenoviral vectors have shown a

**TABLE 1 |** Summarization of advantages and disadvantages in different bioengineering methods.

| Bioengineered methods | Advantages | Disadvantages |
|---|---|---|
| Direct cell reprogramming | • Needs no iPSC stage<br>• Possibility for *in situ* reprogramming<br>• Relatively rapid conversion | • Low efficiency<br>• Unclear cell fate stability<br>• Tumorigenicity risks |
| Indirect cell reprogramming | • High efficiency<br>• iPSC induction from many cell types<br>• Self-renewal of iPSCs<br>• Differentiation condition is modulable<br>• Cell fate stability<br>• Suitable for *ex vivo* manipulations | • Requires iPSC stage<br>• Only can be performed *in vitro*<br>• The CMs are not mature<br>• Tumorigenicity risks |
| Non-viral gene delivery | • Non-pathogenic<br>• Multiple delivery methods. e.g., Naked DNA direct delivery, gene gun, electroporation, ultrasound, lipoplexes and polyplexes etc.<br>• Simplicity in manufacturing<br>• Flexibility in packaging capacity | • Low transduction efficiency<br>• Cytotoxicity<br>• Transient transfection<br>• Tissue damage<br>• Shallow penetration<br>• Immunogenicity |
| Viral gene delivery | • High transduction efficiency<br>• Transient or persistent expression<br>• Multiple viral vector choices | • Difficult to produce high viral titers<br>• Immunogenicity<br>• Limitations in gene packaging capacity<br>• Safety issues<br>• Expensive<br>• |
| Synthetic particles | • High biocompatibility<br>• Cryo-stability<br>• Easy manipulation of particle contents<br>• Cardiac targeting can be achieved<br>• Degradable<br>• Multiple delivery routes<br>• Controlled release of therapeutics | • Hard to control the size and morphology<br>• Requires multiple fabrication steps<br>• Low encapsulation efficiency<br>• Sensitive to operational parameters<br>• Mostly paracrine effects, lack of mechanism to generate new CMs |
| Natural particles (extracellular vesicles and exosomes) | • High biocompatibility<br>• Low immunogenicity<br>• Low tumorigeneicity<br>• Long term stability | • Quality depending on cell batches and culture condition<br>• Variation in batches<br>• Low yield and purity<br>• Difficulty in isolation |
| Non-cellular cardiac patches | • Multiple biomaterial selections<br>• High biocompatibility<br>• Easy manufacturing and off-the-shelf<br>• Suitable for large amount of cargo delivery<br>• Easy storage and transfer | • Hard to transplant *in vivo* (open-chest surgery is required)<br>• Low cardiac integration<br>• Low cardiac penetration<br>• |
| Cellular cardiac patches | • Highly biocompatible<br>• Highly functional<br>• Suitable for both *in vivo* and *in vitro* studies<br>• Multiple designs | • Tumorigenicity<br>• The maturation of CMs in tissue patch<br>• Hard to manufacture<br>• Batch-to-batch variation (depending on cell quality)<br>• Very fragile and hard to transfer or storage<br>• Low vascularization after transplantation<br>• Arrhythmia risks after transplantation |

high transduction rate in both dividing and non-dividing cells (Lee S. et al., 2017). The knockdown of lncRNA through adenovirus-mediated lncRNA approaches lead to the reduction in macrophage infiltration and cardiomyocyte apoptosis in the heart after MI (Wang K. et al., 2017). Although adenovirus vectors were used in clinical trials due to their large tropism profile (Jessup et al., 2011), adenoviral-mediated gene delivery triggers immunogenicity in humans and lacks integration with the host genome, making it an unfavorable choice (Vilaysane and Muruve, 2009; Wasala et al., 2011). Lentiviral vectors are suitable for long-term transgene expression, which integrates their genome into the hosts with a preference for transcriptionally active sites (Bulcha et al., 2021). Lentiviral vectors can also elicit relatively weak immune responses through vector design (Bulcha et al., 2021). Lentiviral-mediated CCND2 gene transfection enhanced the regenerative potency of iPSCs-CMs (Zhu et al., 2018). Additionally, enhanced expression of Gata-4 and Nkz2.5 by lentiviral-mediated prodynorphin vectors resulted in a drastic increase in the CMs' beating activity (Rincon et al., 2015). However, lentiviral vectors are limiting for cardiovascular disease treatments due to their low transduction rate in the myocardium *in vivo* (Rincon et al., 2015). The adeno-associated virus (AVV), as a cardiotropic vector, can be designed as a viral therapeutic to promote cardiac repair after MI (Yoo et al., 2018). AAV6 was reported as the most effective vector to transduce CMs (Ambrosi et al., 2019). For example, AAV6 was designed

to deliver miR-199a to a pig model of MI (Gabisonia et al., 2019). Although the results showed cardiac improvement after 1 month, all pigs died due to subsequent uncontrolled expression of miR-199a that resulted in sudden arrhythmia.

## PARTICLE DESIGN

Stem cell therapy has been a promising approach mediated through paracrine effects (Maghin et al., 2020; Sid-Otmane et al., 2020). However, engraftment of transplanted cells and their low retention limit its therapeutic efficacy. Also, other concerns such as tumorigenicity, immunogenicity, and product stability need to be taken into account (Tang et al., 2018c). Since stem cells secrete a plethora of molecules like cytokines, soluble proteins, and extracellular vesicles that help in cardiac repair and regeneration (Tao et al., 2018), analysis of the cell secretome has gained importance in elucidating therapeutic mechanisms (Ellison-Hughes and Madeddu, 2017).

### Synthetic Particles

Micro-sized synthetic stem cells (SSCs) have been fabricated to mimic the paracrine effects of a live cell through a cell-mimicking microparticle (CMMP) technology (Tang et al., 2017; Huang et al., 2020). Briefly, poly lactic-co-glycolic acid (PLGA) is used to encapsulate the stem cell-derived secretomes. Afterward, microparticles are coated with cell membranes to become SSCs (Tang et al., 2017). This technology not only overcomes the multiple inherent limitations of live-cell therapy (Huang et al., 2020) but also holds a high applicability for different cell lines, for example, both cardiac stromal cells (CSCs) and mesenchymal stem cells (MSCs) have been synthetically created (Luo et al., 2017; Tang et al., 2017; Huang et al., 2020). Additionally, to transfer miR21 into macrophages and ECs, positively charged mesoporous silica nanoparticles (MSNs) are designed to encapsulate miR21 and are injected into the ischemic heart of pigs for treatment (Li Y. et al., 2021). MSNs are reported as a highly biocompatible and transfection-effective nanoparticle that are generated through a classical CTAB-templated, base-catalyzed sol–gel method (Li Y. et al., 2021). These microparticles exert their beneficial effects mainly through mimicking cell paracrine of protein factors and membrane-based cell–cell interaction with injured cells (Luo et al., 2017; Tang et al., 2017). Also, the nanoparticles that are consumed by CMs and fibroblasts release the enveloped miRNAs and proteins to regulate gene expression (Hodgkinson et al., 2015). To fully understand the mechanism, the combination of cell secretomes have to be further studied because the cardiac beneficial results may come from the combination or any of the secretome contents, including miRNAs, protein factors, exosomes, extracellular vesicles, and so on. Moreover, cell secretome is not standardized due to the variation of cell lines, culture conditions, and purity, which makes it even harder to uncover the veil of cell therapy.

### Natural Particles

Exosomes, a type of EVs, are bilipid layered nanovesicles with a diameter of around 35–150 nm that carry encapsulated proteins, membrane-bound proteins, and miRNAs and are capable of triggering various complex function-altering pathways (Li et al., 2017; Sun et al., 2018). Their small size allows them to pass through small capillaries, giving them more access to tissues than transplanted cells (Verweij et al., 2019; Dinh et al., 2020). Exosomes can be extracted and purified through techniques such as immunoaffinity capture, polymeric precipitation, tangential flow ultracentrifugation and size exclusion. Exosomes isolated from several cell lines including MSCs (Huang P. et al., 2019; Hu et al., 2021), iPSCs (Gao et al., 2020), cardiosphere-derived cells (CDCs) (Vandergriff et al., 2015; Gallet et al., 2017), and CPCs (Barile et al., 2017) have demonstrated cardiac protection through neovascularization and anti-inflammation (Teng et al., 2015; Huang P. et al., 2019). MSC-derived exosomes also contain miRNAs (miR-30b, let-7f, miR-424, and miR-30c) that promote angiogenesis For example, MSC-derived exosomal miR-21-5p heightens cardiac contractile strength and calcium handling through PI3K signaling (Mayourian et al., 2018; Qiao et al., 2019).

## CARDIAC TARGETING

Heart stem cell therapy is usually administered intramyocardially *via* open-chest or percutaneous coronary intervention (PCI) (Malliaras and Marbán, 2011). As the invasive nature of this drug delivery is not effective and appealing, researchers focus on developing therapeutics with targeting ability to the injured myocardium. This concept allows drugs to interact specifically with the infracted region and impart therapeutic benefits. Various targeting strategies, such as cardiotropic vector selection, peptide decoration, magnetic reactive carrier, or antibody editing have been employed for efficient drug delivery (Cores et al., 2015; Weinberger and Eschenhagen, 2021).

### Cardiotropic Vector Selection

Cardiac gene therapy requires viral vectors to safely access the heart specifically. So, it is essential to find a cardiotropic vector for gene delivery. For example, although multiple strains of AAVs from serotypes 1 to 9 have been isolated, only AAV9 (Inagaki et al., 2006) and AAV6 (Bish et al., 2008; Gao et al., 2011) showed a higher transduction efficiency. However, these vectors require intrapericardial or intramyocardial administration. Since there is a difference in host specificity (Asokan and Samulski, 2013), it is even harder to evaluate AAV vectors in preclinical models and clinical translation.

### Peptide Targeting

Peptide-based targeting has been achieved by decorating peptide (Kanki et al., 2011) onto therapeutics. A 12-amino acid non-naturally occurring peptide NH2-APWHLSSQYSRT-COOH was reported as a cardiomyocyte-targeting peptide (Feldman and Zahid, 2020). The peptide motif CSTSMLKAC was also identified as a potential tool for heart homing (Shelke et al., 2008; Kanki et al., 2011). For example, CDC-derived exosomes were designed to target the heart injury site *via* cardiac homing peptide CSTSMLKAC through a dioleoylphosphatidylethanolamine *N*-hydroxysuccinimide (DOPE-NHS) linker on the exosomal

membrane (Shelke et al., 2008). Since the prostaglandin E2 (PGE2) receptors are overexpressed in the pathological cardiac microenvironment after ischemic/reperfusion injury (Kim et al., 2008; Zhang et al., 2015), researchers decorated PGE2 on nanoparticles through EDC/NHS coupling chemistry to increase cardiac homing capability (Su et al., 2018b).

### Platelet Targeting

Platelet-based targeting has been designed based on the inherent properties of platelets. Platelet surface receptors such as the GPIb/IX/V complex, GPVI and α2β1, β1, and β3 integrins, are responsible for interactions with exposed injury sites (Li et al., 2018). The platelet membrane has been isolated and coated on either cell (Shen et al., 2016; Tang et al., 2018a), micro- (Li et al., 2020) or nano- (Su et al., 2018b) particles to endow cardiac injury site homing capability (Li et al., 2018). To increase targeting and cellular uptake of nanoparticles on coronary artery stents, scientists activated ECs through binding P-selectin to platelet glycoprotein Ibα (GP Ibα) on platelet-mimicking nanoparticles (Lin et al., 2010).

### Antibody Targeting

There are many cardiac targeting approaches designed to utilize the innate specific binding capability of antibodies. Bispecific antibodies (BsAbs) have been designed to bind two different targets simultaneously by combining variable domains of desired monoclonal antibodies into an integrated structure (Huang et al., 2019a). BsAbs are generated by chemical conjugation, hybridoma fusion, or genetic engineering such as recombinant DNA technology (Parashar et al., 2011). To redirect endogenous bone marrow stem cells (BMSCs) to the injured heart, BsAbs were designed to link F(ab′)2 fragments from monoclonal anti-CD34 and anti-cardiac myosin heavy chain through chemical cycloaddition of AZ-PEG-NHS or DBCO-PEG-NHS on those F(ab′)2 fragments (Huang et al., 2019b). In this study, after G-CSF stimulation, the administration of BsAbs redirected circulating BMSCs to the injured myocardium (Huang et al., 2019b). Additionally, an inhalable platelet-targeting bispecific antibody (PT-BsAb) was designed by linking of CD34 (HSC binding) and CD42b (platelet binding) to redirect stem cells from the lungs to the heart for repair (Liu M. et al., 2021).

To increase the targeting capability of the injury site, a poly (*N*-isopropylacrylamide) nanogel with tissue plasminogen activator (tPA) and cell contractility inhibitor Y-27632 coupled anti-fibrin antibodies on the outside of nanoparticles through an EDC/sulfo-NHA method (Mihalko et al., 2018). The injected nanoparticles were directed by anti-fibrin antibodies to the fibrin-rich site post-MI and released tPA and Y-27632 to the site of injury (Mihalko et al., 2018; Huang et al., 2019b). Besides targeting, antibodies were also decorated on platelet-inspired cardiac-targeting microparticles to neutralize inflammatory cytokines. For example, since IL-1β has been demonstrated as a primary pro-inflammatory cytokine during cardiac remodeling, IL-1β antibodies were linked to platelet membrane on microparticles through 1,2-distearoyl-sn-glycero-3-phosphoethanolamine-poly (ethylene glycol) (DSPE-PEG) (Li et al., 2020).

## CARDIAC PATCH DESIGN

Cardiac patches have been devised to ameliorate the cardiac function post-MI (Mei and Cheng, 2020). A cardiac patch is typically composed of substrate and active therapeutic agents (Yang et al., 2013). Cardiac patches can have therapeutic ingredients ranging from cells, such as iPSCs, myoblasts and MSCs, to bioactive molecules, such as miRNAs, exosomes, and microparticles (Mei et al., 2010; Squillaro et al., 2016; Wang L. L. et al., 2017; Giacomelli et al., 2020).

### Cellular to Non-cellular Patches

Cell-based cardiac patches have been designed to increase the survival ratio of the embedded cells and to ensure cellular retention (Braunwald, 2018; Zhu et al., 2021). For example, a recently developed cardiac patch fabricated with biomimetic microvessels and CSCs in fibrin gel enhanced angiogenesis, CSC retention, and survival rate after heart transplantation (Gao et al., 2018; Su et al., 2018a). Furthermore, non-cellular cardiac patches have been designed to overcome the limitations of live cellular cardiac patches (Tang et al., 2018b; Li Z. et al., 2021). For example, a specific miRNA patch was designed to modulate gene expression during cardiac remodeling (Wang L. L. et al., 2017). For miR-302 cardiac delivery, researchers designed a system by using a cholesterol molecule to decorate miR-302 mimics and using adamantane or cyclodextrin to modify hydrogels. Since the modified hydrogel showed self-assembly into shear-thinning and self-healing gels, the cholesterol on miR-302 mimics interacts with cyclodextrin to achieve sustained release (Wang L. L. et al., 2017; Huang et al., 2019a). To enhance clinical feasibility, an off-the-shelf cardiac patch was designed by embedding synthetic cardiac stromal cells into a decellularized extracellular matrix through a vacuum filtration method (Huang et al., 2020). In addition, exosomes derived from MSCs were integrated into hydrogels, providing a minimally invasive delivery method through intrapericardial injection. This injectable patch revolutionized the delivery of cardiac patches, which normally needs a traumatic open-chest surgery (Zhu and Cheng, 2021; Zhu et al., 2021).

### Tissue Patches

Cardiac tissue patch is one important type of cell-based patches that has been created by culture of embryonic stem cell-derived cardiomyocytes (ESC-CMs) (Chong et al., 2014), iPSC-CMs, or neonatal rodent cardiomyocytes (NRCMs) into a 3D scaffold to form a functional 3D structure (Pomeroy et al., 2020). For example, cardiac tissue patches cultured with multiple layers of iPSC-CMs or NRCMs within hydrogels or other porous polymer scaffolds form a randomly oriented and electromechanically integrated cardiac tissue patch (Shadrin et al., 2017; Pomeroy et al., 2020). In a window chamber model and a rodent MI model, the iPSC-CM 3D cardiac patch showed a preserved structure, electrical function, and successful vascularization (Shadrin et al., 2017; Cui et al., 2020). Implantation of this engineered cardiac tissue patch to the injured heart *in vivo* showed improved vascularization in the infarct region and reduced fibrosis (Wendel

et al., 2014; Iseoka et al., 2018) (Uygun et al., 2010; Dvir et al., 2011; Fleischer et al., 2017).

3D bioprinting enables the production of 3D tissue constructs with precise architecture and integration of various cell types. The microenvironment of printed tissue accurately resembles native conditions, which, in turn, helps promote complex tissue formation *in vitro* (Gu et al., 2020). Different cellular techniques such as inkjet, stereolithography, and extrusion bioprinting are used for the development of cardiovascular tissues (Jana and Lerman, 2015; Duan, 2017). Common cell types used for cardiac tissue printing include MSCs, CSCs, ESCs, iPSCs, and cardiac fibroblasts (Cui et al., 2017). The laser-induced transfer (LIFT)-based cell bioprinting has been used to fabricate EC- and MSC-laden polyester urethane urea (PEUU) cardiac patches (Cui et al., 2018). When compared with non-patterned cardiac patches, patterned patches increased angiogenesis in the border zone of the infarction, as well as preservation of cardiac function after acute MI (Shengjie et al., 2009). 3D bioprinting could facilitate the development of the therapeutic potential of stem cells, which would play an important role in regenerative medicine (Wang et al., 2018; Pomeroy et al., 2020).

## CONCLUSION AND FUTURE DIRECTIONS

Cellular reprogramming is a new paradigm in cell biology and provides a unique and efficient way to generate cell types of interest for cardiac repair by changing one cell fate to another (Wang et al., 2021). Usually, the indirect reprogramming routes require an *in vitro* engineered 3D tissue and then transplant *in vivo* (Querdel et al., 2021). The direct reprogramming bypass early developmental stages and administer the cardiac transcriptional factors directly by viral vectors. From a translational perspective, the technology of direct reprogramming holds great potential as a treatment due to its features including fast turnaround time and feasibility for *in vivo* applications (Wang et al., 2021). However, a large scale of somatic cells could be converted through indirect preprogramming to create a paradigm for *in vitro* CRISPR–Cas9 screening, drug screening, and disease modeling (Wang et al., 2021). Although cell reprogramming showed a potential strategy for the cardiac repair, there are few advantages and disadvantages in both reprogramming routes. Direct reprogramming rarely produces beating CMs after a long culture period (Fu et al., 2013; Nam et al., 2013). In comparison, indirect reprogramming is robust to produce beating CMs that are not in a mature stage. In addition, indirect reprogramming achieves a high conversion efficiency around 70 to even 90% (Pomeroy et al., 2020); however, direct reprogramming has a low conversion efficiency (4.8%) (Engel and Ardehali, 2018) due to the presence of epigenetic barriers such as Bmi1 (Zhou et al., 2016). This low conversion efficiency remains a major hurdle for direct reprogramming, and even the process was already improved by administering cardiac transcriptional factors along with epigenetic modifiers, inhibitors, cytokines, and miRNAs (Engel and Ardehali, 2018).

The goal of gene therapy for cardiac repair is to modify a gene or genetic pathway. Safety and efficacy are important to develop tolerance and ease administration that may be translated to the clinic (Wolfram and Donahue, 2013). For example, adenoviral vectors may trigger acute inflammation, which impacts gene transfer efficacy and may cause host morbidity (Liu and Muruve, 2003). Also, gene delivery through the myocardium or coronary injections has a low cardiac transfection outcome due to the neutralization by existing endogenous antibodies (Jessup et al., 2011). As previously mentioned, long-term expression of target genes may also cause sudden death in pig studies (Gabisonia et al., 2019).

Different types of stem cells have been studied as potential candidates for cardiac regenerative medicine. However, live stem cell delivery has many inherent limitations such as tumorigenicity, immunogenicity, cell death, and low retention after transplantation (Tang et al., 2018c). So, multiple cell-derived secretomes, exosomes, and miRNAs have been engineered as alternatives for heart repair by mimicking paracrine effects of the cell or manipulating gene expression during cardiac remodeling after MI. These cell-derived therapeutics have been combined with different biomaterials to overcome the limitations of low cardiac engraftment/retention, low miRNA stability, and delivery difficulties (Huang et al., 2019a).

Non-targeted cardiac therapeutics with an intravenous delivery usually affects multiple systems, which may cause systemic side effects. Targeted therapeutics, on the other hand, are designed for precise cardiac treatment with one or multiple intravenous injections. The targeting technology is achieved mainly through decorating a cardiac homing molecule on nanosized particles, which are safe in circulation with minimal chance of stimulating coagulations (Dobrovolskaia et al., 2009). Additionally, endogenous stem cells may be stimulated and redirected by BsAbs (Huang et al., 2019b; Liu M. et al., 2021). However, all targeting methods have to be further studied due to the low targeting capability and treatment efficacy.

3D cardiac patches are a promising method in cardiac repair and are either cellular or non-cellular. The cellular patches are generated through seeding of different live cells into various 3D scaffolds. To enhance the survival of the transplanted live cells, the patches have been engineered with mimetic blood vessels (Su et al., 2018a, 2020) or cocultured with ECs (Shadrin et al., 2017). For better integration, the scaffold has been engineered with microneedles (Tang et al., 2018b). Additionally, researchers have manipulated cell growth and differentiation conditions through culture medium optimization to enhance the maturity of iPSC-CMs on tissue patches (Machiraju and Greenway, 2019). Non-cellular patches are generated by seeding different cell derivatives into various 3D scaffolds. Compared with cellular cardiac patches, these patches have better stability, biocompatibility, modifiability, and low tumorigenicity and immunogenicity. 3D bioprinting technology has been widely utilized in cardiac repair by integrating biomaterials with different cell types to precisely pattern a cardiac structure (Liu N. et al., 2021). However, this technology is still in the early stage and needs to be improved (Liu N. et al., 2021).

Additional biotechnologies not mentioned in this review such as cardiac spheroids, single ventricles, bundles, regenerative gene expression, and design of biomaterials also play an important role in the field. Although there are plenty of technologies, it is not easy to get past the bottleneck of heart regenerative medicine, for example, the maturity of iPSC-CMs, the optimized cell protein factor combination, the detailed miRNA regulation mechanism, the key gene for cardiomyocyte regeneration, creation of large-sized cardiac tissue (Gao et al., 2018), and control of drug delivery-caused trauma. To overcome these obstacles, future interdisciplinary cooperation will be the key in the research area. For example, engineering of an injectable material that have controlled gelation speed, biocompatibility, degradative ability, and temperature sensitivity will be essential to create an injectable cardiac patch. Also, screening and designing of cardiotropic viral vectors through structure evolution of capsid variants (Tse et al., 2017) would enhance cardiac gene therapy. Moreover, natural exosomes are not clinically feasible due to many inherent limitations that could be overcome through cell-based pre-isolation exosome engineering and post-isolation exosome engineering (Huang P. et al., 2019; Jafari et al., 2020). Although mainly practiced in research labs today, innovative experimental bioengineering technologies will revolutionize heart repair field in the future.

## AUTHOR CONTRIBUTIONS

MC, DZ, and KH wrote the text of this review article with guidance from KC and KH. All authors have reviewed the final version and approved the content in this manuscript.

## FUNDING

This work was supported by grants from the National Institutes of Health (R01 HL123920, HL137093, HL144002, HL146153, and HL147357 to KC) and the American Heart Association (18TPA34230092 and 19EIA34660286 to KC).

## REFERENCES

Aharonov, A., Shakked, A., Umansky, K. B., Savidor, A., Genzelinakh, A., Kain, D., et al. (2020). ERBB2 drives YAP activation and EMT-like processes during cardiac regeneration. *Nat. Cell Biol.* 22, 1346–1356. doi: 10.1038/s41556-020-00588-4

Al-Dosari, M. S., and Gao, X. (2009). Nonviral gene delivery: principle, limitations, and recent progress. *AAPS J.* 11, 671–681.

Altomare, C., Pianezzi, E., Cervio, E., Bolis, S., Biemmi, V., Benzoni, P., et al. (2016). Human-induced pluripotent stem cell-derived cardiomyocytes from cardiac progenitor cells: effects of selective ion channel blockade. *Europace* 18(Suppl. 4), iv67–iv76.

Ambrosi, C. M., Sadananda, G., Han, J. L., and Entcheva, E. (2019). Adeno-associated virus mediated gene delivery: implications for scalable in vitro and in vivo cardiac optogenetic models. *Front. Physiol.* 10:168. doi: 10.3389/fphys.2019.00168

Asokan, A., and Samulski, R. J. (2013). An emerging adeno-associated viral vector pipeline for cardiac gene therapy. *Hum. Gene Ther.* 24, 906–913. doi: 10.1089/hum.2013.2515

Awada, H. K., Hwang, M. P., and Wang, Y. (2015). Towards comprehensive cardiac repair and regeneration after myocardial infarction: aspects to consider and proteins to deliver. *Biomaterials* 82, 94–112. doi: 10.1016/j.biomaterials.2015.12.025

Barile, L., Moccetti, T., Marbán, E., and Vassalli, G. (2017). Roles of exosomes in cardio protection. *Eur. Heart J.* 38, 1372–1379.

Barreto, S., Hamel, L., Schiatti, T., Yang, Y., and George, V. (2019). Cardiac progenitor cells from stem cells: learning from genetics and biomaterials. *Cells* 8:1536. doi: 10.3390/cells8121536

Bish, L. T., Sleeper, M. M., Brainard, B., Cole, S., Russell, N., Withnall, E., et al. (2008). Percutaneous trans endocardial delivery of self-complementary adeno-associated virus 6 achieves global cardiac gene transfer in Canines. *Mol. Ther.* 16, 1953–1959. doi: 10.1038/mt.2008.202

Bo, B., Zhou, Y., Zheng, Q., Wang, G., Zhou, K., and Wei, J. (2020). The molecular mechanisms associated with aerobic exercise-induced cardiac regeneration. *Biomolecules* 11:19. doi: 10.3390/biom11010019

Braunwald, E. (2018). Cell-based therapy in cardiac regeneration: an overview. *Circ. Res.* 123, 132–137. doi: 10.1161/circresaha.118.313484

Bulcha, J. T., Wang, Y., Ma, H., Tai, P. W. L., Gao, G. (2021). Viral vector platforms within the gene therapy landscape. *Signal Transduct. Target Ther.* 6:53.

Chen, T., and Vunjak-Novakovic, G. (2018). In vitro models of ischemia-reperfusion injury. *Regen. Eng. Transl. Med.* 4 142–153.

Chen, Y., Yang, Z., Zhao, Z.-A., and Shen, Z. (2017). Direct reprogramming of fibroblasts into cardiomyocytes. *Stem Cell Res. Ther.* 8:118.

Chong, J. J. H., Yang, X., Don, C. W., Minami, E., Liu, Y.-W., Weyers, J. J., et al. (2014). Human embryonic-stem-cell-derived cardiomyocytes regenerate non-human primate hearts. *Nature* 510:273.

Cores, J., Caranasos, G. T., and Cheng, K. (2015). Magnetically targeted stem cell delivery for regenerative medicine. *J. Funct. Biomater.* 6, 526–546. doi: 10.3390/jfb6030526

Cui, H., Liu, C., Esworthy, T., Huang, Y., Yu, Z. X., Zhou, X., et al. (2020). 4D physiologically adaptable cardiac patch: a 4-month in vivo study for the treatment of myocardial infarction. *Sci Adv.* 6:eabb5067. doi: 10.1126/sciadv.abb5067

Cui, H., Miao, S., Esworthy, T., Zhou, X., Lee, S.-J., Liu, C., et al. (2018). 3D bioprinting for cardiovascular regeneration and pharmacology. *Adv. Drug Deliv. Rev.* 132, 252–269.

Cui, H., Nowicki, M., Fisher, J. P., and Zhang, L. G. (2017). 3D bioprinting for organ regeneration. *Adv Healthc Mater.* 6:10.1002/adhm.201601118 doi: 10.1002/adhm.201601118

Dinh, P. U. C., Paudel, D., Brochu, H., et al. (2020). Inhalation of lung spheroid cell secretome and exosomes promotes lung repair in pulmonary fibrosis. *Nat. Commun.* 11:1064.

Dobrovolskaia, M. A., Patri, A. K., Zheng, J., Clogston, J. D., Ayub, N., Aggarwal, P., et al. (2009). Interaction of colloidal gold nanoparticles with human blood: effects on particle size and analysis of plasma protein binding profiles. *Nanomedicine* 5, 106–117. doi: 10.1016/j.nano.2008.08.001

Duan, B. (2017). State-of-the-art review of 3D bioprinting for cardiovascular tissue engineering. *Ann. Biomed. Eng.* 45, 195–209. doi: 10.1007/s10439-016-1607-5

D'Uva, G., Aharonov, A., Lauriola, M., Kain, D., Yahalom-Ronen, Y., Carvalho, S., et al. (2015). ERBB2 triggers mammalian heart regeneration by promoting cardiomyocyte dedifferentiation and proliferation. *Nat. Cell Biol.* 17, 627–638. doi: 10.1038/ncb3149

Dvir, T., Timko, B. P., Kohane, D. S., and Langer, R. (2011). Nanotechnological strategies for engineering complex tissues. *Nat. Nanotechnol.* 6, 13–22. doi: 10.1038/nnano.2010.246

Ebert, A. D., Liang, P., and Wu, J. C. (2012). Induced pluripotent stem cells as a disease modeling and drug screening platform. *J. Cardiovasc. Pharmacol.* 60, 408–416. doi: 10.1097/fjc.0b013e318247f642

Ellison-Hughes, G. M., and Madeddu, P. (2017). Exploring pericyte and cardiac stem cell secretome unveils new tactics for drug discovery. *Pharmacol. Ther.* 171, 1–12. doi: 10.1016/j.pharmthera.2016.11.007

Elmén, J., Lindow, M., Schütz, S., Lawrence, M., Petri, A., Obad, S., et al. (2008). LNA-mediated microRNA silencing in non-human primates. *Nature* 452, 896–899. doi: 10.1038/nature06783

Engel, J. L., and Ardehali, R. (2018). Direct cardiac reprogramming: progress and promise. *Stem Cells Int.* 2018:1435746.

Fargnoli, A. S., Katz, M. G., and Bridges, C. R. (2017). A needleless liquid jet injection delivery approach for cardiac gene therapy. *Methods Mol. Biol.* 1521, 219–226. doi: 10.1007/978-1-4939-6588-5_15

Feldman, K. S., and Zahid, M. (2020). In Vivo imaging of transduction efficiencies of cardiac targeting peptide. *J. Vis. Exp.* 11:160.

Fleischer, S., Feiner, R., and Dvir, T. (2017). Cutting-edge platforms in cardiac tissue engineering. *Curr. Opin. Biotechnol.* 47, 23–29. doi: 10.1016/j.copbio.2017.05.008

Fu, J.-D., Stone, N. R., Liu, L., Spencer, C. I., Qian, L., Hayashi, Y., et al. (2013). Direct reprogramming of human fibroblasts toward a cardiomyocyte-like state. *Stem Cell Rep.* 1, 235–247. doi: 10.1016/j.stemcr.2013.07.005

Fu, Y., Huang, C., Xu, X., Gu, H., Ye, Y., Jiang, C., et al. (2015). Direct reprogramming of mouse fibroblasts into cardiomyocytes with chemical cocktails. *Cell Res.* 25, 1013–1024. doi: 10.1038/cr.2015.99

Gabisonia, K., Prosdocimo, G., Aquaro, G. D., Carlucci, L., Zentilin, L., Secco, I., et al. (2019). MicroRNA therapy stimulates uncontrolled cardiac repair after myocardial infarction in pigs. *Nature* 569, 418–422. doi: 10.1038/s41586-019-1191-6

Gallet, R., Dawkins, J., Valle, J., Simsolo, E., de Couto, G., Middleton, R., et al. (2017). Exosomes secreted by cardiosphere-derived cells reduce scarring, attenuate adverse remodeling, and improve function in acute and chronic porcine myocardial infarction. *Eur. Heart J.* 38, 201–211.

Gao, G., Bish, L. T., Sleeper, M. M., Mu, X., Sun, L., Lou, Y., et al. (2011). Trans endocardial delivery of AAV6 results in highly efficient and global cardiac gene transfer in *Rhesus Macaques*. *Hum. Gene Ther.* 22, 979–984. doi: 10.1089/hum.2011.042

Gao, L., Gregorich, Z. R., Zhu, W., Mattapally, S., Oduk, Y., Lou, X., et al. (2018). Large cardiac muscle patches engineered from human induced-pluripotent stem cell–derived cardiac cells improve recovery from myocardial infarction in swine. *Circulation* 137, 1712–1730. doi: 10.1161/circulationaha.117.030785

Gao, L., Wang, L., Wei, Y., Krishnamurthy, P., Walcott, G. P., Menasché, P., et al. (2020). Exosomes secreted by hiPSC-derived cardiac cells improve recovery from myocardial infarction in swine. *Sci. Transl. Med.* 12:eaay1318. doi: 10.1126/scitranslmed.aay1318

Giacomelli, E., Meraviglia, V., Campostrini, G., Cochrane, A., Cao, X., van Helden, R. W. J., et al. (2020). Human-iPSC-derived cardiac stromal cells enhance maturation in 3D cardiac microtissues and reveal non-cardiomyocyte contributions to heart disease. *Cell Stem Cell* 26, 862.e11–879.e11.

Gu, Z., Fu, J., Lin, H., and He, Y. (2020). Development of 3D bioprinting: from printing methods to biomedical applications. *Asian J. Pharm. Sci.* 15, 529–557. doi: 10.1016/j.ajps.2019.11.003

Hashimoto, H., Olson, E. N., and Bassel-Duby, R. (2018). Therapeutic approaches for cardiac regeneration and repair. *Nat. Rev. Cardiol.* 15, 585–600. doi: 10.1038/s41569-018-0036-6

Hodgkinson, C. P., Kang, M. H., Dal-Pra, S., Mirotsou, M., and Dzau, V. J. (2015). MicroRNAs and cardiac regeneration. *Circ. Res.* 116, 1700–1711.

Hu, S., Li, Z., Shen, D., Zhu, D., Huang, K., Su, T., et al. (2021). Exosome-eluting stents for vascular healing after ischaemic injury. *Nat. Biomed. Eng.* doi: 10.1038/s41551-021-00705-0

Huang, K., Hu, S., and Cheng, K. (2019a). A new era of cardiac cell therapy: opportunities and challenges. *Adv. Healthcare Mater.* 8, 1–18. doi: 10.1111/nph.13457

Huang, K., Li, Z., Su, T., Shen, D., Hu, S., and Cheng, K. (2019b). Bispecific antibody therapy for effective cardiac repair through redirection of endogenous stem cells. *Adv. Ther.* 2:1900009. doi: 10.1002/adtp.201900009

Huang, K., Ozpinar, E. W., Su, T., Tang, J., Shen, D., Qiao, L., et al. (2020). An off-the-shelf artificial cardiac patch improves cardiac repair after myocardial infarction in rats and pigs. *Sci. Transl. Med.* 12:eaat9683. doi: 10.1126/scitranslmed.aat9683

Huang, P., Wang, L., Li, Q., Tian, X., Xu, J., Xu, J., et al. (2019). Atorvastatin enhances the therapeutic efficacy of mesenchymal stem cells-derived exosomes in acute myocardial infarction via up-regulating long non-coding RNA H19. *Cardiovasc. Res.* 116, 353–367.

Ieda, M., Fu, J. D., Delgado-Olguin, P., Vedantham, V., Hayashi, Y., Bruneau, B. G., et al. (2010). Direct reprogramming of fibroblasts into functional cardiomyocytes by defined factors. *Cell* 142, 375–386. doi: 10.1016/j.cell.2010.07.002

Inagaki, K., Fuess, S., Storm, T. A., Gibson, G. A., Mctiernan, C. F., Kay, M. A., et al. (2006). Robust systemic transduction with AAV9 vectors in mice: efficient global cardiac gene transfer superior to that of AAV8. *Mol. Ther.* 14, 45–53. doi: 10.1016/j.ymthe.2006.03.014

Iseoka, H., Miyagawa, S., Fukushima, S., Saito, A., Masuda, S., Yajima, S., et al. (2018). Pivotal role of non-cardiomyocytes in electromechanical and therapeutic potential of induced pluripotent stem cell-derived engineered cardiac tissue. *Tissue Eng. Part A* 24, 287–300. doi: 10.1089/ten.tea.2016.0535

Jackman, C. P., Ganapathi, A. M., Asfour, H., Qian, Y., Allen, B. W., Li, Y., et al. (2018). Engineered cardiac tissue patch maintains structural and electrical properties after epicardial implantation. *Biomaterials* 159, 48–58. doi: 10.1016/j.biomaterials.2018.01.002

Jafari, D., Shajari, S., Jafari, R., Mardi, N., Gomari, H., Ganji, F., et al. (2020). Designer exosomes: a new platform for biotechnology therapeutics. *BioDrugs* 34, 567–586. doi: 10.1007/s40259-020-00434-x

Jana, S., and Lerman, A. (2015). Bioprinting a cardiac valve. *Biotechnol. Adv.* 33, 1503–1521. doi: 10.1016/j.biotechadv.2015.07.006

Jayawardena, T. M., Egemnazarov, B., Finch, E. A., Zhang, L., Payne, J. A., Pandya, K., et al. (2012). MicroRNA-mediated in vitro and in vivo direct reprogramming of cardiac fibroblasts to cardiomyocytes. *Circ. Res.* 110, 1465–1473. doi: 10.1161/circresaha.112.269035

Jessup, M., Greenberg, B., Mancini, D., Cappola, T., Pauly, D. F., Jaski, B., et al. (2011). Calcium upregulation by percutaneous administration of gene therapy in cardiac disease (CUPID). *Circulation* 124, 304–313. doi: 10.1161/circulationaha.111.022889

Kanki, S., Jaalouk, D. E., Lee, S., Yu, A. Y. C., Gannon, J., and Lee, R. T. (2011). Identification of targeting peptides for ischemic myocardium by in vivo phage display. *J. Mol. Cell Cardiol.* 50, 841–848. doi: 10.1016/j.yjmcc.2011.02.003

Kim, S. H., Jeong, J. H., Ou, M., Yockman, J. W., Kim, S. W., and Bull, D. A. (2008). Cardiomyocyte-targeted siRNA delivery by prostaglandin E(2)-Fas siRNA polyplexes formulated with reducible poly(amido amine) for preventing cardiomyocyte apoptosis. *Biomaterials* 29, 4439–4446. doi: 10.1016/j.biomaterials.2008.07.047

Kohama, Y., Higo, S., Masumura, Y., Shiba, M., Kondo, T., Ishizu, T., et al. (2020). Adeno-associated virus-mediated gene delivery promotes S-phase entry-independent precise targeted integration in cardiomyocytes. *Sci. Rep.* 10, 1–13.

Lee, C. S., Bishop, E. S., Zhang, R., Yu, X., Farina, E. M., Yan, S., et al. (2017). Adenovirus-mediated gene delivery: potential applications for gene and cell-based therapies in the new era of personalized medicine. *Genes Dis.* 4, 43–63. doi: 10.1016/j.gendis.2017.04.001

Lee, R. T., and Walsh, K. (2016). The future of cardiovascular regenerative medicine. *Circulation* 133, 2618–2625. doi: 10.1161/circulationaha.115.019214

Lee, S., Kim, J. E., Johnson, B., Al, Andukuri, A., and Yoon, Y.-S. (2017). Direct reprogramming into endothelial cells: a new source for vascular regeneration. *Regen. Med.* 12, 317–320. doi: 10.2217/rme-2017-0022

Li, P., Kaslan, M., Lee, S. H., Yao, J., and Gao, Z. (2017). Progress in exosome isolation techniques. *Theranostics* 7, 789–804. doi: 10.7150/thno.18133

Li, X.-H., Li, Q., Jiang, L., Deng, C., Liu, Z., Fu, Y., et al. (2015). Generation of functional human cardiac progenitor cells by high-efficiency protein transduction. *Stem Cells Transl. Med.* 4, 1415–1424. doi: 10.5966/sctm.2015-0136

Li, Y., Chen, X., Jin, R., Chen, L., Dang, M., Cao, H., et al. (2021). Injectable hydrogel with MSNs/microRNA-21-5p delivery enables both immunomodification and enhanced angiogenesis for myocardial infarction therapy in pigs. *Sci. Adv.* 7:eabd6740. doi: 10.1126/sciadv.abd6740

Li, Z., Hu, S., and Cheng, K. (2018). Platelets and their biomimetics for regenerative medicine and cancer therapies. *J. Mater. Chem. B.* 6, 7354–7365. doi: 10.1039/c8tb02301h

Li, Z., Hu, S., Huang, K., Su, T., Cores, J., and Cheng, K. (2020). Targeted anti-IL-1β platelet microparticles for cardiac detoxing and repair. *Sci. Adv.* 6:eaay0589. doi: 10.1126/sciadv.aay0589

Li, Z., Zhu, D., Hui, Q., Bi, J., Yu, B., Huang, Z., et al. (2021). Injection of ROS-responsive hydrogel loaded with basic fibroblast growth factor into the pericardial cavity for heart repair. *Adv. Funct. Mater.* 2021:2004377. doi: 10.1002/adfm.202004377

Lin, A., Sabnis, A., Kona, S., Nattama, S., Patel, H., Dong, J.-F., et al. (2010). Shear-regulated uptake of nanoparticles by endothelial cells and development of endothelial-targeting nanoparticles. *J. Biomed. Mater. Res. A* 93, 833–842.

Liu, M., Lutz, H., Zhu, D., Huang, K., Li, Z., Dinh, P.-U. C., et al. (2021). Bispecific antibody inhalation therapy for redirecting stem cells from the lungs to repair heart injury. *Adv. Sci.* 8:2002127. doi: 10.1002/advs.202002127

Liu, N., Ye, X., Yao, B., Zhao, M., Wu, P., Liu, G., et al. (2021). Advances in 3D bioprinting technology for cardiac tissue engineering and regeneration. *Bioact. Mater.* 6, 1388–1401. doi: 10.1016/j.bioactmat.2020.10.021

Liu, Q., and Muruve, D. (2003). Molecular basis of the inflammatory response to adenovirus vectors. *Gene Ther.* 10, 935–940. doi: 10.1038/sj.gt.3302036

Liu, Z., Wang, L., Welch, J. D., Ma, H., Zhou, Y., Vaseghi, H. R., et al. (2017). Single-cell transcriptomics reconstructs fate conversion from fibroblast to cardiomyocyte. *Nature* 551, 100–104. doi: 10.1038/nature24454

Luo, L., Tang, J., Nishi, K., Yan, C., Dinh, P. U., Cores, J., et al. (2017). Fabrication of synthetic mesenchymal stem cells for the treatment of acute myocardial infarction in mice. *Circ. Res.* 120, 1768–1775. doi: 10.1161/circresaha.116.310374

Machiraju, P., and Greenway, S. C. (2019). Current methods for the maturation of induced pluripotent stem cell-derived cardiomyocytes. *World J. Stem Cells* 11, 33–43. doi: 10.4252/wjsc.v11.i1.33

Maghin, E., Garbati, P., Quarto, R., Piccoli, M., and Bollini, S. (2020). Young at heart: combining strategies to rejuvenate endogenous mechanisms of cardiac repair. *Front. Bioeng. Biotechnol.* 8:447. doi: 10.3389/fbioe.2020.00447

Maiullari, F., Costantini, M., Milan, M., Pace, V., Chirivì, M., Maiullari, S., et al. (2018). A multi-cellular 3D bioprinting approach for vascularized heart tissue engineering based on HUVECs and iPSC-derived cardiomyocytes. *Sci. Rep.* 8, 1–15.

Malliaras, K., and Marbán, E. (2011). Cardiac cell therapy: where we've been, where we are, and where we should be headed. *Br. Med. Bull.* 98, 161–185. doi: 10.1093/bmb/ldr018

Martins, A. M., Vunjak-Novakovic, G., and Reis, R. L. (2014). The current status of iPS cells in cardiac research and their potential for tissue engineering and regenerative medicine. *Stem Cell Rev. Rep.* 10, 177–190. doi: 10.1007/s12015-013-9487-7

Mayourian, J., Ceholski, D. K., Gorski, P. A., Mathiyalagan, P., Murphy, J. F., Salazar, S. I., et al. (2018). Exosomal microRNA-21-5p mediates mesenchymal stem cell paracrine effects on human cardiac tissue contractility. *Circ. Res.* 122, 933–944. doi: 10.1161/circresaha.118.312420

McMurray, J. J., Packer, M., Desai, A. S., Gong, J., Lefkowitz, M. P., Rizkala, A. R., et al. (2014). Angiotensin-neprilysin inhibition versus enalapril in heart failure. *N. Engl. J. Med.* 371, 993–1004.

Mei, X., and Cheng, K. (2020). Recent development in therapeutic cardiac patches. *Front. Cardiovasc. Med.* 7:610364. doi: 10.3389/fcvm.2020.610364

Mei, Y., Saha, K., Bogatyrev, S. R., Yang, J., Hook, A. L., Kalcioglu, Z. I., et al. (2010). Combinatorial development of biomaterials for clonal growth of human pluripotent stem cells. *Nat. Mater.* 9, 768–778. doi: 10.1038/nmat2812

Mihalko, E., Huang, K., Sproul, E., Cheng, K., and Brown, A. C. (2018). Targeted treatment of ischemic and fibrotic complications of myocardial infarction using a dual-delivery microgel therapeutic. *ACS Nano* 12, 7826–7837. doi: 10.1021/acsnano.8b01977

Nam, Y.-J., Song, K., and Olson, E. N. (2013). Heart repair by cardiac reprogramming. *Nat. Med.* 19, 413–415. doi: 10.1038/nm.3147

Nelson, V. L., and Brunt, K. R. (2021). Cutting the molecular brakes to achieve cardiac regeneration. *Cell Death Differ.* 28, 1126–1129. doi: 10.1038/s41418-020-00681-z

Packer, M., Coats, A. J., Fowler, M. B., Katus, H. A., Krum, H., Mohacsi, P., et al. (2001). Carvedilol prospective randomized cumulative survival study group. Effect of carvedilol on survival in severe chronic heart failure. *N. Engl. J. Med.* 344, 1651–1658.

Parashar, A., Sarkar, S., Ganguly, A., Sharma, S. K., and Suresh, M. R. (2011). Bispecific antibodies for diagnostic applications. *Bispec. Antibodies* 349–367. doi: 10.1007/978-3-642-20910-9_19

Pasumarthi, K. B. S., and Field, L. J. (2002). Cardiomyocyte cell cycle regulation. *Circ. Res.* 90, 1044–1054. doi: 10.1161/01.res.0000020201.44772.67

Patel, V., Mathison, M., Singh, V. P., Yang, J., and Rosengart, T. K. (2016). Direct cardiac cellular reprogramming for cardiac regeneration. *Curr. Treat. Options Cardiovasc. Med.* 18:58.

Pianezzi, E., Altomare, C., Bolis, S., Balbi, C., Torre, T., Rinaldi, A., et al. (2020). Role of somatic cell sources in the maturation degree of human induced pluripotent stem cell-derived cardiomyocytes. *Biochim. Biophys. Acta Mol. Cell Res.* 1867:118538. doi: 10.1016/j.bbamcr.2019.118538

Pomeroy, J. E., Helfer, A., and Bursac, N. (2020). Biomaterializing the promise of cardiac tissue engineering. *Biotechnol. Adv.* 42:107353. doi: 10.1016/j.biotechadv.2019.02.009

Qian, L., Huang, Y., Spencer, C. I., Foley, A., Vedantham, V., Liu, L., et al. (2012). In vivo reprogramming of murine cardiac fibroblasts into induced cardiomyocytes. *Nature* 485, 593–598. doi: 10.1038/nature11044

Qiao, L., Hu, S., Liu, S., Zhang, H., Ma, H., Huang, K., et al. (2019). microRNA-21-5p dysregulation in exosomes derived from heart failure patients impairs regenerative potential. *J. Clin. Invest.* 129, 2237–2250. doi: 10.1172/jci123135

Querdel, E., Reinsch, M., Castro, L., Köse, D., Bähr, A., Reich, S., et al. (2021). Human engineered heart tissue patches remuscularize the injured heart in a dose-dependent manner. *Circulation*. 120:047904.

Rao, M. S., and Malik, N. (2012). Assessing iPSC reprogramming methods for their suitability in translational medicine. *J. Cell. Biochem.* 113, 3061–3068. doi: 10.1002/jcb.24183

Raziyeva, K., Smagulova, A., Kim, Y., Smagul, S., Nurkesh, A., and Saparov, A. (2020). Preconditioned and genetically modified stem cells for myocardial infarction treatment. *Int. J. Mol. Sci.* 21:7301. doi: 10.3390/ijms21197301

Rincon, M. Y., VandenDriessche, T., and Chuah, M. K. (2015). Gene therapy for cardiovascular disease: advances in vector development, targeting, and delivery for clinical translation. *Cardiovasc. Res.* 108, 4–20. doi: 10.1093/cvr/cvv205

Rose, E. A., Gelijns, A. C., Moskowitz, A. J., Heitjan, D. F., Stevenson, L. W., Dembitsky, W., et al. (2001). Long-term use of a left ventricular assist device for end-stage heart failure. *N. Engl. J. Med.* 345, 1435–1443.

Sandmaier, S. E., and Telugu, B. P. (2015). MicroRNA-mediated reprogramming of somatic cells into induced pluripotent stem cells. *Methods Mol. Biol.* 1330, 29–36. doi: 10.1007/978-1-4939-2848-4_3

Saparov, A., Ogay, V., Nurgozhin, T., Chen, W. C. W., Mansurov, N., Issabekova, A., et al. (2017). Role of the immune system in cardiac tissue damage and repair following myocardial infarction. *Inflamm. Res.* 66, 739–751. doi: 10.1007/s00011-017-1060-4

Shadrin, I. Y., Allen, B. W., Qian, Y., Jackman, C. P., Carlson, A. L., Juhas, M. E., et al. (2017). Cardiopatch platform enables maturation and scale-up of human pluripotent stem cell-derived engineered heart tissues. *Nat. Commun.* 8:1825.

Shapiro, S. D., Ranjan, A. K., Kawase, Y., Cheng, R. K., Kara, R. J., Bhattacharya, R., et al. (2014). Cyclin A2 induces cardiac regeneration after myocardial infarction through cytokinesis of adult cardiomyocytes. *Sci. Transl. Med.* 6:224ra27. doi: 10.1126/scitranslmed.3007668

Shelke, A. R., Roscoe, J. A., Morrow, G. R., Colman, L. K., Banerjee, T. K., and Kirshner, J. J. (2008). Effect of a nausea expectancy manipulation on chemotherapy-induced nausea: a university of Rochester cancer center community clinical oncology program study. *J. Pain Symptom Manage.* 35, 381–387. doi: 10.1016/j.jpainsymman.2007.05.008

Shen, D., Tang, J., Hensley, M. T., Li, T., Caranasos, T. G., Zhang, T., et al. (2016). Effects of matrix metalloproteinases on the performance of platelet fibrin gel spiked with cardiac stem cells in heart repair. *Stem Cells Transl. Med.* 5, 793–803. doi: 10.5966/sctm.2015-0194

Shengjie, L., Xiong, Z., Wang, X., Yan, Y., Liu, H., and Zhang, R. (2009). Direct fabrication of a hybrid cell/hydrogel construct by a double-nozzle assembling technology. *J. Bioact. Compat. Polym.* 24, 249–265. doi: 10.1177/0883911509104094

Sid-Otmane, C., Perrault, L. P., and Ly, H. Q. (2020). Mesenchymal stem cell mediates cardiac repair through autocrine, paracrine and endocrine axes. *J. Transl. Med.* 18:336.

Song, K., Nam, Y. J., Luo, X., Qi, X., Tan, W., Huang, G. N., et al. (2012). Heart repair by reprogramming non-myocytes with cardiac transcription factors. *Nature* 485, 599–604. doi: 10.1038/nature11139

Squillaro, T., Peluso, G., and Galderisi, U. (2016). Clinical trials with mesenchymal stem cells: an update. *Cell Transpl.* 25, 829–848. doi: 10.3727/096368915x689622

Sridharan, R., and Plath, K. (2011). Small RNAs loom large during reprogramming. *Cell Stem Cell* 8, 599–601. doi: 10.1016/j.stem.2011.05.009

Su, T., Huang, K., Daniele, M. A., Hensley, M. T., Young, A. T., Tang, J., et al. (2018a). Cardiac stem cell patch integrated with microengineered blood vessels promotes cardiomyocyte proliferation and neovascularization after acute myocardial infarction. *ACS Appl. Mater. Interfaces* 10, 33088–33096. doi: 10.1021/acsami.8b13571

Su, T., Huang, K., Ma, H., Liang, H., Dinh, P.-U., Chen, J., et al. (2018b). Platelet-inspired nanocells for targeted heart repair after ischemia/reperfusion injury. *Adv. Funct. Mater.* 0, 1803567. doi: 10.1002/adfm.201803567

Su, T., Huang, K., Mathews, K. G., Scharf, V. F., Hu, S., Li, Z., et al. (2020). Cardiac stromal cell patch integrated with engineered microvessels improves recovery from myocardial infarction in rats and pigs. *ACS Biomater. Sci. Eng.* 6, 6309–6320. doi: 10.1021/acsbiomaterials.0c00942

Sun, Z., Shi, K., Yang, S., Liu, J., Zhou, Q., Wang, G., et al. (2018). Effect of exosomal miRNA on cancer biology and clinical applications. *Mol. Cancer* 17, 1–19. doi: 10.1007/978-3-642-27841-9_7227-1

Tai, Y.-L., Chen, K.-C., Hsieh, J.-T., and Shen, T.-L. (2018). Exosomes in cancer development and clinical applications. *Cancer Sci.* 109, 2364–2374. doi: 10.1111/cas.13697

Tallquist, M. D., and Molkentin, J. D. (2017). Redefining the identity of cardiac fibroblasts. *Nat. Rev. Cardiol.* 14, 484–491. doi: 10.1038/nrcardio.2017.57

Tang, B. L. (2020). Maturing iPSC-derived cardiomyocytes. *Cells* 9:213. doi: 10.3390/cells9010213

Tang, J., Shen, D., Caranasos, T. G., Wang, Z., Vandergriff, A. C., Allen, T. A., et al. (2017). Therapeutic microparticles functionalized with biomimetic cardiac stem cell membranes and secretome. *Nat. Commun.* 8, 1–9. doi: 10.1155/2015/765846

Tang, J., Su, T., Huang, K., Dinh, P. U., Wang, Z., Vandergriff, A., et al. (2018a). Targeted repair of heart injury by stem cells fused with platelet nanovesicles. *Nat. Biomed. Eng.* 2, 17–26. doi: 10.1038/s41551-017-0182-x

Tang, J., Wang, J., Huang, K., Ye, Y., Su, T., Qiao, L., et al. (2018b). Cardiac cell–integrated microneedle patch for treating myocardial infarction. *Sci. Adv.* 4:eaat9365. doi: 10.1126/sciadv.aat9365

Tang, J., Cores, J., Huang, K., Cui, X.-L., Luo, L., Zhang, J.-Y., et al. (2018c). Concise review: is cardiac cell therapy dead? embarrassing trial outcomes and new directions for the future. *Stem Cells Transl. Med.* 0, 354–359. doi: 10.1002/sctm.17-0196

Tao, S. C., Guo, S. C., and Zhang, C. Q. (2018). Modularized extracellular vesicles: the dawn of prospective personalized and precision medicine. *Adv. Sci.* 5:1700449. doi: 10.1002/advs.201700449

Teng, X., Chen, L., Chen, W., Yang, J., Yang, Z., and Shen, Z. (2015). Mesenchymal stem cell-derived exosomes improve the microenvironment of infarcted myocardium contributing to angiogenesis and anti-inflammation. *Cell Physiol. Biochem.* 37, 2415–2424. doi: 10.1159/000438594

Teshigawara, R., Cho, J., Kameda, M., and Tada, T. (2017). Mechanism of human somatic reprogramming to iPS cell. *Lab. Investig.* 97, 1152–1157. doi: 10.1038/labinvest.2017.56

Tohyama, S., Hattori, F., Sano, M., Hishiki, T., Nagahata, Y., Matsuura, T., et al. (2013). Distinct metabolic flow enables large-scale purification of mouse and human pluripotent stem cell-derived cardiomyocytes. *Cell Stem Cell* 12, 127–137. doi: 10.1016/j.stem.2012.09.013

Tse, L. V., Klinc, K. A., Madigan, V. J., Castellanos Rivera, R. M., Wells, L. F., Havlik, L. P., et al. (2017). Structure-guided evolution of antigenically distinct adeno-associated virus variants for immune evasion. *Proc. Natl. Acad. Sci. U.S.A.* 114, E4812–E4821.

Uygun, B., Soto-Gutierrez, A., Yagi, H., et al. (2010). Organ reengineering through development of a transplantable recellularized liver graft using decellularized liver matrix. *Nat. Med.* 16, 814–820. doi: 10.1038/nm.2170

Vandergriff, A. C., Andrade, J. B., Tang, J., Hensley, M. T., Piedrahita, J. A., Caranasos, T. G., et al. (2015). Intravenous cardiac stem cell-derived exosomes ameliorate cardiac dysfunction in doxorubicin induced dilated cardiomyopathy. *Stem Cells Int.* 2015:960926.

Verweij, F. J., Revenu, C., Arras, G., Dingli, F., Loew, D., Pegtel, D. M., et al. (2019). Live tracking of inter-organ communication by endogenous exosomes in vivo. *Dev. Cell.* 48, 573.e4–589.e4.

Vilaysane, A., and Muruve, D. A. (2009). The innate immune response to DNA. *Semin. Immunol.* 21, 208–214.

Wang, H., Yang, Y., Liu, J., et al. (2021). Direct cell reprogramming: approaches, mechanisms and progress. *Nat. Rev. Mol. Cell Biol.* [Epub ahead of print]. doi: 10.1038/s41580-021-00335-z

Wang, K., Gan, T. Y., Li, N., Liu, C. Y., Zhou, L. Y., Gao, J. N., et al. (2017). Circular RNA mediates cardiomyocyte death via miRNA-dependent upregulation of MTP18 expression. *Cell Death Differ.* 24, 1111–1120. doi: 10.1038/cdd.2017.61

Wang, L., Liu, Z., Yin, C., Asfour, H., Chen, O., Li, Y., et al. (2015). Stoichiometry of Gata4, Mef2c, and Tbx5 influences the efficiency and quality of induced cardiac myocyte reprogramming. *Circ. Res.* 116, 237–244. doi: 10.1161/circresaha.116.305547

Wang, L. L., Liu, Y., Chung, J. J., Wang, T., Gaffey, A. C., Lu, M., et al. (2017). Sustained miRNA delivery from an injectable hydrogel promotes cardiomyocyte proliferation and functional regeneration after ischemic injury. *Nat. Biomed. Eng.* 1, 983–992. doi: 10.1038/s41551-017-0157-y

Wang, Z., Lee, S. J., Cheng, H. J., Yoo, J. J., and Atala, A. (2018). 3D bioprinted functional and contractile cardiac tissue constructs. *Acta Biomater.* 70, 48–56. doi: 10.1016/j.actbio.2018.02.007

Wasala, N. B., Shin, J. H., and Duan, D. (2011). The evolution of heart gene delivery vectors. *J. Gene Med.* 13, 557–565. doi: 10.1002/jgm.1600

Weinberger, F., and Eschenhagen, T. (2021). Cardiac regeneration: new hope for an old dream. *Annu. Rev. Physiol.* 83, 1–23.

Wendel, J. S., Ye, L., Zhang, P., Tranquillo, R. T., and Zhang, J. J. (2014). Functional consequences of a tissue-engineered myocardial patch for cardiac repair in a rat infarct model. *Tissue Eng. Part A* 20, 1325–1335. doi: 10.1089/ten.tea.2013.0312

White, H. D., and Chew, D. P. (2008). Acute myocardial infarction. *Lancet* 372, 570–584.

Wilhelm, M. J. (2015). Long-term outcome following heart transplantation: current perspective. *J. Thorac. Dis.* 7, 549–551.

Wolfram, J. A., and Donahue, J. K. (2013). Gene therapy to treat cardiovascular disease. *J. Am. Heart Assoc.* 2:e000119.

World Health Organization (2021). *Global Action Plan for the Prevention and Control of NCDs 2013-2020*. Geneva: World Health Organization.

Wu, P., Chen, H., Jin, R., Weng, T., Ho, J. K., You, C., et al. (2018). Non-viral gene delivery systems for tissue repair and regeneration. *J. Transl. Med.* 16:29.

Xin, M., Olson, E., and Bassel-Duby, R. (2013). Mending broken hearts: cardiac development as a basis for adult heart regeneration and repair. *Nat. Rev. Mol. Cell Biol.* 14, 529–541. doi: 10.1038/nrm3619

Yang, S. Y., O'Cearbhaill, E. D., Sisk, G. C., Park, K. M., Cho, W. K., Villiger, M., et al. (2013). A bio-inspired swellable microneedle adhesive for mechanical interlocking with tissue. *Nat. Commun.* 4, 2–11.

Yoo, S. Y., Jeong, S.-N., Kang, J.-I., and Lee, S.-W. (2018). Chimeric adeno-associated virus-mediated cardiovascular reprogramming for ischemic heart disease. *ACS Omega* 3, 5918–5925. doi: 10.1021/acsomega.8b00904

Zhang, Y., Desai, A., Yang, S. Y., Bae, K. B., Antczak, M. I., Fink, S. P., et al. (2015). Inhibition of the prostaglandin-degrading enzyme 15-PGDH potentiates tissue regeneration. *Science* 348:aaa2340. doi: 10.1126/science.aaa2340

Zhou, Y., Wang, L., Vaseghi, H. R., Liu, Z., Lu, R., Alimohamadi, S., et al. (2016). Bmi1 is a key epigenetic barrier to direct cardiac reprogramming. *Cell Stem Cell* 18, 382–395. doi: 10.1016/j.stem.2016.02.003

Zhu, D., and Cheng, K. (2021). Cardiac cell therapy for heart repair: should the cells be left out? *Cells* 10:641. doi: 10.3390/cells10030641

Zhu, D., Li, Z., Huang, K., Caranasos, T. G., Rossi, J. S., and Cheng, K. (2021). Minimally invasive delivery of therapeutic agents by hydrogel injection into the pericardial cavity for cardiac repair. *Nat. Commun.* 12:1412.

Zhu, W., Zhao, M., Mattapally, S., Chen, S., and Zhang, J. (2018). CCND2 overexpression enhances the regenerative potency of human induced pluripotent stem cell-derived cardiomyocytes: remuscularization of injured ventricle. *Circ. Res.* 122, 88–96. doi: 10.1161/circresaha.117.311504

**Conflict of Interest:** The authors declare that the research was conducted in the absence of any commercial or financial relationships that could be construed as a potential conflict of interest.

frontiers in Bioengineering and Biotechnology

ORIGINAL RESEARCH
published: 11 June 2021
doi: 10.3389/fbioe.2021.674260

# Bioreactor Suspension Culture: Differentiation and Production of Cardiomyocyte Spheroids From Human Induced Pluripotent Stem Cells

*Asher Kahn-Krell[1], Danielle Pretorius[1], Jianfa Ou[1], Vladimir G. Fast[1], Silvio Litovsky[2], Joel Berry[1], Xiaoguang (Margaret) Liu[1]* and Jianyi Zhang[1,3]**

[1] Department of Biomedical Engineering, School of Medicine and School of Engineering, University of Alabama at Birmingham, Birmingham, AL, United States, [2] Division of Anatomic Pathology, Department of Pathology, University of Alabama at Birmingham, Birmingham, AL, United States, [3] Department of Medicine/Cardiovascular Diseases, University of Alabama at Birmingham, Birmingham, AL, United States

OPEN ACCESS

**Edited by:**
Diego Mantovani,
Laval University, Canada

**Reviewed by:**
Diana Massai,
Politecnico di Torino, Italy
Karina Nakayama,
Oregon Health and Science University, United States

***Correspondence:**
Xiaoguang (Margaret) Liu
mliu@uab.edu
Jianyi Zhang
jayzhang@uab.edu

**Specialty section:**
This article was submitted to Tissue Engineering and Regenerative Medicine, a section of the journal Frontiers in Bioengineering and Biotechnology

**Received:** 01 March 2021
**Accepted:** 18 May 2021
**Published:** 11 June 2021

**Citation:**
Kahn-Krell A, Pretorius D, Ou J, Fast VG, Litovsky S, Berry J, Liu X and Zhang J (2021) Bioreactor Suspension Culture: Differentiation and Production of Cardiomyocyte Spheroids From Human Induced Pluripotent Stem Cells. Front. Bioeng. Biotechnol. 9:674260. doi: 10.3389/fbioe.2021.674260

Human induced-pluripotent stem cells (hiPSCs) can be efficiently differentiated into cardiomyocytes (hiPSC-CMs) via the GiWi method, which uses small-molecule inhibitors of glycogen synthase kinase (GSK) and tankyrase to first activate and then suppress Wnt signaling. However, this method is typically conducted in 6-well culture plates with two-dimensional (2D) cell sheets, and consequently, cannot be easily scaled to produce the large numbers of hiPSC-CMs needed for clinical applications. Cell suspensions are more suitable than 2D systems for commercial biomanufacturing, and suspended hiPSCs form free-floating aggregates (i.e., spheroids) that can also be differentiated into hiPSC-CMs. Here, we introduce a protocol for differentiating suspensions of hiPSC spheroids into cardiomyocytes that is based on the GiWi method. After optimization based on cardiac troponin T staining, the purity of hiPSC-CMs differentiated via our novel protocol exceeded 98% with yields of about 1.5 million hiPSC-CMs/mL and less between-batch purity variability than hiPSC-CMs produced in 2D cultures; furthermore, the culture volume could be increased ∼10-fold to 30 mL with no need for re-optimization, which suggests that this method can serve as a framework for large-scale hiPSC-CM production.

**Keywords: pluripotent stem cell, cardiomyocyte, suspension culture, maturation, robust scale-up**

## INTRODUCTION

The experimental manipulation of stem/progenitor cells has led to continuous improvements in cell viability, differentiation efficiency, and functional activity (Laco et al., 2018; Le et al., 2018; Biermann et al., 2019; Cai et al., 2019; Leitolis et al., 2019; Valls-Margarit et al., 2019; Yang et al., 2019; Zhu et al., 2020). Contemporary protocols for differentiating human

induced-pluripotent stem cells (hiPSCs) into cardiomyocytes (hiPSC-CMs) are often based on the GiWi method, which uses small-molecule inhibitors of glycogen synthase kinase (GSK) and tankyrase to alternately activate and then suppress the Wnt signaling pathway (Mazzola and Pasquale, 2020). The remarkable efficiency of the GiWi method has relieved the scarcity of cardiomyocytes for research applications and, consequently, has profoundly impacted the development of cell-based cardiac therapies, including implantable engineered cardiac-tissue patches and hiPSC-CM–derived cell products (e.g., exosomes), as well as in-vitro models for mechanistic studies and drug development (Jackman et al., 2018; Liu et al., 2018; Meyer et al., 2019; Mills et al., 2019; Noor et al., 2019; Yeung et al., 2019; Gao et al., 2020; Pretorius et al., 2020). However, because the GiWi method is typically used to differentiate two-dimensional (2D) cell sheets in 6-well culture plates (Sharma et al., 2015), it may not be sufficiently scalable to produce the number of hiPSC-CMs needed for high-throughput cardiotoxicity assessments or for clinical applications such as the treatment of acute myocardial infarction (MI), which often results in the loss of ∼1 billion cardiomyocytes (Chong et al., 2014; Kropp et al., 2016; Dunn and Palecek, 2018). Higher yields may be achievable with multilayered/stacked flasks or multicarrier-based systems, but neither of these methods have been fully scaled, and both require materials and reagents that are not readily available (Ting et al., 2014, 2018; Breckwoldt et al., 2017; Le and Hasegawa, 2019; Chang et al., 2020; Laco et al., 2020).

When cultured in a three-dimensional (3D) environment, hiPSCs form free-floating suspensions of aggregated cells (i.e., spheroids) that can also be differentiated into hiPSC-CMs with tools that are both widely available and well-characterized. Several groups have used this approach to generate up to 1-L volumes of cardiomyocytes that are more than 90% pure (Chen et al., 2015; Fonoudi et al., 2015; Kempf et al., 2015; Halloin et al., 2019; Hamad et al., 2019), and some evidence suggests that suspension-differentiated hiPSC-CMs may be more mature and, consequently, more suitable for clinical applications, than hiPSC-CMs generated via 2D differentiation protocols (Jeziorowska et al., 2017; Correia et al., 2018). Here, we introduce a novel protocol for differentiating suspensions of hiPSC spheroids into cardiomyocytes that serves as a framework for further scale up to produce the large number of hiPSC-CMs required for clinical applications. We chose a shaker flask based system for this study for both its simplicity and wide availability. This will allow broad application for researchers without advanced bioreactor experience and equipment to expand their culture volumes. However, further scale up for biomanufacturing purposes will require additional optimization and engineering to account for multiple factors including but not limited to oxygen and gas diffusion, mixing and shear stress, as well as temperature and pH monitoring (Amit et al., 2011; Shafa et al., 2011; Abbasalizadeh et al., 2012; Lattermann and Büchs, 2016; Zweigerdt et al., 2016). Our protocol is based on the GiWi method and was optimized for maximum purity and yield by manipulating the initial cell density, reagent concentrations, and other culture conditions. The differentiated hiPSC-CMs were also thoroughly characterized via morphological assessments and by monitoring the expression of cardiomyocyte-specific genes (including maturity markers).

# MATERIALS AND METHODS

## hiPSC Culture and Differentiation

The University of Minnesota Human Subjects Research Institutional Review Board approved all protocols related to cell line establishment in this study. The hiPSCs used in this study were generated from cardiac fibroblasts as previously reported (Zhang et al., 2018) and maintained on Geltrex-coated (Gibco) 6-well plates in mTesR Plus medium (STEMCell Technologies, Canada) with daily medium changes until 90–100% confluent and then prepared for the differentiation protocol over 7 days (i.e., beginning on day-7). The cells were washed once with Dulbecco's Phosphate-Buffered Saline (DPBS) and incubated with 0.5 mL Gentle Cell Dissociation Reagent (GCDR; STEMCell Technologies) for 6 min at 37°C; then, the GCDR was aspirated, and 1 mL TeSR E8 3D medium (STEMCell Technologies) supplemented with 10 μM Y-27632 (BD Biosciences Cat# 562822, RRID:AB_2869435) was gently pipetted into each well to dislodge the cells and disaggregate them into small clumps. Cells from all 6 wells per plate were collected, suspended in 40 mL of TeSR E8 3D Seed medium (STEMCell Technologies), placed in a 125-mL shaker flask (Fisher Scientific), and cultured on a Belly Dancer Shaker (IBI Scientific) at 70 rpm with 5% $CO_2$ at 37°C. On days-6 and 5, 1.2 mL TeSR E8 3D Feed medium (STEMCell Technologies) was added to the culture flasks, and the cells were passaged on day-4. Passaging was performed by disaggregating the cells into smaller clumps and transferring them into a final volume of 80 mL TeSR E8 3D Seed medium; then, the cells were cultured at 50 rpm with daily additions of 2.4 mL TeSR E8 3D Feed medium until day-1, when half of the culture medium was replaced with fresh TeSR E8 3D Seed medium.

Differentiation was initiated on Day 0, and the protocol was optimized by varying the initial cell density (0.26 , 0.67 , 1.1 , 1.6 , 2.1 , and 5.1 $10^6$ cell/mL), CHIR99021 concentration (4, 5, 6, 7, 8, and 9 μM), and shaking speed (0, 20, 55, and 75 rpm). Briefly, 1 mL of the hiPSC-spheroid suspension was collected; then, the cells were dissociated with GCDR and counted to calculate the cell density. The remaining spheroids were washed through a 500 μm filter and collected on a reversible 40 μm filter (pluriSelect) to establish a homogenous population prior to differentiation. The spheroids were washed out with RPMI 1640 supplemented with 1 B27 without insulin (RPMI/B27–) and CHIR99021 with a final volume of 2.5 mL in low attachment 6 well plates (Corning) for optimization and 30 mL in 125 mL flasks (Thermo Fisher Scientific) for subsequent experiments. Twenty-four hours later (i.e., on day 1) the medium was replaced with fresh RPMI/B27–, and the culture volume was increased by 20% and maintained at 1.2 the initial volume for all subsequent medium changes. On day 3, half the medium was replaced with RPMI/B27– containing 10 μM IWR-1, and on day 5, the medium was completely refreshed with RPMI/B27– . On day 7, the medium was completely changed to RPMI 1640 supplemented with B27 with insulin (RPMI/B27+), and

the cells were cultured for two more days until day 9, when the differentiated hiPSC-CMs cells were purified. Purification was performed via metabolic selection: the medium was completely changed to glucose-free RPMI 1640 supplemented with B27 with insulin and 0.12% sodium DL-lactate, and the cells were cultured for 72 h until day 12, when the media was changed back to RPMI/B27+. The purified hiPSC-CMs were maintained in RPMI/B27+ with partial medium changes every 3 days.

## Flow Cytometry

Cells were dissociated into single cells via treatment with cardiomyocyte dissociation media (CMDM, STEMCell Technologies) for 10–20 min at 37°C, resuspended in cardiomyocyte support media (STEMCell Technologies), counted, centrifuged at 300 g for 3 min, washed with DPBS, fixed in 4% paraformaldehyde (PFA) for 20 min, permeabilized with 0.1% Triton-X, blocked with 4% bovine serum albumin (BSA) in 4% fetal bovine serum (FBS), stained with Zenon conjugated anti-Troponin T antibody or primary antibody (**Supplementary Table 1**), incubated for 60 min, and washed with DPBS. Around $5 \times 10^5$ cells were used per sample with spheroids from individual batches analyzed as a single sample. Analysis on an Attune NxT Flow Cytometer (Thermo Fisher) used lasers FSC, SSC, and BL1 with voltages of 80, 310, and 260, respectively. FlowJo (FlowJo, RRID:SCR_008520) was used to gate the single cell population and a threshold was set at $1.3 \times 10^3$ volts for cardiac troponin T positivity with consistent gating used across samples. Each marker was examined in at least 4 independent batches of cells.

## Real-Time Quantitative Reverse-Transcription Polymerase Chain Reaction (RT-qPCR)

Cells were lysed with TRIZOL (Thermo Fisher), and lysates were homogenized by repeatedly drawing/expelling them into/from a pipette; then, the RNA was purified in Direct-zol™ RNA MiniPrep Plus columns (Zymo Research) and treated with DNAase I. Reverse transcription was performed with SuperScript™ IV VILO™ Master Mix (Thermo Fisher) as directed by the manufacturer's protocol, and samples (5 ng with 500 nM primers; **Supplementary Table 2**) were analyzed on a QuantStudio 3 Real-Time PCR System (Applied Biosystems) with PowerUp SYBR Green Master Mix (Applied Biosystems). Measurements were quantified via normalization to measurements of glyceraldehyde phosphate dehydrogenase (GAPDH) RNA abundance in the same sample. Each marker was examined in at least 4 independent batches of cells with GAPDH replicates used to account for measurement error.

## Western Blotting

Protein lysates were collected by treating cells with RIPA buffer (Thermo Fisher Scientific) supplemented with HALT Proteinase Inhibitor (Thermo Fisher Scientific) and homogenized via pipetting. Total protein concentrations were calculated via BCA assay (Fisher Scientific); then, 6 μg of each sample was loaded onto a 4–20% Mini-PROTEAN® TGX™ Precast Protein Gel (Biorad) and run at 100 V for 1 h. Samples were transferred to a nitrocellulose membrane by using the Trans-Blot Turbo System (Biorad), blocked in 5% milk, and then incubated with primary antibody (**Supplementary Table 1**) overnight at 4°C and with secondary antibody for 1 h at room temperature. ECL Chemiluminescent Reagent (GE Healthcare Amersham) was applied to the membrane for 5 min, and then the membrane was exposed on the ChemiDoc Touch Imaging System (Biorad). Each marker was examined in at least 4 independent batches of cells.

## Tissue Preservation

Samples were fixed in 4% formaldehyde (Pierce, Thermo Fisher Scientific, # 28906) for 1 h and then embedded in either optimal cutting temperature (OCT) compound (Fisher Health Care, United States) or paraffin for histological analysis.

## Histochemistry

Sections (10-μm) were deparaffinized, rehydrated, stained in hematoxylin (Mayer's, Merck, 3 min) and eosin Y (2 min) solution, dehydrated, mounted in Permount, and imaged with a bright field microscope (Olympus IX83 epifluorescent microscope). Histological sections were analyzed by a non-blinded clinical cardiac pathologist with expertise in assessing for morphological irregularities and necrotic tissue who was asked to determine the heterogeneity of the cardiac spheroids as well as examine for apoptotic or necrotic regions. Heterogeneity was defined as structural and size differences between cells in different regions of the spheroid.

## Immunostaining

OCT-embedded sections (10-μm) and chamber slides containing live cells were fixed for 20 min in 4% PFA; blocked and permeabilized for 30 min in 10% donkey serum, 10% Tween20, 3% BSA, and 0.05% Triton-X; incubated with primary antibodies (**Supplementary Table 1**) for 1 h at room temperature; washed with PBS (3 washes, 5 min per wash), incubated with fluorescent (4′, 6-diamidino-2-phenylindole [DAPI]) secondary antibodies for 1 h at room temperature; mounted in VECTASHIELD hardset Antifade Mounting Medium; and visualized via confocal laser scanning (Olympus FV3000 confocal microscope). Stains were assessed through visual inspection of at least 4 different spheroids from multiple batches and where used, quantification of TUNEL positive cells was determined via manual counting of all nuclei in a single spheroid cross section.

## Transmission Electron Microscopy (TEM)

Spheroid and monolayer CM cells were dissociated, replated on 0.4-μm pore Transwell Polycarbonate Membranes, and cultured for 7 days; then, the membranes were fixed in 2.5% glutaraldehyde solution for 1 h at 4°C and delivered to the UAB High-Resolution Imaging Facility. Sample blocks were sectioned along the width of the transwells with a diamond knife, and samples were mounted and viewed with a Tecnai Spirit T12 Transmission Electron Microscope. Both monolayer and suspension culture groups consisted of 4 transwells each, with at least 3 subsequent samples per transwell sectioned and

imaged. Each group (monolayer vs. suspension) consisted of at least 12 images each. Sarcomere lengths were determined using ImageJ with the line measure tool and all sarcomeres in an image were measured.

## Statistical Analysis

Data are presented as mean ± SEM, and significance was evaluated via the Student's *t-test* or analysis of variance (ANOVA). Analyses were performed with GraphPad Prism8 software (GraphPad Prism, RRID:SCR_002798), and $p < 0.05$ was considered significant.

# RESULTS

## Optimization of hiPSC-CM Differentiation in Spheroid Suspensions

hiPSCs were cultured in 6-well plates until 90–100% confluent and then in suspension for 7 days before differentiation was induced by culturing the cells in CHIR99021-containing medium for 24 h beginning on Day 0 and then in IWR1-containing medium for 48 h beginning on day 3 (**Figure 1A**). The differentiation protocol was conducted in low attachment 6 well plates with rotational shaking, and the protocol was optimized by varying either the cell density (0.26 , 0.67 , 1.1 , 1.6 , 2.1 , and 5.1 $10^6$ cell/mL), CHIR99021 concentration (4, 5, 6, 7, 8, and 9 μM), or shaking speed (0, 20, 55, and 75 rpm) while holding the other 2 parameters constant. Differentiation efficiency was determined on day 9 via flow cytometry measurements of cTnT expression; optimal results for both the purity (**Figure 1B**) and yield (**Figure 1C**) of cTNT-positive cells was achieved with an initial cell density of 1.6 $10^6$ cells/mL (purity: 92.9 ± 1.8%, yield: 5.08 ± 0.42 $10^6$ hiPSC-CMs), 6 μM CHIR99021 (83.1 ± 4.4%, 4.88 ± 0.96 $10^6$ hiPSC-CMs), and 55 rpm shaking (92.2 ± 1.2%, 4.36 ± 0.32 $10^6$ hiPSC-CMs).

## Characterization of hiPSC-CMs in Suspension-Differentiated Spheroids

Shaker flask suspension culture of iPSC aggregates results in a wide range of spheroid sizes and culture heterogeneity (Otsuji et al., 2014). Therefore, prior to beginning differentiation spheroids were passed through a 500 μm filter and collected on a 40 μm filter to remove large aggregates and small debris. When differentiated under optimized conditions, spheroid sizes remained largely stable: mean diameter was 242.4 ± 3.9 μm before differentiation was initiated, 231.4 ± 4.5 μm on day 12 after 30 days of purification via glucose starvation, and 255.2 ± 4.2 μm on day 30 (**Figure 2A**). Compared with monolayer differentiation (1.08 ± 0.22 $10^6$ CM/mL), the suspension protocol produced greater yields of cells (1.47 ± 0.18 $10^6$ CM/mL), however, the difference did not reach statistical significance ($p = 0.203$) (**Figure 2B**). The most conspicuous changes in spheroid morphology were observed on days 1 and 5, after completion of the 24-h CHIR99021 and 48-h IWR1 culture periods, respectively (**Figure 2C**). Histological (**Figure 2D**) and immunofluorescent (**Figure 2E**) analyses conducted on day 12 indicated that the suspension-differentiated spheroids were composed of homogeneous hiPSC-CM populations that were morphologically similar to fetal cardiomyocytes; displayed no evidence of glandular or other cell populations and no large structural irregularities; consistently expressed cardiac troponin T (cTnT) and alpha-actinin; and had moderately aligned, striated fibers with uniformly distributed spherical nuclei.

One key concern for spheroid culture is whether cells located in the interior of the spheroid are adequately exposed to nutrients and differentiation factors present in the media; thus, spheroid sections were stained for the expression of phosphorylated mixed lineage kinase domain-like protein (pMLKL) (Linkermann et al., 2014; Negroni et al., 2017) and via terminal deoxynucleotidyl transferase dUTP nick-end labeling (TUNEL) to identify necrotic and apoptotic cells, respectively. None of the sections contained pMLKL-positive nuclei (**Figure 3A**) and although 7.7 ± 4.3% of cells were TUNEL-positive (**Figure 3B**) they were evenly distributed throughout the sections rather than localized in the core, which suggests that apoptosis was not caused by lack of access to nutrients in the media. Markers associated with calcium handling and maturation (SERCA, Cx43, JPH2, and MLC2v) were also uniformly expressed throughout spheroid sections and in cardiomyocytes from dissociated spheroids (**Figures 3C–G**) thus, differentiation appeared to be equally efficient throughout the entire volume of the spheroid, including the spheroid interior. Expression of the atrial isoform marker MYL7, however, was noted to appear higher at the edges of the spheroid than in the internal region. Although initially attributed to greater cell density this observation also presents the possibility that subpopulations of more atrial and ventricular cells may be localized to different regions of the spheroid. Further examination using techniques such as single cell sequencing could help elucidate these differences but were outside the scope of this work.

Flow cytometry assessments conducted with cells collected on day 12 indicated that cTnT was expressed by a considerably greater proportion of hiPSC-CMs when the cells were differentiated via the suspension protocol (98.2 ± 0.8%) than in monolayers (89.2 ± 4.8%) (**Figure 4A**) and while expression of the pluripotency markers SOX2, SSEA4, and Tra-1–60 was measurable in suspension-differentiated hiPSC-CMs (SOX2: 0.76 ± 0.18, SSEA4: 2.01 ± 0.22, Tra-1–60 0.75 ± 0.16), the proportion remained at or below that of monolayer-differentiated cells (SOX2: 0.26 ± 0.16, SSEA4: 2.83 ± 0.98, Tra-1–60 2.47 ± 0.74) (**Figure 4B**). RT-qPCR assessments of mRNA levels indicated that pluripotency gene expression declined immediately and rapidly after suspension differentiation was initiated but peaked on day 3 in monolayer-differentiated cells, while expression of the mesoderm genes Brachyury and MESP peaked on days 1 and 3 (respectively), and cardiac gene expression (Gata4, Mef2c, Nkx2–5, and α-MHC) peaked on day 7, with both protocols (**Figure 4C**). Peak levels of mesoderm-gene expression in suspension- and monolayer-differentiated cells were similar, but cells differentiated via the suspension protocol tended to express higher levels of cardiac genes, and the monolayer protocol was associated with greater variability

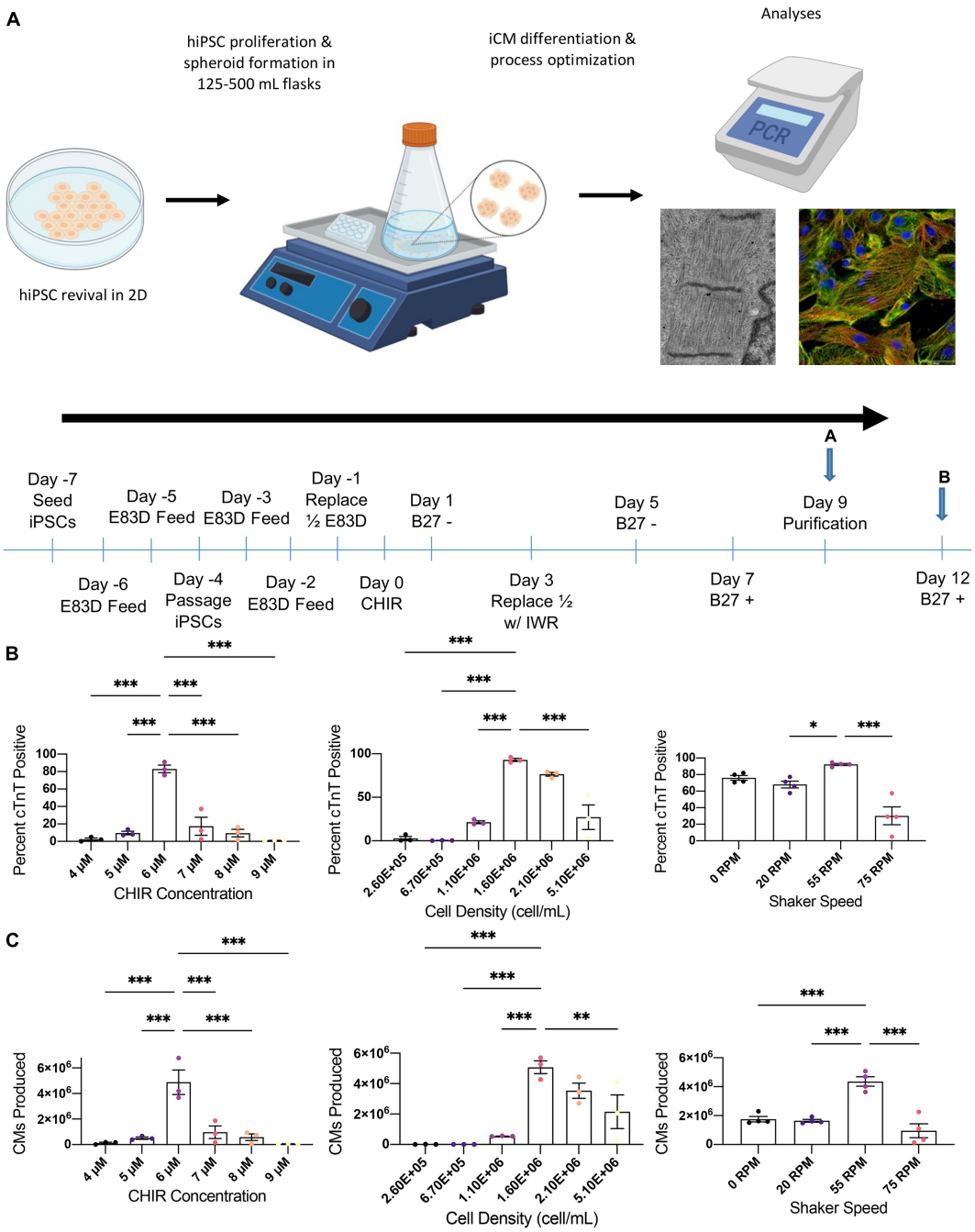


**FIGURE 1 |** Optimization of suspension differentiation protocol. **(A)** Schematic of the overall process and differentiation timeline for cardiac spheroid production pursued in this paper. Monolayer cultured iPSCs were seeded into 3D culture where they were differentiated followed by multimodal biomolecular and functional analysis. After seeding on day-7 cells are cultured in TeSR E8 3D for 7 days with a single passage on day-4. Cell density is calculated on day 0 and spheroids are then cultured in RPMI1640/B27- supplemented with CHIR on day 1 and IWR on day 3. Metabolic purification is initiated on day 9 using RPMI 1640 without glucose supplemented with B27+ and d-lactate. On day 12 and every 3 days thereafter, media is partially changed with fresh RPMI1640/B27+. Optimization studies analyzed cells at point A and all characterization experiments used cells at point B. **(B)** Flow cytometric analysis of cTnT positive cells for optimization of differentiation conditions including CHIR concentration, cell density on day 0, and shaker speed. **(C)** Total cardiomyocytes produced in each differentiation condition during optimization. $*p < 0.05$; $**p < 0.01$; $***p < 0.001$ ($n = 4$).

between samples for all lineage markers (i.e., pluripotency, mesodermal, and cardiac). Notably, when hiPSC-CMs were imaged via TEM, measurements of mean sarcomere length were significantly greater in suspension-differentiated (1.660 ± 0.155 μm) than in monolayer-differentiated (1.406 ± 0.125 μm) cells (**Figure 4D**).

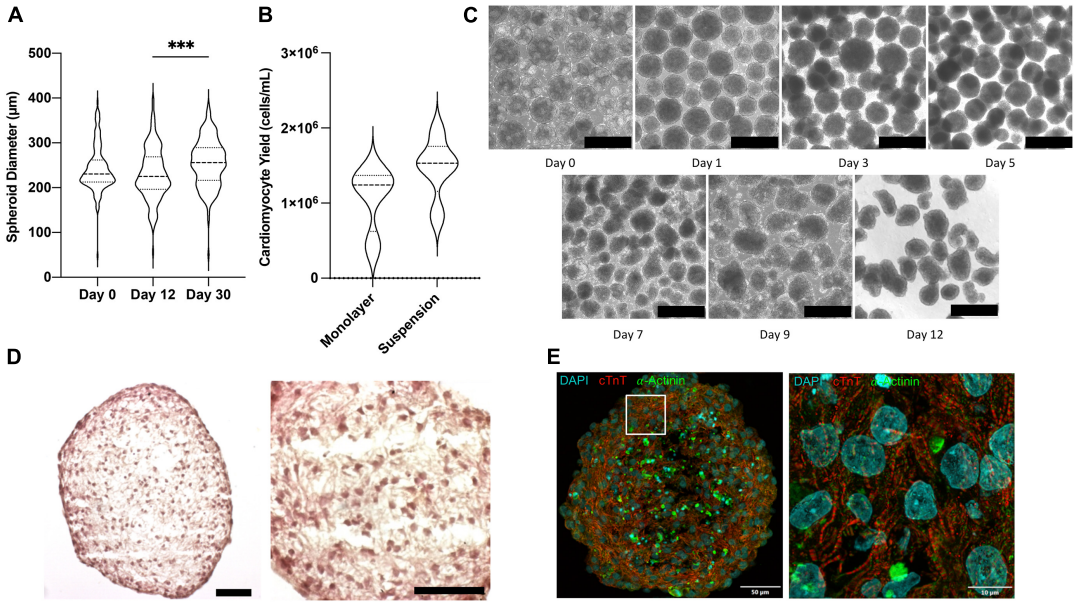


**FIGURE 2 |** Morphological characterization of CM spheroids. **(A)** Violin plot of spheroid size determined from bright field images on day 0, 12, and 30 of differentiation ($n > 150$). **(B)** Violin plot of cardiomyocyte yield on day 12 in monolayer and suspension culture systems determined as cells per volume of media ($n = 4$). **(C)** Bright field photos of differentiating spheroids over time. Scale bar = 500 μm. **(D)** H&E stained parafin sections of day 12 beating cardiomyocyte spheroids. Scale bar = 50 μm. **(E)** Flourescently stained cryosection showing cardiomyocytes muscle fiber striations. $^{***}p < 0.001$.

## Maturity of hiPSC-CMs in Suspension-Differentiated Spheroids

The biological processes associated with cardiomyocyte maturation include changes in the composition of the sarcomere, as well as in the expression of genes involved in cellular metabolism, structural organization, and electrophysiology (e.g., calcium handling). Thus, we evaluated the maturity of suspension- and monolayer-differentiated hiPSC-CMs by conducting RT-qPCR assessments of mRNA abundance for individual genes, or the ratio of mRNA abundance for pairs of genes, that typically increase (Beta-MHC, Beta/Alpha-MHC, MLC-2v, MLC-2/2a, TNNI3, TNNI3/1) or decline (Alpha-MHC, MLC-2a, TNNI1) as cardiomyocytes mature (Guo and Pu, 2020). Assessments conducted in cells collected on day 12 indicated that the ratio of βMHC-to-αMHC expression (Mahdavi et al., 1984; Reiser et al., 2001; Yang et al., 2014; LaBarge et al., 2019), as well as both TNNI3 mRNA levels and the TNNI3-to-TNNI1 ratio (Bedada et al., 2014) were greater in suspension-differentiated hiPSC-CMs than in hiPSC-CMs that were differentiated in monolayers (**Figure 5A**). Furthermore, the same three parameters, as well as MLC2v mRNA levels, the MCL2v-to-MCL2a ratio, and the abundance of CKMT2, LAMA2, PLN, Cx43, NCX1, and Calsequestrin mRNA (Kubalak et al., 1994; Uosaki et al., 2015), increased substantially from days 12 to 30 in suspension-differentiated hiPSC-CMs. Notably, measurements for genes involved in organizational structure (FN1, Col3A1, and ELN) tended to vary more between samples from monolayer-differentiated than suspension-differentiated cells, and the results from Western-blot assessments of protein levels for a subset of key genes were consistent with mRNA measurements (**Figure 5B**) day 12 measurements in suspension- and monolayer-differentiated cells were similar, while both MLC2v protein levels and the ratio of MCL2v-to-MLC2a protein abundance increased from days 12 to 30. Collectively, these observations confirm that hiPSC-CMs were no less mature when differentiated in suspension than in monolayers.

## DISCUSSION

The GiWi method is among the most efficient strategies for differentiating hiPSCs into cardiomyocytes; however, it may not be sufficiently scalable to produce the billions of hiPSC-CMs needed for treatment of myocardial disease or for high-throughput drug-testing, because it is typically conducted with 2D cell sheets in 6-well culture plates (Sharma et al., 2015). hiPSC-CMs can also be produced in suspension culture (Shafa et al., 2011; Kempf et al., 2014, 2015, 2016; Fonoudi et al., 2016; Halloin et al., 2019; Hamad et al., 2019; Chang et al., 2020; Laco et al., 2020; Miwa et al., 2020), which is more compatible with large-scale production, and the GiWi-based suspension-differentiation protocol introduced here incorporates a number of other key innovations, such as (1) the use of hiPSC culture media that was designed specifically for 3D culture and supplied via a fed batch reactor, (2) a filtration step before differentiation to reduce the heterogeneity of the spheroid population, (3) partial media changes on day 3 and from day 12 onward, which reduced processing time, and (4) direct incorporation of metabolic purification, which increased the purity of the differentiated hiPSC-CM populations to > 98%. Furthermore, whereas newly

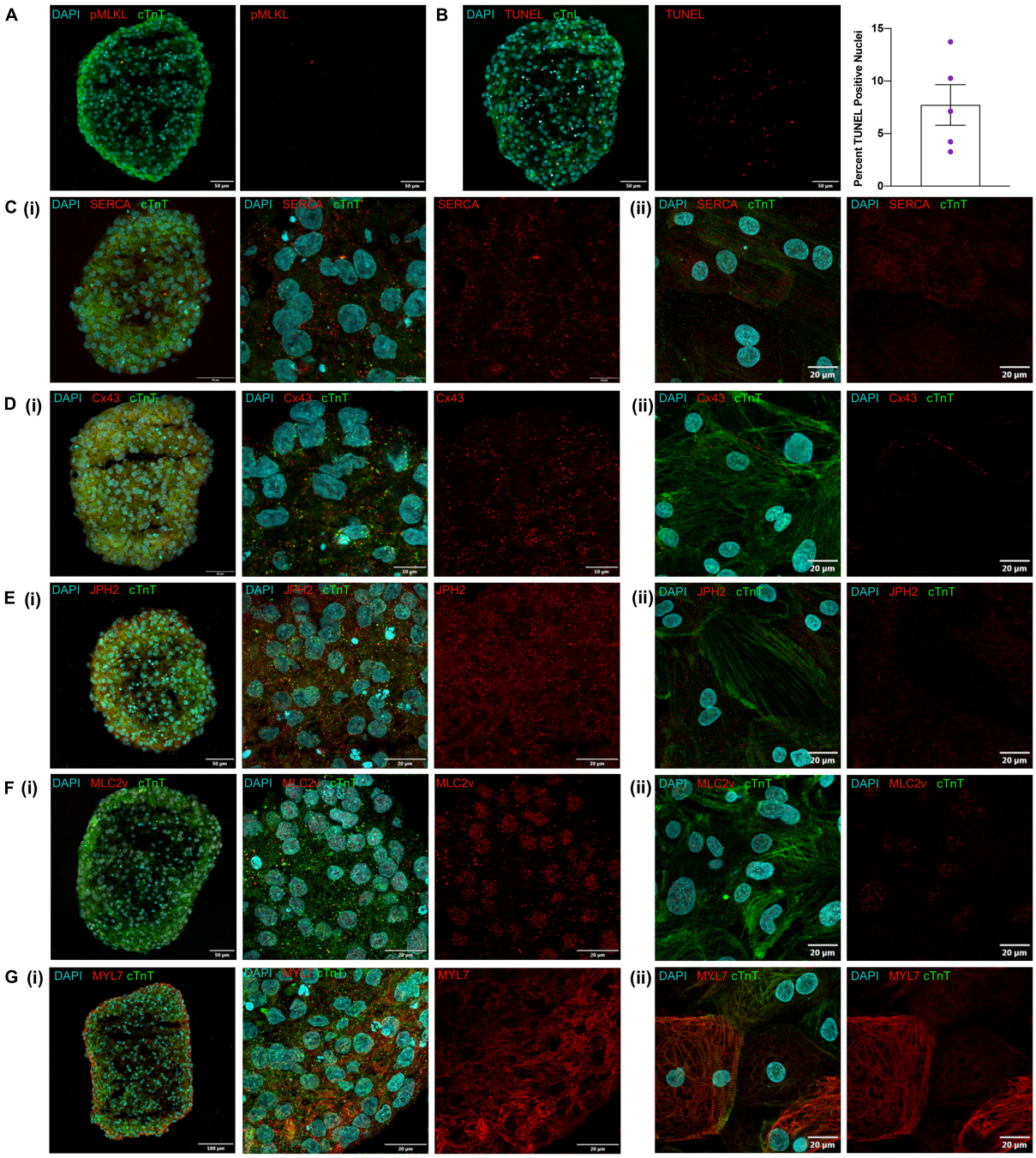


**FIGURE 3 |** Visual characterization of iCMs produced in suspension. **(A)** Day 12 cryosection stained for pMLKL showing no positive nuclei. **(B)** Day 12 cryosection with TUNEL staining and quantification of percent positive nuclei from examination of 5 spheroids. **(C–G)** Immunofluorescent antibody staining of day 12 suspension cardiomyocytes for cTnT and **(C)** SERCA, **(D)** Cx43, **(E)** JPH2, **(F)** MLC2v, and **(G)** MYL7 as (i) cryosections at low and high magnification and (ii) dissociated spheroids cultured for 3 days as monolayers.

differentiated hiPSC-CMs are more phenotypically similar to fetal than to adult cardiomyocytes (Xu et al., 2009; Gupta et al., 2010; Yang et al., 2014; van den Berg et al., 2015), our results suggest that at least some markers for cardiomyocyte maturation tended to be more highly expressed in suspension-differentiated than monolayer-differentiated hiPSC-CMs; this observation is consistent with previous reports that 3D culture conditions appear to promote hiPSC-CM maturity (Correia et al., 2018; Beauchamp et al., 2020; Giacomelli et al., 2020). However, for complete assessment of functional maturity, electrophysiology measurements along with longitudinal studies are needed but were outside the scope of the current work.

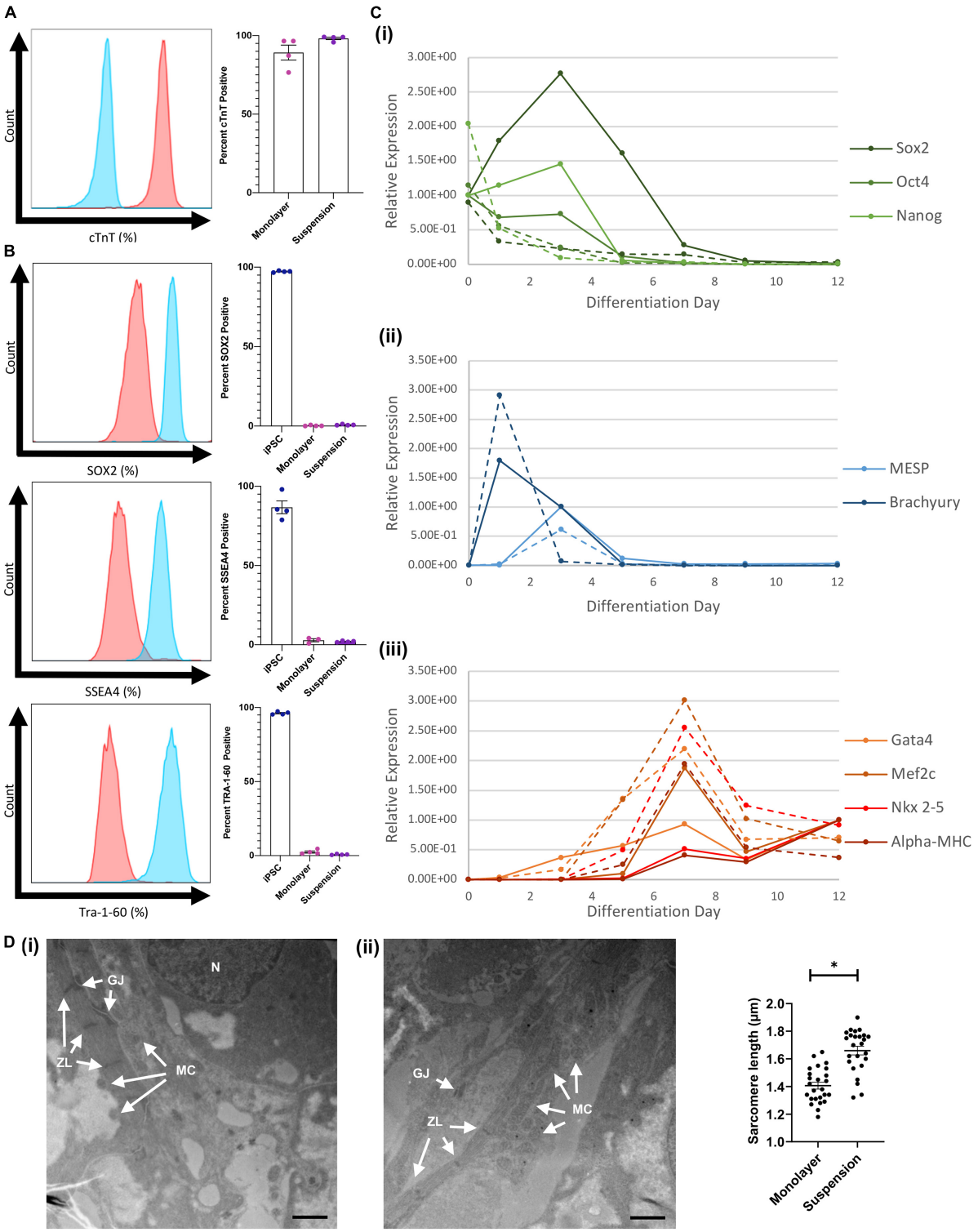


**FIGURE 4 |** Comparison of monolayer and suspension using the optimized protocol. **(A)** Flow cytometry staining for cTnT in suspension differentiated cardiomyoctes (red) compared with antibody isotype control (blue) with corresponding quantification. **(B)** Flow cytometry staining for iPSC markers (SOX2, SSEA4, and Tra-1–60) in monolayer and suspension (red) differentiated cardiomyoctes compared with iPSC (blue) positive control. **(C)** RT-qPCR analysis of (i) stem cell, (ii) mesoderm, and (iii) cardiac gene expression throughout differentiation for monolayer (solid) and suspension (dotted) techniques. **(D)** TEM images of (i) suspension and (ii) monolayer differentiated CMs with labeled characteristic features, N nucleus, GJ gap junction, ZL z-line, and MC mitochondria (Scale bar = 1 μm). Measurements of mean sarcomere length in each condition ($n = 25$). *$p < 0.0001$.

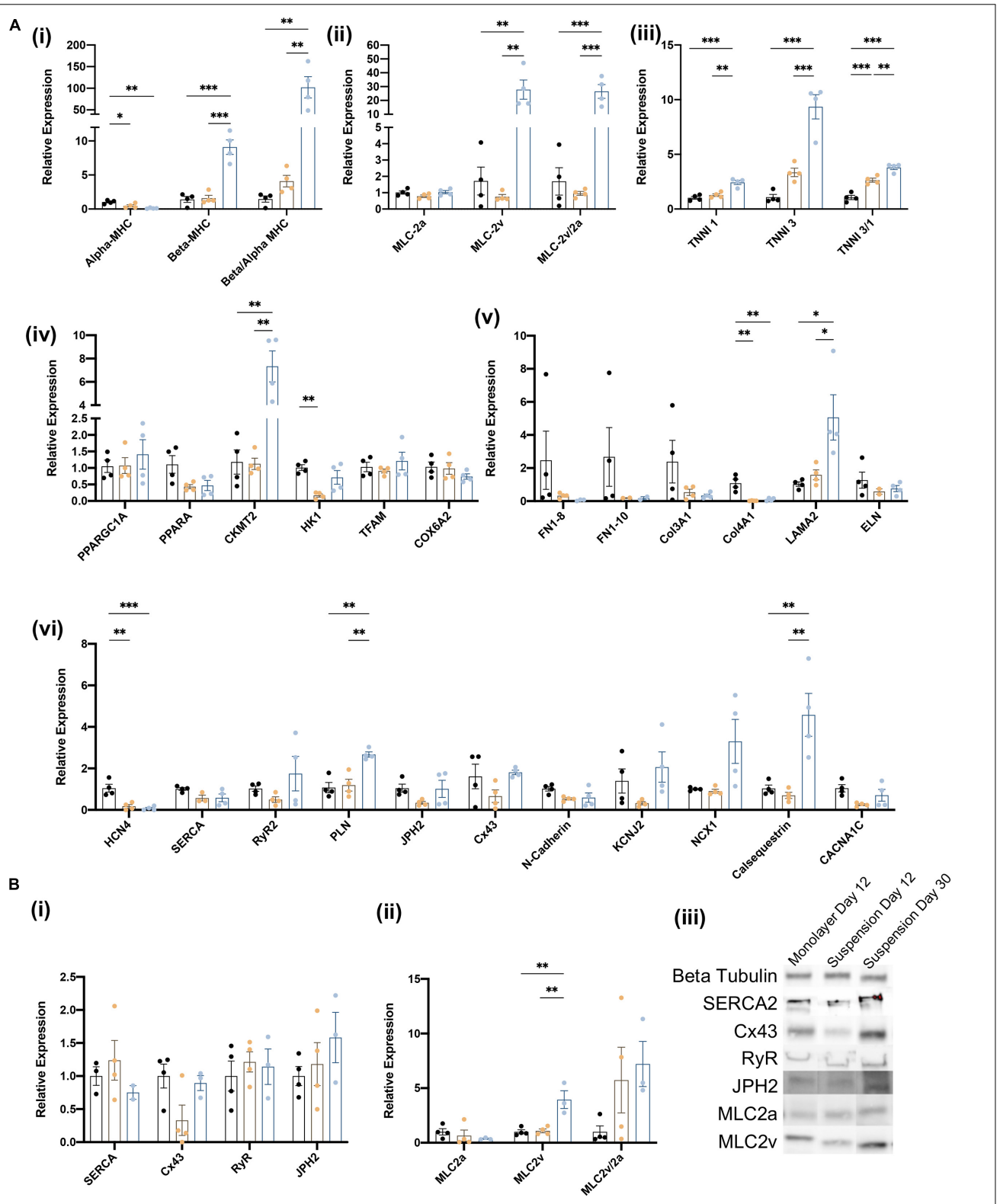


**FIGURE 5 |** Characterization of iCMs produced in suspension vs. monolayer for biochemical markers of maturation. **(A)** RT-qPCR analysis of relative gene expression normalized to GAPDH and monolayer expression on day 12 and 30 for (i) myosin heavy chain isoforms, (ii) myosin light chain isoforms, (iii) troponin I isoforms, (iv) metabolic activity, (v) structural organization, and (vi) calcium handling genes. Groups are as follows, black: monolayer CMs at day 12, blue: suspension CMs at day 12, and yellow: suspension CMs at day 30. **(B)** Western blot quantification of proteins related to (i) CM maturity and (ii) myosin light chain isoforms. (iii) Blot image for selected samples. $^{*}p < 0.05$; $^{**}p < 0.01$; $^{***}p < 0.001$. ($n = 4$).

The efficiency of our differentiation protocol was highly dependent on the initial cell density, CHIR99021 concentration, and shaker speed, but once the optimal conditions were identified, the protocol could be scaled up by ∼10-fold from 3 to 30 mL with no additional optimization. Furthermore, although the efficiencies of the suspension- and monolayer-differentiation protocols were similar, between-batch variation was lower for suspension-differentiated cells, and this consistency across a wide range of culture volumes has important implications for large-scale, commercial biomanufacturing facilities. However, the cumulative evidence from a number of reports suggests that the optimal CHIR99021 concentration can vary depending on which line of hiPSCs is used (Kempf et al., 2015), so our optimization protocol will likely need to be repeated for different hiPSC lines.

In further examining the optimization data, the density dependence most likely results from two competing components, that of limited intercellular communication via soluble factors at low densities and nutrient usage at high densities. This is consistent with our observation that at high seeding densities the final overall cell number was low and significant debris was generated. Additional examination of the concentrations of different signaling factors in the media could help elucidate this further. Cardiac differentiation sensitivity to CHIR concentration has been previously reported and is known to be highly sensitive and variable across cell lines (Lian et al., 2012). Finally, the response to shaker speed variation elucidates a common challenge with pluripotent cell 3D culture that high speeds generate greater sheer stress leading to cell death and low speeds result in aggregation and reduced mixing which negatively effects differentiation potential (Otsuji et al., 2014; Vining and Mooney, 2017). Further scale up and different bioreactor formats will most likely require reassessment of mixing dynamics, but these results provide a framework for determining over or under mixing.

A key limitation and potential for future research is the scalability of the system presented in this work. The simplicity of the shaker flask system with its key advantage in accessibility also provides significant barriers in achieving larger culture volumes. Additional media decreases the surface area to volume ratio requiring advanced gas exchange systems to achieve comparable levels of oxygenation. Further, mass transport dynamics will require alternative vessel formats and mixing such as a stirred tank bioreactor (Kehoe et al., 2010; Olmer et al., 2012). Each of these modifications will require additional engineering and optimization such as the damage that arises with increased shear stress produced by faster impeller speeds. Finally, when considering future clinical applications additional regulatory needs must be met (xeno-free media compatibility and GMP-compliance) as well as manufacturing standardization and automation.

In conclusion, this report introduces an optimized protocol for differentiating suspensions of hiPSC spheroids into cardiomyocytes in a widely available format. Our method produces exceptionally pure (>98%) hiPSC-CM populations with low variation between batches and can function as a groundwork for future bioreactor systems to produce the large number of cells needed for clinical applications.

## DATA AVAILABILITY STATEMENT

The raw data supporting the conclusions of this article will be made available by the authors, without undue reservation.

## AUTHOR CONTRIBUTIONS

AK-K developed the differentiation protocol, designed the experiments, performed histology and imaging, prepared the sample, and wrote the manuscript. DP assisted in experimental design, sample staining, and imaging. JO performed cell culture and assisted in experimental design. VF and JB reviewed the manuscript. SL assisted with histological processing, imaging, and analysis. XL and JZ provided project leadership, funding acquisition, method development and manuscript revisions. All authors contributed to the article and approved the submitted version.

## FUNDING

This research was funded by the National Heart, Lung, and Blood Institute (Grant Nos. R01HL114120, R01HL131017, R01HL149137, and U01HL134764), the American Heart Association (Grant No. 19PRE34380402) to AK-K, the National Institute of General Medical Sciences (Grant No. T32GM008361), and the National Institute of Biomedical Imaging and Bioengineering (Grant No. T32EB023872).

## ACKNOWLEDGMENTS

We would like to thank the UAB Comprehensive Flow Cytometry Core, the UAB High-Resolution Imaging Facility as well as the UAB Pathology Core Lab for their assistance with sample preparation.

## SUPPLEMENTARY MATERIAL

The Supplementary Material for this article can be found online at: https://www.frontiersin.org/articles/10.3389/fbioe.2021.674260/full#supplementary-material

## REFERENCES

Abbasalizadeh, S., Larijani, M. R., Samadian, A., and Baharvand, H. (2012). Bioprocess development for mass production of size-controlled human pluripotent stem cell aggregates in stirred suspension bioreactor. *Tissue Eng. Part C Methods* 18, 831–851. doi: 10.1089/ten.tec.2012.0161

Amit, M., Laevsky, I., Miropolsky, Y., Shariki, K., Peri, M., and Itskovitz-Eldor, J. (2011). Dynamic suspension culture for scalable expansion of undifferentiated

human pluripotent stem cells. *Nat. Protoc.* 6, 572–579. doi: 10.1038/nprot.2011.325

Beauchamp, P., Jackson, C. B., Ozhathil, L. C., Agarkova, I., Galindo, C. L., Sawyer, D. B., et al. (2020). 3D Co-culture of hiPSC-derived cardiomyocytes with cardiac fibroblasts improves tissue-like features of cardiac spheroids. *Front. Mol. Biosci.* 7:14. doi: 10.3389/fmolb.2020.00014

Bedada, F. B., Chan, S. S.-K., Metzger, S. K., Zhang, L., Zhang, J., Garry, D. J., et al. (2014). Acquisition of a quantitative, stoichiometrically conserved ratiometric marker of maturation status in stem cell-derived cardiac myocytes. *Stem Cell Rep.* 3, 594–605. doi: 10.1016/j.stemcr.2014.07.012

Biermann, M., Cai, W., Lang, D., Hermsen, J., Profio, L., Zhou, Y., et al. (2019). Epigenetic priming of human pluripotent stem cell-derived cardiac progenitor cells accelerates cardiomyocyte maturation. *Stem Cells* 37, 910–923. doi: 10.1002/stem.3021

Breckwoldt, K., Letuffe-Brenière, D., Mannhardt, I., Schulze, T., Ulmer, B., Werner, T., et al. (2017). Differentiation of cardiomyocytes and generation of human engineered heart tissue. *Nat. Protoc.* 12, 1177–1197. doi: 10.1038/nprot.2017.033

Cai, W., Zhang, J., Lange, W. J. D., Gregorich, Z. R., Karp, H., Farrell, E. T., et al. (2019). Unbiased proteomics method to assess the maturation of human pluripotent stem cell-derived cardiomyocytes. *Circ. Res.* 125, 936–953. doi: 10.1161/circresaha.119.315305

Chang, S., Finklea, F., Williams, B., Hammons, H., Hodge, A., Scott, S., et al. (2020). Emulsion-based encapsulation of pluripotent stem cells in hydrogel microspheres for cardiac differentiation. *Biotechnol. Progr.* 36:e2986. doi: 10.1002/btpr.2986

Chen, V. C., Ye, J., Shukla, P., Hua, G., Chen, D., Lin, Z., et al. (2015). Development of a scalable suspension culture for cardiac differentiation from human pluripotent stem cells. *Stem Cell Res.* 15, 365–375. doi: 10.1016/j.scr.2015.08.002

Chong, J. J. H., Yang, X., Don, C. W., Minami, E., Liu, Y.-W., Weyers, J. J., et al. (2014). Human embryonic-stem-cell-derived cardiomyocytes regenerate non-human primate hearts. *Nature* 510, 273–277. doi: 10.1038/nature13233

Correia, C., Koshkin, A., Duarte, P., Hu, D., Carido, M., Sebastião, M. J., et al. (2018). 3D aggregate culture improves metabolic maturation of human pluripotent stem cell derived cardiomyocytes. *Biotechnol. Bioeng.* 115, 630–644. doi: 10.1002/bit.26504

Dunn, K. K., and Palecek, S. P. (2018). Engineering scalable manufacturing of high-quality stem cell-derived cardiomyocytes for cardiac tissue repair. *Front. Med.* 5:110. doi: 10.3389/fmed.2018.00110

Fonoudi, H., Ansari, H., Abbasalizadeh, S., Blue, G. M., Aghdami, N., Winlaw, D. S., et al. (2016). Large-scale production of cardiomyocytes from human pluripotent stem cells using a highly reproducible small molecule-based differentiation protocol. *J. Vis. Exp. JOVE* 2016:54276. doi: 10.3791/54276

Fonoudi, H., Ansari, H., Abbasalizadeh, S., Larijani, M. R., Kiani, S., Hashemizadeh, S., et al. (2015). A universal and robust integrated platform for the scalable production of human cardiomyocytes from pluripotent stem cells. *Stem Cell Transl. Med.* 4, 1482–1494. doi: 10.5966/sctm.2014-0275

Gao, L., Wang, L., Wei, Y., Krishnamurthy, P., Walcott, G. P., Menasché, P., et al. (2020). Exosomes secreted by hiPSC-derived cardiac cells improve recovery from myocardial infarction in swine. *Sci. Transl. Med.* 12:eaay1318. doi: 10.1126/scitranslmed.aay1318

Giacomelli, E., Meraviglia, V., Campostrini, G., Cochrane, A., Cao, X., van Helden, R. W. J., et al. (2020). Human-iPSC-derived cardiac stromal cells enhance maturation in 3d cardiac microtissues and reveal non-cardiomyocyte contributions to heart disease. *Cell Stem Cell* 26, 862–879.e11. doi: 10.1016/j.stem.2020.05.004

Guo, Y., and Pu, W. T. (2020). Cardiomyocyte maturation. *Circ. Res.* 126, 1086–1106. doi: 10.1161/circresaha.119.315862

Gupta, M. K., Illich, D. J., Gaarz, A., Matzkies, M., Nguemo, F., Pfannkuche, K., et al. (2010). Global transcriptional profiles of beating clusters derived from human induced pluripotent stem cells and embryonic stem cells are highly similar. *BMC Dev. Biol.* 10:98. doi: 10.1186/1471-213x-10-98

Halloin, C., Schwanke, K., Löbel, W., Franke, A., Szepes, M., Biswanath, S., et al. (2019). Continuous WNT control enables advanced hpsc cardiac processing and prognostic surface marker identification in chemically defined suspension culture. *Stem Cell Rep.* 13, 366–379. doi: 10.1016/j.stemcr.2019.06.004

Hamad, S., Derichsweiler, D., Papadopoulos, S., Nguemo, F., Šarić, T., Sachinidis, A., et al. (2019). Generation of human induced pluripotent stem cell-derived cardiomyocytes in 2D monolayer and scalable 3D suspension bioreactor cultures with reduced batch-to-batch variations. *Theranostics* 9, 7222–7238. doi: 10.7150/thno.32058

Jackman, C. P., Ganapathi, A. M., Asfour, H., Qian, Y., Allen, B. W., Li, Y., et al. (2018). Engineered cardiac tissue patch maintains structural and electrical properties after epicardial implantation. *Biomaterials* 159, 48–58. doi: 10.1016/j.biomaterials.2018.01.002

Jeziorowska, D., Fontaine, V., Jouve, C., Villard, E., Dussaud, S., Akbar, D., et al. (2017). Differential sarcomere and electrophysiological maturation of human ipsc-derived cardiac myocytes in monolayer vs. aggregation-based differentiation protocols. *Int. J. Mol. Sci.* 18:1173. doi: 10.3390/ijms18061173

Kehoe, D. E., Jing, D., Lock, L. T., and Tzanakakis, E. S. (2010). Scalable stirred-suspension bioreactor culture of human pluripotent stem cells. *Tissue Eng. Pt. A* 16, 405–421. doi: 10.1089/ten.tea.2009.0454

Kempf, H., Andree, B., and Zweigerdt, R. (2016). Large-scale production of human pluripotent stem cell derived cardiomyocytes. *Adv. Drug Deliv. Rev.* 96, 18–30. doi: 10.1016/j.addr.2015.11.016

Kempf, H., Kropp, C., Olmer, R., Martin, U., and Zweigerdt, R. (2015). Cardiac differentiation of human pluripotent stem cells in scalable suspension culture. *Nat. Protoc.* 10, 1345–1361. doi: 10.1038/nprot.2015.089

Kempf, H., Olmer, R., Kropp, C., Rückert, M., Jara-Avaca, M., Robles-Diaz, D., et al. (2014). Controlling expansion and cardiomyogenic differentiation of human pluripotent stem cells in scalable suspension culture. *Stem Cell Rep.* 3, 1132–1146. doi: 10.1016/j.stemcr.2014.09.017

Kropp, C., Massai, D., and Zweigerdt, R. (2016). Progress and challenges in large-scale expansion of pluripotent stem cells. *Process. Biochem.* 59, 244–254. doi: 10.1016/j.procbio.2016.09.032

Kubalak, S. W., Miller-Hance, W. C., O'Brien, T. X., Dyson, E., and Chien, K. R. (1994). Chamber specification of atrial myosin light chain-2 expression precedes septation during murine cardiogenesis. *J. Biol. Chem.* 269, 16961–16970. doi: 10.1016/s0021-9258(19)89483-8

LaBarge, W., Mattappally, S., Kannappan, R., Fast, V. G., Pretorius, D., Berry, J. L., et al. (2019). Maturation of three-dimensional, hiPSC-derived cardiomyocyte spheroids utilizing cyclic, uniaxial stretch and electrical stimulation. *PLoS One* 14:e0219442. doi: 10.1371/journal.pone.0219442

Laco, F., Lam, A. T.-L., Woo, T.-L., Tong, G., Ho, V., Soong, P.-L., et al. (2020). Selection of human induced pluripotent stem cells lines optimization of cardiomyocytes differentiation in an integrated suspension microcarrier bioreactor. *Stem Cell Res. Ther.* 11:118. doi: 10.1186/s13287-020-01618-6

Laco, F., Woo, T. L., Zhong, Q., Szmyd, R., Ting, S., Khan, F. J., et al. (2018). Unraveling the inconsistencies of cardiac differentiation efficiency induced by the GSK3β inhibitor CHIR99021 in human pluripotent stem cells. *Stem Cell Rep.* 10, 1851–1866. doi: 10.1016/j.stemcr.2018.03.023

Lattermann, C., and Büchs, J. (2016). "Design and operation of microbioreactor systems for screening and process development: design, operation and novel applications," in *Bioreactors*, ed. C. F. Mandenius (Hoboken NJ: Wiley), 35–76. doi: 10.1002/9783527683369.ch2

Le, M. N. T., and Hasegawa, K. (2019). Expansion culture of human pluripotent stem cells and production of cardiomyocytes. *Bioeng* 6:48. doi: 10.3390/bioengineering6020048

Le, M. N. T., Takahi, M., Maruyama, K., Kurisaki, A., and Ohnuma, K. (2018). Cardiac differentiation at an initial low density of human-induced pluripotent stem cells. *In Vitro Cell. Dev. Biol. Anim.* 54, 513–522. doi: 10.1007/s11626-018-0276-0

Leitolis, A., Robert, A. W., Pereira, I. T., Correa, A., and Stimamiglio, M. A. (2019). Cardiomyogenesis modeling using pluripotent stem cells: the role of microenvironmental signaling. *Front. Cell Dev. Biol.* 7:164. doi: 10.3389/fcell.2019.00164

Lian, X., Hsiao, C., Wilson, G., Zhu, K., Hazeltine, L. B., Azarin, S. M., et al. (2012). Robust cardiomyocyte differentiation from human pluripotent stem cells via temporal modulation of canonical Wnt signaling. *Proc. Natl. Acad. Sci. U.S.A.* 109, E1848–E1857. doi: 10.1073/pnas.1200250109

Linkermann, A., Kunzendorf, U., and Krautwald, S. (2014). Phosphorylated MLKL causes plasma membrane rupture. *Mol. Cell Oncol.* 1:e29915. doi: 10.4161/mco.29915

Liu, B., Lee, B. W., Nakanishi, K., Villasante, A., Williamson, R., Metz, J., et al. (2018). Cardiac recovery via extended cell-free delivery of extracellular vesicles secreted by cardiomyocytes derived from induced pluripotent stem cells. *Nat. Biomed. Eng.* 2, 293–303. doi: 10.1038/s41551-018-0229-7

Mahdavi, V., Lompre, A. M., Chambers, A. P., and Nadal-Ginard, B. (1984). Cardiac myosin heavy chain isozymic transitions during development and under pathological conditions are regulated at the level of mRNA availability. *Eur. Heart J.* 5, 181–191. doi: 10.1093/eurheartj/5.suppl_f.181

Mazzola, M., and Pasquale, E. D. (2020). Toward cardiac regeneration: combination of pluripotent stem cell-based therapies and bioengineering strategies. *Front. Bioeng. Biotechnol.* 8:455. doi: 10.3389/fbioe.2020.00455

Meyer, T., Tiburcy, M., and Zimmermann, W.-H. (2019). Cardiac macrotissues-on-a-plate models for phenotypic drug screens. *Adv. Drug Deliv. Rev.* 140, 93–100. doi: 10.1016/j.addr.2019.03.002

Mills, R. J., Parker, B. L., Quaife-Ryan, G. A., Voges, H. K., Needham, E. J., Bornot, A., et al. (2019). Drug screening in human psc-cardiac organoids identifies pro-proliferative compounds acting via the mevalonate pathway. *Cell Stem Cell* 24, 895–907.e6. doi: 10.1016/j.stem.2019.03.009

Miwa, T., Idiris, A., and Kumagai, H. (2020). A novel cardiac differentiation method of a large number and uniformly-sized spheroids using microfabricated culture vessels. *Regen. Ther.* 15, 18–26. doi: 10.1016/j.reth.2020.04.008

Negroni, A., Colantoni, E., Pierdomenico, M., Palone, F., Costanzo, M., Oliva, S., et al. (2017). RIP3 AND pMLKL promote necroptosis-induced inflammation and alter membrane permeability in intestinal epithelial cells. *Digest Liver Dis.* 49, 1201–1210. doi: 10.1016/j.dld.2017.08.017

Noor, N., Shapira, A., Edri, R., Gal, I., Wertheim, L., and Dvir, T. (2019). 3D printing of personalized thick and perfusable cardiac patches and hearts. *Adv. Sci.* 6:1900344. doi: 10.1002/advs.201900344

Olmer, R., Lange, A., Selzer, S., Kasper, C., Haverich, A., Martin, U., et al. (2012). Suspension culture of human pluripotent stem cells in controlled. stirred bioreactors. *Tissue Eng. Part C Methods* 18, 772–784. doi: 10.1089/ten.tec.2011.0717

Otsuji, T. G., Bin, J., Yoshimura, A., Tomura, M., Tateyama, D., Minami, I., et al. (2014). A 3D sphere culture system containing functional polymers for large-scale human pluripotent stem cell production. *Stem Cell Rep.* 2, 734–745. doi: 10.1016/j.stemcr.2014.03.012

Pretorius, D., Kahn-Krell, A. M., LaBarge, W. C., Lou, X., Kannappan, R., Pollard, A. E., et al. (2020). Fabrication and characterization of a thick, viable bi-layered stem cell-derived surrogate for future myocardial tissue regeneration. *Biomed. Mater.* 16:035007. doi: 10.1088/1748-605x/abc107

Reiser, P. J., Portman, M. A., Ning, X.-H., and Moravec, C. S. (2001). Human cardiac myosin heavy chain isoforms in fetal and failing adult atria and ventricles. *Am. J. Physiol. Heart C* 280, H1814–H1820. doi: 10.1152/ajpheart.2001.280.4.h1814

Shafa, M., Krawetz, R., Zhang, Y., Rattner, J. B., Godollei, A., Duff, H. J., et al. (2011). Impact of stirred suspension bioreactor culture on the differentiation of murine embryonic stem cells into cardiomyocytes. *BMC Cell Biol.* 12:53. doi: 10.1186/1471-2121-12-53

Sharma, A., Li, G., Rajarajan, K., Hamaguchi, R., Burridge, P. W., and Wu, S. M. (2015). Derivation of highly purified cardiomyocytes from human induced pluripotent stem cells using small molecule-modulated differentiation and subsequent glucose starvation. *J. Vis. Exp.* 2015:52628. doi: 10.3791/52628

Ting, S., Chen, A., Reuveny, S., and Oh, S. (2014). An intermittent rocking platform for integrated expansion and differentiation of human pluripotent stem cells to cardiomyocytes in suspended microcarrier cultures. *Stem Cell Res.* 13, 202–213. doi: 10.1016/j.scr.2014.06.002

Ting, S., Lam, A., Tong, G., Chen, A., Wei, H., Wu, J., et al. (2018). Meticulous optimization of cardiomyocyte yields in a 3-stage continuous integrated agitation bioprocess. *Stem Cell Res.* 31, 161–173. doi: 10.1016/j.scr.2018.07.020

Uosaki, H., Cahan, P., Lee, D. I., Wang, S., Miyamoto, M., Fernandez, L., et al. (2015). Transcriptional landscape of cardiomyocyte maturation. *Cell Rep.* 13, 1705–1716. doi: 10.1016/j.celrep.2015.10.032

Valls-Margarit, M., Iglesias-García, O., Guglielmo, C. D., Sarlabous, L., Tadevosyan, K., Paoli, R., et al. (2019). Engineered macroscale cardiac constructs elicit human myocardial tissue-like functionality. *Stem Cell Rep.* 13, 207–220. doi: 10.1016/j.stemcr.2019.05.024

van den Berg, C. W., Okawa, S., Chuva de Sousa Lopes, S. M., van Iperen, L., Passier, R., Braam, S. R., et al. (2015). Transcriptome of human foetal heart compared with cardiomyocytes from pluripotent stem cells. *Development* 142, 3231–3238. doi: 10.1242/dev.123810

Vining, K. H., and Mooney, D. J. (2017). Mechanical forces direct stem cell behaviour in development and regeneration. *Nat. Rev. Mol. Cell Bio.* 18, 728–742. doi: 10.1038/nrm.2017.108

Xu, X. Q., Soo, S. Y., Sun, W., and Zweigerdt, R. (2009). Global expression profile of highly enriched cardiomyocytes derived from human embryonic stem cells. *Stem Cells* 27, 2163–2174. doi: 10.1002/stem.166

Yang, H., Zhong, W., Hamidi, M. R., Zhou, G., and Liu, C. (2019). Functional improvement and maturation of human cardiomyocytes derived from human pluripotent stem cells by barbaloin preconditioning. *Acta Bioch. Bioph. Sin.* 51, 1041–1048. doi: 10.1093/abbs/gmz090

Yang, X., Pabon, L., and Murry, C. E. (2014). Engineering adolescence. *Circ. Res.* 114, 511–523. doi: 10.1161/circresaha.114.300558

Yeung, E., Fukunishi, T., Bai, Y., Bedja, D., Pitaktong, I., Mattson, G., et al. (2019). Cardiac Regeneration using human iPSC-derived BIomaterial-free 3D bioprinted cardiac patch in vivo. *J. Tissue Eng. Regen. M* 13, 2031–2039. doi: 10.1002/term.2954

Zhang, L., Guo, J., Zhang, P., Xiong, Q., Wu, S. C., Xia, L., et al. (2018). Derivation and high engraftment of patient-specific cardiomyocyte sheet using induced pluripotent stem cells generated from adult cardiac fibroblast. *Circ. Hear Fail* 8, 156–166. doi: 10.1161/circheartfailure.114.001317

Zhu, X., Ding, S., Li, H., Zhang, Z., Xu, L., Wu, J., et al. (2020). Disruption of histamine/H1R signaling pathway represses cardiac differentiation and maturation of human induced pluripotent stem cells. *Stem Cell Res. Ther.* 11:27. doi: 10.1186/s13287-020-1551-z

Zweigerdt, R., Andree, B., Kropp, C., and Kempf, H. (2016). "Bioreactors for expansion of pluripotent stem cells and their differentiation to cardiac cells: design, operation and novel applications," in *Bioreactors*, ed. C. F. Mandenius (Hoboken NJ: Wiley), 175–200. doi: 10.1002/9783527683369.ch6

**Conflict of Interest:** The authors declare that the research was conducted in the absence of any commercial or financial relationships that could be construed as a potential conflict of interest.

frontiers in Bioengineering and Biotechnology

REVIEW
published: 20 July 2021
doi: 10.3389/fbioe.2021.683079

# Adhesive Tissue Engineered Scaffolds: Mechanisms and Applications

*Shuai Chen[1], Carmen J. Gil[1], Liqun Ning[1], Linqi Jin[1], Lilanni Perez[1], Gabriella Kabboul[1], Martin L. Tomov[1] and Vahid Serpooshan[1,2,3]**

[1] Department of Biomedical Engineering, Emory University School of Medicine, Georgia Institute of Technology, Atlanta, GA, United States, [2] Department of Pediatrics, Emory University School of Medicine, Atlanta, GA, United States, [3] Children's Healthcare of Atlanta, Atlanta, GA, United States

A variety of suture and bioglue techniques are conventionally used to secure engineered scaffold systems onto the target tissues. These techniques, however, confront several obstacles including secondary damages, cytotoxicity, insufficient adhesion strength, improper degradation rate, and possible allergic reactions. Adhesive tissue engineering scaffolds (ATESs) can circumvent these limitations by introducing their intrinsic tissue adhesion ability. This article highlights the significance of ATESs, reviews their key characteristics and requirements, and explores various mechanisms of action to secure the scaffold onto the tissue. We discuss the current applications of advanced ATES products in various fields of tissue engineering, together with some of the key challenges for each specific field. Strategies for qualitative and quantitative assessment of adhesive properties of scaffolds are presented. Furthermore, we highlight the future prospective in the development of advanced ATES systems for regenerative medicine therapies.

**Keywords: adhesive tissue engineering scaffold, tissue regeneration, scaffold, bone regeneration, cartilage regeneration, nerve regeneration, cardiac regeneration, wound repair**

OPEN ACCESS

***Edited by:***
*Bin Li,*
*Soochow University, China*

***Reviewed by:***
*Aijun Wang,*
*University of California, Davis, United States*
*Joaquim Miguel Oliveira,*
*University of Minho, Portugal*

***Correspondence:**
*Vahid Serpooshan*
*vahid.serpooshan@bme.gatech.edu*

***Specialty section:***
*This article was submitted to Tissue Engineering and Regenerative Medicine, a section of the journal Frontiers in Bioengineering and Biotechnology*

***Received:*** *19 March 2021*
***Accepted:*** *15 June 2021*
***Published:*** *20 July 2021*

***Citation:***
*Chen S, Gil CJ, Ning L, Jin L, Perez L, Kabboul G, Tomov ML and Serpooshan V (2021) Adhesive Tissue Engineered Scaffolds: Mechanisms and Applications. Front. Bioeng. Biotechnol. 9:683079. doi: 10.3389/fbioe.2021.683079*

## INTRODUCTION

Traditionally, adhesive biomaterials are classified into hemostats, sealants, and tissue adhesives (Lauto et al., 2008). Hemostats mainly function by increasing blood coagulation (Hickman et al., 2018). Sealants are the ones that adhere to tissues and act as a barrier to prevent leakage (Sanders and Nagatomi, 2014). Meanwhile tissue adhesives provide stronger adhesive ability to hold tissues together (Burks and Spotnitz, 2014; Ge and Chen, 2020). Conventional tissue adhesives and sealants could be used in cases of blood vessel anastomosis, lung leakage preventions, and incision closure. Examples of tissue adhesives and sealants are cyanoacrylates, albumin, glutaraldehyde, polyethylene glycol (PEG) polymers, and fibrin sealant (Ge and Chen, 2020; Nam and Mooney, 2021). Tissue adhesives and sealants are also used as glue for the application of non-adhesive scaffold devices, aiding to fix the scaffold on the surface of organs and tissues (Ma et al., 2021). However, most tissue adhesives and sealants lack the specific requirements for use as a proper scaffold system for tissue regeneration. Main limitations include: (1) tissue adhesives and sealants are typically used to close incisions but not qualified for filling in larger gaps and defects (Shirzaei Sani et al., 2019); and (2) tissue adhesives and sealants, although showing a degree of biocompatibility and biodegradability, are not specifically designed to support various cellular activities that are needed

for tissue regeneration and usually cause side effects. For example, fibrin sealants may cause viral or infection complications. They also usually lack enough adhesive strength (Spotnitz, 2014). Cyanoacrylate could cause inflammation by toxic degradation products and exothermic reaction by polymerization (Pascual et al., 2016). Also, its stiffness may not be compatible to soft tissues. Albumin and glutaraldehyde have side effects such as infection and delayed wound healing (Furst and Banerjee, 2005). PEG lacks proper biodegradability and may have a chronic inflammation response and potential of swelling up to 350 to 400% of its volume (Lauto et al., 2008; Burks and Spotnitz, 2014; Bhagat and Becker, 2017; Malki et al., 2018). These side effects disqualify most of these materials as proper cell carriers and ECM analogs, and prevent their usage in large quantities when applied to human body.

To address the limitations of traditional adhesive biomaterials, adhesive tissue engineering scaffolds (ATESs) have been developed to repair damaged tissues and guide tissue regeneration after trauma and degeneration (Vermonden et al., 2008; Wiltsey et al., 2015; Ark et al., 2016). As a new generation of adhesive systems, ATESs provide a 3-dimensional (3D) biomimetic and highly biocompatible environment for cell adhesion, growth, differentiation, proliferation, secretion of extracellular matrix (ECM) proteins, as well as remodeling and replacement of the scaffold with regenerated tissue during matrix degradation (Ark et al., 2016; Boyadzhieva et al., 2019). Notably, ATESs can firmly adhere onto the tissue surface without the help of glue, sutures, or other additional fixtures, while providing the desired functions of the scaffolds (Boyadzhieva et al., 2019). ATESs could offer the following benefits: (1) they can be delivered and secured onto narrow or complicated structures in the human body where suturing or gluing might be difficult or impractical (Salzlechner et al., 2020); (2) secondary damages by suturing and bio-incompatibility of commercial glues, such as toxicity of cyanoacrylate or allergies caused by fibrin glues, can be avoided; (3) the delivery of ATESs could be achieved through conduits or syringes, avoiding highly invasive operations; (4) the hindered cell migration between tissues and scaffolds caused by glue or other fixtures with low biocompatibility can be circumvented (Shin et al., 2019); and (5) specific scaffold systems, such as microgel sphere assemblies, can be readily integrated with the surrounding ECM (Xin et al., 2018). Therefore, by combining the advantages of functional scaffolding systems for cell growth and tissue regeneration, and the benefits of intrinsic adhesive products, ATESs can facilitate surgical operations and provide safer medical treatments for patients.

Over the past decade, ATESs have found increasing applications in the repair and regeneration of various organs and tissues, such as cartilage, bone, ocular, nerve, heart, and skin. Adhesive scaffolds can be engineered using different types of biomaterials, including hydrogels, assembled microgel spheres, foams, and electrospun patches. Despite the rapid advancement of the field, there are only a small number of review articles on the ATES systems. For instance, Hozumi and Nomizu reviewed the current progress made on the peptide-conjugated chitosan hydrogel systems as targeted cell-adhesive scaffolds in tissue engineering (Hozumi and Nomizu, 2018). The article mainly focused on the peptide–chitosan matrices and their applications for analyzing cell-biomaterial interactions. Thi et al. published a review on horseradish peroxidase (HRP)-catalyzed hydrogel as adhesive materials. However, the review focuses on the use of HRP-catalyzed hydrogels for hemostasis and drug and cell delivery purposes (Thi et al., 2019). Pei et al. also published a review on the polymer hydrogel bioadhesives, with a small section about bioadhesives for tissue engineering applications (Pei et al., 2021). In this article, we aim to provide a comprehensive review on a variety of tissue engineering scaffolds with adhesive properties. We will elaborate the specific requirements of ATES systems, their adhesion mechanisms, and applications in tissue engineering and regenerative medicine.

# MAIN CHARACTERISTICS AND REQUIREMENTS OF ATESs

## Basic Requirements of ATESs

In general, ATESs are designed to serve two purposes: adhesion (fixation) onto the tissue surfaces and mimicking the ECM niche for cell proliferation, differentiation, growth, to restore tissue structure and function. Based on these primary functions, the following properties are required for a 3D scaffold system to qualify as an ATES (**Table 1**): (1) sufficient adhesive properties to tolerate wet and dynamic *in vivo* environment and the various forces that exist; (2) biocompatibility and low cell toxicity that enable cell survival and function, as well as integration with the surrounding (host) native tissue; (3) proper biodegradation and swelling behavior that accommodates the tissue regeneration rate; (4) incorporated porosity and vasculature that provide sufficient oxygen and nutrients; (5) Young's modulus and stiffness that resemble those of the native tissue; and (6) elasticity or flexibility to withstand tensional or dynamic forces in cases such as nerve or myocardial regeneration (Lauto et al., 2008; Zaokari et al., 2020).

## Adhesion Mechanisms for ATESs

Adhesion to ATES requires interaction between surfaces of the scaffold and the recipient tissue, which could be achieved by molecular interactions and chain penetration and entanglement (**Figure 1**). Generally, binding in the molecular level between the scaffold and tissue can be categorized into ionic, covalent, hydrogen, Van der Waals, and hydrophobic bonding (Korde and Kandasubramanian, 2018). Ionic bonding is based on electrostatic interactions between positive charges of scaffold polymers, such as chitosan, and negative charges on cell surfaces (Gåserød et al., 1998). Covalent bonding, achieved by forming strong bonds through sharing electrons in pairs, is a commonly used strategy to achieve tough and persistent adhesive properties. Functional groups, such as succinimidyl succinate or catechol groups that chemically react with amine moieties on the tissue surface, can be introduced to the back bone of scaffold polymers and anchor the construct to the target tissue (Simson et al., 2013; Han et al., 2017). Hydrogen bonding is weaker than the ionic or covalent bonding, however, it offers the ability to reform after deformation in contrast to most covalent bonds. The hydrogen bond is the driving force of supramolecular adhesives and can

**TABLE 1 |** Main required properties for adhesive tissue engineering scaffolds (ATESs).

| Property | Characterization method | Design considerations | Approach considerations | Target value |
|---|---|---|---|---|
| Adhesive properties | Tensile adhesion test; shear adhesion test; wound closure test; burst pressure test; peeling test | Adhesion firmly after applying and in long term; tolerance of wet condition and stresses | Implying covalent and non-covalent interactions | Adhesion strength 1KPa–1MPa |
| Biocompatibility and low cell toxicity | AlamarBlue; MTT; *in vivo* compatibility tests | Low cell and tissue toxicity that allow cell growth and tissue regeneration | Using bio-compatible materials and adhesion mechanisms | Usually higher cell survival rates are preferred. |
| Biodegradation and swelling behavior | *In vivo* and *in vitro* degradation and swelling tests | Low swelling ratios that do not affect design pattern or exert pressure to tissue; proper degradation behavior that accommodates tissue regeneration rate | Choosing proper materials with intrinsic low swelling behavior and proper degradation rate; proper crosslink density; proper chain length for polymers | Low swelling ratio is preferred; 20–25% of materials is left after 4 weeks of degradation *in vivo* |
| Porosity and vasculature | SEM; microscopy | Incorporation of vasculature or choosing materials with adequate porosity | 3D printed vascular system or choosing a proper base material and proper concentration and crosslink density | Optimal porosity and pore size highly depend on the tissue type and the specific application |
| Young's modulus and stiffness | Mechanical tests: indentation test; compression test | Strong enough for bone and cartilage repair; soft enough for patient comfort for corneal repair; ability to withstand tensile stress for nerve repair | Choosing proper material, concentration, and crosslink density | 1 KPa–100 MPa for cartilage and bone; 100 Pa – 100 KPa for corneal; and typically 100 Pa – 100 KPa for other tissues |

also be used as a supplemental force when scaffold material is protein or polysaccharide based. Van der Waals bond is even weaker than hydrogen bonding and provides supplementary force for tissue adhesion. Hydrophobic bonding is the entropy induced molecular interaction and aggregation within non-polar molecules under aqueous environment. Hydrophobic domains on scaffolds could interact with fibronectin and fibrillin in the ECM, on the surface of tissues, and improve adhesive strength (Nishiguchi et al., 2019; Nishiguchi and Taguchi, 2020). Specifically, such effect can improve adhesive properties under wet conditions by decreasing water layer at the interface between the scaffold and host tissue through repelling water molecules, which helps addressing one of the most challenging issues for adhesion *in vivo* (Wang B. et al., 2018). In a more recent effort, an adhesive hydrogel, consisting of polyacrylic acid, chitosan, tannic acid, and $Al^{3+}$, demonstrated strong and reversible underwater adhesion properties, owing to its electrostatic interactions and dynamic catechol chemistry (Duarte et al., 2020).

In addition to introducing functional groups, positive charges, and hydrophobic domains, increasing chain penetration into tissue is another way to achieve higher adhesive efficiency. One example is incorporating free PEG polymers that can increase adhesive potentials through free chain interpenetration into mucosa surfaces (Huang et al., 2000). It should be noted that in the design of ATESs, the introduction of adhesive properties should not affect biocompatibility, cell affinity, porosity, and biodegradation characteristics of the scaffold system for the optimal regenerative effects.

When applied *in vivo*, the interaction of the scaffold with body fluids and blood could affect its adhesive properties. Water molecules can form a boundary between the adhesive scaffold and tissue, mask the functional groups, and thus hinder adhesion processes. Non-covalent interactions can also be affected (Hou et al., 2020a). Efforts have been made to improve underwater adhesive properties through mimicking the mechanism that are active in marine animals such as mussels and sandcastle worms (Zhao et al., 2017). The keys to achieve underwater adhesion ability are the incorporation of L-3,4-dihydroxyphenylalanine (Dopa) and complex coacervation. Dopa provides a reversible chelation as well as covalent bonding with thiols and amines after oxidation. In complex coacervation, a denser liquid phase, separated from two fluid phases containing oppositely charged polyelectrolytes, binds to the wetted surface and triggers the underwater adhesion (Oh et al., 2014). In addition to these key mechanisms, other methods to enhance adhesion *in vivo* include hydrophobic interaction, double layer adhesion by zwitterions, increased surface unevenness of hydrogels (improves contact with adherends by repellence of liquid), incorporation of polymers that interpenetrate into the adherend and form interactions with chains of the substrate, and water absorbable dehydrated gelatin and poly (acrylic acid) films (Laura et al., 2017; Nishiguchi et al., 2019; Yuk et al., 2019; Hou et al., 2020a). In the case of ATESs, compatibility with native cells and tissues and the feasibility to form a 3D shaped construct should be also considered when selecting optimal methods for *in vivo* adhesion ability under wet conditions.

Adhesion under dynamic forces has been also a challenging concept. Adhesive cardiac scaffolds [i.e., cardiac patches (Serpooshan et al., 2013b, 2014; Serpooshan and Ruiz-Lozano, 2014)] applied to the surface of a beating heart are an example (Lin et al., 2019; Walker et al., 2019). The irregular and dynamic

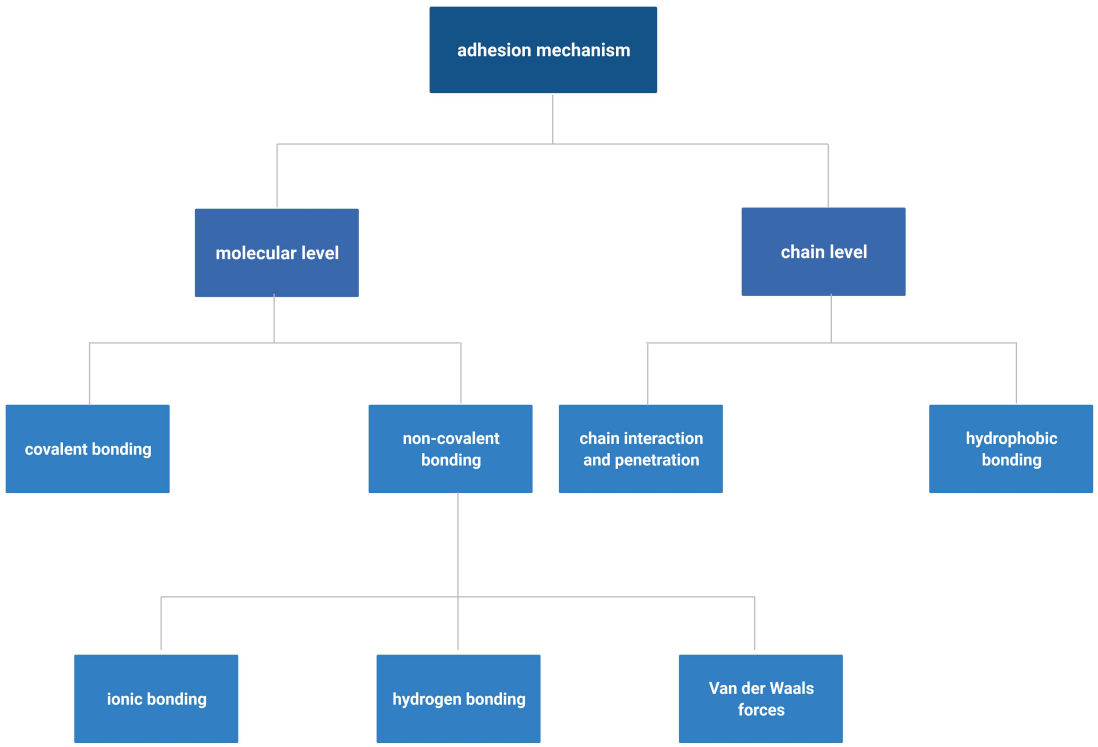


**FIGURE 1 |** Summary of different mechanisms of adhesion of tissue engineering scaffolds. Created with BioRender.com.

shape of the heart complicates maintaining the patch biomaterial in place, before curing and bonding formation with the tissue (Walker et al., 2019). The slippery wet surface together with the pulsatile motion make the cardiac patch adhesion one of the most challenging tasks, which requires strong adhesion and short curing and adhesion times under wet conditions. In the next section we will discuss advanced material options that been developed to meet such requirements.

Other mechanical requirements for ATES devices include tolerance to tension in applications such as nerve repair (Du et al., 2018), and to compression in cartilage and bone regeneration (Serpooshan et al., 2010, 2013a). Further, flexibility and elasticity of the scaffold are prominent in applications for lung and gastrointestinal adhesion (Tsuchiya et al., 2020). Also, harsh conditions in diseased states or post-surgery should be taken into account for *in vivo* applications (Zaokari et al., 2020). Such harsh conditions, such as low pH, oxidative environment, and high immune response, can affect degradation rate, swelling ratio, and cohesive strength of scaffolds, leading to a diminished adhesive strength in the long term (Taboada et al., 2020). In particular, lower pH can block amines on the tissue surface by amine protonation and hinder scaffold adhesive behavior based on covalent bonding with amine groups (Taboada et al., 2020). In summary, to manufacture an optimal ATES device for clinical and translational applications, the following material requirements must be fulfilled: (1) strong and durable adhesive properties; (2) the ability to form adhesion under wet conditions; (3) sufficient adhesive properties after partial degradation and swelling; (4) tolerance to tensile, compressive, and dynamic forces; and (5) sufficient adhesive strength under inflammatory conditions.

## Measurement of Adhesion Properties of ATESs

Adhesive strength is the core property of the ATESs. A variety of mechanical tests such as tensile strength, shearing strength, burst pressure, wound closure, and peeling adhesion tests are primarily used to probe adhesive strength of biomaterials (**Figure 2**; Shin et al., 2015). Tensile test is employed when the adhesive scaffold is used to provide a linkage, such as in nerve repairing implants (Muzhou et al., 2012; Assmann et al., 2017; Xin et al., 2017; Jouan and Constantinescu, 2018; Chandrasekharan et al., 2019; Hong et al., 2019; Yuk et al., 2019; Cadena et al., 2020). Tensile test to measure adhesive properties is conducted by attaching the scaffold between the target tissues that are connected to the two probes of a tensile tester. After sufficient time for adhesion, the probe is pulled at a determined speed and the tensile strength is recorded (Shin et al., 2015). For shearing adhesive strength, different setups are used based on variable geometries and ways of applying the shearing forces. A single lap shear test, thick adherent shear test, and the Arcan device (butterfly shape) transform tensile movement to shear forces, while napkin ring test uses a torsion loading mode (Muzhou et al., 2012; Jouan and Constantinescu, 2018). Burst pressure test investigates the

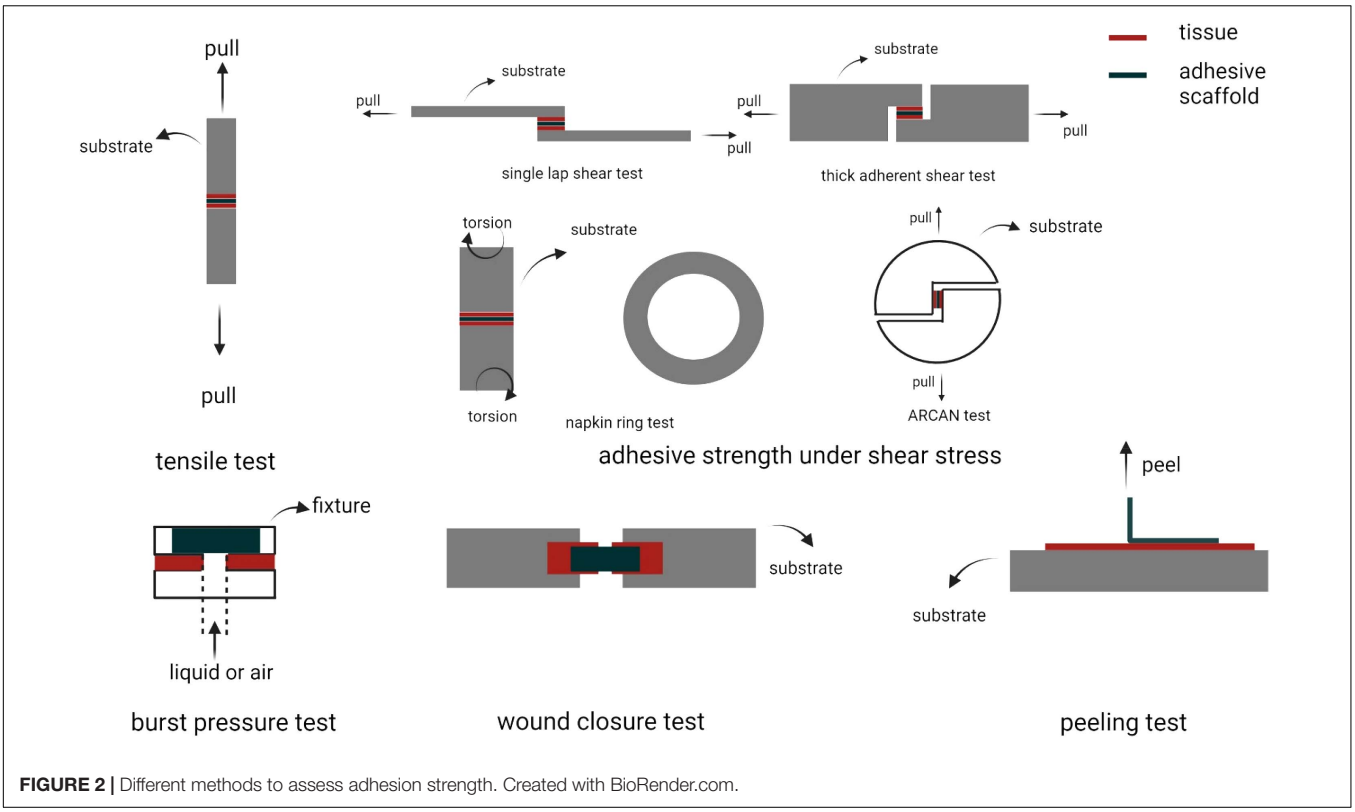


**FIGURE 2 |** Different methods to assess adhesion strength. Created with BioRender.com.

capability of scaffold to withstand air or fluid pressure. The tissue is fixed onto a device linked to a syringe pump. Subsequently, an incision of certain size is made in the tissue. After application of adhesive material to the damaged region and certain time for adhesive curing, liquid or air is applied with increasing pressure to the sample until bursting. The burst pressure is recorded as the highest pressure that the adhesive material could withstand before breakage (Assmann et al., 2017; Hong et al., 2019). Wound closure test can be examined according to ASTM F2458-05 standard. Two ends of a tissue piece for testing are glued to two slides and left with a gap. After incision in the middle, the tissue is re-united with adhesive material and then pulled by tensile stress until detachment (Chandrasekharan et al., 2019). Peeling test is used to measure interfacial adhesion toughness and is measured from the plateau force for either 180-degree or 90-degree peel test (Xin et al., 2017; Yuk et al., 2019).

Qualitative (or semi-quantitative) methods such as lifting heavy objects by adhesive material or twisting or bending the bound materials are also frequently used to demonstrate adequate adhesive properties (Liu X. et al., 2017). To better mimic the *in vivo* environment, tests could be conducted in aqueous solutions or by pre-wetting tissue scaffolds (Shoo and Stewart, 2010). Humid chambers could also be used to maintain moisture content and prevent dehydration (Mehdizadeh et al., 2012). Considering the complex geometries of tissues and the diverse loading types that can be applied to the adhesion site, a combination of multiple adhesion tests may be a better strategy for comprehensive analysis of the binding strength. Other properties such as swelling ratio, mechanical properties, biodegradability, porosity, and biocompatibility are extensively examined for ATES systems (Zhou et al., 2016; Han et al., 2018).

## APPLICATIONS OF ATESs

Due to many unique advantages that discussed above, ATES systems are being increasingly used in a variety of tissue engineering applications (**Table 2**). Here we review six of the most common fields of tissue engineering that have utilized adhesive scaffolds. For each case, we discuss the necessity of regenerative treatments, the challenges that current therapies face in each field, and the significance and the outlook of applying ATES devices as an alternative approach. Benefits of these adhesive scaffold systems in comparison to conventional tissue engineering strategies are elaborated.

### Nerve Regeneration

Peripheral nerve defect is a common injury and often lead to partial or complete loss of sensation or even permanent disability (Ichihara et al., 2008). Although nerves have an inherent regenerative capacity, transected nerves typically show hindered regeneration. Such damages often require surgical interventions (Soucy et al., 2018). Methods such as autografts have shown success in treating the damaged nerve, but they have limitations such as surgical incisions, donor site morbidity, and limited graft supply (Ray and Mackinnon, 2010). As an alternative, tissue scaffolds, or conduits, have been fabricated

**TABLE 2 |** List of various adhesive tissue engineering scaffold (ATES) systems along with the scaffold type, adhesion mechanism, and applications.

| Organ, Tissue | Scaffold type | Adhesion mechanism | Material(s) | Application(s) | |
|---|---|---|---|---|---|
| Nerve | Hydrogel | Covalent bonding (reaction between methacrylates and amines) | GelMA and MeTro | *In vitro* support of Schwann cell growth, outgrowth of encapsulated dorsal root ganglia | (Soucy et al., 2018) |
| | | Hydrogen bonds, π-cation, and electrostatic interactions | Chitosan and catechol modified ε-polylysine | *In vivo* repair of transected nerve fiber | (Zhou et al., 2016) |
| Cartilage | Hydrogel | Covalent bonding (Schiff's reaction) | Gelatin, borax, and oxidized alginate | *In vitro* support of chondrocyte proliferation and migration | (Balakrishnan et al., 2014) |
| | | Covalent bonding (conjugation of tyramines and tyrosines) | Sulfate and tyramine modified alginate | *In vitro* support of viability and re-differentiation of chondrocytes, *in vivo* support of secretion of chondrocytes | (Ztürk et al., 2020) |
| | | Covalent bonding (reaction between methacrylates and amines) | elastin-like polypeptide (ELP) combined with methacrylate modified hyaluronic acid (MeHA) | *In vitro* support of proliferation and migration of hMSCs and NIH-3T3 cells | (Shirzaei Sani et al., 2018) |
| | | Covalent bonding (reaction between quinone groups and amine, imidazole, and thiol groups) | Gelatin and tyramine modified hyaluronic acid | *In vitro* support of viability, proliferation, and promotion of rabbit meniscus fibro-chondrocytes | (Kim et al., 2018) |
| | | Covalent bonding (Schiff's reaction) for PNIPAAm-g-CS combined with aldehyde-modified chondroitin sulfate; hydrogen bonding and ionic bonding for PNIPAAm-g-CS with calcium alginate particles | Chondroitin sulfate grafted poly(N-isopropylacrylamide) (PNIPAAm-g-CS) combined with aldehyde-modified chondroitin sulfate; or PNIPAAm-g-CS with calcium alginate particles | *In vitro* support of viability of adipose derived stem cells and HEK-293 cells | (Wiltsey et al., 2015) |
| | | Covalent bonding (reaction between quinone groups and amino groups) | Catechol containing poly(2-alkyl-2-oxazoline) based polymers and fibrinogen | *In vitro* support of chondrocyte penetration, secretion, and cartilage tissue regeneration | (Berberich et al., 2019) |
| | | Hydrogen bonds, π-cation and electrostatic interactions | Polydopamine-chondroitin complex and polyacrylamide | *In vitro* support of proliferation and gene expression of bone marrow stem cells and chondrocytes; *in vivo* cartilage repair | (Han et al., 2018) |
| | | Covalent bonding (reaction between quinones and amino groups and between methacrylates and amines) | Methacrylate and 3,4-dihydroxyphenylalanine modified hyaluronic acid | *In vitro* adhesion to mouse hind limbs and support of 17IA4 cell viability | (Salzlechner et al., 2020) |
| | Micro-particles | Covalent bonding (Schiff's reaction) | N-(2-aminoethyl)-4-(4-(hydroxymethyl)-2-methoxy-5-nitrosophenoxy) butanamide decorated silk fibroin microparticles | *In vivo* cartilage regeneration | (Zhang et al., 2020) |
| | | Covalent bonding (reaction between PEG-NHS and amines) | norbornene-modified gelatin crosslinked by thiol-modified PEG | *In vitro* support of viability and secretion of hBMSCs. and cartilage tissue regeneration | (Fanyi et al., 2018) |

*(Continued)*

**TABLE 2 |** Continued

| Organ, Tissue | Scaffold type | Adhesion mechanism | Material(s) | Application(s) | |
|---|---|---|---|---|---|
| Cornea | Hydrogel | Covalent bonding (reaction between methacrylates and amines) | GelMA | *In vivo* repair of stromal and re-epithelialization of corneal defects | (Shirzaei Sani et al., 2019) |
| | | Hydrogen bonds, π-cation and electrostatic interactions | Dopamine modified hyaluronic acid | *In vitro* support of viability and expression of hASCs and LESC | (Koivusalo et al., 2019) |
| Skin | Hydrogel | Covalent bonding (reaction between methacrylates and amines) | GelMA | *In vivo* repair of wounds and promotion of vascularization | (Saleh et al., 2019) |
| | | Covalent bonding (amide bonds) | N-hydroxysuccinimide modified chondroitin sulfate cross-linked by PEG–$(NH_2)_6$ | *In vitro* support of viability of chondrocytes | (Strehin et al., 2010) |
| | | Hydrogen bonds and electrostatic interactions | polyurethane-poly(acrylamide) | *In vivo* repair of wounds | (Hou et al., 2020b) |
| | | Non-covalent hydrogen bonding generated between urethane esters and tissues | poly(ethylene glycol)and poly(sulfamethazine ester urethane) copolymer | *In vivo* repair of wounds | (Duy et al., 2018) |
| | | Hydrogen bonds and ionic interactions | Gelatin connected PCLA-bPEG-b-PCLA | *In vivo* repair of wounds | (Turabee et al., 2019) |
| Heart | Hydrogel | Covalent bonding (reaction between quinone groups and amino groups) | Catechol modified hyaluronic acid | *In vivo* treatment of myocardial infarction | (Shin et al., 2019) |
| | Electro-spun Patch | Covalent bonding (reaction between methacrylates and amines) and ionic bonds | choline-based bio-ionic liquid conjugated Gel MA | *In vivo* treatment of myocardial infarction | (Walker et al., 2019) |
| | | Denatured protein interlock | Albumin | *In vivo* adhesion to the heart surface | (Malki et al., 2018) |
| Bone | Hydrogel | Covalent bonding (reaction between methacrylates and amines), together with hydrogen bonds, π-cation and electrostatic interactions | Dopamine modified methacrylated alginate | *In vivo* bone regeneration | (Hasani-Sadrabadi et al., 2020) |
| | | Covalent bonding (Schiff's reaction) | Aldehyde modified hyaluronic acid | *In vitro* proliferation of hMSC | (Bermejo-Velasco et al., 2019) |
| | | Non-covalent nucleophile-phenolic bonding and $Ca^{2+}$-phenolic coordination bonds | Hydroxyapatite, tannic acid and silk fibroin | *In vitro* growth and differentiation of rat bone MSCs and *in vivo* repair of bone | (Bai et al., 2020) |
| | Foam | Non-covalent hydrogen bonding generated between urethane esters and tissues | Polyurethane | *In vivo* bone repair | (Lei et al., 2019) |

and used as bridges for damaged nerve reconnection. They have shown great promise to facilitate and guide the regrowth of neurites (Stephanie et al., 2017; Ning et al., 2019). The standard approach to connect the transected nerve with a scaffold is suturing which can mechanically fixate the artificial structure into the nerve (Barton et al., 2014). However, suturing has inadequate capacity for sealing the nerves, and also could cause secondary damages to the injured tissue and increase tension, which would lead to reduced angiogenesis, one of the key requirements for nerve regeneration (Kehoe et al., 2012; Bahm et al., 2018). Therefore, sutureless approaches, such as bioadhesives, have been developed and attracted increasing attention. They seal the sectioned nerves and bind the two tissue ends together. Among these adhesives, fibrin-based glues have been extensively used (Sameem et al., 2011; Wang W. et al., 2018). The infilled fibrin glues could further guide the growing direction of neurites with orientated microfibers, while inhibiting the encroachment of scar tissue (Liqun et al., 2018). However, fibrin glues do not fulfill the mechanical and adhesive strength requirements for neural repair under sutureless conditions due to their inherently low stiffness. Also, these glue materials pose a high risk of infection which further limits its applications (Mehall et al., 2002). Compared to fibrin, cyanoacrylate gules overcome the infection risks, but their inferior biocompatibility could lead to possible foreign body reaction and fibrosis (Wieken et al., 2003). Another hydrogel-type glue, PEG, has also been used in nerve repair (Robinson and Madison, 2016). PEG glue has the potential of incorporating bioactive molecules through covalent reaction and has short binding time under initiation of visible light. The major concern for using PEG-based glues is the low degradation rate, hence, the possibility of persisting graft years after implantation (Barton et al., 2014).

As an alternative to these conventional suturing and glue methods, ATESs can be used as an advanced approach that offers greater biocompatibility, lower secondary damage, adjustable adhesive and mechanical strength, and tunable shapes. For instance, composite scaffold systems have been made by photocrosslinking two natural polymers, gelatin-methacryloyl (gelMA), and methacryloyl-substituted tropoelastin (MeTro) (Soucy et al., 2018). The gelMA/MeTro scaffold demonstrated tunable physicochemical properties, such as degradation rate, that could be regulated to match the nerve growth rate. These hydrogels exhibited a remarkable adhesive strength to the nerve tissue, 15-fold greater than the control fibrin glue. Another example is a chitosan and catechol modified ε-polylysine (PL) based adhesive hydrogel. The adhesion ability comes from non-covalent hydrogen bonding, π-cation and ionic interactions formed between catechol and lysine groups with nerve epineurium. *In vivo* tests demonstrated the ability of re-connecting and repairing of transected nerve fiber (**Figure 3**; Zhou et al., 2016).

Future steps to further improve the function of ATESs in nerve regeneration include designing structures that could direct neural growth, incorporation of growth factors to promote cellular proliferation and/or function and integrating electrical stimulators or conductors. Also, the accuracy of axon reconnection with their original end-organ targets is essential because otherwise the generated nerve could be functionally compromised.

## Use of ATESs in Cartilage Repair

Cartilage regeneration is vital for mitigating osteoarthritis, orthopedic trauma, meniscus damage, and other degenerative diseases (Kim et al., 2018). The lack of vasculature and nerve system, together with limited migration ability of chondrocytes, impair cartilage self-regeneration capacity. When left untreated, these conditions lead to loss of mobility and advance into chronic diseases (Fanyi et al., 2018). One effective therapy could be scaffolds that are biocompatible and adhere to the entire damaged tissue, and can maintain encapsulated cells, promote chondrocyte proliferation, and activate glycosaminoglycan (GAG) and collagen secretion. Traditional scaffold grafting methods are suturing and glue. In the case of cartilage, suturing can cause loss of chondrocytes and proteoglycans, induced by insertion of the suturing needle, fissures in the wall of the suture channels, and propagation of exiting cracks under mechanical forces acting on the joint (Hunziker and Stähli, 2008). Glues could also cause various complication that were described in previous sections. For maxillofacial cartilage specifically, material fixation methods should bring minimal physical damage to nerves, have low infection rate, and be non-toxic considering their short distance to the brain. Therefore, conventional suture and glue methods are often challenging for the fixation of materials onto the maxillofacial cartilage. ATESs can solve this problem by offering great biocompatibility, minimally invasive delivery approach through syringes, and tunable and short adhesion time post-delivery (Salzlechner et al., 2020). For instance, a hyaluronic acid (HA) hydrogel, modified with both MA and Dopa groups, was applied under aqueous conditions, demonstrating a rapid gelation using a standard surgical light and an adequate adhesion to the muscle tissue (Salzlechner et al., 2020). The catechol functional groups in dopamine can bind to organic and inorganic substrates through covalent and non-covalent interactions and are frequently used in bio-adhesive materials as dopamine can be readily incorporated into the backbone of polymers. Another type of catechol based ATESs is fabricated by polydopamine-chondroitin complex and polyacrylamide, with the adhesion property coming from the non-covalent interactions brought by catechol (Han et al., 2018). The hydrogel supports proliferation and gene expression of bone marrow stem cells and chondrocytes *in vitro*. Further, *in vivo* experiments demonstrated the ability of the adhesive hydrogel to repair cartilage defects (**Figure 4A**).

Injectable hydrogels also offer a minimally invasive nature and could fit into complex and irregular geometries of the degenerated cartilage (Liu M. et al., 2017). Hydrogel scaffolds could provide protection against shear forces during injection and increase retention rate of cells as well as support cell migration, proliferation, and function (Liu M. et al., 2017; Li et al., 2019). The intrinsic adhesive ability of injectable hydrogels is essential for fixation of deposited biomaterial onto the damaged cartilage. Polymers such as gelatin, HA, and alginate could be used to develop injectable hydrogels with intrinsic adhesive

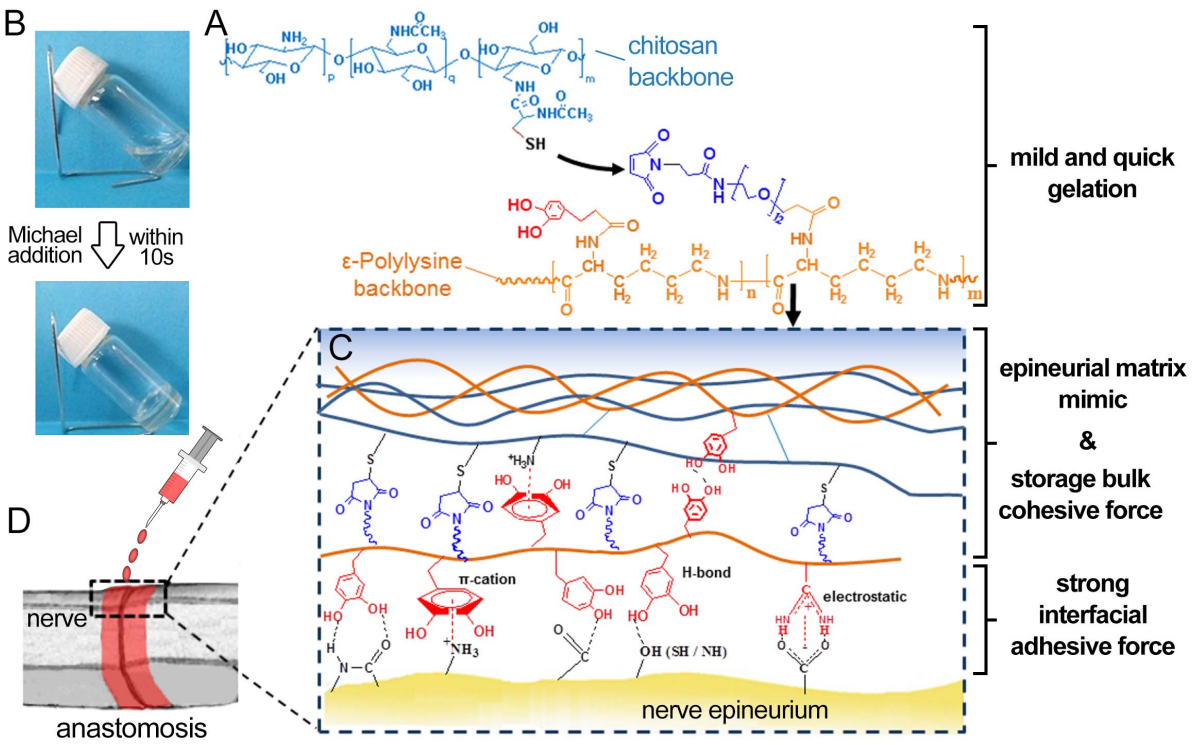


**FIGURE 3 |** Application of adhesive tissue engineering scaffold (ATES) in nerve repair. **(A)** Mechanism of Hydrogel Formation. **(B)** Transforming from prepolymer solution to hydrogel state. **(C)** Mechanism of adhesion between the hydrogel and the nerve epineurium. **(D)** Schematic demonstrating the application of ATES *in vivo*. Reconstructed with permission from Zhou et al. (2016).

properties. Functional groups in these polymers are used for the incorporation of crosslinkable moieties that can form covalent bonding with chemical groups, such as primary amines, on the cartilage tissue. For instance, oxidation can create functional groups such as aldehydes in alginate polymers. An adhesive injectable hydrogel scaffold composed of oxidized alginate, gelatin, and borax (as crosslinker) has been used to encapsulate chondrocytes (Balakrishnan et al., 2014). Alginate induced chondrocytes re-differentiation and gelatin promoted hydrogel-chondrocyte interaction. Aldehyde groups in oxidized alginate reacted with amine groups in gelatin and the surrounding tissue to elicit crosslinking of hydrogel and adhesion to the cartilage (Balakrishnan et al., 2014). In more recent works, an catechol modified chondroitin sulfate based adhesive hydrogel was fabricated for cartilage regeneration (Shin et al., 2021). Further, an injectable catechol group modified poly(2-alkyl-2-oxazoline) and fibrinogen based material was developed to treat cartilage defects (Berberich et al., 2019). Results from these studies suggested that injectable adhesive hydrogels solutions may provide an optimal solution for cartilage (and other) tissue repair due to their high tunability.

In another study, tyramine (TA) conjugated HA (TA-HA) combined with gelatin was used to form adhesive injectable hydrogel by tyrosinase (TYR)-mediated crosslinking and adhesion. HA is one of the major components of cartilage ECM and could help with cell proliferation, migration, and tissue regeneration. TA can be oxidized by TYR to generate quinone groups. These groups covalently bond with other phenolic moieties or amine, thiol, and imidazole groups in gelatin, for crosslinking, and with groups on tissue for adhesion (Kim et al., 2018). These adhesive injectable hydrogels encapsulated with cells can facilitate tissue regeneration through minimally invasive procedures.

To further facilitate nutrient and waste exchange within the ATES structure, microgel spheres have been also adapted as scaffold systems for articular cartilage repair (**Figure 4B**; Fanyi et al., 2018). To achieve rapid bonding between microgels for assembling into higher order structures, and also the adhesion between microgels and the surrounding tissue, 4-arm poly (ethylene glycol)-Nhydroxysuccinimide (NHS) has been used as a crosslinker (Fanyi et al., 2018). NIH forms covalent bonds with primary amines on gelatin based microgels and with the protein-rich cartilage tissue. Human bone marrow derived mesenchymal stem cells (hBMSCs) were encapsulated in these microgel assemblies exhibited significantly increased chondrogenic gene expression.

In summary, ATESs can aid cartilage regenerative processes by offering a minimally invasive delivery, a simplified surgical grafting operation, flexibility to treat small or complex defects, steady fixation without secondary damages or cytotoxicity, protection and retention of cells, and support of cellular proliferation and differentiation. In addition to these benefits,

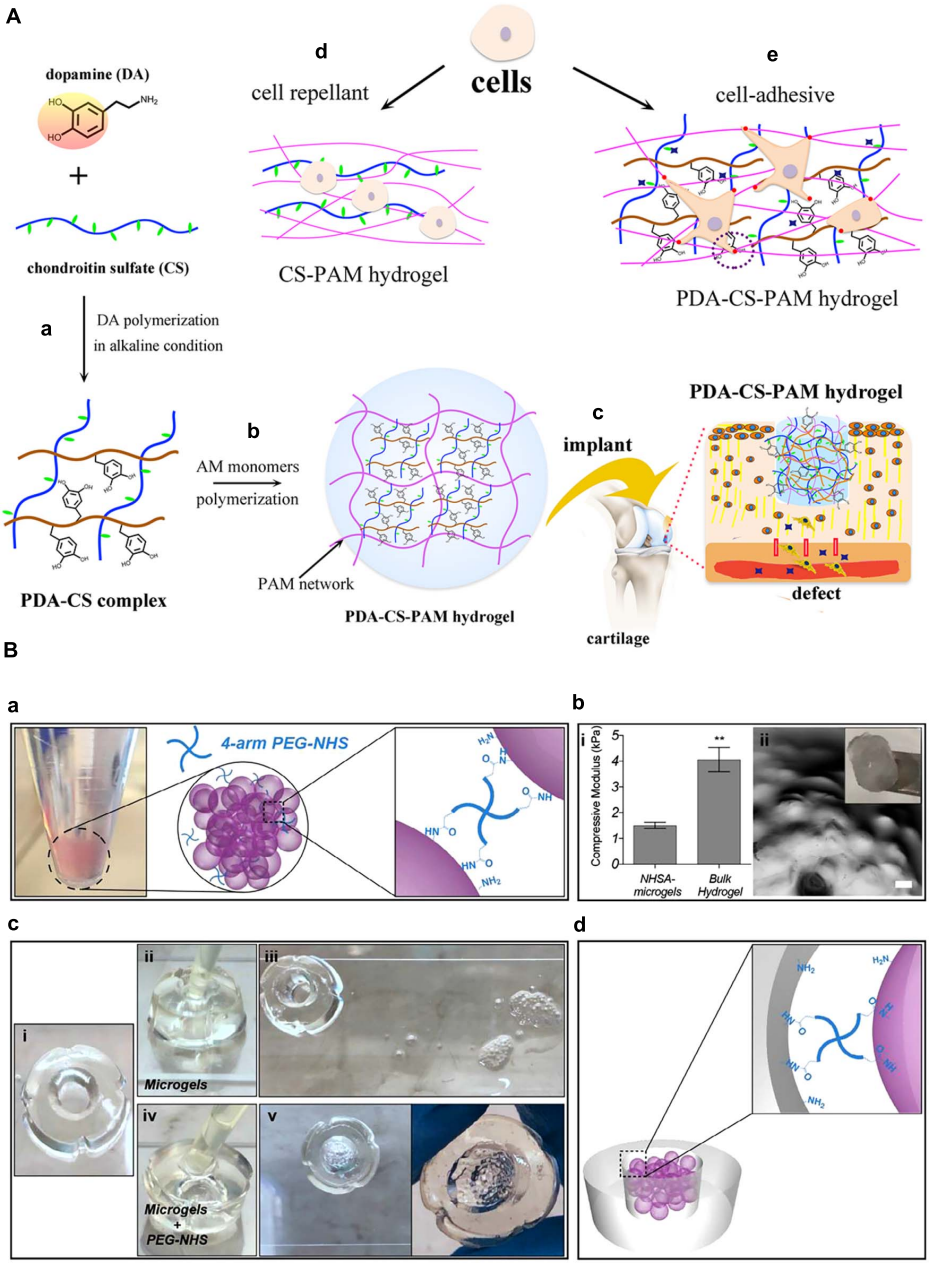


**FIGURE 4 |** Application of adhesive tissue engineering scaffolds (ATESs) in cartilage repair. **(A)** PDA-CS-PAM adhesive scaffold to regenerate cartilage. **(a)** Mechanism of PDA-CS complex fabrication. **(b)** Mechanism of PDA-CS-PAM hydrogel formation. **(c)** Schematic demonstration of the application of adhesive scaffold *in vivo*. **(d)** Cell repellence of CS-PAM hydrogel. **(e)** Promotion of cell adhesion to the hydrogel by addition of PDA. **(B)** Adhesive microgel systems for cartilage tissue engineering. **(a)** Assembly of microspheres induced by 4-arm PEG-NHS. **(b)** Assembled NHSA-microgels: **(i)** Compressive modulus of NHSA micro and bulk hydrogels by unconfined compression test; **(ii)** NHSA microgels on a spatula and under microscope (scale bar: 100 μm). **(c)** *In vitro* testing of adhesion ability: (**i**) Hollow gelatin hydrogel; **(ii,iii)** Injection of untreated microgels into the middle of the hollow hydrogel and no adhesion after 90 min; **(iv,v)** Injection of PEG-NHS treated microgel suspension into the middle of the hollow hydrogel and adhesion after incubation. **(d)** Demonstration of adhesion mechanism between microgels and tissue. $^{**}P < 0.01$. Reconstructed with permissions from Fanyi et al. (2018) and Han et al. (2018).

an ideal scaffold for cartilage repair should also demonstrate adequate tolerance to certain levels of forces and maintain effective adhesive strength under dynamic movements. These requirements must be addressed in the future endeavors on biomaterial selection and development.

## Corneal Regeneration Using ATESs

If left untreated, corneal injuries and infections might lead to eye shape deformations and even vision loss. Tissue grafting and corneal transplantation are standard treatments for corneal stromal defects (Yorston and Garg, 2009). Tissue grafting is

limited by the need for donor tissues, special equipment, and advanced skills, as well as potential transplant complications and rejection. Corneal transplantation has drawbacks brought by donor tissue shortage and high expense of transplantation surgery. Also, if suturing is applied, the process not only requires high skill levels from the surgery team and a relatively long time for operation, but can also cause multiple complications including inflammation, astigmatism, suture breakage, secondary neovascularization, microbial infection, as well as the lack of control of disease recurrence (Chan and Boisjoly, 2004; Bhatia, 2006; Grinstaff, 2007; Romano et al., 2016; Santiago et al., 2019). Ocular adhesives used as an alternative for the above treatments typically consist of synthetic materials, such as cyanoacrylate-based, PEG-based, and dendrimer-based adhesives, and naturally derived materials, such as protein-based and polysaccharide-based adhesives (Park et al., 2011; Koivusalo et al., 2019; Santiago et al., 2019). In particular, cyanoacrylate-based glues, PEG-based adhesives, and fibrin glues have been most commonly used in treatments for various ocular conditions (Santiago et al., 2019).

Cyanoacrylates are one of the earliest ocular adhesive solutions used. However, their cytotoxicity, rough texture, poor biodegradability and bioabsorbability, inflexibility after solidification, and lack of transparency impose major limitations on their application in clinical treatments (Ciapetti et al., 1994; Kaufman et al., 2003; Chan and Boisjoly, 2004; Bhatia, 2006; Chen et al., 2007; Park et al., 2011). An FDA-approved PEG-based adhesive for ocular repair, ReSure®, has already been used in cataract surgery and laser-assisted *in situ* keratomileusis (LASIK) surgery (Masket et al., 2014; Ramsook and Hersh, 2015; Tong et al., 2018). But this hydrogel adhesive requires rapid operation, has limited stability, cannot seal large leaky incisions, or fill in stromal defects (Park et al., 2011). The drawbacks of fibrin glue mainly lie in its poor adhesion ability to wet surfaces, difficulty to control product quality, and potential risks of viral contamination and immunological problems (Shirzaei Sani et al., 2019).

For an optimal alternative adhesion strategy for corneal tissue grafting or transplantation, the following biomaterial requirements must be fulfilled: long time stability onto the tissue, transparency, biocompatibility and biodegradability, appropriate stiffness, support of cell growth, simplified application procedure, and the ability to elicit tissue regeneration (Ahearne et al., 2020). ATESs are considered a proper candidate, as they can support tissue regeneration, have designable degradation rates and stiffness, and avoid suturing and glues, which is essential when it comes to vision recovery (**Figure 5**). Adhesive scaffolds are also able to fill larger stromal defects and help reduce surgery difficulties with intrinsic bonding ability. For instance, a modified photo-crosslinkable gelatin material, called GelCORE (gel for corneal regeneration), has been shown to adhere to the cornea tissue within a short-time exposure to visible light (**Figure 5**; Shirzaei Sani et al., 2019). While an adhesion strength higher than the commercially available adhesives was obtained, this ATES also maintained transparency. GelCORE was compatible with corneal cells and promoted cell integration. It effectively sealed corneal defect and promoted re-epithelialization (Shirzaei Sani et al., 2019). Another ATES product was based on modified HA. Two components, aldehyde modified HA and carbodihydrazide and dopamine modified HA, were mixed to fabricate a transparent hydrogel (Koivusalo et al., 2019). Aldehyde groups formed covalent bonding with the surrounding tissue, while dopamine groups augmented the adhesion strength and promoted human adipose-derived stem cell (hASC) culture by facilitating the conjugation of cell-adhesive proteins to the hydrogel surface. One novelty of this approach was the co-encapsulation of two cell types, hASCs and human embryonic stem cells (hESCs) into the ATES, with hASCs buried within the hydrogel to elicit regeneration of corneal stroma and hESCs on the surface of for regeneration of epithelium (Koivusalo et al., 2019).

For corneal regeneration, aside from basic requirements such as biocompatibility and biodegradability, transparency and appropriate stiffness for patient comfort are key factors for an optimal scaffold design. ATESs can help avoid complications caused by suturing, such as astigmatism and extensive neovascularization, as well as circumvent the inability of glue products in filling the stromal defects. Transparent ATESs with adjustable mechanical strength that could adhere to the tissue for long periods of time offer great promise as a desirable tissue engineering device for ocular regeneration.

## ATESs in Skin Regeneration

While treatments for acute skin wounds can be effective, chronic wounds can be difficult to fully treat (Subhamoy and Baker, 2016). Further, diabetes, severe burning, or other severe conditions may obstruct the natural healing process of the skin, highlighting the need for enhanced clinical interventions (Chouhan et al., 2019). Among alternative strategies, cultured epithelial autograft (CEA) sheets, skin grafts, skin substitutes, wound dressings, and injectable hydrogels are commonly used to facilitate wound healing (Vig et al., 2017). CEA sheets limitations include relatively long preparation time and poor function in full thickness wounds. Skin grafts are invasive and may cause complications such as scarring and infection (Tottoli et al., 2020). Skin substitutes are tissue engineered products that are designed to replace or mimic the form and function of the skin (Krishna et al., 2014). Wound dressings work as a barrier for maintaining moisture and keeping out bacterial infections (Zoe et al., 2019). Engineered scaffolds are commonly used as skin substitutes and wound dressings and can facilitate healing process through providing a reservoir of cells and growth factors to mediate angiogenesis, inflammation, antibacterial properties (**Figure 6**). At the same time, these ATESs can regulate cell infiltration, proliferation, and replacement of the lost tissue (Boateng et al., 2008). Adhesive properties of tissue engineering scaffolds can have several benefits for their application in wound healing: (1) these constructs are able to conform to uneven, curved, or folded surfaces of complex skin wounds or wounds near joints; (2) can reduce the risk of wound exposure to bacterial invasion; (3) avoid the use of sutures and staples that can cause secondary damages to the tissue; and (4) the adhesive *in situ* forming hydrogels can be applied to longitudinal wounds to protect them from the external environment (Saleh et al., 2019; Hou et al., 2020b). Also, adhesion ability combined with *in situ* gelling ability can be used to fabricate injectable hydrogels that can fill wounds with

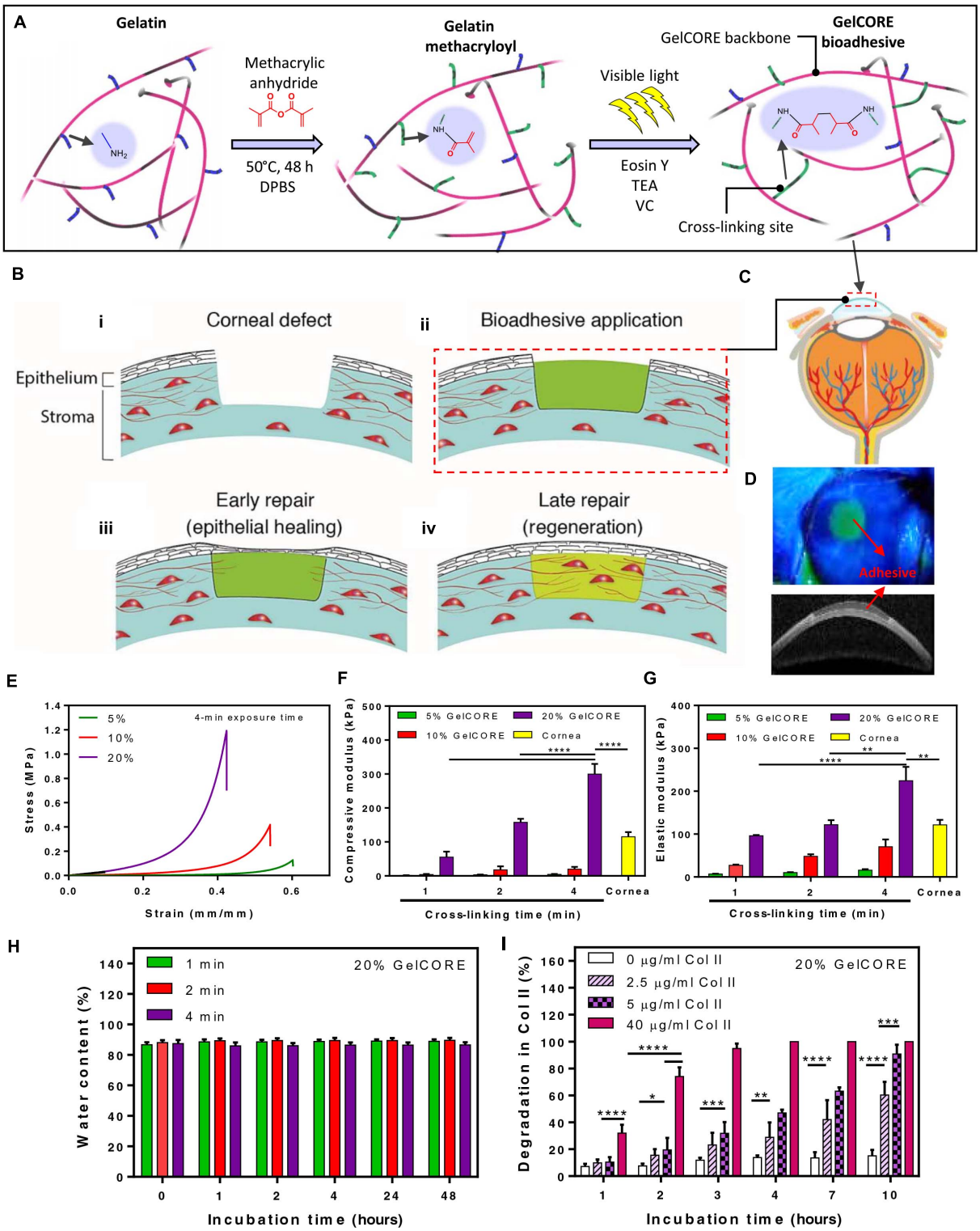


**FIGURE 5 |** Application of adhesive tissue engineering scaffolds (ATESs) in cornea repair. **(A)** Mechanism of hydrogel formation. **(B)** Application of ATES: **(i)** Corneal defect; **(ii)** Scaffold application; **(iii)** Epithelial healing; **(iv)** Regeneration. **(C)** Injection of prepolymer into injured cornea. **(D)** Demonstration of GelCORE hydrogel. **(E–G)** Compressive stress-strain curve **(E)**, compressive moduli **(F)**, and elastic moduli **(G)** for GelCORE hydrogels at varied concentration and crosslinking time. **(H)** Water content of GelCORE hydrogel after different crosslinking times at 37°C. **(I)** GelCORE degradation in collagenase type II at 37°C. $^{*}P < 0.05$, $^{**}P < 0.01$, $^{***}P < 0.001$, and $^{****}P < 0.0001$. Reconstructed with permission from Shirzaei Sani et al. (2019).

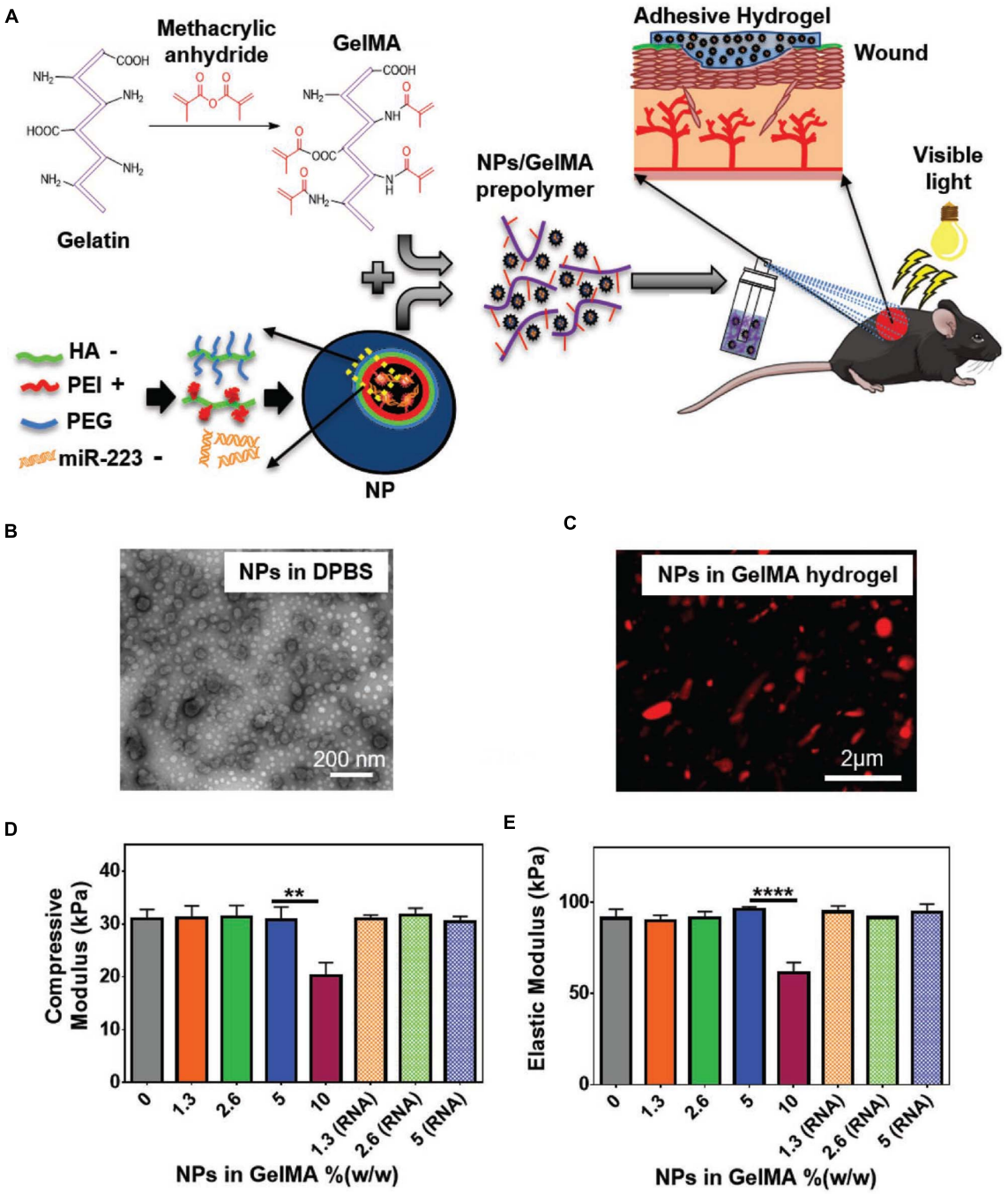


**FIGURE 6 |** Application of adhesive tissue engineering scaffolds (ATESs) in skin tissue repair. **(A)** GelMA hydrogel formation and application to skin wounds. **(B)** Representative TEM image of HA/miR-223* NPs with ratio of 325:1 (w/w) in DPBS. **(C)** Representative confocal image of Cy5.5-labeled (red) NPs in hydrogel. **(D)** Elastic modulus of hydrogels containing different NP concentrations. **(E)** Compressive modulus of hydrogels with different NP concentrations. $^{**}P < 0.01$ and $^{****}P < 0.0001$. Reconstructed with permission from Saleh et al. (2019).

irregular shapes and provide a customized coverage (Subhamoy and Baker, 2016; Duy et al., 2018).

Patch shaped polyurethane-poly(acrylamide) (PU-PAAm) hydrogels can be UV cured to demonstrate tissue adhesion functionality that is introduced by electrostatic interactions between hydrogel and the skin (Hou et al., 2020b). Further, the interpenetration of PU and PAAm gives stretchability and ductility to the hydrogel. The adhesion property, along with the flexibility, allow this ATES to fit into complex wounds and prevent bacterial invasion. The hydrogel shows remarkable

skin regenerative capacity and easy removal (Hou et al., 2020b). Compared with control group, the hydrogel treatment groups showed decreased inflammatory cells infiltration and enhanced vascularization and epithelialization. UV-crosslinkable gelMA-based hydrogels that are supportive of cell attachment, infiltration, and proliferation, can be also used to mediate wound re-epithelialization and healing (**Figure 6**; Saleh et al., 2019). The adhesion strength is brought by mechanical interlocking between gelMA and the native tissue, as well as covalent bonding triggered by radicals generated during photo-crosslinking.

Injectable adhesive hydrogels can also fill irregular shape wounds by *in situ* gelation and adhesion that could be used to heal longitudinal wounds. An example is a multiblock copolymer, comprised of PEG and pH- and temperature-sensitive poly(sulfamethazine ester urethane) (PSMEU), which can change from sols into stable gel by transitioning from *in vitro* (8.5, 23°C) to *in vivo* conditions (7.4, 37°C) (Duy et al., 2018). The adhesion ability came from the presence of urethane esters that interact with the tissue. Quantitative measurement of wound closure rate, breaking strength, and collagen content suggested that the adhesive hydrogel effectively homed the cells, facilitated cell migration, and provided a suitable environment for neo-tissue formation (Duy et al., 2018). Another example is poly (ε-caprolactone-*co*-lactide)-*b*-poly-(ethylene glycol)-*b*-poly (ε-caprolactone-*co*-lactide) (PCLA-*b*-PEG-*b*-PCLA, called in short PCLA) which is a biodegradable temperature sensitive polymer. PCLA/gelatin hydrogels with cell affinity and porous structure are used to seal the wounds and promote wound healing (Li et al., 2020). The adhesive ability can come from the interfacial hydrogen bonding between hydrogels and skin tissue. The presence of gelatin could improve the adhesion strength due to the ionic interactions between free amine groups on the gelatin chains and the skin tissue. In one study, the PCLA/gelatin hydrogel treated groups showed well organized collagen fiber and complete re-epithelialization after 7 days in a simple liner wound model with a 1 cm cut (Turabee et al., 2019). Further, treatment of a full thickness wound model with a 1 cm × 1 cm excisional wound showed granular tissue formation, dermis deposition, and enhanced collagen remodeling, suggesting that the scaffold provides a suitable environment for neovascularization and tissue regeneration (Turabee et al., 2019). More recently, a polydopamine-sodium alginate–polyacrylamide (PDA–SA–PAM)-based hydrogel with multi-functions was developed for skin tissue engineering (Suneetha et al., 2019). These hydrogels can be used as drug delivery systems for targeted and sustained release, hence, reducing systemic drug toxicity.

In sum, the application of ATESs in the fields of wound healing and skin tissue engineering has shown great promise. Future works could focus on developing an optimal adhesive scaffold with the following properties: (1) ability to adsorb wound exudates while maintaining moisture; (2) ability to protect the wound from the external environment, bacteria, and other pathogens; (3) flexibility and adaptability to complex wound shapes that enable complete and customized coverage; (4) applicability to all healing phases; and (5) basic functions such as biocompatibility, biodegradability, low cytotoxicity, and oxygen permeability, cost effectiveness, availability, and easy storage and application (Rezaie et al., 2019).

## The Use of ATESs in Cardiac Tissue Repair

Adult cardiomyocytes have limited capacity for replication, which leads to the requirement of effective therapies to help regenerate damaged heart tissue (Ruvinov and Cohen, 2013; Doppler et al., 2017). A variety of tissue engineering therapies have been investigated for myocardial repair, including cell-based and scaffold-based approaches. Each strategy has its own challenges. The limitations of cell injections include the low cell survival and retention rate, limited interaction between the transplanted cells and the host tissue, and the possibility of inducing or exacerbating arrhythmias post injection (Soler-Botija et al., 2012; Huang et al., 2018, 2019). Injectable hydrogels might cause secondary damages and hemorrhage to the already weakened heart, and also limit the amount of therapeutics and cells that can be delivered to the tissue due to the hydrogel-induced pressure (Shin et al., 2019). Cell sheets face the challenge of electromechanical isolation from the native myocardium, as well as vascularization resistance when the construct contains four or more cell layers (Zhang and Jianyi, 2015). Cardiac patch devices are an alternative for the treatment of cardiovascular tissues after severe injuries (Serpooshan and Ruiz-Lozano, 2014; Serpooshan et al., 2014; Mei and Cheng, 2020). These engineered scaffolds can act as a depository of regenerative factors and a matrix to aid targeted therapeutic delivery and sustained release (Tomov et al., 2019). In comparison to other types of treatments, patch devices can offer the following benefits: (1) pre-designed structure that could be patient-specific, incorporate vasculature and contain patterned cells according to desired function (Noor et al., 2019); (2) full coverage of the entire damaged area (and the area at risk) that is specifically important for drug delivery and mechanical support (Ravichandran et al., 2015); (3) the ability of adhesive scaffolds to reduce secondary damages to the injured tissue, which is typically associated with gluing or intramyocardial injection methods. Using adhesive and glue materials is typically associated with challenges such as the inhibition of cell migration from the patch to damaged tissue, inadequate stiffness, cytotoxicity and exothermic reaction by polymerization of cyanoacrylates, complications related to viral infections, and low adhesion ability of fibrin sealants (Shin et al., 2019).

A ready-to-use tissue-adhesive catechol or pyrogallol modified HA patch has been developed and used for cardiac cell and drug delivery (Shin et al., 2019). The phenolic HA patches were lyophilized before use and simply applied by placing the hydrogel onto the cardiac tissue surface. Tissue adhesion and polymer crosslinking were initiated by oxidation of catechol or pyrogallol through spraying oxidizing solution (4.5 mg/mL of $NaIO_4$). Rat BMSCs were transplanted by seeding onto the adhered patches. The lyophilized patch soaked up water molecules and formed a hydrogel after adhesion. The lyophilization step significantly enhanced the adhesion ability of the hydrogel. Application of the adhesive patch prevented LV dilatation and cardiac hypertrophy,

and improved angiogenesis in a rat model of myocardial infarction (MI) (Shin et al., 2019).

Electrospun fibrillar patches can also serve as ATESs for cardiac tissue regeneration. The benefits of using fibrillar scaffolds include high surface area to volume ratios, defined spatial density, 3D anisotropic organization, and recapitulation of the fibrillar topography of the native myocardium (Kim and Cho, 2016; Streeter et al., 2019). For instance, a gelMA-based fibrillar patch was developed that could adhere to the heart tissue via photo-crosslinking, during which, MA groups of gelMA formed covalent bonds with amine groups of the tissue (**Figure 7**; Walker et al., 2019). To restore electrical conductivity at the site of MI, a choline-based bio-ionic liquid (Bio-IL) was covalently bound to the gelMA patch during photocrosslinking. The Bio-IL contributed to the adhesion ability through electrostatic interactions between its positive charges and negative charges of carboxyl groups in the cardiac tissue. After *in vivo* implantation, both gelMA and gelMA/Bio-IL scaffolds demonstrated tissue ingrowth, suggesting that they could both provide a cell-supportive microenvironment to reduce adverse cardiac remodeling post MI (**Figure 7**; Walker et al., 2019).

Fibrillar scaffolds can also adhere to the tissue through near IR irradiation, which results in hear generation and partial and local melting (denaturing) of the scaffold polymer to evoke binding and adhesion. An example is an electrospun albumin-based scaffold, encapsulating gold nanorods (AuNRs) (Malki et al., 2018). AuNRs absorb near IR radiation and generate heat, while simultaneously can help increasing electrical conductivity of the hydrogel matrix grafted onto the MI tissue. To inhibit potential damage of the localized heat to tissue, the patch was irradiated to attach to the heart tissue only on the peripheral areas, resulting in a strong fixation of the construct for the entire duration of assays (Malki et al., 2018).

In summary, adhesion to the heart tissue is a difficult task due to the presence of a high density of blood vessels and the highly dynamic forces. In addition to adequate adhesive strength, several other essential factors must be considered in fabrication of optimal cardiac ATES. These include electromechanical coupling of the patch with the host tissue, proper cell type, density, and distribution within the scaffold, and sufficient mass transport properties. Efforts should be made to integrate intrinsic adhesive properties, with other key requirements specific to cardiac tissue grafts. 3D bioprinting technologies that have already shown great promise in customization of cardiac patch structure and function (Hu et al., 2017; Serpooshan et al., 2018), could be an important tool in the design and development of cardiac ATES systems. For instance, an *in vivo* printed gelMA based adhesive scaffold was developed and used for skeletal muscle tissue repair (Quint et al., 2021).

## ATES Solutions for Bone Repair

Regeneration of bone tissue when its remodeling capacity cannot compensate the tissue destruction remains a challenge in clinical practice (Yin et al., 2019; Bai et al., 2020). Treatment of such bone defects typically requires filling by autologous or allogenic grafts, as well as stabilization by screws, cages, or rods (Duarte et al., 2020). Limitations of autografts include excessive pain, donor site morbidity, cost, and limited supply. Allografts, with abundant source, are challenged by the uncertainty of compatibility and suboptimal osteoinductivity which may result in delayed or incomplete bone regeneration, immunogenic reactions, risk of infection, and possible disease transmission (Stevens et al., 2010; Gibbs et al., 2016). Complications associated with metal tools such as screws are potential over-tightening and bone stripping, fixture dislocation, fractures from holes, bone resorption by stress shielding, foreign-body reactions, growth disturbance, and the possible surgery for their removal (Schreader et al., 2012; Lei et al., 2019; Bai et al., 2020). Traditional bone adhesives, as an alternative, help with the spread of force over the whole contact area and thus minimize stress shielding effects. However, commonly used poly (methyl methacrylate) (PMMA) bone cement has low biocompatibility, no intrinsic adhesion ability to the bone, toxic monomers, poor bioresorbability, and possible thermal damage during polymerization. Fibrin glue is limited by its low mechanical properties and risk of inducing allergies. Calcium phosphate bone cements (CPCs) often lack proper mechanical properties and adhesive ability (Lei et al., 2019; Bai et al., 2020; Duarte et al., 2020). Advanced tissue engineering scaffolds with adhesive properties in wet environment, can replace autologous or allogenic bone grafts by offering sufficient biocompatibility and biodegradability. Further, ATESs will serve as a reservoir for cells and growth factors, as well as a suitable microenvironment that directs cell proliferation and differentiation toward bone regeneration (Leberfinger et al., 2017; Hasani-Sadrabadi et al., 2020).

An inorganic–organic hybrid scaffold consisting of tannic acid (TA), silk fibroin (SF), and hydroxyapatite (HAP) has been developed as an ATES for bone regeneration (**Figure 8**; Bai et al., 2020). This SF@TA@HAP system was inspired by the human bone, where inorganic nanoparticles are glued into organic collagen by proteins and proteoglycans. The bone hierarchical organization uses calcium-mediated sacrificial bonds for energy dissipation, ensuring high mechanical strength and healing properties. In the case of this bone-mimetic hybrid hydrogel, tannic acid acts as the glue to combine inorganic HAP and organic SF to form a scaffold with robust water-resistant structure (Bai et al., 2020). The adhesion ability comes from $Ca^{2+}$ – phenolic bonds and other nucleophile-phenolic non-covalent interactions between the scaffold and the collagen proteins and HAP of bone tissue. The scaffold, embedded with bone morphogenetic protein-2 (BMP-2), guided MSCs toward osteogenic differentiation and mineralization *in vitro*. Further, application of the ATES in a rat femoral defect model resulted in enhanced bone regeneration bridging across the defect (Bai et al., 2020). Another ATES device was developed using dopamine–modified alginate and used to deliver cells and guide mineralization (Hasani-Sadrabadi et al., 2020). Moreover, a porous room-temperature-cured foam-like adhesive scaffold, based on polyurethane, was tested *in vivo,* demonstrating extensive cellular infiltration and newly generated bone, forming a connected structure after 24 weeks of osteotomy (Lei et al., 2019). More recently, an injectable

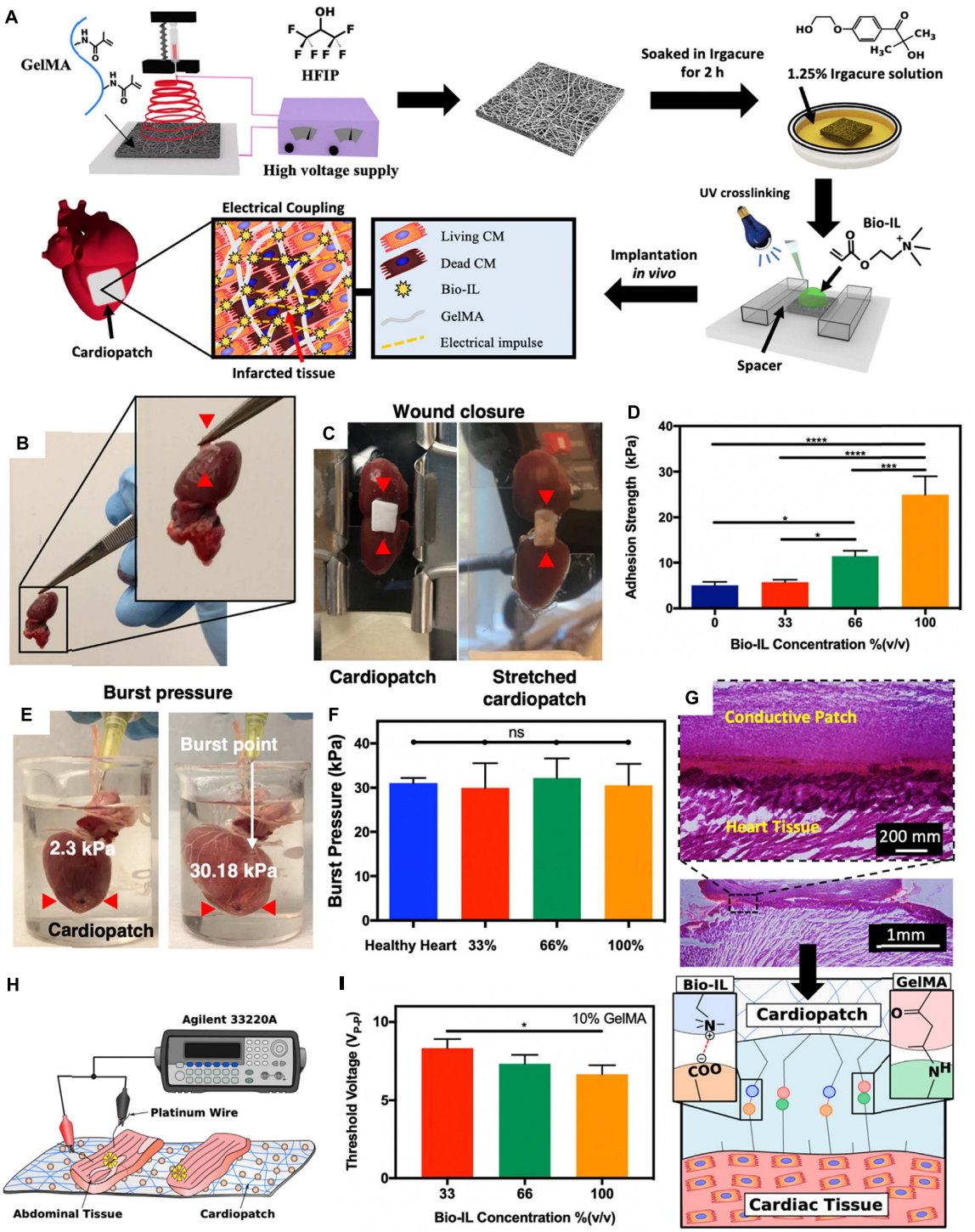


**FIGURE 7 |** Application of adhesive tissue engineering scaffolds (ATESs) in cardiac tissue repair. **(A)** Fabrication of electrospun cardiopatches, soaking in Irgacure solution, addition of Bio-IL, followed by UV crosslinking for 5 min. **(B)** GelMA/Bio-IL cardiopatch photo-crosslinked on explanted rat heart, demonstrating adequate adhesion (red arrows) to the heart tissue. **(C)** Wound closure test to test the adhesion strength of cardiopatches on the explanted rat heart (as substrate). **(D)** Quantification of the patch adhesion strength, consisting of 10% (w/v) gelMA and at varying concentrations of Bio-IL. **(E)** Images of gelMA/Bio-IL cardiopatch with 10% gelMA and 66% Bio-IL, crosslinked onto the defect site of explanted rat heart, to measure the burst pressure. **(F)** Quantification of the burst pressure. **(G)** H&E staining of patch-tissue interface, demonstrating a strong bonding of the hydrogel to the murine myocardium. **(H,I)** *Ex vivo* analysis of the threshold voltage of gelMA/Bio-IL cardiopatches at varying Bio-IL concentrations. $^{*}P < 0.05$, $^{****}P < 0.001$ and $^{****}P < 0.0001$. Reconstructed with permission from Walker et al. (2019).

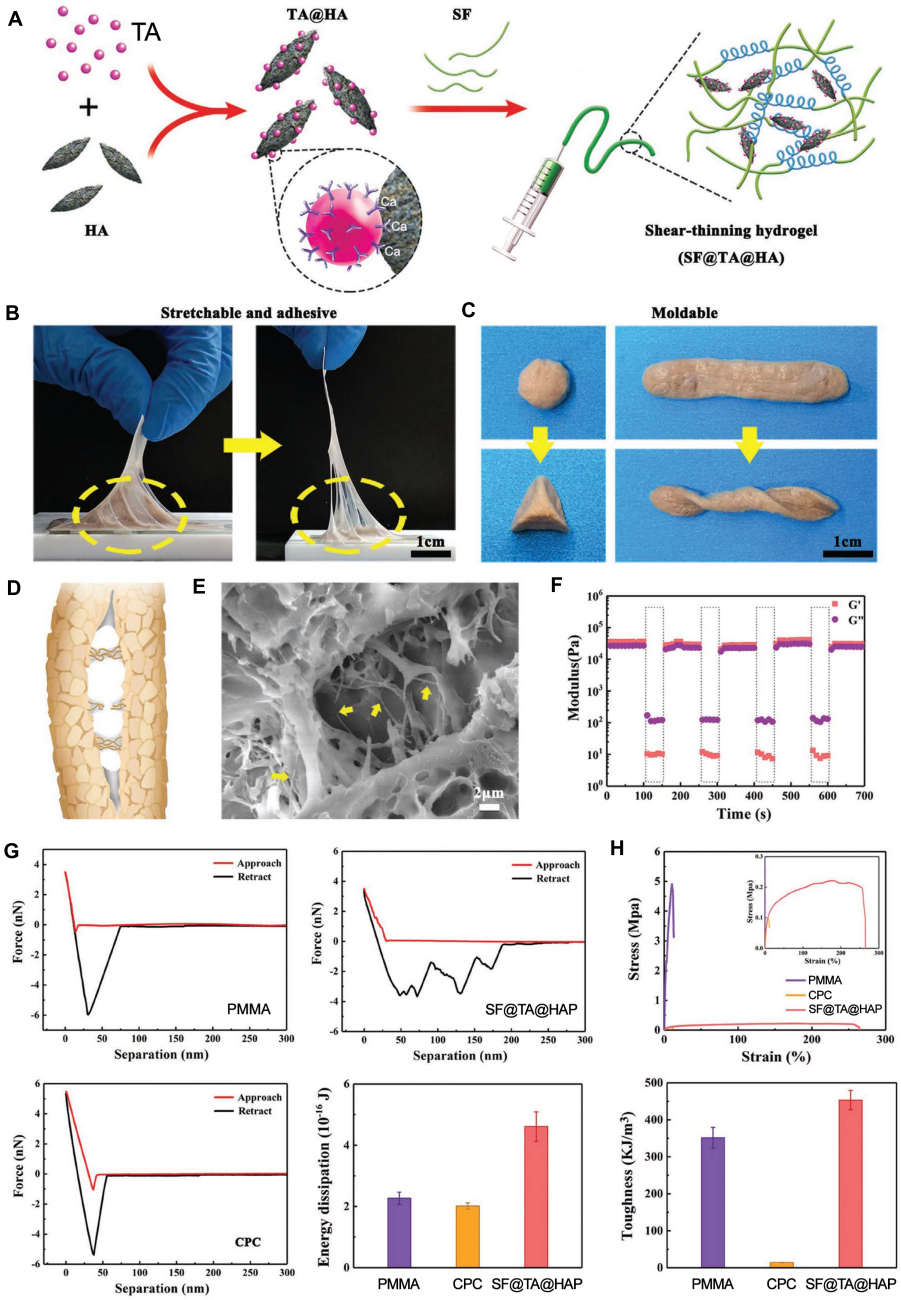


**FIGURE 8 |** Application of adhesive tissue engineering scaffolds (ATESs) in bone tissue engineering. **(A)** Demonstration of SF@TA@HAP hydrogel formation. **(B)** Demonstration of adhesion and stretchability of SF@TA@HAP scaffold. **(C)** Demonstration of the flexibility and malleability of the hydrogel. **(D)** Glue filaments in the bone structure, connecting mineralized collagen fibrils. **(E)** Representative SEM image of the filaments in the SF@TA@HAP hydrogel. **(F)** Modulus of SF@TA@HAP hydrogel under repeated application of 100 and 0.1% strain. **(G)** AFM mechanical testing of SF@TA@HA, PMMA, and CPC. Bar graphs show the quantified values of dissipated energy during the separation step. **(H)** Results of mechanical testing of SF@TA@HA, PMMA, and CPC samples. Bar graphs show the quantified toughness. Reconstructed with permission from Bai et al. (2020).

alginate based adhesive hydrogel, laden with mesenchymal stem cells, was developed for craniofacial tissue engineering (Hasani-Sadrabadi et al., 2020).

In summary, ATESs could offer a highly attractive alternative therapy to substitute autologous or allogenic bone grafts, as well as serving as a highly tunable bone adhesive, replacing screws and other metallic devices for fracture stabilization. An ideal adhesive scaffold in the future should be able to adhere under wet conditions, while exhibiting adequate mechanical strength, especially compressive strength.

## CURRENT CHALLENGES AND FUTURE PROSPECTIVE

Design and development of ATESs have attracted increasing attention in recent years. Recent works have successfully created scaffold systems that fulfill the basic requirements (elastic modulus, adhesion strength and mechanism, degradation rate, and biocompatibility) for diverse tissue engineering applications. However, efforts are still needed to enable and enhance clinical translation of these products in the future. Current adhesive scaffolds are mostly made through traditional scaffold fabrication methods, such as *in situ* gelation from liquid pre-gel. Integration of advanced scaffold fabrication methods, such as 3D printing and bioprinting, could be considered for enhanced cell-biomaterial arrangement, vessel incorporation, and personalized designs. Maintaining proper adhesion properties under wet conditions is still a challenge. New mechanisms that help tolerating such harsh conditions should be investigated for successful clinical translation. Also, methods for less invasive delivery of adhesive scaffolds should be adopted for each specific tissue and organ. Since additional fixation is not required for adhesive scaffolds, delivery through minimally invasive conduits (e.g., catheters) could be considered.

Effective application of ATES devices in different tissue engineering applications currently face many challenges. ATESs for all different types of tissues face challenges such as wet environment where water molecules form a boundary and mask functional groups, low pH, oxidative environment, high immune response under trauma and post-surgery. For the nerve scaffolds, significant tensile stresses are another challenge. In cartilage and bone, dynamic compressive stresses would complicate the adhesion requirements. In the case of corneal tissue engineering, the ATES must also exhibit adequate transparency and patient comfort. Finally, for the cardiac scaffolds, dynamic loading exerted by the beating heart and the lack of reservoir which requires quick adhesion, are some of the key limitations.

Future research on adhesive scaffold devices could focus on two specific directions: (1) advanced adhesion properties that can maintain the secured device attachment under harsh conditions such as bleeding, dynamic (pulsatile) loading such as beating heart, or in the presence of strong immune responses; (2) Incorporation of adhesive hydrogel (biomaterial) technologies into advanced tissue biomanufacturing techniques. In particular, adhesive scaffold devices can be 3D bioprinted to provide a more targeted and personalized structure, while incorporating more functional features such as perfusable vascular networks and heterogeneous cellular populations that more closely mimic the native human tissue.

## CONCLUSION

Adhesive tissue engineering scaffolds are advanced medical treatments to replace traditional fixation strategies such as sutures or bio-glues to circumvent their drawbacks such as morbidity, toxicity, potential allergies, and operation inconveniences especially for treating complex tissue defects. Adhesive scaffolds can help with more effective cell migration and engraftment between implanted construct and the host tissue. They can also significantly reduce operation trauma and pain for patients by providing minimally invasive delivery (e.g., injection) and immediate fixation. There are substantial differences between ATESs and adhesive products. Adhesives are used for holding tissues together, while ATESs are scaffolds with *intrinsic* adhesion properties for tissue regeneration. These two functions could be held at the same time, but many adhesives lack the ability for tissue regeneration due to their low biocompatibility, insufficient mechanical properties, and improper degradation rate. Future works in ATES will focus on improving the under-water adhesion properties and simultaneously improving mechanical properties, flexibility, and other functions that are specific to each tissue and organ. For instance, scaffolding biomaterials with enhanced optical properties will be needed for corneal regeneration. Adhesion ability under dynamic forces and adequate electrical conductivity will be required to manufacture cardiac ATES devices. Furthermore, for more effective development of adhesive scaffolds, standardized testing procedures should be defined for measuring the strength of adhesion to specific tissues and organs. More insight into the adhesion mechanisms between the scaffold and tissue surfaces would be of great significance. The successful development of functional ATES products, with potential for clinical translation, could help significantly reduce patients' pain and morbidity and therefore, is expected to draw increasing attention in the coming years.

## AUTHOR CONTRIBUTIONS

SC, CG, LN, LJ, LP, GK, and MT contributed to writing different sections and subsections of the work, and designed and generated the figures and tables. SC led the writing tasks. VS conceived the concept, designed the overall article structure, and edited the manuscript. All authors contributed to the article and approved the submitted version.

## FUNDING

This research was funded by the NIH Grant Nos. R00HL127295 and R01 MH126195 (to VS).

## REFERENCES

Ahearne, M., Fernández-Pérez, J., Masterton, S., Madden, P. W., and Bhattacharjee, P. (2020). Designing scaffolds for corneal regeneration. *Adv. Funct. Mater.* 30:1908996. doi: 10.1002/adfm.201908996

Ark, M., Boughton, P., Lauto, A., Tran, G. T., Chen, Y., Cosman, P. H., et al. (2016). Characterisation of a novel light activated adhesive scaffold: potential for device attachment. *J. Mech. Behav. Biomed. Mater.* 62, 433–445. doi: 10.1016/j.jmbbm.2016.05.029

Assmann, A., Vegh, A., Ghasemi-Rad, M., Bagherifard, S., Cheng, G., Sani, E. S., et al. (2017). A highly adhesive and naturally derived sealant. *Biomaterials* 140, 115–127. doi: 10.1016/j.biomaterials.2017.06.004

Bahm, J., Esser, T., Sellhaus, B., El-Kazzi, W., and Schuind, F. (2018). *Tension in Peripheral Nerve Suture*. London: IntechOpen. doi: 10.5772/intechopen.78722

Bai, S., Zhang, X., Lv, X., Zhang, M., Huang, X., Shi, Y., et al. (2020). Bioinspired mineral-organic bone adhesives for stable fracture fixation and accelerated bone regeneration. *Adv. Funct. Mater.* 30:1908381. doi: 10.1002/adfm.201908381

Balakrishnan, B., Joshi, N., Jayakrishnan, A., and Banerjee, R. (2014). Self-crosslinked oxidized alginate/gelatin hydrogel as injectable, adhesive biomimetic scaffolds for cartilage regeneration. *Acta Biomater.* 10, 3650–3663. doi: 10.1016/j.actbio.2014.04.031

Barton, M. J., Morley, J. W., Stoodley, M. A., Lauto, A., and Mahns, D. A. (2014). Nerve repair: toward a sutureless approach. *Neurosurg. Rev.* 37, 585–595. doi: 10.1007/s10143-014-0559-1

Berberich, O., Blhbaum, J., Hlscher-Doht, S., Meffert, R. H., and Groll, J. (2019). Catechol-modified Poly(oxazoline)s with tunable degradability facilitate cell invasion and lateral cartilage integration. *J. Ind. Eng. Chem.* 80, 757–769. doi: 10.1016/j.jiec.2019.06.038

Bermejo-Velasco, D., Kadekar, S., Costa, M. V. T. D., Oommen, O. P., and Varghese, O. P. (2019). First aldol cross-linked hyaluronic acid hydrogel: fast and hydrolytically stable hydrogel with tissue adhesive properties. *ACS Appl. Mater. Interfaces* 11, 38232–38239. doi: 10.1021/acsami.9b10239

Bhagat, V., and Becker, M. L. (2017). Degradable adhesives for surgery and tissue engineering. *Biomacromolecules* 18, 3009–3039. doi: 10.1021/acs.biomac.7b00969

Bhatia, S. S. (2006). Ocular surface sealants and adhesives. *Ocular Surface* 4, 146–154. doi: 10.1016/S1542-0124(12)70041-1

Boateng, J. S., Matthews, K. H., Stevens, H. N. E., and Eccleston, G. M. (2008). Wound healing dressings and drug delivery systems: a review. *J. Pharmaceut.* 97, 2892–2923. doi: 10.1002/jps.21210

Boyadzhieva, S., Sorg, K., Danner, M., Fischer, S. C. L., Hensel, R., Schick, B., et al. (2019). A self-adhesive elastomeric wound scaffold for sensitive adhesion to tissue. *Polymers* 11:942. doi: 10.3390/polym11060942

Burks, S., and Spotnitz, W. (2014). Safety and usability of hemostats. Sealants, and adhesives. *Aorn J.* 100, 160–176. doi: 10.1016/j.aorn.2014.01.026

Cadena, M., Ning, L., King, A., Hwang, B., Jin, L., Serpooshan, V., et al. (2020). 3D bioprinting of neural tissues. *Adv. Healthc. Mater.* doi: 10.1002/adhm.202001600 [Epub ahead of print].

Chan, S. M., and Boisjoly, H. L. N. (2004). Advances in the use of adhesives in ophthalmology. *Curr. Opin. Ophthalmol.* 15, 305–310. doi: 10.1097/00055735-200408000-00005

Chandrasekharan, A., Seong, K.-Y., Yim, S.-G., Kim, S., Seo, S., Yoon, J., et al. (2019). In situ photocrosslinkable hyaluronic acid-based surgical glue with tunable mechanical properties and high adhesive strength. *J. Polymer Sci. Part A Polym. Chem.* 57, 522–530. doi: 10.1002/pola.29290

Chen, W. L., Lin, C. T., Hsieh, C. Y., Tu, I. H., Chen, W. Y. W., and Hu, F. R. (2007). Comparison of the bacteriostatic effects, corneal cytotoxicity, and the ability to seal corneal incisions among three different tissue adhesives. *Cornea* 26, 1228–1234. doi: 10.1097/ICO.0b013e3181506129

Chouhan, D., Dey, N., Bhardwaj, N., and Mandal, B. B. (2019). Emerging and innovative approaches for wound healing and skin regeneration: current status and advances. *Biomaterials* 216:119267. doi: 10.1016/j.biomaterials.2019.119267

Ciapetti, G., Stea, S., Cenni, E., Sudanese, A., Marraro, D., Toni, A., et al. (1994). Cytotoxicity testing of cyanoacrylates using direct contact assay on cell cultures. *Biomaterials* 15, 63–67. doi: 10.1016/0142-9612(94)90199-6

Doppler, S. A., Deutsch, M. A., Serpooshan, V., Li, G., Dzilic, E., Lange, R., et al. (2017). Mammalian heart regeneration: the race to the finish line. *Circ. Res.* 120, 630–632. doi: 10.1161/CIRCRESAHA.116.310051

Du, J., Chen, H., Qing, L., Yang, X., and Jia, X. (2018). Biomimetic neural scaffolds: a crucial step towards optimal peripheral nerve regeneration. *Biomater. Sci.* 6, 1299–1311. doi: 10.1039/C8BM00260F

Duarte, R. M., Correia-Pinto, J., Reis, R. L., and Duarte, A. R. C. (2020). Advancing spinal fusion: interbody stabilization by in situ foaming of a chemically modified polycaprolactone. *J. Tissue Eng. Regen. Med.* 14, 1465–1475. doi: 10.1002/term.3111

Duy, L. T. M., Trang, D. H. T., Thavasyappan, T., Giang, P. V. H., Hoon, J. J., and Sung, L. D. (2018). Bioinspired pH- and temperature-responsive injectable adhesive hydrogels with polyplexes promotes skin wound healing. *Biomacromolecules* 19, 3536–3548. doi: 10.1021/acs.biomac.8b00819

Fanyi, L., Truong, V. X., Philipp, F., Clara, L., Veronica, G., Marcy, Z. W., et al. (2018). Cartilage tissue formation through assembly of microgels containing mesenchymal stem cells. *Acta Biomater.* 77, 48–62. doi: 10.1016/j.actbio.2018.07.015

Furst, W., and Banerjee, A. (2005). Release of glutaraldehyde from an albumin-glutaraldehyde tissue adhesive causes significant in vitro and in vivo toxicity. *Ann. Thorac. Surg.* 79, 1522–1528; discussion 1529. doi: 10.1016/j.athoracsur.2004.11.054

Gåserød, O., Jolliffe, I. G., Hampson, F. C., Dettmar, P. W., and Skjåk-Bræk, G. (1998). The enhancement of the bioadhesive properties of calcium alginate gel beads by coating with chitosan. *Int. J. Pharmaceut.* 175, 237–246. doi: 10.1016/S0378-5173(98)00277-4

Ge, L., and Chen, S. (2020). Recent advances in tissue adhesives for clinical medicine. *Polymers* 12:939. doi: 10.3390/polym12040939

Gibbs, D. M. R., Black, C. R. M., Dawson, J. I., and Oreffo, R. O. C. (2016). A review of hydrogel use in fracture healing and bone regeneration. *J. Tissue Eng. Regen. Med.* 10, 187–198. doi: 10.1002/term.1968

Grinstaff, M. W. (2007). Designing hydrogel adhesives for corneal wound repair. *Biomaterials* 28, 5205–5214. doi: 10.1016/j.biomaterials.2007.08.041

Han, L., Lu, X., Liu, K., Wang, K., Fang, L., Weng, L. T., et al. (2017). Mussel-inspired adhesive and tough hydrogel based on nanoclay confined dopamine polymerization. *Acs Nano* 11:2561. doi: 10.1021/acsnano.6b05318

Han, L., Wang, M., Li, P., Gan, D., Yan, L., Xu, J., et al. (2018). Mussel-inspired tissue-adhesive hydrogel based on the polydopamine-chondroitin sulfate complex for growth-factor-free cartilage regeneration. *ACS Appl. Mater. Interfaces* 10, 28015–28026. doi: 10.1021/acsami.8b05314

Hasani-Sadrabadi, M. M., Sarrion, P., Pouraghaei, S., Chau, Y., and Moshaverinia, A. (2020). An engineered cell-laden adhesive hydrogel promotes craniofacial bone tissue regeneration in rats. *Ence Transl. Med.* 12:eaay6853. doi: 10.1126/scitranslmed.aay6853

Hickman, D. A., Pawlowski, C. L., Sekhon, U. D. S., Marks, J., and Gupta, A. S. (2018). Biomaterials and advanced technologies for hemostatic management of bleeding. *Adv. Mater.* 30:10.1002/adma.201700859. doi: 10.1002/adma.201700859

Hong, Y., Zhou, F., Hua, Y., Zhang, X., and Ouyang, H. (2019). A strongly adhesive hemostatic hydrogel for the repair of arterial and heart bleeds. *Nat. Commun.* 10:2060. doi: 10.1038/s41467-019-10004-7

Hou, Y., Deng, X., and Xie, C. (2020a). Biomaterial surface modification for underwater adhesion. *Smart Mater. Med.* 1, 77–91. doi: 10.1016/j.smaim.2020.07.003

Hou, Y., Jiang, N., Sun, D., Wang, Y., Chen, X., Zhu, S., et al. (2020b). A fast UV-curable PU-PAAm hydrogel with mechanical flexibility and self-adhesion for wound healing. *RSC Adv.* 10, 4907–4915. doi: 10.1039/C9RA10666A

Hozumi, K., and Nomizu, M. (2018). Mixed peptide-conjugated chitosan matrices as multi-receptor targeted cell-adhesive scaffolds. *Int. J. Mol. Sci.* 19:2713. doi: 10.3390/ijms19092713

Hu, J. B., Hu, D. A., Buikema, J. W., Chirikian, O., Venkatraman, S., Serpooshan, V., et al. (2017). Bioengineering of vascular myocardial tissue; a 3D bioprinting approach. *Tissue Eng. Part A* 23, S158–S159.

Huang, K., Hu, S., and Cheng, K. (2019). A new era of cardiac cell therapy: opportunities and challenges. *Adv. Healthcare Mater.* 8:1801011. doi: 10.1002/adhm.201801011

Huang, N. F., Serpooshan, V., Morris, V. B., Sayed, N., Pardon, G., Abilez, O. J., et al. (2018). Big bottlenecks in cardiovascular tissue engineering. *Commun. Biol.* 1:199. doi: 10.1038/s42003-018-0202-8

Huang, Y., Leobandung, W., Foss, A., and Peppas, N. A. (2000). Molecular aspects of muco- and bioadhesion: tethered structures and site-specific surfaces. *J. Control. Release* 65, 63–71. doi: 10.1016/S0168-3659(99)00233-3

Hunziker, E. B., and Stähli, A. (2008). Surgical suturing of articular cartilage induces osteoarthritis-like changes. *Osteoarthr. Cartil.* 16, 1067–1073. doi: 10.1016/j.joca.2008.01.009

Ichihara, S., Inada, Y., and Nakamura, T. (2008). Artificial nerve tubes and their application for repair of peripheral nerve injury: an update of current concepts. *Injury Int. J. Care Injured* 39, 29–39. doi: 10.1016/j.injury.2008.08.029

Jouan, A., and Constantinescu, A. (2018). A critical comparison of shear tests for adhesive joints. *Int. J. Adhes. Adhes.* 84, 63–79. doi: 10.1016/j.ijadhadh.2018.02.035

Kaufman, H. E., Insler, M. S., Ibrahim-Elzembely, H. A., and Kaufman, S. C. (2003). Human fibrin tissue adhesive for sutureless lamellar keratoplasty and scleral

patch adhesion: a pilot study. *Ophthalmology* 110, 2168–2172. doi: 10.1016/S0161-6420(03)00832-7

Kehoe, S., Zhang, X. F., and Boyd, D. (2012). FDA approved guidance conduits and wraps for peripheral nerve injury: a review of materials and efficacy. *Injury* 43, 553–572. doi: 10.1016/j.injury.2010.12.030

Kim, P.-H., and Cho, J.-Y. (2016). Myocardial tissue engineering using electrospun nanofiber composites. *BMB Rep.* 49, 26–36. doi: 10.5483/BMBRep.2016.49.1.165

Kim, S. H., An, Y. H., Kim, H. D., Kim, K., Lee, S. H., Yim, H. G., et al. (2018). Enzyme-mediated tissue adhesive hydrogels for meniscus repair. *Int. J. Biol. Macromol. Struct. Funct. Interact.* 110, 479–487. doi: 10.1016/j.ijbiomac.2017.12.053

Koivusalo, L., Kauppila, M., Samanta, S., Parihar, V. S., Ilmarinen, T., Miettinen, S., et al. (2019). Tissue adhesive hyaluronic acid hydrogels for sutureless stem cell delivery and regeneration of corneal epithelium and stroma. *Biomaterials* 225:119516. doi: 10.1016/j.biomaterials.2019.119516

Korde, M. J., and Kandasubramanian, B. (2018). Biocompatible alkyl cyanoacrylates and their derivatives as bio-adhesives. *Biomater. Sci.* 6, 1691–1711. doi: 10.1039/C8BM00312B

Krishna, Vyas, Henry, and Vasconez. (2014). Wound healing: biologics, skin substitutes, biomembranes and scaffolds. *Healthcare* 2, 356–400. doi: 10.3390/healthcare2030356

Laura, C., Bradley, Nathan, D., Bade, Lisa, M., Mariani, et al. (2017). Rough adhesive hydrogels (RAd gels) for underwater adhesion. *Acs Appl. Mater. Interfaces* 9, 27409–27413. doi: 10.1021/acsami.7b08916

Lauto, A., Mawad, D., and Foster, J. L. R. (2008). Adhesive biomaterials for tissue reconstruction. *J. Chem. Technol. Biotechnol.* 83:464. doi: 10.1002/jctb.1771

Leberfinger, A. N., Ravnic, D. J., Dhawan, A., and Ozbolat, I. T. (2017). Concise review: bioprinting of stem cells for transplantable tissue fabrication. *Stem Cells Transl. Med.* 6, 1940–1948. doi: 10.1002/sctm.17-0148

Lei, K., Zhu, Q., Wang, X., Xiao, H., and Zheng, Z. (2019). In vitro and in vivo characterization of a foam-like polyurethane bone adhesive for promoting bone tissue growth. *ACS Biomater. Eng.* 5, 5489–5497. doi: 10.1021/acsbiomaterials.9b00918

Li, J., Chen, G., Xu, X., Abdou, P., Jiang, Q., Shi, D., et al. (2019). Advances of injectable hydrogel-based scaffolds for cartilage regeneration. *Regen. Biomater.* 6, 129–140. doi: 10.1093/rb/rbz022

Li, Y., Yang, H. Y., and Lee, D. S. (2020). Advances in biodegradable and injectable hydrogels for biomedical applications. *J. Control Release* 330, 151–160. doi: 10.1016/j.jconrel.2020.12.008

Lin, X., Liu, Y., Bai, A., Cai, H., Bai, Y., Jiang, W., et al. (2019). A viscoelastic adhesive epicardial patch for treating myocardial infarction. *Nat. Biomed. Eng.* 3, 632–643. doi: 10.1038/s41551-019-0380-9

Liqun, N., Haoying, S., Tiphanie, L., Romain, G., Ning, Z., Schreyer, D. J., et al. (2018). 3D bioprinting of scaffolds with living Schwann cells for potential nerve tissue engineering applications. *Biofabrication* 10:035014. doi: 10.1088/1758-5090/aacd30

Liu, M., Zeng, X., Ma, C., Yi, H., Ali, Z., Mou, X., et al. (2017). Injectable hydrogels for cartilage and bone tissue engineering. *Bone Res.* 5:17014. doi: 10.1038/boneres.2017.14

Liu, X., Zhang, Q., Gao, Z., Hou, R., and Gao, G. (2017). A bio-inspired adhesive hydrogel driven by adenine and thymine. *Acs Appl. Mater. Interfaces* 9, 17645–17652. doi: 10.1021/acsami.7b04832

Ma, Z., Bao, G., and Li, J. (2021). Multifaceted design and emerging applications of tissue adhesives. *Adv. Mater.* 33:e2007663. doi: 10.1002/adma.202007663

Malki, M., Fleischer, S., Shapira, A., and Dvir, T. (2018). Gold nanorod-based engineered cardiac patch for suture-free engraftment by near IR. *Nano Lett.* 18, 4069–4073. doi: 10.1021/acs.nanolett.7b04924

Masket, S., Hovanesian, J. A., Levenson, J., Tyson, F., Flynn, W., Endl, M., et al. (2014). Hydrogel sealant versus sutures to prevent fluid egress after cataract surgery. *J. Cataract Refract. Surg.* 40, 2057–2066. doi: 10.1016/j.jcrs.2014.03.034

Mehall, J. R., Saltzman, D. A., Jackson, R. J., and Smith, S. D. (2002). Fibrin sheath enhances central venous catheter infection. *Crit. Care Med.* 30, 908–912. doi: 10.1097/00003246-200204000-00033

Mehdizadeh, M., Weng, H., Gyawali, D., Tang, L., and Yang, J. (2012). Injectable citrate-based mussel-inspired tissue bioadhesives with high wet strength for sutureless wound closure. *Biomaterials* 33, 7972–7983. doi: 10.1016/j.biomaterials.2012.07.055

Mei, X., and Cheng, K. (2020). Recent development in therapeutic cardiac patches. *Front. Cardiovasc. Med.* 7:610364. doi: 10.3389/fcvm.2020.610364

Muzhou, Wang, Julia, A., and Kornfield. (2012). Measuring shear strength of soft-tissue adhesives. *J. Biomed. Mater. Res. Part B Appl. Biomater.* 100B, 618–623. doi: 10.1002/jbm.b.31981

Nam, S., and Mooney, D. (2021). Polymeric tissue adhesives. *Chem. Rev.* [Epub ahead of print] . doi: 10.1021/acs.chemrev.0c00798

Ning, L., Zhu, N., Mohabatpour, F., Sarker, M. D., Schreyer, D. J., and Chen, X. (2019). Bioprinting Schwann cell-laden scaffolds from low-viscosity hydrogel compositions. *J. Mater. Chem. B* 7, 4538–4551. doi: 10.1039/C9TB00669A

Nishiguchi, A., Kurihara, Y., and Taguchi, T. (2019). Underwater-adhesive microparticle dressing composed of hydrophobically-modified Alaska pollock gelatin for gastrointestinal tract wound healing. *Acta Biomater.* 99, 387–396. doi: 10.1016/j.actbio.2019.08.040

Nishiguchi, A., and Taguchi, T. (2020). Designing an anti-inflammatory and tissue-adhesive colloidal dressing for wound treatment. *Colloids Surfaces B Biointerfaces* 188:110737. doi: 10.1016/j.colsurfb.2019.110737

Noor, N., Shapira, A., Edri, R., Gal, I., Wertheim, L., and Dvir, T. (2019). 3D printing of personalized thick and perfusable cardiac patches and hearts. *Adv. Sci.* 6:1970066. doi: 10.1002/advs.201900344

Oh, D. X., Shin, S., Yoo, H. Y., Lim, C., and Hwang, D. S. (2014). Surface forces apparatus and its applications for nanomechanics of underwater adhesives. *Korean J. Chem. Eng.* 31, 1306–1315. doi: 10.1007/s11814-014-0136-x

Park, H. C., Champakalakshmi, R., Panengad, P. P., Raghunath, M., and Mehta, J. S. (2011). Tissue adhesives in ocular surgery. *Expert Rev. Ophthalmol.* 6, 631–655. doi: 10.1586/eop.11.64

Pascual, G., Sotomayor, S., Rodriguez, M., Perez-Kohler, B., Kuhnhardt, A., Fernandez-Gutierrez, M., et al. (2016). Cytotoxicity of cyanoacrylate-based tissue adhesives and short-term preclinical in vivo biocompatibility in abdominal hernia repair. *PLoS One* 11:e0157920. doi: 10.1371/journal.pone.0157920

Pei, X., Wang, J., Cong, Y., and Fu, J. (2021). Recent progress in polymer hydrogel bioadhesives. *J. Polymer Sci.* 1–26. doi: 10.1002/pol.20210249

Quint, J. P., Mostafavi, A., Endo, Y., Panayi, A., Russell, C. S., Nourmahnad, A., et al. (2021). In vivo printing of nanoenabled scaffolds for the treatment of skeletal muscle injuries. *Adv. Healthc. Mater.* 10:e2002152. doi: 10.1002/adhm.202002152

Ramsook, S. S., and Hersh, P. S. (2015). Use of a hydrogel sealant in epithelial ingrowth removal after laser in situ keratomileusis. *J. Cataract Refract. Surg.* 41, 2768–2771. doi: 10.1016/j.jcrs.2015.11.024

Ravichandran, R., Venugopal, J. R., Mukherjee, S., Sundarrajan, S., and Ramakrishna, S. (2015). Elastomeric core/shell nanofibrous cardiac patch as a biomimetic support for infarcted Porcine myocardium. *Tissue Eng. Part A* 21, 1288–1298. doi: 10.1089/ten.tea.2014.0265

Ray, W. Z., and Mackinnon, S. E. (2010). Management of nerve gaps: autografts, allografts, nerve transfers, and end-to-side neurorrhaphy. *Exp. Neurol.* 223, 77–85. doi: 10.1016/j.expneurol.2009.03.031

Rezaie, F., Momeni-Moghaddam, M., and Naderi-Meshkin, H. (2019). Regeneration and repair of skin wounds: various strategies for treatment. *Int. J.Lower Extrem. Wounds* 18, 153473461985921. doi: 10.1177/1534734619859214

Robinson, G. A., and Madison, R. D. (2016). Polyethylene glycol fusion repair prevents reinnervation accuracy in rat peripheral nerve. *J. Neurosci. Res.* 94:636. doi: 10.1002/jnr.23734

Romano, V., Cruciani, M., Conti, L., and Fontana, L. (2016). Fibrin glue versus sutures for conjunctival autografting in primary pterygium surgery. *Cochrane Database Syst. Rev.* 12:CD011308. doi: 10.1002/14651858.CD011308.pub2

Ruvinov, E., and Cohen, S. (2013). Engineering biomaterials for myocardial regeneration and repair. *Israel J. Chem.* 53, 695–709. doi: 10.1002/ijch.201300050

Saleh, B., Dhaliwal, H. K., Portillo *mm* Ara, R., Sani, E. S., and Annabi, N. (2019). Local immunomodulation using an adhesive hydrogel loaded with mirna *mm* aden nanoparticles promotes wound healing. *Small* 15:e1902232. doi: 10.1002/smll.201902232

Salzlechner, C., Haghighi, T., Huebscher, I., Walther, A. R., and Gentleman, E. (2020). Adhesive hydrogels for maxillofacial tissue regeneration using minimally invasive procedures. *Adv. Healthcare Mater.* 9:1901134. doi: 10.1002/adhm.201901134

Sameem, M., Wood, T. J., and Bain, J. R. (2011). A systematic review on the use of fibrin glue for peripheral nerve repair. *Plast. Reconstruct. Surg.* 127, 2381–2390. doi: 10.1097/PRS.0b013e3182131cf5

Sanders, L., and Nagatomi, J. (2014). Clinical applications of surgical adhesives and sealants. *Crit. Rev. Biomed. Eng.* 42, 271–292. doi: 10.1615/CritRevBiomedEng.2014011676

Santiago, T. D., Sharifi, R., Yue, K., Sani, E. S., Kashaf, S. S., Alvarez, M. M., et al. (2019). Ocular adhesives: design, chemistry, crosslinking mechanisms, and applications. *Biomaterials* 197, 345–367. doi: 10.1016/j.biomaterials.2019.01.011

Schreader, K. J., Bayer, I. S., Milner, D. J., Loth, E., and Jasiuk, I. (2012). A polyurethane-based nanocomposite biocompatible bone adhesive. *J. Appl. Polymer* 127, 4974–4982. doi: 10.1002/app.38100

Serpooshan, V., Hu, J. B., Chirikian, O., Hu, D. A., Mahmoudi, M., and Wu, S. M. (2018). "Chapter 8 - 4D printing of actuating cardiac tissue," in *3D Printing Applications in Cardiovascular Medicine*, eds S. J. Al'aref, B. Mosadegh, S. Dunham, and J. K. Min (Boston: Academic Press), 153–162. doi: 10.1016/B978-0-12-803917-5.00008-0

Serpooshan, V., Julien, M., Nguyen, O., Wang, H., Li, A., Muja, N., et al. (2010). Reduced hydraulic permeability of three-dimensional collagen scaffolds attenuates gel contraction and promotes the growth and differentiation of mesenchymal stem cells. *Acta Biomater.* 6, 3978–3987. doi: 10.1016/j.actbio.2010.04.028

Serpooshan, V., Quinn, T. M., Muja, N., and Nazhat, S. N. (2013a). Hydraulic permeability of multilayered collagen gel scaffolds under plastic compression-induced unidirectional fluid flow. *Acta Biomater.* 9, 4673–4680. doi: 10.1016/j.actbio.2012.08.031

Serpooshan, V., and Ruiz-Lozano, P. (2014). Ultra-rapid manufacturing of engineered epicardial substitute to regenerate cardiac tissue following acute ischemic injury. *Methods Mol. Biol.* 1210, 239–248. doi: 10.1007/978-1-4939-1435-7_18

Serpooshan, V., Zhao, M., Metzler, S. A., Wei, K., Shah, P. B., Wang, A., et al. (2013b). The effect of bioengineered acellular collagen patch on cardiac remodeling and ventricular function post myocardial infarction. *Biomaterials* 34, 9048–9055. doi: 10.1016/j.biomaterials.2013.08.017

Serpooshan, V., Zhao, M., Metzler, S. A., Wei, K., Shah, P. B., Wang, A., et al. (2014). Use of bio-mimetic three-dimensional technology in therapeutics for heart disease. *Bioengineered* 5, 193–197. doi: 10.4161/bioe.27751

Shin, J., Choi, S., Kim, J. H., Cho, J. H., Jin, Y., Kim, S., et al. (2019). Tissue tapes—phenolic hyaluronic acid hydrogel patches for off-the-shelf therapy. *Adv. Funct. Mater.* 29:1903863. doi: 10.1002/adfm.201903863

Shin, J., Kang, E. H., Choi, S., Jeon, E. J., Cho, J. H., Kang, D., et al. (2021). Tissue-adhesive chondroitin sulfate hydrogel for cartilage reconstruction. *ACS Biomater. Sci. Eng.* [Epub ahead of print]. doi: 10.1021/acsbiomaterials.0c01414

Shin, J., Lee, J. S., Lee, C., Park, H. I., and Cho, S. O. (2015). Tissue adhesive catechol-modified hyaluronic acid hydrogel for effective, minimally invasive cell therapy. *Adv. Funct. Mater.* 25, 3814–3824. doi: 10.1002/adfm.201500006

Shirzaei Sani, E., Kheirkhah, A., Rana, D., Sun, Z., Foulsham, W., and Sheikhi, A. (2019). Sutureless repair of corneal injuries using naturally derived bioadhesive hydrogels. *Sci. Adv.* 5:eaav1281. doi: 10.1126/sciadv.aav1281

Shirzaei Sani, E., Portillo-Lara, R., Spencer, A., Yu, W., Geilich, B. M., Noshadi, I., et al. (2018). Engineering adhesive and antimicrobial hyaluronic acid/elastin-like polypeptide hybrid hydrogels for tissue engineering applications. *Acs Biomater. Sci. Eng.* 4, 2528–2540. doi: 10.1021/acsbiomaterials.8b00408

Shoo, H., and Stewart, R. J. (2010). Biomimetic underwater adhesives with environmentally triggered setting mechanisms. *Adv. Mater.* 22, 729–733. doi: 10.1002/adma.200902380

Simson, J. A., Strehin, I. A., Allen, B. W., and Elisseeff, J. H. (2013). Bonding and fusion of meniscus fibrocartilage using a novel chondroitin sulfate bone marrow tissue adhesive. *Tissue Eng. Part A* 19, 1843–1851. doi: 10.1089/ten.tea.2012.0578

Soler-Botija, C., Bagó, J. R., and Bayes-Genis, A. (2012). A bird's-eye view of cell therapy and tissue engineering for cardiac regeneration. *Ann. N. Y. Acad. Sci.* 1254, 57–65. doi: 10.1111/j.1749-6632.2012.06519.x

Soucy, J. R., Shirzaei Sani, E., Portillo Lara, R., Diaz, D., Dias, F., Weiss, A. S., et al. (2018). Photocrosslinkable gelatin/tropoelastin hydrogel adhesives for peripheral nerve repair. *Tissue Eng. Part A*. 24, 1393–1405. doi: 10.1089/ten.tea.2017.0502

Spotnitz, W. D. (2014). Fibrin sealant: the only approved hemostat, sealant, and adhesive-a laboratory and clinical perspective. *ISRN Surg.* 2014, 203943. doi: 10.1155/2014/203943

Stephanie, E., Ajay, R., David, J. S., and Xiongbiao, C. (2017). Bioprinted fibrin-factor XIII-hyaluronate hydrogel scaffolds with encapsulated Schwann cells and their in vitro characterization for use in nerve regeneration. *Bioprinting* 5, 1–9. doi: 10.1016/j.bprint.2016.12.001

Stevens, B., Yang, Y., Mohandas, A., Stucker, B., and Nguyen, K. T. (2010). A review of materials, fabrication methods, and strategies used to enhance bone regeneration in engineered bone tissues. *J. Biomed. Mater. Res. Part B Appl. Biomater.* 85b, 573–582. doi: 10.1002/jbm.b.30962

Streeter, B. W., Xue, J., Xia, Y., and Davis, M. E. (2019). Electrospun nanofiber-based patches for the delivery of cardiac progenitor cells. *ACS Appl. Mater. Interfaces* 11, 18242–18253. doi: 10.1021/acsami.9b04473

Strehin, I., Nahas, Z., Arora, K., Nguyen, T., and Elisseeff, J. (2010). A versatile pH sensitive chondroitin sulfate-PEG tissue adhesive and hydrogel. *Biomaterials* 31, 2788–2797. doi: 10.1016/j.biomaterials.2009.12.033

Subhamoy, D., and Baker, A. B. (2016). Biomaterials and nanotherapeutics for enhancing skin wound healing. *Front. Bioeng. Biotechnol.* 4:82. doi: 10.3389/fbioe.2016.00082

Suneetha, M., Rao, K. M., and Han, S. S. (2019). Mussel-inspired cell/tissue-adhesive, hemostatic hydrogels for tissue engineering applications. *ACS Omega* 4, 12647–12656. doi: 10.1021/acsomega.9b01302

Taboada, G. M., Yang, K., Pereira, M. J. N., Liu, S. S., and Lee, Y. (2020). Overcoming the translational barriers of tissue adhesives. *Nat. Rev. Mater.* 5, 1–20. doi: 10.1038/s41578-019-0171-7

Thi, T., Lee, Y., Le, P., and Park, K. D. (2019). Engineered horseradish peroxidase-catalyzed hydrogels with high tissue adhesiveness for biomedical applications. *J. Ind. Eng. Chem.* 78, 34–52. doi: 10.1016/j.jiec.2019.05.026

Tomov, M. L., Gil, C. J., Cetnar, A., Theus, A. S., Lima, B. J., Nish, J. E., et al. (2019). Engineering functional cardiac tissues for regenerative medicine applications. *Curr. Cardiol. Rep.* 21:105. doi: 10.1007/s11886-019-1178-9

Tong, A. Y., Gupta, P. K., and Kim, T. (2018). Wound closure and tissue adhesives in clear corneal incision cataract surgery. *Curr. Opin. Ophthalmol.* 29, 14–18. doi: 10.1097/ICU.0000000000000431

Tottoli, E. M., Dorati, R., Genta, I., Chiesa, E., and Conti, B. (2020). Skin wound healing process and new emerging technologies for skin wound care and regeneration. *Pharmaceutics* 12:735. doi: 10.3390/pharmaceutics12080735

Tsuchiya, T., Doi, R., Obata, T., Hatachi, G., and Nagayasu, T. (2020). Lung microvascular niche, repair, and engineering. *Front. Bioeng. Biotechnol.* 8:105. doi: 10.3389/fbioe.2020.00105

Turabee, M. H., Thambi, T., and Lee, D. S. (2019). Development of injectable tissue-adhesive hybrid hydrogel for growth factor-free tissue integration in advanced wound regeneration. *ACS Appl. Biol. Mater.* 2, 2500–2510. doi: 10.1021/acsabm.9b00204

Vermonden, T., Fedorovich, N. E., Van Geemen, D., Alblas, J., Van Nostrum, C. F., Dhert, W. J., et al. (2008). Photopolymerized thermosensitive hydrogels: synthesis, degradation, and cytocompatibility. *Biomacromolecules* 9, 919–926. doi: 10.1021/bm7013075

Vig, K., Chaudhari, A., Tripathi, S., Dixit, S., Sahu, R., Pillai, S., et al. (2017). Advances in skin regeneration using tissue engineering. *Int. J. Mol. Sci.* 18, 789. doi: 10.3390/ijms18040789

Walker, B. W., Lara, R. P., Yu, C. H., Sani, E. S., and Annabi, N. (2019). Engineering a naturally-derived adhesive and conductive cardiopatch. *Biomaterials* 207, 89–101. doi: 10.1016/j.biomaterials.2019.03.015

Wang, B., Lee, J. S., Jeon, Y. S., Kim, J., and Kim, J. H. (2018). Hydrophobicity enhanced adhesion of novel biomimetic biocompatible polyaspartamide derivative glues. *Polymer Int.* 67, 557–565. doi: 10.1002/pi.5544

Wang, W., Degrugillier, L., Tremp, M., Prautsch, K., Sottaz, L., Schaefer, D. J., et al. (2018). Nerve repair with fibrin nerve conduit and modified suture placement. *Anat. Rec. Adv. Integr. Anat. Evol. Biol.* 301, 1690–1696. doi: 10.1002/ar.23921

Wieken, K., Angioi-Duprez, K., Lim, A., Marchal, L., and Merle, M. (2003). Nerve anastomosis with glue: comparative histologic study of fibrin and cyanoacrylate glue. *J. Reconstruct. Microsurg.* 19, 017–020. doi: 10.1055/s-2003-37186

Wiltsey, C., Christiani, T., Williams, J., Scaramazza, J., Van Sciver, C., Toomer, K., et al. (2015). Thermogelling bioadhesive scaffolds for intervertebral disk tissue engineering: preliminary in vitro comparison of aldehyde-based versus

alginate microparticle-mediated adhesion. *Acta Biomater.* 16, 71–80. doi: 10.1016/j.actbio.2015.01.025

Xin, Liu, Qin, Zhang, Guanghui, and Ga. (2017). Bioinspired adhesive hydrogels tackified by nucleobases. *Adv. Funct. Mater.* 27:1703132. doi: 10.1002/adfm.201703132

Xin, S., Wyman, O. M., and Alge, D. L. (2018). Assembly of PEG microgels into porous cell-instructive 3D scaffolds via thiol-ene click chemistry. *Adv. Healthcare Mater.* 7:1800160. doi: 10.1002/adhm.201800160

Yin, S., Zhang, W., Zhang, Z., and Jiang, X. (2019). Recent advances in scaffold design and material for vascularized tissue⊥ngineered bone regeneration. *Adv. Healthcare Mater.* 8:e1801433. doi: 10.1002/adhm.201801433

Yorston, D., and Garg, P. (2009). Corneal grafting: what eye care workers need to know. *Commun. Eye Health* 22, 44–45.

Yuk, H., Varela, C. E., Nabzdyk, C. S., Mao, X., and Zhao, X. (2019). Dry double-sided tape for adhesion of wet tissues and devices. *Nature* 575, 169–174. doi: 10.1038/s41586-019-1710-5

Zaokari, Y., Persaud, A., and Ibrahim, A. (2020). Biomaterials for adhesion in orthopedic applications: a review. *Eng. Regen.* 1, 51–63. doi: 10.1016/j.engreg.2020.07.002

Zhang, J., Zhang, X., Hong, Y., Fu, Q., He, Q., Mechakra, A., et al. (2020). Tissue-adhesive paint of silk microparticles for articular surface cartilage regeneration. *ACS Appl. Mater. Interfaces* 12, 22467–22478. doi: 10.1021/acsami.0c01776

Zhang, and Jianyi. (2015). Engineered tissue patch for cardiac cell therapy. *Curr. Treatment Options Cardiovasc. Med.* 17, 1–10. doi: 10.1007/s11936-015-0399-5

Zhao, Y., Wu, Y., Wang, L., Zhang, M., and Wang, Z. (2017). Bio-inspired reversible underwater adhesive. *Nat. Commun.* 8:2218. doi: 10.1038/s41467-017-02387-2

Zhou, Y., Zhao, J., Sun, X., Li, S., Hou, X., Yuan, X., et al. (2016). Rapid gelling chitosan/polylysine hydrogel with enhanced bulk cohesive and interfacial adhesive force: mimicking features of epineurial matrix for peripheral nerve anastomosis. *Macromolecules* 17, 622–630. doi: 10.1021/acs.biomac.5b01550

Zoe, M. R., Elizabeth, W. Z., June, C. A., and Louise, F. B. (2019). Development and use of biomaterials as wound healing therapies. *Burns Trauma* 7:2. doi: 10.1186/s41038-018-0139-7

Ztürk, E., Stauber, T., Levinson, C., Cavalli, E., Arlov, Y., and Zenobi-Wong, M. (2020). Tyrosinase-crosslinked, tissue adhesive and biomimetic alginate sulfate hydrogels for cartilage repair. *Biomed. Mater.* 15:045019. doi: 10.1088/1748-605X/ab8318

**Conflict of Interest:** The authors declare that the research was conducted in the absence of any commercial or financial relationships that could be construed as a potential conflict of interest.

frontiers in Bioengineering and Biotechnology

REVIEW
published: 02 August 2021
doi: 10.3389/fbioe.2021.673477

# Bioengineering the Cardiac Conduction System: Advances in Cellular, Gene, and Tissue Engineering for Heart Rhythm Regeneration

*Nataliia Naumova and Laura Iop**

*Department of Cardiac Thoracic Vascular Sciences and Public Health, University of Padua, Padua, Italy*

Heart rhythm disturbances caused by different etiologies may affect pediatric and adult patients with life-threatening consequences. When pharmacological therapy is ineffective in treating the disturbances, the implantation of electronic devices to control and/or restore normal heart pacing is a unique clinical management option. Although these artificial devices are life-saving, they display many limitations; not least, they do not have any capability to adapt to somatic growth or respond to neuroautonomic physiological changes. A biological pacemaker could offer a new clinical solution for restoring heart rhythms in the conditions of disorder in the cardiac conduction system. Several experimental approaches, such as cell-based, gene-based approaches, and the combination of both, for the generation of biological pacemakers are currently established and widely studied. Pacemaker bioengineering is also emerging as a technology to regenerate nodal tissues. This review analyzes and summarizes the strategies applied so far for the development of biological pacemakers, and discusses current translational challenges toward the first-in-human clinical application.

**Keywords: biological pacemaker, cardiac conduction system, cardiac diseases, bioengineering, gene engineering, tissue engineering**

OPEN ACCESS

***Edited by:***
*Vahid Serpooshan, Emory University, United States*

***Reviewed by:***
*Gerard J. J. Boink, University of Amsterdam, Netherlands*
*Wuqiang Zhu, Mayo Clinic Arizona, United States*

****Correspondence:***
*Laura Iop*
*laura.iop@unipd.it*

***Specialty section:***
*This article was submitted to Tissue Engineering and Regenerative Medicine, a section of the journal Frontiers in Bioengineering and Biotechnology*

***Received:*** *27 February 2021*
***Accepted:*** *24 June 2021*
***Published:*** *02 August 2021*

***Citation:***
*Naumova N and Iop L (2021) Bioengineering the Cardiac Conduction System: Advances in Cellular, Gene, and Tissue Engineering for Heart Rhythm Regeneration. Front. Bioeng. Biotechnol. 9:673477. doi: 10.3389/fbioe.2021.673477*

## INTRODUCTION

Cardiac and cardiovascular diseases are globally increasing due to the aging of populations. The total number of electronic cardiac pacemaker implantations has risen accordingly (Mensah et al., 2019; Bai et al., 2020; Peters et al., 2020; Virani et al., 2020). However, even with continuous technological improvements, current-generation electronic pacemakers still have significant limitations and complications regarding the clinical application. Electronic pacemaker implantations are accompanied with numerous challenges, such as the risk of various infections, a relatively short battery life, lead failure/repositioning, pacemaker material allergy, electronic interference, an occasional component failure, vascular, and other complications (Nishii, 2016). Several cardiac conditions require additional non-device approaches as in the case of a congenital heart block, which cannot be treated using electronic pacemakers, or in the case of a contraindication to reimplantation before effective antibiosis is established. A congenital heart block and other congenital cardiac conditions could result in fetal death or stillbirth and, in most cases, require *in utero* pacing (Gutiérrez et al., 1989; DeSimone and Sohail, 2018; Manolis et al., 2020).

Biological pacemakers could be, therefore, a new promising therapeutic alternative to current electronic devices, being the advanced, effective biotechnology to counter these challenges. The concept of biological pacemakers is based on bioengineering and biotechnology approaches for the production and implantation of different pacemaker cellular components for the electrical pacing of heart. As of date, numerous studies are conducted, and methodologies are proposed to create clinically relevant biological pacemakers as an alternative to the artificial cardiac devices.

## ANATOMY, BIOLOGY, AND PHYSIOLOGY OF THE CARDIAC CONDUCTION SYSTEM

The mammalian cardiac conduction system can be figured as an electrical path able to generate the impulse and transfer it across the heart, where it triggers the electromechanical force at the base of the pump function. In this electrical path, several stations with a precise functional hierarchy are present: firstly, the sinoatrial node (SAN); then, the atrioventricular node (AVN), the His bundle, the left and right bundle branches; and, finally, the Purkinje fibers (Park and Fishman, 2011; Persson and Persson, 2012).

### The Sinoatrial Node

SAN is a natural pacemaker of the heart, i.e., the specialized myocardial tissue responsible for our 2-billion heartbeats in the lifespan. Described for the first time by Keith and Flack in 1907 as a "wonderful structure" Keith and Flack (1907), the SAN is the heart conduction system's primary station.

In almost all mammals, SAN is localized sub-epicardially in the *sulcus terminalis*, namely the terminal groove, in the junctional region between the right atrium and superior vena cava (Liu et al., 2007). In most cases, it displays a tadpole shape with a length varying from 1.5 mm in mouse to 15 mm in humans (James, 1961; Liu et al., 2007), but large variability in size and localization has been observed in intraspecies and interspecies anatomical comparisons (James, 1977).

Being already distinguishable from 6 to 8 weeks of embryonic development, this specialized tissue has a particular composition in cells and extracellular matrix elements, rendering it very particular with respect to the working myocardium and other adjacent structures. An intricate network of collagens surrounds, in humans, the cells responsible for the generation of the impulse, the so-called pacemaker cells (PCs), and other cytotypes, i.e., the transitional cells. Each PC displays a clear cytoplasmic zone around a large, centrally located nucleus with little glycogen amount and randomly oriented myofibrils and small mitochondria. Proximity to and arrangement in clusters or grapes are mainly observed among PCs, but the interconnection is poor with the absence of intercalated disks and tight junctions (James, 1977). During SAN depolarization, the spontaneous release of $Ca^{2+}$ from the sarcoplasmic reticulum through the ryanodine receptor 2 (RYR2) activates the five distinct ionic currents of PCs, i.e., (1) the voltage-dependent outward current $I_k$, generated by ERG channels, (2) the inward current carried by $Na^+$ and $K^+$ ions, the so-called funny current $I_f$, dependent on HCN1/4 channels, (3) the L-type $Ca^{2+}$ current, i.e., $I_{Ca,L}$, generated by Cav1.2/1.3; (4) the T-type $Ca^{2+}$ current, i.e., $I_{Ca,T}$ mediated by Cav3.1/3.2 channels, and, finally, (5) the inward $Na^+$-$Ca^{2+}$ exchange current, i.e., $I_{NaCa}$ due to the NCX1 channels. All these membrane ion channels concur to the physiological automaticity of SAN, but a long debate is still going on the predominant one in controlling the spontaneous diastolic depolarization (DD) (Lakatta and DiFrancesco, 2009; DiFrancesco, 2020). $I_f$ current is largely considered the electrophysiological hallmark of SAN. It was discovered as an inward current in 1979 by the electrophysiological analysis of the cell preparation of a rabbit sinoatrial node. Indeed, an inward current was previously observed in the hearts of mammals and amphibians (Noma and Irisawa, 1976; Brown et al., 1977): however, its relevance was not immediately recognized, nor the contributing ion channel(s) were distinguished. The unusual behavior and features of the just identified current induced its discoverers Brown and colleagues to describe it as "funny." It was, in fact, unprecedented that an ionic current was revealed to be activated by hyperpolarization at a very low threshold, works at the voltage range that includes the DD voltage diapason (from −40/50 to −100 mV), and display kinetics characterized by reverse at about −10/−20 mV thanks to the $Na^+/K^+$ channel permeability (Brown et al., 1979). Not only $I_f$ was demonstrated to possess these unique properties, but also showed responsiveness to adrenergic and muscarinic stimulations. All the fundamental requisites for DD generation and heart rate modulation are indicative of the pacemaking ability of $I_f$ current. Lately, another feature was found to render $I_f$ unique, namely its physiological retrieval in almost no other body tissues than SAN (Liu et al., 2007). Another inward current gained interest as a possible "intracellular $Ca^{2+}$ clock," i.e., $I_{NaCa}$: $Ca^{2+}$ cycling at the sarcolemmal membrane is particularly relevant for normal pacemaker automaticity and, hence, it could represent another mechanism of pacemaking (Maltsev and Lakatta, 2008). During DD, in fact, NCX channels become activated by the spontaneous, local $Ca^{2+}$ releases after the opening of RYR2. As a consequence, the depolarization of the membrane potential is increased until the threshold for the next action potential is reached. Uncertainty still remains about the relative roles of $I_f$ (membrane voltage clock) and $I_{NaCa}$ (intracellular $Ca^{2+}$ clock) in the normal total pacemaker clock (Lakatta and DiFrancesco, 2009). Conversely, the conclusive phase of the action potential in PCs has been more defined, with $Ca^{2+}$ re-uptaking in the sarcoplasmic reticulum *via* $Ca^{2+}$ ATPase SERCA2 (Irisawa et al., 1993; Mangoni et al., 2006; Maltsev and Lakatta, 2008; Chandler et al., 2009).

Around PC grape-like clusters, transitional cells distribute in the outer half part of SAN. Despite a similar elongated aspect to working myocardial cells, transitional elements are smaller in size, very interweaved, abundant in glycogen, less rich in myofibrils and mitochondria, distributed in an arranged fashion. Transitional cells are much higher in number than PCs and are responsible for transmitting the sinus impulse to the ordinary myocardium. These SAN cells have an embryonic origin in

the *sinus venosus* as other cell types composing the node, i.e., fibroblasts and nerve cells.

An important component of SAN is its main artery, prevalently originating from the right coronary artery as its first branch. The SAN artery crosses the node centrally and is widely interconnected with the right and circumflex coronary tree, thus supplying blood to the atrium and the same node. A copious net of capillaries, arterioles, and venules supports the vascularization of the whole SAN.

Due to its proximity and arterial connection to the aorta, SAN also exerts a sensor role for monitoring central aortic pressure and pulse, a servomechanism stabilizing pulse and impulse. Moreover, adrenergic and cholinergic nerves operate as further functional stabilizers in the beat-to-beat frame and in the longest time. In particular, the balanced autonomic innervation contributes to the stable performance of SAN in its postnatal maturity (James, 1970).

## The Atrioventricular Node

AVN lies at the conjunction of the right atrium and the right ventricle. For this purpose, Tawara (1906) described it as the sole electrical connection between the upper and lower chambers of heart as he first observed in several mammalian species. This anatomical hypothesis was confirmed after 1 year by Keith and Flack (1907) and further elaborated 7 years later by Kent (1913) as a multiple, muscular atrioventricular path. Knowledge about AVN was progressively re-evaluated with an increase in interest not only by anatomists and histologists but also by molecular/clinical cardiologists and electrophysiologists (Anderson and Siew, 2002).

This second station of the conduction system appears as a small spindle-shaped structure localized in humans at the apex of the Koch triangle, an endocardial region ideally defined by the coronary sinus orifice, the Todaro tendon, and the septal leaflet of the tricuspid valve. AVN receives blood supply *via* the right coronary artery in the right heart dominance case (Kurian et al., 2010; Anderson et al., 2020). Besides a compact nodal area, a transitional region is present. Two electrophysiologically distinct conduction pathways connect SAN to AVN. The pathways were described first in 1971 (Spach et al., 1971) as the "fast AVN" and the "slow AVN" ones as they are the fastest and slowest pathways for the action potential *via* AVN (Dobrzynski et al., 2013). Therefore, AVN is characterized by a "dual-pathway electrophysiology": the route *via* the interatrial septum connects to the fast (normal) pathway, and the route *via* the terminal crest connects to the slow pathway (Meijler and Janse, 1988; Dobrzynski et al., 2013).

The inferior extension of AVN is much debated, which recently has been better characterized in human hearts (Anderson et al., 2020; Cabrera et al., 2020). In particular, wide variability was described in terms of dimension and penetration degree for the AVN conduction tracts entering the myocardium as well as for the subsequent part of the conduction system, i.e., the bundle of His (further details in the next subchapter). Intrahuman variability has been observed for many AVN components, such as the nodal region morphology and the connections of atrial myocardium (Anderson et al., 2020; Sternick and Sánchez-Quintana, 2021).

AVN generates cardiac automaticity only as a subsidiary to SAN and with different characteristics from the first conduction system station. AVN shows a filtering activity protecting the ventricles from supraventricular tachycardia. Its conduction velocity is slower (AVN delay); thus, the potential action transmission is highly controlled, and the atrial and ventricular excitation–contraction cycle is very coordinated also in the case of atrial fibrillation or tachycardia. AVN-generated automaticity is only subordinate to SAN and might impose only with the dysfunctional pacemaking of the latter (Meijler and Janse, 1988). It has been reported that a minimum of three different functional regions and five different cell types constitute AVN. From AVN cell types, cell junctions with ventricular bundle branch and His cells are established. Like SAN PCs, midnodal cells are very packed in the so-called Tawara's "Knote" or N region, display scarce myofibrils, and rarely establish junctional relationships (Meijler and Janse, 1988). They express HCN4 (Huang et al., 2013; Xia et al., 2020) and depend on voltage-gated L-type Cav1.3 and T-type Cav3.1 $Ca^{2+}$ channels, too (Baudot et al., 2020), through which pacemaking can be controlled when required. Transitional cells derive their name from the AVN midnodal region transition toward the atrial myocardium. In the rabbit heart, where they have been deeply studied, three transitional cell types have been distinguished mainly depending on their location (Anderson et al., 1974). Lower nodal cells are arranged in a bundle parallel to AVN and display a smaller size than atrial cells (Meijler and Janse, 1988). The NH region identifies the cells that connect with the His bundle and are thought to be the sites of AVN automaticity. The AVN nodal delay depends on the transmission through these multiple bundles and a peculiar arrangement of connexins in the nodal cells. In addition, the diameter of these latter concurs in the transmission delay as well as the possible presence of passive electrical properties (Pollack, 1976; Meijler and Janse, 1988; LeBlanc and Dubé, 1993; Choi and Salama, 1998). The typical connexins of the physiologic human myocardium, namely Cx43, 45, 40, and 31.9, show a differential distribution in AVN by combining in specific ratios and in a reduced number of gap junctions. For example, Cx43, being very abundant in the working myocardium, is only expressed in the AVN penetrating bundle, whereas Cx45 is present in both the compact node and inferior extension (Dobrzynski et al., 2013).

The AVN delay might be related to the relative paucity of connexins, especially Cx43, as well as to the reduced number of $Na_v1.5$ channels and hence, the dependence on a slow inward ion current, as firstly hypothesized by Rougier et al. (1969) in the frog atrium and by Zipes and Mendez (1973) in the isolated rabbit heart.

## The His Bundle, Bundle Branches, and Purkinje Fibers

The discovery of the His bundle by its homonymous researcher dates to almost 15 years before identifying SAN and AVN. It was

only at the beginning of the 1970s that James and Sherf (1971) differentiated histologically the regions belonging to AVN and the His bundle.

Anatomically, the His bundle appears as a group of fibers with surrounding electrical isolation provided by the central fibrous body. This fascicle exits AVN, and mainly enters the membranous septum at the apex of the Koch triangle to continue afterward into the left and right bundle branches. Through its triple ramification, the thicker left bundle branch is responsible for the excitation of the mid-septal area and the regions of the anterolateral and the posteromedial papillary muscles. The right bundle branch travels toward the moderator band and the anterolateral papillary muscle. Lastly, they both culminate in the sub-endocardium, respectively, in the left and the right ventricles, by connecting with Purkinje fibers that contribute to the transmission of the electrical signal to the endocardial ventricular regions (Padala et al., 2021).

Compared to the surrounding cells, Purkinje cells are histologically distinguishable thanks to their clear cytoplasm, as observed first by Jan Purkinje in 1839 (Cavero et al., 2017). Unlike the cells composing the upper portions of the conduction system, Purkinje fibers display no electrical isolation from the rest of the cardiac tissues although they equally propagate the electrical impulse and show pacing and triggered activity but to a minimal extent. Interestingly, the type and distribution of connexins, namely Cx40 and 43, are peculiar to Purkinje cells with respect to the cells constituting the His bundle. Moving from the His bundle toward Purkinje fibers, the expression of Cx40 increases. Cx43 cellular localization becomes membranous and copious only in Purkinje cells that interact among themselves and not with other sub-endocardial cells (Dun and Boyden, 2008). Regarding action potentials, the duration is longer than in ventricular cells due to prolonged cell repolarization mainly dependent on $I_{KAch}$, but depolarization is short thanks to very rapid, $I_{Na}$-related maximal upstroke velocity (Gintant et al., 1984; Yang et al., 1996). Other differences can be identified in the electrophysiological behavior of Purkinje cells, as reviewed by Dun and Boyden (2008).

## APPROACHES FOR THE ENGINEERING OF BIOLOGICAL PACEMAKERS

With such a sophisticated composition and functionality, both congenital and acquired cardiac rhythm disturbances may originate from a heterogeneous spectrum of pathophysiological mechanisms (Persson and Persson, 2012). Therefore, effective anti-arrhythmic therapeutic approaches are more and more in demand for both pediatric and adult patients.

When pharmacological treatment is inefficacious to treat arrhythmias, artificial devices must be implanted to control pacing and prevent lethal consequences. These artificial treatments are lifesaving but show many shortcomings associated with a possible generator malfunction, the lack of autonomic responsiveness, a short battery lifespan, undesirable interactions with strong magnetic fields, device-related infections, etc. (Cingolani et al., 2018; Co et al., 2021; Joury et al., 2021). Additional challenges are related to artificial device implantation in children during the existence of the conditions of rapid growth, small body size, and/or anatomical variations associated with congenital heart defects (Cingolani et al., 2018; Taleski and Zafirovska, 2021). Other limitations are associated to the cardiac patients' required continuous monitoring and implementation of early interventions (Joury et al., 2021; Taleski and Zafirovska, 2021).

Various strategies have been progressively designed and improved to restore physiological cardiac pacing through natural solutions. The first attempt to restore physiological pacing was realized in several mammal species at the end of the 1920s by transplanting autologous, allogeneic, or xenogeneic conduction system tissue, namely a pedicle of the right atrium containing SAN, in the ventricular myocardium. The intervention was disclosed generally successful in case of autologous transplantation with the established rhythm between 6 h and 5 days from heterotopic grafting. Although effective for the first hours, allogeneic and xenogeneic grafts became progressively dysfunctional and underwent fibrosis (Rylant, 1927). About 40 years later, several preclinical studies were proposed to re-establish the electrical conduction between the right auricle and ventricle in a canine model of normal heart or complete block. By applying the same pedicle technique, autologous SAN tissues demonstrated to pace only after 2 months from the implantation in the normal heart (Ernst and Paulson, 1962). After a stable, complete heart block, the implanted autologous SANs established no influence on the recipient's preexistent idioventricular rhythm (Starzl et al., 1963). Uncertainties on the validity of the surgical technique applied and other technological difficulties related to the implantation and monitoring of the conduction tissue (e.g., pacemaker malfunctions) were also evident with further investigation (Morishita et al., 1981). Although not completely clear in the eyes of the scientists who tried it first, this initial approach could not be successful for many reasons, starting with a possible immune response to the allogeneic/xenogeneic tissue (foreign body reaction) up to the difficulties to achieve electrical integration and coupling with recipient's myocardium. With the current knowledge, one of the main causes of this unsuccess—besides immunoreaction—was the phenomenon of core necrosis (Rouwkema et al., 2009), which is a consequence of the blood supply insufficiency and a sign of failed tissue integration, very well-known to bioengineers.

In the path toward natural rhythm restoration (**Figure 1**), several technological advances are deeply contributing to an increased understanding of conductance (patho)physiology (Franco and Icardo, 2001; Goodyer et al., 2019; van Eif et al., 2020; Padala et al., 2021), as well as to its more feasible addressing for resolution. Methodologies based on naturally pacing cells, stem cell differentiation, gene engineering, tissue engineering, and/or their combination have been rehearsed so far *in vitro* and *in vivo* with varying success rates in restoring adequate cardiac pacing and conduction.

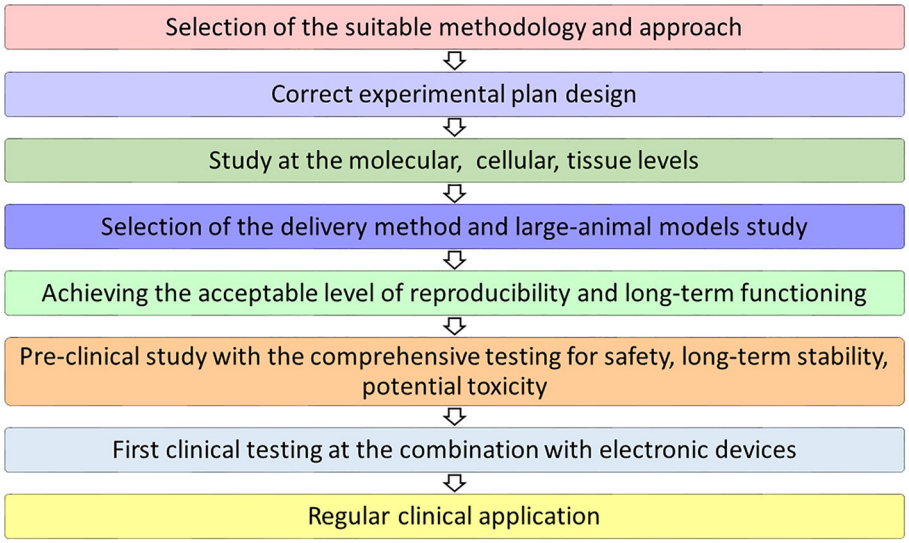


**FIGURE 1 |** Milestones for the clinical translation of a bioengineered pacemaker.

## Cell-Based Approaches Using SAN Cells

After the initial unsuccessful, autologous, allogeneic, and xenogeneic transplantation trials of the SAN tissue (Rylant, 1927; Ernst and Paulson, 1962; Starzl et al., 1963; Morishita et al., 1981), subsequent attempts were realized using the methodologies characterized by an inferior technical demand.

One of the first approaches utilized to re-establish the biological pacemaker function was the cell-based one, relying on the concept of transplanting not a complete SAN tissue, but only its cells, possibly mixed with atrial cardiomyocytes. Typically, these methodologies are focused on the intrinsically electrogenic ability of the injected cells, which are expected to act as an ectopic pacemaker after functional electrical coupling with host working cardiomyocytes (**Table 1**).

Ruhparwar et al. (2002) dissociated the fetal canine atrial cardiomyocytes and injected them into the left ventricle of an adult dog model of X-linked muscular dystrophy. Successful electrical and mechanical coupling between host and donor cardiomyocytes was disclosed. Later, in 2005, the similar results were reported with a cell preparation of human atrial cardiomyocytes containing SAN PCs. When the mixed human atrial cells were injected into the porcine left ventricles, functional junctions, effective pacing, and an optimal autonomic response between donor cells and host cardiomyocytes were identified (Lin et al., 2005).

In another preclinical study, autologous SAN cells were injected into the myocardial wall of the right ventricle in a dog model after a complete heart block and the implantation of an electronic pacemaker. In spite of preserving the electrical activity, they showed different pacing features compared to their originating conduction system station. This observation highlights the relevant role of substrate conditioning in cell pacemaking activity (Zhang et al., 2011) and, hence, the still poorly studied but specific modulatory effect exerted by local cellular and extracellular microenvironments on the phenotype of exogenously introduced cells.

Although these initial cell-based strategies did not reach any clinical translation, they served as proof-of-concept for more advanced stem cell-based therapies and the next generation of pacemakers with optimal functioning after implantation in the selected regions of the heart.

## Cell-Based Approaches Using Pluripotent Stem Cell-Derived Cardiomyocytes

Pluripotent stem cells (PSCs), i.e., embryonic stem cells (ESCs) and induced PSCs (iPSCs), are considered the most promising stem cell types regarding their ability to differentiate into a virtually unlimited number of body cell types, including those derived from the cardiac lineage (Rajala et al., 2011; Kadota et al., 2020). An accurate methodology for cardiomyocyte differentiation and/or PC specification from human PSCs (hPSCs) is based on the features and patterns of the embryonic cardiac development and aims to recapitulate *in vitro* the stage-specific modulation of its signaling pathways. It includes experimental tactics of embryoid body development (Yang et al., 2008) or monolayer attachment culture with specific biochemical conditioning (Laflamme et al., 2007). Yet, the differentiation of PSCs to cardiomyocytes mainly results in a mixture of atrial, ventricular, and nodal cells; therefore, the ultimate goal to guide the differentiation into a desired subtype and to create the biological pacemaker appears challenging (**Table 2**) (Xu et al., 2002; He et al., 2003; Yang et al., 2008; Jung et al., 2012, 2014; Mandel et al., 2012; Müller et al., 2012; Christoforou et al., 2013; Birket et al., 2015; Protze et al., 2016; Chauveau et al., 2017; Dorn et al., 2018; Zhang and Huang, 2019; Zhang et al., 2019a; Yechikov et al., 2020).

Human ESCs (hESCs) are widely utilized in stem cell-based methodologies due to their ability to differentiate

**TABLE 1 |** Cell-based biopacemaking approaches using SAN cells.

| SAN cells | Methodology and experimental details | References |
|---|---|---|
| Canine, mixed atrial cardiomyocytes | Dissociated fetal canine atrial cardiomyocytes were transplanted into the left ventricle of an adult dog model of X-linked muscular dystrophy. Electrical and mechanical coupling between the host and donor cardiomyocytes were observed. | Ruhparwar et al., 2002 |
| Human, mixed atrial cardiomyocytes | Dissociated human atrial cardiomyocytes containing SAN PCs were injected into porcine left ventricles. Functional junctions, effective pacing, and optimal autonomic reaction between the donor cells and host cardiomyocytes were identified. | Lin et al., 2005 |
| Canine SAN cells | SAN cells were injected into the right ventricle subepicardial free wall and dogs were monitored for 2 weeks. Pacemaker function was assessed by overdrive pacing and IV epinephrine challenge. SAN cells expressed a time-dependent inward current (If) activating on hyperpolarization. Brisk catecholamine responsiveness occurred. However, dogs implanted with autologous SAN cells manifested biological pacing properties dissimilar from those of the anatomic tissue, thus evidencing a correlation between the substrate environment and phenotype modification in injected cells. | Zhang et al., 2011 |

*SAN, sinoatrial node; PCs, pacemaker cells.*

**TABLE 2 |** Cell-based biopacemaking approaches by PSC differentiation into cardiomyocytes.

| PSCs | Methodology and experimental details | References |
|---|---|---|
| hESCs | Electrically active hESC-derived cardiomyocytes were transplanted into guinea pig hearts. Functional integration and pacing generation were achieved. | Xue et al., 2005 |
| | Cardiomyocyte cell grafts were generated from hESC *in vitro* using the embryoid body differentiating system, this tissue formed structural and electromechanical connections with cultured rat cardiomyocytes. *In vivo* integration was shown in a large animal model of slow heart rate. The transplanted hESC-derived cardiomyocytes paced the hearts of swine with complete atrioventricular block. | Kehat et al., 2004 |
| | hESC-derived cardiomyocytes were used to form scaffold-free patches (implanted on the epicardium) and micro-tissue particles (delivered by intramyocardial injection) into the ischemia/reperfusion injured athymic rat heart. | Gerbin et al., 2015 |
| hiPSCs | SAN-like pacemaker cells from hiPSCs were identified as NKX2-5-negative, SIRPA-positive cardiomyocytes displaying pacemaker action potentials, ion current profiles, and chronotropic responses. When transplanted into the apex of rat hearts, SAN-like cells demonstrated pacemaking activity. | Protze et al., 2016 |
| | hiPSC-derived cardiomyocytes were integrated into the host myocardium of AVN-blocked dogs and induced a biological pacemaking activity. | Chauveau et al., 2017 |

*PSCs, pluripotent stem cells; hESCs, human embryonic stem cells; hiPSCs, human induced pluripotent stem cells; SAN, sinoatrial node; AVN, atrioventricular node.*

into spontaneously beating cardiomyocytes, which functionally express HCN channels (Kehat et al., 2001; Xu et al., 2002; He et al., 2003). For example, the functional integration and generation of the pacemaker activity were achieved in the transplantation experiments of electrically active hESC-derived cardiomyocytes into guinea pig hearts. Comprehensive optical mapping of the epicardial surface of these guinea pig hearts integrated with hESC-derived cardiomyocytes proved the extent of membrane depolarization being effective from the injection site to an adjacent myocardium as a bona fide sign of syncytium formation (Xue et al., 2005).

Indeed, human iPSCs (hiPSCs) are finding larger applications for the generation of PCs-like cardiomyocytes. Modern protocols currently allow to effectively generate hiPSCs-derived cardiomyocytes with the typical cardiac physiological features: a variety of ion channels, specific contracting apparatus, excitation, propagation, etc. (Xu et al., 2002; He et al., 2003; Yang et al., 2008; Jung et al., 2012; Mandel et al., 2012; Christoforou et al., 2013; Burridge et al., 2014; Birket et al., 2015; Dorn et al., 2018; Zhang and Huang, 2019). Moreover, biological pacing ability was demonstrated *in vitro* and *in vivo* (e.g., Protze et al., 2016; Chauveau et al., 2017).

Most approaches aiming at re-establishing the pacemaker activity relied on the injection of a heterogenous cardiomyocyte population derived from iPSC cardiac differentiation. For instance, after the delivery of iPSC-derived cardiomyocytes derived from embryoid body differentiation into AV block canine hearts in open thoracotomy, Chauveau et al. (2017) observed that these cells were integrated into the host heart tissue and were able to pace. However, this approach should be additionally optimized to increase the yield in the number of iPSC-derived PCs and reach a critical mass for effective and sustained pacing.

Notably, only a few studies attempted to overcome this issue by focusing on deriving SAN-like cells from the cardiac differentiation and pacemaker specification of hiPSCs (Müller et al., 2012; Birket et al., 2015; Protze et al., 2016; Zhang and Huang, 2019; Yechikov et al., 2020). Calcium-activated potassium channels were demonstrated in hPSCs as a valid target to generate an enriched population of PC-like cells by conditioning with 1-ethyl-2-benzimidazolinone (1-EBIO). After an initial induction of early mesodermal and cardiac genes (Brachyury, Isl1, and Myh6), conditioned cells displayed a small size, a high expression of the nodal marker HCN4, and a reduced content of myofibrils (Müller et al., 2012). Similarly,

1-EBIO might activate an atrial/PC cell differentiation program in conditioned ESCs and iPSCs. Birket et al. (2015) took advantage of lineage tracing to isolate the population of PCs from NKX2.5$^{eGFP/w}$ hESCs. Upon cardiac differentiation through a doxycycline-inducible MYC transgene and/or fibroblast growth factor (FGF)/bone morphogenetic proteins (BMP) signaling modulation, they observed that eGFP-negative cells were expectedly NKX2.5-negative but also expressed ISL1 and the posterior heart field marker podoplanin (PDPN) at high levels. This pattern of expression in these cardiac progenitors is typical of the native SAN during development. After further differentiation, these cells also showed a strong induction of TBX3, SHOX2, TBX18, and HCN4 and displayed the electrophysiological features of PCs. So-selected eGFP-negative, ISL1-positive, and NKX2.5-negative cardiac progenitors were demonstrated to be clonogenic and multipotent (Birket et al., 2015), therefore opening the way to further studies on development and disease modeling. However, the reliance of this PC generating system on a MYC transgene moves away from the clinical path and may require alternative strategies for a regenerative medicine application in humans.

A promising transgene-independent method for generating pure SAN-like PCs from hiPSCs was proposed by Protze et al. (2016) by a stage-specific manipulation of developmental signaling pathways. In these experiments, iPSC cardiac differentiation and PC specification were induced by time-controlled administration of several transcription factors, as first BMP4, Activin A, and bFGF, and, hence, the inhibitors of Wnt production 2 (IWP2) and vascular endothelial growth factor (VEGF), in order to induce cardiac mesoderm and cardiomyocyte generation. SAN-like PCs were selected in the whole population as NKX2.5-negative, SIRPA-positive cardiomyocytes expressing the typical SAN lineage markers (TBX18, SHOX2, TBX3, and ISL1), classic ion current profiles (e.g., $I_f$ and $I_{KAch}$), chronotropic responses, and the ability to fire pacemaker action potentials and pace ventricular cardiomyocytes *in vitro*. After the transfer into the apex of rat hearts submitted to AV block, these SAN-like cardiomyocytes demonstrated pacing activity in the host tissue and were able to function as a biological pacemaker (Protze et al., 2016).

Zhang et al. (2019b) disclosed the outcomes of a double-reporter system based on TBX5$^{Clover2}$ and NKX2.5$^{TagRFP}$ developed with CRISPR-Cas9 technology to isolate TBX5-positive, NKX2.5-negative cardiac progenitors from the differentiated hiPSCs. These progenitors were identified as epicardial, by expressing the markers WT1 and TBX18, and they were found also positive for SHOX2, TBX3, HCN1, HCN4, and KCNJ3. PC-like cells differentiated from these progenitors showed a typical action potential morphology (in 80% of the total cells) and distinctive parameters (Zhang et al., 2019a). Unfortunately, this characterization did not identify a specific surface marker, which could be suitable to enrich this TBX5-positive, NKX2.5-negative subset of progenitors independently from the reporter system.

More recently, Yechikov et al. (2020) attempted to investigate the PC-like specification through Nodal inhibition. In the development of cardiac mesoderm, the inhibition of Nodal signaling downregulates a transcription factor, PITX2c, which represses SAN formation in the left atrium. Based on this rationale, iPSC-cardiomyocytes were submitted to Nodal signaling repression by the specific inhibitor SB431542. This conditioning actually induced the generation of a mixed population, also with nodal-like electrophysiological characteristics and higher expression of the transcription factors TBX3 and TBX18 (Yechikov et al., 2020), but not enriched or pure PCs.

Eventually, the identification of an effective specification protocol and/or a surface selection marker to enrich PC-like cells after PSC differentiation could anticipate the clinical application. As described previously, hPSC-cardiomyocytes, including enriched PC-like cells, were extensively investigated in various animal models (mouse, rat, guinea pig, pig, and primates) for the prospective of clinical transplantation (Kadota et al., 2020). In France, the phase I ESCORT trial by Menasché and colleagues evaluated the feasibility and safety to differentiate hESCs into ISL1-positive, CD15-positive cardiac progenitors for a clinical-grade therapeutic approach for the severe dysfunction of the left ventricle. No teratomas or arrhythmias were observed in the median of 18 months (Menasché et al., 2018). The first trial based on human allogeneic iPSCs started in Japan in 2019 to study the short-term efficacy of severe ischemic cardiomyopathy treatment by combining the derived cardiac progenitors and cell sheet technology (ClinicalTrials.gov Identifier: NCT04696328). As such, other clinical applications of PSC-derived cardiomyocytes are expected, including biopacemaking. However, challenging aspects for restoring pacing—apart from the relative pureness of hiPS-derived PCs—remain the delivery modality and cell injection substrate. Different approaches of hPSC-cardiomyocytes transplantation into the recipient cardiac tissue are currently tested (e.g., direct intramuscular injection or cell sheet epicardial patch techniques), which were often proved to allow for the formation of gap junctions between added cells and recipient tissues, and electrical coupling (Zhang et al., 2001; Hamdi et al., 2011; Kawamura et al., 2013; Narita et al., 2013; Tano et al., 2014; Gerbin et al., 2015; Kadota et al., 2020). It is still to be confirmed whether these methods could be equally suitable to guarantee adequate and functional integration also for hPSC-derived PC-like cells.

## Gene-Based Approaches

Gene delivery was long time studied for the potential application in biological pacemaker regeneration methodologies (**Table 3**). It aims at overexpressing a gene codifying for an ion channel or another protein relevant in PC electrophysiology by adopting viral or non-viral transfer strategies.

*De facto*, the first effective gene-based approach for the generation of a biological pacemaker was applied by Miake et al. (2002) by using the viral gene transfer to transform quiescent heart-muscle cells into PCs. This study was focused on the inhibition of the endogenous inward rectifier potassium current ($I_{K1}$) to prevent the automaticity suppression in guinea pig ventricular myocytes. Reduction in the number of inward rectifier potassium ion channels (encoded by the KIR2 gene

**TABLE 3 |** Gene-based biopacemaking approaches.

| Genetic engineering | Methodology and experimental details | References |
|---|---|---|
| Dominant-negative inhibition of Kir2-encoded inward-rectifier potassium channels | *In vivo* viral gene transfer to transform quiescent heart-muscle cells into PCs was performed. After the construct injection into the left ventricular cavity of guinea pigs, successful generation of spontaneous, rhythmic electrical activity in the ventricle was achieved. | Miake et al., 2002 |
| Human β2-adrenergic receptor transfection | The effects of β2-adrenergic receptor transfer were studied: *in vitro* (murine embryonic cardiac myocytes transient transfection with plasmid constructs), *ex vivo* (murine neonatal cardiac transplantation model), and *in vivo* (injection into the right atrium of the endogenous heart). | Edelberg et al., 1998 |
| | Plasmids encoding human β2-adrenergic receptor were injected into the right atria of native Yorkshire pig hearts. A significant increase of chronotropy compared with control injections was achieved. | Edelberg, 2001 |
| HCN1 gene overexpression | HCN1 mutant (three deleted residues: HCN1-AAA) showed activation kinetics similar to SAN and induced pacing activity in porcine models. | Tse et al., 2006 |
| HCN2 gene overexpression | HCN2 gene overexpression increased the heart rate and generated biological pacemaker activity in canine models. | Qu et al., 2003 |
| Dual gene constructs HCN2/SkM1 | Dual gene constructs HCN2/SkM1 were transduced into the left bundle branches in the models of complete AVN block dogs. Complete restoration of the heart rate was demonstrated. | Boink et al., 2013 |
| Adenylate cyclase type VI (AC-VI) overexpression | Adenoviral gene transfer of AC-VI induced pacemaker activity in the AVN block model in adult pigs. | Ruhparwar et al., 2010 |
| Adenoviral vector cocktail (K(AAA) + H2), expressing Kir2.1AAA and HCN2 genes | An adenoviral vector cocktail (K(AAA) + H2), expressing Kir2.1AAA and HCN2 genes, was injected into the AV junctional region in a model of AV block in pigs. | Cingolani et al., 2012 |
| AC1 or HCN2/AC1 overexpression | $Ca^{2+}$-stimulated adenylyl cyclase AC1 or HCN2/AC1 overexpression in left bundle branches provides highly efficient biological pacing and greater sensitivity to autonomic modulation than HCN2 alone. | Boink et al., 2012b |

*PCs, pacemaker cells; SAN, sinoatrial node; AVN, atrioventricular node.*

family; KCNJ2) in the myocardium by overexpressing a KIR2.1-dominant-negative construct (KIR2.1AAA) was adopted. The suppression of $I_{K1}$ induced ventricular cardiomyocytes to depolarize spontaneously, thus producing pacemaker activity (Miake et al., 2002). Further research focused on the KIR2.1AAA-based approach indicated that the overexpression of KIR2.1AAA not only prompts spontaneous membrane depolarization but also additionally triggers the action potential prolongation in case of lower mutant gene overexpression (Miake et al., 2003). However, there are some limitations regarding the use of Kir2.1-induced suppression as it could be associated with the heterogeneous expression of the ion channel between transduced and non-transduced regions, and, hence, arrhythmogenic electrical instability could be triggered (Miake et al., 2003; Sekar et al., 2009).

A growing body of evidence supports the hypothesis that the upregulation of exogenous β2-adrenergic receptors in the right atrium might cause an increase in the heart rate (Edelberg et al., 1998; Edelberg, 2001; Greene et al., 2012). Experimental data demonstrated that upon the atrial injection of the β2-adrenergic receptor construct, cardiac chronotropy enhanced up to 40% in mice (Edelberg et al., 1998) and up to 50% in pigs (Edelberg, 2001). In fact, this targeted, non-viral overexpression of β2-adrenergic receptors increases the protein availability for binding to endogenous catecholamines. Additional research confirmed that β2-adrenergic receptors colocalize with some ion channels, which are crucial for the correct cardiac function and heart rate. It was also established that β2-adrenergic receptors could create protein complexes with the pacemaker HCN4 channel and other subtypes of HCN channels (Greene et al., 2012). Nevertheless, this approach has only a chronotropic effect and does not increase the number of pacemaker channels. Moreover, uncertainties associated with the duration of construct expression might impede β2-adrenergic receptor overexpression from being effectively translated in the clinics.

A locally enhanced chronotropic activity might potentially be achieved through the HCN overexpression in the subsidiary atrial pacemaker tissue, which is physiologically bradycardic but shares several characteristics with SAN, including the differential expression of TBX3, HCN1, Nav1.5, and Cx43 with respect to the right atrium. It was shown, in fact, that pacing could be accelerated by the localized HCN2 or HCN212 overexpression (Morris et al., 2013), hence, advancing proof-of-concept for the clinical use of this subsidiary atrial pacemaker tissue for biopacemaking in the treatment of sick sinus syndrome. Translational interest was also dedicated to unravel the molecular basis of the link between the HCN repression and decreased heart rate. D'Souza et al. (2017) first demonstrated a prominent role for a microRNA, i.e., miR-423-5p, in the downregulation of HCN4 during bradycardia. Such a finding could explain the reduced heart rate observed in athletes and, ultimately, the sinus nodal dysfunction often diagnosed in elders who played sports at competitive levels. Yanni et al. (2020) similarly evidenced in models of heart failure with sinus bradycardia that the downregulation of the pacemaker ion channel HCN4 and its corresponding ionic current $I_f$ is associated with the upregulation of another microRNA (miR-370-3p). Thus, the regulation of these specific miRs deserves more attention for possible pharmacological targeting in therapeutic strategies preventing the irreversible dysfunction of SAN.

Due to the extreme relevance of $I_f$ current on pacemaking, additional gene-based approaches for the bioengineering of

biological pacemakers are focused on the local transfer of a unique HCN gene (Qu et al., 2003; Tse et al., 2006; Plotnikov et al., 2008; Boink et al., 2013). HCN2 gene overexpression can increase the heart rate as well as generate biological pacemaker activity, as first demonstrated by Qu et al. (2003) in a canine model. In this experiment, adenoviral HCN2 constructs were injected by open thoracotomy into the left atrial appendage. After suppressing sinus rhythm by vagal stimulation, a spontaneous rhythm was observed on day 4 after the injection (Qu et al., 2003). In dogs with a complete AV block, Bucchi et al. (2006) demonstrated that the biological pacemaker obtained by the gene transfer of mE324A, a mutant of murine HCN2 (mHCN2) genes, in the left bundle branch could function in tandem with electronic pacemakers, reducing the number of their beats, and conferring sympathetic responsiveness. Moreover, they showed that mE324A was more effective than mHCN2 in activating the pacemaker current and providing catecholamine sensitivity (Bucchi et al., 2006). In a porcine model of sick sinus syndrome (SAN radiofrequency ablation) supported by electronic pacemaker implantation, Tse et al. (2006) observed that the overexpression of an engineered HCN1 construct through a somatic gene transfer could restore a physiological heart rate and reliable pacing of the myocardium by reducing the need for electronic pacing.

Shortcomings associated with the sole HCN-based genetic engineering for the biological pacing generation are related to relatively low autonomic sensitivity and can be overcome by dual-gene overexpression strategies with the skeletal muscle $Na^+$ channel (SkM1) or adenylyl cyclase (AC) genes (Boink et al., 2012b, 2013). Adenoviral dual gene construct HCN2/SkM1 transduction into left bundle branches was demonstrated to restore the heart rate in complete AV block dogs. It was proved that upon the local overexpression of HCN2 and SkM1, no dependency on the electronic reserved pacing as well as better autonomic responsiveness were established (Boink et al., 2013). *In vivo* adenoviral gene transfer of AC type VI was demonstrated to induce pacemaker activity in an AVN block model in adult pigs (Ruhparwar et al., 2010). However, this rhythm was initiated only after isoprenalin administration and, thus, limiting the suitability of this approach only to preclinical study. Another AC overexpression-based modality using AC1 gene in combination with HCN2 revealed superior biological pacing and a higher degree in autonomic modulation than HCN2 alone (Boink et al., 2012b).

A different dual delivery strategy was applied by Piron et al. (2008) that, through a non-viral system (poloxamines), overexpressed HCN2 and β2-adrenergic receptor genes in the ventricular myocardium of a mouse model of AV block. Functional pacemaking and chronotropic regulation were achieved for a relatively long experimental period (Piron et al., 2008).

## Combined Gene-Cell Approaches

Gene-cell combinations explore the transfer of cells together with pacemaker genes into the heart to generate biopacemaking. The cells act, therefore, as delivery platforms for PC ion channels (**Table 4**).

Pioneering studies on this approach were advanced in 2007: their experimental concept was based on the chemically induced fusion of cardiomyocytes and syngeneic fibroblasts, which had been manipulated to express HCN1 pacemaker channels. HCN1-expressing fibroblasts were conditioned to fuse with freshly isolated guinea pig ventricular myocytes to form fibroblast-myocyte heterokaryons displaying biological pacemaker activity (Cho et al., 2007).

Apart from cell fusion, another system to deliver pacemaker genes in the heart revealed its potential: genetically modified human mesenchymal stem cells (hMSCs) were proved to express functional cardiac pacemaker HCN2 channels and induce spontaneous pacemaker activity, triggering the contraction of ventricle cardiomyocytes *in vitro*, as well *in vivo* when injected into the sub-epicardial left ventricular wall (Potapova et al., 2004). With a similar approach, Boink et al. (2012a) effectively used canine mesenchymal stem cells (cMSCs) to deliver SkM1 channels and their derived current into the injected epicardial border zones. Normal conduction and no arrhythmias were achieved by this cell-mediated delivery. As a further proof of the efficacy of SkM1-based approaches, functional delivery of HCN2/SkM1 *via* another platform, namely human cardiomyocyte progenitor cells (CPCs), was recently demonstrated in bradycardia models. In particular, the lentiviral transduction of HCN2 and SkM1 was more efficient than their nucleofection-mediated gene transfer. Moreover, virally transduced cells survived better *in vivo* (Végh et al., 2021). These notable pieces of evidence are supportive of the high translational potential of this gene delivery modality in the treatment of SAN bradycardic pathologies. Nevertheless, the use of lentiviral vectors is not free from safety issues due to the tumorigenic risks associated with random insertion in the cell genome.

In other animal studies based on hMSCs transduced with HCN1, HCN2, or HCN4, the ability of electrical coupling with cardiomyocytes and the generation of $I_f$ current were also confirmed (Zhang et al., 2012; Nong et al., 2013; Zhou et al., 2013). As recently reviewed by Pittenger et al. (2019), hMSCs have aroused an incredible translational interest in many cell therapy applications due to their peculiar repertoire of major histocompatibility complex (MHC) molecules, anti-inflammatory paracrine effect, and ability to suppress mixed lymphocyte reactions, which render them immunotolerated in allogeneic donations, too. However, some experimental and clinical complications could be related to the possible migration of MSCs from injection sites and their differentiation into other cardiomyocytes or cardiac cells (Quinn and Flake, 2008; Li, 2012). Such a type of occurrence could cause a gradual, time-dependent loss of pacing. Further research should focus on biotechnological modalities to encapsulate MSCs and/or anchor cell clusters for the site-specific delivery of HCN2 and SkM1 ion channels. In all the cases, permanent and stable coupling between HCN-transduced MSCs and the working myocardium should be achieved for further clinical applications (Boheler, 2004; Li, 2012). These issues could be solved by using other cellular delivery platforms that can guarantee the sustained pacemaker

**TABLE 4 |** Combined gene-cell biopacemaking approaches.

| Gene-cell approach | Methodology and experimental details | References |
|---|---|---|
| HCN1-expressing fibroblasts fused with freshly isolated myocytes | HCN1-expressing fibroblasts were fused with freshly isolated guinea pig ventricular myocytes and formed fibroblast-myocyte heterokaryons with biological pacemaker activity. | Cho et al., 2007 |
| HCN1-expressing hMSCs | Genetically-engineered MSCs transfected with the human HCN1 gene expressed pacemaker $I_f$ current. The effect of the hHCN1-transfected MSCs on cardiomyocyte excitability was determined by coculturing genetically engineered MSCs with neonatal rabbit ventricular myocytes. | Zhou et al., 2013 |
| HCN2-expressing hMSCs | Genetically modified hMSCs expressed functional cardiac pacemaker gene HCN2 and induced spontaneous pacemaker activity triggering the contraction of ventricle cardiomyocytes *in vitro* and *in vivo*. | Potapova et al., 2004 |
| | HCN2-expressing hMSCs were introduced into the right ventricular apex in dogs and biological pacemaker activity was obtained. Pacing was stable for 6 weeks with no cellular or humoral rejection. | Plotnikov et al., 2007 |
| HCN4-expressing rabbit MSCs | *In vivo* integration and pacing function were achieved after the transplantation of mHCN4-modified rabbit MSCs into the rabbit left ventricle free wall epicardium. Pacing function of the modified MSCs persisted for at least 4 weeks after transplantation. | Zhang et al., 2012 |
| HCN4-expressing rat MSCs | Genetically modified rat MSCs carrying HCN channels expressed pacemaker $I_f$ current *in vitro*. Pacemaking activity was observed after transplantation into the rat host heart. | Nong et al., 2013 |
| TBX18-expressing cardiomyocytes | The conversion of rodent cardiomyocytes to SAN cells *in vitro* and *in vivo* using the expression of Tbx18 was performed. Focal Tbx18 gene transfer in the guinea-pig ventricle induced ectopic pacemaker activity, correcting a bradycardic disease phenotype. | Kapoor et al., 2013 |
| SHOX2-overexpression in ESCs | The overexpression of SHOX2 induced the differentiation of ESCs into pacemaker cells and the transplantation of embryoid bodies from SHOX2-transduced ESCs into the left ventricles of rat hearts with a complete heart block. Consistent pacing ability was demonstrated. | Ionta et al., 2015 |
| HCN2/SkM1-overexpression in CPCs | Functional delivery of HCN2/SkM1 *via* human CPCs demonstrated effectiveness in bradycardia models. In particular, the lentiviral transduction of HCN2 and SkM1 was more efficient than their nucleofection-mediated gene transfer. Moreover, virally transduced cells survived better *in vivo*. | Végh et al., 2021 |

*MSCs, mesenchymal stem cells; hMSCs, human MSCs; SAN, sinoatrial node; ESCs, embryonic stem cells; CPCs, cardiomyocyte progenitor cells.*

function. As an example, the aforementioned human CPCs are an endogenous cell population of the heart and showed the survival and functional integration in the injected peri-ischemic cardiac sites in a long-term follow-up (Smits et al., 2009), thus being a valid alternative to hMSCs for biopacemaker gene delivery (Végh et al., 2019, 2021).

## Transcription Factor-Based Reprogramming Approaches

An advanced approach for pacemaker bioengineering is based on transcription factor manipulations and is currently extensively studied with a view to clinical translation. The transfer of genes encoding different fundamental transcription factors in conduction system development could have the prospective to generate faithful replicas of actual PCs (**Table 5**).

Even though directed cardiomyogenesis from fibroblasts was significantly enhanced in the last few years by reprogramming with several cardiopoietic transcription factor combinations (Ieda et al., 2010; Inagawa et al., 2012; Protze et al., 2012; Qian et al., 2012; Christoforou et al., 2013), targeted differentiation of fibroblasts or working cardiomyocytes into PCs, particularly SAN and AVN cells, remains to be poorly studied. It is known that PC development and differentiation are significantly modulated by specific transcriptional regulators, among them SHOX2, TBX3, TBX5, and TBX18 (Blaschke et al., 2007; Christoffels et al., 2010; Munshi, 2012; Cho, 2015; Gorabi et al., 2019a,b; Raghunathan et al., 2020; van Eif et al., 2020).

Hoogaars et al. (2007) performed a fundamental study on the role of the transcriptional repressor TBX3 in the development of the cardiac conduction system. TBX3 expression defines the SAN region, which initiates a distinct gene expression program compared to the adjacent atrial cells. Lineage segregation of TBX3-negative atrial and TBX3-positive SAN precursor cells was observed after atrial gene program initiation. TBX3-dependent SAN specification and formation as well as the regulation of the pacemaker gene expression program were proved. Later, Bakker et al. (2012) established the effect of TBX3 on the adult heart in the context of its ability to reprogram terminally differentiated working cardiomyocytes into PCs: reduced intercellular coupling and $I_{K1}$ density, but no ectopic pacemaking and $I_f$ current were revealed. The pro-pacemaking ability of the transcriptional factor TBX3 was also tested by its *in vitro* overexpression in ESCs. Forward specification of PSCs with the nodal cell inducer TBX3 was used in combination with Myh6-promoter-based antibiotic selection as a successful strategy to increase PC enrichment. In fact, 80% of the selected cells exhibited nodal-like electrophysiological characteristics, enhanced HCN4 levels, and fired spontaneous action potentials (Jung et al., 2014).

Embryonic T-box transcription factor TBX18 is another crucial PC transcriptional factor: it is necessary to develop the SAN head (right caval vein myocardium) and induce the differentiation of SAN myocardium (Wiese et al., 2009). The first successful realization of a genetic engineering methodology based on this transcriptional factor was introduced in 2013 and

**TABLE 5 |** Reprogramming biopacemaking approaches.

| Reprogramming approach | Methodology and experimental details | References |
|---|---|---|
| TBX3-induced reprogramming | TBX3 overexpression in rat cardiomyocytes *in vivo* induced the reduction of intercellular coupling and $I_{K1}$ density, but failed to establish ectopic pacemaking and $I_f$ current. | Bakker et al., 2012 |
| TBX18-induced reprogramming | The conversion of rodent cardiomyocytes to SAN cells *in vitro* and *in vivo* by the expression of Tbx18 was performed. Focal Tbx18 gene transfer in the guinea pig ventricle induced ectopic pacemaker activity, correcting a bradycardic disease phenotype. | Kapoor et al., 2013 |
| | TBX18 gene transfer created biological pacemaker activity *in vivo* in a complete heart block in pigs. | Hu et al., 2014 |
| | TBX18 gene delivery resulted in antegrade conduction rescue in a preclinical model of right ventricular pacing-induced cardiomyopathy. | Dawkins et al., 2019 |

*SAN, sinoatrial node.*

2014 by overexpressing the gene encoding the human TBX18 to induce the conversion of adult ventricular cardiomyocytes into SAN-like cells (Kapoor et al., 2013; Hu et al., 2014). The latter displayed various phenotypic and functional characteristics of the native PCs. They not only initiated a biological pacemaker rhythm from the site of injection but also were shown to be sensitive to catecholamines (Kapoor et al., 2013). In other experiments, TBX18-expressing adenoviruses were delivered into the interventricular septa of pigs with a complete heart block: TBX18 overexpression enhanced the heart rate and also resulted in automaticity originating from the focal site of gene injection (Hu et al., 2014). However, biopacemaking was maintained as sustained for no more than 2 weeks due to the reasons that were not investigated but hypothesized as related to inflammation, immune reactions, or unintended reprogramming of AVN cells. These studies were only the pioneering ones in the biological pacing generation through TBX18 reprogramming, and, currently, the attempts for the successful realization of this methodology continue. TBX18 gene-based reprogramming into PC-like cells was demonstrated *in vitro* starting from neonatal rat fibroblasts, vascular smooth muscle cells from ascending aorta, and adipose tissue MSCs (Yang et al., 2016; Quan and Huang, 2018; Wang et al., 2019). Experiments with TBX18 gene overexpression in hiPSC-cardiomyocytes to induce PC-like cells demonstrated the effectiveness of this approach independently from the gene delivery modality (Gorabi et al., 2019b). The essential role of TBX18 was also demonstrated recently by Dawkins et al. (2019) in a preclinical model of right ventricular pacing-induced cardiomyopathy. It was shown that it is possible to prevent and reverse cardiomyopathy signs by the strategy of antegrade conduction rescue *via* TBX18 biological pacing. Despite the promise generated by TBX18 gene delivery for pacemaking restoring, several concerns for its safe clinical application remain in addition to the aforementioned unsolved issue of temporary effect. Whenever a permanent overexpression will be reached, the risk of interference with epithelial-mesenchymal transition can be hypothesized depending on the gene delivery site. Such a consequence cannot be excluded because TBX18, together with Wilms' tumor homolog 1 (WT1), is upregulated in the developing epicardium and injury-activated epicardial stem cells, giving rise, through the epithelial-mesenchymal transition, to the fibroblasts and smooth muscle cells of the coronary arteries (Takeichi et al., 2013) and/or cardiomyocytes (Smart et al., 2011).

The ability of the transcriptional factor SHOX2 to activate PC differentiation was tested *in vitro* by the adenoviral transfer of human SHOX2 into mouse ESCs. The transplantation of embryoid bodies from SHOX2-transduced ESCs into the left ventricles of rat hearts with a complete heart block demonstrated the consistent pacing ability nascent from the injection sites, as recorded by *ex vivo* optimal mapping 2–4 days after injection (Ionta et al., 2015). Despite the short window of evaluation, SHOX2-transduced embryoid bodies proved to immediately integrate with the host ventricular myocardium. Notably, neither SHOX2 gene delivery nor mouse embryoid bodies appeared to trigger an immune response in this discordant, immunocompetent transplantation model. Longer follow-up of these SHOX2-transduced embryoid bodies in the rat heart as well as direct *in vivo* reprogramming using SHOX2 adenoviral construct could shed more light on possible safety complications.

ISL1 transcriptional factor was also studied for its ability to initiate the PC differentiation: ISL1 overexpression in ESCs and in *Xenopus laevis* embryos stimulates the increase of the cardiomyocyte precursors' differentiation toward prevalently nodal cells. Enhanced HCN4 expression and increased cellular automaticity were also observed (Dorn et al., 2015). These outcomes confirmed in two systems are suggestive for the potential use of ISL1 as a pro-pacemaking transcriptional factor *in vivo*. Although no animal investigation has been performed yet, another *in vitro* study on adipose tissue-derived MSCs demonstrated the obtainment of PC-like cells through lentiviral delivery of ISL1 combined with TBX18. Transfected cells expressed TBX3, HCN4, cTnT, and Cx45; moreover, they possessed a functional $I_f$ current (Zhang and Huang, 2019). Even if the used lentiviral gene expression system opens up many safety concerns, the fact that ISL1/TBX18 double gene transfer may be effective in initiating the SAN program also on mesodermal (stem) cells can be seen as further evidence of the validity of this approach in somatic cell reprogramming *in vivo*.

As it can be noted from these studies, investigation on a multifactorial gene strategy for direct reprogramming of somatic cells into PCs with transcription factors is still missing. Nam et al. (2014) played on the combination of transcription factors

demonstrated efficacious for cardiomyocyte induction (Ieda et al., 2010; Protze et al., 2012; Qian et al., 2012). By adopting a highly reliable HCN-GFP reporter for PC tracking, they observed that the genetic cocktail of the selected cardiogenic transcription factors, including GATA4, HAND2, MEF2c, and TBX5, induced nearly 30% of bona fide PCs in transgenic fibroblasts without passing through a cardiac progenitor intermediate (Nam et al., 2014). Obviously, such a transcriptional gene transfer system cannot be clinically translated for a reliable biopacemaking as 70% of the induced cardiomyocytes were atrial or ventricular. However, the *in vitro* mechanistic platform developed in this study might possess strong prediction ability in identifying other combinations of transcription factors more effective in SAN program reactivation.

The reprogramming of somatic cells, such as cardiac fibroblasts, atrial, and ventricular cardiomyocytes, into functional hiPSC-pacemaking cardiomyocytes with adequate PC-like electrophysiological activity using various transcriptional factors might be likely the most straightforward approach for human cell-based biopacemaker engineering. Nevertheless, further studies are still required to find the suitable gene cocktails able to specifically initiate SAN program *in vitro*, test their validity, long-term efficacy, as well as possible concerns *in vivo*. In addition, careful attention should also be addressed in preclinical studies to evaluate improved and minimally invasive delivery modalities to be translated into the clinics with ease and safety.

## Tissue Engineering and Biohybrid Approaches

The multidisciplinary field of tissue engineering and regenerative medicine revealed its potentiality in many cardiovascular applications, such as the generation of heart valve replacements and cardiac tissue constructs (e.g., Iop et al., 2009, 2014, 2018; Dal Sasso et al., 2020; Zouhair et al., 2020). Tissue engineering is increasingly utilized for the development of biopacemakers (**Table 6**). Due to the architectural and functional complexity of nodal tissues, such a strategy might fully regenerate cardiac conduction by combining scaffolds and cells opportunely in biomimetic, bioequivalent tissue constructs. However, the drawbacks of the first SAN tissue transplantation experiments (Starzl et al., 1963; Morishita et al., 1981) as core necrosis, immune response, and non-integration might hamper the success of tissue engineering approaches and have to be excluded to prevent any condition leading to graft failure.

A first tissue engineering effort to generate an AVN pacemaker was realized by Choi et al. (2006): a liquid mixture of skeletal myoblasts, collagen, and Matrigel was cast into molds, allowed to solidify, and statically cultured before being implanted into the cardiac atrioventricular groove of syngeneic rats. In 70% of the animals, AV conduction was not re-established. In the rest of the animals, it was permanently conveyed thanks to an implanted viable construct, promptly vascularized *in vivo*. This approach, however, is barely transferrable to human therapy for its low clinical grade (an xenogeneic material such as Matrigel) and reliance on non-specialized components (incompletely differentiated, non-cardiac cells, and immature, xenogeneic scaffold). Zhang et al. (2019b) reported the outcomes of the atrioventricular groove implantation of a tissue-engineered construct composed of collagen sponges and cardiac progenitors derived from the human embryonic heart tubes. Around 60% of the implanted rats survived, and the pacing was maintained for about 3 months *in vivo*. Again, such an approach could have difficult translation into the clinics depending on the ethical questions and legislative limitations on using human embryos issued by each country.

Cardiac organoid models were generated by inserting an iPSC-derived embryoid body into the engineered heart tissue (Schulze et al., 2019) by recapitulating the cell and extracellular matrix functional connections typically observed in the native nodal tissues.

The differentiation through the embryoid body method is possibly spontaneous and relatively easy to perform but might be associated with high yield variability in the achievement of cardiac progenitors with PC features and consequently to excessive system costs. A layer-by-layer cell coating technique has been proposed by Sasano et al. (2020) to more efficiently differentiate hiPSCs into a hierarchical cardiac tissue-mimetic structure.

Three-dimensional cardiac pacemaker spheroids were tissue-engineered by adopting somatic gene transfer technology of TBX18 (Grijalva et al., 2019). These tissue constructs spontaneously fired action potentials and induced cell contraction in co-cultured cardiomyocytes *in vitro*.

Vascularization is an important feature of a functional node. Cardiac pacemakers tissue-engineered with cardiac progenitors were promptly vascularized by adding *in vitro* endothelial progenitor cells to the cell component of the constructs realized with Matrigel and proved pacing activity in a rat model of SAN dysfunction (Zhang et al., 2017).

Through the STARS program BIOSAN, we also develop biological pacemakers based on the combination of natural scaffolds and induced PCs.

Alternatively, applying a biohybrid approach mixing smart polymers and electronic devices could respond to the immediate need to render an artificial pacemaker more natural-like for the body (**Table 5**; Feiner and Dvir, 2020). Such a strategy could prevent fibrotic reactions associated with the implantable device (Robotti et al., 2020), but it may not overcome other related limitations, as the lack of neuroautonomic responsiveness.

# TRANSLATIONAL CHALLENGES TOWARD THE CLINICAL APPLICATION OF BIOLOGICAL PACEMAKERS

Despite the variety of approaches that have been tested in different models, extensive and comprehensive additional studies are still necessary for further development and potential clinical application of biological pacemakers. For all current approaches, investigation on the optimization and the evaluation of safety, potential toxicity, long-term stability, and a variety of crucial parameters is definitely mandatory (**Figure 1**). Regarding recent

**TABLE 6 |** Tissue engineering and hybrid biopacemaking approaches.

| Tissue engineering | Methodology and experimental details | References |
|---|---|---|
| Tissue engineered cardiac pacemakers | A liquid mixture of skeletal myoblasts, collagen, and Matrigel was cast into molds, allowed to solidify, and statically cultured before being implanted into the cardiac atrioventricular groove of syngeneic rats. In 30% of the treated animals, the pacing was established. | Choi et al., 2006 |
| | Cardiac and endothelial progenitors were opportunely mixed with Matrigel to obtain vascularized tissue-engineered pacemakers *in vitro*, which proved pacing activity in a rat model of SAN dysfunction. | Zhang et al., 2017 |
| | A tissue-engineered construct composed of collagen sponges and cardiac progenitors derived from the human embryonic heart tubes was implanted in the rat atrioventricular groove. Around 60% of the implanted rats survived, and the pacing was maintained for about 3 months *in vivo*. | Zhang et al., 2019b |
| Biohybrid pacemaker devices | A biohybrid strategy combining smart coating biopolymers and cardiac electronic devices prevented the formation of fibrotic adherences *in vivo*. | Robotti et al., 2020 |

*SAN, sinoatrial node.*

studies and the obtained results, biological pacing therapy is much closer to the clinical application; however, numerous challenges still exist in this field (Rosen et al., 2011; Cingolani et al., 2018).

*In vitro* studies are fundamental to evaluate the proof-of-principle of novel biopacing concepts, but the ultimate efficacy test is on the animal model. Animal studies were performed with the primary goal to evaluate the efficacy, safety, stability, and other parameters of the different biological pacemaker approaches. Biological pacemaking was achieved in the majority of these models, which vary depending on the animal, duration of observation, delivery method, and time stability (Edelberg et al., 1998; Edelberg, 2001; Miake et al., 2002; Ruhparwar et al., 2002, 2010; Qu et al., 2003; Plotnikov et al., 2004, 2007, 2008; Potapova et al., 2004; Lin et al., 2005; Xue et al., 2005; Bucchi et al., 2006; Tse et al., 2006; Cai et al., 2007; Cho et al., 2007; Piron et al., 2008; Shlapakova et al., 2010; Zhang et al., 2011, 2012; Boink et al., 2012a,b; Cingolani et al., 2012; Kapoor et al., 2013; Morris et al., 2013; Nong et al., 2013; Hu et al., 2014; Ionta et al., 2015; Protze et al., 2016; Chauveau et al., 2017; Choudhury et al., 2018; Dawkins et al., 2019; Gorabi et al., 2019a; Végh et al., 2019, 2021).

Significant issues could prevent the successful adoption of the biopacing technologies in clinics: challenging delivery of genes and cells, inefficient integration and coupling, the risks of pro-arrhythmic effects of biological pacemakers, the possible teratogenic effects of stem cells or/and transcription factor-based approaches, and, not lastly, the ethical issues derived from the use of hESCs derivatives. One of the main concerns and potential limitations of biologic-driven automaticity is the possibility of ventricular arrhythmias and related life-threatening consequences.

Specific limitations might depend first on the delivery methods used to deploy genes, cells, or tissue-engineered constructs at the selected site. For all approaches pursued for biopacemaking, it is fundamental to find adequate delivery modalities that are easy to perform, minimally invasive, associated with low peri-intervention risks, and able to guarantee the sustained effect *in vivo*. Most gene or cell delivery methods are still invasive (open chest or thoracotomy), representing less attractive options for the future clinical application in humans (Miake et al., 2002; Ruhparwar et al., 2002, 2010; Qu et al., 2003; Potapova et al., 2004; Lin et al., 2005; Xue et al., 2005; Choi et al., 2006; Tse et al., 2006; Cai et al., 2007; Cho et al., 2007; Plotnikov et al., 2007; Boink et al., 2012a, 2013; Zhang et al., 2012; Kapoor et al., 2013; Nong et al., 2013; Ionta et al., 2015; Protze et al., 2016; Chauveau et al., 2017; Gorabi et al., 2019a). The development of minimally invasive, safer, and well-controlled delivery methods is a current research priority of biological pacemakers in the field of regenerative medicine. A catheter-based injection, especially when combined with fluoroscopic guiding, offered a safe and an effective option to deliver genes and cells with minimal invasiveness in preclinical biological pacing (Edelberg, 2001; Plotnikov et al., 2004, 2008; Bucchi et al., 2006; Cingolani et al., 2012; Hu et al., 2014). In particular, such a low invasive deployment modality for gene delivery causes minimum blood loss and pain and has a significantly lower risk of stroke due to the catheter insertion into the right-sided circulation. It is unquestionably a routine approach for many clinical applications and could be easily translated in humans for gene- and cell-based biopacemaking strategies, too.

Once the deployment has been performed, the initiation of biopacemaking is subordinate at first glance to the establishment of an immunotolerant state with respect to injected cells, genes, or tissue-engineered constructs. While MSCs are able to induce such a state (Pittenger et al., 2019), other cell types used as delivery platforms are considered immunogenic, as in the case of hESCs derivatives or SAN cell preparations from allogeneic donors (Drukker and Benvenisty, 2004). The adoption of iPSCs has allowed to partially skip this issue by employing patient-specific cells for reprogramming to pluripotency. PC-, atrial-, and ventricular-like cardiomyocytes differentiated from iPSCs were shown to display the same MHC repertoire as the somatic cells of the patient (Park et al., 2013). Although MHC-matched allogeneic iPSCs were recently reported to be well-tolerated in preclinical studies in immunocompetent animal models (Ishigaki et al., 2021), much concern related to several cases of rejection remains, leading to focus research on developing hypoimmunogenic iPSC lines (Deuse et al., 2019). Immunorejection might also happen with gene delivery, especially with viral constructs. The application of viral gene delivery strategies, particularly the ones depending on lentiviral vectors, might be more efficient than non-viral approaches to

reach adequate overexpression of ion channels, other proteins essential to generate PC currents, and transcription factors relevant to start SAN program; however, the risks related to immunogenicity, but also random genome integration, and tumorigenicity cannot be underestimated at all. Some clinical trials with gene therapy, also combined with cell platforms, were stopped due to adverse events, as it was recently disclosed during the application of autologous hematopoietic stem cells transduced with a *BCL11A* mRNA-encoding lentiviral vector for the treatment of sickle cell disease (Esrick et al., 2021; Statement on NHLBI decision to pause the Pilot and Feasibility Study of Hematopoietic Stem Cell Gene Transfer for Sickle Cell Disease | NHLBI, NIH, 2021). As proposed by Végh et al. (2019), insertional mutagenesis could be prevented by adopting self-inactivating lentivirus or promoters with a weak-to-moderate activity. Non-viral strategies for gene delivery or reprogramming might be spare of some of these issues, but possible epigenetic modifications and genetic instabilities need to be investigated in depth, as they were observed also in hiPSCs reprogrammed with non-integrating methods (Schlaeger et al., 2015). Even if no data are available still regarding non-integrating gene delivery for *in vivo* biopacemaking, the strategies of microRNA-therapeutic silencing after myocardial infarction revealed to be immunotolerated in animal models (Liao et al., 2021). As far as concerning bioengineered conduction tissues, immunotolerance establishment depends both on scaffolds and cells, as well as on cell culture conditions (e.g., the use of xenogeneic reagents), employed to fabricate them; therefore, a careful selection of non-immunogenic components and/or manipulations for the antigenic moiety removal are required to prevent immune rejection, as in other cardiovascular tissue engineering applications (Iop et al., 2018).

Once biopacemaking has been activated, most of the gene- and cell-based approaches showed shortcomings in the mid-term maintenance of sustained performance. Such a limitation can be expected for tissue-engineered conduction bioequivalents, too. As mentioned before, yet a few biopacemaking studies demonstrated *in vivo* pacing for around 45 days while most of them reported function for no longerthan 2–4 weeks or did not assess pacing performance during longer follow-up (for instance, Plotnikov et al., 2007, 2008; Piron et al., 2008; Kapoor et al., 2013; Hu et al., 2014). Often, an increase in heart rhythm is reported after some days from the treatment but tends to decrease just as quickly. Some studies disclosed a loss of PC-like cells over time, as after transcription factor gene overexpression (Kapoor et al., 2013). Whether this time-limited efficiency is, due to late-onset immune reactions elicited against gene constructs or exogenous cells, transient gene expression (gene delivery), unintended cell targeting (gene delivery), reduced survival (cells), inability to integrate, core necrosis (tissue-engineered constructs), migration events, interference with other biological activities (e.g., epithelial-mesenchymal transition), conditioning from local microenvironment at the injection site (inflammatory state and/or region-specific electrophysiological characteristics), or a combination of these causes, it still remains to be fully elucidated.

Delivery constructs that target a specific cell type of the heart are not yet available, and vehiculated genes are, therefore, introduced at the site of injection where they are randomly inserted. It has been speculated that a non-targeted gene delivery might have a causative role in the unsustained activity at the AV level whether native, functional AVN PCs are the objects of the forced expression of channel proteins (Hu et al., 2014). Nanotechnology concepts applied in the cell targeting for cancer therapies (e.g., chimeric antigen receptor T-cell or CAR-T) (Ma et al., 2020) could be translated in the context of biopacemaking to induce the expression of the exogenous gene in a selected cell type, e.g., cardiac fibroblasts. Transient gene expression is related to the vector used to vehiculate the gene of interest. Lentiviral and retroviral delivery strategies are reliable for gene overexpression, also in the long term (Tse et al., 2006; Nong et al., 2013; Gorabi et al., 2019a; Végh et al., 2019, 2021), but might induce insertional mutagenesis as discussed before. The adenoviral transfer is non-integrating and efficient, but the expression is limited in time (Miake et al., 2002; Qu et al., 2003; Bucchi et al., 2006; Tse et al., 2006; Cho et al., 2007; Plotnikov et al., 2008; Ruhparwar et al., 2010; Cingolani et al., 2012; Kapoor et al., 2013; Hu et al., 2014; Ionta et al., 2015; Choudhury et al., 2018; Dawkins et al., 2019; Grijalva et al., 2019), and, thus, it cannot be considered as an option to be employed in the clinic for sustained biopacemaking. As advanced by Cingolani et al. (2018), this time-limited overexpression might, conversely, be ideal to establish temporary, hardware-free pacing in patients with device-related infections (bridge to device implantation), chronic atrial fibrillation, and congenital AVN block (*in utero*).

Inability to stably integrate, poor cell viability, and core necrosis phenomena might be a consequence of the lack of effective oxygen and nutrient supply, which is particularly problematic when transplanting thick tissues, as observed in the first trials with native SANs (Ernst and Paulson, 1962; Starzl et al., 1963; Morishita et al., 1981) and expected for tissue-engineered conduction constructs. Vascularization must be promptly established to prevent ischemic conditions and necrosis, also envisaging the *in vitro* creation of vessel networks in tissue engineering approaches (Zhang et al., 2017; Shah Mohammadi et al., 2020).

Another issue regarding the maintenance of biopacing is related to possible cell migration. Considering that the native conduction system possesses electrical insulation (Choi and Salama, 1998), all delivery strategies, including the ones intending to transplant tissue-engineered biopacemakers, should be developed considering this as one of the main prerequisites in order to prevent migration and dilution-like effects that could be possibly responsible for mid/long-term loss of function. Several strategies might be applied to avert migration. Anchoring modalities should be developed to maintain the cells at the site of injection. Encapsulation in biocompatible and semipermeable membranes could be advantageous, especially for cell-based approaches to favor viability and immunoisolation as already advanced clinically (Hardin-Young et al., 2000; Carlsson et al., 2018), as long as they do not prevent the creation of opportune electrical coupling for biopacemaking.

Alternatively, for the strategies depending on cell delivery platforms, the use of cells belonging to the heart as cardiac stem cells might be resolutive (Végh et al., 2021). In conduction system tissue engineering, the combination with scaffolds characterized by slow biodegradation kinetics could be helpful. Mimicking or reproducing the natural electrical insulation of SAN and AVN should be pursued to prevent migration side effects as possible interferences with other biological functions and/or dedifferentiation/transdifferentiation.

Finally, suboptimal differentiation/specification and electromechanical coupling of the introduced or induced PC-like cells might be responsible for discontinuous pacing or the generation of arrhythmic foci (Plotnikov et al., 2008; Boink et al., 2012b; Shiba et al., 2014).

In order to deeply investigate these aspects, as well as safety and teratogenicity, accurate and long-term monitoring is essential. Typically, biological pacemaker activity and pro-arrhythmic effects were monitored by *in vivo* and *ex vivo* assessment. ECG, serial Holter monitoring, pacemaker log recordings, patch clamp, non-fluoroscopic magnetic electroanatomic system (CARTO), and optical mapping of the epicardial electrical activity in perfused, excided hearts are often employed to analyze biopacing activity (Miake et al., 2002, 2003; Ruhparwar et al., 2002, 2010; Qu et al., 2003; Xue et al., 2005; Choi et al., 2006; Tse et al., 2006; Plotnikov et al., 2007, 2008; Shlapakova et al., 2010; Zhang et al., 2012, 2017; Kapoor et al., 2013; Nong et al., 2013; Gorabi et al., 2019a). *In vivo* evaluations are more indicative of the induced biopacemaking activity because they allow to study electrical function in the living animal and assess the global function. More reliable results can be achieved by performing real-time, continuous ECG telemetry as it was done in the experiments with the model of complete heart block in pigs (Edelberg, 2001; Hu et al., 2014). Such continuous monitoring should be performed and extended for long-term follow-up in all large animal studies to evaluate any time-related dynamic change of the biological pacemaker. The most extended evaluation has been performed with a tissue-engineered biopacemaker (from 2 weeks to maximum 3 years), but unfortunately, no *in vivo* electrical assessment has been realized (Choi et al., 2006), which could have provided valuable information on the fate of the whole graft and its composing cells. Despite the abundance of animal studies, a comprehensive evaluation of safety, long-term stability, arrhythmogenicity, and toxicity remains still to be realized to date. Various *in vivo* dysfunctional rhythm models were successfully created to simulate, e.g., bradyarrhythmia, sick sinus syndrome, and AV block (Qu et al., 2003; Kehat et al., 2004; Plotnikov et al., 2004, 2007, 2008; Bucchi et al., 2006; Tse et al., 2006; Shlapakova et al., 2010; Zhang et al., 2012; Hu et al., 2014), by allowing to effectively test any one of the developed biopacemaker therapeutic concepts.

Another outstanding question in the clinical application of a biopacemaking therapy is related to ethics and costs. Most approaches so far explored rely on components, the in-human application of which might be estimated as controversial due to the derivation (e.g., ESCs and Matrigel) or associated health risks (viral delivery vectors, especially the integrating ones). With a considerable level of technology implemented in these approaches, the manufacturing costs are particularly high, representing a critical barrier for distribution in both industrialized and non-industrialized countries. As for other advanced therapeutic medicinal hypotheses, the balancing between benefits and risks associated to any biopacemaking approach must be critically valued in healthcare management programs to prevent any harmful exposure of patients affected by the disturbances of the conduction system. Indeed, the possibility of clinically testing these hypotheses depends on the local sanitary legislation, as well as on government/federal funding allocated, and, finally, on the consent of the patient. In the cases where no available treatment options are suitable to (re)establish rhythm functionality as for fetal subjects with congenital AV block or adult patients with device-related infections (Cingolani et al., 2018), compassionate use might eventually be authorized.

With the current level of knowledge and technology, a complete recovery of the physiological heart rate has not been achieved yet by using stem cell- and reprogramming-based approaches, but is confirmed at least temporarily using other methodologies as gene transfer. The delivery of genes codifying for essential proteins in PC electrical function or transcription factors initiating the conduction system program needs further optimization regarding the employed vectors and identification of effective cocktails. Cell-based approaches (mixed or pure SAN cell preparations or PC-like cells from the differentiated PSCs) and tissue engineering strategies will also require additional investigation before reaching the clinical application: the acceptable level of reproducibility and long-term functioning is not yet achieved. Although the biological pacing created by gene transfer showed hitherto to be the most successful biopacemaking strategy in short-term preclinical evaluations, the application of tissue engineering principles is expected to keep its promises to overcome all the limitations shown by the other approaches to clinically replace electronic pacemakers.

At the present moment, the best strategy for the first clinical testing of a biological pacemaker appears to be its combination with electronic devices (Plotnikov et al., 2004, 2008; Bucchi et al., 2006). Preliminary and first-stage biological pacing could be realized in the clinical conditions of permanent atrial fibrillation in combination with AV block or other complicated cases (Cingolani et al., 2018). Patients with sinus bradycardia could also be the candidates for the biological pacing with SAN transcription factor or microRNA (miRNA) reprogramming of atrial subsidiary pacemaker sites (Morris et al., 2013; D'Souza et al., 2017; Choudhury et al., 2018; Yanni et al., 2020).

## CONCLUSIONS

We overviewed a significant progress in the field of biological pacemaker development in the last few years. We have every reason to believe that modern biological pacing technology

will demonstrate its validity in preclinical investigation *in vitro*, in long-term animal studies *in vivo*, and, finally, in the clinic. Various methodologies for biological pacemaker generation are being currently studied and show potentialities for further preclinical and clinical applications: cell-based, gene-based, combined gene-cell-based, transcription factor-induced reprogramming, and tissue engineering applications. Though all these approaches are focused on effective and safe biological pacing generation, they are founded on diverse strategies and delivery methods. In addition, limitations and crucial points for further clinical introduction (safety, long-term stability, and potential toxicity) differentiate them. Nevertheless, each of them potentially could be safe and effective and more promising compared to artificial electronic devices, so far clinically applied. In summary, biological pacemakers are expected to improve and expand the spectrum of the therapeutic strategies for the treatment of disorders in the cardiac conduction system.

## AUTHOR CONTRIBUTIONS

LI conceived the manuscript. NN and LI contributed to the article and approved the submitted version.

## FUNDING

This work was funded by the University of Padua under the STARS Grants program (BIOSAN, The development of a tissue-engineered BIOpacemaker based on acellular SAN and iPSCs derived nodal cells for pharmacological screening), DOR 2017, and BIRD 2019.

## ACKNOWLEDGMENTS

We acknowledge the University of Padua for the financial support provided with the funds DOR 2017, BIRD 2019, and STARS Program.

## REFERENCES

Anderson, R. H., Janse, M. J., van Capelle, F. J., Billette, J., Becker, A. E., and Durrer, D. (1974). A combined morphological and electrophysiological study of the atrioventricular node of the rabbit heart. *Circ. Res.* 35, 909–922. doi: 10.1161/01.RES.35.6.909

Anderson, R. H., Sanchez-Quintana, D., Mori, S., Cabrera, J. A., and Sternick, E. B. (2020). Re-evaluation of the structure of the atrioventricular node and its connections with the atrium. *Europace* 22, 821–830. doi: 10.1093/europace/euaa031

Anderson, R. H., and Siew, Y. H. (2002). The morphology of the specialized atrioventricular junctional area: the evolution of understanding. *PACE Pacing Clin. Electrophysiol.* 25, 957–966. doi: 10.1046/j.1460-9592.2002.00957.x

Bai, W., Suzuki, H., Huang, J., Francis, C., Wang, S., Tarroni, G., et al. (2020). A population-based phenome-wide association study of cardiac and aortic structure and function. *Nat. Med.* 26, 1654–1662. doi: 10.1038/s41591-020-1009-y

Bakker, M. L., Boink, G. J. J., Boukens, B. J., Verkerk, A. O., van den Boogaard, M., den Haan, A. D., et al. (2012). T-box transcription factor TBX3 reprogrammes mature cardiac myocytes into pacemaker-like cells. *Cardiovasc. Res.* 94, 439–449. doi: 10.1093/cvr/cvs120

Baudot, M., Torre, E., Bidaud, I., Louradour, J., Torrente, A. G., Fossier, L., et al. (2020). Concomitant genetic ablation of L-type Cav1.3 (α1D) and T-type Cav3.1 (α1G) Ca2+ channels disrupts heart automaticity. *Sci. Rep.* 10, 1–19. doi: 10.1038/s41598-020-76049-7

Birket, M. J., Ribeiro, M. C., Verkerk, A. O., Ward, D., Leitoguinho, A. R., den Hartogh, S. C., et al. (2015). Expansion and patterning of cardiovascular progenitors derived from human pluripotent stem cells. *Nat. Biotechnol.* 33, 970–979. doi: 10.1038/nbt.3271

Blaschke, R. J., Hahurij, N. D., Kuijper, S., Just, S., Wisse, L. J., Deissler, K., et al. (2007). Targeted mutation reveals essential functions of the homeodomain transcription factor Shox2 in sinoatrial and pacemaking development. *Circulation* 115, 1830–1838. doi: 10.1161/CIRCULATIONAHA.106.637819

Boheler, K. R. (2004). Functional markers and the 'homogeneity' of human mesenchymal stem cells. *J. Physiol.* 554, 592–592. doi: 10.1113/jphysiol.2003.057224

Boink, G. J. J., Duan, L., Nearing, B. D., Shlapakova, I. N., Sosunov, E. A., Anyukhovsky, E. P., et al. (2013). HCN2/SkM1 gene transfer into canine left bundle branch induces stable, autonomically responsive biological pacing at physiological heart rates. *J. Am. Coll. Cardiol.* 61, 1192–1201. doi: 10.1016/j.jacc.2012.12.031

Boink, G. J. J., Lu, J., Driessen, H. E., Duan, L., Sosunov, E. A., Anyukhovsky, E. P., et al. (2012a). Effect of skeletal muscle Na + channel delivered via a cell platform on cardiac conduction and arrhythmia induction. *Circ. Arrhythmia Electrophysiol.* 5, 831–840. doi: 10.1161/CIRCEP.111.969907

Boink, G. J. J., Nearing, B. D., Shlapakova, I. N., Duan, L., Kryukova, Y., Bobkov, Y., et al. (2012b). Ca 2+ -stimulated adenylyl cyclase AC1 generates efficient biological pacing as single gene therapy and in combination with HCN2. *Circulation* 126, 528–536. doi: 10.1161/CIRCULATIONAHA.111.083584

Brown, H. F., Difrancesco, D., and Noble, S. J. (1979). How does adrenaline accelerate the heart? [13]. *Nature* 280, 235–236. doi: 10.1038/280235a0

Brown, H. F., Giles, W., and Noble, S. J. (1977). Membrane currents underlying activity in frog sinus venosus. *J. Physiol.* 271, 783–816. doi: 10.1113/jphysiol.1977.sp012026

Bucchi, A., Plotnikov, A. N., Shlapakova, I., Danilo, P., Kryukova, Y., Qu, J., et al. (2006). Wild-type and mutant HCN channels in a tandem biological-electronic cardiac pacemaker. *Circulation* 114, 992–999. doi: 10.1161/CIRCULATIONAHA.106.617613

Burridge, P. W., Matsa, E., Shukla, P., Lin, Z. C., Churko, J. M., Ebert, A. D., et al. (2014). Chemically defined generation of human cardiomyocytes. *Nat. Methods* 11, 855–860. doi: 10.1038/nmeth.2999

Cabrera, J. Á., Anderson, R. H., Macías, Y., Nevado-Medina, J., Porta-Sánchez, A., Rubio, J. M., et al. (2020). Variable arrangement of the atrioventricular conduction axis within the triangle of koch: implications for permanent his bundle pacing. *JACC Clin. Electrophysiol.* 6, 362–377. doi: 10.1016/j.jacep.2019.12.004

Cai, J., Yi, F.-F., Li, Y.-H., Yang, X.-C., Song, J., Jiang, X.-J., et al. (2007). Adenoviral gene transfer of HCN4 creates a genetic pacemaker in pigs with complete atrioventricular block. *Life Sci.* 80, 1746–1753. doi: 10.1016/j.lfs.2007.02.006

Carlsson, P. O., Espes, D., Sedigh, A., Rotem, A., Zimerman, B., Grinberg, H., et al. (2018). Transplantation of macroencapsulated human islets within the bioartificial pancreas βAir to patients with type 1 diabetes mellitus. *Am. J. Transplant.* 18, 1735–1744. doi: 10.1111/ajt.14642

Cavero, I., Guillon, J. M., and Holzgrefe, H. H. (2017). Reminiscing about Jan Evangelista Purkinje: a pioneer of modern experimental physiology. *Adv. Physiol. Educ.* 41, 528–538. doi: 10.1152/advan.00068.2017

Chandler, N. J., Greener, I. D., Tellez, J. O., Inada, S., Musa, H., Molenaar, P., et al. (2009). Molecular architecture of the human sinus node insights into the function of the cardiac pacemaker. *Circulation* 119, 1562–1575. doi: 10.1161/CIRCULATIONAHA.108.804369

Chauveau, S., Anyukhovsky, E. P., Ben-Ari, M., Naor, S., Jiang, Y.-P., Danilo, P., et al. (2017). Induced pluripotent stem cell–derived cardiomyocytes provide *in vivo* biological pacemaker function. *Circ. Arrhythmia Electrophysiol.* 10:4502. doi: 10.1161/CIRCEP.116.004508

Cho, H. C. (2015). Pacing the Heart with Genes: Recent Progress in Biological Pacing. *Curr. Cardiol. Rep.* 17, 65. doi: 10.1007/s11886-015-0620-x

Cho, H. C., Kashiwakura, Y., and Marbán, E. (2007). Creation of a biological pacemaker by cell fusion. *Circ. Res.* 100, 1112–1115. doi: 10.1161/01.RES.0000265845.04439.78

Choi, B. R., and Salama, G. (1998). Optical mapping of atrioventricular node reveals a conduction barrier between atrial and nodal cells. *Am. J. Physiol. Hear. Circ. Physiol.* 274, H829–H845. doi: 10.1152/ajpheart.1998.274.3.h829

Choi, Y.-H., Stamm, C., Hammer, P. E., Kwaku, K. F., Marler, J. J., Friehs, I., et al. (2006). Cardiac conduction through engineered tissue. *Am. J. Pathol.* 169, 72–85. doi: 10.2353/ajpath.2006.051163

Choudhury, M., Black, N., Alghamdi, A., D'Souza, A., Wang, R., Yanni, J., et al. (2018). TBX18 overexpression enhances pacemaker function in a rat subsidiary atrial pacemaker model of sick sinus syndrome. *J. Physiol.* 596, 6141–6155. doi: 10.1113/JP276508

Christoffels, V. M., Smits, G. J., Kispert, A., and Moorman, A. F. M. (2010). Development of the pacemaker tissues of the heart. *Circ. Res.* 106, 240–254. doi: 10.1161/CIRCRESAHA.109.205419

Christoforou, N., Chellappan, M., Adler, A. F., Kirkton, R. D., Wu, T., Addis, R. C., et al. (2013). Transcription Factors MYOCD, SRF, Mesp1 and SMARCD3 Enhance the Cardio-Inducing Effect of GATA4, TBX5, and MEF2C during direct cellular reprogramming. *PLoS ONE* 8:63577. doi: 10.1371/journal.pone.0063577

Cingolani, E., Goldhaber, J. I., and Marbán, E. (2018). Next-generation pacemakers: from small devices to biological pacemakers. *Nat. Rev. Cardiol.* 15, 139–150. doi: 10.1038/nrcardio.2017.165

Cingolani, E., Yee, K., Shehata, M., Chugh, S. S., Marbán, E., and Cho, H. C. (2012). Biological pacemaker created by percutaneous gene delivery via venous catheters in a porcine model of complete heart block. *Hear. Rhythm* 9, 1310–1318. doi: 10.1016/j.hrthm.2012.04.020

Co, M. L., Khouzam, J. P., Pour-Ghaz, I., Minhas, S., and Basu-Ray, I. (2021). Emerging technologies in cardiac pacing from leadless pacers to stem cells. *Curr. Probl. Cardiol.* 46, 100797. doi: 10.1016/j.cpcardiol.2021.100797

Dal Sasso, E., Menabò, R., Agrillo, D., Arrigoni, G., Franchin, C., Giraudo, C., et al. (2020). RegenHeart: a time-effective, low-concentration, detergent-based method aiming for conservative decellularization of the whole heart organ. *ACS Biomater. Sci. Eng.* 6, 5493–5506. doi: 10.1021/acsbiomaterials.0c00540

Dawkins, J. F., Hu, Y.-F., Valle, J., Sanchez, L., Zheng, Y., Marbán, E., et al. (2019). Antegrade conduction rescues right ventricular pacing-induced cardiomyopathy in complete heart block. *J. Am. Coll. Cardiol.* 73, 1673–1687. doi: 10.1016/j.jacc.2018.12.086

DeSimone, D. C., and Sohail, M. R. (2018). Infection management. *Card. Electrophysiol. Clin.* 10, 601–607. doi: 10.1016/j.ccep.2018.04.002

Deuse, T., Hu, X., Gravina, A., Wang, D., Tediashvili, G., De, C., et al. (2019). Hypoimmunogenic derivatives of induced pluripotent stem cells evade immune rejection in fully immunocompetent allogeneic recipients. *Nat. Biotechnol.* 37, 252–258. doi: 10.1038/s41587-019-0016-3

DiFrancesco, D. (2020). A brief history of pacemaking. *Front. Physiol.* 10:1599. doi: 10.3389/fphys.2019.01599

Dobrzynski, H., Anderson, R. H., Atkinson, A., Borbas, Z., D'Souza, A., Fraser, J. F., et al. (2013). Structure, function and clinical relevance of the cardiac conduction system, including the atrioventricular ring and outflow tract tissues. *Pharmacol. Ther.* 139, 260–288. doi: 10.1016/j.pharmthera.2013.04.010

Dorn, T., Goedel, A., Lam, J. T., Haas, J., Tian, Q., Herrmann, F., et al. (2015). Direct nkx2-5 transcriptional repression of isl1 controls cardiomyocyte subtype identity. *Stem Cells* 33, 1113–1129. doi: 10.1002/stem.1923

Dorn, T., Kornherr, J., Parrotta, E. I., Zawada, D., Ayetey, H., Santamaria, G., et al. (2018). Interplay of cell-cell contacts and RhoA/MRTF-A signaling regulates cardiomyocyte identity. *EMBO J.* 37:e98133. doi: 10.15252/embj.201798133

Drukker, M., and Benvenisty, N. (2004). The immunogenicity of human embryonic stem-derived cells. *Trends Biotechnol.* 22, 136–141. doi: 10.1016/j.tibtech.2004.01.003

D'Souza, A., Pearman, C. M., Wang, Y., Nakao, S., Logantha, S. J. R. J., Cox, C., et al. (2017). Targeting miR-423-5p reverses exercise training–induced HCN4 channel remodeling and sinus bradycardia. *Circ. Res.* 121, 1058–1068. doi: 10.1161/CIRCRESAHA.117.311607

Dun, W., and Boyden, P. A. (2008). The Purkinje cell; 2008 style. *J. Mol. Cell. Cardiol.* 45, 617–624. doi: 10.1016/j.yjmcc.2008.08.001

Edelberg, J. M. (2001). Molecular enhancement of porcine cardiac chronotropy. *Heart* 86, 559–562. doi: 10.1136/heart.86.5.559

Edelberg, J. M., Aird, W. C., and Rosenberg, R. D. (1998). Enhancement of murine cardiac chronotropy by the molecular transfer of the human beta2 adrenergic receptor cDNA. *J. Clin. Invest.* 101, 337–343. doi: 10.1172/JCI1330

Ernst, R. W., and Paulson, D. L. (1962). Pedicle grafting of the sino-auricular node to the right ventricle for the treatment of complete atrioventricular block. *J. Thorac. Cardiovasc. Surg.* 44, 681–686. doi: 10.1016/S0022-5223(19)32933-2

Esrick, E. B., Lehmann, L. E., Biffi, A., Achebe, M., Brendel, C., Ciuculescu, M. F., et al. (2021). Post-transcriptional genetic silencing of BCL11A to treat sickle cell disease. *N. Engl. J. Med.* 384, 205–215. doi: 10.1056/NEJMoa2029392

Feiner, R., and Dvir, T. (2020). Engineering smart hybrid tissues with built-in electronics. *iScience* 23:833. doi: 10.1016/j.isci.2020.100833

Franco, D., and Icardo, J. M. (2001). Molecular characterization of the ventricular conduction system in the developing mouse heart: topographical correlation in normal and congenitally malformed hearts. *Cardiovasc. Res.* 49, 417–429. doi: 10.1016/S0008-6363(00)00252-2

Gerbin, K. A., Yang, X., Murry, C. E., and Coulombe, K. L. K. (2015). Enhanced electrical integration of engineered human myocardium via intramyocardial versus epicardial delivery in infarcted rat hearts. *PLoS ONE* 10:e0131446. doi: 10.1371/journal.pone.0131446

Gintant, G. A., Datyner, N. B., and Cohen, I. S. (1984). Slow inactivation of a tetrodotoxin-sensitive current in canine cardiac Purkinje fibers. *Biophys. J.* 45, 509–512. doi: 10.1016/S0006-3495(84)84187-9

Goodyer, W. R., Beyersdorf, B. M., Paik, D. T., Tian, L., Li, G., Buikema, J. W., et al. (2019). Transcriptomic profiling of the developing cardiac conduction system at single-cell resolution. *Circ. Res.* 125, 379–397. doi: 10.1161/CIRCRESAHA.118.314578

Gorabi, A. M., Hajighasemi, S., Khori, V., Soleimani, M., Rajaei, M., Rabbani, S., et al. (2019a). Functional biological pacemaker generation by T-Box18 protein expression via stem cell and viral delivery approaches in a murine model of complete heart block. *Pharmacol. Res.* 141, 443–450. doi: 10.1016/j.phrs.2019.01.034

Gorabi, A. M., Hajighasemi, S., Tafti, H. A., Atashi, A., Soleimani, M., Aghdami, N., et al. (2019b). TBX18 transcription factor overexpression in human-induced pluripotent stem cells increases their differentiation into pacemaker-like cells. *J. Cell. Physiol.* 234, 1534–1546. doi: 10.1002/jcp.27018

Greene, D., Kang, S., Kosenko, A., and Hoshi, N. (2012). Adrenergic regulation of HCN4 channel requires protein association with β2-adrenergic receptor. *J. Biol. Chem.* 287, 23690–23697. doi: 10.1074/jbc.M112.366955

Grijalva, S. I., Gu, J., Li, J., Fernandez, N., Fan, J., Sung, J. H., et al. (2019). Engineered cardiac pacemaker nodes created by TBX18 gene transfer overcome source–sink mismatch. *Adv. Sci.* 6:1901099. doi: 10.1002/advs.201901099

Gutiérrez, M., Figueroa, F., Rivero, S., Salles, J. P., Arnaiz, P., Cruzat, L., et al. (1989). [Maternal connective tissue disease associated with congenital AV block]. *Rev. Med. Chil.* 117, 789–93.

Hamdi, H., Planat-Benard, V., Bel, A., Puymirat, E., Geha, R., Pidial, L., et al. (2011). Epicardial adipose stem cell sheets results in greater post-infarction survival than intramyocardial injections. *Cardiovasc. Res.* 91, 483–491. doi: 10.1093/cvr/cvr099

Hardin-Young, J., Teumer, J., Ross, R. N., and Parenteau, N. L. (2000). "Chapter 23 - Approaches to transplanting engineered cells and tissues," in *Tissue Engineering Intelligence Unit, Principles of Tissue Engineering (Second Edition)*, eds R. P. Lanza, R. Langer, and J. Vacanti (Academic Press), 281–291. doi: 10.1016/B978-012436630-5/50027-1

He, J.-Q., Ma, Y., Lee, Y., Thomson, J. A., and Kamp, T. J. (2003). Human embryonic stem cells develop into multiple types of cardiac myocytes. *Circ. Res.* 93, 32–39. doi: 10.1161/01.RES.0000080317.92718.99

Hoogaars, W. M. H., Engel, A., Brons, J. F., Verkerk, A. O., de Lange, F. J., Wong, L. Y. E., et al. (2007). Tbx3 controls the sinoatrial node gene program and imposes pacemaker function on the atria. *Genes Dev.* 21, 1098–1112. doi: 10.1101/gad.416007

Hu, Y.-F., Dawkins, J. F., Cho, H. C., Marbán, E., Cingolani, E., Marban, E., et al. (2014). Biological pacemaker created by minimally invasive somatic reprogramming in pigs with complete heart block. *Sci. Transl. Med.* 6, 245ra94–245ra94. doi: 10.1126/scitranslmed.3008681

Huang, C., Kaza, A. K., Hitchcock, R. W., and Sachse, F. B. (2013). Identification of nodal tissue in the living heart using rapid scanning fiber-optics confocal

microscopy and extracellular fluorophores. *Circ. Cardiovasc. Imaging* 6, 739–746. doi: 10.1161/CIRCIMAGING.112.000121

Ieda, M., Fu, J. D., Delgado-Olguin, P., Vedantham, V., Hayashi, Y., Bruneau, B. G., et al. (2010). Direct reprogramming of fibroblasts into functional cardiomyocytes by defined factors. *Cell* 142, 375–386. doi: 10.1016/j.cell.2010.07.002

Inagawa, K., Miyamoto, K., Yamakawa, H., Muraoka, N., Sadahiro, T., Umei, T., et al. (2012). Induction of cardiomyocyte-like cells in infarct hearts by gene transfer of Gata4, Mef2c, and Tbx5. *Circ. Res.* 111, 1147–1156. doi: 10.1161/CIRCRESAHA.112.271148

Ionta, V., Liang, W., Kim, E. H., Rafie, R., Giacomello, A., Marbán, E., et al. (2015). SHOX2 overexpression favors differentiation of embryonic stem cells into cardiac pacemaker cells, improving biological pacing ability. *Stem Cell Rep.* 4, 129–142. doi: 10.1016/j.stemcr.2014.11.004

Iop, L., Bonetti, A., Naso, F., Rizzo, S., Cagnin, S., Bianco, R., et al. (2014). Decellularized allogeneic heart valves demonstrate self-regeneration potential after a long-term preclinical evaluation. *PLoS ONE* 9:e99593. doi: 10.1371/journal.pone.0099593

Iop, L., Palmosi, T., Dal Sasso, E., and Gerosa, G. (2018). Bioengineered tissue solutions for repair, correction and reconstruction in cardiovascular surgery. *J. Thorac. Dis.* 10, S2390–S2411. doi: 10.21037/jtd.2018.04.27

Iop, L., Renier, V., Naso, F., Piccoli, M., Bonetti, A., Gandaglia, A., et al. (2009). The influence of heart valve leaflet matrix characteristics on the interaction between human mesenchymal stem cells and decellularized scaffolds. *Biomaterials* 30, 4104–4116. doi: 10.1016/j.biomaterials.2009.04.031

Irisawa, H., Brown, H. F., and Giles, W. (1993). Cardiac pacemaking in the sinoatrial node. *Physiol. Rev.* 73, 197–227. doi: 10.1152/physrev.1993.73.1.197

Ishigaki, H., Pham, V. L., Terai, J., Sasamura, T., Nguyen, C. T., Ishida, H., et al. (2021). No tumorigenicity of allogeneic induced pluripotent stem cells in major histocompatibility complex-matched cynomolgus macaques. *Cell Transplant.* 30:66. doi: 10.1177/0963689721992066

James, T. N. (1961). Anatomy of the human sinus node. *Anat. Rec.* 141, 109–139. doi: 10.1002/ar.1091410205

James, T. N. (1970). Cardiac conduction system: fetal and postnatal development. *Am. J. Cardiol.* 25, 213–226. doi: 10.1016/0002-9149(70)90581-3

James, T. N. (1977). The sinus node. *Am. J. Cardiol.* 40, 965–986. doi: 10.1016/0002-9149(77)90048-0

James, T. N., and Sherf, L. (1971). Fine structure of the His bundle. *Circulation* 44, 9–28. doi: 10.1161/01.CIR.44.1.9

Joury, A., Bob-Manuel, T., Sanchez, A., Srinithya, F., Sleem, A., Nasir, A., et al. (2021). Leadless and wireless cardiac devices: the next frontier in remote patient monitoring. *Curr. Probl. Cardiol.* 46:100800. doi: 10.1016/j.cpcardiol.2021.100800

Jung, C. B., Moretti, A., Mederos y Schnitzler, M., Iop, L., Storch, U., Bellin, M., et al. (2012). Dantrolene rescues arrhythmogenic RYR2 defect in a patient-specific stem cell model of catecholaminergic polymorphic ventricular tachycardia. *EMBO Mol. Med.* 4, 180–191. doi: 10.1002/emmm.201100194

Jung, J. J., Husse, B., Rimmbach, C., Krebs, S., Stieber, J., Steinhoff, G., et al. (2014). Programming and isolation of highly pure physiologically and pharmacologically functional sinus-nodal bodies from pluripotent stem cells. *Stem Cell Rep.* 2, 592–605. doi: 10.1016/j.stemcr.2014.03.006

Kadota, S., Tanaka, Y., and Shiba, Y. (2020). Heart regeneration using pluripotent stem cells. *J. Cardiol.* 76, 459–463. doi: 10.1016/j.jjcc.2020.03.013

Kapoor, N., Liang, W., Marbán, E., and Cho, H. C. (2013). Direct conversion of quiescent cardiomyocytes to pacemaker cells by expression of Tbx18. *Nat. Biotechnol.* 31, 54–62. doi: 10.1038/nbt.2465

Kawamura, M., Miyagawa, S., Fukushima, S., Saito, A., Miki, K., Ito, E., et al. (2013). Enhanced survival of transplanted human induced pluripotent stem cell-derived cardiomyocytes by the combination of cell sheets with the pedicled omental flap technique in a porcine heart. *Circulation* 128, S87–S94. doi: 10.1161/CIRCULATIONAHA.112.000366

Kehat, I., Kenyagin-Karsenti, D., Snir, M., Segev, H., Amit, M., Gepstein, A., et al. (2001). Human embryonic stem cells can differentiate into myocytes with structural and functional properties of cardiomyocytes. *J. Clin. Invest.* 108, 407–414. doi: 10.1172/JCI12131

Kehat, I., Khimovich, L., Caspi, O., Gepstein, A., Shofti, R., Arbel, G., et al. (2004). Electromechanical integration of cardiomyocytes derived from human embryonic stem cells. *Nat. Biotechnol.* 22, 1282–1289. doi: 10.1038/nbt1014

Keith, A., and Flack, M. (1907). The form and nature of the muscular connections between the primary divisions of the vertebrate heart. *J Anat Physiol.* 41, 172–189.

Kent, A. F. S. (1913). Observations on the auriculo-ventricular junction of the mammalian heart. *Q. J. Exp. Physiol* 7, 193–195.

Kurian, T., Ambrosi, C., Hucker, W., Fedorov, V. V., and Efimov, I. R. (2010). Anatomy and electrophysiology of the human AV node. *PACE Pacing Clin. Electrophysiol.* 33, 754–762. doi: 10.1111/j.1540-8159.2010.02699.x

Laflamme, M. A., Chen, K. Y., Naumova, A. V., Muskheli, V., Fugate, J. A., Dupras, S. K., et al. (2007). Cardiomyocytes derived from human embryonic stem cells in pro-survival factors enhance function of infarcted rat hearts. *Nat. Biotechnol.* 25, 1015–1024. doi: 10.1038/nbt1327

Lakatta, E. G., and DiFrancesco, D. (2009). What keeps us ticking: a funny current, a calcium clock, or both? *J. Mol. Cell. Cardiol.* 47, 157–170. doi: 10.1016/j.yjmcc.2009.03.022

LeBlanc, A. R., and Dubé, B. (1993). Propagation in the AV node: a model based on a simplified two-dimensional structure and a bidomain tissue representation. *Med. Biol. Eng. Comput.* 31, 545–556. doi: 10.1007/BF02441800

Li, R. A. (2012). Gene- and cell-based bio-artificial pacemaker: what basic and translational lessons have we learned? *Gene Ther.* 19, 588–595. doi: 10.1038/gt.2012.33

Liao, Y., Li, H., Cao, H., Dong, Y., Gao, L., Liu, Z., et al. (2021). Therapeutic silencing miR-146b-5p improves cardiac remodeling in a porcine model of myocardial infarction by modulating the wound reparative phenotype. *Protein Cell* 12, 194–212. doi: 10.1007/s13238-020-00750-6

Lin, G., Cai, J., Jiang, H., Shen, H., Jiang, X., Yu, Q., et al. (2005). Biological pacemaker created by fetal cardiomyocyte transplantation. *J. Biomed. Sci.* 12, 513–519. doi: 10.1007/s11373-005-6794-2

Liu, J., Dobrzynski, H., Yanni, J., Boyett, M. R., and Lei, M. (2007). Organisation of the mouse sinoatrial node: structure and expression of HCN channels. *Cardiovasc. Res.* 73, 729–738. doi: 10.1016/j.cardiores.2006.11.016

Ma, W., Zhu, D., Li, J., Chen, X., Xie, W., Jiang, X., et al. (2020). Coating biomimetic nanoparticles with chimeric antigen receptor T cell-membrane provides high specificity for hepatocellular carcinoma photothermal therapy treatment. *Theranostics* 10, 1281–1295. doi: 10.7150/thno.40291

Maltsev, V. A., and Lakatta, E. G. (2008). Dynamic interactions of an intracellular Ca2+ clock and membrane ion channel clock underlie robust initiation and regulation of cardiac pacemaker function. *Cardiovasc. Res.* 77, 274–284. doi: 10.1093/cvr/cvm058

Mandel, Y., Weissman, A., Schick, R., Barad, L., Novak, A., Meiry, G., et al. (2012). Human embryonic and induced pluripotent stem cell–derived cardiomyocytes exhibit beat rate variability and power-law behavior. *Circulation* 125, 883–893. doi: 10.1161/CIRCULATIONAHA.111.045146

Mangoni, M. E., Traboulsie, A., Leoni, A. L., Couette, B., Marger, L., Le Quang, K., et al. (2006). Bradycardia and slowing of the atrioventricular conduction in mice lacking CaV3.1/α1G T-type calcium channels. *Circ. Res.* 98, 1422–1430. doi: 10.1161/01.RES.0000225862.14314.49

Manolis, A. A., Manolis, T. A., Melita, H., and Manolis, A. S. (2020). Congenital heart block: pace earlier (Childhood) than later (Adulthood). *Trends Cardiovasc. Med.* 30, 275–286. doi: 10.1016/j.tcm.2019.06.006

Meijler, F. L., and Janse, M. J. (1988). Morphology and electrophysiology of the mammalian atrioventricular node. *Physiol. Rev.* 68, 608–647. doi: 10.1152/physrev.1988.68.2.608

Menasché, P., Vanneaux, V., Hagège, A., Bel, A., Cholley, B., Parouchev, A., et al. (2018). Transplantation of human embryonic stem cell–derived cardiovascular progenitors for severe ischemic left ventricular dysfunction. *J. Am. Coll. Cardiol.* 71, 429–438. doi: 10.1016/j.jacc.2017.11.047

Mensah, G. A., Roth, G. A., and Fuster, V. (2019). The global burden of cardiovascular diseases and risk factors. *J. Am. Coll. Cardiol.* 74, 2529–2532. doi: 10.1016/j.jacc.2019.10.009

Miake, J., Marbán, E., and Nuss, H. B. (2002). Biological pacemaker created by gene transfer. *Nature* 419, 132–133. doi: 10.1038/419132b

Miake, J., Marbán, E., and Nuss, H. B. (2003). Functional role of inward rectifier current in heart probed by Kir2.1 overexpression and dominant-negative suppression. *J. Clin. Invest.* 111, 1529–1536. doi: 10.1172/JCI17959

Morishita, Y., Poirier, R., a., and Rohner, R. F. (1981). Sino-Atrial Node Transplantation in the Dog. *Vasc. Endovascular Surg.* 15, 388–393. doi: 10.1177/153857448101500603

Morris, G. M., D'Souza, A., Dobrzynski, H., Lei, M., Choudhury, M., Billeter, R., et al. (2013). Characterization of a right atrial subsidiary pacemaker and acceleration of the pacing rate by HCN over-expression. *Cardiovasc. Res.* 100, 160–169. doi: 10.1093/cvr/cvt164

Müller, M., Stockmann, M., Malan, D., Wolheim, A., Tischendorf, M., Linta, L., et al. (2012). Ca2+ activated K channels-new tools to induce cardiac commitment from pluripotent stem cells in mice and men. *Stem Cell Rev. Rep.* 8, 720–740. doi: 10.1007/s12015-011-9324-9

Munshi, N. V. (2012). Gene regulatory networks in cardiac conduction system development. *Circ. Res.* 110, 1525–1537. doi: 10.1161/CIRCRESAHA.111.260026

Nam, Y.-J., Lubczyk, C., Bhakta, M., Zang, T., Fernandez-Perez, A., McAnally, J., et al. (2014). Induction of diverse cardiac cell types by reprogramming fibroblasts with cardiac transcription factors. *Development* 141, 4267–4278. doi: 10.1242/dev.114025

Narita, T., Shintani, Y., Ikebe, C., Kaneko, M., Campbell, N. G., Coppen, S. R., et al. (2013). The use of scaffold-free cell sheet technique to refine mesenchymal stromal cell-based therapy for heart failure. *Mol. Ther.* 21, 860–867. doi: 10.1038/mt.2013.9

Nishii, N. (2016). Arrhythmia management after device removal. *J. Arrhythmia* 32, 287–292. doi: 10.1016/j.joa.2015.09.004

Noma, A., and Irisawa, H. (1976). Membrane currents in the rabbit sinoatrial node cell as studied by the double microelectrode method. *Pflügers Arch. Eur. J. Physiol.* 364, 45–52. doi: 10.1007/BF01062910

Nong, Y., Zhang, C., Wei, L., Zhang, Z., Cheng, J., Wen, L., et al. (2013). *In situ* investigation of allografted mouse HCN4 gene–transfected rat bone marrow mesenchymal stromal cells with the use of patch-clamp recording of ventricular slices. *Cytotherapy* 15, 905–919. doi: 10.1016/j.jcyt.2013.03.010

Padala, S. K., Cabrera, J. A., and Ellenbogen, K. A. (2021). Anatomy of the cardiac conduction system. *PACE Pacing Clin. Electrophysiol.* 44, 15–25. doi: 10.1111/pace.14107

Park, D. S., and Fishman, G. I. (2011). The cardiac conduction system. *Circulation* 123, 904–915. doi: 10.1161/CIRCULATIONAHA.110.942284

Park, K. M., Cha, S. H., Ahn, C., and Woo, H. M. (2013). Generation of porcine induced pluripotent stem cells and evaluation of their major histocompatibility complex protein expression *in vitro*. *Vet. Res. Commun.* 37, 293–301. doi: 10.1007/s11259-013-9574-x

Persson, A. B., and Persson, P. B. (2012). Cardiac electrophysiology: what is behind our two-billion heart beats? *Acta Physiol.* 206, 90–93. doi: 10.1111/j.1748-1716.2012.02466.x

Peters, C. H., Sharpe, E. J., and Proenza, C. (2020). Cardiac pacemaker activity and aging. *Annu. Rev. Physiol.* 82, 21–43. doi: 10.1146/annurev-physiol-021119-034453

Piron, J., Quang, K., Le, B.riec, F., Amirault, J.-C., and Leoni, A.-L., Desigaux, L., et al. (2008). Biological pacemaker engineered by nonviral gene transfer in a mouse model of complete atrioventricular block. *Mol. Ther.* 16, 1937–1943. doi: 10.1038/mt.2008.209

Pittenger, M. F., Discher, D. E., Péault, B. M., Phinney, D. G., Hare, J. M., and Caplan, A. I. (2019). Mesenchymal stem cell perspective: cell biology to clinical progress. *NPJ Regen. Med.* 4:22. doi: 10.1038/s41536-019-0083-6

Plotnikov, A. N., Bucchi, A., Shlapakova, I., Danilo, P., Brink, P. R., Robinson, R. B., et al. (2008). HCN212-channel biological pacemakers manifesting ventricular tachyarrhythmias are responsive to treatment with If blockade. *Hear. Rhythm* 5, 282–288. doi: 10.1016/j.hrthm.2007.09.028

Plotnikov, A. N., Shlapakova, I., Szabolcs, M. J., Danilo, P., Lorell, B. H., Potapova, I. A., et al. (2007). Xenografted adult human mesenchymal stem cells provide a platform for sustained biological pacemaker function in canine heart. *Circulation* 116, 706–713. doi: 10.1161/CIRCULATIONAHA.107.703231

Plotnikov, A. N., Sosunov, E. A., Qu, J., Shlapakova, I. N., Anyukhovsky, E. P., Liu, L., et al. (2004). Biological pacemaker implanted in canine left bundle branch provides ventricular escape rhythms that have physiologically acceptable rates. *Circulation* 109, 506–512. doi: 10.1161/01.CIR.0000114527.10764.CC

Pollack, G. H. (1976). Intercellular coupling in the atrioventricular node and other tissues of the rabbit heart. *J. Physiol.* 255, 275–298. doi: 10.1113/jphysiol.1976.sp011280

Potapova, I., Plotnikov, A., Lu, Z., Danilo, P., Valiunas, V., Qu, J., et al. (2004). Human mesenchymal stem cells as a gene delivery system to create cardiac pacemakers. *Circ. Res.* 94, 952–959. doi: 10.1161/01.RES.0000123827.60210.72

Protze, S., Khattak, S., Poulet, C., Lindemann, D., Tanaka, E. M., and Ravens, U. (2012). A new approach to transcription factor screening for reprogramming of fibroblasts to cardiomyocyte-like cells. *J. Mol. Cell. Cardiol.* 53, 323–332. doi: 10.1016/j.yjmcc.2012.04.010

Protze, S. I., Liu, J., Nussinovitch, U., Ohana, L., Backx, P. H., Gepstein, L., et al. (2016). Sinoatrial node cardiomyocytes derived from human pluripotent cells function as a biological pacemaker. *Nat. Biotechnol.* 35, 56–68. doi: 10.1038/nbt.3745

Qian, L., Huang, Y., Spencer, C. I., Foley, A., Vedantham, V., Liu, L., et al. (2012). *In vivo* reprogramming of murine cardiac fibroblasts into induced cardiomyocytes. *Nature* 485, 593–598. doi: 10.1038/nature11044

Qu, J., Plotnikov, A. N., Danilo, P., Shlapakova, I., Cohen, I. S., Robinson, R. B., et al. (2003). Expression and function of a biological pacemaker in canine heart. *Circulation* 107, 1106–1109. doi: 10.1161/01.CIR.0000059939.97249.2C

Quan, D., and Huang, H. (2018). In vitro study of the effects of reprogramming neonatal rat fibroblasts transfected with TBX18 on spontaneous beating in neonatal rat cardiomyocytes. *Mol. Med. Rep.* 18, 5520–5526. doi: 10.3892/mmr.2018.9566

Quinn, C., and Flake, A. W. (2008). *In vivo* differentiation potential of mesenchymal stem cells: prenatal and postnatal model systems. *Transfus. Med. Hemotherapy* 35, 239–247. doi: 10.1159/000129129

Raghunathan, S., Islas, J. F., Mistretta, B., Iyer, D., Shi, L., Gunaratne, P. H., et al. (2020). Conversion of human cardiac progenitor cells into cardiac pacemaker-like cells. *J. Mol. Cell. Cardiol.* 138, 12–22. doi: 10.1016/j.yjmcc.2019.09.015

Rajala, K., Pekkanen-Mattila, M., and Aalto-Setäl,ä, K. (2011). Cardiac differentiation of pluripotent stem cells. *Stem Cells Int.* 2011, 1–12. doi: 10.4061/2011/383709

Robotti, F., Sterner, I., Bottan, S., Monné Rodríguez, J. M., Pellegrini, G., Schmidt, T., et al. (2020). Microengineered biosynthesized cellulose as anti-fibrotic *in vivo* protection for cardiac implantable electronic devices. *Biomaterials* 229:119583. doi: 10.1016/j.biomaterials.2019.119583

Rosen, M. R., Robinson, R. B., Brink, P. R., and Cohen, I. S. (2011). The road to biological pacing. *Nat. Rev. Cardiol.* 8, 656–666. doi: 10.1038/nrcardio.2011.120

Rougier, O., Vassort, G., Gargouil, Y. M., and Coraboeuf, E. (1969). Existence and role of a slow inward current during the frog atrial action potential. *Pflügers Arch. Eur. J. Physiol.* 308, 91–110. doi: 10.1007/BF00587018

Rouwkema, J., Koopman, B. F. J. M., Blitterswijk, C. A. V., Dhert, W. J. A., and Malda, J. (2009). Supply of nutrients to cells in engineered tissues. *Biotechnol. Genet. Eng. Rev.* 26, 163–178. doi: 10.5661/bger-26-163

Ruhparwar, A., Kallenbach, K., Klein, G., Bara, C., Ghodsizad, A., Sigg, D. C., et al. (2010). Adenylate-cyclase vi transforms ventricular cardiomyocytes into biological pacemaker cells. *Tissue Eng. Part A* 16, 1867–1872. doi: 10.1089/ten.tea.2009.0537

Ruhparwar, A., Tebbenjohanns, J., Niehaus, M., Mengel, M., Irtel, T., Kofidis, T., et al. (2002). Transplanted fetal cardiomyocytes as cardiac pacemaker. *Eur. J. Cardiothorac. Surg.* 21, 853–857. doi: 10.1016/s1010-7940(02)00066-0

Rylant, P. (1927). "Contribution à l'ètude de l'automatisme et de la conduction dans le coeur," in *Bulletin de l'Académie royale de médecine de Belgique* (Bulletin de l'Académie royale de médecine de Belgique), 161–200.

Sasano, Y., Fukumoto, K., Tsukamoto, Y., Akagi, T., and Akashi, M. (2020). Construction of 3D cardiac tissue with synchronous powerful beating using human cardiomyocytes from human iPS cells prepared by a convenient differentiation method. *J. Biosci. Bioeng.* 129, 749–755. doi: 10.1016/j.jbiosc.2020.01.001

Schlaeger, T. M., Daheron, L., Brickler, T. R., Entwisle, S., Chan, K., Cianci, A., et al. (2015). A comparison of non-integrating reprogramming methods. *Nat. Biotechnol.* 33, 58–63. doi: 10.1038/nbt.3070

Schulze, M. L., Lemoine, M. D., Fischer, A. W., Scherschel, K., David, R., Riecken, K., et al. (2019). Dissecting hiPSC-CM pacemaker function in a cardiac organoid model. *Biomaterials* 206, 133–145. doi: 10.1016/j.biomaterials.2019.03.023

Sekar, R. B., Kizana, E., Cho, H. C., Molitoris, J. M., Hesketh, G. G., Eaton, B. P., et al. (2009). I K1 heterogeneity affects genesis and stability of spiral waves in cardiac myocyte monolayers. *Circ. Res.* 104, 355–364. doi: 10.1161/CIRCRESAHA.108.178335

Shah Mohammadi, M., Buchen, J. T., Pasquina, P. F., Niklason, L., Alvarez, L. M., and Jariwala, S. H. (2020). Critical considerations for

regeneration of vascularized composite tissues. *Tissue Eng. Part B Rev.* doi: 10.1089/ten.teb.2020.0223. [Epub ahead of print].

Shiba, Y., Filice, D., Fernandes, S., Minami, E., Dupras, S. K., Van Biber, B., et al. (2014). Electrical integration of human embryonic stem cell-derived cardiomyocytes in a guinea pig chronic infarct model. *J. Cardiovasc. Pharmacol. Ther.* 19, 368–381. doi: 10.1177/1074248413520344

Shlapakova, I. N., Nearing, B. D., Lau, D. H., Boink, G. J. J., Danilo, P., Kryukova, Y., et al. (2010). Biological pacemakers in canines exhibit positive chronotropic response to emotional arousal. *Hear. Rhythm* 7, 1835–1840. doi: 10.1016/j.hrthm.2010.08.004

Smart, N., Bollini, S., Dubé, K. N., Vieira, J. M., Zhou, B., Davidson, S., et al. (2011). *De novo* cardiomyocytes from within the activated adult heart after injury. *Nature* 474, 640–644. doi: 10.1038/nature10188

Smits, A. M., Van Laake, L. W., Den Ouden, K., Schreurs, C., Szuhai, K., Van Echteld, C. J., et al. (2009). Human cardiomyocyte progenitor cell transplantation preserves long-term function of the infarcted mouse myocardium. *Cardiovasc. Res.* 83, 527–535. doi: 10.1093/cvr/cvp146

Spach, M. S., Barr, R. C., Serwer, G. S., Johnson, E. A., and Kootsey, J. M. (1971). Collision of excitation waves in the dog purkinje system. *Circ. Res.* 29, 499–511. doi: 10.1161/01.RES.29.5.499

Starzl, T. E., Hermann, G., Axtell, H. K., Marchioro, T. L., and Waddell, W. R. (1963). Failure of sino-atrial nodal transplantation for the treatment of experimental complete heart block in dogs. *J. Thorac. Cardiovasc. Surg.* 46, 201–5.

Statement on NHLBI decision to pause the Pilot and Feasibility Study of Hematopoietic Stem Cell Gene Transfer for Sickle Cell Disease | NHLBI, NIH. (2021). Available online at: https://www.nhlbi.nih.gov/education-and-awareness/sickle-cell/statement-study-gene-transfer-scd (accessed May 3, 2021).

Sternick, E. B., and Sánchez-Quintana, D. (2021). Critical assessment of the concepts and misconceptions of the cardiac conduction system over the last 100 years: the personal quest of robert H. *J. Cardiovasc. Dev. Dis.* 8:5. doi: 10.3390/jcdd8010005

Takeichi, M., Nimura, K., Mori, M., Nakagami, H., and Kaneda, Y. (2013). The transcription factors Tbx18 and Wt1 control the epicardial epithelial-mesenchymal transition through bi-directional regulation of slug in murine primary epicardial cells. *PLoS ONE* 8:e57829. doi: 10.1371/journal.pone.0057829

Taleski, J., and Zafirovska, B. (2021). Strategies to promote long-term cardiac implant site health. *Cureus* 13:e12457. doi: 10.7759/cureus.12457

Tano, N., Narita, T., Kaneko, M., Ikebe, C., Coppen, S. R., Campbell, N. G., et al. (2014). Epicardial placement of mesenchymal stromal cell-sheets for the treatment of ischemic cardiomyopathy; *in vivo* proof-of-concept study. *Mol. Ther.* 22, 1864–1871. doi: 10.1038/mt.2014.110

Tawara, S. (1906). Die topographie und histologie der bruckenfasern.Ein beitrag zur lehre von der bedeutung der Purkinjeschen faden. *Zentralbl Physiol* 19, 70–76.

Tse, H.-F., Xue, T., Lau, C.-P., Siu, C.-W., Wang, K., Zhang, Q.-Y., et al. (2006). Bioartificial sinus node constructed via *in vivo* gene transfer of an engineered pacemaker HCN channel reduces the dependence on electronic pacemaker in a sick-sinus syndrome model. *Circulation* 114, 1000–1011. doi: 10.1161/CIRCULATIONAHA.106.615385

van Eif, V. W. W., Protze, S. I., Bosada, F. M., Yuan, X., Sinha, T., van Duijvenboden, K., et al. (2020). Genome-wide analysis identifies an essential human TBX3 pacemaker enhancer. *Circ. Res.* 127, 1522–1535. doi: 10.1161/CIRCRESAHA.120.317054

Végh, A. M. D., den Haan, A. D., Cócera Ortega, L., Verkerk, A. O., Sluijter, J. P. G., Bakker, D., et al. (2019). Cardiomyocyte progenitor cells as a functional gene delivery vehicle for long-term biological pacing. *Molecules* 24:181. doi: 10.3390/molecules24010181

Végh, A. M. D., Verkerk, A. O., Cócera Ortega, L., Wang, J., Geerts, D., Klerk, M., et al. (2021). Toward biological pacing by cellular delivery of Hcn2/SkM1. *Front. Physiol.* 11:588679. doi: 10.3389/fphys.2020.588679

Virani, S. S., Alonso, A., Benjamin, E. J., Bittencourt, M. S., Callaway, C. W., Carson, A. P., et al. (2020). Heart disease and stroke statistics–2020 update: a report from the american heart association. *Circulation* 141:757. doi: 10.1161/CIR.0000000000000757

Wang, F., Zhao, H., Yin, L., Tang, Y., Wang, X., Zhao, Q., et al. (2019). Transcription factor TBX18 reprograms vascular smooth muscle cells of ascending aorta to pacemaker-like cells. *DNA Cell Biol.* 38, 1470–1479. doi: 10.1089/dna.2019.4940

Wiese, C., Grieskamp, T., Airik, R., Mommersteeg, M. T. M., Gardiwal, A., de Gier-de Vries, C., et al. (2009). Formation of the sinus node head and differentiation of sinus node myocardium are independently regulated by Tbx18 and Tbx3. *Circ. Res.* 104, 388–397. doi: 10.1161/CIRCRESAHA.108.187062

Xia, R., Vlcek, J., Bauer, J., Kääb, S., Ishikawa-Ankerhold, H., van den Heuvel, D. A., et al. (2020). Whole-mount immunofluorescence staining, confocal imaging and 3D reconstruction of the sinoatrial and atrioventricular node in the mouse. *J. Vis. Exp.* 166:e62058. doi: 10.3791/62058

Xu, C., Police, S., Rao, N., and Carpenter, M. K. (2002). Characterization and enrichment of cardiomyocytes derived from human embryonic stem cells. *Circ. Res.* 91, 501–508. doi: 10.1161/01.RES.0000035254.80718.91

Xue, T., Cho, H. C., Akar, F. G., Tsang, S.-Y., Jones, S. P., Marbán, E., et al. (2005). Functional integration of electrically active cardiac derivatives from genetically engineered human embryonic stem cells with quiescent recipient ventricular cardiomyocytes: insights into the development of cell-based pacemakers. *Circulation* 111, 11–20. doi: 10.1161/01.CIR.0000151313.18547.A2

Yang, L., Soonpaa, M. H., Adler, E. D., Roepke, T. K., Kattman, S. J., Kennedy, M., et al. (2008). Human cardiovascular progenitor cells develop from a KDR+ embryonic-stem-cell-derived population. *Nature* 453, 524–528. doi: 10.1038/nature06894

Yang, M., Zhang, G. G., Wang, T., Wang, X., Tang, Y. H., Huang, H., et al. (2016). TBX18 gene induces adipose-derived stem cells to differentiate into pacemaker-like cells in the myocardial microenvironment. *Int. J. Mol. Med.* 38, 1403–1410. doi: 10.3892/ijmm.2016.2736

Yang, Z. K., Boyett, M. R., Janvier, N. C., McMorn, S. O., Shui, Z., and Karim, F. (1996). Regional differences in the negative inotropic effect of acetylcholine within the canine ventricle. *J. Physiol.* 492, 789–806. doi: 10.1113/jphysiol.1996.sp021346

Yanni, J., D'Souza, A., Wang, Y., Li, N., Hansen, B. J., Zakharkin, S. O., et al. (2020). Silencing miR-370-3p rescues funny current and sinus node function in heart failure. *Sci. Rep.* 10:11279. doi: 10.1038/s41598-020-67790-0

Yechikov, S., Kao, H. K. J., Chang, C.-W., Pretto, D., Zhang, X.-D., Sun, Y.-H., et al. (2020). NODAL inhibition promotes differentiation of pacemaker-like cardiomyocytes from human induced pluripotent stem cells. *Stem Cell Res.* 49:102043. doi: 10.1016/j.scr.2020.102043

Zhang, H., Lau, D. H., Shlapakova, I. N., Zhao, X., Danilo, P., Robinson, R. B., et al. (2011). Implantation of sinoatrial node cells into canine right ventricle: biological pacing appears limited by the substrate. *Cell Transpl.* 20, 1907–1914. doi: 10.3727/096368911X565038

Zhang, J., and Huang, C. (2019). A new combination of transcription factors increases the harvesting efficiency of pacemaker-like cells. *Mol. Med. Rep.* 19, 3584–3592. doi: 10.3892/mmr.2019.10012

Zhang, J. Z., Termglinchan, V., Shao, N. Y., Itzhaki, I., Liu, C., Ma, N., et al. (2019a). A human iPSC double-reporter system enables purification of cardiac lineage subpopulations with distinct function and drug response profiles. *Cell Stem Cell* 24, 802–811.e5. doi: 10.1016/j.stem.2019.02.015

Zhang, L., Li, X., Yu, X., Li, Y., Sun, A., Huang, C., et al. (2017). Construction of vascularized pacemaker tissues by seeding cardiac progenitor cells and endothelial progenitor cells into Matrigel. *Life Sci.* 179, 139–146. doi: 10.1016/j.lfs.2017.05.007

Zhang, M., Methot, D., Poppa, V., Fujio, Y., Walsh, K., and Murry, C. E. (2001). Cardiomyocyte grafting for cardiac repair: graft cell death and anti-death strategies. *J. Mol. Cell. Cardiol.* 33, 907–921. doi: 10.1006/jmcc.2001.1367

Zhang, W., Li, X., Sun, S., and Zhang, X. (2019b). Implantation of engineered conduction tissue in the rat heart. *Mol. Med. Rep.* 19, 2687–2697. doi: 10.3892/mmr.2019.9933

Zhang, Z., Song, Z., Cheng, J., Nong, Y., Wei, L., and Zhang, C. (2012). The integration and functional evaluation of rabbit pacing cells transplanted into the left ventricular free wall. *Int. J. Med. Sci.* 9, 513–520. doi: 10.7150/ijms.4971

Zhou, Y.-F., Yang, X.-J., Li, H.-X., Han, L.-H., and Jiang, W.-P. (2013). Genetically-engineered mesenchymal stem cells transfected with human HCN1 gene to create cardiac pacemaker cells. *J. Int. Med. Res.* 41, 1570–1576. doi: 10.1177/0300060513501123

Zipes, D. P., and Mendez, C. (1973). Action of manganese ions and tetrodotoxin on atrioventricular nodal transmembrane potentials in isolated rabbit hearts. *Circ. Res.* 32, 447–454. doi: 10.1161/01.RES.32.4.447

Zouhair, S., Sasso, E. D., Tuladhar, S. R., Fidalgo, C., Vedovelli, L., Filippi, A., et al. (2020). A comprehensive comparison of bovine and porcine decellularized pericardia: new insights for surgical applications. *Biomolecules* 10:371. doi: 10.3390/biom10030371

**Conflict of Interest:** The authors declare that the research was conducted in the absence of any commercial or financial relationships that could be construed as a potential conflict of interest.

**Publisher's Note:** All claims expressed in this article are solely those of the authors and do not necessarily represent those of their affiliated organizations, or those of the publisher, the editors and the reviewers. Any product that may be evaluated in this article, or claim that may be made by its manufacturer, is not guaranteed or endorsed by the publisher.

# Advantages of publishing in Frontiers

**OPEN ACCESS**
Articles are free to read for greatest visibility and readership

**FAST PUBLICATION**
Around 90 days from submission to decision

**HIGH QUALITY PEER-REVIEW**
Rigorous, collaborative, and constructive peer-review

**TRANSPARENT PEER-REVIEW**
Editors and reviewers acknowledged by name on published articles

**Frontiers**
Avenue du Tribunal-Fédéral 34
1005 Lausanne | Switzerland

**Visit us:** www.frontiersin.org
**Contact us:** frontiersin.org/about/contact

**REPRODUCIBILITY OF RESEARCH**
Support open data and methods to enhance research reproducibility

**DIGITAL PUBLISHING**
Articles designed for optimal readership across devices

**FOLLOW US**
@frontiersin

**IMPACT METRICS**
Advanced article metrics track visibility across digital media

**EXTENSIVE PROMOTION**
Marketing and promotion of impactful research

**LOOP RESEARCH NETWORK**
Our network increases your article's readership